

# Global Venting, Midwater, and Benthic Ecological Processes

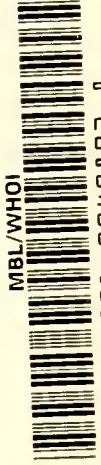
Michael P. De Luca and Ivar Babb  
Editors

July 1988



U.S. DEPARTMENT OF COMMERCE  
National Oceanic and Atmospheric Administration  
Oceanic and Atmospheric Research  
Office of Undersea Research





MBL/WHOI

0 0301 0040892 8

# Global Venting, Midwater, and Benthic Ecological Processes

Michael P. De Luca and Ivar Babb  
Editors

July 1988



**U.S. DEPARTMENT OF COMMERCE**  
C. William Verity, Secretary

**National Oceanic and Atmospheric Administration**  
William E. Evans, Under Secretary

**Oceanic and Atmospheric Research**  
Joseph O. Fletcher, Assistant Administrator

**Office of Undersea Research**  
David B. Duane, Director



## Table of Contents

	Page
PREFACE.....	vii
 CHAPTER I. GLOBAL VENT PROCESSES	
Session Summary: Global Vent Processes Stephen R. Hammond.....	1
Gorda Ridge and Mid-Atlantic Ridge: New Frontiers for Undersea Research. Peter A. Rona.....	3
The Geochemistry of Submarine Venting Fluids at Axial Volcano, Juan de Fuca Ridge: New Sampling Methods and a Vents Program Rationale. Gary J. Massoth, Hugh B. Milburn, Stephen R. Hammond, David A. Butterfield, Russell E. McDuff, & John E. Lupton .....	29
The Caldera of Axial Volcano--Remote Sensing and Submersible Studies of a Hydrothermally Active Submarine Volcano. R. W. Embley, S. R. Hammond & K. Murphy.....	61
Seabeam Backscatter Analysis Applied to the Classification of Deep-Sea Volcanic Terrains. Christopher G. Fox & Marijke van Heeswijk.....	71
The Presence and Potential Impact of Geothermal Activity on the Chemistry and Biology of Yellowstone Lake, Wyoming. J. Val Klump, Charles C. Remsen, & Jerry L. Kaster.....	81
Biological Influences on Mineral Deposition at Deep-Sea Hydrothermal Vents. S. Kim Juniper, Verena Tunnicliffe, & A. R. Fontaine.....	99
Gulf of Mexico Hydrocarbon Seep Ecosystem Studies. James M. Brooks, Eric N. Powell, Mahlon C. Kennicutt, II, Robert S. Carney, Ian R. MacDonald, Susanne J. McDonald, Robert R. Bidigare, & Terry L. Wade.....	119
Biology and Ecology of the Oregon Continental Shelf Edge Associated With the Accretionary Prism. Andrew G. Carey, Jr., David L. Stein, Gary L. Taghon, & Anne E. DeBevoise.....	137

Fluid Venting Structures on the Northern Oregon Continental Shelf. LaVerne D. Kulm, Erwin Suess, & Parke D. Snavely, Jr.....	151
Energy and Carbon Sources for Endosymbioses Between Bacteria and Marine Invertebrates. James J. Childress & Charles R. Fisher.....	177
Initial Microbiological and Chemical Investigations of Pele's Vent, Loihi Seamount. David M. Karl, Andrew Brittain, & Bronte Tilbrook.....	187
Sulfide, Sediment, and Biological Zonation at Ashes Vent Field, Axial Volcano. Alexander Malahoff, Anne M. Arquit, & Gary M. McMurtry.....	235

## CHAPTER II. DEEP WATER ECOLOGY

Session Summary: Deep Water Ecology. Larry Madin.....	247
Effects of Boundary-Layer Flow on the Settlement of Organisms onto Flat Plates: Preliminary Results From Cross Seamount. L. S. Mullenax, C. A. Butman, & C. M. Fuller.....	251
Midwater Community Studies off New England Using the <u>Johnson Sea-Link</u> Submersibles. Ronald J. Larson, G. Richard Harbison, Phillip R. Pugh, John A. Janssen, Robert H. Gibbs, James E. Craddock, Claudia E. Mills, Richard L. Miller, & Ronald W. Gilmer.....	265
The Effect of Plant Material on a Benthic Community of the Bermuda Continental Slope. J. Frederick Grassle, Paul V. R. Snelgrove, James R. Weinberg, & Robert B. Whitlatch .....	283
Beebe Project: Zooplankton Studies in the 1987 Field Season. Laurence P. Madin.....	291
Quantitative Analysis of the Abundance, Swimming Behavior, and Interactions of Midwater Organisms. W. M. Hamner, C. T. Prewitt, & E. Kristof.....	307

## CHAPTER III. OCEAN SERVICES/BIOLOGICAL PRODUCTIVITY

Session Summary: Ocean Services/Biological Productivity. Ivar Babb.....	319
Hazards to Divers in Polluted Waters. Kelly Cunningham & Rita R. Colwell.....	321
Recent Progress in Experimental Saltwater Tilapia Culture in the Caribbean. Wade O. Watanabe, Robert I. Wicklund, Bori L. Olla, & Douglas H. Ernst .....	337
Preliminary Studies on the Early Life History of the Queen Conch <u>Strombus gigas</u> in the Exuma Cays, Bahamas. Robert I. Wicklund, Lucinda J. Hepp, & Geraldine A. Wenz .....	347
Diel Patterns of Growth, Nitrogen Content, Herbivory, and Chemical Versus Morphological Defenses: Can Tropical Seaweeds Reduce Herbivory by Growing at Night? Mark E. Hay, Valerie J. Paul, Sara M. Lewis, Kirk Gustafson, Jane Tucker, & Robbin N. Trindell .....	365
Preliminary Observations on the Capture of Flatfish by Trawls. C. G. Bublitz .....	403
Manned Submersible and ROV Assessment of Ghost Gillnets on Jeffreys and Stellwagen Banks, Gulf of Maine. Richard A. Cooper, H. Arnold Carr, & Alan H. Hulbert.....	429



## PREFACE

The National Oceanic and Atmospheric Administration's Office of Undersea Research supports in-situ research utilizing a variety of systems including manned submersibles, saturation habitats, remotely operated vehicles (ROV's) and scuba. There are currently five National Undersea Research Centers (NURC's) that operate on grants from NOAA to universities and private research centers. These centers are located at the Caribbean Marine Research Center in the Bahamas, the University of Connecticut at Avery Point, Fairleigh Dickinson University's West Indies Laboratory, the University of Hawaii, and the University of North Carolina at Wilmington.

NOAA's Office of Undersea Research provides facilities for scientists to conduct research supporting NOAA's mission objectives in the areas of: global oceanic processes, pathways and fate of materials in the ocean and Great Lakes, coastal oceanic and estuarine processes, ocean lithosphere and mineral resources, biological productivity and living resources, ocean technology, and diving safety and physiology.

The series of papers presented in this volume are the result of an Undersea Science Symposium held at the National Undersea Research Center at the University of Connecticut at Avery Point on October 21-23, 1987. The symposium addressed four major research themes that fall under NOAA's research mission including: marine resources in the Gulf of Maine, global vent processes, deep-water ecology, and ocean technology/biological productivity. This volume addresses research on global vent processes and benthic ecology. A companion volume (National Undersea Research Program Research Report 88-3) presents the remaining papers. In many cases, the papers presented herein represent a report to the Office of Undersea Research on preliminary results of funded research and should not preclude publication in peer-reviewed journals.

Michael P. De Luca  
Program Scientist  
Office of Undersea Research  
NOAA  
6010 Executive Boulevard  
Suite 805  
Rockville, MD 20852

Ivar G. Babb  
Science Coordinator  
Gulf of Maine  
National Undersea Research Center  
University of Connecticut at  
Avery Point  
Groton, CT 06340



## SESSION SUMMARY: GLOBAL VENT PROCESSES

Stephen R. Hammond  
NOAA VENTS Program  
Pacific Marine Environmental Laboratory  
Marine Resources Research Division  
Hatfield Marine Science Center  
Newport, OR 97365

On October 22, 1987, as part of NOAA's Office of Undersea Research (OUR), an Undersea Science Symposium was convened to report on the status and results of diverse investigations having as a broad, common goal, gaining an understanding of the distribution, causes, and the physical, chemical and biological effects of submarine venting. A number of the presentations also address the application of technology rapidly being developed with enhanced capabilities for carrying out these studies in what are, in many instances, unusually harsh undersea environments.

During the past decade, there has been a dramatic increase in the number of scientific investigations focused on venting, and associated, processes. This is happening, in part, because of the growing recognition that submarine venting, rather than simply resulting in localized geological, geochemical, or biological anomalies, is instead a worldwide, fundamental, and quantitatively important means for transferring heat and/or mass from the earth's mantle to the earth's crust, hydrosphere, and perhaps even to the atmosphere. These processes are now known to have been responsible for the generation of economically significant deposits of continental metal ores; they provide a unique environment for the evolution of extensive animal communities which appear to be completely independent of a photosynthetic link with the earth's surface and all other known earth life forms. These same processes appear to govern the budgets of some of the important hydrothermal activity preserved in the geological record and have been linked with long-term climate changes.

Initially, it was the discovery of hydrothermal venting - which can now be reliably predicted to occur throughout the global ocean along the worldwide seafloor spreading-center system - that sparked international interest in venting processes. Now, not only is ridgecrest research flourishing, but the papers included in this Symposium also illustrate that the geographic and scientific scope of venting research has been extended to include other important geological environments, e.g., active submarine volcanoes and subaerial hot springs associated with mantle hotspots and the subducting edges of crustal plates. NOAA's Office of Undersea Research is providing a means for carrying out this important research by providing critical

national support for the facilities needed to visit and sample active vents as well as for initial scientific labors which perforce follow utilization of these facilities. As the papers engendered by the Global Vent Processes Symposium session illustrate, OUR is providing a leadership role in the development and support of not only critical facilities such as submersibles and ROVs but of state-of-the-art instrumentation which will eventually be used to equip remote, unmanned seafloor laboratories. Such efforts are clearly called for in the not-too-distant future in order to make the kinds of long-term measurements necessary to model and then predict the global consequences of seafloor venting.

GORDA RIDGE AND MID-ATLANTIC RIDGE: NEW FRONTIERS  
FOR UNDERSEA RESEARCH

Peter A. Rona

National Oceanic and Atmospheric Administration  
Miami, Florida 33149

ABSTRACT

Investigations of the Gorda Ridge within the proclaimed U.S. Exclusive Economic Zone off northern California and southern Oregon, and the Mid-Atlantic Ridge extending along the center of the Atlantic ocean, have received new impetus from the discovery of hot black smokers, sizeable polymetallic massive sulfide deposits, and vent animals at the Mid-Atlantic Ridge by the NOAA VENTS Program in 1985. Prior to that time, the oceanographic community focused investigations of seafloor venting at the faster-spreading oceanic ridges of the Pacific Ocean including the East Pacific Rise, the Galapagos spreading center and the Juan de Fuca Ridge because a consensus held that the faster spreading rates at these ridges were necessary to supply the heat to drive high-temperature black smoker-type venting. As the only oceanic ridge in the Pacific with slow-spreading characteristics, the Gorda Ridge is an outlier of the slow-spreading ridge system that extends through the Atlantic Ocean and western Indian Ocean comprising more than half the 55,000 km length of the globe-encircling oceanic ridge system.

In response to recent discoveries at the Mid-Atlantic Ridge the oceanographic community is shifting more of its activity to investigation of hydrothermal venting and related processes at slow-spreading oceanic ridges. The discovery cruise by a team of NOAA and university scientists in 1985 followed by DSRV Alvin dives by a NOAA-WHOI-MIT team in 1986, supported by NOAA's Office of Undersea Research and the National Science Foundation, revealed that the black smokers emanate from the center of a mound the size and shape of the Houston Astrodome. The mound is constructed primarily of polymetallic massive sulfides and situated in the rift valley of the Mid-Atlantic Ridge near 26°N, 45°W. Massive sulfide samples from the mound exhibit supergene enrichment of gold attaining the highest grade (16ppm; 0.5 oz per ton) yet found in such seafloor deposits. The chemistry, heat content, and dynamics of the venting solutions exhibit similarities and differences with Pacific vents. The vent animals differ from those of the Pacific.

The northern two-thirds of the 300 km long Gorda Ridge is sediment-starved like the Mid-Atlantic Ridge. Evidence for past and present high-temperature black smoker-type venting was detected at the northern Gorda Ridge by a NOAA-Oregon State

University-U.S. Geological Survey research team in 1985 and 1986. The southern one-third of the Gorda Ridge is sediment-filled. Polymetallic massive sulfides hosted in the sediment of the Escanaba Trough of the southern Gorda Ridge were discovered by USGS scientists in 1985. By analogy with the Mid-Atlantic Ridge, the discovery of black smokers, additional massive sulfide and related types of hydrothermal deposits, and vent animals is anticipated at various sites along the Gorda Ridge. The recent discoveries described have opened the Gorda Ridge and the Mid-Atlantic Ridge as new frontiers for investigation of hydrothermal mineralization, chemical and thermal effects of venting on the ocean environment, and the adaptation of vent organisms.

## INTRODUCTION

The Gorda Ridge and the Mid-Atlantic Ridge were largely bypassed by the scientific community in the past and have only recently become frontiers for undersea research (Fig. 1). The Mid-Atlantic Ridge is the classic example of a slow-spreading oceanic ridge. It was the site of the earliest systematic investigations of an oceanic ridge by several projects including the Canadian Hudson Geotraverse at latitude 45°N between 1960 and 1975 (Loncarevic et al., 1966; Loncarevic, 1976), the French American Mid-Ocean Undersea Study (FAMOUS) near latitude 37°N between 1971 and 1974 (Heirtzler and van Andel, 1977) and the Trans-Atlantic Geotraverse (TAG) Project near latitude 26°N between 1970 and 1975 (Rona, 1970, 1976). The first active hydrothermal field at an oceanic ridge in an open ocean basin was discovered at the Mid-Atlantic Ridge by the TAG Project in 1972 (Rona, 1973; Rona and Scott, 1974; M. R. Scott et al., 1974; R. B. Scott et al., 1974). However, the evidence at that time was for the presence of warm springs and low-temperature mineral deposits. When massive sulfides deposited from high-temperature solutions were discovered at latitude 21°N at the fast-spreading East Pacific Rise in 1978 (CYAMEX, 1979), followed by the discovery of hot black smoker-type vents (350°C) at the same site in 1979 (RISE Project Group, 1980), the oceanic ridge research "bandwagon" shifted from the Atlantic Ocean to the Pacific Ocean.

With the shift in emphasis of oceanic ridge research to the Pacific in 1979, most attention was devoted to the faster spreading East Pacific Rise, Galapagos spreading center, and Juan de Fuca Ridge in the belief that faster spreading thermal regimes were necessary to sustain high-temperature hydrothermal activity. The Gorda Ridge with slow-spreading characteristics received relatively little attention (e.g., Raff and Mason, 1961; McManus 1966; Moore, 1970; Atwater and Mudie, 1973; Riddihough, 1980; Malahoff, 1985). The proclamation of the U.S. Exclusive Economic Zone in 1983 drew attention to the Gorda Ridge as the only oceanic ridge off the conterminous United States within that zone. The discovery of polymetallic massive sulfide deposits,

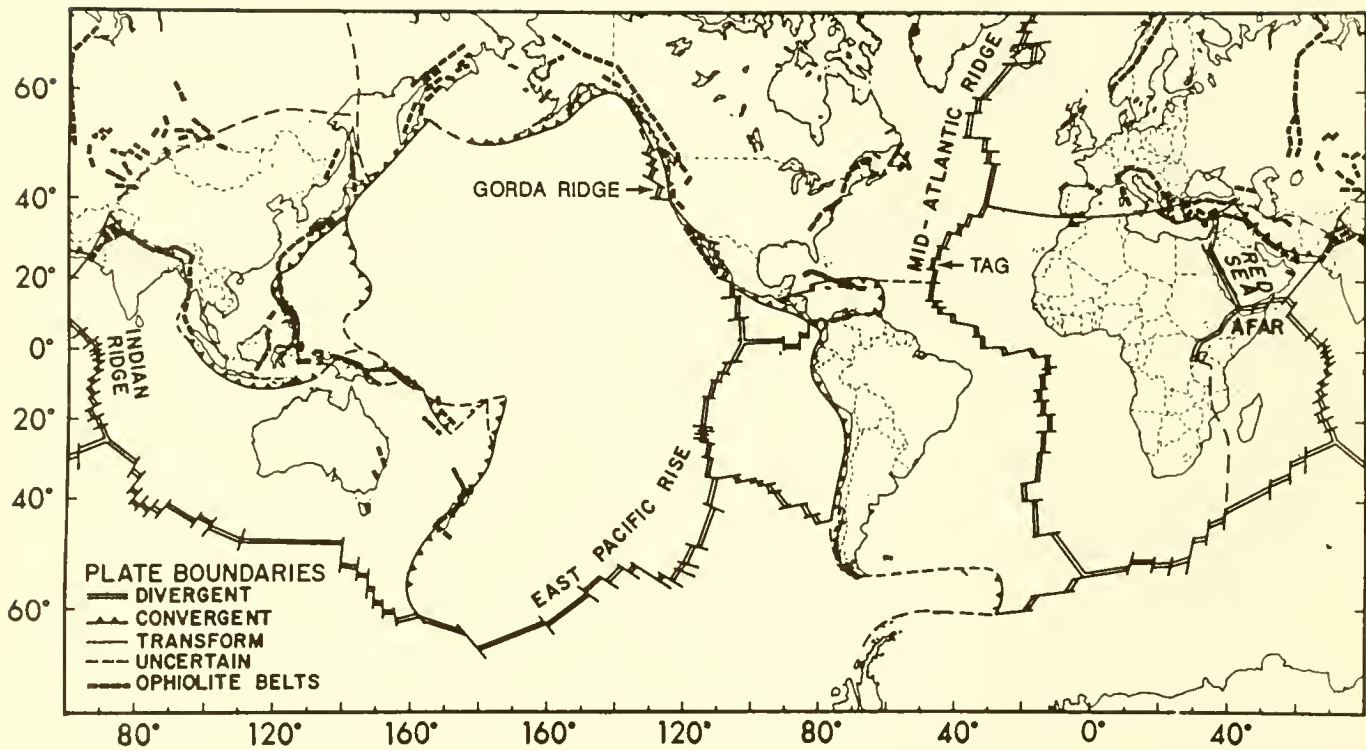


Figure 1. World map showing the oceanic ridge system (divergent plate boundaries where seafloor spreading occurs) and other types of plate boundaries. The oceanic ridges in the Atlantic Ocean and western Indian Ocean are slow-spreading (full-rate  $\leq 4$  cm/y). The oceanic ridges in the eastern Indian Ocean and Pacific Ocean are faster-spreading with the exception of the Gorda Ridge which has slow-spreading characteristics similar to the Mid-Atlantic Ridge. Locations of the TAG Hydrothermal Field at the Mid-Atlantic Ridge and the Gorda Ridge are noted.

hot black smokers and vent animal communities at the Mid-Atlantic Ridge in 1985 (Rona et al., 1986; Ocean Drilling Program Leg 106 Scientific Party, 1986) dramatically changed perception of the role of hydrothermal activity at slow-spreading oceanic ridges. This change initiated a redress of the imbalance in research emphasis between the Pacific Ocean and the Atlantic Ocean and, at the same time, positioned the Gorda Ridge and the Mid-Atlantic Ridge at the leading edge of undersea research.

## SEAFLOOR HYDROTHERMAL ACTIVITY

### Process

A major factor driving research at oceanic ridges is interest in seafloor hydrothermal activity, because such activity has wide ramifications on basic and applied levels. The ocean basins are leaky as containers of the oceans. Cold, dense seawater penetrates kilometers downward through permeable fractures in oceanic crust. In most places in the ocean basin where this penetration occurs it is a one-way trip downward and the water is assimilated into the crust which is about 5 km thick, and into the underlying upper mantle. In localized areas where heat sources exist within the oceanic crust in the form of magma chambers and related offshoots of hot volcanic rock the down-welling seawater is heated, thermally expands, and buoyantly upwells as a less dense hot solution forming a subseafloor convective circulation system which discharges as hot springs at the seafloor (Fig. 2). Subseafloor hydrothermal convection systems are highly efficient in exchanging chemicals and heat between the ocean and the oceanic crust. A two-way chemical exchange occurs between the circulating seawater and the rocks. During circulation certain elements and compounds are removed from the seawater and other elements, notably metals, are dissolved from mineral phases in the fractured volcanic rocks (Table 1; Fig. 2).

The major locus of heat sources that drive hydrothermal circulation in oceanic crust is an intermittent line of magma chambers and hot volcanic rock generated in the process of seafloor spreading at the submerged volcanic mountain ranges of the oceanic ridge system. The submerged volcanic mountain ranges are divergent plate boundaries that extend some 55,000 km through all the ocean basins of the world (Fig. 1). Other volcanic heat sources that drive hydrothermal circulation in oceanic crust are associated with volcanic island arcs such as those that lie along the western margin of the Pacific Ocean and comprise convergent plate boundaries where oceanic crust and upper mantle is reassimilated into the Earth's interior (Fig. 1). Certain volcanic islands like Hawaii, isolated from plate boundaries, are

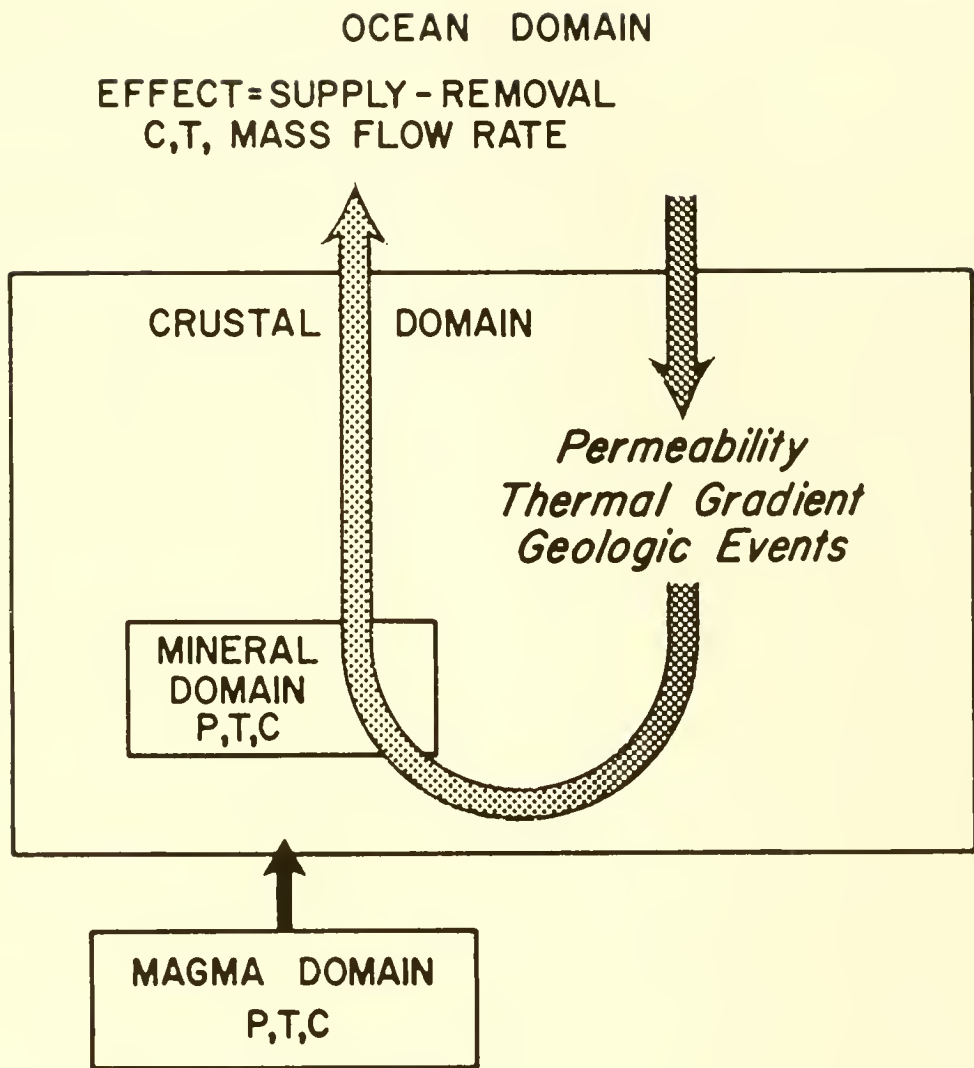


Figure 2. Simple sketch of the components of a subseafloor hydrothermal circulation system. The system involves: 1) down-welling of cold, dense, alkaline, metal-poor seawater through permeable, fractured oceanic crust; 2) heating by flow near magmatic heat sources; 3) upwelling of hot, thermally expanded, lighter seawater; 4) reaction of the heated seawater with minerals under prevailing pressure (P), temperature (T), and composition (C) fields to evolve acid, metal-rich hydrothermal solutions; 5) precipitation of metallic minerals beneath and on the seafloor; and 6) discharge of hot springs into the ocean; the effect of the hot springs on the ocean environment is related to their composition (C), temperature (T), and mass flow rate.

Table 1. Chemical exchange between seawater and basalt in a high-temperature (200-400°C) subseafloor hydrothermal circulation system (Edmond et al., 1980; Thompson, 1983).

Constituent	Basalt	Seawater	Oceanic Ridge/River*
Copper (Cu)	-	+	---
Iron (Fe)	-	+	---
Manganese (Mn)	-	+	1
Zinc (Zn)	-	+	---
Potassium (K)	-	+	2/3
Lithium (Li)	-	+	10
Rubidium (Rb)	-	+	---
Barium (Ba)	-	+	2/3
Calcium (Ca)	-	+	1
Silica (SiO <sub>2</sub> )	-	+	2/3
Magnesium (Mg)	+	-	1
Sulfate (SO <sub>4</sub> )	+	-	1
Sodium (Na)	+	-	Variable
Chlorine (Cl)	?	?	Variable

- = removal.

+= addition.

\* = Ratio of oceanic ridge flux to river input.

also loci of heat sources that may drive subseafloor hydrothermal circulation.

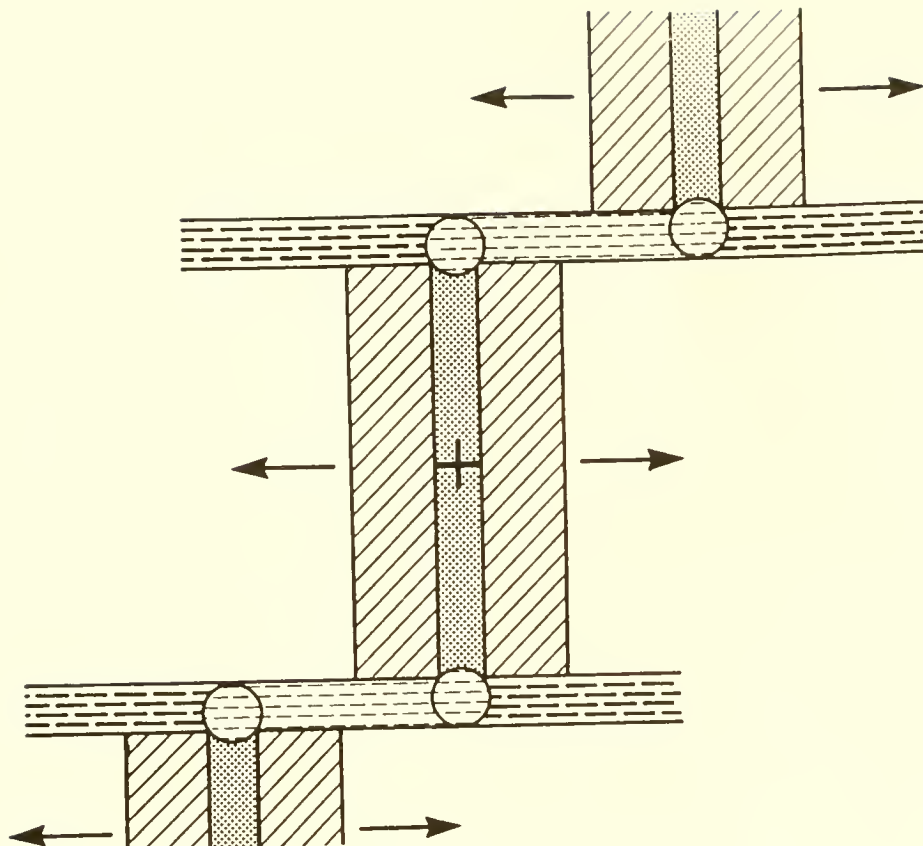
### Significance

Subseafloor hydrothermal circulation is important for several reasons. The Earth is a water-cooled planet and some 20 percent of its internal heat is dissipated by hydrothermal circulation at oceanic ridges (Williams and Von Herzen, 1974; Wolery and Sleep, 1976). The two-way chemical exchange between seawater and oceanic crust in hydrothermal circulation systems at oceanic ridges is a significant influence on the composition of seawater supplying certain metals in amounts comparable to the input by rivers of material weathered from the continents (Table 1; Fig. 1; Edmond et al., 1980). This finding changes the role of the ocean basins from passive sinks to active sources of certain chemical elements and compounds which affect the entire ocean environment. A byproduct of this chemical exchange is mineralization in which metals present in trace quantities in oceanic crust are concentrated into mineral deposits beneath and on the seafloor by precipitation from the hydrothermal solutions triggered by chemical and physical gradients (Rona, 1984). The mineral deposits are analogs of certain ancient polymetallic sulfides and related types of deposits uplifted from the seafloor onto land where they are mined. Accordingly, the seafloor sites are both natural laboratories for the observation of mineralization processes as well as resources for the future. The adaptation of animal communities at the seafloor vents to a food net based on utilization by bacteria of certain dissolved compounds in the hot springs entirely dependent on subseafloor chemical exchanges is the subject of intensive biologic study, as well as the evolution of the vent organisms and their possible relation to the origin of life (Grassle, 1983).

## HYDROTHERMAL ACTIVITY AT THE MID-ATLANTIC RIDGE

### Characteristics

The Mid-Atlantic Ridge extends about 15,000 km along the center of the North Atlantic and South Atlantic Oceans between latitudes 65°N and 55°S and is the prototype slow-spreading oceanic ridge with full-rates up to about 4 cm/y (full-rate is the sum of spreading rates to either side of spreading axis). It exhibits features common to all oceanic ridges (Fig. 3) as well as features specific to slow-spreading ridges. A common feature of oceanic ridges parallel to their axes is a segmented structure comprised of linear segments of the order of 10 km long which are the loci of seafloor spreading, alternating with various types of discontinuities including transform faults that may offset the linear segments by distances up to hundreds of kilometers (Fig. 3). A feature perpendicular to the axis common to all oceanic ridges is a zone of volcanic extrusion of the



- Axial Zone of Volcanic Extrusion
- ▨ Marginal Zone of Active Extension
- ▨ Transform Fault
- ▨ Fracture Zone
- ✚ Topographic High
- Topographic Low
- Direction of Seafloor Spreading

Figure 3. Schematic plan view of features of all seafloor spreading centers (not to scale; Rona, 1984). The linear segments of the spreading axis between offsets at transform faults and other deviations from axial linearity are typically of the order of 10 km long.

order of 1 kilometer wide centered at the axis and bounded by marginal zones of active extension where the newly formed oceanic crust is faulted and undergoes differential uplift. Specific features of the Mid-Atlantic Ridge and most other slow-spreading oceanic ridges is the presence of a well-defined rift valley with widths up to about 30 km between crests of flanking rift mountains and relief up to 3 km from rift valley floor to the mountain crests (Fig. 4). A well-defined rift valley is absent in intermediate-spreading oceanic ridges like the Juan de Fuca Ridge and the Galapagos spreading center, and intermediate- to fast-spreading ridges like the East Pacific Rise.

### Mineralization

The TAG Hydrothermal field where the first hot black smokers, polymetallic massive sulfide deposits and vent animals in the Atlantic Ocean were discovered in 1985 is situated along a linear segment of the rift valley of the Mid-Atlantic Ridge at  $26^{\circ}08'N$ ,  $44^{\circ}49'W$  (Rona et al., 1986a). The field occupies a 6 by 8 km area of the rift valley including the floor and the east wall (Fig. 5). The area encompasses warm springs and low-temperature mineral deposits on the east wall between depths of 2300 and 3300 m, and hot springs associated with vent animals and high-temperature deposits on the lower portion of the east wall and floor of the rift valley between depths of 3300 and 3900 m. The low-temperature deposits comprise stratiform layered manganese oxides and iron oxides, hydroxides and silicates in patches up to tens of meters in diameter distributed along faults trending subparallel to the ridge axis at mid-depth on the east wall (Table 2; Rona et al., 1984; Thompson et al., 1985).

The high-temperature deposits of the TAG Hydrothermal Field are primarily massive sulfides that occur in mound shapes (Rona et al., 1986a; Thompson et al., 1988). One mound is inactive and is about 1500 m wide by 100 m high, rising from a depth of 3400 m near the base of the east wall (Rona et al., 1986b). A second mound is hydrothermally active and is about 250 m wide, rising 50 m from a depth of 3670 m at the juncture between the base of the east wall and the floor of the rift valley (Fig. 5). Massive sulfide samples recovered from the hydrothermally active mound include copper-, iron- and zinc-rich varieties (Table 2) similar to massive sulfides from Pacific sites. The copper-iron massive sulfides from the active mound have relatively high content of free native gold (16 ppm; 0.5 oz. per ton; Hannington et al., 1988). The gold is inferred to have been concentrated by a secondary supergene process involving circulation of low-temperature seawater through the massive sulfides initially precipitated from high-temperature solutions, similar to the process that has concentrated gold recovered from some ancient massive sulfide deposits on land. This is the highest content of gold and the first occurrence of secondary enrichment reported in massive sulfide deposits anywhere on the seafloor. The discovery

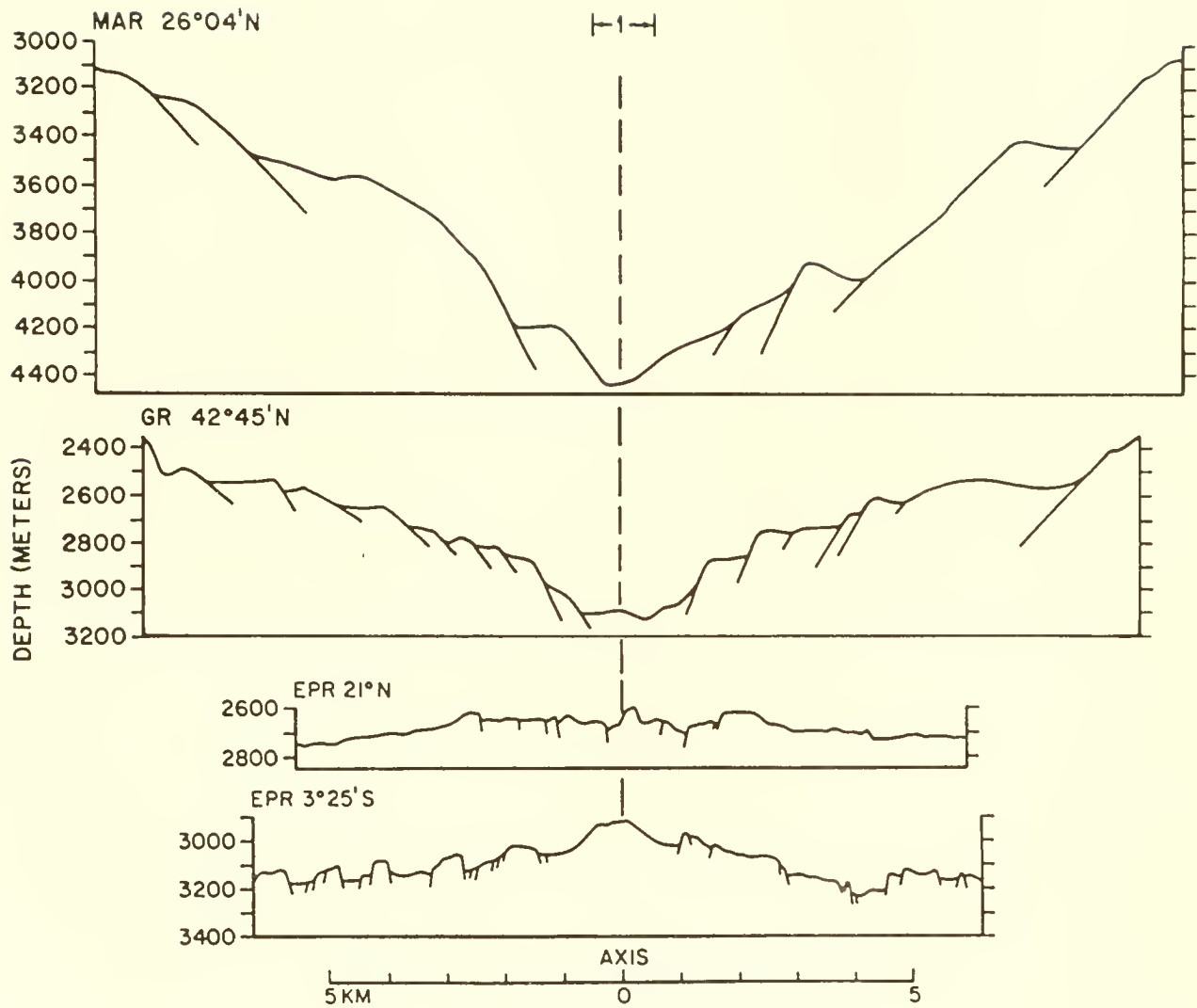


Figure 4. Bathymetric profiles of slow- (full rate  $\leq 4$  cm/y; Mid-Atlantic Ridge [MAR],  $26^{\circ}04'N$ ), intermediate- (full rate  $> 4-8$  cm/y; Gorda Ridge [GR],  $42^{\circ}45'N$ ; East Pacific Rise [EPR]  $21^{\circ}N$ ), and fast- (full rate  $> 8$  cm/y East Pacific Rise [EPR],  $3^{\circ}25'S$ ) spreading oceanic ridges. Topographic relief decreases with increase of spreading rate (Fig. 1). An axial zone of volcanic extrusion ( $\sim 1$  km wide) is bounded by marginal zones of active extension ( $\sim 10$  km wide). Vertical exaggeration is 4:1.

## TAG HYDROTHERMAL FIELD

### HYDROTHERMAL FIELD

RIFT VALLEY FLOOR

EAST WALL

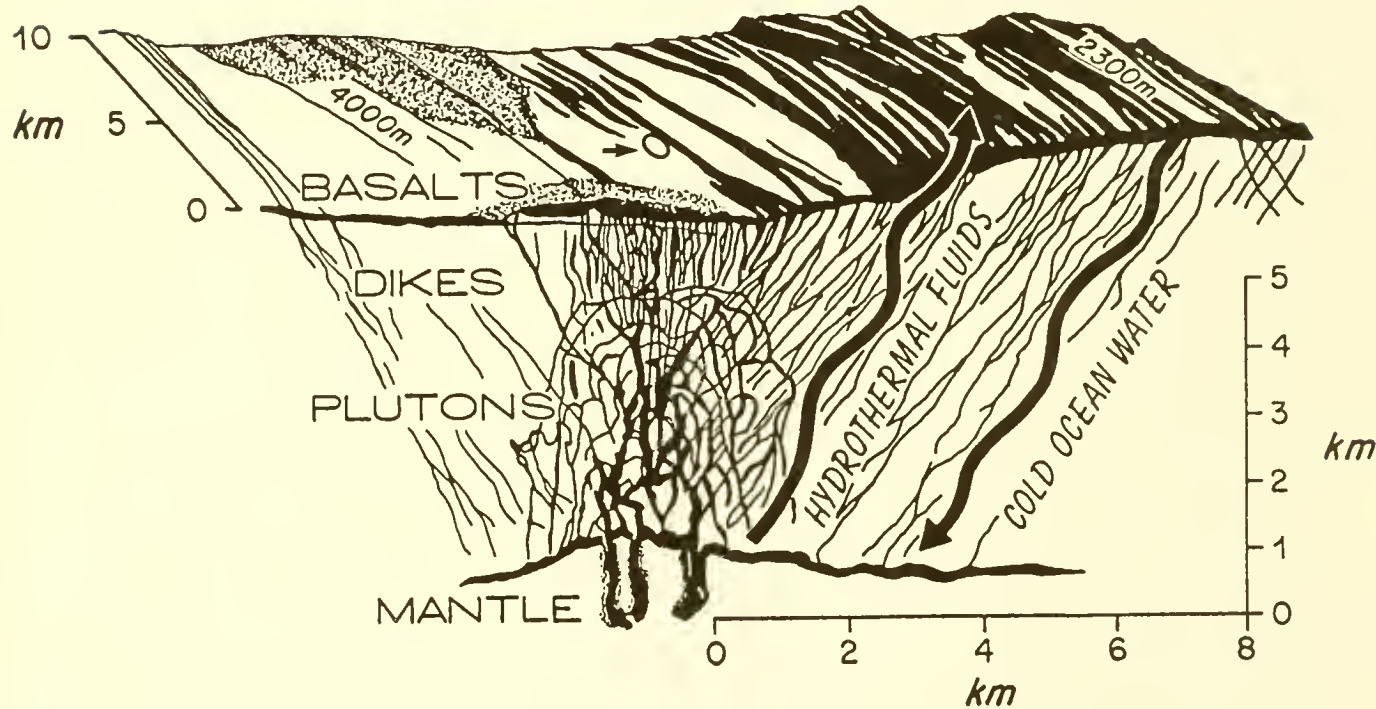


Figure 5. Simplified block diagram showing the geologic setting of subseafloor hydrothermal circulation system at the TAG Hydrothermal Field in the rift valley of the Mid-Atlantic Ridge (Fig. 1; modified by G. Thompson from slide by R.B. Scott). The arrow on the rift valley floor points to a mound the size and shape of the Houston Astrodome where black smokers are venting. The mound is constructed of polymetallic massive sulfides precipitated from the hot springs.

Table 2. Metal content of hydrothermal mineral samples recovered from the TAG site at the Mid-Atlantic Ridge (Thompson et al. 1985, 1988) and the NESCA and SESCA sites in the Escanaba Trough of the southern Gorda Ridge (Fig. 6; Koski et al. 1988).

Metal (wt. %)	TAG Hydrothermal Field, Mid-Atlantic Ridge		Escanaba Trough, Gorda Ridge	
	Manganese Oxides <sup>1</sup>	Massive Sulfides <sup>2</sup>	Massive Sulfides <sup>3</sup>	Barite Crusts
Cu	≤ 0.01	0.1-42.6	-----	-----
Fe	< 0.01	16.3-43.2	-----	-----
Mn	39.2-52.3	< 0.01	-----	-----
Pb	< 0.01	< 0.01-0.25	≤ 7.6	≤ 14
Zn	< 0.01	0.03-21.6	≤ 43	≤ 17
Ag (ppm)	-----	< 5-285	≤ 700	≤ 390
Au (ppm)	-----	0.8-16.4	-----	≤ 2

<sup>1</sup> Scott et al. 1974, Thompson et al. 1985

<sup>2</sup> Rona et al. 1986, Thompson et al. 1988, Hannington et al. 1988

<sup>3</sup> Koski et al. 1988, Table 3

significantly increases the resource potential of seafloor sulfides.

### Hydrothermal Activity

The active mound at the TAG Hydrothermal Field can be visualized as a feature the size and shape of the Houston Astrodome (Fig. 5). It is surrounded by a field of predominantly pillow lava flows, veneered with light tan sediment, indicating that the flows are not fresh. Near the edges of the mound the lava flows are fractured by faults in the marginal zone of active extension that may create permeable pathways for upwelling hydrothermal solutions. An abrupt boundary exists between the lava flows and the outer edge of the mound, composed of talus of massive sulfide fragments with surfaces oxidized to hues of red and orange. Hot spring activity progressively increases in temperature and intensity with changes in surface morphology from edge to center of the mound. Warm springs with estimated temperatures of tens of degrees Celsius above ambient and diffuse discharge emanate as shimmering water from areas of talus and relict chimney-like forms up to several meters high, composed of massive sulfides in the outer one-third of the mound; white anemones and crabs are the predominant animals present. Proceeding toward the center, the next one-third of the mound exhibits similar diffuse flow with the addition of organized flow of white and blue-white smoke from bulbous-shaped chimneys 1 to 2 m high. Temperatures up to 300°C are inferred for the solutions containing the smoke by analogy with white smokers at Pacific sites and from the zinc sulfide-rich composition of the recovered chimney (Thompson et al., 1988). The central one-third of the mound consists of an edifice constructed of massive sulfides surmounted by a group of about 10 chimney-like forms up to 20 m high vigorously discharging black smoke at flow rates up to several meters per second. Black smoke also discharges at slower flow rates from numerous cracks around the base of the central edifice. Layers of calcium sulfate (anhydrite) up to several meters thick interspersed with massive sulfides crop out around the base of the central edifice. Eel-like grey fish typically about 0.5 m long live in crevices of the irregular surface of the mound. Swarms of grey shrimp, between 2 and 5 cm long of a new genus (Williams and Rona, 1986), cover the sulfide surfaces of all active black smoker cracks and chimneys where they are inferred to be feeding on bacteria chemosynthetically growing in the hot spring environment (Van Dover et al., 1987).

### Solution Properties

A plume of hydrothermal solutions buoyantly rises from the central area of the mound. The hydrothermal plume entrains surrounding seawater as it rises until its density equals that of surrounding seawater and attains equilibrium in a layer between 200 and 350 m above the venting zone extending about 6 km along

the rift valley axis (Rona and Speer, 1987, and in preparation). A minimum estimate of the convective heat flux from the black smokers in the central area of the mound is  $10^7$  W. This value is intermediate between the values of  $10^6$  W and  $10^8$  W estimated for small to large hydrothermal fields at the fast-spreading East Pacific Rise (Macdonald et al., 1980; Converse et al., 1984; Little et al., 1987). The composition of the solutions discharging from the black smokers exhibits both similarities and differences from those discharging from black smokers at the East Pacific Rise (Table 3). The concentration in the solutions of major elements including iron, manganese and silicon are similar to those at the East Pacific Rise site at  $21^{\circ}\text{N}$  (Edmond et al., 1986). Minor elements including the rare earths and certain isotopes including boron are different indicating differences in the evolution of the solutions (Klinkhammer et al., 1986; Edmond et al., 1986; Campbell et al., 1988a). Reconnaissance of an 1800 km section of the rift valley of the Mid-Atlantic Ridge between the TAG Hydrothermal Field at latitude  $26^{\circ}\text{N}$  and  $12^{\circ}\text{N}$  using geological, geophysical, and geochemical indicators suggests that other hydrothermal sites are present at a spacing of tens of kilometers (Rona et al., 1982; Rona, 1984; Klinkhammer et al., 1985).

## HYDROTHERMAL ACTIVITY AT THE GORDA RIDGE

### Characteristics

The Gorda Ridge is a 300 km long volcanic mountain range situated between 200 and 300 km west of northern California and southern Oregon (Fig. 6). On the north it is separated from the faster-spreading Juan de Fuca Ridge (full-rate 6 cm per year) by the Blanco Fracture Zone and it terminates on the south at the Mendocino Fracture Zone. The Gorda Ridge has been interpreted as part of a deformation zone that accommodates differential motion between the Juan de Fuca plate to the north and the Pacific plate to the south and west (Fig. 6; Wilson, 1986; Stoddard, 1987). The ridge is divided into three sections by right-lateral structural discontinuities near  $42^{\circ}26'\text{N}$  and  $41^{\circ}26'\text{N}$  (Fig. 5). The northern section is spreading at an intermediate full-rate of 5.5 cm per year (Riddiough, 1980), although its morphologic and petrologic characteristics are more like those of the slow-spreading Mid-Atlantic Ridge (full-rate  $< 4$  cm/y) than any other oceanic ridge in the Pacific (Fig. 4). Both the northern Gorda Ridge and Mid-Atlantic Ridge have well-defined rift valleys, although the width and relief of the rift valley of the northern Gorda Ridge are about one-half that of the Mid-Atlantic Ridge and the floor is 1 to 2 km shoaler. Spatially and temporally closely associated lava types at the northern Gorda Ridge exhibit a diversity in range of percentage of melting and degree of compositional evolution similar to that of the Mid-Atlantic Ridge (Davis and Clague, 1987).

Table 3. Hydrothermal solution chemistry of selected Atlantic and Pacific sites.

Measurements ( $\mu$ or mmol/kg)	East Pacific Rise <sup>1</sup> (21°N)	Mid-Atlantic Ridge <sup>2</sup> (26°N and 23°N)	Seawater
<b>Transition metals</b>			
Cu ( $\mu$ )	< 0.02-44	-----	0.007
Fe ( $\mu$ )	1800	1848-2136	< 0.001
Mn ( $\mu$ )	610	483-506	< 0.001
Zn ( $\mu$ )	40-104	-----	0.01
<b>Alkali metals</b>			
K (m)	24	-----	10
Li ( $\mu$ )	820	-----	26
Na (m)	450	-----	464
Rb ( $\mu$ )	26	-----	1.3
<b>Alkaline earth metals</b>			
Ca (m)	16	-----	10
Mg (m)	0	0	53
Sr ( $\mu$ )	90	-----	87
<b>Anions</b>			
SiO <sub>4</sub> (m)	16-22	18	0.16
Cl (m)	550	558-559	541
SO <sub>4</sub> (m)	0	0	-----
S (m)	6.5	6	-----
pH	3.3-3.8	3.7-4.0	7.8
Alkalinity (m eq/kg)	-0.5 to -0.2	-0.2 to -0.1	2.3

<sup>1</sup> Von Damm et al. 1985

<sup>2</sup> Campbell et al. 1988

The central and southern sections of the Gorda Ridge are spreading at slow rates (full-rate 2.2-2.4 cm/y; Atwater and Mudie, 1973; Riddihough, 1980) and exhibit a well-defined rift valley characteristic of slow-spreading oceanic ridges. The rift valley is sediment-starved to latitude 41°15'N where the southern 100 km is filled with terrigenous sediment up to 500 m thick. A series of volcanic centers consisting of irregular domes projecting upwards through the sediment fill are spaced at 15 to 20 km intervals along this southernmost section which is part of the Escanaba Trough (Fig. 6).

### Hydrothermal Activity and Mineralization

A survey of chemical and physical properties of the water column over the rift valley of the Gorda Ridge to determine the state of hydrothermal activity was carried out cooperatively by investigators from NOAA, Oregon State University and the University of California and coordinated by the Gorda Ridge Technical Task Force of the Minerals Management Service in 1985 (Baker et al., 1987). The survey comprised ten widely spaced stations along the length of the Gorda Ridge (Fig. 6) utilizing CTD (conductivity, temperature, depth)-transmissometer (light attenuation by suspended particulate matter) profiles and water samples for analysis of chemical indicators of hydrothermal activity (dissolved manganese, particulate aluminum/iron ratio, methane, radon-222, helium-3). The survey revealed ongoing hydrothermal venting at the two stations at the northern section of the Gorda Ridge (station GR-14 at 42°44.7'N, 126°43.7'W; station GR-15 at 42°56.7'N, 126°35.6'W), ambiguous values of the various hydrothermal indicators at the stations in the central section, and no hydrothermal signal at the single station over the Escanaba Trough at the southern section of the Gorda Ridge. More detailed water column work at the two northernmost stations confirmed the hydrothermal activity (Collier et al., 1986; Kadko, 1986), and recovered suspended mineral particles (anhydrite, atacamite) indicative of high-temperature black smoker-type venting (Nelsen, 1987). Recent dives with DSRV Alvin in the NESCA area of the Escanaba Trough found and sampled active hot springs associated with massive sulfide deposits at the flanks of a volcanic center (Fig. 5; Campbell et al., 1988b; Zierenberg et al., 1988).

### Northern Gorda Ridge

The 10 by 10 km area centered on station GR-14 at the northern section of the Gorda Ridge was investigated with bathymetry, seafloor photography and video, and dredging by NOAA and U.S. Geological Survey (USGS) cruises in 1986 building on a prior seafloor data base of NOAA Sea Beam work (Malahoff, 1985) and USGS-University of Hawaii SeaMARC II side-scan sonar imagery (Clague et al., 1984; Clague and Holmes, 1987). Inactive and active hydrothermal sites were identified within this area and

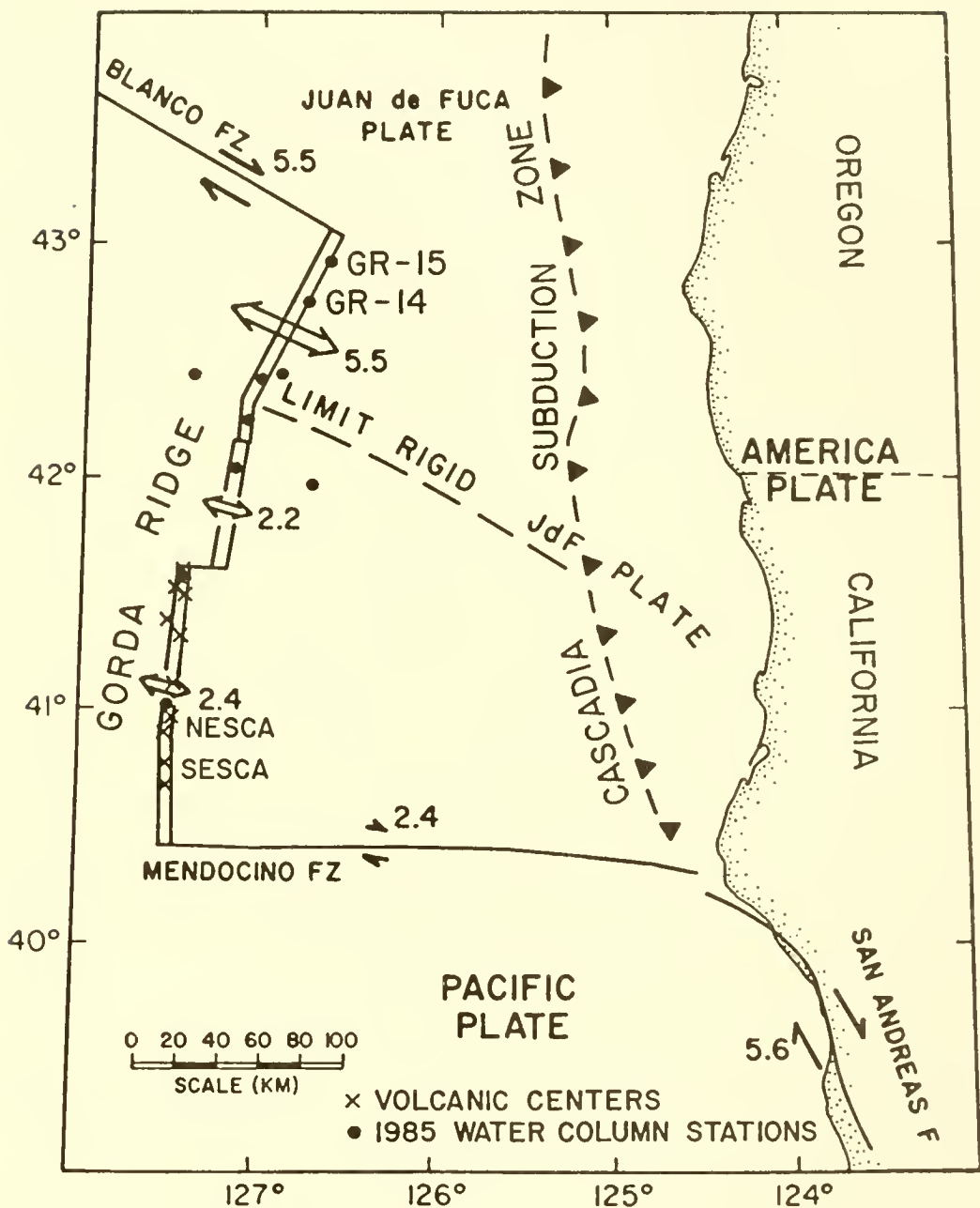


Figure 6. Map of the Gorda Ridge region showing features described in the text (modified from Riddihough, 1980; Wilson, 1986). Full-rates of seafloor spreading (cm/y; arrows at Gorda Ridge) and relative rates of plate motion (cm/y; opposed paired arrows) are indicated.

related to focusing of hydrothermal upwelling through fractured oceanic crust with enhanced permeability at the intersection of two regional tectonic trends (Rona and Clague, 1986, 1989). A predominant tectonic trend common to all oceanic ridges (Fig. 3) is represented by fault scarps subparallel to the  $022^{\circ}$  orientation of the rift valley axis. A subsidiary anomalous tectonic trend related to the regional stress field of the northern Gorda Ridge is represented by faults and fissures with a  $350^{\circ}$  orientation. The presently inactive hydrothermal site occurs where the two tectonic trends intersect at the east side of the rift valley floor at a depth of 3100 m near  $42^{\circ}44'N$ ,  $126^{\circ}44.5'W$ . An assemblage of features is present within a small area (c.  $1 \times 1$  km) at this location comprising sheet flows, fissures, partially altered talus at the base of fault scarps, and material with the appearance in photographs of hydrothermal precipitates. Facets of angular talus composed of fresh pillow fragments recovered by dredging are coated white with the mineral boehmite formed by high-temperature alteration of the basalt (Howard and Fisk, 1988). The active hydrothermal site occurs where the two tectonic trends intersect at mid-depth on the east wall of the rift valley. A linear ridge surmounted by a row of hills centered at  $42^{\circ}45.5'N$ ,  $126^{\circ}42.2'W$  about 1.5 km long parallel to the valley axis by 0.5 km wide rises up to 80 m above the 2700 m isobath. This ridge directly underlies the chemical and physical anomalies indicative of hydrothermal activity measured in the overlying water column (Collier et al., 1986; Kadko et al., 1986; Baker et al., 1987). The hills surmounting the ridge are formed by fractured pillow lava flows. Relatively dark sediment inferred to be metalliferous, biological debris, and numerous fish recorded on video images at the southern end of the hills suggests proximity to black smoker-type venting from faults and fractures (Rona and Clague, 1986, 1989). Hydrothermal phenomena in the GR-14 area of the northern Gorda Ridge are targeted for a scheduled 1988 dive series with DSV Sea Cliff.

#### Southern Gorda Ridge

Polymetallic massive sulfide samples were recovered, their surface distribution partially mapped and evidence of relatively recent hydrothermal and volcanic activity was found at sites in the southern section of the Gorda Ridge. The massive sulfides were initially recovered by dredging at the flanks of one of the volcanic centers at  $40^{\circ}45'N$  in the Escanaba Trough on a USGS cruise in 1985 (Morton et al., 1987). Seafloor photography, dredging and heat flow measurements conducted on that cruise at two of the volcanic centers revealed fresh pillow lava flows and anomalously high heat flow values through adjacent sediment (Abbott et al., 1986). Surface ship and submersible observations with the U.S. Navy DSV Sea Cliff in 1986 provided additional information. Multiple sulfide occurrences were observed in two areas each about 5 by 10 km along the sediment-filled axis of the northern (NESCA site centered at latitude  $41^{\circ}00'N$ , longitude

127°30'W) and southern (SESCA site centered at latitude 40°45'N, longitude 127°30'N) portions of the Escanaba Trough (Koski et al., 1988). Active hot springs associated with a community of vent animals were found at one of the volcanic centers in the NESCA area by DSRV Alvin in 1988 (Campbell et al., 1988b). Additional dives are scheduled in 1988 with DSV Sea Cliff at the two areas in the Escanaba Trough.

Ten relatively large massive sulfide occurrences as wide as 200 m and numerous smaller occurrences were found in the NESCA and SESCA areas. The sulfide occurrences are spatially associated with the basaltic edifices at the volcanic centers that intrude and uplift the sediment fill composed of terrigenous turbidites (Morton et al., 1987; Morton and Holmes, 1987). In both areas the larger deposits occur at faults around the base of sediment-capped hills composed of basaltic sheet and pillow lava flows. The occurrences consist of constructional ledges and mounds of massive sulfides tens of meters in diameter and several meters high that are capped by occasional chimney-like structures and surrounded by an apron of sulfide talus. The massive sulfides typically contain higher contents of zinc ( $\leq$  43 percent), lead ( $\leq$  7.6 percent), and silver ( $\leq$  700 ppm) than massive sulfides at sediment-starved oceanic ridges, reflecting additional provenance of these metals by dissolution from the terrigenous sediments (Table 2; Koski et al., 1988). Samples of the massive sulfides are impregnated with asphaltic petroleum formed by cracking of organic matter in the underlying sediments by upwelling hydrothermal solutions (Koski and Kvenvolden, 1986). The presence of intact small sulfide chimneys on sediment and fresh pillow flows indicates recent hydrothermal activity. Subsurface mineralization is evidenced by sulfide veinlets in sediment cores and sulfide-cemented sediment. The overall size of the deposits present in the two areas of the southern section of the Gorda Ridge depends on whether the distribution of sulfides is limited to faults which penetrate the sediment or is laterally extensive through the layers of sediment. This question will require drilling to resolve.

## CONCLUSIONS

The Mid-Atlantic Ridge and the Gorda Ridge have moved to the forefront of research investigating hydrothermal and related processes at oceanic ridges. The recent discovery of black smokers, sizeable polymetallic sulfide deposits, and vent animals at the Mid-Atlantic Ridge stimulates investigation of slow-spreading oceanic ridges in general and the Gorda Ridge in particular owing to its slow-spreading characteristics and accessible location. The sediment-starved northern section and possibly the central section of the Gorda Ridge are tectonically and volcanically active settings favorable for hydrothermal activity anticipated to be associated with mineralization and vent animals at sites localized by the intersection of structural

trends near magmatic heat sources. The sediment-filled southern section of the Gorda Ridge is a setting for hydrothermal mineralization associated with active venting and vent animals at sites localized by the development of volcanic centers. Geologic diversity along the long length of the Mid-Atlantic Ridge and the short length of the Gorda Ridge favors future discoveries that will produce new insights and practical benefits with reference to the thermal regime of the Earth, chemical and thermal controls of the ocean environment, seafloor mineralization, and adaptation of organisms.

The 1988 DSV Sea Cliff dive series discovered a high-temperature hydrothermal field with black smokers, mineral deposits, and vent biota where predicted (Rona and Clague, 1986, 1989) on the east wall of the rift valley of the northern Gorda Ridge in the GR-14 area (Fig. 6; Federal/State Gorda Ridge Task Force Working Group B, 1988). The scientific team that made the dives has proposed the name "Sea Cliff Hydrothermal Field" for this new site. The name reflects the location of the field perched on cliffs between water depths of 2700 and 2800 m about 300 m above the floor of the rift valley and also recognizes the Navy submersible Sea Cliff and its complement for their invaluable contribution to the success of the program.

#### ACKNOWLEDGMENTS

NOAA's Office of Undersea Research is acknowledged for support of submersible investigations at the Mid-Atlantic Ridge and for participation in the 1987 Undersea Science Symposium. The Gorda Ridge Technical Task Force of the Minerals Management Service is acknowledged for coordination of the cooperative work at the Gorda Ridge and for participation in the 1987 Gorda Ridge Symposium. The U.S. Navy provided outstanding support on the 1986 Gorda Ridge Expedition of DSV Sea Cliff. Thanks to the NOAA VENTS Program for funding and the opportunity to investigate the Gorda Ridge.

#### LITERATURE CITED

Abbott, D. 1986. Heat Flow Results from the Gorda Ridge. Open-File Rept. 0-86-12. Portland, Oreg., Oregon Department of Geology and Mineral Industries. 10 pp.

Atwater, T., and J. D. Mudie. 1973. Detailed Near-Bottom Geophysical Study of the Gorda Rise. J. Geophys. Res., Vol. 78, No. 35, pp. 8665-8686.

Baker, E. T., G. J. Massoth, R. W. Collier, J. H. Trefrey, D. Kadko, T. A. Nelsen, P. A. Rona, and J. E. Lupton. 1987. Evidence for High-Temperature Hydrothermal Venting on the Gorda Ridge, Northeast Pacific Ocean. Deep-Sea Res., Vol. 34, No. 8, pp. 1461-1476.

Campbell, A. C., M. R. Palmer, G. P. Klinkhammer, T. S. Bowers, J. M. Edmond, J. R. Lawrence, J. F. Casey, G. Thompson, S. Humphris, P. Rona, and J. A. Karson. 1988a. Chemistry of Hot Springs on the Mid-Atlantic Ridge. Nature, Vol. 335, No. 6190, pp. 514-519.

Campbell, A. C., C. German, M. R. Palmer, and J. M. Edmond. 1988b. Preliminary Report of the Chemistry of Hydrothermal Fluids From the Escanaba Trough. EOS, Trans. Amer. Geophys. U., Vol. 69, No. 44, p. 1271.

Carey, A. G., G. L. Taghon, D. L. Stein, and P. A. Rona. 1989. Distributional Ecology of Benthic Mega-Epifauna and Fishes in the Gorda Axial Valley. Gorda Ridge Symp. Proceed. New York, N.Y., Springer-Verlag (in press).

Clague, D. A., W. Friesen, P. Quinterno, L. Morgenson, M. Holmes, J. Morton, J. R. Bouse, and A. Davis. 1984. Preliminary Geological, Geophysical, and Biological Data from the Gorda Ridge. Geol. Surv. Open-File Rept. 84-364, 31 pp.

Clague, D. A., and M. L. Holmes. 1987. Geology, Petrology, and Mineral Potential of the Gorda Ridge. In: D. W. Scholl, A. Grantz, and J. G. Vedder (eds.), Geology and Resource Potential of the Continental Margin of Western North American and Adjacent Ocean Basins-Beaufort Sea to Baja California. Circum-Pacific Council for Energy and Mineral Resources. Circum-Pacific Earth Sci. Ser., Vol. 6, pp. 563-580.

Collier, R. W., S. H. Holbrook, and J. M. Robbins. 1986. Studies of Trace Metals and Active Hydrothermal Venting on the Gorda Ridge. Portland, Oreg., Oregon Dept. of Geology and Min. Industries, Open-File Rept. 0-86-13. 36 pp.

Converse, D. R., H. D. Hollard, and J. Edmond. 1984. Flow Rates in the Axial Hot Springs of the East Pacific Rise (21°N): Implications for the Heat Budget and the Formation of Massive Sulfide Deposits. Earth Planet. Sci. Lett., Vol. 69, No. 1, pp. 159-175.

CYAMEX Scientific Team: J. Francheteau, H. D. Needham, P. Choukroune, T. Juteau, M. Siguret, R. D. Ballard, P. J. Fox, W. R. Normark, A. Carranza, D. Cordoba, J. Guerrero, and C. Rangin. 1979. Massive Deep Sea Sulfide Ore Deposits Discovered on the East Pacific Rise. Nature, Vol. 277, No. 5697, pp. 523-528.

Davis, A. S., and D. A. Clague. 1987. Geochemistry, Mineralogy and Petrogenesis of Basalt from the Gorda Ridge. J. Geophys. Res., Vol. 92, No. B10, pp. 10467-10483.

Detrick, R. S., J. Honnorez, A. C. Adamson, G. Brass, K. M. Gillis, S. E., Humphris, C. Mevel, P. Meyer, N. Petersen, M. Rautenschlein, T. Shibata, H. Staudigel, K. Yamamoto, and A. L. Woolridge. 1986. Ocean Drilling Program Leg 106 Scientific Party, Drilling the Snake Pit Hydrothermal Sulfide Deposit on the Mid-Atlantic Ridge, latitude 23°22'N. Geology, Vol. 14, No. 12, pp. 1004-1007.

Edmond, J. M., C. Measures, R. E. McDuff, L. H. Chan, R. Collier, B. Grant, L. I. Gordon, and J. B. Corliss. 1979. Ridge Crest Hydrothermal Activity and the Balances of the Major and Minor Elements in the Ocean: The Galapagos Data. Earth Planet. Sci. Lett., Vol. 46, No. 1, pp. 1-18.

Federal/State Gorda Ridge Technical Task Force Working Group B: P. Rona, R. Denlinger, M. Fisk, K. Howard, K. Klitgord, J. McClain, G. McMurray, G. Taghon, and J. Wiltshire. 1988. Hydrothermal Activity on the Gorda Ridge. EOS, Trans. Amer. Geophys. U., Vol. 69, No. 47, p. 1588.

Grassle, J. F. 1983. Introduction to the biology of hydrothermal vents. In: P. A. Rona, K. Bostrom, L. Laubier, and K. L. Smith, Jr. (eds.), Hydrothermal Processes at Seafloor Spreading Centers. New York, N.Y., Plenum Press, NATO Conference Series, Series IV: Mar. Sci., Vol. 12, pp. 665-675.

Hannington, M. D., G. Thompson, P. A. Rona, and S. D. Scott. 1988. Gold and Native Copper in Supergene Sulfides from the Mid-Atlantic Ridge. Nature, Vol. 333, No. 6168, pp. 64-66.

Heirtzler, J. R., and T. H. van Andel. 1977. Project FAMOUS: Its Origin, Programs, and Setting. Geol. Soc. Amer. Bull., Vol. 88, No. 4, pp. 481-487.

Howard, K. J., and M. R. Fisk. 1988. Hydrothermal Alumina-Rich Clays and Boehmite on the Gorda Ridge. Geochim. Cosmochim. Acta, Vol. 52, No. 9, pp. 2269-2279.

Kadko, D. 1986. Radon-222 as a Real-Time Tracer of Hydrothermal Activity on the Gorda Ridge. Portland, Oreg., Oregon Dept. of Geology and Min. Industries., Open-File Rept. 0-86-14. 19 pp.

Karlin, R., and M. K. Lyle. 1986. Sediment Studies on the Gorda Ridge. Portland, Oregon Dept. of Geology and Min. Industries, Open-File Rept. 0-86-19. 76 pp.

Klinkhammer, G., J. M. Edmond, H. Elderfield, and M. Greaves. 1986. A Comparison of REE Data for Hydrothermal Fluids from the MAR and EPR. EOS, Trans. Amer. Geophys. U., Vol. 67, No. 44, p. 1021.

Klinkhammer, G., P. A. Rona, M. Greaves, and H. Elderfield. 1985. Hydrothermal Manganese Plumes in the Mid-Atlantic Ridge Rift Valley. Nature, Vol. 314, No. 6013, pp. 727-731.

Koski, R. A., and K. A. Kvenvolden. 1986. Polymetallic Sulfide Associated with Asphaltic Petroleum at the Gorda Ridge Spreading Center, Offshore Northern California. EOS, Trans. Amer. Geophys. U., Vol. 67, No. 44, p. 1283.

Koski, R. A., W. C. Shanks, III, W. A. Bohrson, and R. L. Oscarson. 1988. The Composition of Massive Sulfide Deposits from the Sediment-covered Floor of Escanaba Trough, Gorda Ridge: Implications for Depositional Processes. Canad. Mineral., Vol. 26, No. 3, pp. 655-675.

Little, S. A., K. D. Stolzenbach, and R. P. Von Herzen. 1987. Measurements of Plume Flow from a Hydrothermal Vent Field. J. Geophys. Res., Vol. 92, No. B3, pp. 2587-2596.

Loncarevic, B. D. 1976. Brief Review of Exploration of the Mid-Atlantic Ridge Near Latitude 45°N, and Partly Annotated Bibliography of the Study Area. In: P. A. Rona (ed.), Mid-Atlantic Ridge, Geol. Soc. Amer., Microform Publ. 5, Part 2, pp. 457-470.

Macdonald, K. C., K. Becker, R. N. Spiess, and R. D. Ballard. 1980. Hydrothermal Heat Flux of the "Black Smoker" Vents on the East Pacific Rise. Earth Planet. Sci. Lett., Vol. 48, No. 1, pp. 1-7.

Malahoff, A. 1985. Hydrothermal Vents and Polymetallic Sulfides of the Galapagos and Gorda/Juan de Fuca Ridge Systems and of Submarine Volcanoes. Biol. Soc. Wash. Bull., No. 6, pp. 19-41.

McManus, D. A. 1966. Physiography of Cobb and Gorda Rises, Northeast Pacific Ocean. Geol. Soc. Amer. Bull., Vol. 78, No. 4, pp. 527-546.

Moore, G. W. 1970. Seafloor Spreading at the Junction Between Gorda Rise and Mendocino Ridge. Geol. Soc. Amer. Bull., Vol. 81, No. 9, pp. 2817-2824.

Morton, J. L., and M. L. Holmes. 1987. Distribution of Sediment-Hosted Sulfide Deposits, Escanabe Trough, Gorda Ridge. Portland, Oreg., Oregon Dept. Geology and Min. Industries, Gorda Ridge Symp., Abstracts with Program, p. 19.

Morton, J. L., M. L. Holmes, and R. A. Koski. 1987. Volcanism and Massive Sulfide Formation at a Sedimented Spreading Center, Escanaba Trough, Gorda Ridge, Northeast Pacific Ocean. Geophys. Res. Lett., Vol. 14, No. 7, pp. 769-772.

Nelsen, T. A., N. Iricanin, and J. H. Trefry. 1987. Suspended and Bottom Sediments from the Gorda Ridge. Gorda Ridge Symp., Abstracts with Program, p. 24.

Ocean Drilling Program Leg 106 Scientific Party: R. S. Detrick, J. Honnorez, A. C. Adamson, G. Brass, K. M. Gillis, S. E. Humphris, C. Mevel, P. Meyer, N. Petersen, M. Rautenschlein, T. Shibata, H. Staudigel, K. Yamamoto, and A. L. Woolridge. 1986. Drilling the Snake Pit Hydrothermal Sulfide Deposit on the Mid-Atlantic Ridge, latitude 23°22'N. Geology, Vol. 14, No. 12, pp. 1004-1007.

Riddihough, R. P. 1980. Gorda Plate Motions from Magnetic Anomaly Analysis. Earth Planet. Sci. Lett., Vol. 51, No. 1, pp. 163-170.

RISE Project Group: F. N. Speiss, K. D., Macdonald, T. Atwater, R. Ballard, A. Carranza, D. Cordoba, C. Cox, V. M. Diaz Garcia, J. K. Francetuau, J. Guerrero, J. Hawkins, R. Hayman, R. Hessler, T. Juteau, M. Kastner, R. Larson, B. Luyendyk, J. D. Macdougall, S. Miller, W. Normark, J. Oncutt, and C. Rangin. 1980. East Pacific Rise: Hot Springs and Geophysical Experiments. Science, Vol. 207, No. 4438, pp. 1421-1444.

Raff, A. D., and R. G. Mason. 1961. Magnetic Survey off the West Coast of North America, 40°N Latitude to 52°N Latitude. Geol. Soc. Amer. Bull., Vol. 72, No. 8, pp. 1267-1270.

Rona, P. A. 1970. Comparison of Continental Margins of Eastern North America at Cape Hatteras and Northwestern Africa at Cape Blanc. Amer. Assoc. Petrol. Geol. Bull., Vol. 54, No. 1, pp. 129-157.

Rona, P. A. 1973. New Evidence for Seabed Resources from Global Tectonics. Ocean Manage., Vol. 1, pp. 145-159.

Rona, P. A., editor. 1976. Mid-Atlantic Ridge. Geol. Soc. Amer., Microform Pub. 5, 470 pp.

Rona, P. A. 1984. Hydrothermal Mineralization at Seafloor Spreading Centers. Earth-Sci. Rev., Vol. 20, No. 1, pp. 1-104.

Rona, P. A., and D. A. Clague. 1986. Geologic Setting of Hydrothermal Activity at the Northern Gorda Ridge. EOS, Trans. Amer. Geophys. U., Vol. 67, No. 44, p. 1028.

Rona, P. A., and D. A. Clague. 1989. Geologic Controls of Hydrothermal Discharge on the Northern Gorda Ridge. Geology (submitted).

Rona, P. A., and R. B. Scott. 1974. Convenors, Symposium: Axial Processes of the Mid-Atlantic Ridge. EOS, Trans. Amer. Geophys. U., Vol. 55, No. 12, pp. 292-295.

Rona, P. A., and K. G. Speer. 1987. Hydrothermal Plume Characteristics and Heat Transfer at the TAG Area, Mid-Atlantic Ridge Rift Valley near 26°N. EOS, Trans. Amer. Geophys. U., Vol. 68, No. 44, p. 1325.

Rona, P. A., G. Klinkhammer, T. A. Nelsen, J. H. Trefry, and H. Elderfield. 1986a. Black Smokers, Massive Sulfides and Vent Biota at the Mid-Atlantic Ridge. Nature, Vol. 321, No. 6065, pp. 33-37.

Rona, P. A., R. A. Pockalny, and G. Thompson. 1986b. Geologic Setting and Heat Transfer at Black Smokers at TAG Hydrothermal Field, Mid-Atlantic Ridge 26°N. EOS, Trans. Amer. Geophys. U., Vol. 67, No. 44, p. 1021.

Rona, P. A., K. Bostrom, L. Widenfalk, D. S. Cronan, W. J. Jenkins, and M. Mallette. 1982. Hydrothermal Mineralization of Mid-Atlantic Ridge 0-27°N. Geol. Soc. Amer., Vol. 14, No. 7, p. 602. Abstracts with Program, 1982 Annual Meeting.

Scott, M. R., R. B. Scott, P. A. Rona, L. W. Butler, and A. J. Nalwalk. 1974. Rapidly Accumulating Manganese Deposit from the Median Valley of the Mid-Atlantic Ridge. Geophys. Res. Lett., Vol. 1, No. 8, pp. 355-358.

Scott, R. B., P. A. Rona, B. A. McGregor, and M. R. Scott. 1974. The TAG Hydrothermal Field. Nature, Vol. 251, No. 5473, pp. 301-302.

Speiss, F. N., K. D. Macdonald, T. Atwater, R. Ballard, A. Carranza, D. Cordoba, C. Cox, V. M. Diaz Garcia, J. K. Francetuau, J. Guerrero, J. Hawkins, R. Hayman, R. Hessler, T. Juteau, M. Kastner, R. Larson, B. Luyendyk, J. D. Macdougall, S. Miller, W. Normark, J. Oncutt, and C. Rangin, RISE Project Group. 1980. East Pacific Rise: Hot Springs and Geophysical Experiments. Science, Vol. 207, No. 4438, pp. 1421-1444.

Stoddard, P. R. 1987. A Kinematic Model for the Evolution of the Gorda Plate. J. Geophys. Res., Vol. 92, No. B11, pp. 11524-11532.

Thompson, G. 1983. Basalt-seawater interaction. In: P. A. Rona, K. Bostrom., L. Laubier, and K. L. Smith, Jr. (eds.). Hydrothermal Processes at Seafloor Spreading Centers, New York, N.Y., Plenum Press, NATO Conference Series, Series IV: Mar. Sci., Vol. 12, pp. 225-278.

Thompson, G., M. J. Mottl, and P. A. Rona. 1985. Morphology, Mineralogy and Chemistry of Hydrothermal Deposits from the TAG Area, 26°N Mid-Atlantic Ridge. Chem. Geol., Vol. 49, pp. 243-257.

Thompson, G., S. E. Humphris, B. Schroeder, M. Sulanowska, and P. A. Rona. 1988. Active Vents and Massive Sulfides at 26°N (TAG) and 23°N (Snake Pit) on the Mid-Atlantic Ridge. Canad. Mineral., Vol. 26, No. 4, pp. 697-711.

Van Dover, C. L., and B. Fry, J. F. Grassle, S. Humphris, and P. A. Rona. 1988. Feeding Biology of the Shrimp Rimicar Exoculata at Hydrothermal Vents on the Mid-Atlantic Ridge. Mar. Biol., Vol. 98, No. 2, pp. 209-216.

von Damm, K. L., and J. M. Edmond, B. Grant, C. I. Measures, B. Walden, and R. F. Weiss. 1985. Chemistry of Submarine Hydrothermal Solutions at 21°N, East Pacific Rise. Geochim. Cosmochim. Acta, Vol. 49, No. 11, pp. 2197-2220.

Williams, A. B., and P. A. Rona. 1986. Two New Caridean Shrimps (Bresiliidae) from a Hydrothermal Field on the Mid-Atlantic Ridge. J. Crust. Biol., Vol. 6, No. 3, pp. 446-462.

Williams, D. L., and R. P. Von Herzen. 1974. Heat Loss from the Earth: New Estimate. Geology, Vol. 2, No. 7, pp. 327-328.

Wilson, D. S. 1986. A Kinematic Model for the Gorda Deformation Zone as a Diffuse Southern Boundary of the Juan de Fuca Plate. J. Geophys. Res., Vol. 91, No. B10, pp. 10259-10269.

Wolery, T. J. and N. H. Sleep. 1976. Hydrothermal Circulation and Geochemical Flux at Mid-Ocean Ridges. J. Geol., Vol. 84, No. 3, pp. 249-275.

Zierenberg, R. A., R. A. Koski, W. C. Shanks, III, and J. F. Slack. 1988. Preliminary Results of ALVIN Dives on Active Sediment-hosted Massive Sulfide Deposits in the Escanaba Trough, Southern Gorda Ridge. EOS, Trans. Amer. Geophys. U., Vol. 69, No. 44, pp. 1488.

THE GEOCHEMISTRY OF SUBMARINE VENTING FLUIDS  
AT AXIAL VOLCANO, JUAN DE FUCA RIDGE:  
NEW SAMPLING METHODS AND A VENTS PROGRAM RATIONALE

Gary J. Massoth<sup>1</sup>, Hugh B. Milburn<sup>1</sup>, Stephen R. Hammond<sup>2</sup>,  
David A. Butterfield<sup>3</sup>, Russell E. McDuff<sup>3</sup>, and  
John E. Lupton<sup>4</sup>

<sup>1</sup>NOAA/PMEL, Seattle, WA 98115

<sup>2</sup>Mark O. Hatfield Marine Science Center, Newport, OR 98195

<sup>3</sup>School of Oceanography, University of Washington,  
Seattle, WA 98195

<sup>4</sup>Marine Science Institute, University of California,  
Santa Barbara, CA 93106

ABSTRACT

Observations of vent fluids collected in 1986 with the submersible Pisces IV from the ASHES vent field at Axial Volcano, Juan de Fuca Ridge suggest that hydrothermal fluids similar to those vented at other sediment-starved ridgecrest sites are being discharged along with unprecedented Cl-poor, gas-enriched fluids that are likely the result of phase separation. Anomalously low concentrations of silica, calcium, manganese and iron were also observed in the Cl-poor vent fluids. New sampling tools and protocols conceived to overcome the interpretive limitations inherent to conventional vent fluid data were tested during 1987 using the Deep Submersible Alvin. A Submersible-coupled In situ Sensing and Sampling System (SIS<sup>3</sup>) enabled a more efficient collection of high quality vent fluid samples coincident with the sensing of temperature. An In Situ Chemical Analyzer (ISCA), based on the technology of flow injection analysis and configured to monitor the chemical output of a warm spring vent for H<sub>2</sub>S, Fe<sup>2+</sup>, pH, and temperature, was deployed with partial success for 3 days at the ASHES vent field. The integral role of vent fluid studies in testing the hypothesis that hydrothermal venting along the Juan de Fuca/Explorer/Gorda Ridge system plays a major role in controlling the chemistry of the northeastern Pacific Ocean is identified and supported.

INTRODUCTION

The operating hypothesis of the NOAA VENTS Program as formulated within its Implementation Plan is: Hydrothermal venting along the Juan de Fuca/Explorer/Gorda Ridge system plays a major role in controlling the chemistry of the northeastern Pacific Ocean. Fundamental to the testing of this hypothesis are determinations of the chemical source strengths of hydrothermal

emissions from throughout the ridgecrest system and an assessment of the temporal variability of these emissions. We present here the preliminary results of our efforts to quantify the chemical source strengths and variabilities associated with hydrothermal venting from a single component of the northeastern Pacific ridgecrest system: the Axial Volcano segment of the Juan de Fuca Ridge (Fig. 1). In addition, sampling protocols conceived and implemented as a result of the interpretive limitations inherent to conventional vent fluid data are discussed in the context of the VENTS hypothesis.

Neutrally buoyant hydrothermal plumes characterized by large chemical and thermal anomalies have been observed over seven regions of the Juan de Fuca/Explorer/Gorda Ridge (Figs. 1 and 2; Massoth et al., 1982; Lupton et al., 1985; Baker and Massoth, 1987; Baker et al., 1987a-c; McConachy and Scott, 1987). The sharply defined portions of these plumes, which we shall henceforth refer to as proximal plumes, typically extend no more than a few kilometers from the venting site and lie within a single near-bottom layer 100-250 m thick. In contrast to this common distribution pattern, the chemical signals associated with these plumes can be significantly different (Massoth et al., 1985, Baker and Massoth, 1987). Because of this chemical diversity, characteristic and often unique, linear relationships result when plume elemental concentrations are compared to the respective thermal anomalies. The collective element-temperature relationships for a given plume are defined here as the "proximal plume signature." It has been shown that this signature for plumes overlying the Cleft Segment of the Juan de Fuca Ridge is not simply related to the high-temperature fluids venting at that site (Baker and Massoth, 1986, Baker et al., 1987, Massoth et al., in preparation). For example, the concentrations of  $^{3}\text{He}$ , Si, Mn, and Fe determined by extrapolation of plume data to endmember temperatures differ by factors of 2-15 from the concentrations determined directly from the vent fluid data. Factors which contribute to the disparity between the proximal plume and discrete vents are: the regional integration of chemically distinct low- and high-temperature vent fluids by buoyancy induced mixing processes, the formation of "black smoker" particulates and their subsequent local deposition (Feely et al., 1987), and the scavenging of the oxyanions of phosphorous and several trace metals from seawater by Fe-oxyhydroxides (Massoth, manuscript in preparation). It is important to distinguish, especially relative to the goals of the VENTS Program, that it is the more chemically evolved proximal plume chemistry that is dispersed into the regional ocean (Massoth et al., 1984, 1985). Thus, knowledge of the proximal plume signature is required to predict the distributions and effects of hydrothermal effluents in the far-field.

Accordingly, since 1985 VENTS investigators have conducted systematic regional assessments of the thermal and chemical

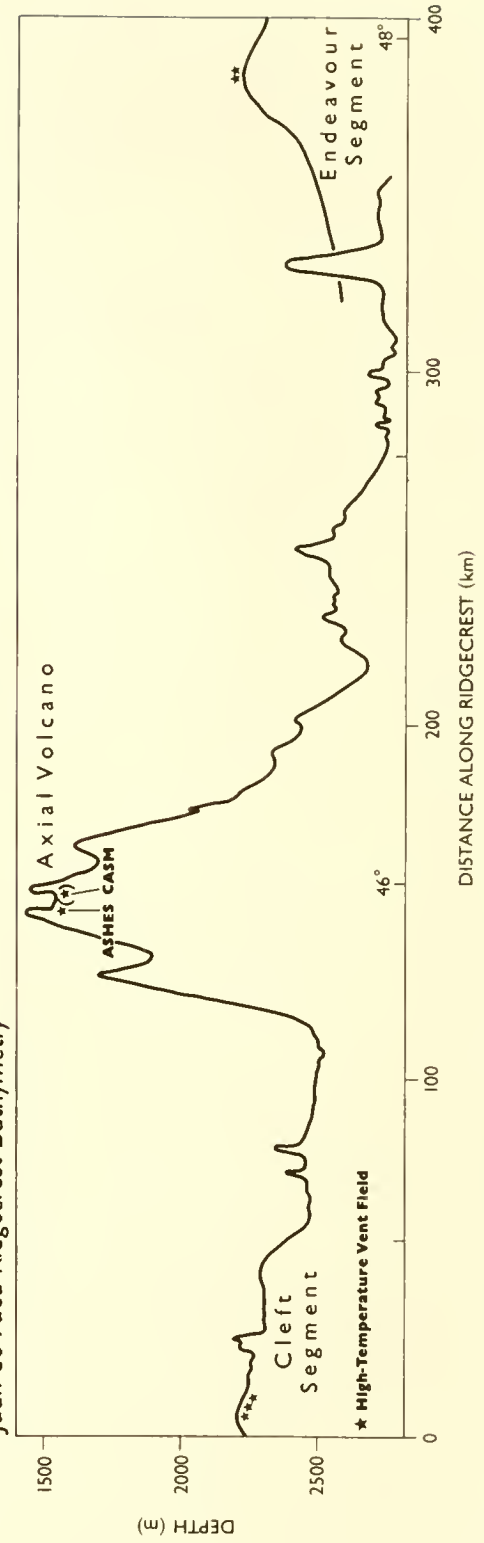
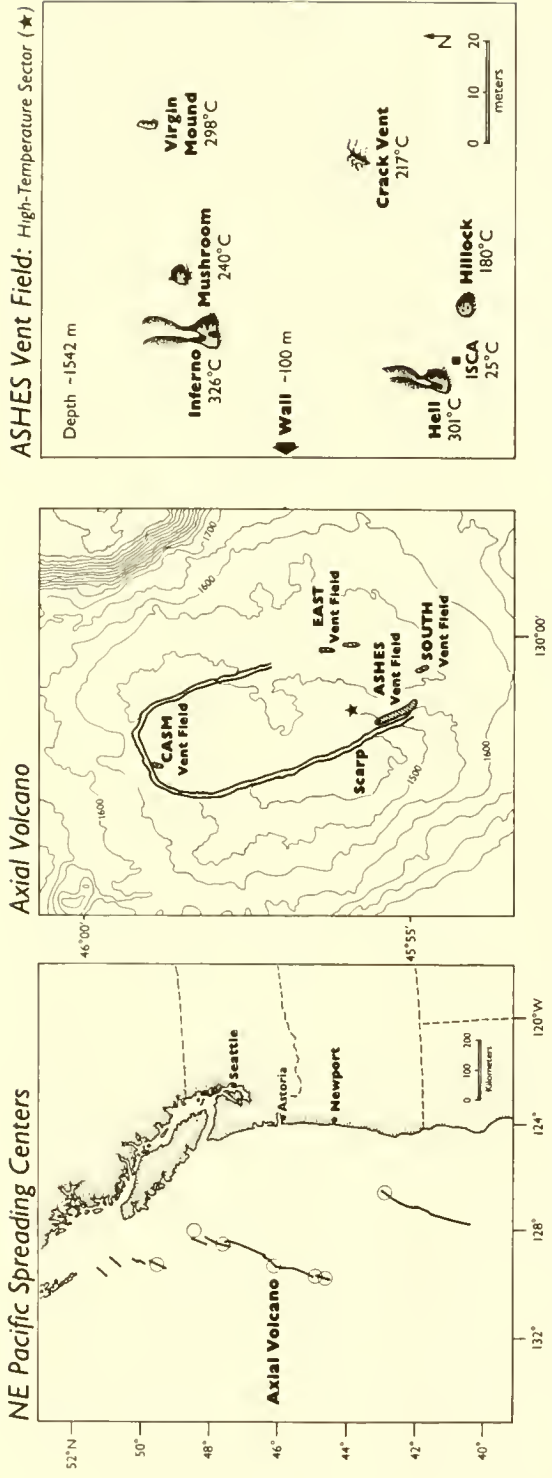


Figure 1. Location charts for Axial Volcano along the Juan de Fuca ridgecrest (top-right), the ASHES vent field within the caldera of Axial Volcano (top-center), individual vents within the ASHES vent field (top-left), and a Juan de Fuca ridgecrest bathymetric profile (bottom). Circles along ridgecrest in upper right-hand panel denote the sites of hydrothermal plumes. Stars represent high-temperature vent fields (with the exception of the CASM site, at which a maximum temperature of 100°C has been observed).

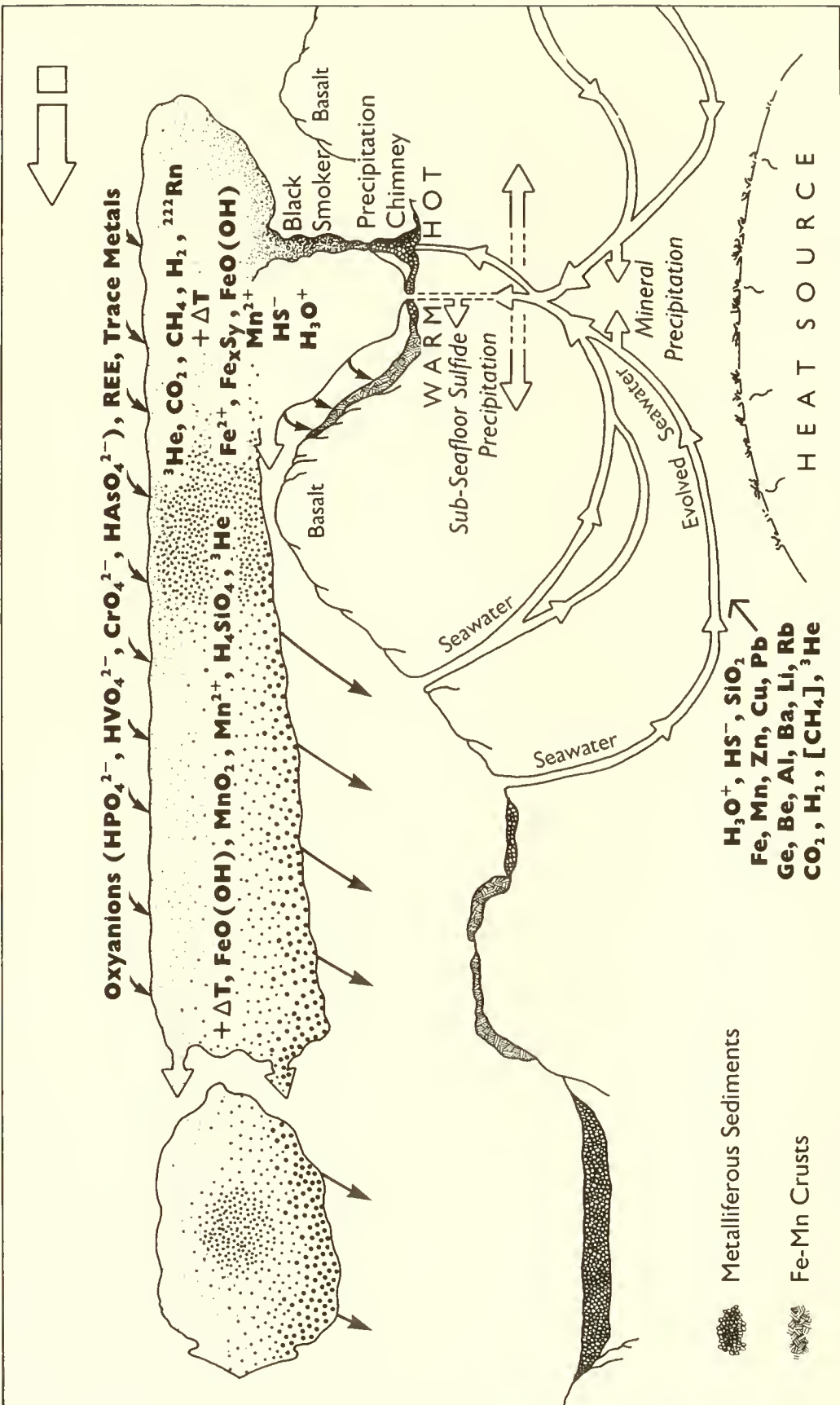


Figure 2. Cartoon representation of hydrothermal system at a ridgecrest spreading center. Note the warm and high-temperature vent sources, buoyant plume, neutrally-buoyant proximal plume, and discontinuous distal plume.

anomalies within the proximal plumes overlying vents, fields of vents, and entire segments of ridgecrest. The resulting inventories have been coupled with measurements of ambient advection to provide estimates of the hydrothermal fluxes transported away from the respective ridgecrest regions (Baker and Massoth, 1986, 1987). Thus, the emphasis within the VENTS Program relative to the determination of chemical source strengths has been on the assessment of plume fluxes rather than on vent fluid fluxes.

Why, then, should we pursue a costly and labor-intensive vent fluid sampling program? From a geochemical perspective, a four-fold rationale guides our serious efforts in this regard:

- o We need to understand better the relationship between the proximal plume and its precursors: high-temperature ( $T > 100^{\circ}\text{C}$ ) vent fluids, the heretofore much-neglected low-temperature vent fluids, and ambient seawater.
- o We need to know the composition of the parent hydrothermal fluids.
- o We need to assess the magnitude of the "invisible plume," and,
- o We need to establish a statistical basis upon which we can extend our instantaneous measurements of vent fluid and plume chemistry to time scales appropriate to the basin-wide effects that we propose to validate.

We expand on these in the following text.

The answers to such questions as: "What are the relative chemical, thermal, and mass contributions of each of the parent reservoirs to the overlying plume?" and, even more basic, "Are the chemical signatures of the respective reservoirs significantly different?" remain unsatisfyingly incomplete. Yet, these answers and the attendant implications are fundamental to our understanding of submarine hydrothermal circulation processes and our assessment of source strengths. Directly analyzing samples from these reservoirs provides information needed to attain these answers. Relating this information to the proximal plume, however, is complicated by the dissolved-to-particulate phase transformations that occur within the buoyant plume. These phase transformations provide significant sinks for some vented species such as reduced sulphur and the chalcophilic metals (e.g., Fe, Cu, and Zn) which combine to form dense particulates that rapidly settle from the plume. Consequently, data must be gathered by submersible at closely spaced intervals throughout the steep geochemical and thermal gradients typical of the buoyant plume in order to track both the mixing and phase transformation processes. Finally, there is an expanding vent fluid data base arising from ongoing research at hydrothermally active sites located throughout the global ridgecrest system. In order for us to extend plume-based predictive capabilities to these study regions a firm

understanding of the links between the proximal plume and its sources is required.

Knowledge of the composition of parent hydrothermal fluids permits estimation by modeling of the sub-seafloor sinks for hydrothermally cycled species which may be important in some elemental mass-balance determinations (Mg, for example). Venting fluid/parent fluid comparisons are also important in the resolution of multiple sub-seafloor endmembers resulting from phase separation and segregation (Von Damm, 1988) which may provide dramatic enhancements in the mobilization and transport of heavy metals (e.g., Fe, Mn, and Zn) within both the brine and vapor phases of hydrothermal fluids (Bischoff et al., 1981; Bischoff and Rosenbauer, 1987). Lastly, changes over time in the composition of the primary fluid may, by inferences drawn from modeling, provide insight into the geophysical underpinnings of hydrothermalism.

Venting fluids are commonly diluted several thousand-fold with ambient seawater during the formation of the proximal plume (7000X, Lupton et al., 1985; 8500X, Baker and Massoth, 1986). Plume anomalies for elements vented at concentrations within an order of magnitude of that of seawater are, therefore, essentially mixed beyond detection by all but the most precise analytical techniques and, thus, are effectively "invisible." Elements within this category and for which hydrothermal processes play a significant role in the respective global mass balances (e.g., Mg, S, Li, Rb, B, Ca, and K) are thus more efficiently studied by examination of vent fluids. These elements are important relative to the VENTS rationale simply by virtue of their imprint on the composition of seawater. The time-scales and processes by which seawater concentrations are buffered relative to these elements, however, are metered relative to seawater (8-10 Ma) and lithosphere (100-1000 Ma) hydrothermal cycling times whereas the observable plume anomaly related effects occur over days to the 100's of years typical of ocean basin mixing times.

We know very little about the temporal variability of venting. Time-series observations of vent fluid chemistry have been reported for only two sites: the East Pacific Rise at 21°N and Guaymas Basin where measurements were obtained at less than annual frequencies extending over four to six years (Campbell et al., in press). While the chemical concentrations of most major vent fluid constituents remained essentially constant over this interval, two-fold variations were documented for Mn and Fe which are among the primary modulators of the chemical state of hydrothermal plumes. The need for additional and higher frequency time-series information can be addressed in part by looking through the temporal window afforded by in situ chemical monitoring of venting fluids. Using state-of-the-art technology, such as flow-injection analysis linked to a variety of chemical detectors (e.g., Johnson et al., 1985, 1986a,b), it is conceivable

that we can measure via unattended in situ chemical analyzers (ISCA's) the chemical variability of venting over time spans of hours to months or longer. Although a deep-submersible is required to deploy this instrumentation, recovery is possible from a surface ship using acoustic release technology. It would be difficult to obtain the temporally comparative information from observations of the proximal plume over the short-term because of smearing caused by local current variability (at semi-diurnal frequencies and longer) and over the long-term because of the cost of surface-ship time. It is this long-term monitoring, however, that is especially relevant to the interpretation of distal plume data. For example, along a transect normal to the Southern Juan de Fuca Ridge, Massoth et al. (1985) and Massoth, Lupton et al. (manuscript in preparation) observed a discontinuity in the plume distributions of He, Mn, and Fe at an off-axis distance temporally equivalent to at least several months transit time from the nearest known source sites. It remains ambiguous whether this discontinuity was due to a hiatus in vent output or was an artifact of advective processes, e.g., the bisection of a gyre-like plume flow-path by the sampling transect or the crossing of this transect by the dispersal routes of plumes originating from different sites. One way of reducing this ambiguity during future off-axis plume studies is by coupling our knowledge of the temporal variability of plume sources, gained by in situ monitoring, with that of the three dimensional chemical structure of the plume, thus allowing us to distinguish source variations from advective processes. Lastly, the coupling of in situ chemical monitoring instrumentation with similar geophysical monitoring instrumentation may provide the data necessary to better understand some of the short-term interconnections between hydrothermal venting and the tectonic/volcanic processes that drive it.

#### Study Site

The Axial Volcano study site, located 260 nautical miles due west of Astoria, Oregon (Fig. 1) sits atop an active submarine volcano which is distinguished by a relatively large rectangular-shaped caldera (3 by 8 km wide, 80-100 m deep) through which the central segment of the actively spreading Juan de Fuca Ridgecrest is thought to pass. The geology of this site has been discussed by Embley et al. (this volume). Venting at Axial Volcano occurs at depths ranging between 1450 and 1600 m. This is at least one-half km shallower than the venting observed at other sites along the Juan de Fuca Ridge (Fig. 1; the Explorer Ridge vent fields, not shown on the bathymetric profile, lie at about 1850 m) and is the shallowest known high-temperature vent site along the global mid-ocean ridgecrest system.

Patchy, low-temperature venting and regional accumulations of orange-yellow colored sediments demarcate the boundaries of the approximately 1 km long, 200 m wide ASHES vent field. Low-

temperature venting has also been observed at the CASM, east and south vent fields (Fig. 1; Canadian American Seamount Expedition, 1985; ASHES Expedition, 1986; and NOAA Alvin Dive Program, 1987, unpublished data). Sulfide deposits, which are evidence of past high-temperature discharge, have been recovered from the CASM and east vent fields. Water column anomalies indicative of high-temperature venting were observed by Massoth et al. (1982) at a depth of about 1600 near the north flank of Axial Volcano in 1981, but were missing during repeat visits to that region in 1983 and 1986 (Massoth, unpublished data). The thermal and particulate anomalies normally associated with Juan de Fuca ridgecrest hydrothermal plumes are greatly attenuated within the water column overlying the caldera of Axial Volcano (Baker and Massoth, unpublished data). The anomalies for dissolved Mn and  $^{3}\text{He}$ , however, are moderately and greatly elevated, respectively (Massoth and Lupton, unpublished data).

The only high-temperature venting that has been observed at Axial Volcano occurs within a 60 m diameter area located near the northern end of the ASHES vent field (Fig. 1). The flat and shallow (1542  $\pm$  1 m) caldera floor in this region consists of lobate and broken sheet flows that are nearly devoid of sediment cover. Sitting directly on these basalts, i.e., without a supporting basement and surrounding blanket of metalliferous sediment, are four sulfide structures, each of which have multiple chimneys discharging high-temperature fluids. The largest of these structures are the Inferno and Hell vents which are about 5 m and 4 m high, respectively, and several meters in diameter. Buoyant plumes of brown and black particulate smoke form above cm-scale orifices located at the top and sides of these vents. Clear, high-temperature fluids flow vigorously through vent orifices located near the base of Inferno vent. These fluids appear to flow laterally after about one meter of vertical rise and form a white particulate smoke beginning a meter or so downstream. The Mushroom and Hilloch vents are sulfide mounds of 1-2 m height and width. High-temperature fluids which form an opaque smoke rise from spires imbedded within a dense covering of tube worms on Mushroom vent. Black smoke was observed to rise from a vent on the side of Hilloch. Two high-temperature vents within the ASHES field are not visibly associated with sulfide structures. Virgin Mound vent is a white, spire-like edifice 0.5-0.8 m high composed almost entirely of anhydrite. Clear fluids gush vigorously through its several cm wide orifice and ascend beyond view in a smokeless plume. A cms-thick, 2 m-diameter apron of anhydrite which surrounds the vent is apparently the result of frequent structural failures of the chimney and reflects an equilibrium between venting-induced chimney formation and anhydrite dissolution (Feely et al., 1987). Near Virgin Mound, high temperature fluids issue from a pair of merging cracks approximately 5-10 cm wide and about 10-15 m in overall length which are collectively known as Crack vent. Chunks of anhydrite overflow from these cracks, which, like Virgin Mound, give rise to

buoyant and smokeless plumes. Shimmering water (low temperature discharge) is associated with patches of tube worms located throughout the high-temperature sector and is also ubiquitous about the bases and sides of the sulfide structures.

## METHODS

### Pisces-IV

The vent fluid data reported here were determined from samples collected during a joint Canadian-U.S. sponsored series of 15 dives on Axial Volcano conducted during July-August 1986 using the Research Submersible Pisces IV and tender ship Pandora II. Submersible navigation was performed relative to an acoustic transponder net. Vent water temperatures were initially determined by commercially available platinum resistance thermometers. After three of these mechanically failed during immersion in high-temperature vent fluids, an impromptu thermo-couple system was fabricated from a thermal sensor borrowed from the propulsion system of the Pandora II. Temperatures were not measured coincidentally with the collection of vent fluids: typically, the spatial location of maximum temperature sensor output was memorized by the submersible pilot during a thermal search of the vent fluid flowstream after which the temperature probe was returned to its holster, the sampler of choice was picked up by the manipulator arm, and its snorkel maneuvered into position for sampling. Venting fluids were collected in paired 755 mL titanium syringes (Major Samplers) described by Von Damm et al. (1985) which were available to us courtesy of the Alvin Group, WHOI. One sample was collected explicitly for vent fluid gases in a UCSB Gas-Tight Bottle designed by J.E. Lupton. Because of space and loading constraints on Pisces, only a single titanium sampler pair was filled during any given dive. Additional water samples were collected in selectable plastic reservoirs indexed upon demand into the flowstream of the Pisces slurp gun.

Determinations of vent fluid alkalinity and pH were performed shipboard. The methods, precisions and laboratories associated with these as well as the shore based determinations of  $^{3}\text{He}$ ,  $\text{Mg}^{2+}$ ,  $\text{H}_4\text{SiO}_4$ ,  $\text{H}_2\text{S}$ ,  $\text{Cl}^-$ ,  $\text{Ca}^{2+}$ ,  $\text{Mn}^{2+}$ , and  $\text{Fe}^{2+}$  are given in Table 1.

### Alvin

A second series of 11 dives at the ASHES vent field was conducted using Alvin/Atlantis II during September-October 1987. The chemical data for 27 water and 11 gas samples collected during this expedition are presently being determined and will be reported elsewhere. Temperatures were measured at each of the high-temperature vents at ASHES using a platinum resistance thermometer which was an integral part of a combined sampling and sensing system for vent fluids that will be discussed later in this report. Drift in the calibration of this system was

Table 1. Analytical techniques for vent water analyses

<u>Analyte</u>	<u>Method</u>	<u>Reference</u>
Alkalinity	Potentiometric, end point by titration (1 $\sigma$ : 0.2%, PMEL, shipboard)	Dyrssen (1965)
$\text{H}_3\text{O}^+$	Potentiometric, NBS buffers, 25°C (1 $\sigma$ : <0.25% as pH, PMEL, shipboard)	Zirino (1975)
$^3\text{He}$	Mass spectrometry (1 $\sigma$ : 1.0%, UCSB)	Lupton et al. (1980)
$\text{Mg}^{2+}$	EDTA titration (1 $\sigma$ : 0.5%, UW)	Gieskes (1974)
$\text{H}_4\text{SiO}_4$	Colorimetric-flow injection, silico-molybdate complex (1 $\sigma$ : 1.0%, UW)	Thomsen et al. (1983)
$\text{H}_2\text{S}$	Colorimetric, methylene blue, samples preserved as ZnS (1 $\sigma$ : 5%, UW)	Cline (1969)
$\text{Cl}^-$	Potentiometric titration (1 $\sigma$ : 0.1%, UW)	McDuff (1985)
$\text{Ca}^{2+}$	EGTA titration (1 $\sigma$ : 0.5%, UW)	Gieskes (1974)
$\text{Mn}^{2+}$	Flame atomic absorption spectrophotometry (1 $\sigma$ : 5%, PMEL)	Perkin Elmer Manual
$\text{Fe}^{2+}$	Flame atomic absorption spectrophotometry (1 $\sigma$ : 5%, PMEL)	Perkin Elmer Manual

periodically assessed at sea using a field temperature calibrator. Temperature offsets within the 0° to 400°C calibration range were never greater than 2.0°C.

## RESULTS

The chemical data determined from vent fluids collected in the titanium samplers are given in Table 2. Endmembers (estimated by extrapolation to "0" Mg along linear element:Mg mixing lines) for the respective analytes at Axial Volcano and for several other sediment-starved ridgecrest spreading center sites are also given. Graphic representations of the Axial Volcano Cl:Mg, H<sub>2</sub>S:Mg and Mn:Mg, Fe:Mg, and Fe:Mn relations are shown in Figures 3 and 4, respectively. Also shown in these figures are the data determined from water samples collected with the PISCES slurp gun (not given in Table 2). Because of sample mixing problems, the slurp gun data were not as reliable as that from the titanium samplers, and, hence, were not used in the determinations of endmembers.

Venting fluids at Inferno were collected exclusively from the basal outlet discharging the clear fluids described previously. Local currents combined with the single manipulator configuration of Pisces to preclude vent fluid collection from orifices beyond the reach of a bottom-anchored submersible. At Mushroom and Virgin Mound vent fluids were collected directly above the spires and within the anhydrite chimney orifice, respectively.

Because of calibration uncertainties (as shown previously) the temperature data listed in Table 1 are given only for relative comparison. The temperature maxima determined at these vents during the 1987 Alvin dives are shown in Figure 1.

## DISCUSSION

The Axial Volcano ASHES vent field data set presented here is rather sparse with respect to the number of data points and their spread along the seawater-hydrothermal fluid mixing line (the most hydrothermally enriched sample contained only 33% pure vent fluid based on the premise that the latter is characterized by a "0" Mg value). Nevertheless, several preliminary observations are offered while we await the results of determinations presently underway on the 1987 vent fluid collection.

The Axial data fall into two clearly distinct categories, which are apparent from the plots of chloride, hydrogen sulfide, manganese, and iron versus magnesium (Figs. 3 and 4). In each of these plots we can distinguish two mixing lines: one between seawater and a "normal" hydrothermal fluid endmember and another between seawater and a low-salinity, metal-depleted, gas-enriched fluid endmember. The elemental concentrations for the normal hydrothermal fluid endmember at Axial Volcano fall within the range of previously published data on ridgecrest hydrothermal

Table 2. Axial volcano vent fluid chemistry

Sample	Location	Temp. °C	Hydro-thermal eq	pH	$^3\text{He}$ pmol	$\text{Mg}^{2+}$ mmol	$\text{H}_4\text{SiO}_4$ mmol	$\text{H}_2\text{S}$ mmol	$\text{Cl}^-$ mmol	$\text{Ca}^{2+}$ mmol	$\text{Mn}^{2+}$ $\mu\text{mol}$	$\text{Fe}^{2+}$ $\mu\text{mol}$
1721-3	Inferno	(330)	22	1.66	5.44	41.0	3.10	1.21	54.0	18.0	27.8	247
1721-4	Inferno	(330)	18	1.73	5.51	42.9	2.68	1.16	54.1	16.9	25.5	218
1727-3	Inferno	(145)	14	5.50		45.2	2.19		53.7	15.1	19.4	16.9
1727-4	Inferno	(145)	13	1.90		45.8	2.28		54.3	14.6	19.1	127
1729-UCSB	Inferno	(283)			5.5	50.8	0.48	0.19	53.1	10.8	2.3	28
1722-3	Mushroom	(283)	3	2.21	6.12	51.1	0.49	0.17	53.3	10.7	2.1	27
1722-4	Mushroom	(283)	3	2.27	6.09	51.1	0.49	2.00	42.3	10.5	4.0	5
1733-3	V. Mound	(250)	33	1.63	4.80	(11.1)	35.2		42.8	10.6	4.1	6
1733-4	V. Mound	(250)	32	3.90		35.9	3.60		53.9	10.3	.0005	.001
Seawater	1600 m	2.32	0	2.35	7.47	.004	52.4	0.17				

## Endmembers ("0" Mg)

Axial Volcano	Excluding Virgin Mound	100	-.85		0.0	14.4	5.8	56.6	47.5	141.5	120.6	
	Virgin Mound + Seawater	100	.16		0.0	11.2	17.2	11.1	12.6	12.6	17	
Cleft Segment, JFR <sup>1</sup>		100	0.0	3.2	9.5	0.0	22.7-	3.5-	89.6-	77.3-	261.0-	
							23.3	4.4	108.7	96.4	448.0	10300-18700
Endeavour Segment, JFR <sup>2</sup>		100		4.5	0.0	4-	4.0	42.0	36.0	240-	920-	
						22.5				980	2880	
East Pacific Rise, 21° N <sup>3</sup>		100	-.19-	3.3-3.8	5.8	0.0	15.6-	6.6-	48.9-	11.7-	69.9-	75.0-
			-.50				19.5	8.4	57.9	20.8	100.2	242.9
East Pacific Rise, 13° N <sup>4</sup>		100		3.8	0.0	22			74.0	55	800-	1050-1850
										1200		
Mid-Atlantic Ridge, TAG <sup>5</sup>		100			0.0	22			65.9	26	1000	1640
Galapagos Spreading Center <sup>6</sup>		100	0.0		7.7	0.0	21.9	+	+/-	24.6-	360-	+
										40.2	140.0	

<sup>1</sup> All data but  $^3\text{He}$  is from Von Damm and Bischoff (1987); <sup>2</sup> He from Kennedy (1985); <sup>3</sup> He from Russell E. McDuff (unpublished data), Gary J. Massoth (unpublished data); <sup>4</sup> All data but <sup>3</sup>He is from Von Damm et al. (1985); <sup>5</sup> He from Lupton et al. (1980); <sup>6</sup> Michard et al. (1984); <sup>7</sup> Edmond et al. (1986); <sup>8</sup> Edmond et al. (1979a, b); units are per kilogram unless specifically noted.

## Axial Volcano/PISCES 86

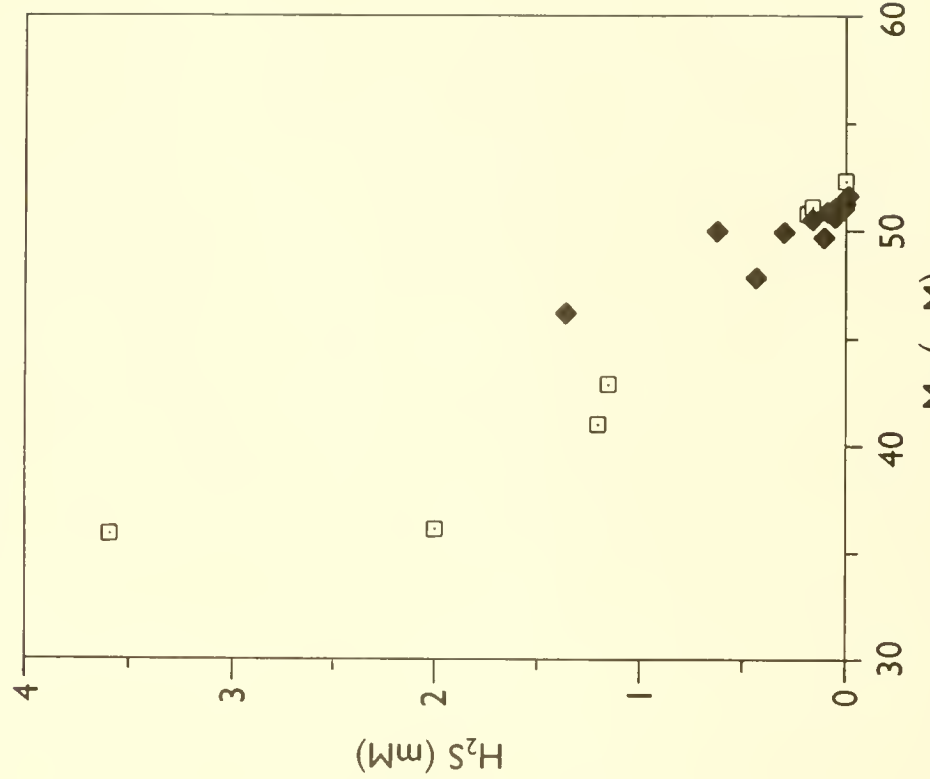
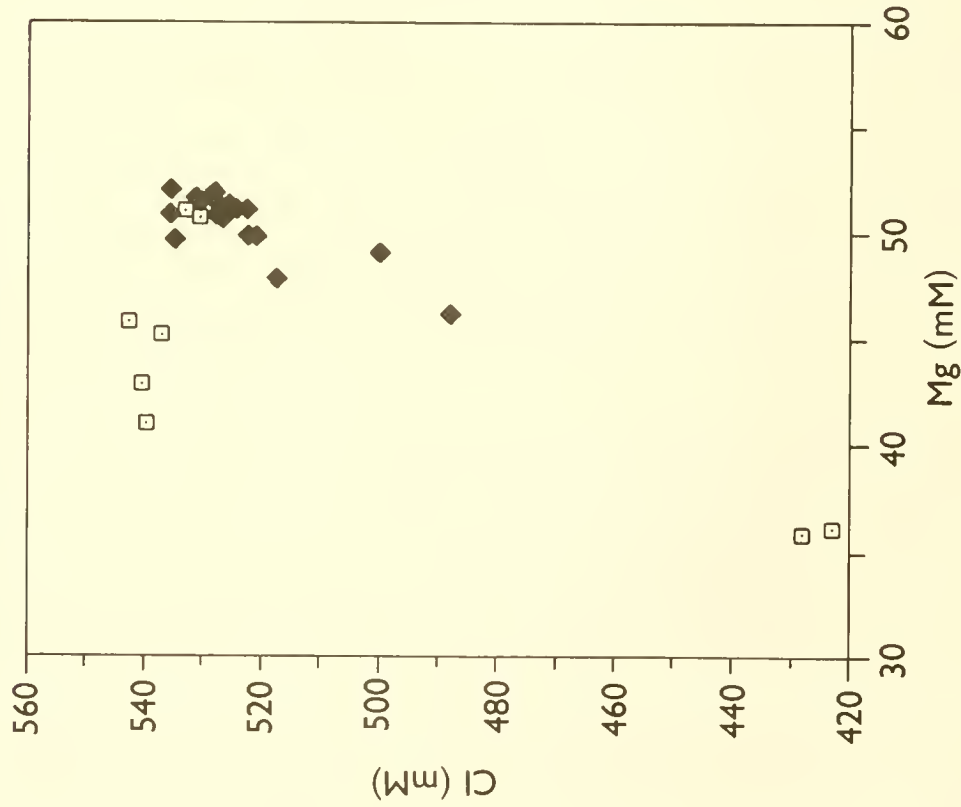


Figure 3. Chloride vs. magnesium (left) and hydrogen sulfide vs. magnesium (right) for Axial Volcano, ASHES vent field samples collected in 1986. Open squares are for fluids collected in Major Samplers. Closed diamonds represent fluids collected with the PISCES slurp gun.

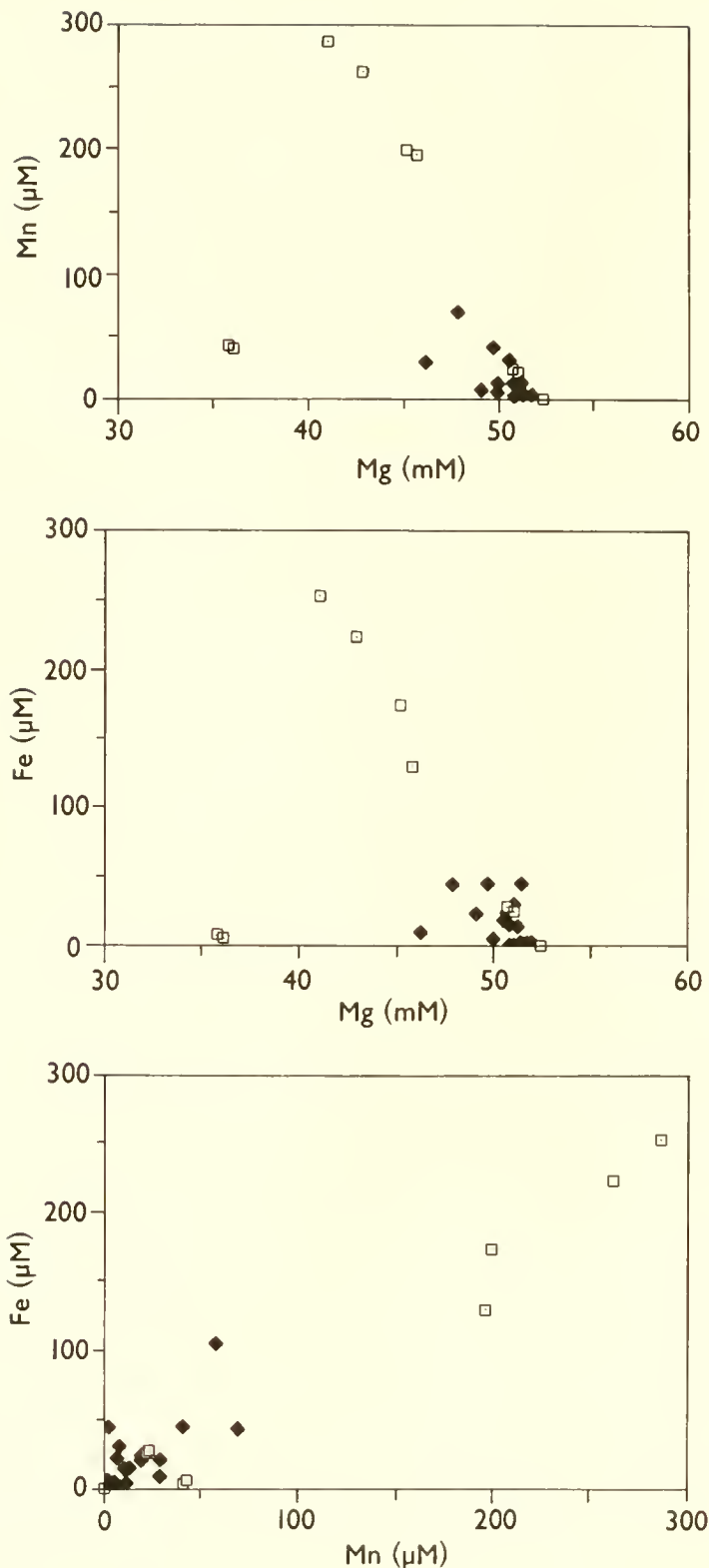


Figure 4. Manganese vs. magnesium (top), iron vs. magnesium (center), and iron vs. manganese (bottom) for the Axial Volcano, ASHES vent field samples collected in 1986. Symbols as in Figure 3.

fluids (e.g., East Pacific Rise, 21°N, Galapagos Spreading Center, and Mid-Atlantic Ridge TAG site, Table 2 and references therein). The chloride concentration of the normal Axial endmember is within the range of variability normally ascribed to mineralogic control (Von Damm, 1988). Silicate levels are consistent with quartz solubility control (Von Damm and Bischoff, 1987) and calcium appears slightly elevated relative to other hydrothermal fluids with similar chloride concentrations. The normal Axial endmember is represented by samples from the Inferno, Mushroom and Hell vents.

Mixing lines connecting the Virgin Mound data with the seawater endmember define a second data group. All of the non-volatile element concentrations are consistently and significantly lower in this low-salinity endmember than in the normal endmember. The chloride endmember concentration, for example, corresponds to a chlorinity only one-third that of seawater and is significantly lower than reported values for any other ridgecrest spreading center. The Fe and Mn concentrations are also abnormally low and preferentially depleted in Fe relative to Mn (Fig. 4).

In contrast to the non-volatile elements, the volatile elements are highly enriched in the low-salinity fluids of Virgin Mound. These fluids effervesced vigorously as they were expelled from the titanium syringe samplers which were observed to leak gas bubbles during ascent from dive 1733. As the only gas analysis for the Virgin Mound data group is from one of these syringes, caution must be exercised in the interpretation of the gas data. Nonetheless, if we assume that most of the measured condensable gas ( $1.28 \text{ cc g}^{-1}$ ) is  $\text{CO}_2$ , then the Virgin Mound  $\text{CO}_2$  endmember concentration ( $173 \text{ mmol kg}^{-1}$ ) is about 15 to 30 times that estimated for the Galapagos Spreading Center and East Pacific Rise, 21°N endmembers, respectively (Craig et al., 1980). The  $\text{H}_2\text{S}$  data from Virgin Mound and a related vent extrapolate to a zero-magnesium endmember of approximately  $11 \text{ mmol kg}^{-1}$ , while the Inferno and related vents endmember concentration is about  $6 \text{ mmol kg}^{-1}$ .

The maximum observed discharge temperature at Axial Volcano is  $326^\circ\text{C}$ , compared to the predicted boiling point of  $348^\circ\text{C}$  (Bischoff and Rosenbauer, 1984) for the local seafloor pressure. The proximity of measured temperatures to the boiling temperature together with the elevated volatile content and depleted chloride in samples from Virgin Mound are consistent with the hypothesis that the hydrothermal fluid rising through the ocean crust underwent subcritical phase separation, which generated a low salinity vapor phase. This vapor phase then must have become partially segregated from its parent hydrothermal fluid to eventually exit the seafloor at the anomalous Virgin Mound vent. That the phase separation occurred late in the circulation cycle, temporally and spatially close to venting, is supported by the proximity of the measured temperature and pressure to the boiling

curve for seawater and the close physical proximity of the two chemistries.

When we compare the results of our work at Axial Volcano with recent experimental results on the chemical effects of phase separation of hydrothermal fluids (Bischoff and Rosenbauer, 1987), there are some differences, but the major trends are the same. The pseudo-conservative element chloride is somewhat higher in the low-salinity Axial endmember than found in the experimental vapor phase, while the Axial volatile components are considerably elevated over the levels in the experimental vapor phase. Some of the factors which contribute to the differences between the experimental results and our field results are: 1) different pressure and temperature conditions, 2) incomplete segregation of vapor phase from parent fluid in the field, 3) differences in chemistry of the basalt and evolved hydrothermal fluid between the experiment and the field, and 4) closed experimental system versus possible open-system boiling in the field.

It is anticipated that the complete analysis of the much larger 1987 vent fluid data set will help to align the above observations with a single, self-consistent model for the Axial hydrothermal system.

#### Submersible-coupled In situ Sensing and Sampling System (SIS<sup>3</sup>)

Two rather obvious weaknesses of the 1986 Axial vent fluid data set are the lack of relatively undiluted (i.e., > 90% hydrothermal,  $Mg < 5 \text{ mmol kg}^{-1}$ ) vent fluid samples and reliable temperature data, especially temperatures measured coincident with sample collection. Near-pure hydrothermal fluid data substantially enhances our ability to extrapolate to endmember values and, in fact, may serve as reasonable direct measures of these. For non-conservatively behaving plume species, like Fe and Ba, undiluted vent fluid data are essential to a nonambiguous endmember determination. The vent fluid data set assembled by Karen Von Damm (1983) for the East Pacific Rise (EPR), 21°N hydrothermal fields is one of the most complete yet reported. The Fe versus Mg data for this site are shown in Figure 5. By the aforementioned criteria, only 27% (n=20) of the vent fluid samples were suitable for use in the determination of the endmembers for Fe (and, similarly, Mn, Co, Ni, Cu, Zn, Ag, Cd, Pb, Hg,  $H_2S$ , As, Se, pH, and Alkalinity). It is likely that some of the more diluted samples shown in Figure 5 are artifacts of sampling: i.e., the sampler snorkel tip was not in the position of highest temperature, hence, maximum fluid purity, during piston retraction. The sensing of temperature during sampling would increase the efficiency with which undiluted fluids are recovered.

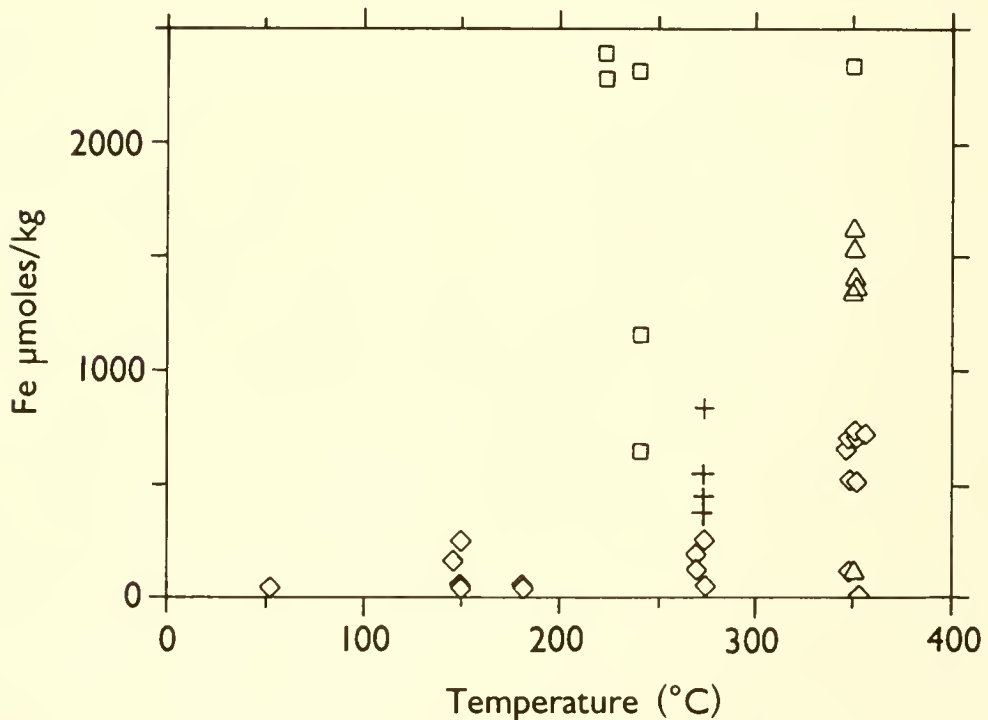
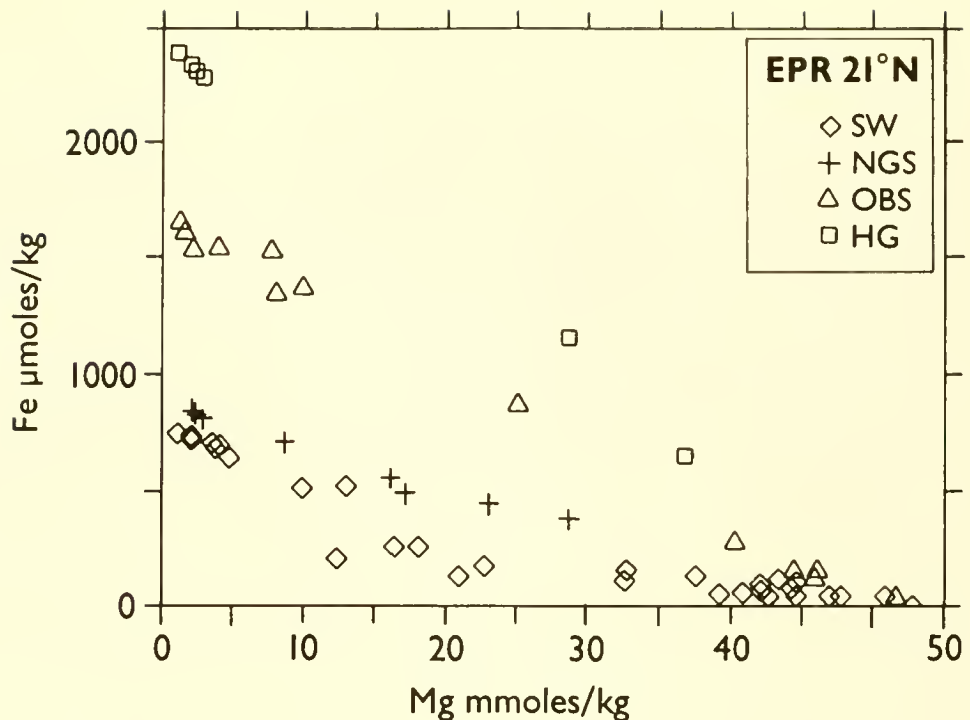


Figure 5. Iron vs. magnesium (top), and iron vs. temperature (bottom) for samples collected at the East Pacific Rise, 21°N in 1981. SW, NGS, OBS, and HG are different vent fields at the 21°N site. Data from Von Damm (1983) and replotted here courtesy of Karen Von Damm.

The cornerstone of our approach to the assessment of plume fluxes are the element/heat ratios determined for the highly diluted proximal plume waters. To attain the desired understanding of the linkages between venting fluids and these plumes, these ratios must also be determined for the venting fluids. Because of the high thermal gradients within the cm-scale vent fluid sampling zone, it is difficult to ensure that collected fluids and (independently) measured temperatures precisely correspond. A sense of this can be seen in the Fe versus temperature data for 21°N, EPR (Fig. 5). The uncertainties of the element/heat ratios produced by separate measurements of chemistry and temperature make it impractical to use these data to track mixing processes into the near-field.

Fluid-correlated and accurate (to within 1°C) temperature data is also needed for thermodynamic applications and for detecting subtle temporal changes in venting behavior (Campbell et al., 1988; Bowers et al., 1988). Furthermore, laboratory studies (Seyfried and Janecky, 1985) and thermodynamic modeling calculations (Janecky and Seyfried, 1984; Bowers et al., 1985) suggest that the compositions of some major vent fluid constituents are extremely variable at temperatures near the critical point for the discharging fluids. For example, the experiments of Seyfried and Janecky (1985) show that a 25°C increase in temperature from 400°C to 425°C at 400 bars leads to approximately 4 to 10-fold increases in concentrations of Fe and Mn and equally large or larger decreases for Cu, Zn, and H<sub>2</sub>S. Last, the calibration of chemical geothermometers (e.g., those for Na-K-Ca and Na-Li) for submarine hydrothermal systems await reliable vent fluid temperature data (Von Damm, 1988).

To address some of these sampling concerns, Submersible-coupled In situ Sensing and Sampling System (SIS<sup>3</sup>) was conceived by a group of vent fluid chemists (R.E. McDuff, J.E. Lupton, M. Lilley of the University of Washington, and G.J. Massoth) and marine engineers (H.B. Milburn and B. Walden of the Alvin Group/WHOI) and fabricated at PMEL under the auspices of the NOAA VENTS Program and Office of Undersea Research. The guiding concept was that fluids needed to be sampled in a way that both the elemental concentration and the temperature at the precise point of sampling would be known. Real-time temperature and chemical data would provide valuable guidance in sampling. The system would have to be effective over a wide range of temperatures and flow rates. Specific improvements included: 1) the ability to sample and sense both high-temperature and warm spring vent fluids with a single system configuration, 2) the ability to insure in realtime that sample quality is maximized by precise control of sampling flow rate and the monitoring of in situ temperatures along the system's flow path, 3) more "pilot-friendly" manipulator requirements during sampling operations, 4) more basket payload and space available for other operations

due to a near-hull attachment of most of the system components, 5) shipboard calibration facilities for the system's temperature sensors, and 6) in-line ports available for easy incorporation of additional flow stream sensors or samplers (such as the ISCA, as follows, in a "SCANNER" (Submersible Chemical Analyzer) mode in the fashion of Johnson et al., 1986).

The SIS<sup>3</sup>, as shown pictorially in Figure 6, was tested during the 1987 Alvin dives. The manifold portion of the system was designed to fit close under the forward section of the Alvin sphere to keep weight as far aft as possible and to preclude interference with other activities that utilize the basket and manipulators. The flow path was fabricated in a manner to minimize contamination and preserve heat between the inlet and the samplers. The tubing, joints, and fittings were made from commercially pure titanium, with alumina ceramic liners in the tubing sections.

The inlet nozzle is free to rotate in two dimensions and is gripped by the T-handle with the manipulator arm. The nozzle is closed on the bottom and slotted on the sides to reduce clogging during the excavating often associated with sampling. The tip of the inlet temperature probe is located directly above the intake slots. The arm, which is extensible and free to rotate, is comprised of two titanium tubes with internal ceramic liners carefully sized to slide together and sealed at the central ceramic joint with a silicone O-ring. The shoulder joint on the manifold is located directly below the port manipulator arm of ALVIN and is also free to rotate in two dimensions. The 100 cm long titanium manifold is lined with 3.1 cm ID ceramic tubing, and is fitted with 8 outlet ports along the sides through which the samples are drawn. The starboard end of the tube is fitted with another temperature probe to monitor manifold temperature. The flow is channeled from the bottom of the end plate of the manifold into a cooling coil to dissipate heat and then to a turbine flow meter for monitoring flow rates. Vinyl tubing connects the flow meter to the main suction pump, which is a rubber impeller driven by a pressure-balanced DC motor.

Water samples are drawn through sampling ports into one of four possible major samplers on the forward side of the manifold. The tripping mechanism on the samplers is actuated by a small hydraulic cylinder connected to the submersible's hydraulic system. Two UCSB Gas-Tight samplers are fitted on the aft side of the manifold and are also actuated by hydraulic cylinders. Both of these types of samplers have purge ports on the intake valves that are used to flush the dead volume behind the valve body. A flushing pump, identical in type to the main suction pump, is connected to these ports via a collection manifold. Additionally, two 500 mL polycarbonate syringes fitted with teflon inline filter

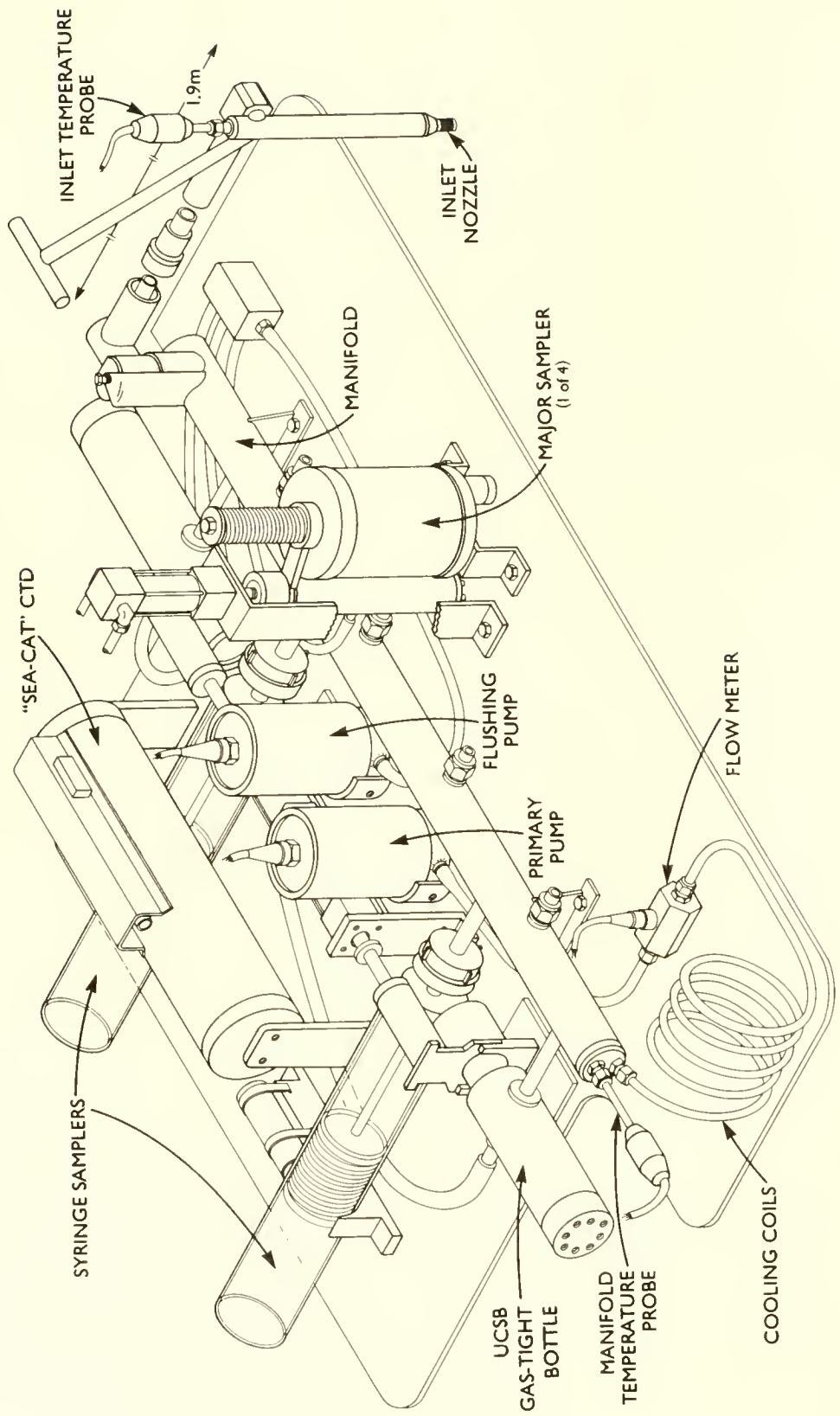


Figure 6. The Submersible-coupled *In situ* Sensing and Sampling System (SIS<sup>3</sup>) as it would be viewed from a point off the starboard bow of ALVIN.

holders are located aft of the manifold. The syringes are actuated by energizing an electric solenoid which releases a compressed spring on the plunger arm.

The sensor and control lines were passed through the Alvin hull penetration system and connected to a terminal strip inside the sphere. Custom designed interface electronics were installed in the equipment rack, and the data display and logging were performed on a laptop computer with a backlit LCD display. The software, which was written in Forth, displayed an analog plot of the two temperatures, and a digital display of all other parameters. Data was stored on internal floppy discs.

During operation when the submersible is adjacent to a vent, the pumps are switched on as the pilot removes the nozzle from a holster attached to the basket. As the nozzle is manipulated within the venting fluid flow stream, the observer guides the pilot by watching the display of temperatures on the computer. The data shown in Figure 7 are representative of the real time display. When the highest temperature has been found, time is allowed for the system to come to thermal equilibrium and to allow complete flushing of the system. At the nominal flow rate of 5 liters/min through each pump, this requires approximately 1 minute. At this point the pumping rate can be modulated to ensure that the sample is not being diluted with ambient seawater. When equilibrium has been achieved, as exemplified by the manifold temperature reaching a maxima, the pumps are turned off and a sampler is activated. When the nozzle has been removed from the vent, the pumps are again turned on to flush the entire system.

The system has shown the importance of measuring temperature at the inlet of the sampler. Very small motions of the manipulator arm by the pilot can cause temperature changes of hundreds of degrees and the guidance of the observer is necessary to obtain the highest temperature water at a particular vent. Typically the nozzle is obscured from view during sampling by "black smoke" or resuspended sediments. Relying on visual means to position the sampler in most cases would result in dilution of vent fluids with ambient sea water.

#### In Situ Chemical Analyzer (ISCA)

The 1987 Alvin dive series also provided an opportunity to test a second type of instrument new to the VENTS Program: an In Situ Chemical Analyzer (ISCA) which was designed to determine the chemical output of low-temperature vents over time periods of days. This was conceived to be a first step toward the establishment of an in situ chemical monitoring capability that will eventually provide the information necessary to temporally extend instantaneous plume and vent fluid measurements to time scales appropriate for testing the VENTS Program's ocean basin scale hypothesis.

holders are located aft of the manifold. The syringes are actuated by energizing an electric solenoid which releases a compressed spring on the plunger arm.

The sensor and control lines were passed through the Alvin hull penetration system and connected to a terminal strip inside the sphere. Custom designed interface electronics were installed in the equipment rack, and the data display and logging were performed on a laptop computer with a backlit LCD display. The software, which was written in Forth, displayed an analog plot of the two temperatures, and a digital display of all other parameters. Data was stored on internal floppy discs.

During operation when the submersible is adjacent to a vent, the pumps are switched on as the pilot removes the nozzle from a holster attached to the basket. As the nozzle is manipulated within the venting fluid flow stream, the observer guides the pilot by watching the display of temperatures on the computer. The data shown in Figure 7 are representative of the real time display. When the highest temperature has been found, time is allowed for the system to come to thermal equilibrium and to allow complete flushing of the system. At the nominal flow rate of 5 liters/min through each pump, this requires approximately 1 minute. At this point the pumping rate can be modulated to ensure that the sample is not being diluted with ambient seawater. When equilibrium has been achieved, as exemplified by the manifold temperature reaching a maxima, the pumps are turned off and a sampler is activated. When the nozzle has been removed from the vent, the pumps are again turned on to flush the entire system.

The system has shown the importance of measuring temperature at the inlet of the sampler. Very small motions of the manipulator arm by the pilot can cause temperature changes of hundreds of degrees and the guidance of the observer is necessary to obtain the highest temperature water at a particular vent. Typically the nozzle is obscured from view during sampling by "black smoke" or resuspended sediments. Relying on visual means to position the sampler in most cases would result in dilution of vent fluids with ambient sea water.

#### In Situ Chemical Analyzer (ISCA)

The 1987 Alvin dive series also provided an opportunity to test a second type of instrument new to the VENTS Program: an In Situ Chemical Analyzer (ISCA) which was designed to determine the chemical output of low-temperature vents over time periods of days. This was conceived to be a first step toward the establishment of an in situ chemical monitoring capability that will eventually provide the information necessary to temporally extend instantaneous plume and vent fluid measurements to time scales appropriate for testing the VENTS Program's ocean basin scale hypothesis.

## DIVE 1910

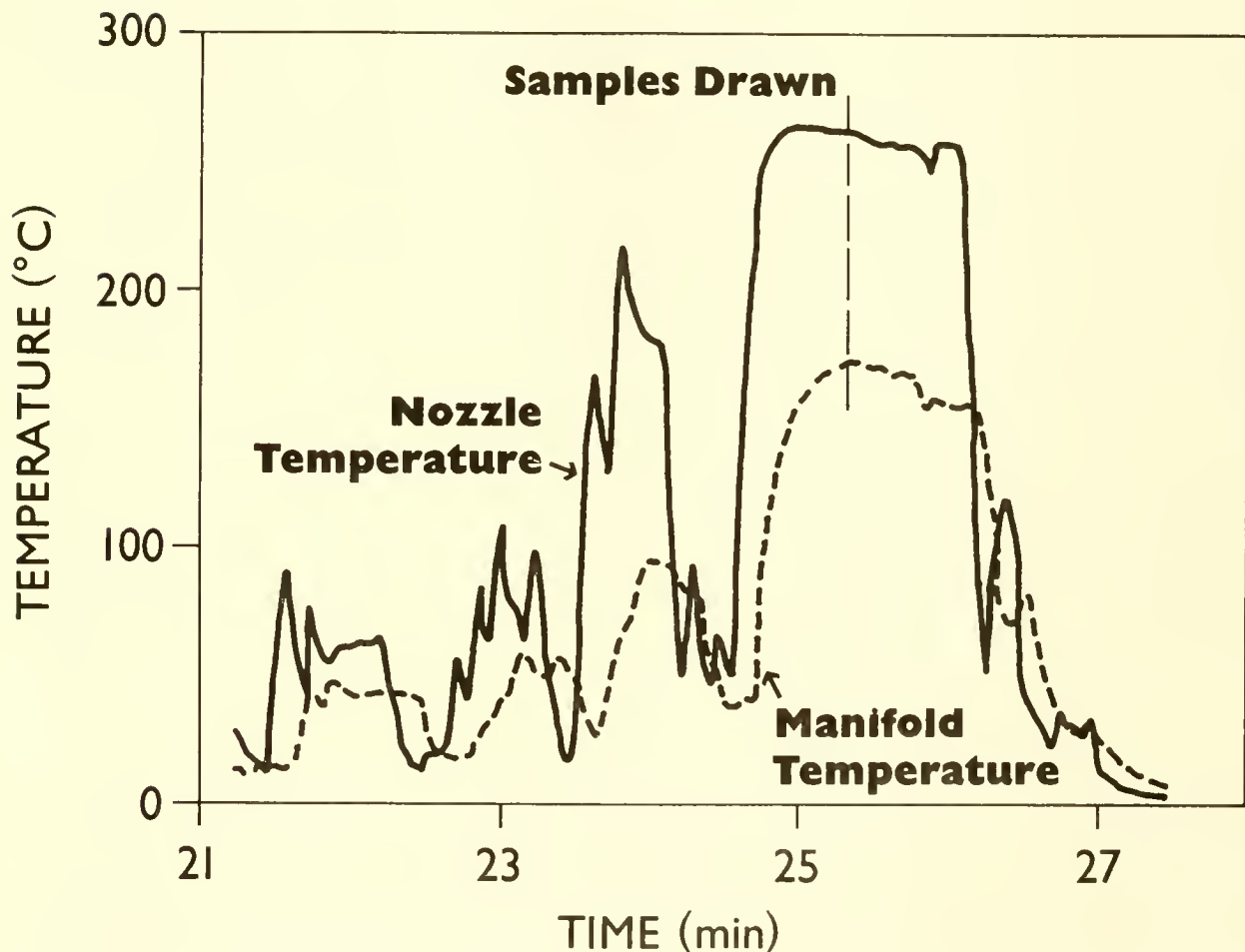


Figure 7. Reproduction of lap-top computer display of temperature vs. time during sampling with SIS<sup>3</sup>. Note hysteresis in manifold temperature profile (short dashes) relative to that for the temperature sensor in the nozzle (solid line). The temperature range displayed is easily selectable during sampling. Digital information is also displayed in real time (not shown).

The ISCA is the chemical outgrowth of vent fluid temperature and flow monitoring instrumentation first deployed by researchers from the University of Washington during a 1984 Alvin dive program (MERGE Group, 1984). The design of the ISCA draws heavily upon the relatively new technology of flow injection analysis (FIA) and the pioneering work of Johnson et al. (1986b) who made *in situ* chemical measurements from Alvin with a SCANNER. A block diagram of the ISCA is shown in Figure 8. The instrument is capable of determining solutes that can be measured by colorimetric detection at wavelengths in the range 550-900 nm. It consists of a peristaltic pumping system that propels sample (or standard) and reagent streams through a reactor manifold and a simple photometric detector consisting of a light-emitting diode and phototransistor. These components are subjected to *in situ* pressures, with electrical components (motors and solenoids) isolated in fluid-filled, pressure-compensating housings. Controlling electronics and battery supplies are contained in a pressure case. The controlling electronics are built around a low power data logger with 28K of user partitioned memory, an on-board BASIC operating system and an RS-232 interface. All of the components are contained within an aluminum frame, 18" x 18" x 26." Chemical modules were built to determine  $H_4SiO_4$ ,  $H_2S$ ,  $Fe^{2+}$ ,  $Fe^{3+}$  and pH. Two or three of these can be used at once. Temperature is also monitored (by thermistor) with a  $0.1^{\circ}C$  resolution. The system can be used in two modes. The monitor mode involves measuring fluids periodically over several days under computer control, deploying and recovering the system with Alvin. The scanning mode involves analyzing fluids during the course of an Alvin dive, with the system controlled via an RS-232 link into the submersible.

The system was configured to determine  $H_2S$ ,  $Fe^{2+}$ , pH and temperature during a 3-day deployment at a low-temperature vent at the ASHES site (Fig. 1). The data recorded indicate that the motor driving the pump was running erratically and eventually stopped. While this failure was disappointing, the test had many positive aspects. Sufficient data was obtained to determine that all other components worked as expected. Alvin had no problem in deploying or recovering the instrument. Several ways of improving the design were identified. We are confident that the problem with the motor will be resolved and look forward to our next opportunity for deployment and to extension of the time span for *in situ* chemical monitoring.

In conclusion, we have presented the preliminary results of our ongoing studies to understand the submarine hydrothermal venting system at the ASHES site on Axial Volcano and its contribution to the integrated venting source strength of the Juan de Fuca ridgecrest. The vent fluid data for this site are unique with respect to the low Cl values encountered at a single anomalous vent within a small vent field. The likelihood that phase separation is responsible for the anomalous vent fluid

## Standard and Reagent Reservoirs

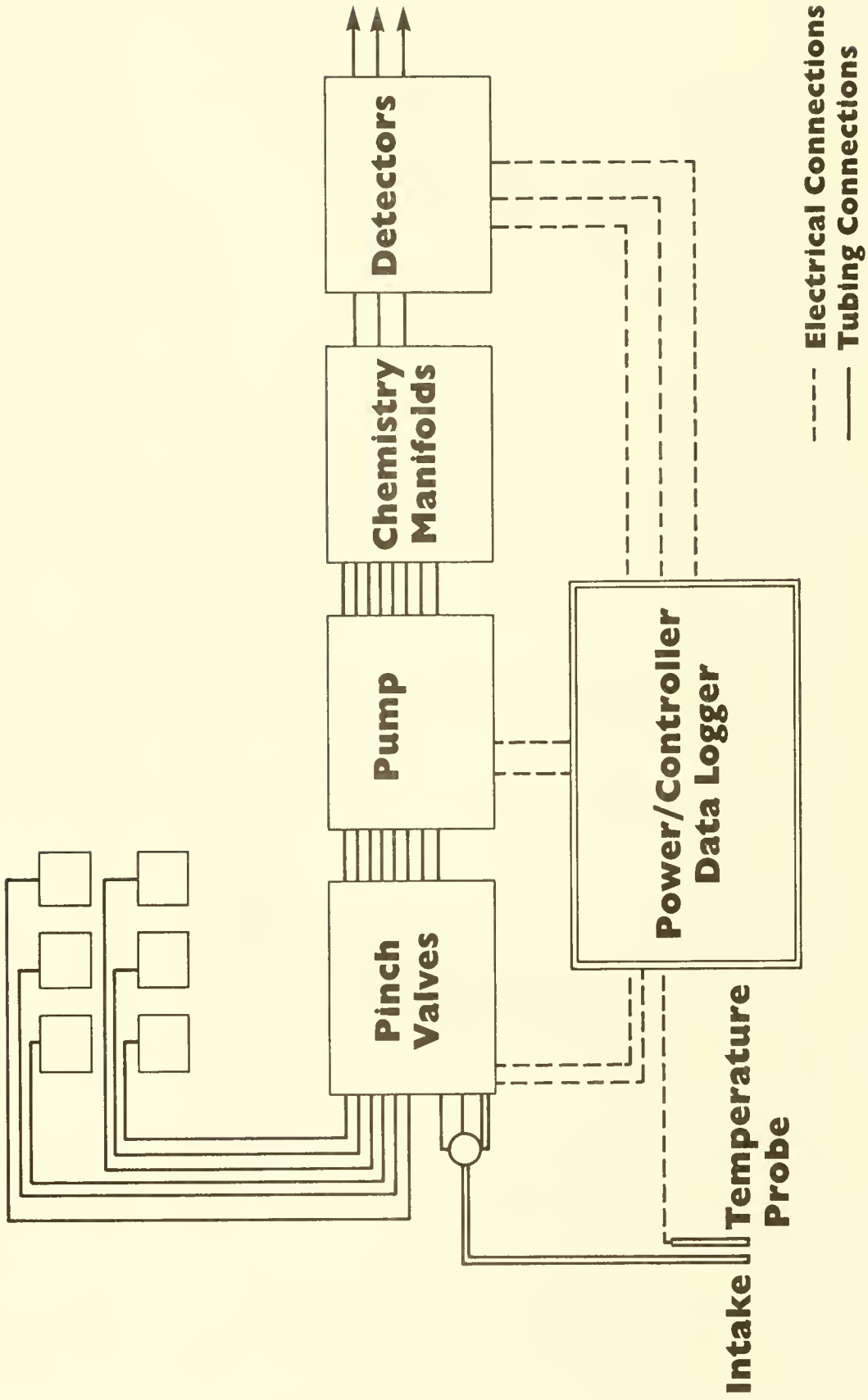


Figure 8. Block diagram of the major components of the *In Situ* Chemical Analyzer (ISCA).

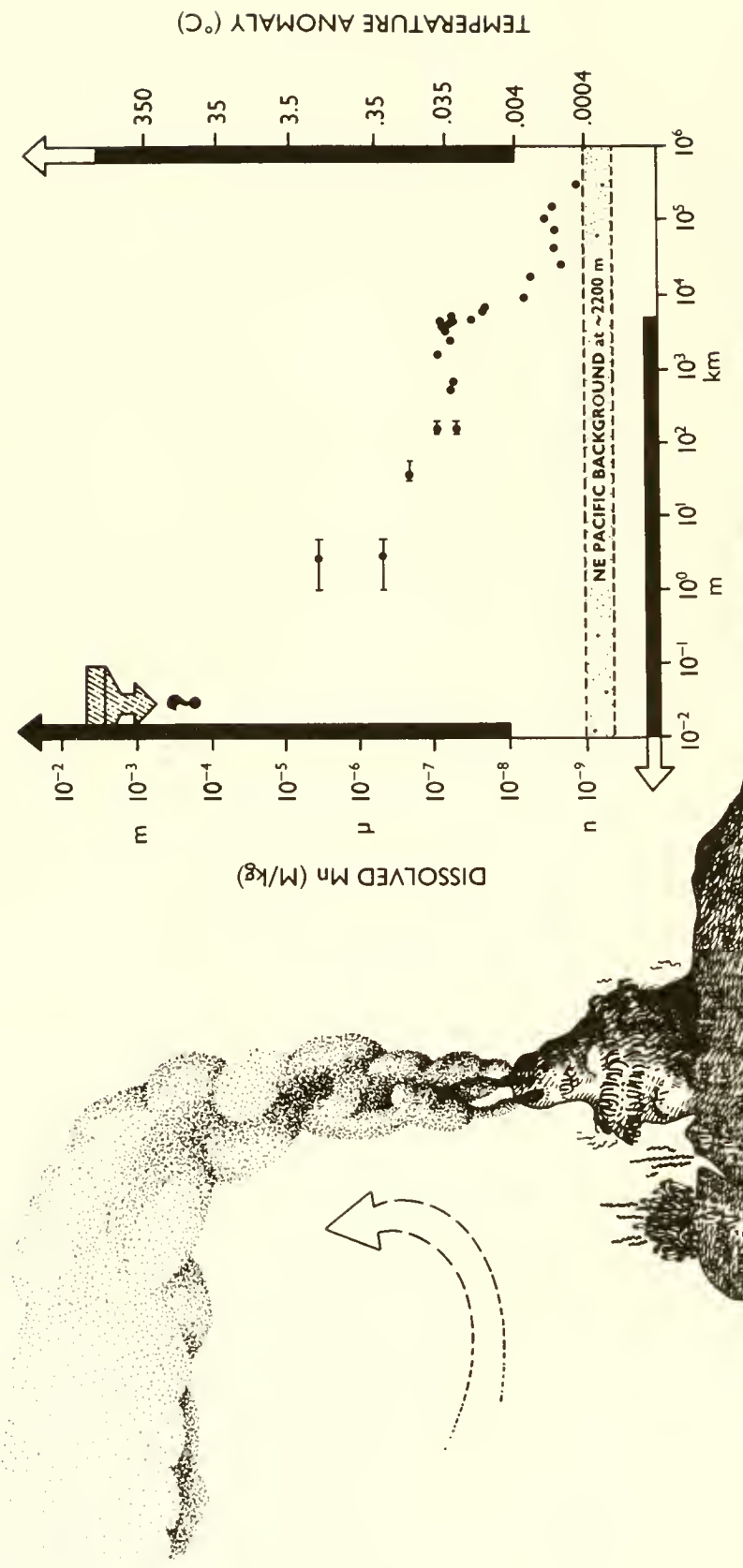


Figure 9. An example (right panel), using the major hydrothermal fluid component dissolved Mn, data shown here from a transect westward of the Southern Juan de Fuca Ridge) of the elemental concentration, temperature, spatial, and temporal scales over which studies of the post-venting portion of hydrothermal systems are conducted. The heavy bars along the axes delimit the venting fluid-proximal plume regions discussed in the text. Displayed in the left panel are cartoon representations of system components: vent orifice (crack in basalt, ubiquitous "diffuse" flow, and high-temperature chimneys), buoyant plume, neutrally buoyant plume, and ambient water motion (including entrainment).

chemistry is suggested. New sampling methods have been formulated, and the instrumentation required to implement them tested. A rationale for submersible-based vent fluid sampling within the overall context of the VENTS Program has been explained. Vent fluids occupy an important part of the elemental concentration, temperature, spatial, and temporal scales (Fig. 9) over which hydrothermal effects investigations are made. The integration of the results obtained from throughout these scales is required to test the VENTS hypothesis.

#### ACKNOWLEDGMENTS

We thank the officers and crews of R/V Pandora II AND R/V Atlantis II, and the Pisces IV and Alvin pilots for valuable guidance at sea. Marvin Lilley, Barrie Walden, Patrick McLain and Dennis Holzer contributed significantly to the design, fabrication, and testing of the SIS<sup>3</sup>. Ken Johnson and Susie Kalhorn assisted with the design and fabrication of the ISCA. Kevin Roe performed the determinations of Mn and Fe in the vent fluids. Karen Thornberry assisted with the <sup>3</sup>He determinations.

#### LITERATURE CITED

ASHES Expedition. 1986. PISCES submersible exploration of a high-temperature vent field in the caldera of Axial Volcano, Juan de Fuca Ridge. EOS, Vol. 67, No. 44, p. 1027.

Baker, E. T., and G. J. Massoth. 1986. Hydrothermal plume measurements: a regional perspective. Science, Vol. 234, pp. 980-982.

Baker, E. T., and G. J. Massoth. 1987. Characteristics of hydrothermal plumes from two vent fields on the Juan de Fuca Ridge, northeast Pacific Ocean. Earth Planet. Sci. Lett., Vol. 85, pp. 59-73.

Baker, E. T., G. J. Massoth, and R. A. Feely. 1987a. Cataclysmic hydrothermal venting on the Juan de Fuca Ridge. Nature, Vol. 329, No. 6135, pp. 149-151.

Baker, E. T., G. J. Massoth, R. W. Collier, J. H. Trefrey, D. Kadko, T. A. Nelson, P. A. Rona, and J. E. Lupton. 1987b. Evidence for high-temperature hydrothermal venting on the Gorda Ridge, northeast Pacific Ocean. Deep Sea Res., Vol. 34, No. 8, pp. 1461-1476.

Baker, E. T., R. A. Feely, and G. J. Massoth. 1987c. Hydrographic and chemical survey of hydrothermal plumes of the Middle Valley vent field, Juan de Fuca Ridge. EOS, Vol. 68, No. 44, p. 1325.

Bischoff, J. L., A. S. Radtke, and R. J. Rosenbauer. 1981. Hydrothermal alteration of graywacke by brine and seawater: Roles of alteration and chloride complexing on metal solubilization at 200° and 350°C. Econ. Geol., Vol. 76, pp. 659-676.

Bischoff, J. L., and R. J. Rosenbauer. 1984. The critical point and two-phase boundary of seawater, 200-500°C. Earth Planet. Sci. Lett., Vol. 68, pp. 172-180.

Bischoff, J. L., and R. J. Rosenbauer. 1987. Phase separation in seafloor geothermal systems: An experimental study of the effects on metal transport. Am. Jour. Sci., Vol. 287, pp. 953-978.

Bowers, T. S., K. L. Von Damm, and J. M. Edmond. 1985. Chemical evolution of mid-ocean ridge hot springs. Geochim. Cosmochim. Acta, Vol. 49, No. 11, pp. 2239-2252.

Bowers, T. S., A. C. Campbell, C. I. Measures, A. J. Spivack, M. Khadem, and J. M. Edmonds. 1988. Chemical controls on the composition of vent fluids at 11°-13°N and 21°N, East Pacific Rise. J. Geophys. Res., Vol. 93, No. 5, pp. 4522-4536.

Campbell, A. C., T. S. Bowers, C. I. Measures, K. K. Falkner, M. Khadem, and J. E. Edmonds. 1988. A time series of vent fluid compositions from 21°N, EPR (1979, 1981, 1985) and the Guaymas Basin, Gulf of California (1982, 1985). J. Geophys. Res., Vol. 93, No. 5, pp. 4537-4549.

Canadian American Seamount Expedition. 1985. Hydrothermal vents on an axis seamount of the Juan de Fuca Ridge. Nature, Vol. 313, No. 5999, pp. 212-214.

Cline, J.D. 1969. Spectrophotometric determination of hydrogen sulfide in natural waters. Limnol. Oceanogr., Vol. 14, No. 3, pp. 454-458.

Craig, H., J. A. Welhan, K. Kim, R. Poreda, and J. E. Lupton. 1980. Geochemical studies of the 21°N EPR hydrothermal fields. EOS, Vol. 61, No. 46, p. 992.

Dyrssen, D. 1965. A Gran titration of sea water on board Sagitta. Acta Chem. Scand., Vol. 19, No. 5, p. 1265.

Edmond, J. M., C. Measures, R. E. McDuff, L. H. Chan, R. Collier, B. Grant, L. I. Gordon and J. B. Corliss. 1979a. Ridge crest hydrothermal activity and the balances of the major and minor elements in the ocean: the Galapagos data. Earth Planet. Sci., Vol. 46, pp. 1-18.

Edmond, J. M., C. Measures, B. Mangum, B. Grant, F. R. Sclater, R. Collier, A. Hudson, L. I. Gordon, and J. B. Corliss. 1979b. On the formation of metal-rich deposits at ridge crests. Earth Planet. Sci. Lett., Vol. 46, pp. 19-30.

Edmond, J. M., A. C. Campbell, M. R. Palmer, and G. P. Klinkhammer. 1986. Preliminary report on the chemistry of hydrothermal fluids from the Mid-Atlantic Ridge (abstract). EOS, Vol. 67, No. 44, p. 1021.

Embley, R. W., S. R. Hammond, and K. Murphy. 1988. The caldera of Axial Volcano remote sensing and submersible studies of a hydrothermally active submarine volcano. In: Michael P. De Luca and Ivar Babb (eds.), Global Venting, Midwater, and Benthic Ecological Processes. National Undersea Research Program Research Report 88-4, pp. 61-70. Rockville, Md., NOAA Undersea Research Program.

Feely, R. A., M. Lewison, G. J. Massoth, G. Robert-Baldo, J. W. Lavelle, R. H. Byrne, K. L. Von Damm, and H. C. Curl, Jr. 1987. Composition and dissolution of black smoker particulates from active vents on the Juan de Fuca Ridge. J. Geophys. Res., Vol. 92, No. 11, pp. 11,347-11,363.

Gieskes, J. M. 1974. Interstitial water studies, Leg 25. In: E. S. W. Simpson, R. Schlich, et al., Initial Reports of the Deep Sea Drilling Project, Vol. 25, pp. 361-394. Washington, D.C., U.S. Government Printing Office.

Janecky, D. R., and W. E. Seyfried, Jr. 1984. Formation of massive sulfide deposits on oceanic ridge crests: Incremental reaction models for mixing between hydrothermal solutions and seawater. Geochim. Cosmochim. Acta, Vol. 48, No. 12, pp. 2723-2738.

Johnson, K. S., R. L. Petty, and J. Thomsen. 1985. Flow-injection analyses for seawater micronutrients. In: A. Zirino, (ed.), Mapping Strategies in Chemical Oceanography. American Chemical Society, Washington, D.C., pp. 7-30.

Johnson, K. S., C. L. Beehler, and C. M. Sakamoto-Arnold. 1986a. A submersible flow analysis system. Anal. Chim. Acta, Vol. 179, pp. 245-257.

Johnson, K. S., C. L. Beehler, C. M. Sakamoto-Arnold, and J. J. Childress. 1986b. In situ measurements of chemical distributions in a deep-sea hydrothermal vent field. Science, Vol. 231, pp. 1139-1141.

Kennedy, B. M. 1985. Noble gases in vent fluids from the southern Juan de Fuca Ridge. EOS, Vol. 66, No. 46, p. 929.

Lupton, J. E., G. P. Klinkhammer, W. R. Normark, R. Haymon, K. C. MacDonald, R. F. Weiss and H. Craig. 1980. Helium-3 and manganese at the 21°N East Pacific Rise hydrothermal site. Earth Planet. Sci. Lett., Vol. 50, pp. 115-127.

Lupton, J. E., J. R. Delaney, H. P. Johnson, and M. K. Tivey. 1985. Entrainment and vertical transport of deep-ocean water by buoyant hydrothermal plumes. Nature, Vol. 316, No. 6029, pp. 621-623.

Massoth, G. J., R. A. Feely and H. C. Curl, Jr. 1982. Hydrothermal manganese over the Juan de Fuca and Gorda Ridges (abstract). EOS, Vol. 63, No. 45, p. 999.

Massoth, G. J., E. T. Baker, R. A. Feely, and H. C. Curl, Jr. 1984. Hydrothermal signals away from the southern Juan de Fuca Ridge. EOS, Vol. 65, No. 45, p. 1112.

Massoth, G. J., E. T. Baker, J. P. Cowen, K. K. Roe, and P. Y. Appriou. 1985. The chemical diversity of Juan de Fuca Ridge hydrothermal plumes. EOS, Vol. 66, No. 46, p. 929.

McConachy, T. F., and S. D. Scott. 1987. Real-time mapping of hydrothermal plumes over southern Explorer Ridge, NE Pacific Ocean. Marine Mining, Vol. 6, pp. 181-204.

McDuff, R. E. 1985. The chemistry of interstitial waters, Deep Sea Drilling Project, Leg 86. In: G. R. Heath, L. H. Burckle, et al., Initial Reports of the Deep Sea Drilling Project, Vol. 86, pp. 675-687. Washington, D.C., U.S. Government Printing Office.

MERGE Group. 1984. Regional setting and local character of hydrothermal field/sulfide deposit on the Endeavour segment of the Juan de Fuca Ridge (abstract). EOS, Vol. 65, No. 45, p. 1111.

Michard, G., F. Albarede, A. Michard, J. F. Minster, J. L. Charlou, and N. Tan. 1984. Chemistry of solutions from the 13°N East Pacific Rise site. Earth Planet. Sci. Lett., Vol. 67, pp. 297-307.

Seyfried, W. E., Jr. and D. R. Janecky. 1985. Heavy metal and sulfur transport during subcritical and supercritical hydrothermal alteration of basalt: Influence of fluid pressure and basalt composition and crystallinity. Geochim. Cosmochim. Acta, Vol. 49, No. 12, pp. 2545-2560.

Thomsen, J., K. S. Johnson, and R. L. Petty. 1983. Determination of reactive silicate in seawater by flow injection analysis. Anal. Chem., Vol. 55, No. 14, pp. 2378-2382.

Von Damm, K. L. 1983. Chemistry of submarine hydrothermal solutions at 21°N, East Pacific Rise and Guaymas Basin, Gulf of California. Ph.D Thesis, MIT. 240 pp.

Von Damm, K. L., J. M. Edmond, C. I. Measures, B. Walden, and R. F. Weiss. 1985. Chemistry of submarine hydrothermal solutions at 21°N, East Pacific Rise. Geochim. Cosmochim. Acta, Vol. 49, No. 11, pp. 2197-2220.

Von Damm, K. L., and J. L. Bischoff. 1987. Chemistry of hydrothermal solutions from the southern Juan de Fuca Ridge. Geophys. Res., Vol. 92, No. 11, pp. 11,334-11,346.

Von Damm, K. L. 1988. Systematics of and postulated controls on submarine hydrothermal solution chemistry. J. Geophys. Res., Vol. 93, No. 5, pp. 4551-4561.

Zirino, A. 1975. Measurement of the apparent pH of seawater with a combination microelectrode. Limnol. Oceanogr., Vol. 20, No. 4, pp. 654-657.



THE CALDERA OF AXIAL VOLCANO--REMOTE SENSING AND SUBMERSIBLE STUDIES OF A HYDROTHERMALLY ACTIVE SUBMARINE VOLCANO

R. W. Embley, S. R. Hammond and K. Murphy  
National Oceanic and Atmospheric Administration  
Pacific Marine Environmental Laboratory  
Hatfield Marine Science Center  
Newport, OR 97365

INTRODUCTION

The establishment of the NOAA VENTS program in 1984 provided a focus for several NOAA research groups that had been working on aspects of ocean hydrothermal systems. The evolution of the program during the past few years has led to a focus on the vent systems of the northeast Pacific spreading centers and their effect on the chemistry of the northeast Pacific Ocean. Using the existing data base (as of 1984) consisting of Sea Beam bathymetry, reconnaissance side-scan sonar, bottom photography, water column studies and Alvin dives, a program of systematic geologic and geochemical mapping of vent sites was begun in 1985. The ultimate goal is to understand the hydrothermal "source function" of the ridge system in terms of geographic and temporal variability and to relate this function to the near-, mid-, and far-field water column hydrothermal effects.

The first site chosen for this systematic approach was Axial Volcano (Fig. 1). This was selected as the initial site because there was a need for a shallow, relatively small vent area to use as a seafloor laboratory to test hypotheses concerning: (1) chemical and physical variability, (2) particulate fallout models, and (3) near-field plume dynamics. The shallow depth of the vent field (1545 m) is within range of both Fishes class submersibles and Alvin. Its small size (suspected on the basis of reconnaissance Alvin dives in 1984) ensured a manageable problem in terms of seafloor instrumentation, flux calculations, etc.

Axial volcano is the youngest volcanic edifice in the Cobb-Eikelberg seamount chain which extends from the central segment of the Juan de Fuca Ridge several hundred kilometers into the Pacific Plate (Fig. 1). The volcano and its caldera were initially mapped with the Sea Beam sonar during 1981 as part of NOAA's effort to discover and map active hydrothermal venting sites along the entire Juan de Fuca Ridge system (Malahoff, 1985, Crane et al., 1985). The Sea Beam bathymetry of the central Juan de Fuca Ridge shows that the Axial Volcano Edifice (volcano plus rift zones or AVE) is a morphologically complex structure that is superimposed on the generally linear 020°N seafloor-spreading fabric of the Juan de Fuca Ridge (Fig. 2). The volcano's major features include: (1) the central shoal area (1450 m minimum

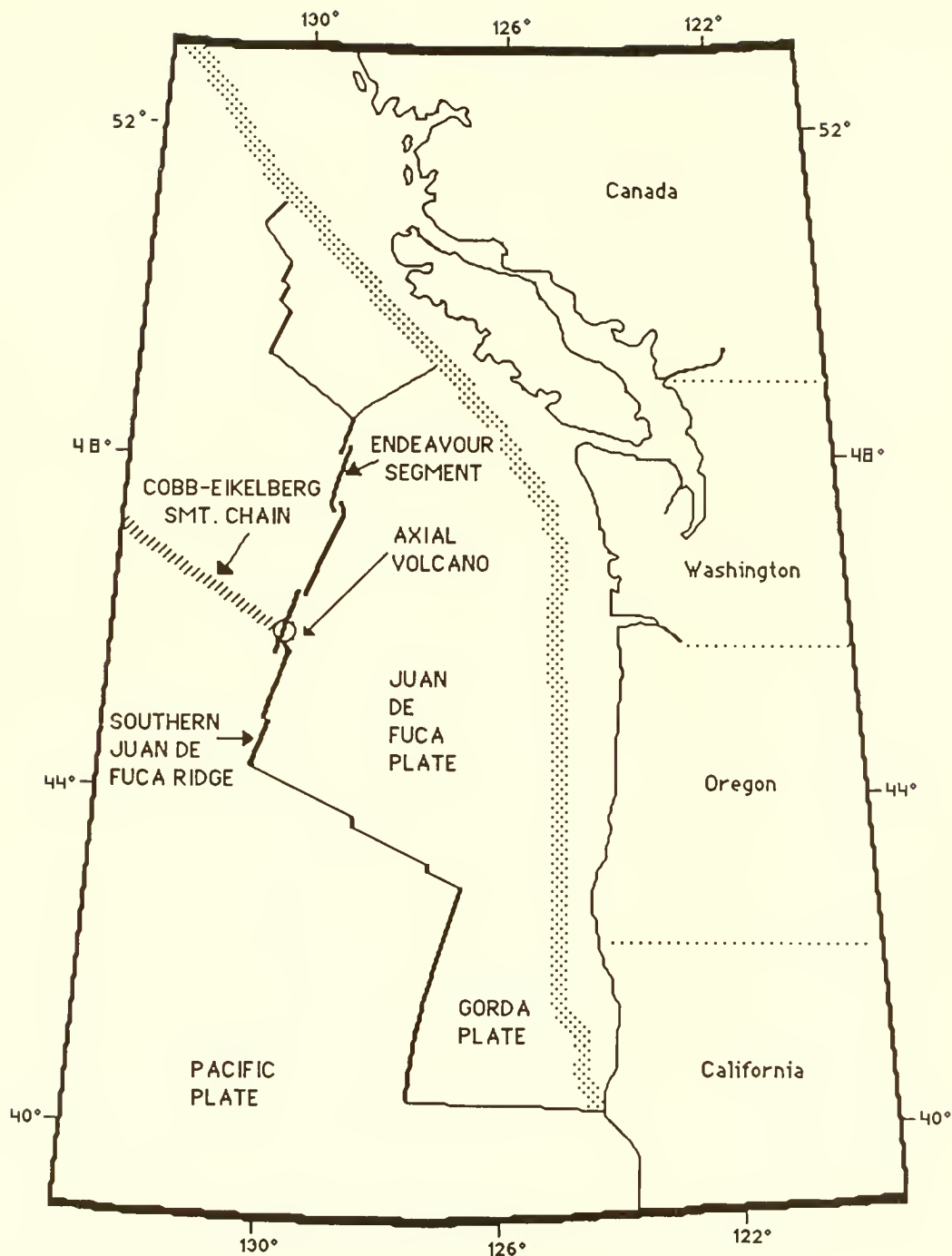


Figure 1. Location map of Northeast Pacific.

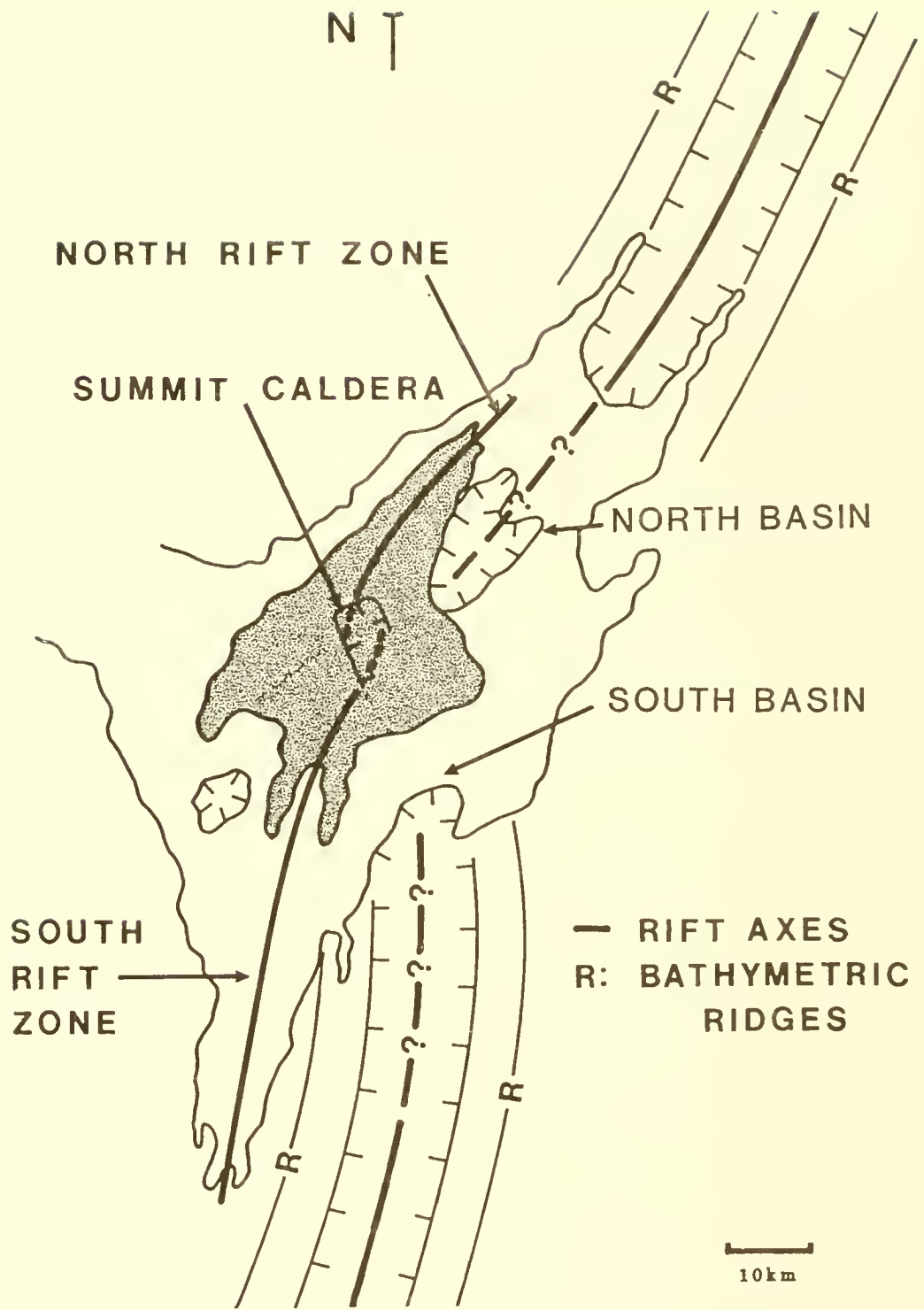


Figure 2. Physiographic sketch map of Central Juan de Fuca and Axial Volcano. North Basin is also known as Helium Basin.

depth), (2) two long, linear highs extending northeast and south from the summit area, (3) several smaller ridges extending along similar azimuths and (4) several closed and open basins indenting the edifice on the north and south sides. The total relief of the volcanic edifice is about 700 meters relative to the mean depth of the seafloor spreading axis to the north and south.

The summit of Axial Volcano is marked by an unusual rectangular shaped 3 km x 8 km caldera that lies in an apparent offset region between the two rift zones (Figs. 2 and 3). The caldera and the proximal portions of the north and south rift zones have been extensively surveyed during NOAA cruises in 1985-86 by Sea Marc I sidescan (5 km, 2 km and 1 km swath widths) and deep-sea cameras navigated within a long-term transponder net. The primary focus of the surveys was to determine the geologic setting of the hydrothermal vent fields within the caldera. The first submersible expedition to the volcano in 1983 discovered warm water vents with associated vent-specific animal communities in the northern end of the caldera (CASM, 1985). In 1984, as part of NOAA's Alvin dive program to investigate suspected active hydrothermal sites, four dives were made in the caldera along the southern wall. During one of these dives (1411), an active high-temperature vent was briefly observed and sampled. These vent fields have been a primary focal point of submersible studies undertaken by the NOAA VENTS program with support from the Office of Undersea Research in 1986 and 1987.

#### METHODS

In anticipation of more submersible dives in 1986 and beyond, the 1985 field season was devoted to beginning a comprehensive geological survey of the caldera and vicinity. In order to facilitate the mapping effort and to ensure accurate intercalibration of the various data sets, a long-baseline transponder net was established and has been maintained to the present. The two primary data sets obtained during the 1985 field season were digital side-scan sonar and bottom photography. This combination of precision navigation, side-scan sonar and bottom photography has enabled us to begin to construct an accurate representation of the caldera and rift zone geology.

A Sea Marc IA, 30 kHz digital side-scan sonar was used in 1985, 1986 and 1987 to collect data from the caldera and vicinity as well as the south rift zone and southern Juan de Fuca Ridge. This system has an adjustable scan width ranging from 5 km to 0.5 km. The resolution of the digital data is inversely proportional to the scan width. For example, the pixel size of a 5 km and a 0.5 km scan is, respectively, 2.5 m and 0.25 m. The higher resolution scans were used in the vicinity of the vent fields. The side-scan sonar system has a built-in processor that corrects the data for both slant range distortion and speed. Post-processing software assigns each pixel an x-y value relative

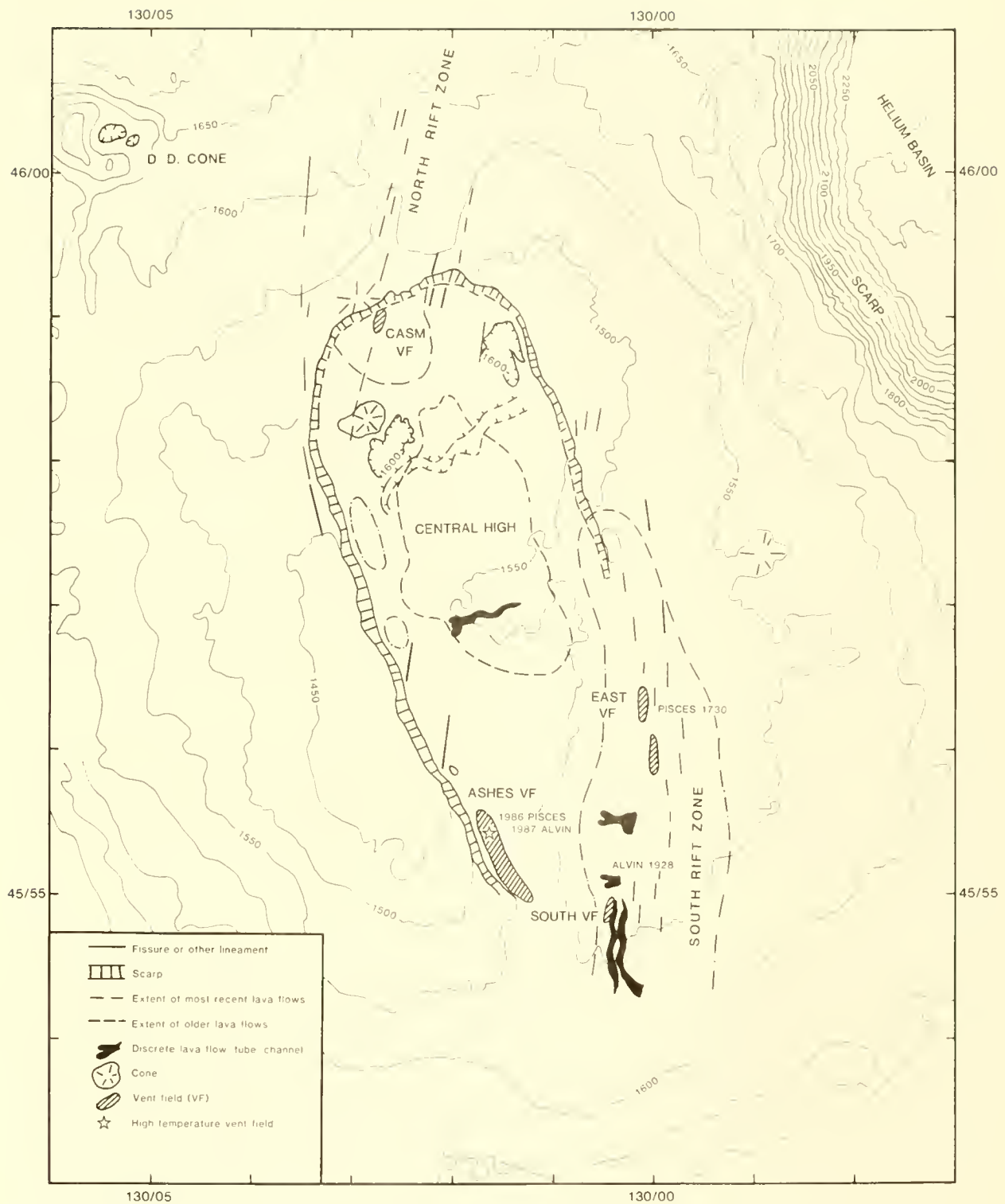


Figure 3. Sea Beam bathymetry (m) of summit of Axial Volcano, showing major geologic features.

to the transponder grid. In addition, various image enhancement schemes are presently being applied to the data at a special image processing facility established at the Newport lab.

The side-scan sonar provides an image of seafloor texture derived from acoustic backscatter. However, the relationship of the backscatter to the seafloor geology can only be determined by direct observation, either from towed cameras or from submersibles. During the 1985 and subsequent field seasons, more than 27,000 35 mm photographs of the seafloor were taken in and near the caldera. The photographic coverage in the vicinity of the ASHES vent field is shown (Fig. 4). To integrate and manipulate the photographic data, a data base scheme was developed that allows key parameters (such as lava type, hydrothermal indicators etc.) to be plotted along the track. Two sets of data can be plotted along track at its actual scaled size (see Fox et al., 1988 for details). Superimposition of these data on the sidescan image allows identification of geological associations with the major backscatter patterns.

In 1986 and 1987, 28 submersible dives were made in Axial Caldera. Of these 28 dives, 24 were located in and around the southwest vent field, primarily in the ASHES high temperature field, 1 dive revisited the CASM area, and 3 dives mapped and sampled the south rift vent fields. Some of the methods and initial results from the water chemistry program (the major emphasis of the dives) are reported in Massoth et al. (this volume). Other major experiments and data collected on these dives include: (1) a time lapse camera deployed for 28 days in 1986 (Johnson and Tunnicliffe, 1986) and for a year beginning in September, 1987, (2) sulfide samples, (3) basalt collections, (4) biological collection, (5) photographic and video surveys, and (6) near-bottom heat-flow surveys.

## RESULTS

The caldera is defined on three sides by a steep wall with up to 150 m relief. The caldera wall generally marks a sharp backscatter boundary on the side-scan records; a low amplitude return characterizes the more heavily sedimented area outside the caldera. Sidescan, camera, and submersible observation show that the wall is a fault structure with extensive outcrop of truncated lava flows. Talus piles have developed in some places along the base of the wall, whereas in other places lavas directly abut the wall. These relationships reflect an interplay between mass wasting and faulting along the wall as well as volcanic episodes within the caldera. The interior of the caldera (Fig. 3) is covered by lava flows ranging from young, glassy and/or thinly sedimented jumbled sheet and lobate flows, which characterize the central high of the caldera. The side-scan sonar records resolve differences in backscatter between at least three types of lava

## CAMERA TOW TRACKLINE COVERAGE

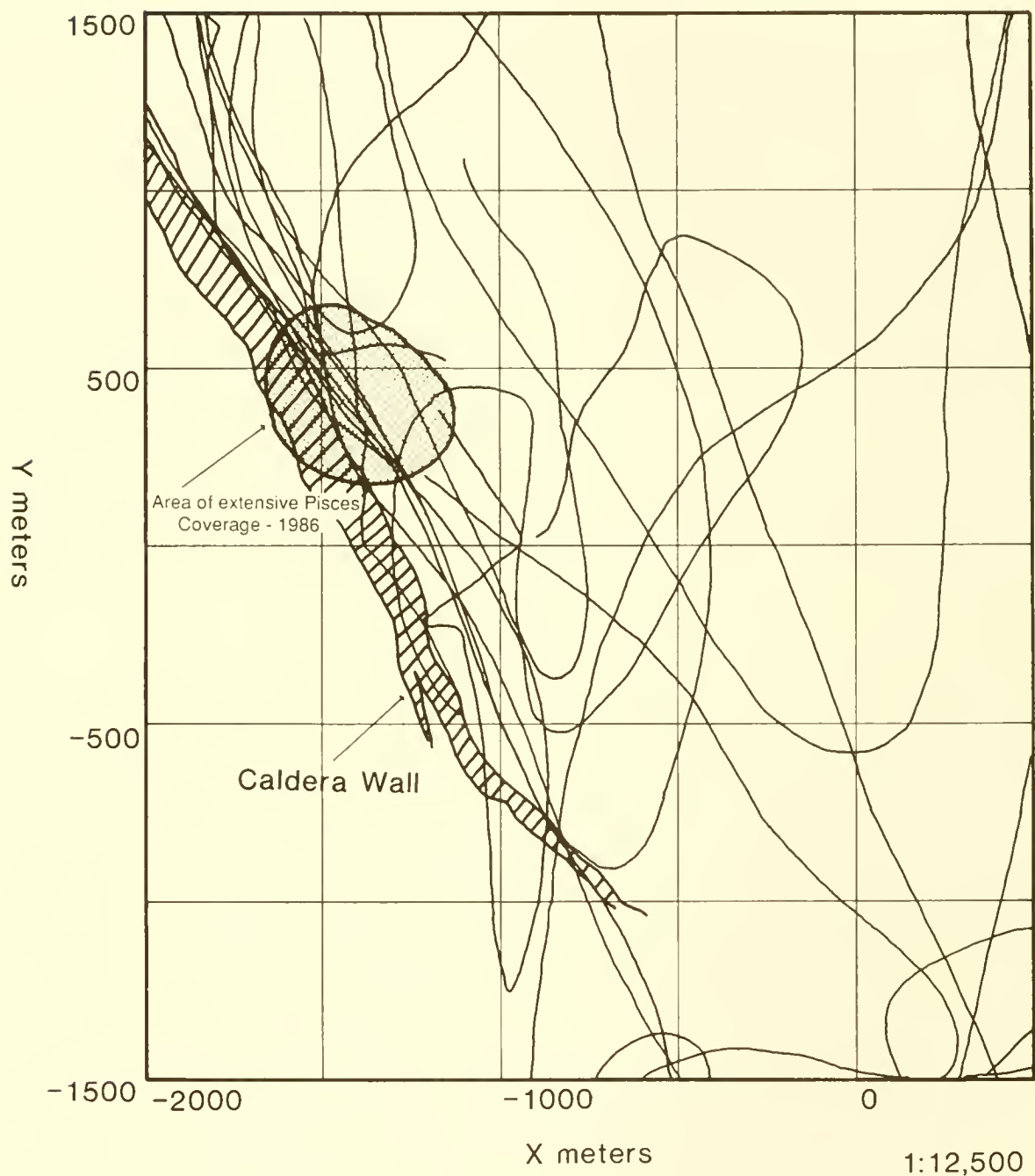


Figure 4. Transponder maps of ASHES vent field area showing coverage by towed cameras and submersible dives.

flows (ropy sheet, jumbled sheet, and lobate) but resolution of age relationships between lava flows is more difficult.

Within the caldera, areas of lowest amplitude return signal (not including shadow zones caused by volcanic topography) are usually associated with lava pond characterized by ropy sheet flows. The relatively low microrelief of these lavas ( $<0.25$  m) and associated evenly distributed sediments gives rise to, respectively, low backscatter and high acoustic absorption relative to the other lava types. The highest signal return (excluding reflections off tectonic scarps or flow fronts) is associated with the jumbled sheet flows. The presence of numerous sharp ridges and the absence of any continuous sediment cover provides a combination of high microrelief (0.5 m - 1.0 m) and low acoustic absorption. The lobate flows are associated with intermediate return signal strength but tend to grade into the other two types. Pillow lavas are not common in the caldera, but where they do occur (predominantly in the middle of the caldera) they are associated with either discrete volcanic cones (northwestern caldera) or "lumpy" appearing forms. Since extensive fields of pillow lavas tend to be associated with larger edifices, their appearance on the sidescan is not strictly comparable with the other lava types, which occur in flatter areas.

The hydrothermal vents are associated with primary structural features of the caldera, i.e., the rift zones and fault-bounded wall. The low-temperature vent areas are characterized by a diverse vent fauna and patches of silica/nontronite exhalite. The CASM vent field (north end of caldera) is primarily located within a discrete rift zone, although some extinct sulfide chimneys occur about 100 m to the east of the rift zone. The ASHES vent field, which is probably structurally controlled by fracturing associated with the base of the southwestern caldera wall, consists of a 1000 m by 200 m wide area of semicontinuous low temperature ( $<35^{\circ}\text{C}$  water) exhalite and patchy vent fauna (Fig. 5). At the northern end of the vent field there is a 100 m-diameter area characterized by high-temperature venting. This was the site of comprehensive interdisciplinary studies using the Pisces IV submersible in 1986 and Alvin in 1987. Active low-temperature venting also occurs on the wall adjacent to the high-temperature area. All of the high-temperature (both active and extinct) vents within the caldera appear to be immature, that is, there are no basal sulfide mounds present; the chimneys protrude directly from the basalt flows. Water temperatures of up to  $330^{\circ}\text{C}$  were measured in clear fluids exiting from chimney structures apparently made predominantly of anhydrite.

Pervasive low-temperature venting was also discovered along the southeastern side of the caldera (Fig. 3). These vents were initially found by towed-camera surveys in 1985 and 1986 and were

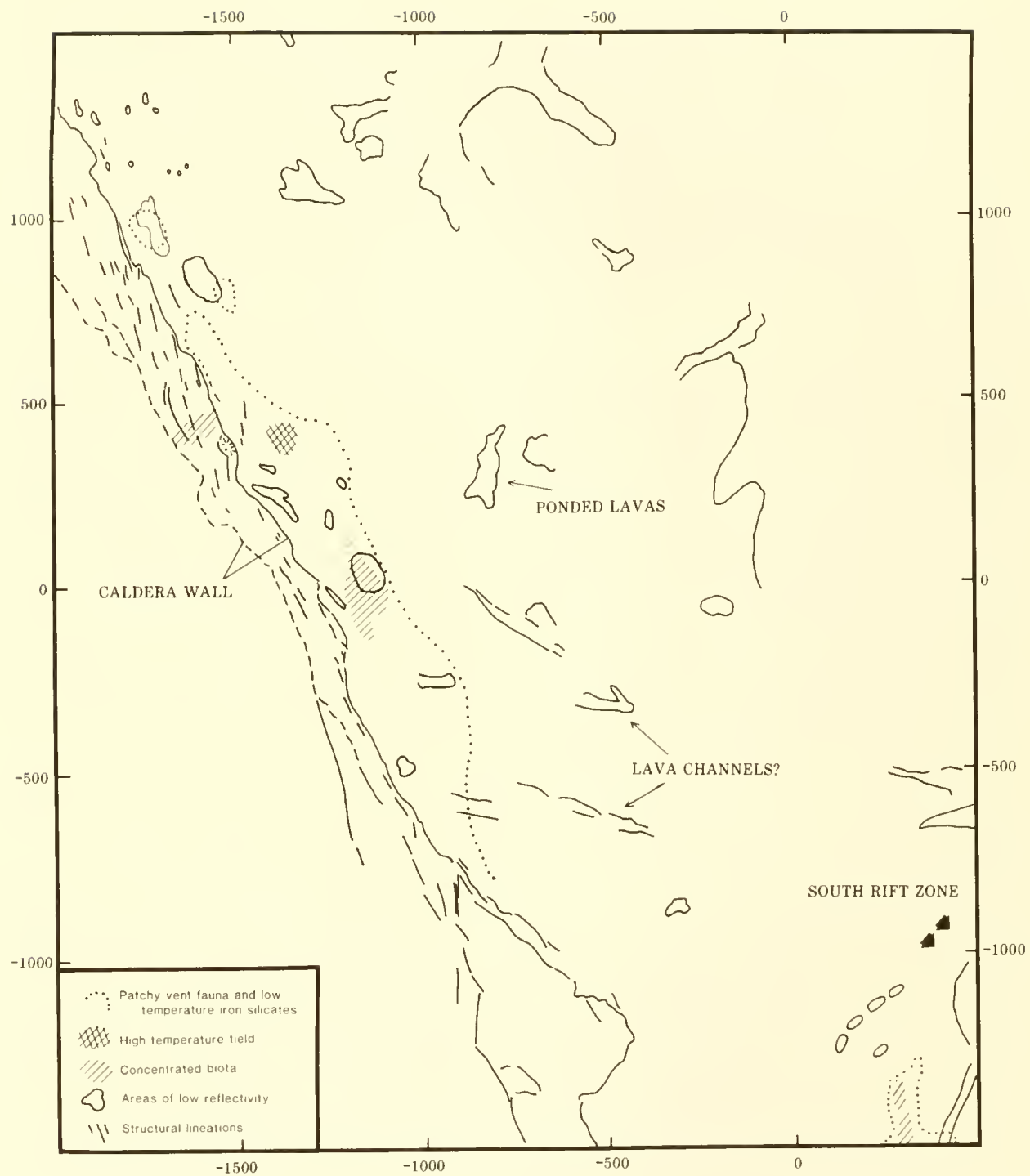


Figure 5. Map of southwestern caldera showing major sidescan backscatter targets and the locations of vent areas. Scale is in meters (transponder coordinates).

visited by Pisces IV (dive 1730) and Alvin (dives 1925 and 1928). The vents, usually associated with small collapses, cracks and boundaries between the flow lobes, are characterized by widespread bacterial colonies and isolated colonies of larger animals. Although no high-temperature venting (maximum measured temperature was 25°C) was observed during these dives, an isolated 1 m pyritic chimney recovered on Pisces dive 1730 suggests that there have been localized, short-lived episodes of high-temperature venting within this field.

#### DISCUSSION AND CONCLUSIONS

An understanding of the volcanic and hydrothermal processes occurring in and around the caldera are important to developing a better model of the dynamics of submarine volcano evolution and concomitant hydrothermalism. Some of the major questions relating to the interplay between volcanic and hydrothermal processes may be addressed at Axial Volcano. For example, the lack of large high-temperature vent fields (and consequent lack of a significant plume) is probably due to some combination of factors related to the frequency of volcanism, present stage of the volcano-tectonic cycle, and the physics and chemistry of the hydrothermal process active at the water depth and environment of Axial Volcano. Because of its shallow depth (and consequent accessibility to both Alvin and Pisces submersibles) and its manageable size, the ASHES vent field is becoming a laboratory for developing better quantitative models of near-field vent processes and testing vent monitoring devices. Axial Volcano is a critical seafloor feature for study both of the evolution of a still active (volcanically and hydrothermally) submarine volcano and in its role in the recent evolution of the Juan de Fuca Ridge.

#### LITERATURE CITED

CASM, 1985. Hydrothermal vents on an axial seamount on the Juan de Fuca Ridge. Nature, Vol. 313, No. 5999, pp. 212-214.

Crane, F. Aikman, R. W. Embley, S. Hammond and A. Malahoff, 1985. The distribution of geothermal fields on the Juan de Fuca Ridge. J. Geophys. Res., Vol. 90, No. B1, pp. 727-744.

Fox, C. G., K. M. Murphy and R. W. Embley, 1987. Automated display and statistical analysis of interpreted deep-sea bottom photographs. Mar. Geol., Vol. 78, pp. 199-216.

Malahoff, A., 1985. Hydrothermal vents and polymetallic sulfides of the Galapagos and Gorda/Juan de Fuca Ridge systems and of submarine volcanos. Bull. Biol. Soc. of Washington, No. 6, pp. 19-42.

SEABEAM BACKSCATTER ANALYSIS APPLIED TO THE  
CLASSIFICATION OF DEEP-SEA VOLCANIC TERRAINS

Christopher G. Fox and Marijke van Heeswijk

National Oceanic and Atmospheric Administration  
Pacific Marine Environmental Laboratory  
Hatfield Marine Science Center  
Newport, OR 97365

ABSTRACT

Hull-mounted sonar systems, such as Sea Beam, are typically used for mapping the bathymetry of the deep-sea floor. The same digital information that is used for the measurement of depth can be evaluated for the backscattering properties of the seafloor. The unique morphologies and petrologies of volcanic and hydrothermal terrains may produce identifiable backscatter signatures. The Alvin support vessel Atlantis II is equipped for digitally acquiring Sea Beam backscatter energy traces, allowing sonar remote sensing and submersible exploration to be performed in tandem. An experiment funded by the National Undersea Research Program, at Axial Seamount, Juan de Fuca Ridge, has produced the most extensive data set to date from a known hydrothermal area, and these data are being calibrated using the large groundtruth data base collected by NOAA's VENTS research program.

INTRODUCTION

Hull-mounted sonar sounding systems have been used since the 1920's for mapping the bathymetry of the deep-sea floor. The technique involves projecting monochromatic sound (usually 12 kHz in modern systems) directly downward from the ship and recording the two-way travel time of the sound as it echoes from the seafloor. By assuming a mean sound velocity for the water column, the depth can be inferred. Since the 1960's, digital systems have been available which allow both a narrow beam pattern to be generated, and the automated acquisition of the returned acoustic energy to be processed via computer. In the 1970's, a multibeam sounding system (Sea Beam) was made commercially available. This system allows a wide swath of individual soundings to be collected simultaneously. Tyce (1986) describes many of the various sonar instruments currently available with a historical perspective of their development.

In conducting a typical Sea Beam bathymetric survey, the returning acoustic pulse (backscatter echo) is digitized and automatically analyzed to determine the arrival time of the maximum (bottom) return. Following this determination for each beam, the backscatter information is normally discarded and the

subsequent return recorded. Although this normal operation is adequate for bathymetric mapping, substantial insight into the physical properties and microtopography of the bottom can be derived from the interpretation of the character of the return pulse.

#### SYSTEM DESCRIPTION

Sea Beam is a multibeam sounding system developed and manufactured by General Instruments Corporation. The geometry of the system is described by Glenn (1970) and is illustrated (Fig. 1). The hull mounted array uses 20 acoustic projectors mounted along ship and 40 receiving hydrophones mounted athwartship to perform 16 beams of 2-2/3' solid angle dimension and spacing. The 54' range of the beam pattern allows ensonification of the seafloor for a width equal to approximately 75 percent of the water depth. The pings for the current experiment were transmitted at constant time intervals of 6 or 12 seconds. Throughout the ping cycle, sensors are interrogated to record the ship's attitude (roll, pitch and yaw). All of the information is transferred to the shipboard processing computer for analysis.

The backscatter recording system, developed and described by deMoustier (1986), accesses this information for recording to magnetic tape. The backscatter envelope from each of the 16 beams is digitized and recorded with 512 samples at 2 millisecond intervals centered on a window about the bottom return. During post-processing, numerous corrections must be performed on this recorded data. A time varying gain function is applied to account for spherical spreading of the acoustic wave front. The Sea Beam hardware assures that the outgoing pulse is near vertical over the relatively short duration (7 milliseconds) of projection. However, the ship's roll angle can vary substantially during the receiving cycle, and must be modelled and compensated. The corrected backscatter data from each beam, when combined with ship's navigation, become the fundamental information for sea-floor classification.

#### GENERAL PRINCIPLES

The physics of acoustic bottom interaction is a complex and much studied subject and is described in some detail by Urick (1983), Clay and Medwin (1977), and others. Research is currently underway to study the physics of interaction of Sea Beam with the seafloor (Robert C. Tyce, personal communication, 1987). The principles discussed here are greatly simplified, however as will be shown later, the perspective is adequate for the approach taken for this study.

For the purposes of discussion, the outgoing acoustic signal will be assumed to be an instantaneous planar wavefront. In theory, the more complex form of this wavefront could be modelled

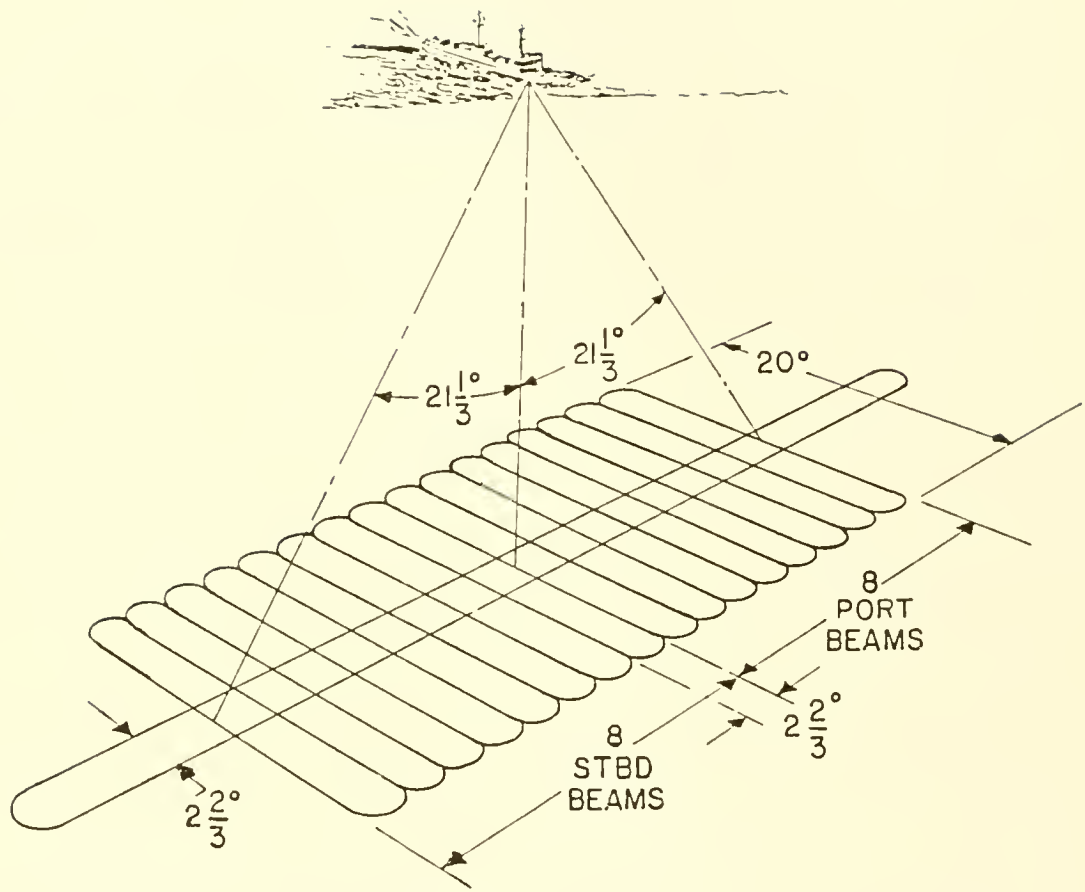


Figure 1. Geometry of the Sea Beam multibeam sounding system.

and deconvolved with the received echo, however this level of signal processing will not be attempted for the planned study. Volume scattering of sound in the water column will also be ignored. The primary remaining effects relate to the nature of the seafloor ensonified; the relative orientation of the incident wavefront with the bottom, the reflection coefficient of the bottom, the roughness of the seafloor within the footprint, and the interference of subsurface reflectors. Since the current study area is dominated by fresh lavas, the subsurface interference can be ignored.

The relative orientation of incident waves and the reflecting surface has a primary effect on the nature of the return pulse. For a vertical incident wave (whether the center beam on a flat bottom or a sidebeam on a properly sloping area of the bottom) the reflected energies are directed toward the receiving array. At any other angle, the primary energies are directed away from the ship, with the majority of the energies being forward scattered and the remainder back scattered. Because the Sea Beam system provides a complete two dimensional model of the seafloor, the orientation for the spatial wavelengths sampled can be directly calculated. As described by Fox and Hayes (1985), seafloor topography is composed of a continuum of wavelengths, and therefore the boundary between the "orientation" and "roughness" wavelengths of the seafloor are purely artificial.

For vertically incident acoustic energy reflecting from a perfectly smooth surface, the amount of energy returned depends upon the physical properties of the reflecting surface and the transmission medium. More specifically, the reflection coefficient is a function of the relative densities and compressional wave velocities of the two media. The properties of the bottom water are essentially constant for most study areas and the varying properties of the bottom generally control the reflection coefficient. DeMoustier (1985) was able to map the distribution of manganese nodules in a sedimentary environment using these properties by mapping the peak amplitude of the center beam return. The variations in rock properties for the current study are probably minimal, being a neo-volcanic terrain.

The microtopographic roughness of the seafloor within the sonar footprint is the final primary factor affecting the nature of the acoustic return. For a vertically incident plane wave, the return pulse represents the convolution of an impulse function with the distributions of depths within the footprint. For a smooth bottom, the variance of depths is small and therefore the returned energy is coherently received as a narrow energy envelope. For a rough bottom, the variance of depths is larger and the returned energy is spread out in time. For the rough bottom case, additional energy is lost to scattering, which with the spreading of the signal, results in a substantially

reduced amplitude for that condition, independent of the reflection coefficient.

For side beams, the degree of bottom roughness directly affects the amount of energy returned. Smooth bottoms allow the majority of the incident energy to forward scatter away from the source. Rough surfaces, on the other hand, provide inward facing facets which allow increased percentages of energy to be back scattered toward the source. Therefore, while rough surfaces tend to decrease the energy returned in vertically incident waves, they also tend to increase the energy received from nonvertically incident waves. The multi-beam configuration of Sea Beam allows this effect to be incorporated into bottom characterization studies. Figure 2 illustrates a typical backscatter record from Sea Beam.

#### INTERPRETIVE METHOD

Before attempting to categorize the backscatter energy character for seafloor mapping, it is necessary to develop a concise description of the energy envelopes associated with each beam. Each gather produces over 8,000 data points, which at a six second ping rate results in an enormous data set for analysis. Therefore, after the various corrections are applied to the data, a curvilinear model is fitted via least squares to each beam using iterative techniques described in van Heeswijk and Fox (1988). For the center beams, a simple Gaussian function appears to be an adequate model for the energy envelope. For the outer beam, the distribution becomes skewed, requiring a more elaborate function. The Rician probability density function has been proposed as the appropriate general model by Stanton (1984).

The fitted Gaussian curves describe each center beam with terms relating to the amplitude, dispersion, and total integrated energy. As the previous discussion indicated, these various model parameters are intercorrelated. In order to best discern the potential groupings of pings independent of correlated parameters, the data are rotated into an orthogonal vector space through principal components techniques. Figure 3 illustrates a typical data set from the Mid-Atlantic Ridge projected on its first three principal components. The clustering of the samples into groups is apparent. These principal components scores would next be subjected to a clustering algorithm to automatically select distinct groupings.

Whether these grouping have geological meaning requires that the resulting groups be spatially coherent. Therefore, the next stage of analysis would be to attempt to map the data back onto the earth and investigate the resulting patterns. If such patterns result, ground truth geological data from bottom photography or submersible observations are required to relate the mathematical properties of the return pulses to the physical

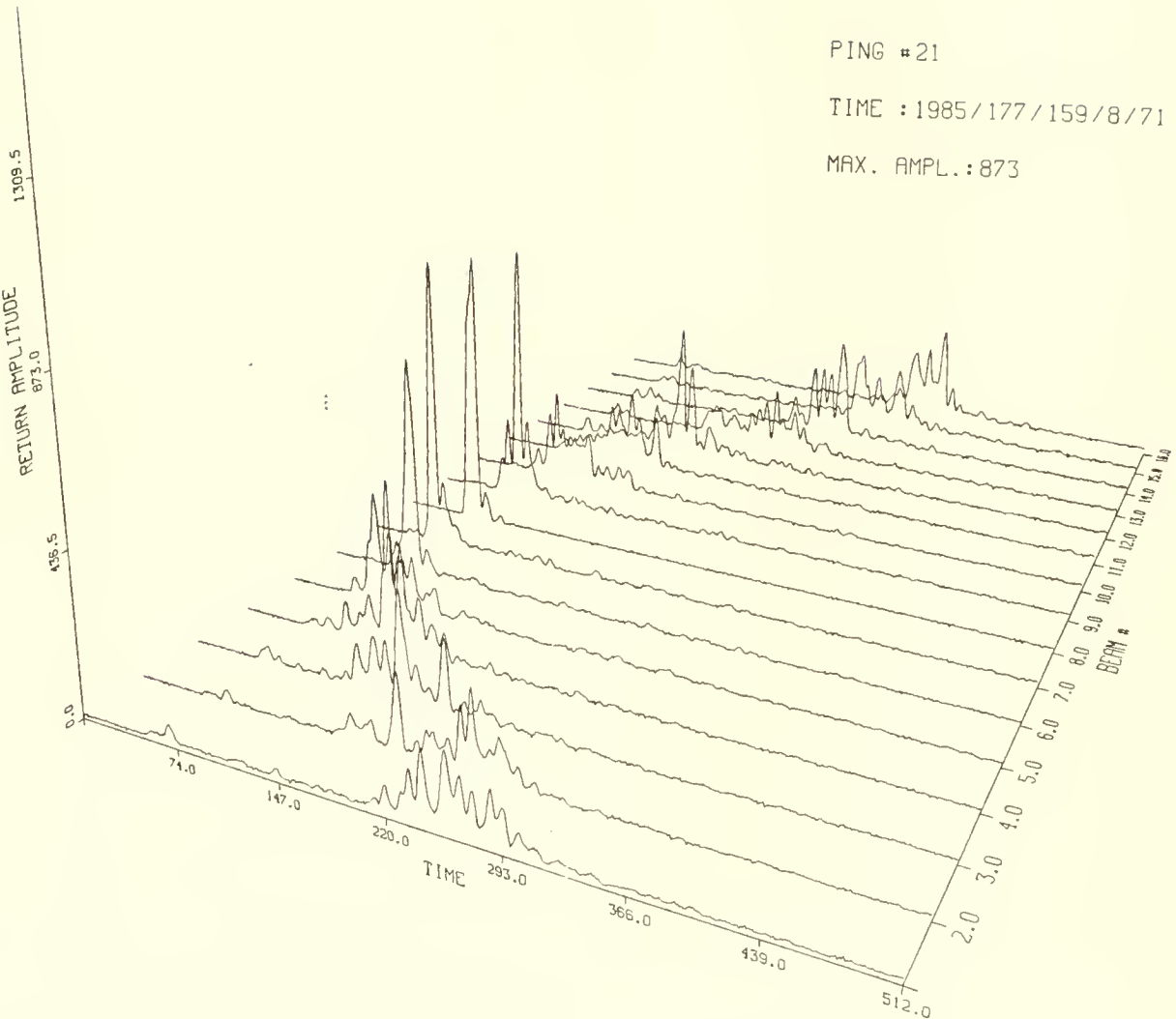


Figure 2. Acoustic backscatter return pulse for a typical Sea Beam ping. The envelopes recorded on the center beams (7 & 8) are narrow and high amplitude, while the outer beams are successively delayed in time due to longer travel paths.

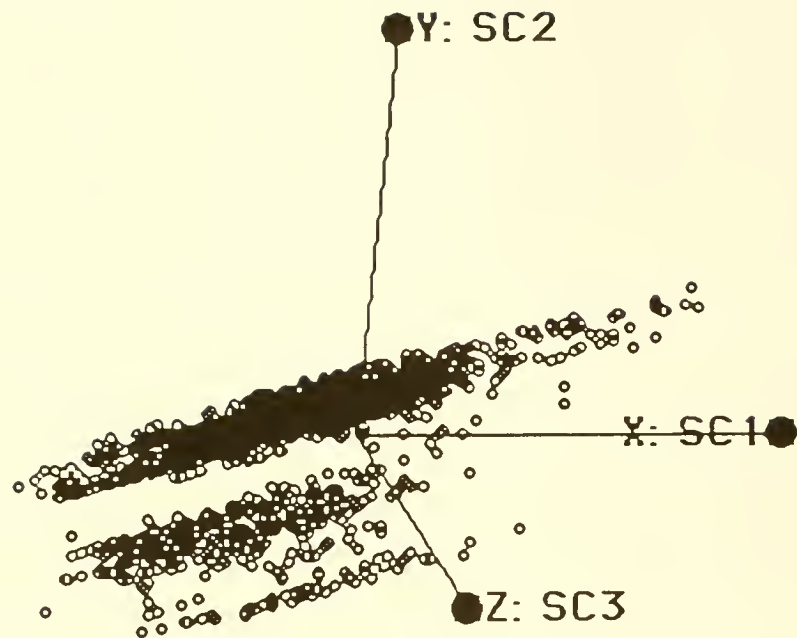


Figure 3. Resulting component scores from a principal components analysis of a Sea Beam backscatter survey at the Mid-Atlantic Ridge. The samples appear to cluster into distinct groups.

properties of the terrain. The few data sets collected to date have not provided sufficient coverage nor adequate ground truth information to allow such a comparison.

#### DISCUSSION OF 1987 NURP SPONSORED PROGRAM

During the September-October 1987 Alvin expedition sponsored by NURP and the NOAA VENTS program, a simultaneous experiment was funded by NURP to collect a complete Sea Beam backscatter data set at Axial Seamount. Axial Seamount is located on the central Juan de Fuca Ridge and has been the focus of extensive geological and geophysical investigations by NOAA's VENTS research program (see Embley et al., Chapter II, this volume). The experiment resulted in over 2.5 gigabytes of backscatter data concentrated at Axial Caldera. In addition to a full coverage survey of the seamount summit, an intensive, transponder-navigated survey of the ASHES hydrothermal vent field within the caldera was conducted.

These data, collected within transponder coordinates over an area with tens of thousands of bottom photographs also transponder navigated, provide the best controlled data set to date for relating acoustic backscatter information to the controlling physical properties. Since the data were collected only weeks before the Undersea Symposium, no results are available at this time. The method may prove particularly applicable to NURP's future submersible operations.

The presence of hydrothermal sediment and extreme black smoker terrains associated with the ASHES vent field may produce a very distinctive backscatter signature. Since much of the current submersible-based research being conducted in the deep ocean involves the investigation of hydrothermal systems, the technique may provide a remote sensing tool for identifying hydrothermal areas. As the Sea Beam equipment and Alvin reside on the same platform, the two systems may be used in tandem for exploration.

#### LITERATURE CITED

Clay, C. S., and H. Medwin. 1977. Acoustical Oceanography: Principles and Applications. New York, N.Y., John Wiley & Sons. 544 pp.

deMoustier, C. 1986. Beyond bathymetry: mapping acoustic backscatter from the deep seafloor with Sea Beam. J. Acoust. Soc. Amer., Vol. 79, No. 2, pp. 316-331.

deMoustier, C. 1985. Inference of manganese nodule coverage from Sea Beam acoustic backscatter data. Geophysics, Vol. 50, No. 6, pp. 989-1001.

Embley, R. W., S. R. Hammond, and K. M. Murphy. 1988. The caldera of Axial Volcano--remote sensing and submersible studies of a hydrothermally active submarine volcano. In: Michael P. De Luca and Ivar Babb (eds.), Global Venting, Midwater, and Benthic Ecological Processes. National Undersea Research Program Research Report 88-4, pp. 61-70. Rockville, Md., NOAA Undersea Research Program.

Fox, C. G., and D. E. Hayes. 1985. Quantitative methods for describing the roughness of the seafloor. Rev. Geophys. and Space Phys., Vol. 23, No. 1, pp. 1-48.

Glenn, M. F. 1970. Introducing an operational multi-beam array sonar. Interna. Hydrographic Rev., Vol. 47, No. 1, pp. 35-39.

Stanton, T. K. 1984. Sonar estimates of microroughness. J. Acoust. Soc. Amer., Vol. 75, p. 809-818.

Tyce, Robert C. 1986. Deep seafloor mapping systems - a review. Mar. Tech. Soc. J., Vol. 20, No. 4, pp. 4-16.

Urick, R. J. 1983. Principles of Underwater Sound. 3rd Edition. New York, N.Y., McGraw-Hill. 384 pp.

van Heeswijk, M. and C. G. Fox. 1988. Iterative method and FORTRAN code for non-linear curve fitting. Computers and Geosci., Vol. 14, No. 4, pp. 489-503.



THE PRESENCE AND POTENTIAL IMPACT OF GEOTHERMAL ACTIVITY ON THE CHEMISTRY AND BIOLOGY OF YELLOWSTONE LAKE, WYOMING

J. Val Klump<sup>1,2</sup>, Charles C. Remsen<sup>1</sup>, and Jerry L. Kaster<sup>1</sup>

Center for Great Lakes Studies

<sup>1</sup>Department of Biological Sciences

<sup>2</sup>Department of Geological and Geophysical Sciences

University of Wisconsin--Milwaukee

Milwaukee, WI 53201

ABSTRACT

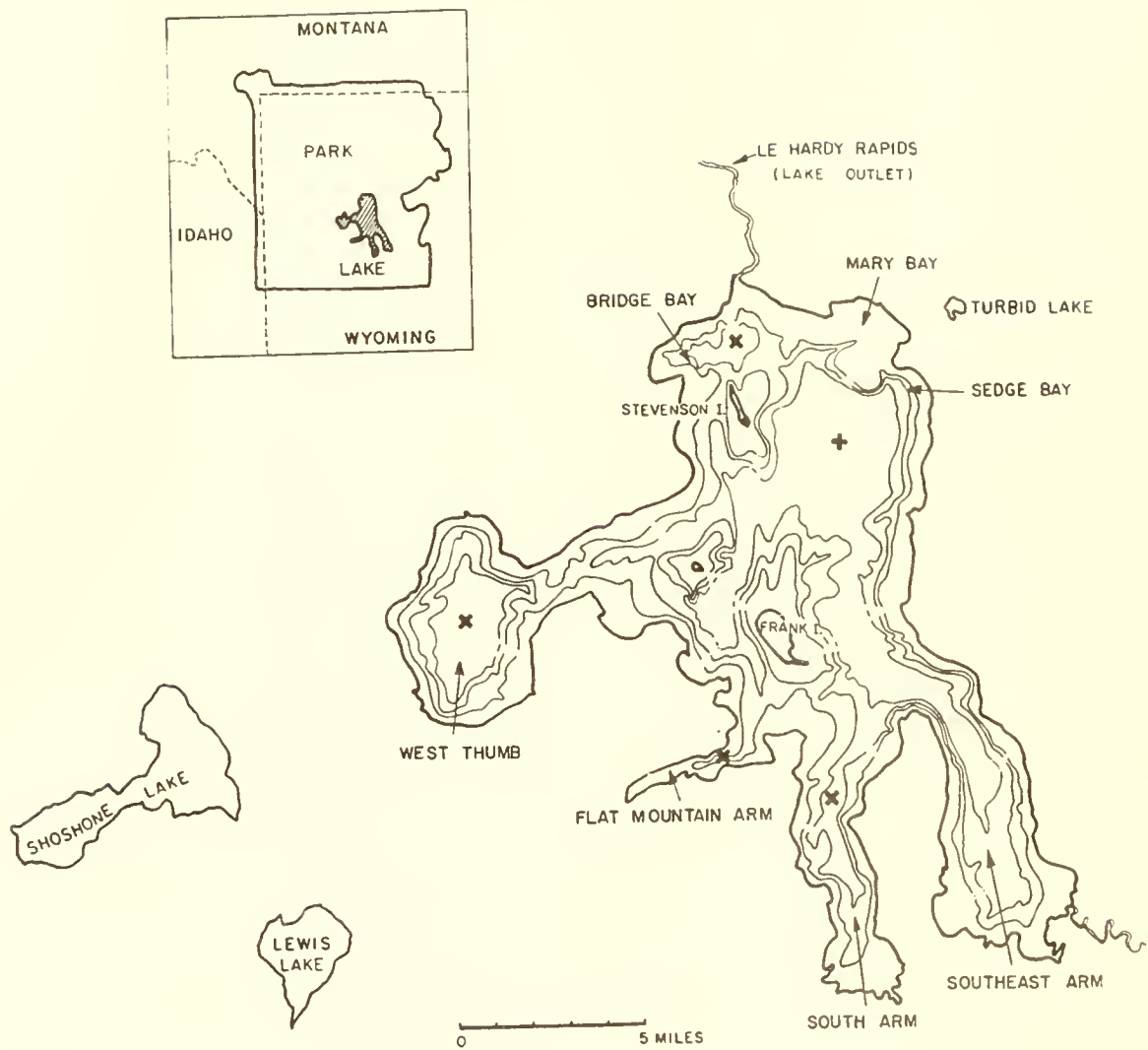
Yellowstone Lake, Wyoming is located in a tectonic "hot spot" and lies within the Yellowstone caldera, a region with some of the highest measured geothermal heat fluxes in the world. Geothermal gradients within the lake bed are consequently very high and hydrothermal springs and hot gas fumaroles occur within the lake itself. These features are unique in limnology and indications are that they may have a significant impact on the chemistry, nutrient dynamics and biology of this oligotrophic system. Observations to date have revealed nearshore regions with widespread gas ebullition, numerous small springs or seeps, and elevated (95° C) substrate temperatures. Gases are primarily carbon dioxide, with traces of methane and hydrogen sulfide. Hydrothermal waters reaching 70° C are anoxic and high in dissolved nutrients. Enhanced biological activity surrounds these vents with mats of microbial heterotrophs and photo- and chemo-lithotrophs, hydroponic-like algal growth and dense congregations of aquatic worms. Geophysical evidence indicates that hydrothermal activity may be widespread. ROV observations demonstrated directly that geothermal activity was present in the deepest areas of the lake as well as in the shallow nearshore zones.

INTRODUCTION

The Yellowstone System

Yellowstone Lake (Fig. 1), the largest high altitude lake in North America, is situated in Yellowstone National Park, one of the most tectonically active regions in the world. Like the Hawaiian Islands, Yellowstone represents a hot spot in the earth's crust. The Yellowstone plateau, with an average elevation of ~ 2000 meters, overlies magma chambers which are the source of heat for the well known geothermal features in the Park: geysers, hot springs, fumaroles, and mud pots.

Over the last 2 million years, there have been 3 major volcanic episodes in Yellowstone (Christiansen and Blank 1972).



## YELLOWSTONE LAKE

✖ STATIONS  
AUGUST 83

DEPTH CONTOUR IN FEET

— 80  
— 160  
— 240

Figure 1. Yellowstone Lake in Yellowstone National Park is the largest high altitude lake in North America at an elevation of 2357 meters.

The most recent of these occurred approximately 600,000 years ago. Following a period of substantial uplift of the Yellowstone plateau, more than 900 km<sup>3</sup> of rhyolitic pumice and ash erupted resulting in the collapse of a 75 km by 45 km area and the formation of the Yellowstone Caldera (Eaton et al. 1975). The magnitude of this explosion was immense. By way of comparison, the famous Krakatoa eruption of 1883 created a caldera less than 7 km across, yet sent enough dust into the atmosphere to have a measurable effect on global climate. Immediately following this collapse, resurgence within the magma chamber uplifted the floor of the caldera and formed two resurgent domes within the caldera boundary (Fig. 2). Today, most of the thermal features within the Park are clustered around the rim of this caldera as surface and ground waters circulate along systems of deep fractures at the caldera rim and at the intersection of tectonic faults with the rim fractures (Smith and Christiansen 1980). Yellowstone is one of the most seismically active regions of the world, with micro-earthquakes recorded daily (W. Hamilton, pers. comm.).

Yellowstone Lake is situated largely within the caldera, although the South and Southeast Arms lie outside it (Fig. 2). The lake itself is of glacial origin. The region was covered by ice during the last glaciation ~ 15,000 years ago. The hydrologic outflow of the lake at Le Hardy Rapids on the Yellowstone river flows directly across one of the two resurgent domes within the caldera. Active doming has been raising this outfall nearly 2.5 cm per year since the 1920's when the first elevations were taken, and short term doming/subsidence events have raised this region as much as 20 cm in 3 to 4 weeks (Hamilton 1987).

The limnological history of the lake is not well known. Studies by Brian Shero on the diverse diatom record in sediment cores representing the last 1500 years (Shero and Parker 1976) led him to hypothesize that the productivity of the lake was decreasing with time. Both diatom abundance and sedimentation were lower in recent sediments. More detailed studies of sediments deposited in the last 200 years, however, show a more complicated picture (Kaster et al. 1987, Klump et al. 1987). While sediment accumulation rates determined via Pb-210 dating have remained nearly constant, the deposition of biogenic silica has varied by as much as 30% over the last 100 to 150 years (Fig. 3). A variety of factors have been hypothesized as having a role in controlling the productivity of Yellowstone and other lakes in the region. These include nutrient input from forest fires, climate, ecosystem (food web) dynamics, and anthropogenic influences. Given the geological setting of the lake, however, and the potential impact of ground water inputs, particularly geothermally heated and reacted ground waters, we believe that fluctuations in hydrothermal inputs to the lake may be important to the biology and chemistry of the system.



Figure 2. Map of Yellowstone National Park showing the extent of the Yellowstone Caldera and the resurgent domes near Old Faithful and Le Hardy Rapids. Areas of geothermal activity are shown in black (after Smith and Christiansen 1980). Yellowstone Lake lies within this active region.

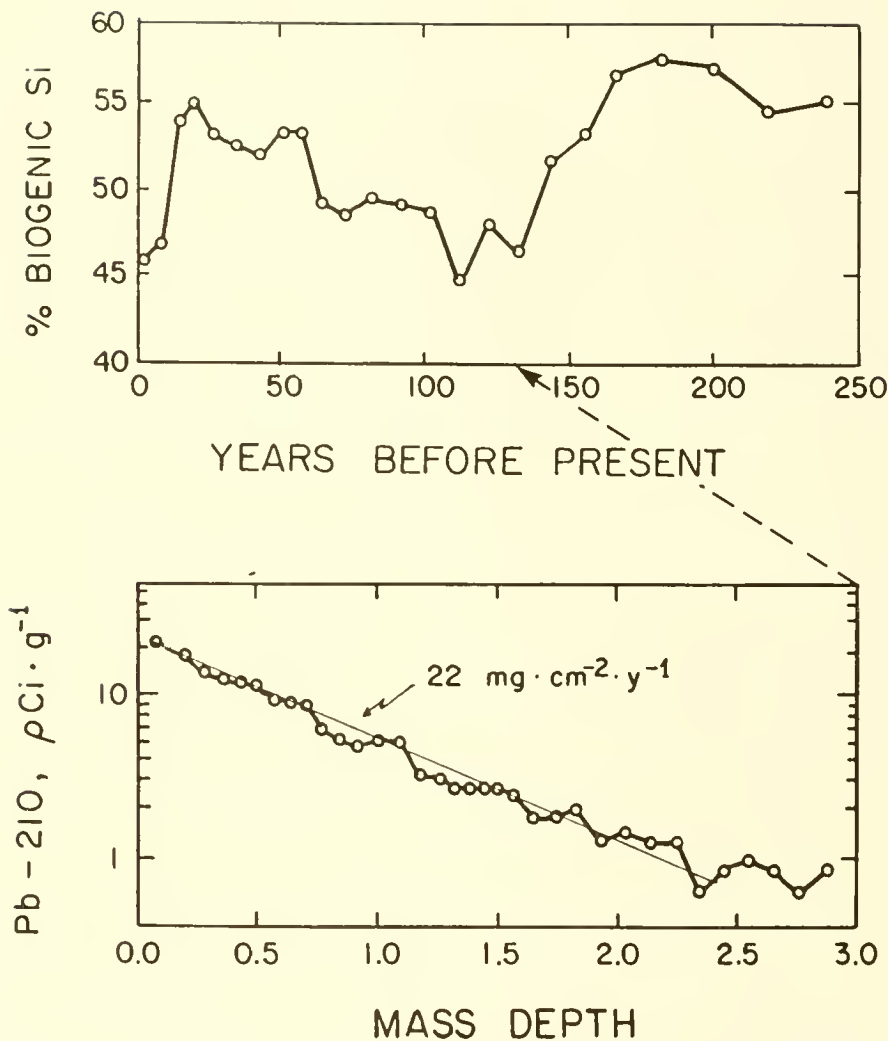


Figure 3. Top: During this time the biogenic silica content (diatom frustules) has varied nearly 30 percent. Such fluctuations may result from changes in productivity through time, perhaps induced by changes in hydrothermal inputs of nutrients as tectonic shifts alter the sublacustrine "plumbing" of the Yellowstone systems. Other hypothesized causes include climatic changes, forest fire history and changing food web dynamics; bottom: A Pb-210 profile from a core collected in the deep basin in West Thumb. Sedimentation rates have been relatively constant here at approximately  $22 \text{ mg dry sediment cm}^{-2} \cdot \text{y}^{-1}$  over the last 100 to 120 years.

## Evidence of Hydrothermal Activity Within the Lake

In 1974, Morgan et al. (1977) undertook the first studies of thermal gradients within the lake floor in order to study the existence of the mantle derived intrusives in the upper crust beneath Yellowstone. More recently, Morgan and Blackwell have significantly increased the data base on thermal gradients within the lake sediments and have calculated for the major portion of the lake, the flow of heat resulting from the gradients observed. For the Rockies in general, the average heat flow is  $\sim 60$  MW per  $m^2$ . In Yellowstone Lake the range is from 100 to over 40,000 MW  $m^{-2}$  (personal communication, Morgan, Northern Arizona State University, 1987). The regions of highest heat flux are in Mary Bay, the site of a relatively recent explosion crater (Wold et al. 1977), southwest West Thumb and in deep water east of Stevenson Island. Temperature gradients in Mary Bay, for example, reach as high as a  $50^\circ$  C increase in temperature per meter depth into the sediment. The magnitude of these gradients and heat fluxes are indicative of hydrothermal activity throughout much of the lake. The topography of the lake bottom is complex and poorly known. At least some of the high temperature anomalies appear to be associated with downfaulted sediment structure and small fissures or troughs on the lake floor (personal communication, Morgan, Northern Arizona State University, 1987). Continuous bottom water temperature recorders placed at several locations in the lake by the Morgan and Blackwell group in conjunction with the thermal gradient studies showed a gradual and steady increase of  $\sim 1^\circ$  C in water temperature during the winter ice cover period from December to May.

## METHODS

Direct observations were made in both shallow and deep water via a MiniRover MKI. To facilitate the measurement of thermal anomalies, the movable claw on the ROV was replaced with a rotating drum to which was mounted an  $\sim 40$  cm aluminum rod holding a high precision well logging thermister loaned to us by Dr. Paul Morgan of N. Arizona State University. The drum and rod were configured so that the thermister could be held vertically and then rotated through 90 degrees to the horizontal, allowing the probe to be inserted up to 5 to 10 cm in the sediment.

Water samples of hydrothermal solutions were collected by SCUBA divers using a tube (with attached temperature probe) connected to a peristaltic pump at the surface or by using hand held 50 ml syringes. Samples of microbial mats were similarly collected using sterile 10 ml disposable plastic syringes.

Samples for chemical analysis were held on ice until brought back to the laboratory. The cations: Na, K, Mg, Ca and the anions: Cl and  $SO_4$  were separated via single column ion chromatography on a dual channel Wescan Mdl 261 IC. To date, Ca

and Mg have also been analyzed on a few samples via AAS with agreement to within 10%. Dissolved silica (APHA 1985) and ammonium (Koroleff 1969) were determined colorimetrically. Total dissolved inorganic carbon was analyzed via the syringe stripping method of Stainton (1973) on a Gow Mac 150 gas chromatograph.

Water for radon-222 analysis was collected with a 30 liter niskin sampler into 20 liter evacuated sample bottles. Radon was extracted and counted following Broecker (1965). Supported radon-222 concentrations have been determined on re-extracted samples following ingrowth and are less than 0.06 dpm/l. Water column temperature profiles were measured with a YSI in situ probe.

## RESULTS AND DISCUSSION

### ROV Observations

In 1987 direct observations of the bottom of Yellowstone Lake were made for the first time using a ROV. Over a period of six days, 22 dives were made in Mary Bay, Sedge Bay, West Thumb, and in the deepest portion of the lake near Stevenson Island. All of these locations represented areas suspected of having a high probability of hydrothermal activity based upon geothermal gradient data, surface observations of gas ebullition, or proximity to onshore thermal areas. With the exception of one dive, evidence of geothermal activity was observed at all sites.

In the deeper depositional areas of the lake, the most frequently observed features were small (approximately a few cm in diameter) depressions or openings in bottom sediments from which an occasional gas bubble was emitted. These small holes were also frequently surrounded by a white mat or precipitate assumed to result from the growth of a Thiothrix-like organism commonly observed in shallow waters in association with sulfide emanations. Gas bubbles were not always seen. It was assumed that, based upon the loose, flocculent nature of these sediments, that some relatively recent and persistent physical disturbance would be required to prevent covering over and filling in with sediment. Occasionally, warm water was observed flowing from a fissure or hole in the bottom, creating a shimmering effect against the backdrop of cooler waters. The most dramatic example of this was observed at over 98 meters in a narrow >112 meter deep depression in the main basin of the lake near Stevenson Island. This small deep defile represented a sounding more than 15 meters deeper than any before recorded. Sediments throughout these regions were warmer than bottom waters by approximately 1° C, and warmer still near presumed thermal features.

Seismic profiles of the bottom in this region indicated apparent downfaulting and offsets in sediment stratigraphy of up

to 3 meters in what would appear to be actively accumulating sediments (Blackwell, pers. comm. 1987, see also Otis et al. 1977). Present sediment deposition rates determined by Pb-210 dating in Yellowstone Lake are on the order of 10 to 20 mg cm<sup>-2</sup>.y<sup>-1</sup>, or roughly a mm per year. These offsets frequently extended to the sediment surface, the implication being that these "faults" represent contemporary events and that the bottom experiences major shifts in response to continuing tectonic activity.

ROV observations of the bottom revealed steep topography, sediment slumping and "outcrops" of exposed sediment strata. If our estimates of deposition rates apply, these sediments are young, no more than a few hundred to a couple of thousand years old at most. They appeared to be very well lithified, however, in contrast to sediments collected in other deep areas of the lake in cores nearly a meter in length. The sediments in Yellowstone are a diatomaceous ooze consisting of up to 50% to 60% biogenic silica and having an organic carbon content of ~ 3%. It is possible that these exposed "outcrops" represent older sediments or that they have undergone accelerated diagenesis and lithification due to heating from below.

Geothermal activity in nearshore areas was much more readily observable and more dramatic. In Mary Bay, for example, gas ebullition from submerged fumaroles was widespread and extremely active. Curtains of gas bubbles, consisting largely of carbon dioxide, were observed emanating from barren sandy sediments which reached temperatures of nearly 100° C at 4 or 5 cm below the sediment surface. Submerged fumaroles were also found in Sedge Bay. Sediment temperatures here were cooler, however, and macrophyte (primarily aquatic mosses) and attached algal growth was well established and appeared, in some instances, to be enhanced by the high CO<sub>2</sub> content of the fumarole gas.

Growth of a Thiothrix-type organism was commonly observed as white filamentous material covering rocks and plants growing in fumarole effluents containing hydrogen sulfide. The absence of these sulfide oxidizers around some gas vents is assumed to indicate the absence of hydrogen sulfide as well. In some shallow areas, dense and colorful microbial mats grew in bands approximately 1 meter in width and extended for 10's of meters across silty-sand bottoms. These mats apparently followed subsurface thermal features generating steep thermal and chemical gradients.

#### Preliminary Observations on the Chemistry of Submerged Hydrothermal Springs in a Nearshore Region: Sedge Bay

While submerged fumaroles were the most prevalent feature observed in these shallow near shore areas, occasional small hydrothermal springs and seeps occurred in association with gas

vents. Temperatures of these springs ranged from 35 to 80°C, but cooled very rapidly upon mixing with ambient lake water at 12 to 15°C. These waters were clear, anoxic and contained elevated concentrations of nutrients and major dissolved anions and cations. Because of the relatively low flow rates of these vents and immediate mixing with lake water, pure hydrothermal solutions were not obtained. Figure 4 shows the concentrations of a variety of dissolved constituents as a function of the estimated temperature of the hydrothermal fluids for a set of samples collected in 3 to 10 meters of water in Sedge Bay. Lack of a good thermal stoichiometry may result from both different sources for the waters collected and the difficulty, with the simple techniques employed, in obtaining an accurate temperature in situ without cooling. The chemical stoichiometry is somewhat more coherent (Fig. 5) with most dissolved constituents covarying linearly.

The chemistry of hot springs has been used extensively to predict subterranean conditions in Yellowstone and other geothermal systems (Mazor and Thompson 1982, Fournier 1979, and others). Using chemical geothermometers, Fournier and co-workers (1979, 1974a,b, 1973, 1970, 1966) have estimated the underground temperatures of the source reservoirs for hot springs and the temperature of the last rock-water interaction. Hot springs often emanate from hydrologically complex systems which include intermediate reservoirs, mixing with water from other sources, and both conductive and adiabatic cooling. Enthalpy-chloride relationships have been shown by Fournier (1979) to be useful in resolving some of these complexities. The hydrothermal fluids collected to date, however, are low in chloride (bicarbonate being the principle anion), thus confounding the application of these relationships. Application of the two most commonly used chemical geothermometers, silica (Fournier and Rowe 1966) and Na-K-Ca (Fournier and Truesdell 1973) result in maximum estimated temperatures for the Sedge Bay sublacustrine springs of 150 to 180°C and 196 to 211°C, respectively. The higher temperature is generally considered more reliable, however, because of the possibilities for mixing with multiple reservoirs and heating by steam and hot gases, the reliability of these estimates is currently unknown.

Concentrations of almost all constituents in these warm waters were significantly elevated above that of ambient lake water (Table 1). The nutrients: dissolved silica, ammonium, and total inorganic carbon were as much as 2 orders of magnitude more concentrated in the warm hydrothermal waters collected in Sedge Bay than in the overlying lake water. Yellowstone Lake is characterized as an oligotrophic system and is assumed to be nitrogen limited, although no year-round data on the chemistry of the lake currently exists. Dissolved inorganic nitrogen is undetectable in the epilimnion and a mid to late summer bloom of the nitrogen-fixing alga, Anabena, is an annual phenomena (R.

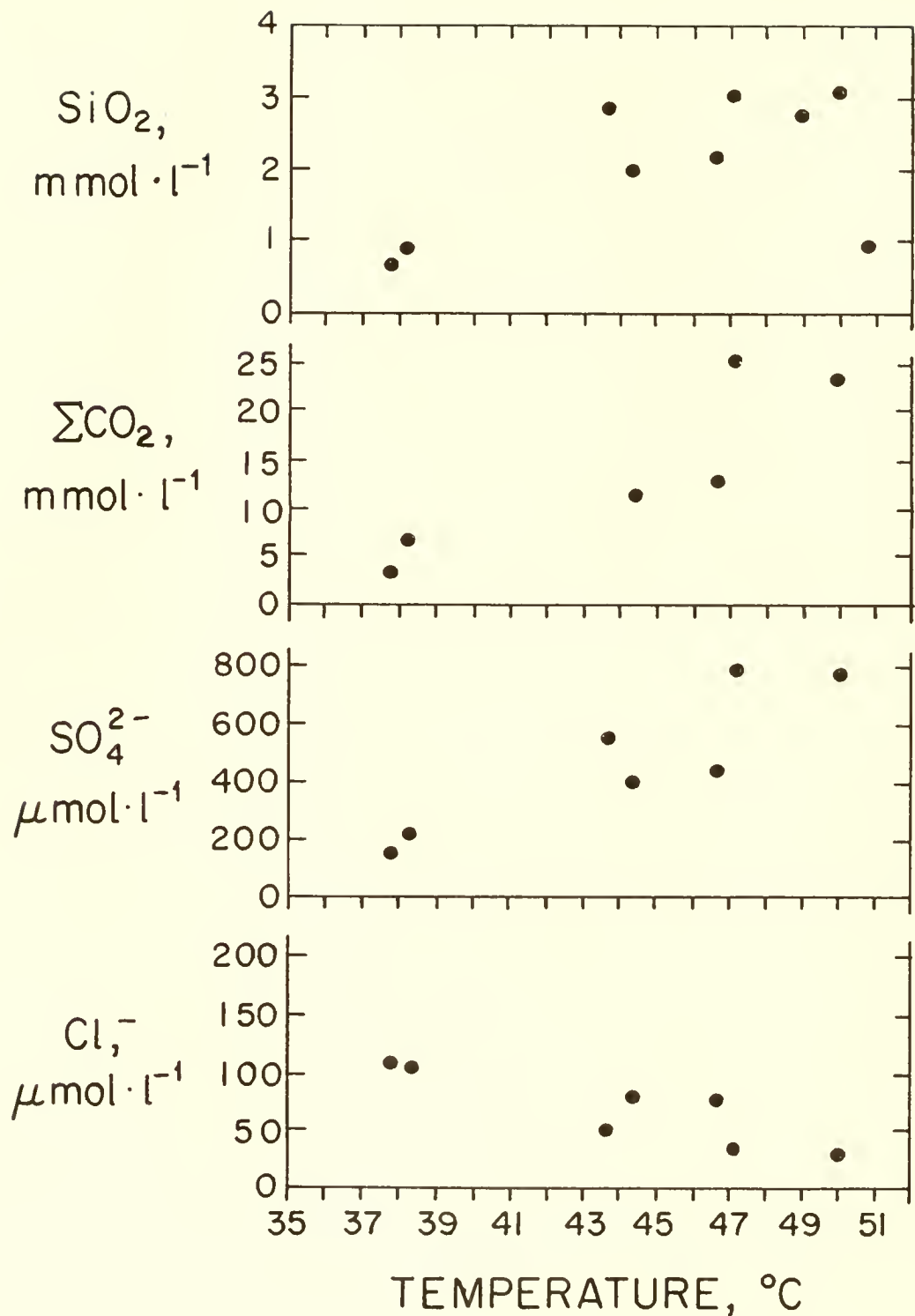


Figure 4. Plot of concentration vs. temperature for a variety of chemical constituents in Sedge Bay hydrothermal waters.

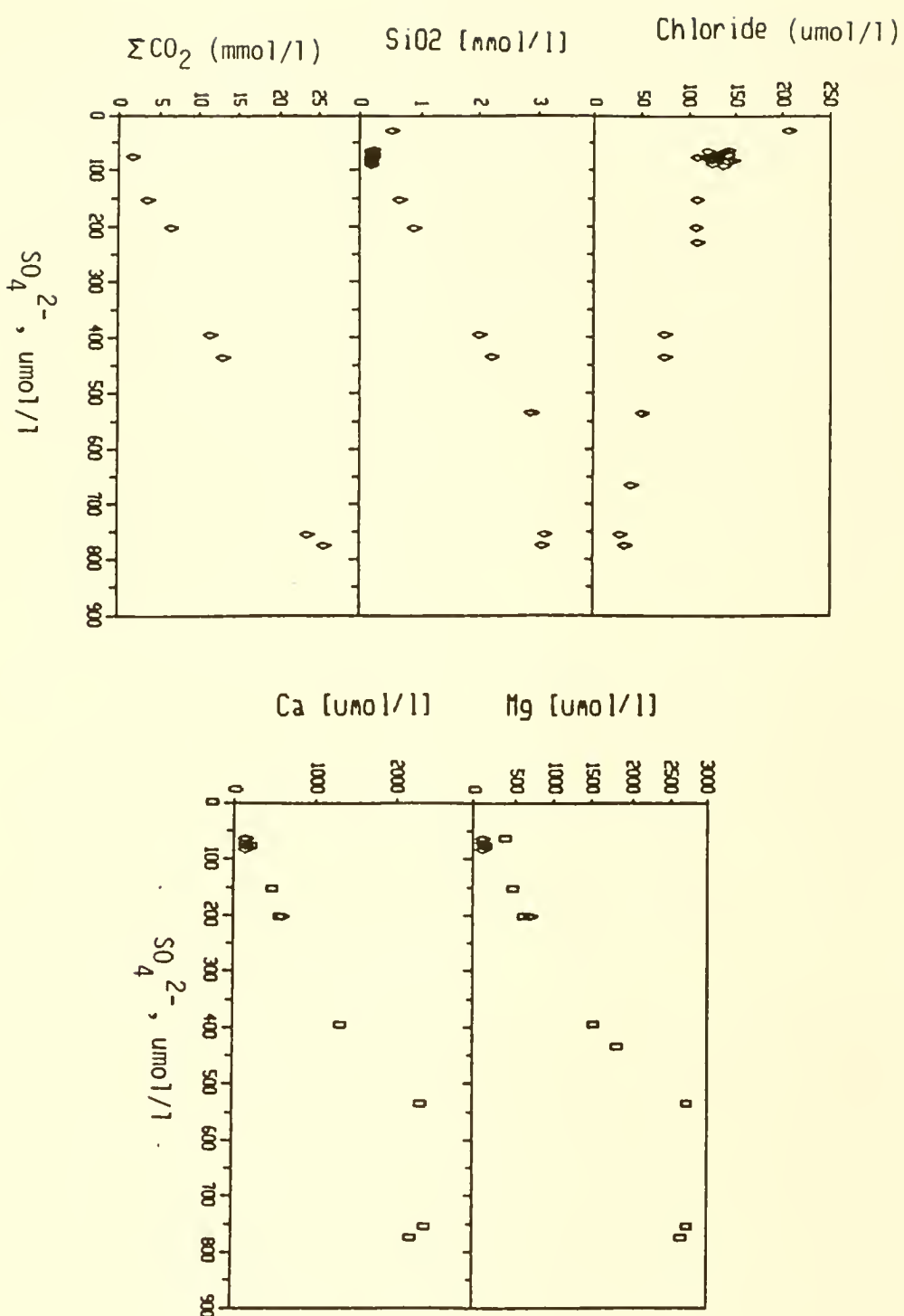


Figure 5. Stoichiometric relationships between chemicals dissolved in vent water are frequently constant as a result of dilution with ambient lake water.

Table 1. Concentrations of major ions and nutrients dissolved in surface waters and hydrothermal vent waters found in Yellowstone Lake, Wyoming.

Sample	Cl <sup>-</sup>	SO <sub>4</sub> <sup>2-</sup>	Mg <sup>2+</sup>	Ca <sup>2+</sup>	Na <sup>+</sup>	K <sup>+</sup>	SiO <sub>2</sub>	NH <sub>4</sub> <sup>+</sup>	ΣCO <sub>2</sub>
	(umol·l <sup>-1</sup> )						(mmol·l <sup>-1</sup> )		
<b>Vent water (Sedge Bay):</b>									
4	97	113			425	73	27	19.9	
5	100	99	176	196	532	63	150	2.2	
6	99	592	2900	2300	4100	535	2429	17.9	28.9
8	102	734	2700	2300		510	2429	23.2	26.6
9	113	442	1900	1600	3200	401	2429	93.1	10.1
10	68	566					1829	33.7	19.2
11	94	634					2429	22.7	25.9
12	179	187					341	27.3	5.25
13	95	556	2400	2000	3800	519	3172	36.8	
14	87	503			3800	496	3074	39.7	
15	79	532	2300	1900	3700	501	3152	53.8	19.4
16	193	348	2900	2400	4700	606	3290	23.1	25.6
17	211	349	2700	2200	4400	528	3310	74.3	24.1
19	659	173	1700	1000	4600	536	3113	80.4	16.0
20	950	98	395	290	3600	420	2033	218	6.34
22	179	366	2800	2200	4400	554	3211	0.0	25.5
23	156	286	2000	1600	3200	413	2387	41.6	14.5
<b>Lake water: [avg. all samples]</b>									
±	149	80	102	143	490	46	167	0.15	0.66
	24	6	2	3	27	3	8	0.25	0.06

Gresswell, pers. comm.). Given the high concentrations of nutrients in hydrothermal solutions and the evidence for the relatively widespread occurrence of hydrothermal vents, geothermally heated and reacted ground water inputs may prove to have a significant impact on the chemistry and limnology of the lake.

An indication of possible hydrothermal fluxes into the lake may be seen in the high excess radon-222 concentrations measured in bottom waters of a small hole in the outer portion of Mary Bay. Radon-222 was measured in the water column in both Mary Bay and in the deep basin off Stevenson Island (Fig. 6). In a 98 meter deep water column near Stevenson Island measured Rn-222 concentrations ranged from 0.06 dpm/l at the surface (close to the supported Rn-222 concentration of ~0.03 dpm/l) to 18 dpm/L one to two meters above the bottom. In the Mary Bay Rn-222 concentrations as high as 70 to 110 dpm/l were measured in the hypolimnion of a small steep sided hole which dropped off quickly from less than 20 meters to nearly 40. The bottom in this area was complex with steep and variable topography. The hypolimnetic water here was also warm, ~12.5° C.

The source of this high excess Rn-222 is unknown. Water samples taken from the surface of a shallow thermal pond (temperature = 35° C) less than a 100 meters onshore in Mary Bay yielded extremely high Rn-222 concentrations of 1400-1800 dpm/l. More detailed Rn-222 profiles and an estimate of diffusive emanation from sediments, as well as measurements of the possible sources, hydrothermal fluids and fumarole gases, may allow future estimates of hydrothermal/geothermal inputs.

### Biota Associated with Thermal Activity in the Lake

#### Microbial communities

The microbial communities associated with these thermal features are diverse. Samples collected from mats, vent waters and glass slides incubated over fumaroles and vents were inoculated into a variety of enrichment media. A summary of the results of those enrichments, to date, are shown in Table 2. In addition, samples were tested for growth at high temperature (70° C). Of the 13 samples incubated, 6 yielded growth of thermo-philic colonies. The thermophilic bacteria of the terrestrial hot springs have been extensively studied (see Brock 1978, for review) and are one of the unique features of the thermal systems in Yellowstone. The enrichments have produced a diverse group of heterotrophic and autotrophic (both lithotrophic and phototrophic) microorganisms. A Thiothrix-type sulfide oxidizing bacteria was very common in fumaroles and produced many large filamentous colonies which frequently covered entire plants. A positive enrichment for Beggiatoa was also obtained. Mats of purple sulfur bacteria, Chromatium and

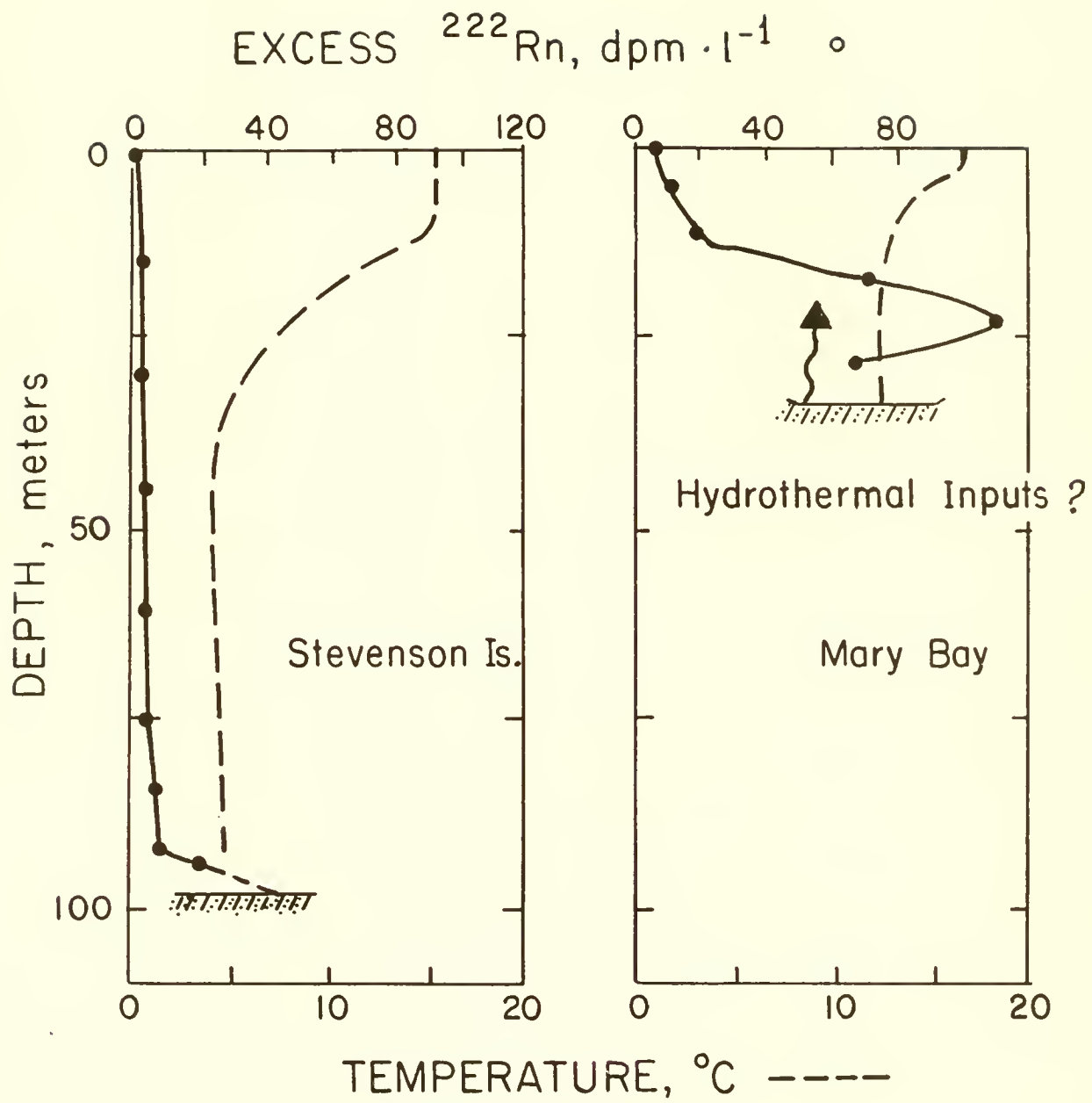


Figure 6. Temperature and radon-222 profiles for two stations in Yellowstone Lake: A Mary Bay basin (~34 meters max. depth), and a basin near Stevenson Island (~98 meters max. depth). Supported radon-222 concentrations are  $< 0.06 \text{ dpm/l}$ .

Table 2. Summary of microbial enrichments from Sedge Bay, Summer 1987.

---

Sedge Bay Mat Samples:

Photosynthetic bacteria-	<u>Chromatium</u> sp.
Cyanobacteria-	<u>Thiocystis</u> sp.
SO <sub>4</sub> -Reducers	<u>Synechococcus</u> sp. Unknown sp.

Vent Samples:

Thiosulfate-oxidizers	Unknown sp.
SO <sub>4</sub> -Reducers	<u>Desulfovibrio</u> sp.
Heterotrophic Thiosulfate	Unknown sp. (fat rods)
Oxidizers	Unknown sp. (Thiobacillus type)
	Unknown sp. (Pseudomonas type)

Glass slides:

Sulfide oxidizers-	<u>Beggiatoa</u> sp.
SO <sub>4</sub> -Reducers	<u>Thiothrix</u> sp. Unknown sp.

---

Thiocystis spp., were also abundant over warm sediments. Several different enrichments for sulfate reducing bacteria have been obtained, and sulfate reducers were found in all three sample types.

#### Macrofauna

In addition to the prolific and colorful microbial communities, dense populations of oligochaete worms were also occasionally found congregated near fumaroles in warm sediments. Worm densities in these small patches were an order of magnitude higher than in the cool sandy sediments only a few cm away. These "colonies" consisted of three tubificid species, Limnodrilus hoffmeisteri, L. udekemianus and L. profundicola, and an occasional solitary, exceptionally large (for freshwater) lumbriculid oligochaete of the genus Lumbriculus. The latter represents either a new species or a particularly robust L. variegatus, as it is twice the typical size reported for the species (Brinkhurst and Jamieson 1971). Presumably the worms are attracted by the healthy bacterial flora upon which they feed. The fact that these worms live near their thermal limits in sediments that reach 80° C at 3 to 4 cm depth is a unique situation for these organisms.

#### ACKNOWLEDGMENTS

This work was supported by grants from the NOAA National Undersea Research Program, the National Geographic Society, and the Graduate School of the University of Wisconsin--Milwaukee. This work could not have been carried out without the excellent cooperation and assistance of R. Jones and R. Gresswell of the U.S. Fish and Wildlife Service. The authors would also like to thank W. Hamilton and the National Park Service for their cooperation and interest, P. Anderson, F. Binkowski, M. Kapinski, J. Krezowski, J. Maki and R. Paddock for their help and collaboration in the field and laboratory, and Dave and Rebecca Lovalvo of Eastern Oceanics Inc. for their very capable operation of the ROV. This is the Center for Great Lakes Studies Contribution Number 309.

#### LITERATURE CITED

American Public Health Association, American Water Works Association, and Water Pollution Control Federation. 1985. Automated method for molybdate-reactive silica. In: Standard Methods for the Examination of Water and Wastewater, 16th Ed., APHA, Washington, D.C., pp. 461-463.

Brinkhurst, R. O. and B. G. M. Jamieson. 1971. Aquatic Oligochaetes of the World. Toronto, Univ. of Toronto Press. 860 pp.

Brock, T.D. 1978. Thermophilic microorganisms and life at high temperatures. New York, N.Y., Springer-Verlag. 465 pp.

Broecker, W. S. 1965. An application of natural radon to problems in ocean circulation. In: Symposium on Diffusion in Oceans and Fresh Waters. Lamont Geol. Obs., Palisades, NY, pp. 116-145.

Christiansen, R. L. H. R. Blank, Jr. 1972. Volcanic stratigraphy of the quaternary rhyolite plateau in Yellowstone National Park. USGS Prof. Paper 729-B. Government Printing Office, Washington, D.C.

Eaton, G. P., R. L. Christiansen, H. M. Iyer, A. N. Pitt, D. R. Mabey, H. R. Blank, Jr., I. Zietz, and M. E. Gettings, M. E. 1975. Magna beneath Yellowstone National Park. Science, Vol. 188, No. 4190, pp. 787-796.

Fournier, R. O. 1979. Geochemical and hydrologic considerations and the use of enthalpy-chloride diagrams in the prediction of underground conditions in hot-spring systems. J. Volcan. Geotherm. Res., Vol. 5, pp. 1-16.

Fournier, R. O. and A. H. Truesdell. 1974. Geochemical indicators of subsurface temperature. 2. Estimation of temperature and fraction of hot water mixed with cold water. U.S. Geol. Surv. J. Res., Vol. 2, pp. 263-270.

Fournier, R. O. and A. H. Truesdell. 1973. An empirical Na-K-Ca geothermometer for natural waters. Geochim. Cosmochim. Acta., Vol. 37, pp. 1255-1275.

Fournier, R. O. and A. H. Truesdell. 1970. Chemical indicators of subsurface temperature applied to hot spring waters of Yellowstone National Park, Wyoming, U.S.A. Geothermics, Vol. 2, No. 1, pp. 529-535.

Fournier, R. O. and J. J. Rowe. 1966. Estimation of underground temperatures from the silica content of water from hot springs and wet-steam wells. Am. J. Sci., Vol. 264, pp. 685-697.

Fournier, R. O., D. E. White, and A. H. Truesdell. 1974. Geochemical indicators of subsurface temperature. I. Basic assumptions. U.S. Geol. Surv. J. Res., Vol. 2, pp. 259-262.

Hamilton, W. L. 1987. Water level records used to evaluate deformation within the Yellowstone Caldera, Yellowstone National Park. J. Volcan. Geotherm. Res., Vol. 31, pp. 205-215.

Kaster, J. L., J. V. Klump, and C. C. Remsen. 1987. The recent paleolimnology of Yellowstone Lake: Climate, tectonics or ...? Abstract, Internat. Assoc. Great Lakes Res. Annual Meeting. May 11-14, 1987.

Klump, J. V., J. L. Kaster, and C. C. Remsen. 1987. Possible climatic and hydrothermal impacts on the limnology of Yellowstone Lake, Wyoming. Abstract, ASLO Annual Meeting, June 14-18, 1987.

Koroleff, F. 1969. Direct determination of ammonia in natural waters as indophenol blue. ICES, C. M. 1969/C:9 (mimeo).

Mazor, E. and Thompson, J. M. 1982. Evolution of geothermal fluids deduced from chemistry plots: Yellowstone National Park (U.S.A.). J. Volcan. Geotherm. Res., Vol. 12, pp. 351-360.

Morgan, P., D. D. Blackwell, R. E. Spafford, and R. B. Smith. 1977. Heat flow measurements in Yellowstone Lake and the thermal structure of the Yellowstone Caldera. J. Geophys. Res., Vol. 82, No. 26, pp. 3719-3732.

Otis, R. M., R. B. Smith, and R. J. Wold. 1977. Geophysical surveys of Yellowstone Lake, Wyoming. J. Geophys. Res., Vol. 82, No. 26, pp. 3705-3717.

Shero, B. R. and M. Parker. 1976. Limnological changes in Yellowstone Lake as indicated by sediment diatoms. Contract Report No. 43-8329. U. S. Dept. of Interior National Park Service.

Smith, R. B. and R. L. Christiansen. 1980. Yellowstone as a window on the earth's interior. Sci. Am., Vol. 242, No. 2, pp. 104-117.

Smith, R. B., R. T. Shuey, J. R. Pelton, and J. P. Bailey. 1977. Yellowstone Hot Spot: Contemporary tectonics and crustal properties from earthquakes and aeromagnetic data. J. Geophys. Res., Vol. 82, No. 26, pp. 3665-3676.

Stainton, M. P. 1973. A syringe gas-stripping procedure for gas chromatographic determination of dissolved inorganic and organic carbon in fresh water and carbonates in sediments. J. Fish. Res. Bd. Canada, Vol. 30, pp. 1441-1445.

Wold, R. J., M. A. Mayhew, and R. B. Smith. 1977. Bathymetric and geophysical evidence for a hydrothermal explosion crater in Mary Bay, Yellowstone Lake, Wyoming. J. Geophys. Res., Vol. 82, No. 26, pp. 3733-3738.

BIOLOGICAL INFLUENCES ON MINERAL DEPOSITION  
AT DEEP-SEA HYDROTHERMAL VENTS

S. Kim Juniper, Verena Tunnicliffe, and A. R. Fontaine  
Department of Biology, University of Victoria  
Victoria, British Columbia  
CANADA V8W 2Y2

ABSTRACT

The intimate association of biological and mineral deposition processes at hydrothermal vents in the northeast Pacific provides opportunity for study of their interaction. Three on-going investigations are reviewed. 1) Iron encrustation on vestimentiferan tubes appears to be initiated by iron-accumulating sheathed bacteria that colonize tube surfaces. At one site growth of such encrustations within clumps of tube worms leads to the formation of mini-spires of iron oxide. 2) Mucus secreted in large quantities by an alvinellid polychaete accumulates mineral particles and trace elements. Mucous tubes on smoker chimneys may affect chimney growth by reducing wall porosity. 3) Examination of filamentous iron/silica deposits formed from sulfide-depleted fluids suggests that their formation may depend on the prior existence of filamentous bacterial mats. Mineral deposition on biological surfaces is potentially deleterious to most vent organisms, although encrustations on vestimentiferan tubes may protect them from predation. While many mechanisms of bio-enhancement of mineral deposition are becoming apparent, their overall quantitative significance remains to be determined.

INTRODUCTION

The hydrothermal vent environment is a milieu of intense geochemical activity where oxidation/reduction reactions lead to the precipitation of sulfide, sulfate and oxide minerals. Most activity is confined to a narrow zone near hot water openings where element-rich hydrothermal fluid mixes with ambient seawater. This same zone bounds a unique ecosystem driven by energy released in the oxidation of  $H_2S$  and other reducing substances present in venting fluids. In their exploitation of hydrothermal fluids vent organisms create structures and produce debris that alter the vent fluid/seawater mixing regime and form a complex mosaic of microenvironments (Juniper 1988, Tunnicliffe et al. 1985). A recent study by Johnson et al. (1986) suggests that the metabolism of vent organisms (Vestimentifera) can significantly influence geochemical gradients around vent openings. Such passive and active biological effects on geochemical processes are of interest to the earth sciences as they can influence the formation of mineral deposits.

Extensive mineral deposition at vent sites in the northeast Pacific has created a habitat where vent organisms live in close intimacy with the processes of deposit formation (Fig. 1). This area is an ideal natural laboratory for observation and experimental study of the interaction of life processes with the formation of mineral deposits. In this paper we describe three on-going investigations of biological influences on mineral deposition. Our approach has been one of combining *in situ* observation and sampling with electron microscopic and mineralogical analyses of preserved specimens. The major aim has been to identify and describe organism-mineral interactions and to develop hypotheses for future experimental and quantitative investigations.

#### **VESTIMENTIFERAN TUBES: SURFACE AND STRUCTURAL EFFECTS**

The most common, and often largest animal found at vents is the tube-worm; these are the famous gutless Vestimentifera with symbiotic bacteria. After frequently observing vestimentiferan tubes partially or completely incorporated into hydrothermal mineral deposits (Fig. 2; also see Koski et al. 1984), we are investigating mechanisms by which tubes are first encrusted by minerals and then eventually entombed in growing deposits. The central question is whether the tubes locally enhance mineral deposition or whether they are simply being engulfed by processes upon which they have little effect. In the laboratory the microenvironment of the worm tube surface is investigated by electron microscopy combined with energy dispersive x-ray analysis. Structural effects such as alteration of vent fluid-seawater mixing, leading to enhancement of mineral deposition within tube worm aggregations are studied *in situ* with a time-lapse camera, by monitoring growth of chimneys associated with Vestimentifera.

##### Processes At The Tube Surface

Samples for electron microscopy of tube surfaces were collected from vents on the southern Juan de Fuca site (Fig. 1) (U.S. Geological Survey Juan de Fuca Study Group 1986). Some of the most striking examples of mineral encrustation on tube surfaces and chimney growth around tubes can be found at this site (Fig. 3a). So called "clear" tubes from a vent where little mineral deposition or encrustation was occurring (Fig. 3b) were compared with samples from vents where occupied tubes were frequently encrusted from the base to near the tube opening. Examination of "clear" tubes with little encrustation revealed a diverse bacterial flora colonizing the tube surface (Fig. 4a). The most abundant members of this flora were sheathed bacteria which frequently had accumulated minute Fe particles in the

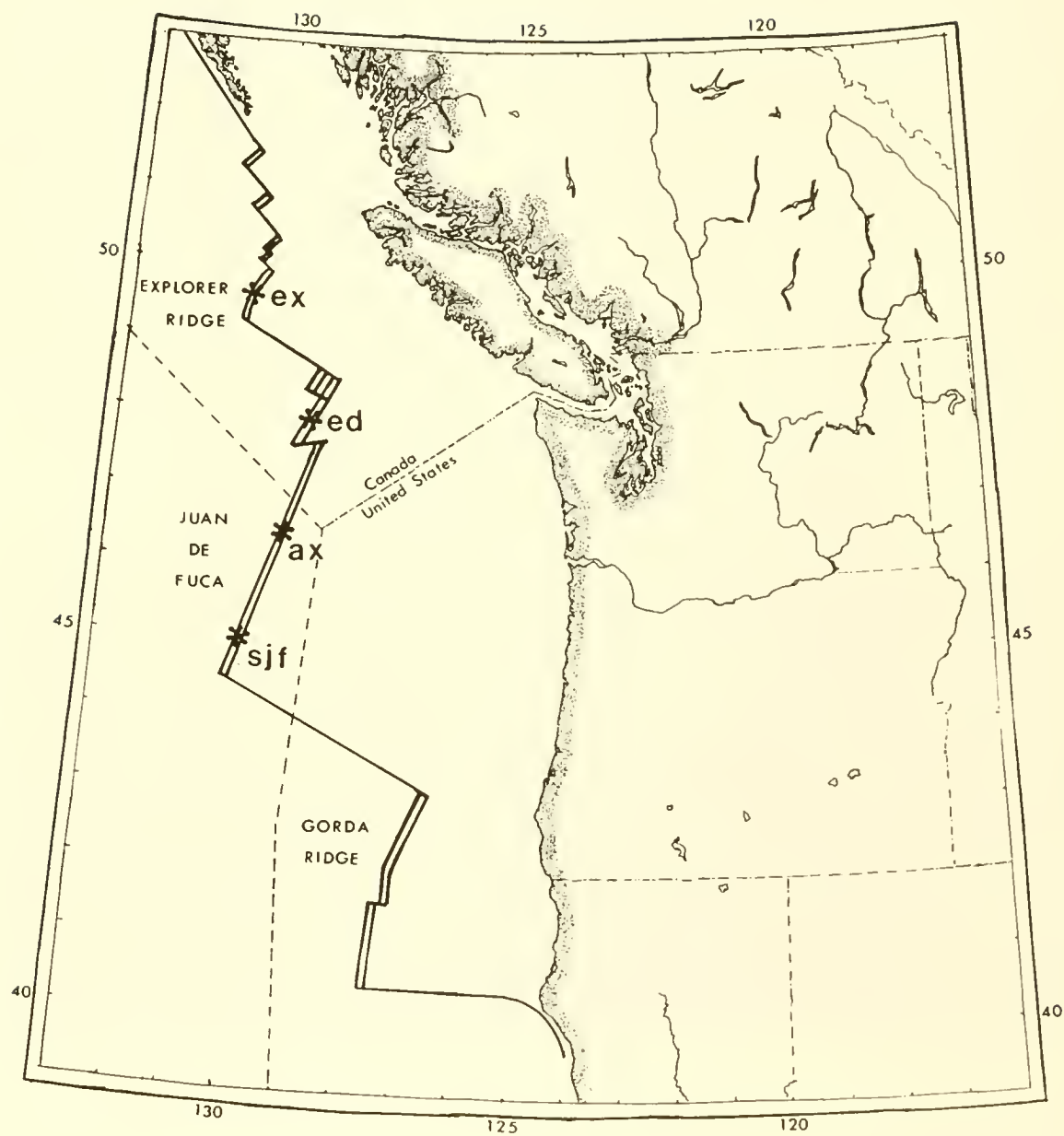


Figure 1. Map of northeast Pacific spreading centers showing hydrothermal sites explored by submersible to date. ex- Explorer Ridge; ed - Endeavor Segment; Juan de Fuca Ridge; ax - Axial Seamont, sjf - Southern Juan de Fuca site.

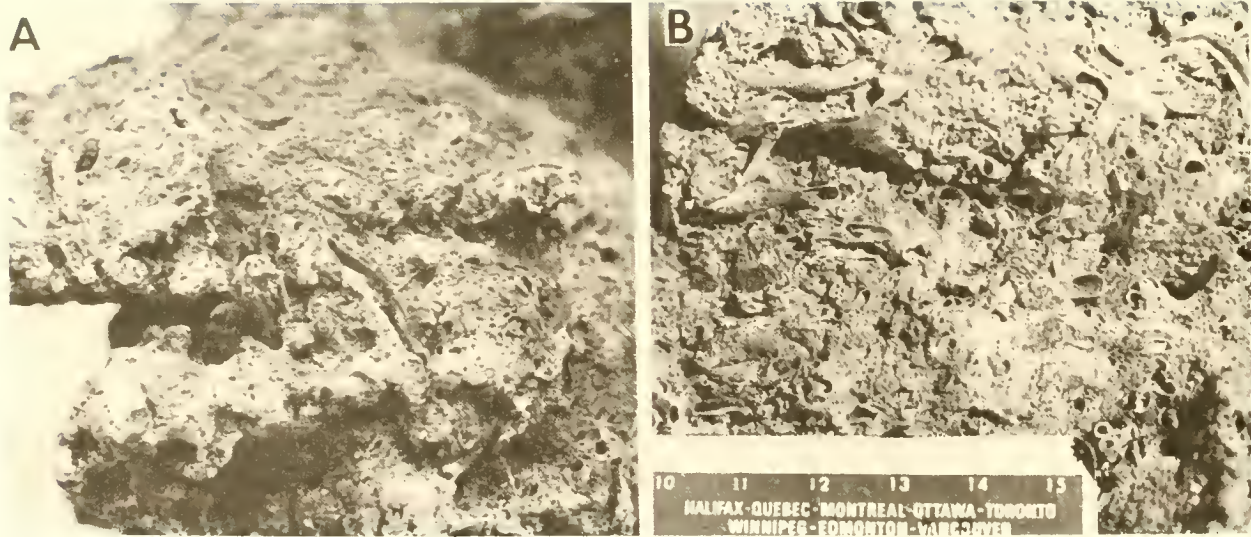


Figure 2. Traces of vent fauna in sulfide chimney sample recovered from Axial Seamount (A, B). Such samples often contain hundreds of fossilized worm tubes embedded in the sulfide matrix. Photo B is a closer view of the sample shown in A (scale in B in cm).

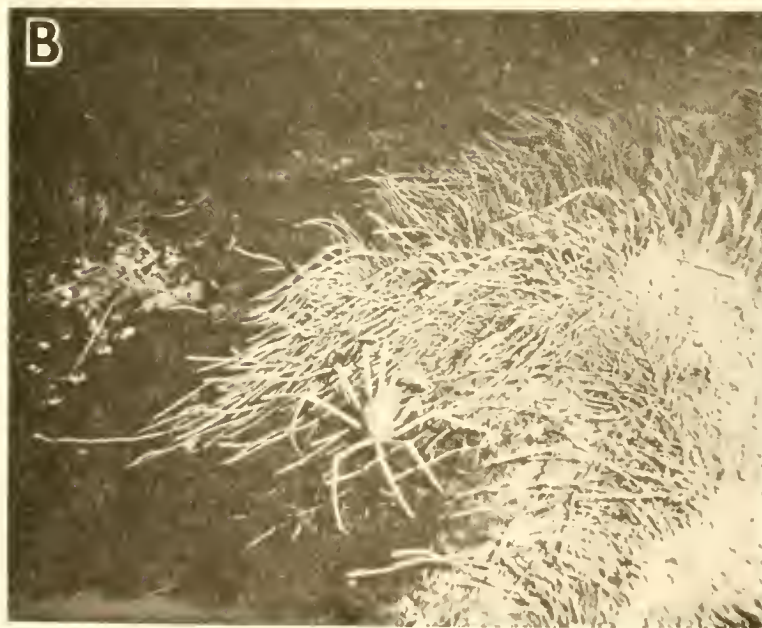


Figure 3. (A) Coalescing of heavily encrusted empty vestimentiferan tubes forms small spires of iron oxide. (B) "Plume Vent" site where encrustation is negligible and tubes are a clear white color.

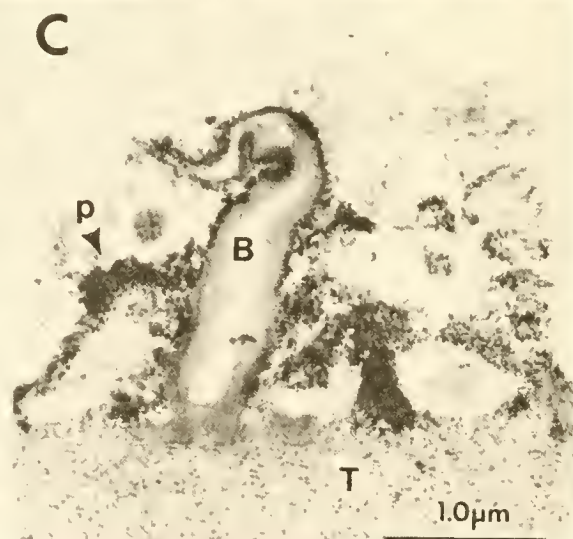
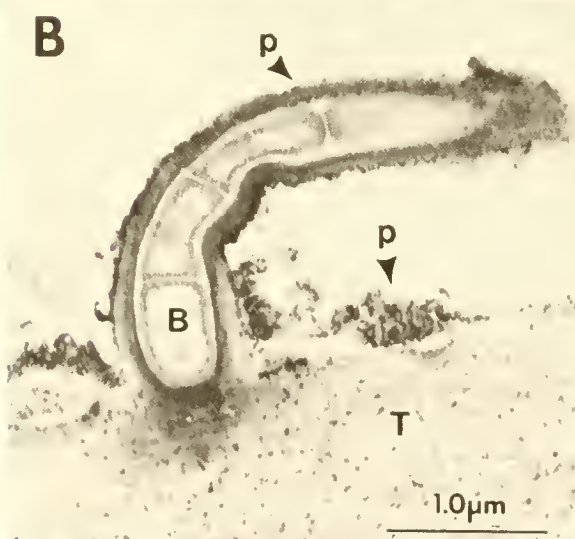


Figure 4. Electron micrographs of vestimentiferan tube surfaces from Plume Vent. (A) SEM photo of tube surface with light colonization by sheathed bacteria; (B) TEM photo showing iron particle (P) accumulation in sheath of bacterium (B) attached to tube surface (T); and (C) Extensive iron particle (P) accumulation in extracellular matrix around bacterium (B) on tube surface (T).

matrix of their sheaths (Fig. 4b and c). This observation later proved important in interpretation of iron-rich encrustations on tubes from sites where mineral deposition was much heavier. Tubes from these areas were encrusted with a red-orange material which qualitative EDS analyses revealed to consist mainly of Fe and P (Fig. 5a). Sheathed bacteria accumulating Fe were abundant on these tubes (Fig. 5b), as were aggregations of sheathed bacteria that formed rounded Fe-rich particles of 6-8 m diameter. Tunnicliffe and Fontaine (1987) have proposed that formation of iron encrustations is initiated by the process observed on the "clear" tubes, that is, accumulation of fine iron particles by the sheathed bacteria. Where sheathed bacteria are more abundant and more closely spaced, as they are on the encrusted tubes, fine Fe particles will begin to accumulate between sheaths and then accumulate in a non-specific way on the growing Fe particle. This type of autocatalytic accumulation of metals following biocatalysis is known from a variety of aquatic habitats. Ghiorse (1984) in a review of Fe and Mn accumulating bacteria describes how iron can associate non-specifically with acidic extracellular polymers (bacterial slime), such that once iron oxides have been formed by microbial biocatalysis further binding and oxidation of iron can occur autocatalytically. The tube-surface microflora and iron encrustations are most developed at sites where iron deposition is heaviest and presumably venting fluids are transporting the most reduced iron. The relationship between microbial growth and ambient iron concentration remains to be investigated.

### Structural Effects

Growth of tube worm assemblages over or adjacent to hot water openings clearly affects the mixing of vent fluid and bottom seawater. Tunnicliffe et al. (1985) used a simple series of point temperature measurements to illustrate the retention of vent fluid within a tube worm thicket. At vents where mineral deposition is significant there are a number of mechanisms by which it can be enhanced within the microenvironment formed by tube worm aggregations. Surface effects such as those described in the preceding section would be magnified since tube structures both provide extensive surface area and retard dilution of metals being transported in vent fluids. Partial retention of venting waters within this microenvironment may also increase cooling of the fluids, further facilitating chemical saturation and precipitation of metals. Unoccupied tubes appear to persist for a long time. Groves of empty tubes seen in a 1984 cruise were still present at the same vent in 1987 (personal communication, Wm. Normark, U.S. Geological Survey, 1987); micro-spires of sulfides were forming around these tubes. Presently this effect is being studied using a time-lapse camera to record the relationship between the location of worm tubes on a growing sulfide mound and the addition of new sulfides to this deposit.

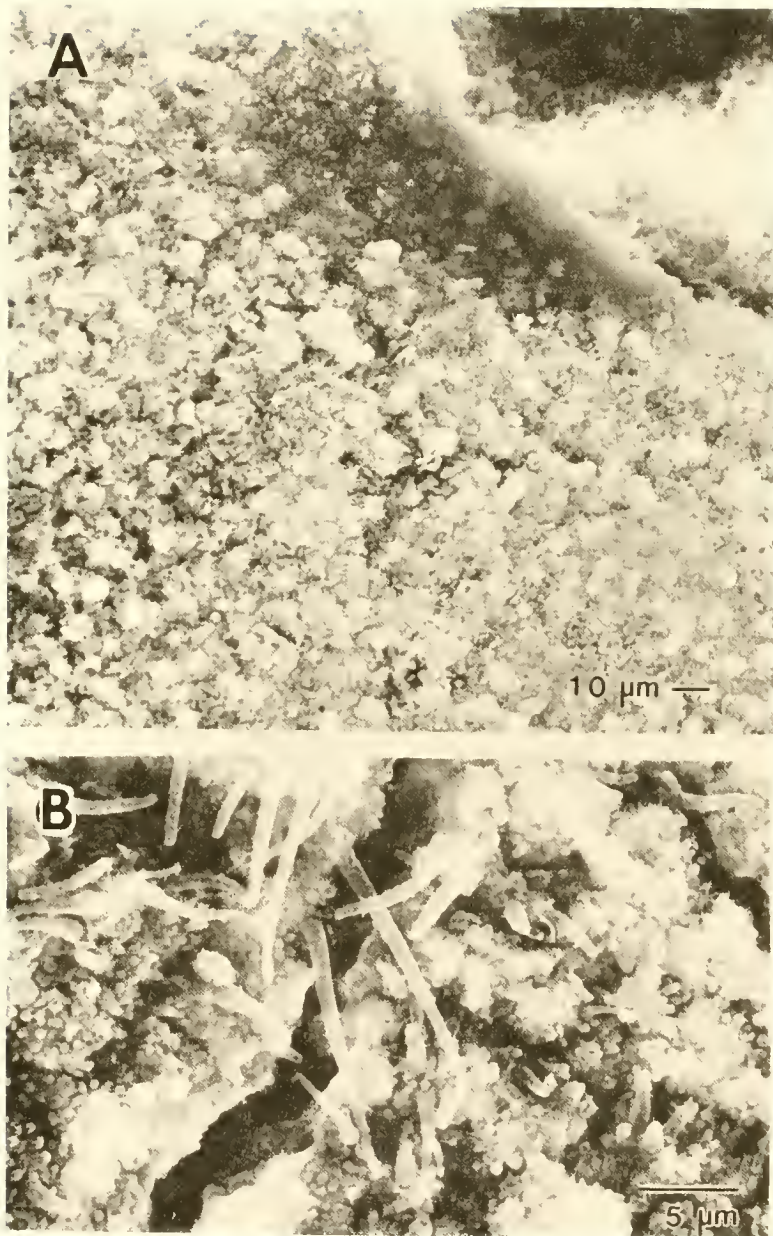


Figure 5. SEM photos of heavy iron oxide encrustation on vestimentiferan tubes: (A) Low magnification view of encrusted tube surface; (B) Surface of fractured encrustation revealing abundance of sheathed bacteria.

## PALM WORM MUCUS: ACCUMULATION OF MINERALS AND TRACE ELEMENTS

The Alvinellidae is a new polychaete family known exclusively from hydrothermal vents (Desbruyères and Laubier 1986). The palm worm, Paralvinella palmiformis (Desbruyères and Laubier), is an alvinellid found in large numbers at most hydrothermal vents in the northeast Pacific. It has a very flexible life habit, adopting a semi-erect posture with its caudal end coiled around vestimentiferan tubes, freely ranging over surfaces of sulfide chimneys, living partially buried in sulfide sediments; it also dwells in muco-particulate tubes on the sides of high temperature smokers much like the pompeii worm of East Pacific Rise vents (Desbruyères and Laubier 1980). Common to all these modes of life is the secretion of large quantities of mucus that has the effect of clearing the worm's epidermal surface of mineral particles that constantly precipitate in the vent environment (Fig. 6a). A protective barrier of mucus remains at all times on the epidermal surface. As mineral particles accumulate a layer of mucus is shed and replaced by newly secreted material (Juniper et al. 1986). Three states of mucus alteration are identifiable in situ and in submersible grab samples of vent fauna (Fig. 6a): (1) a transparent layer of freshly produced mucus with no visible mineral accumulations; (2) a bright yellow layer of mucus containing oxidized iron and large quantities of elemental sulfur; and (3) thick grey or grey-black wrappings of mineral-laden mucus in the process of being shed by the worm. Shed mucus is highly insoluble in seawater and persists for significant periods of time in the vent environment where it continues to accumulate mineral particles, likely until it is incorporated into growing mineral deposits (Juniper et al. 1986, Juniper 1988). It adheres to vestimentiferan tubes (Fig. 6a) and sulfides. Remarkably large quantities of shed mucus have been recovered with vent faunal grab samples. Approximately 25 percent of a 2 kg (wet wt.) biomass sample from a vent on Axial Seamount consisted of palm worm mucus (Tunnicliffe et al. 1985).

### Mineral Particle Accumulation

Organic matter generally comprises less than 10% of the total mass of shed mucus. The most significant components are elemental sulfur and mineral particles (Fig. 6b). Samples containing up to 60% elemental sulfur are not uncommon (Juniper et al. 1986, Juniper unpublished data). The origin of the mucus elemental sulfur is not known. Histological examination has so far failed to reveal internal sulfur accumulation in the worm or evidence of sulfur transport to the epidermal surface. A direct linear relationship between mucus carbon and sulfur contents (Juniper et al. 1986) suggests that an organic/elemental sulfur matrix develops before or soon after the mucus is secreted. The carbon and sulfur contents are progressively diluted as mineral particles are occluded, to the point where the material no longer

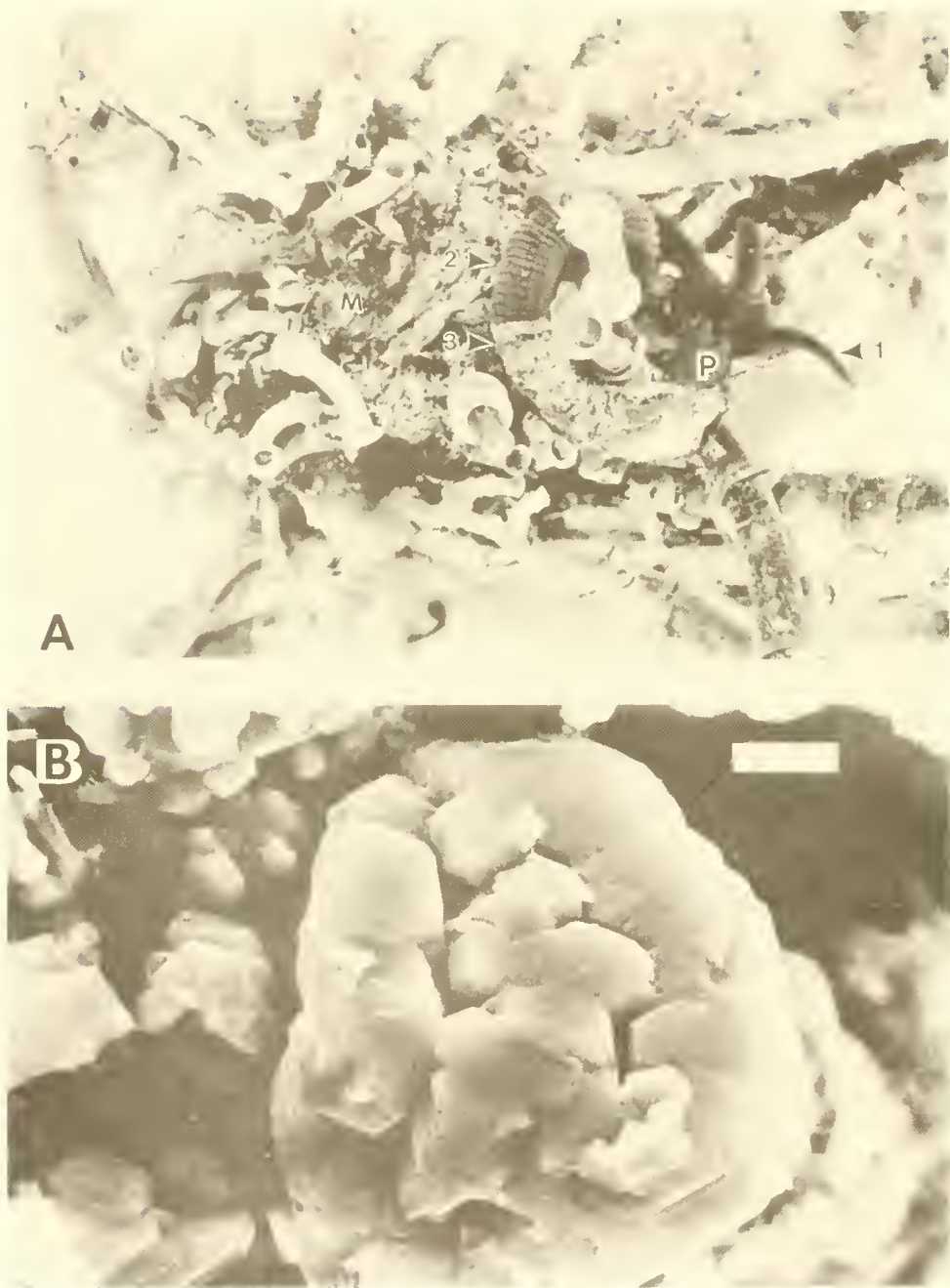


Figure 6. (A) Palm worm (P) in vent faunal grab collected by submersible. Three forms of mucus are visible: (1) branchiae are coated in transparent mucus; (2) upper and lower body segments are coated in an iron oxide rich, orange colored mucus; and (3) gray mucus, laden with mineral particles, is wrapped around the worm's midsection. Quantities of shed gray mucus (m) adhere to vestimentiferan tubes in the sample. (B) Aggregate of chalcopyrite crystals occluded in shed mucus.

resembles mucus. A variety of sulfide and sulfate minerals have been identified by X-ray diffraction and corresponding mineral grains can be located in mucus using a scanning electron microscope equipped with an energy dispersive X-ray analyzer. The quantitative contribution of mucus-aggregated minerals to the mass of deposits forming in the palm worm's immediate environment is not yet clear. The next stage of this investigation will be directed toward acquiring quantitative data on mucus production by palm worm populations and developing a means of identifying traces of mucus within consolidated mineral deposits.

Mucus produced by tube-dwelling palm worms has a somewhat different fate in the vent environment. Palm worms that colonize smoker chimneys use secreted mucus to aggregate mineral particles into tubes which are attached to the sides of these edifices (Fig. 7). How long such tubes remain inhabited has not been established, although abandoned tubes are frequently observed. Tube building palm worms appear to be the pioneer colonizers of new smoker chimneys. A recent return visit to vents on Axial Seamount has revealed year-old smoker chimneys to be extensively covered in palm worm tubes (V. Tunnicliffe, personal observation). Extensive coating of chimney walls by mucus-cemented minerals may reduce wall porosity enough to effect chimney growth and mineralization. Haymon (1983) has pointed out the importance of wall porosity in the transition from sulfate dominated to sulfide dominated stages in the growth of black smoker chimneys. Repeat visits to vents at 13° N EPR have revealed tube building activity by the pompeii worm to affect development of smoker chimneys (Fustec et al. 1987). The influence of palm worm tube building on the growth and evolution of smoker chimneys is presently being monitored *in situ* with a time-lapse camera. Rates of anhydrite accumulation, sulfide consolidation, palm worm colonization, and mucus cycling will be studied over the course of a year.

#### Trace Element And Heavy Metal Accumulation

In addition to mineral particle aggregation, palm worm mucus has two other geochemically interesting properties. Many samples have been found to contain unusually high concentrations of uranium, some in excess of 100 mg/kg (Juniper et al. 1986) compared to the average crustal abundance of 3 mg/kg and vent fluid and seawater concentrations of <0.5 to 3.00 mg/kg (Juniper et al. 1986). Uranium is known to be adsorbed and complexed by organic material under reducing or mild hydrothermal conditions. Similar uranium concentrations have been observed in the Galapagos hydrothermal mounds (Lalou et al. 1980). Another unusual property of the mucus is that its muco-polysaccharide matrix contains significant quantities of thiolic proteins that preliminary analysis suggest are metal-binding proteins. The exact nature of these proteins and the metals that they react with remain to be determined. The interesting point is that the

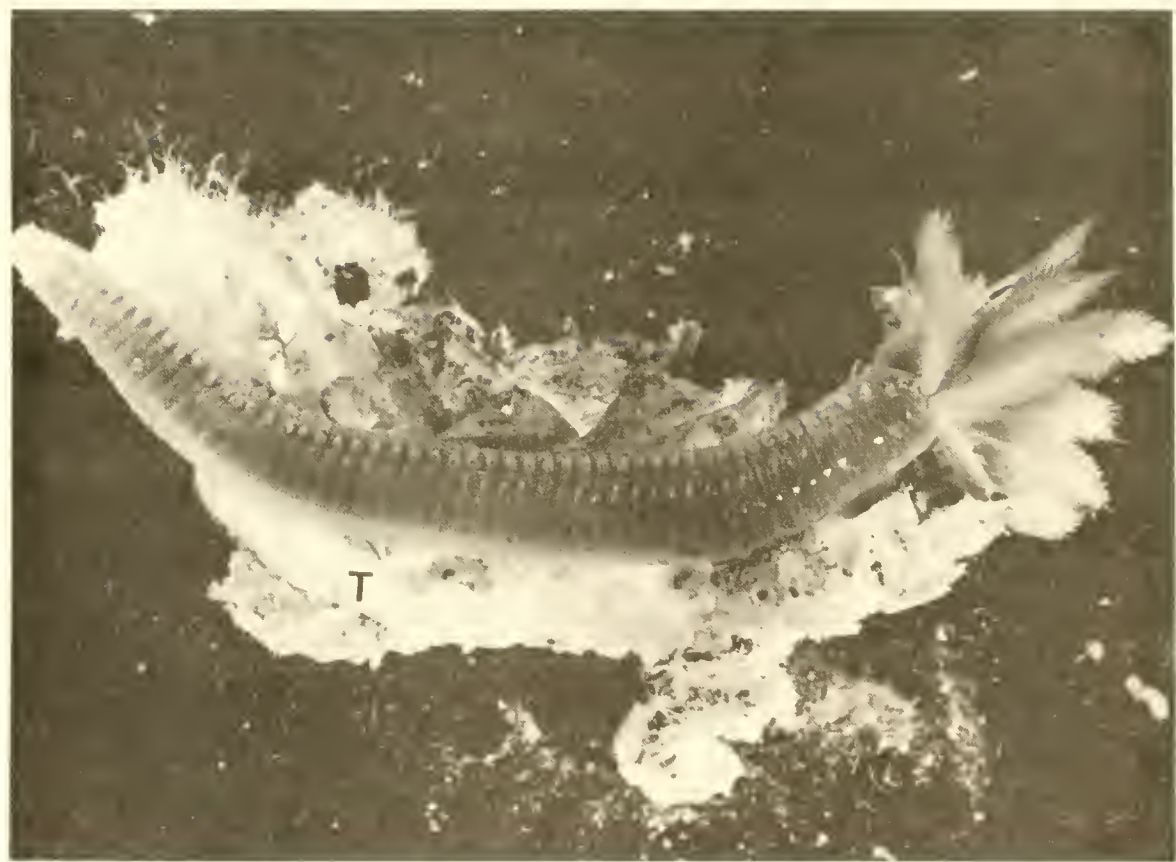


Figure 7. Tube-dwelling palm worm removed from its muco-particulate tube (T).

worm is possibly secreting significant quantities of proteins into the vent environment that actively complex heavy metals such as Cd, Zn and Cu which are locally very abundant.

#### FILAMENTOUS FE/SI DEPOSITS: MINERAL OR MICROBIAL ORIGIN?

Orange-red deposits of iron/silica are formed by low-temperature venting at a number of sites in the northeast Pacific and along the length of the EPR (Juniper and Fouquet 1988). Vent-specific organisms such as *Vestimentifera*, alvinellid polychaetes and bivalves are not usually found in association with this type of venting, as the fluids contain little or no H<sub>2</sub>S, the major energy source for vent faunal-microbial symbioses. Although well known to geologists this form of hydrothermal activity has received little attention in the literature, likely because of the highly oxidized nature of the venting fluids, the lack of economically interesting minerals and the total absence of vent fauna.

Iron/silica deposits form either on top of sulfides deposited by previous higher temperature venting or directly on basalt where they can occur as chimney structures (Fig. 8). The iron is mainly in a highly oxidized form, giving the deposits their distinct orange-red color. Associated silica is an amorphous oxide, Opal A. An active 1.5 m high chimney on Explorer Ridge was composed of 73 percent silica, 7 percent iron, and 1.3 percent organic carbon along a number of minor constituents (Juniper and Fouquet 1988). The chimney was emitting a 27°C fluid enriched in Fe and Si over ambient seawater but containing no detectable H<sub>2</sub>S (Tunnicliffe et al. 1986). In a routine scanning electron microscopic survey of geological samples from Explorer Ridge, we discovered this chimney to be formed of hollow microbial-like filaments. This observation together with the presence of organic carbon led to an investigation of the possible role of micro-organisms in mineral precipitation. Work to date has been limited to re-examination of geological samples from the northeast Pacific and the EPR.

All examined samples were porous and consisted of aggregates of branching filaments of iron frequently covered in amorphous silica (Opal A) (Fig. 9). Frequently distinct mineralogical zonation was visible, indicating local variation in redox conditions during deposit formation. Consistent among all samples was the fact that iron was deposited in a filamentous arrangement before the deposition of silica. Filaments of iron were occasionally observed to be coated in concentric layers of amorphous silica (Fig. 9e). Silica often filled inter-filament spaces as well, further consolidating the deposits.

No strictly mineralogical explanation satisfactorily accounts for the filamentous morphology of these deposits. Spherical and tubular structures are known to form during the



Figure 8. Iron oxide deposit on Axial Seamount. Deposit consists of metalliferous sediment and small edifices.

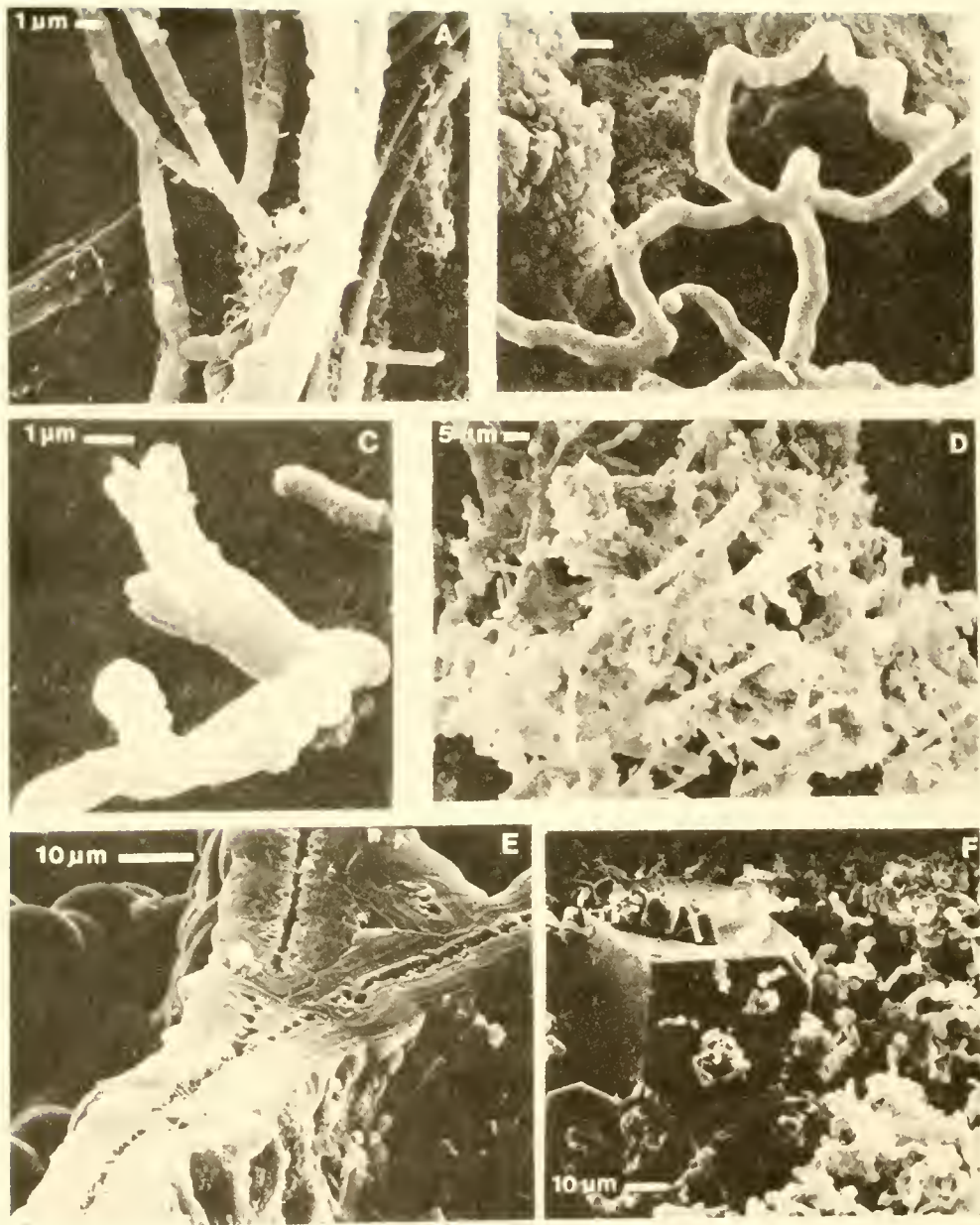


Figure 9. Scanning electron micrographs of dilamentous iron/silica deposits: (A-C) Filament morphology varies from long and short branching filaments to hyphae-like filament networks; (D) Low magnification view of sample from filamentous Fe/Si deposit; (E) Longitudinal section of filament coated in concentric layers of silica; and (F) Short, simply branching filaments with cubic crystal of pyrite.

crystallization of siliceous gels (Lebedev 1967), but the solutions forming such gels are dense viscous liquids of much greater silica concentration than modern hydrothermal fluids. As well, in the present example the formation of filamentous silica is directly linked to the morphology of the underlying support of iron-oxide filaments upon which the silica precipitates. The formation of dendrites, filaments of iron-oxide, also requires the presence of a solid support. Thus, it is difficult to explain the upward growth of filamentous iron/silica deposits without invoking the prior existence of a filamentous structure that would have acted as a support for mineral precipitation. The similarity of these filaments in size and shape to those produced by bacteria has led us to consider how the deposits could have formed within a filamentous structure provided by micro-organisms.

Filamentous micro-organisms are very abundant around hydrothermal vents, as this morphology is common in groups of sulfur and metal-oxidizing bacteria (Jannasch and Wirsen 1981). Branching filaments are best known among the iron and manganese oxidizing taxa. It is quite conceivable that mat-like aggregations of iron-accumulating bacteria could have existed at the sites where the described deposits were formed. Growth of microbial mats around vent openings would result in the diffusion of hydrothermal fluid through the filamentous structure. A combination of bio-catalysis and autocatalysis similar to that proposed above for vestimentiferan tubes could lead to iron accumulation on the filaments. Mineralogical zonation observed in the deposits could result from differential mixing of vent fluid and ambient seawater with the mat structure (Juniper and Fouquet 1988). Similar physico-chemical gradients have been observed in seafloor mats of the filamentous sulfur bacteria Beggiatoa (Nelson et al. 1986; Moller et al. 1985).

The precipitation of amorphous silica from hydrothermal fluid requires more than a structural support. The inorganic formation of Opal A is rare because it requires a medium saturated in silica (Bertine and Keen 1974, Kastner 1979, Wollast 1974). While hydrothermal fluids are rich in silica, cooling by mixing with seawater does not normally result in silica precipitation because the resulting dilution prevents saturation (Wollast 1974). Substantial conductive cooling is necessary to precipitate silica from hydrothermal fluids. The microenvironment provided by a porous filamentous structure, partially filled by iron-oxide precipitation could sufficiently limit mixing and allow enough conductive cooling to permit silica saturation and Opal A precipitation to occur. A similar process is likely responsible for in-filling of porous sulfide chimneys by amorphous silica. The fact that silica deposition occurs consistently after iron suggests that it is the slower process.

We have yet to sample the living micro-organisms at vents where these iron/silica deposits are forming, and no traces of bacterial cellular constituents have been observed in existing samples. Nonetheless, the precipitation of iron and silica on an existing filamentous structure offers an explanation of the nature of these deposits. Further study of this problem will require *in situ* sampling to verify the presence or non-presence of living microbial filaments.

## OVERVIEW

Vent organisms are able to both actively and passively influence mineral deposition. Active effects, that is direct chemical transformation of mineral forming elements, result from organism metabolism and detoxication. Passive effects are produced by the physical presence of biological structures and debris which trap mineral particles, control geochemical gradients and provide surfaces for mineral precipitation. In the few examples we have studied to date, passive effects appear to have a greater quantitative influence on mineral deposition than active effects. Even where possible active effects were identifiable, such as in iron deposition by bacteria on worm tubes or within filamentous mats, they occurred in conjunction with surface or structural effects that likely greatly enhanced their quantitative significance.

Biological effects are most evident at sites where mineral deposition is the greatest, rather than where biomass is highest. In fact, biomass is usually greater where little deposition is occurring and physico-chemical conditions are less severe. Thus, the importance of biomimetication appears to depend on the potential of a vent to deposit minerals, which is likely related to the properties of vent fluids (Tunnicliffe and Fontaine 1987).

The intimate involvement of vent organisms with mineral deposition has both positive and negative effects on their ability to survive and reproduce. Negative effects are the most apparent. Mineral particle fouling of branchial surfaces has been observed in *Vestimentifera* (unpublished observation) and probably affects the respiratory surfaces of most vent organisms. The abundance of mineral particles likely poses detoxication problems for grazing and deposit feeding animals that ingest a variety of metals along with particulate organic material (Tunnicliffe et al. 1985). Although entombment of live vent organisms by mineral deposition has never been observed, this process may be an important cause of mortality for sessile organisms in areas of heavy mineral deposition. A certain degree of mineralization can have fortuitous positive effects. There are noticeably fewer signs of predation in northeast Pacific *vestimentifera* populations that have visibly mineralized tubes (V. Tunnicliffe, unpublished observation). The major predator of these tube-worms

is a large majid crab that ingests the tubes along with soft body parts (Tunnicliffe and Jensen 1987).

All examples discussed in this paper are from sites where hydrothermal venting occurs on a sediment-starved volcanic terrain. Even the largest mineral deposits found in this setting are much smaller than some recently discovered sediment-hosted deposits where hydrothermal fluids pass through a seafloor sediment cover before venting into the water column. Physical and chemical interaction between sediments and hydrothermal fluids forms and traps minerals within the sediment blanket. In this environment biological influences on mineral deposition will clearly be insignificant compared to the effect of the sediments. Nonetheless, it is interesting to point out that some of the mechanisms by which sediment cover enhances mineral deposition - restriction of vent fluid-seawater mixing, abundance of solid surfaces for mineral nucleation, etc. - are similar to those proposed for biological structures.

#### ACKNOWLEDGMENTS

In addition to support from the National Undersea Research Program, this work was supported by the University of Victoria, the Natural Sciences and Engineering Research Council (Canada), the Department of Fisheries and Oceans (Canada), IFREMER (France), and the French Ministère des Relations Extérieures. We thank C.L. Singla for preparation of specimens for electron microscopy and Tom Gore for photographic plates.

#### LITERATURE CITED

Bertine, K. K. and J. B. Keene 1974. Submarine barite-opal rocks of hydrothermal origin. Science, Vol. 188, No. 4184, pp. 150-152.

Desbruyères, D. and L. Laubier. 1986. Les Alvinellidae, une famille nouvelle d'annélides polychètes inféodés aux sources hydrothermales sous-marines: systématique, biologie et écologie. Can. J. Zool., Vol. 64, No. 10, pp. 2227-2245.

Desbruyères, D. and L. Laubier. 1980. Alvinella pompejana gen. sp. nov., Ampharetidae aberrant des sources hydrothermales de la ride Est-Pacifique. Oceanologica Acta, Vol. 3, No. 3, pp. 267-274.

Fustec, A., D. Desbruyères, and S. K. Juniper. 1987. Deep-sea hydrothermal vent communities at 13° N on the East Pacific Rise: Microdistribution and temporal variations. Biol. Oceanogr., Vol. 4, No. 2, pp. 121-164.

Ghiorse, W. C. 1984. Biology of iron- and manganese-depositing bacteria. Ann. Rev. Microbiol., Vol. 38, pp. 515-550.

Haymon, R. M. 1983. Growth history of hydrothermal black smoker chimneys. Nature, Vol. 301, No. 5902, pp. 695-698.

Johnson, K. S., C. L. Beehler, C. M. Sakamoto-Arnold, and J. J. Childress. 1986. In situ measurements of chemical distributions in a deep-sea hydrothermal vent field. Science, Vol. 231, No. 4742, pp. 1139-1141.

Juniper, S. K. 1988. Geochimie et ecologie d'un microenvironnement hydrothermal: Les secrétions de mucus de Paralvinella palmiformis. Oceanologica Acta, Special Issue No. 8, pp. 167-172.

Juniper, S. K., J. A. J. Thompson, and S. E. Calvert. 1986. Accumulation of minerals and trace elements in biogenic mucus at hydrothermal vents. Deep-Sea Res., Vol. 33, No. 3, pp. 401-412.

Juniper, S. K., and Y. Fouquet. 1988. Filamentous iron-silica deposits from modern and ancient hydrothermal sites. The Canadian Mineralogist, Vol. 26, Part 3, pp. 859-869.

Kastner, M. 1979. Silica polymorphs. In: Reviews in Mineralogy, Vol. 6, Marine Minerals. Mineralogical Society of America, Washington, DC. Chapter 3, pp. 99-109.

Koski, R. A., Clague, D. A. and E. Oudin 1984. Mineralogy and chemistry of massive sulfide deposits from the Juan de Fuca Ridge. Geol. Soc. Amer. Bull., Vol. 95, No. 8, pp. 930-945.

Lalou, C., and E. Brichet. 1980. Anomalously high uranium contents in the sediment under Galapagos hydrothermal mounds. Nature, Vol. 284, No. 5753, pp. 251-253.

Lebedev, Lev M. 1967. Metalloids in Endogenic Deposits. New York, N.Y., Plenum Press. 297 pp.

Moller, M. M., L. P. Neilson, and B. B. Jergensen. 1985. Oxygen responses and mat formation by Beggiatoa spp. Appl. and Environ. Microbiol., Vol. 50, No. 2, pp. 373-382.

Nelson, D. C., B. B. Jergensen, and N. P. Revsbech. 1986. Growth pattern and yield of chemoautotrophic Beggiatoa sp. in oxygen-sulfide microgradients. Appl. and Environ. Microbiol., Vol. 52, No. 2, pp. 225-233.

Tunnicliffe, V., and A. R. Fontaine. 1987. Faunal composition and organic surface encrustations at hydrothermal vents on the southern Juan de Fuca Ridge. J. Geophys. Res., Vol. 92, No. B11, pp. 303-311.

Tunnicliffe, V., S. K. Juniper, and M. E. de Burgh. 1985. Biological communities of the Juan de Fuca hydrothermal vents. In: M. L. Jones (ed.), Hydrothermal Vents of the Eastern Pacific: An Overview. Biol. Soc. of Washington Bull. 6, pp. 453-464.

Tunnicliffe, V. and R. G. Jensen. 1987. Distribution and behavior of the spider crab Macroregonia macrochira Sakai (Brachyura) around the hydrothermal vents of the northeast Pacific. Can. J. Zool., Vol. 65, No. 10, pp. 2443-2449.

U.S. Geological Survey Juan de Fuca Study Group. 1986. Submarine fissure eruptions and hydrothermal vents on the southern Juan de Fuca ridge: Preliminary observations from the submersible Alvin. Geology, Vol. 14, No. 10, pp. 823-827.

Wollast, R. 1974. The silica problem. In: The Sea, Volume 5, New York, N.Y., pp 359-392.

## GULF OF MEXICO HYDROCARBON SEEP ECOSYSTEM STUDIES

James M. Brooks<sup>1</sup>, Eric N. Powell<sup>2</sup>, Mahlon C. Kennicutt II<sup>3</sup>,  
Robert S. Carney<sup>2</sup>, Ian R. MacDonald<sup>2</sup>, Susanne J. McDonald<sup>1</sup>,  
Robert R. Bidigare<sup>1</sup>, and Terry L. Wade<sup>1</sup>

1 - Geochemical and Environmental Research Group  
Texas A&M University  
College Station, TX 77840

2 - Department of Oceanography  
Texas A&M University  
College Station, TX 77840

3 - Coastal Ecology Institute  
Louisiana State University  
Baton Rouge, LA 70803

### ABSTRACT

The northern Gulf of Mexico continental slope is the site of a number of unique discoveries in the last few years. Active seepage of oil to the sea surface has been observed in the Green Canyon-184/185 and 190/234 areas. In at least one of these areas, extensive molecular and isotopic analyses have demonstrated that the petroleum in shallow sediments and surface oil slicks is derived from reservoirs more than 2500 m deep in the subsurface. Ten locations on the Louisiana slope (530 to 2400 m water depth) have currently been identified that contain either biogenic or thermogenic gas hydrates in shallow sediments (<8 m). Analyses of bitumens from several thousand cores from the continental slope suggest that seepage is a widespread phenomena on the Gulf of Mexico continental slope. This seepage drives large populations of chemosynthetic organisms. A number of new species of tube worms and bivalves are being described from the trawl and submersible collections at these sites.

### INTRODUCTION

The northern Gulf of Mexico continental slope has been the site of a number of recent discoveries that have dramatically altered our understanding of chemical, biological and geological processes on the continental slope. The Geochemical and Environmental Research Group at Texas A&M University reported the first occurrence of thermogenic gas hydrates in oil-stained cores in deep ocean sediments in 1984 (Brooks et al., 1984). Trawling in these areas has identified tube worms and bivalves containing

chemosynthetic, bacterial endosymbionts (Kennicutt et al., 1985; Brooks et al., 1985, 1987a,b). These discoveries significantly expand the geographic area of the deep ocean where one might expect to encounter dense populations of vent-type taxa. Subsequent studies on the upper Gulf of Mexico continental slope using submersibles and surface ships have:

- (1) Identified chemosynthetic organisms or their remains (either tube worms, mussels and/or clams) at 17 northwestern Gulf of Mexico continental slope sites (Fig. 1);
- (2) Confirmed, based on enzyme activities, elemental sulfur content and electron microscopy, that tubeworms and clams from these sites do contain chemoautotrophic, bacterial endosymbionts (Brooks et al., 1987b);
- (3) Found a mussel that is potentially capable of utilizing methane as its sole carbon and energy source, the first demonstrated symbiosis between a methanotrophic bacteria and an animal (Childress et al., 1986);
- (4) Identified shallow seismic "wipe-out" zones as high probability sites for chemosynthetic ecosystems (Fig. 2);
- (5) Shown that active oil seepage is associated with all of the chemosynthetic ecosystems described on the Gulf of Mexico slope (Fig. 3);
- (6) Demonstrated that carbon, nitrogen and sulfur isotopes can be useful in differentiating heterotrophic, sulfur-based and methane-based ecosystems (Brooks et al., 1987b);
- (7) Confirmed the transfer of carbon from the chemosynthetic organisms to background heterotrophic organisms;
- (8) Discovered ten gas hydrate and several active oil seepage locations in the Gulf of Mexico; and,
- (9) Determined that shell beds are being produced in and around areas of petroleum seepage.

## METHODS

Three series of dives have been conducted at the hydrocarbon seep communities. The first six dives aboard

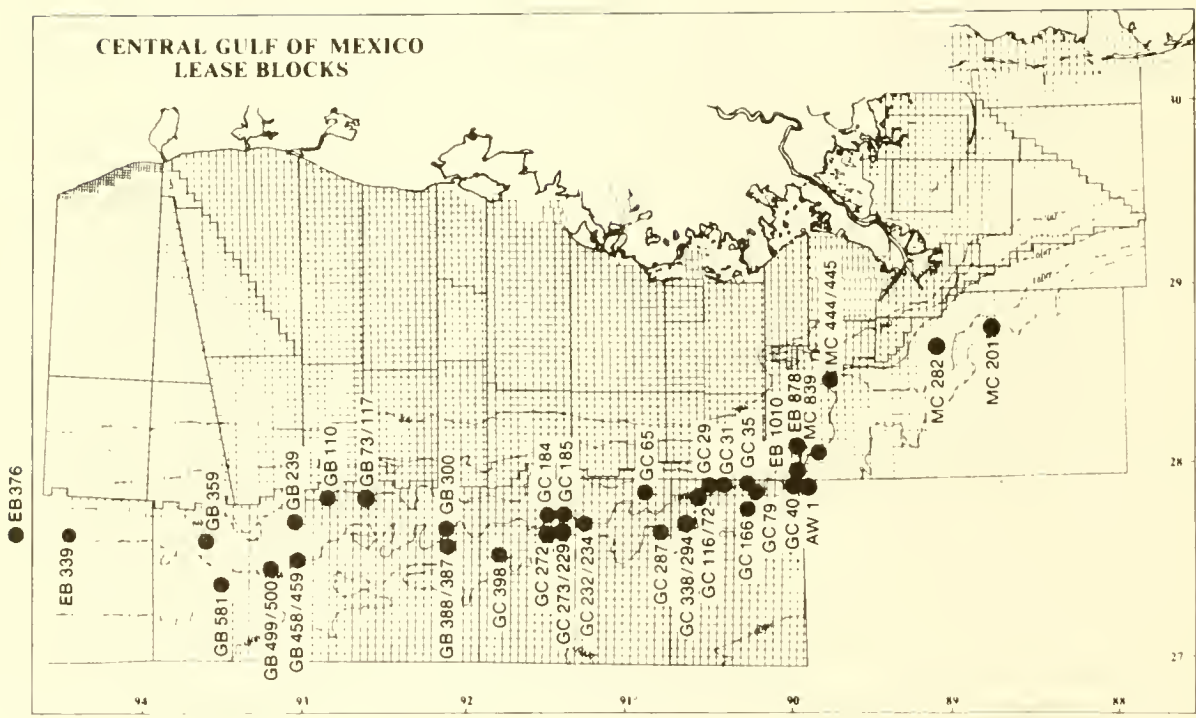


Figure 1. Locations of seismic "wipe-out" zones on the upper Gulf of Mexico continental slope. Trawling at these sites have indicated that at least 17 of these sites contain chemosynthetic organisms or their remains (e.g., tube worms, bivalves and/or mussels).

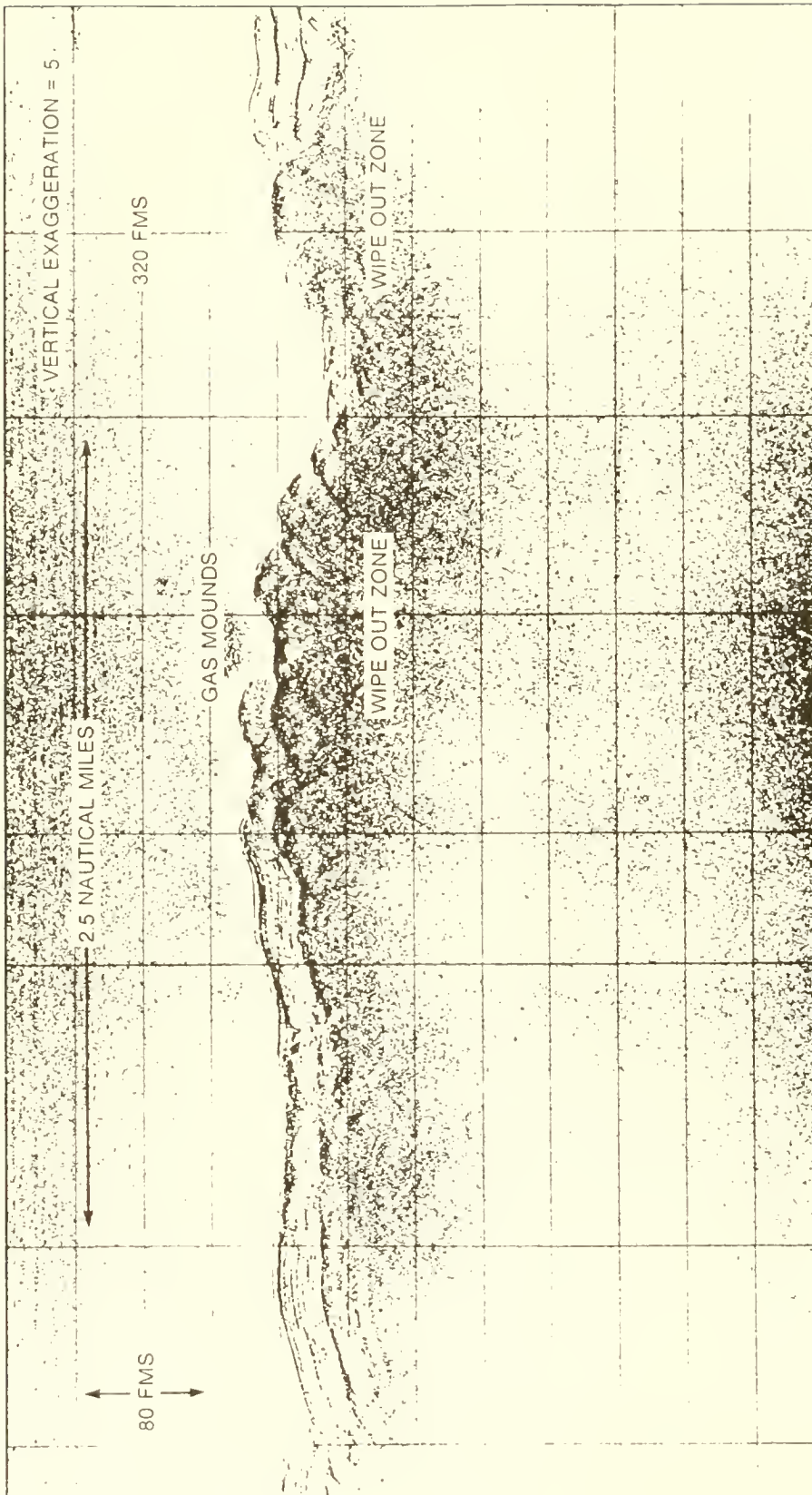


Figure 2. Typical seismic "wipe-out" zone in the Gulf of Mexico. These areas are characterized by oil seepage, gas hydrates and/or gas-charged sediments. These are also the sites of all known chemosynthetic ecosystems in the Gulf of Mexico.

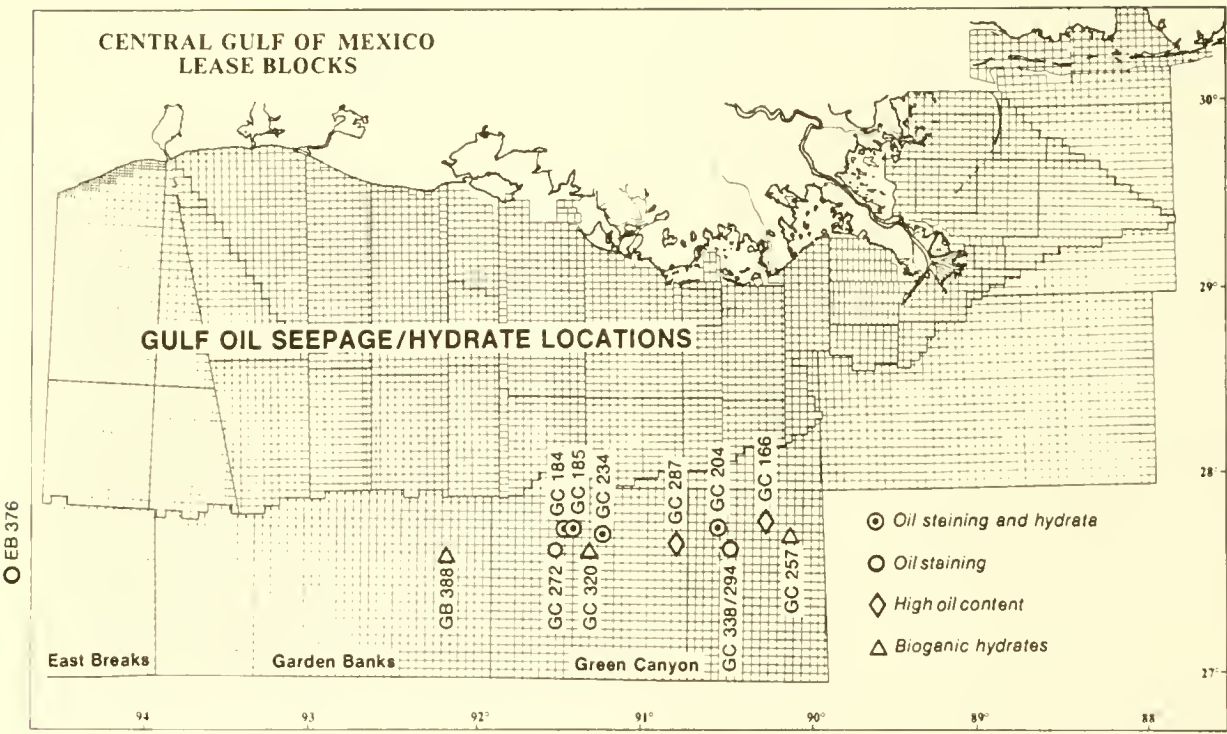


Figure 3. Known sites of oil seepage and gas hydrates in the Gulf of Mexico as identified by the Geochemical and Environmental Research Group at Texas A&M University. Most of these sites are associated with chemosynthetic ecosystems and shallow seismic "wipe-out" zones.

the Johnson Sea Link were funded by the Mineral Management Service (MMS) in September 1986. These dives were followed by a larger survey using the NR-1 (March 1987). Based on these results, the National Undersea Research Program (NURP) funded a series of dives (Dives 2053-2077) in June 1987 aboard the Johnson Sea Link. The goals of these dives were continued studies to refine the description of the distribution and abundance of organisms around the seep sites; description of the sediment, water and hydrocarbon chemistry around the animals; and documentation of the importance of chemosynthesis to these communities using biochemical, physiological and isotopic methods. The ecological components of the Sea-Link series of dives were designed to describe the distribution of organisms within these ecosystems and the factors controlling the observed distributions.

## RESULTS AND DISCUSSION

### Ecology (Including Isotopes)

Four sites have been intensively surveyed by the Johnson Sea Link and a broader regional survey was conducted by the NR-1. The Johnson Sea Link dives produced 87 video tapes (20 minute tapes) of faunal transects and of assemblage structure. Eighteen (18) rolls of 35 mm film were taken to provide high-resolution spatial data. At present, data from Dives 2052 to 2056 have been analyzed and work is progressing on other samples.

Significant progress was made in better understanding the relationship between background, heterotrophic fauna and chemosynthetic fauna. Progress in this area is one of the most exciting aspects of the NURP-sponsored Johnson Sea Link cruise. The mussel and tubeworm clumps form distinct assemblages which are exploited by "background" browsers and predators. Due to the relative ease of sampling the mussel assemblages, the best information is currently available about this system (Fig. 4). Both sessile suspension feeders (gorgonians), epifaunal browsers (urchins) and predators can derive carbon from the chemosynthetic community.

The composition and spatial distribution of the faunal assemblages in the seep area were found to be more complex than previously suspected. Whereas it is increasingly clear that methane and petroleum support and regulate these communities, why the different assemblages are distributed as they are over a topographically complex landscape is not clear. On a smaller scale, it is not known what controls variations within assemblage clumps. However, there appear to be important ecological differences between the tubeworm and mussel assemblages. High mussel cover density is significantly correlated to methane levels in the water

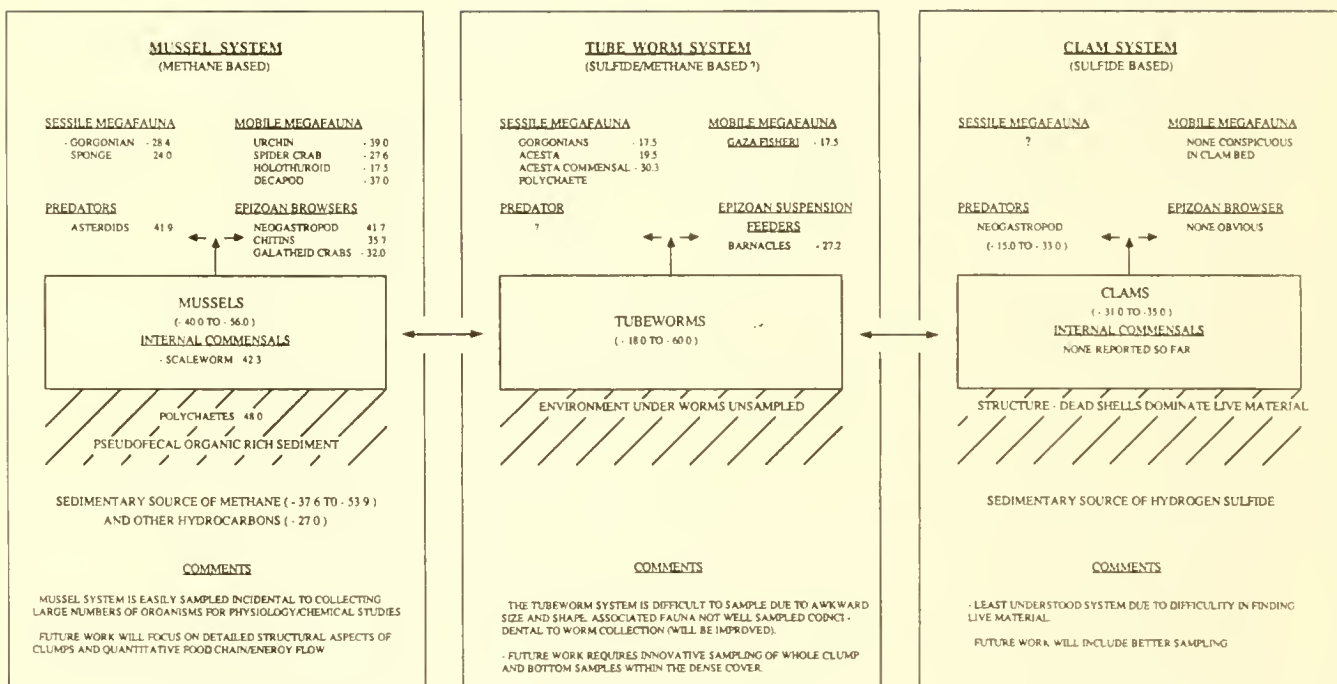


Figure 4. Initial isotopic measurements on the 1987 Johnson Sea Link cruise samples showing relationships between system components. Values represent carbon isotope values in per mil (‰) relative to the PDB standard.

column. Tubeworm cover does not show a significant correlation with methane concentrations, but it does correlate with extractable organic material (EOM) in the sediments; a pattern not shared by mussels. In both cases (mussels-methane and tubeworms--extractable organic compounds), the significant correlation is localized to a radius of less than 7.5 m from the high methane or EOM sites. The EOM is predominantly liquid petroleum.

Observations made during the June 1987 dive series showed that the spatial variation of the various assemblages was greater than anticipated from earlier work. At least five basic assemblage types were encountered: mussel beds, tube worm clumps, clam beds, epifaunal brachiopod-solitary coral assemblages, and gorgonian fields. In some instances, some of these assemblages overlapped in space, and initial isotopic data suggests some shared dependence upon chemosynthetic sources.

### Chemical Studies

Twelve discrete streams of gas bubbles were collected and analyzed. As a percent of C1 to C5 hydrocarbons, all gases collected were predominantly methane (Table 1). Other than the hydrate, methane accounted for more than 94% of the C1 to C5 hydrocarbon gases. The hydrate gases contained ~ 30% C2 to C5 gases. The highest percentage of methane gas (99.4%) and the second isotopically lightest gas (-52.9 ‰) was collected at GC-272. In general the isotopically heavier gases were collected at GC-184 and GC-234, but a substantial range in values was observed (-37.6 to -53.9 ‰). The gases sampled as discrete streams of gas bubbles were a mixture of thermogenic and biogenic gases. Analyses are not complete enough to evaluate variations in mussel tissue carbon isotopic composition as a function of variations in the source methane carbon isotopic composition.

### Hydrocarbon Metabolism in Seep Organisms

A variety of seep organisms (including mussels, clams, tubeworms and neogastropods) were surveyed for evidence of mixed function oxidase (MFO) mediated hydrocarbon metabolism (Tables 2, 3 and 4). Not surprisingly, mussels exhibited much higher MFO activity than did the other species. Mussels live in closer contact with active petroleum seepage than other species. Of the mussel tissues assayed (gills, mantle, food, digestive gland and gonad), only the gills exhibited significant MFO activity. This is very unusual in molluscs, since MFO activity normally is concentrated in their digestive glands. The gills are also the site where the methylotrophic symbiotic bacteria are located.

Table 1. Molecular and carbon isotopic compositions of bubbling gas seeps collected near-bottom on the 1987 NURP Sea-Link dives. The one gas hydrate gas sample was collected with a grab sample and sampled on the surface ship.

Sea Link Dive #	Dive Location	Site Description	Methane (%)	Ethane (%)	Propane (%)	C1/(C2+C3)	C-13-CH4 (‰)
2057	GC-234		97.996	1.310	0.540	53.0	-53.9
2061	GC-234	Hydrate	69.342	11.702	12.297	2.9	-44.2,-44.3
2061	GC-234	Mussel & Tubeworms	95.134	3.390	0.881	22.3	-37.6,-37.6
2061	GC-234		95.412	3.252	0.822	23.4	
2062	GC-234		94.595	3.404	1.021	21.4	-51.8,-50.7
2062	GC-234	Mussel site	95.123	3.211	0.906	23.1	-47.0,-46.6
2062	GC-234	Mussel site	94.987	3.270	0.934	22.6	-53.0,-50.8
2063	GC-234	Tubeworm site	95.851	2.985	0.675	26.2	-51.8,-51.8
2063	GC-234	Tubeworm site	95.791	3.031	0.696	25.7	-47.6
2071	GC-272	Clam site	99.446	0.479	0.043	190.6	-52.9,-51.3
2074	GC-184		94.590	3.344	1.435	19.8	-51.3
2074	GC-184	Mussel site	94.452	3.413	1.471	19.3	-46.8,-46.8

Table 2. Mixed-function oxidase (MFOase) metabolite counts extracted from tissues isolated from a whole mussel incubated with  $^{14}\text{C}$ -labelled benzo(a)pyrene.

GILL	DIGESTIVE GLAND	FOOT	MANTLE	ABDUCTOR MUSCLE
(counts per minute per gm dry weight)				
13,695	7,534	4,456	3,301	0

Table 3. Mixed-function oxidase (MFOase) metabolite counts extracted from excised mussel gill tissue incubated with  $^{14}\text{C}$ -labelled benzo(a)pyrene.

MUSSEL 1	MUSSEL 2	MUSSEL 3	MUSSEL 4
(Counts per minute per mg protein)			
50	1000	120	190

Table 4. Mixed-function oxidase (MFOase) metabolite counts extracted from mussel-gill bacterial slurry incubated with  $^{14}\text{C}$ -labelled benzo(a)pyrene.

EXPERIMENTAL CONDITIONS	COUNTS PER MG PROTEIN
CONTROL (no inhibitor)	860
+ MFOASE INHIBITOR (7,8 benzoflavone)	194
+ METHANE MONOOXYGENASE INHIBITOR (n-servc)	718

Symbiotic bacteria were separated from mussel gill tissue through a series of filtration steps and assayed for hydrocarbon metabolizing activity. Initial results from these experiments indicate that the bacteria and not the gill tissue are responsible for the observed hydrocarbon metabolites. Preliminary results from inhibitor studies have shown that metabolite production is inhibited by use of MFO inhibitors. Some aromatic hydrocarbons are co-oxidized by bacteria during the oxidation of methane; however, the aromatic hydrocarbon metabolite inhibition data using a methane mono-oxygenase inhibitor is inconclusive in this study.

Mussels and sediment were collected from a variety of sites of varying levels of petroleum seepage, and preserved for hydrocarbon analysis. Hydrocarbon loads in the mussels appear to be variable with respect to location and tissue, as would be expected for animals living over a wide range of hydrocarbon exposure levels. Some mussels have exhibited significantly higher hydrocarbon levels in the gills, particularly in the naphthalene range, than in the rest of the body while in others a more even distribution of polynuclear aromatic hydrocarbons (PAHs) was observed (Table 5).

Various species were also assayed for the presence of oxygen detoxificatory enzymes, catalase and superoxide dismutase (Table 6). Again mussels exhibited significantly higher activities than clams, gastropods or tube worms. Methane oxidation probably produces oxygen radicals. All catalases were inhibited by 3-amino-1,2,4-triazole indicating that they are normal catalases (some sulfur dependent metazoans have a modified catalase not inhibited by 3-amino-1,2,4-triazole).

#### Taphofacies Analysis

The first year of submersible activity at the petroleum seep sites have helped to address several major avenues of investigation. A higher shell accumulation rate at seep locations compared with continental shelf localities has been documented. Shells clearly accumulate at seeps in greater quantities than at any other shelf, slope or bay site in the western Gulf, except oyster reefs. Only here are shell beds formed that are not "event" deposits. Coupled with the large accumulation of shell material is an apparently high dissolution rate which indicates that net productivity (calcium carbonate accumulation) is greater than shell loss in spite of the acidic environment. Clearly mussels are rarely preserved. Hence, fossil analogues should be dominated by clams. Indeed that is the case at Tepee Buttes. It is known that mussel shells are poorly preserved at all locations. The question is: "Why are

Table 5. Polynuclear aromatic hydrocarbon (PAH) concentrations in mussel tissues (gill and body) collected near hydrocarbon seep sites.

Compound	Mussel	
	Body	Gill
Naphthalene	*	277.6
2-Methyl Naphthalene	*	162.2
1-Methyl Naphthalene	*	388
Biphenyl	*	*
Dimethyl Naphthalene #1	*	*
Dimethyl Naphthalene #2	*	63.6
Dimethyl Naphthalene #3	*	225.7
Dimethyl Naphthalene #4	*	118.4
Dimethyl Naphthalene #5	*	136.2
Dimethyl Naphthalene #6	*	*
Acenaphthene	*	53.4
Fluorene	*	*
Phenanthrene	59.1	26.1
Anthracene	*	*
3-Methyl Phenanthrene	52.6	33.6
2-Methyl Phenanthrene	52.6	38.9
9-Methyl Phenanthrene	52.6	35.7
1-Methyl Phenanthrene	52.6	*
Fluoranthene	*	*
Pyrene	33	*
Benz(a)anthracene	*	*
Chrysene	*	*
Benzo(e)pyrene	*	*
Benzo(a)pyrene	*	*
Perylene	23.3	132.6
Dibenz(a,h)anthracene	*	*

\* Concentration less than 20 ppb

Table 6. Catalase activity in petroleum seep organisms.

Taxon	Catalase Activity (units/mg protein)	Number Animals Assayed
<i>Lucinoma</i> sp.		
Whole Body	0.448	1
Gill only	0.544 $\pm$ 0.185	4
Residual (body w/o gills)	0.674 $\pm$ 0.690	6
<i>Bathymodiolus</i> -like sp.		
Gill	22.590	1
Foot	14.290	1
Mantle	6.160	1
Hepatopancreas	10.120	1
<i>Lamellibranchia</i> sp.		
Trophosome	1.177 $\pm$ 0.314	4
Vest	0.352 $\pm$ 0.189	2
<i>Escarpia</i> -like sp.		
Trophosome	1.805 $\pm$ 0.233	2
Vest	0.690	1
<i>Vesicomya</i> sp.		
Gill	0.828	1
Foot	1.220	1
Gonad	1.012	1

clams preserved so well in spite of the relatively low population levels in many portions of the clam beds?" One possibility is that, when active seepage stops, dissolution rates also drop, so that shells still remaining can be indefinitely preserved. We have developed a method to date time-since-death for molluscs based on the rate of protein decomposition in the shell and will apply that method to dating the age of seep sites and to look at the relative ages of shells in active and inactive areas of seepage within the sites. This is, in effect, a variant of time averaging, since patch migration on the sea floor results in a much wider distribution of shell material of many different ages than would be expected from the current distribution of the living fauna. The shells are, however, stratigraphically equivalent.

#### SUMMARY

Chemosynthetic ecosystems composed of tube worms, mussels and/or clams are widely distributed on the Gulf of Mexico continental slope. The distribution of these ecosystems are controlled by the seepage of oil and gas which provides the driving energy. The chemosynthetic mussels which can utilize methane as a result of symbiotic bacteria in their gills (Childress et al., 1986) are in most cases associated closely with bubbling gas seepage. The tubeworms and clams are associated more closely with the presence of high sediment concentrations of oil. The chemosynthetic communities represent extremely high biomass densities for the deep-sea benthos and isotope evidence indicates that chemosynthetically produced carbon is being transferred into the background deep-sea fauna (e.g., crabs, crustaceans) at the seep sites. The ecology, physiology, chemistry, and geology of these ecosystems and sites are very complex requiring coordinated multidisciplinary studies.

#### LITERATURE CITED

Brooks, J. M., M. C. Kennicutt II, R. R. Fay, T. J. McDonald, and R. A. Sessen. 1984. Thermogenic gas hydrates in the Gulf of Mexico. Science, Vol. 225, pp. 409-411.

Brooks, J. M., M. C. Kennicutt II, R. R. Bidigare and R. R. Fay. 1985. Hydrates, oil seepage and chemosynthetic ecosystems on the Gulf of Mexico slope. EOS, Vol. 66, No. 10, p. 105.

Brooks, J. M., M. C. Kennicutt II, R. R. Bidigare, T. L. Wade, E. Powell, G. J. Denoux, R. R. Fay, J. J. Childress, C. R. Fisher, I. Rosman, and G. Boland. 1987a. Chemosynthetic ecosystems, hydrates, and oil seepage on the Gulf of Mexico slope: An update. EOS, Vol. 68, No. 18, pp. 498-499.

Brooks, J. M., M. C. Kennicutt II, C. R. Fisher, S. A. Macko, K. Cole, J. J. Childress, R. R. Bidigare, and R. D. Vetter. 1987b. Deep-Sea Hydrocarbon Seep Communities: evidence for energy and nutritional carbon sources. Science, Vol. 238, p. 1142.

Childress, J. J., C. R. Fisher, J. M. Brooks, M. C. Kennicutt II, R. R. Bidigare, and A. Anderson. 1986. A methanotrophic marine molluscan symbiosis: mussels fueled by gas. Science, Vol. 233, pp. 1306-1308.

Kennicutt, M. C. II, J. M. Brooks, R. R. Bidigare, R. R. Fay, T. L. Wade, and T. J. McDonald. 1985. Vent type taxa in a hydrocarbon seep region on the Louisiana slope. Nature, Vol. 317, No. 6035, pp. 351-353.



## BIOLOGY AND ECOLOGY OF THE OREGON CONTINENTAL SHELF EDGE ASSOCIATED WITH THE ACCRETIONARY PRISM

Andrew G. Carey, Jr., David L. Stein, Gary L. Taghon,  
and Anne E. DeBevoise  
College of Oceanography  
Oregon State University  
Corvallis, OR 97331-5503

### ABSTRACT

As part of an exploratory study of the geology and biology of the upper Oregon subduction zone, we undertook submersible reconnaissance dives on the northern continental shelf edge and upper slope. Our objectives were: (1) to ascertain the structure of the benthic assemblages present, and (2) to study assemblages associated with possible active vents. Although direct observations and photography demonstrated that abundant calcium carbonate slabs and chimneys occur on Nehalem Bank, there are now no active subduction-driven vents. Presumably, methane from extensive past venting geochemically formed the calcium carbonate edifices. The vent field appears to be extinct; however, hard deposits produced by venting have changed the nature of the animal community in the area by providing substrate for hard bottom organisms. In addition to a typical outer continental shelf fine sand-mud community, a hard substrate epifaunal community is also present.

### INTRODUCTION

In plate convergence zones where oceanic crust is being subducted, methane is expelled from faults and permeable zones within accreted sediments (Kulm et al., 1986; Boulegue et al. 1987). In 1984 investigators from Oregon State University discovered vents and faunal communities associated with the subduction zone on the lower continental slope at depths of 2000 to 2400 m off central Oregon (Suess et al. 1985; Kulm et al. 1986). During dives with the research submersible Alvin, methane-enriched bottom waters (182-428 ml/l) were sampled. These sites contain methane-derived authigenic carbonate slabs and chimneys, and the surrounding sandstone rocks contain carbonate cement clearly derived from methane (Kulm et al. 1986, Ritger et al. 1987).

The 1985 discovery of calcium carbonate chimneys at 247 m depth on the northern Oregon shelf edge by commercial fishermen aboard F/V Kodiak and other vessels suggested that fluids are expelled along the entire width of the accretionary complex of the subduction zone (Schroeder et al. 1987; Kulm et al. submitted, this volume; Fig. 1). This conclusion is supported by collections from earlier benthic trawls and dredges on the Oregon

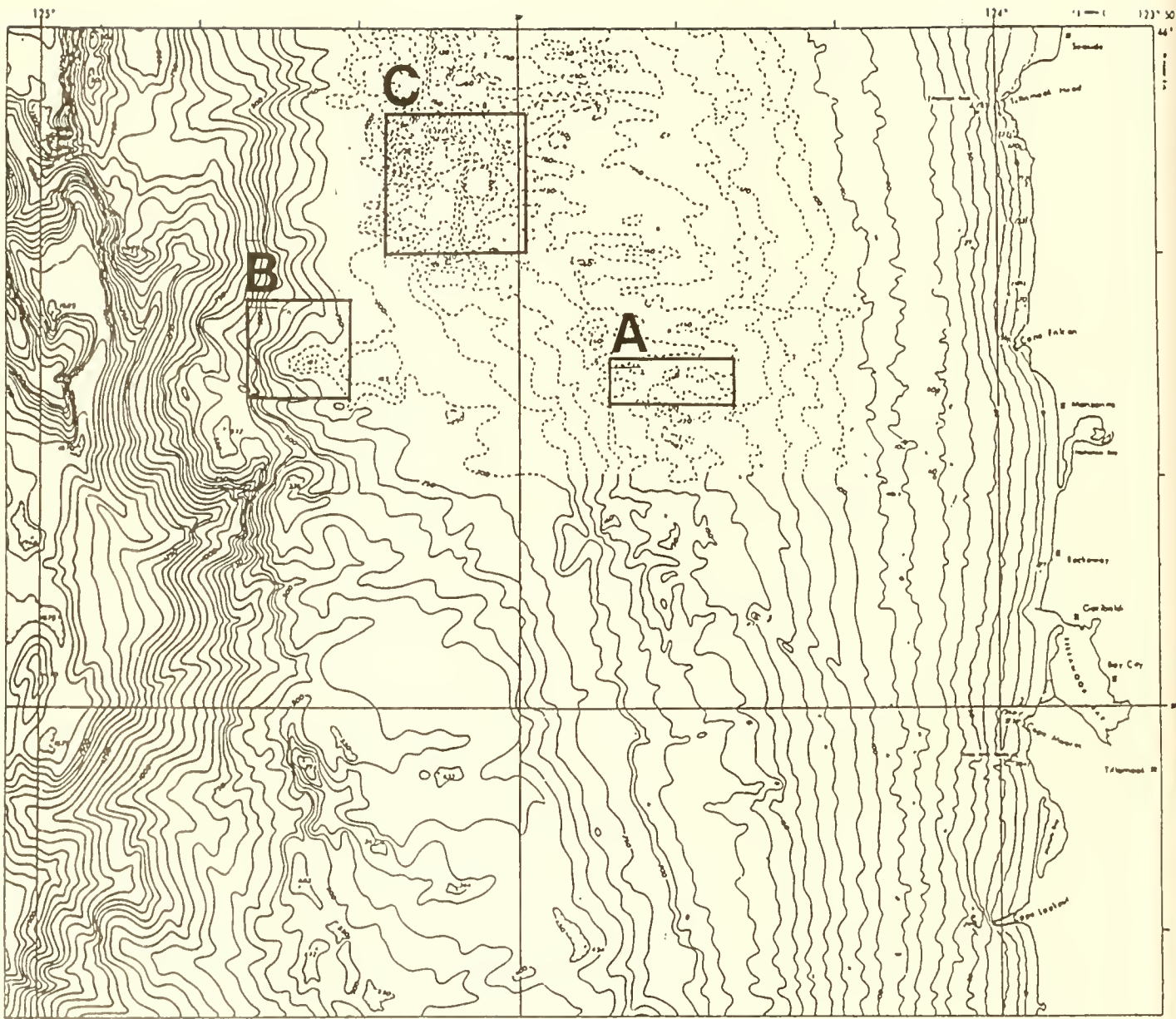


Figure 1. Location map of 1987-1988 dive sites on the northern Oregon continental shelf where subduction-driven venting was suspected. Station B was the location of two 1987 DSV Mermaid-II dives and three ROV (Recon-IV) deployments; Stations A, B, and C were the sites for 11 DSV Delta dives in 1988. Station B includes Nehalem Bank and the initial chimney find by commercial fishermen on board the F/V Kodiak.

continental shelf and slope, which include the gutless clam, Solemya johnsoni Dall, and the vestimentiferan, Lamellibrachia barhami Webb, (Fig. 2). Lamellibrachia occurs at the deeper vents at the base of the continental slope. Specimens of Solemya johnsoni have been frequently collected along the continental slope, as well as just seaward of the shallow-water chimney site (Carey, unpublished data; Fig. 1). Calyptogena pacifica Dall 1891, also found at vent sites, has been collected from the upper slope. Solemya clams are associated with active vents in deeper waters and with sulfide-rich sediments (Cavanaugh 1985; Suess et al. 1985), and are present at the active vents found on the lower slope (Kulm et al. 1986; Suess et al. 1985). Solemya sp. also occurs in great abundance to the exclusion of other animals along fault zones where fluids are being expelled (Suess et al. 1985). Such fault zones are common within the accretionary complex on the continental margin; Solemya may be associated with these faults in many localities along the margin.

Similarities between the Oregon lower slope methane-derived  $\text{CaCO}_3$  chimneys and slabs and underlying geological structure strongly suggest that the same geological and geochemical processes also operate in shallow water (Schroeder et al. 1987). Vent fluids from the lower Oregon subduction zone contain high concentrations of methane, suggesting that shallow vent effluents would also expel methane (Kulm et al. 1986; Ritger et al. 1987).

Our integrated research program on the northern Oregon continental margin proposed to determine if active subduction-driven vents were present. Furthermore, we planned to define the geology, biology, and geo-biological interactions in subduction-driven vent fields of the upper accretionary complex. Dives with the DSV Mermaid-II in 1987 and DSV Delta in 1988 showed that the vent field we examined is extinct. However, active venting of methane-rich fluids did occur in the area and formed abundant  $\text{CaCO}_3$  slabs and chimney edifices. This paper documents the effects of these formations on the nature of the local benthic fauna.

## METHODS

During August 1987, we utilized the DSV Mermaid-II to survey the chimney field on Nehalem Bank (Fig. 1). In September 1988 we undertook dives with DSV Delta for additional, more detailed searches on and around Nehalem Bank off northern Oregon. During many of the 1988 DSV Delta dives, the PHOTOSEA camera system, loaded with 200 ASA Ektachrome film, took still photographs every 30 seconds. A hand-held video camera was used for continuous recording of portions of the dives.

Photographs ( $n = 444$ ) from 8 DSV Delta 1988 dives were analyzed for distribution of invertebrate fauna and fishes by

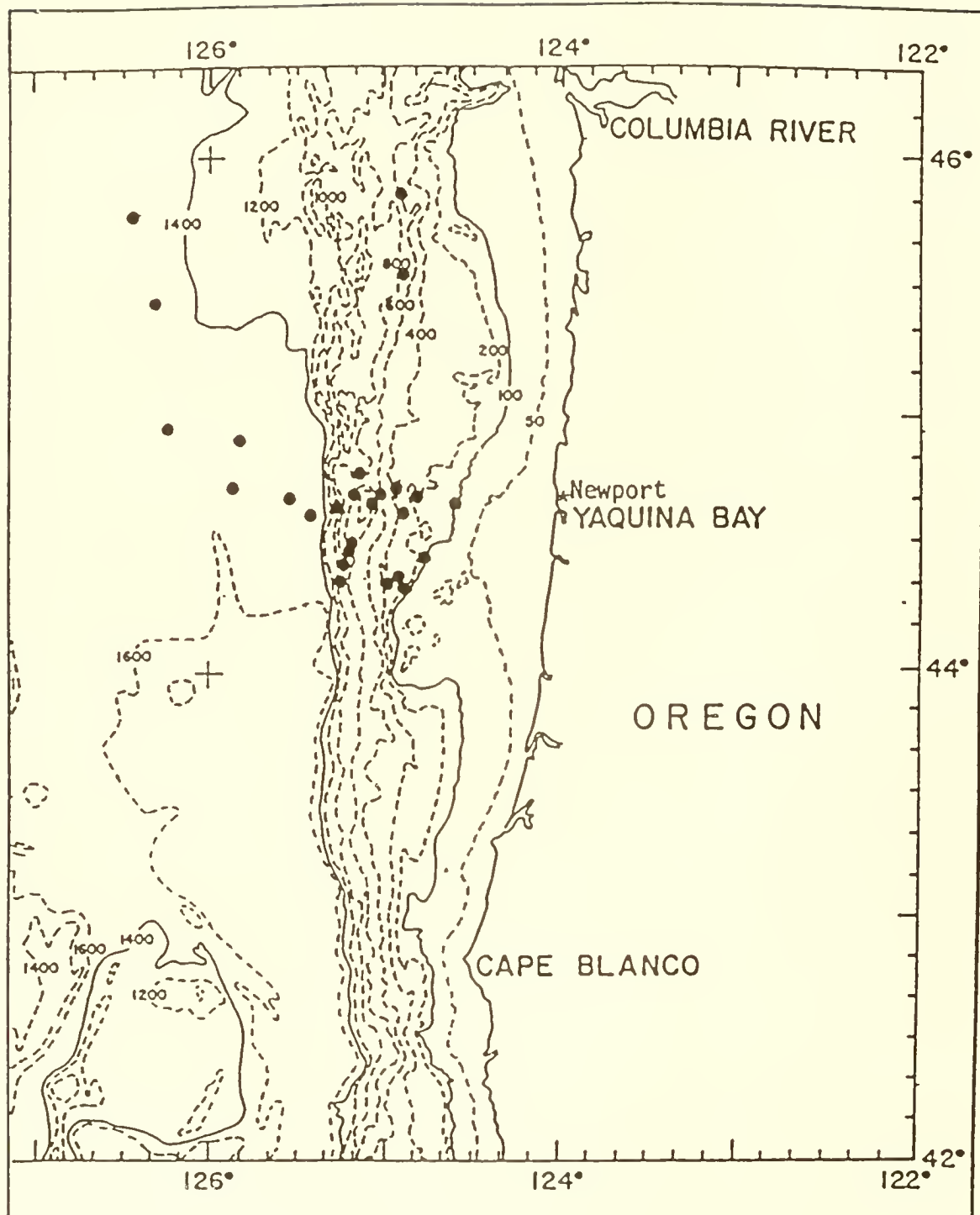


Figure 2. Location map of collections of *Solemya johnsoni* (solid circles) and *Lamellibrachia barhami* (triangle) by trawl and dredge (1962-1970). Depth contours in fathoms. (1 fath. = 1.83 m.) (Carey, unpublished data).

substrate. Substrate was either fine sandy mud, characteristic of the continental shelf edge off Oregon, or rock ( $\text{CaCO}_3$ ). Four substrate categories were designated for analysis of invertebrates and fishes to determine if the presence of hard substrate affects composition of shelf benthos; these were: (1) mud, (2) mud near rock, (3) rock near mud, and (4) rock.

Caution is necessary in considering the "all mud" category, because rock could have been present just beyond the photograph. Because photographic coverage was not evenly distributed, numbers of observations do not indicate frequency of occurrence and are, therefore, not included. Because quantitative transects were not made, these data represent only presence or absence of fish and invertebrate taxa (identified to lowest possible taxon) in still photographs taken at varying altitudes and spatial intervals.

In 1987, we also utilized a remotely operated vehicle (ROV Recon-IV) for surveys of the chimney field. Also in 1987, animal and rock collections were made with the submersible manipulator arms and a 7.1 m otter trawl with 1.3 cm mesh towed from R/V Aloha at 1.5 to 2.0 knots.

## RESULTS

The invertebrates living on the sediments of Nehalem Bank are similar to those in other regions of the Oregon continental slope and outer shelf (Appendix 1). Many of the same species of asteroids, holothuroids, and echinoids were present. Echinoids, Allocentrotus fragilis and Brisaster townsendi, are common in the Nehalem Bank sedimentary environment; the holothuroid Parastichopus californicus occurs on the sediment surface in low abundance. B. latifrons is a burrowing sea urchin that can be observed breaking the sediment surface, leaving characteristic wide, meandering burrow patterns. Ophiuroids are abundant in some areas. We observed an alcyonarian (Anthomastus ritteri ?) never collected by us with conventional sampling gear that, in Oregon waters, may be restricted to rocky environments. Rockfishes (family Scorpaenidae) were observed throughout the area (Table 1).

The fauna collected from the rocky substrate was noticeably different from our previous collections from the Oregon shelf edge, probably an indication of the difficulty of trawling in this rugged environment during past research projects. Typically, commatulid crinoids, psolid holothuroids, chitons, ophiuroids, brachiopods, corals, sponges, actiniarians and other hard substrate epifauna cover the surface of calcium carbonate slabs and chimneys (Table 2). Occasionally, predaceous starfish, such as Luidea foliolata and Pisaster sp., occur on the rock surfaces. One large actiniarian inhabiting the rocky substrate is new, to our knowledge, off Oregon; it resembles a white sphere

Table 1. Fish taxa identified from 1987 ROV videotapes on Nehalem Bank on the northern Oregon shelf-edge.

---

Family Rajidae  
Raja rhina

Family Zoarcidae  
Lycodes corteziatus

Family Scorpaenidae  
Sebastolobus sp.

Sebastes babcocki  
Sebastes ?caurinus  
Sebastes helvomaculatus  
Sebastes zacentrus

Family Agonidae  
unidentified spp.

Family Pleuronectidae  
Glyptocephalus zachirus  
Microstomus pacificus

---

Table 2. Substrate preference of common mega-epifaunal invertebrates and fish species on Nehalem Bank off the northern Oregon coast. Occurrence of fish species identified from the vent field.

Species	SUBSTRATE			
	All mud	Mud rock	nr. mud	Rock nr. mud
				All rock
<b>INVERTEBRATES</b>				
<u>Psolus chitonoides</u>				X
<u>Pisaster</u> sp.				X
<u>Ophiophthalmus diplasia</u>				X
<u>Florometra serratissima</u>				X
Decapoda shrimp sp. a				X
<u>Solaster</u> sp.		X		X
<u>Pennatulacea</u> sp.		X		
<u>Pteraster</u> sp.		X		
<u>Heterozonias</u> sp.		X		
<u>Parastichopus californicus</u>	X	X		
<u>Allocentrotus fragilis</u>	X	X		
<u>Brisaster latifrons</u>	X	X		
<u>Pandalus</u> sp.	X	X		
Decapoda shrimp sp. b	X			
<b>FISH</b>				
<u>Sebastes zacentrus</u>	X	X	X	X
<u>Sebastes helvomaculatus</u>	X	X	X	X
<u>Sebastes</u> spp.	X	X		X
<u>Ophiodon elongatus</u>				X
<u>Microstomus pacificus</u>	X	X		
Agonidae spp.	X	X		
<u>Sebastolobus alascanus</u>	X	X		
Unident. Pleuronectidae	X			
Cottidae spp.	X	X		
<u>Raja</u> spp.	X	X		
Zoarcidae spp.	X			
<u>Eptatretus</u> sp.			X	
<u>Sebastes elongatus</u>	X			

10 to 30 cm in diameter with polyp-like protuberances evenly spaced around its surface. There appeared to be no difference in the assemblages living on the  $\text{CaCO}_3$  slabs versus the chimneys.

The invertebrates associated with hard substrate are suspension feeders and carnivores. The psolid sea cucumber Psolus chitonoides uses branched, dendritic tentacles to capture detrital particles from the water; these oral tentacles are arrayed dorsally above the animal. The comatulid crinoid Florometra serratissima suspension-feeds with highly pinnulated arms projected into the overlying water layer (Hyman 1955; Barnes 1980). There are also abundant unidentified small actiniarians on the hard substrate surfaces. Photographs document that a shrimp species utilizes rock overhangs for protection; they are, therefore, associated with the rocky environment. Occasionally, carnivorous asteroids (e.g. Luidia foliolata, Solaster sp., Pisaster sp.) clung to the rock surface, presumably feeding (Carey 1972).

Several soft bottom invertebrates occurred in dense patches. All box crabs seen (Lopholithodes foraminatus) occurred in large, extremely dense patches (up to 25 individuals per  $\text{m}^2$ ); one patch was at Station A on a broad stretch of sandy mud (Fig. 1). We observed the other aggregation at Station C on mud in both shallow depressions and on small ridge tops. The crabs were facing in one direction and moving their mouthparts rapidly, probably feeding. Though ophiuroids occurred over much of the study area, an extensive, dense patch (up to 285 individuals per  $\text{m}^2$ ) of at least two species was observed at Station B. Less dense echinoid patches occurred on featureless stretches of sediment (7 individuals per  $\text{m}^2$ ).

Clear differences exist between fish species assemblages in the different habitats. Many more species were identified from all mud and mud near rock than from rock near mud and all rock substrates (Table 2). Flatfishes, zoarcids, agonids, cottids, skates, and thornyheads did not occur on rock. Both species identified from all rock substrates (sharpchin and rosethorn rockfish) occurred over all mud. The greatest concentrations of fish occurred on jumbled carbonate mounds, although a few individual rockfish used small donut-shaped vent chimneys for shelter.

All rocky habitat fishes seen were Sebastes spp. Other species probably occur also. The most common rockfish was the sharpchin, S. zacentrus. It occurred whenever rock was present, often in substantial numbers. Unlike Heceta Bank rocky areas (Pearcy et al. in press), no small juvenile rockfishes were present. Although it is not evident from the still photographs, visual observational notes and video tapes suggest that neither of the two rocky habitat species identified stray far from rock.

Soft substrate fishes included all other taxa listed. During ROV deployment #1 in 1987, agonids appeared to be the most common taxon occurring on all soft bottom. During ROV #2, although agonids were still common, zoarcids (probably L. cortezianus) were relatively more common. Individual Sebastolobus alascanus, which appear to be quite sedentary, occurred in shallow pits. Whether the fish excavate these or simply take advantage of existing irregularities is unknown.

#### DISCUSSION AND CONCLUSIONS

The reason for dense invertebrate aggregations we observed is unknown. Food concentration, reproductive behavior, or gregarious interactions could be the causes of these. Although there was no apparent environmental difference where box crabs, ophiuroids, and echinoids were clumped, currents or eddies may have caused concentrations of particulate organic materials in the bottom water layer or at the sediment-water interface. Reproductive pheromones released in the water by sexually mature individuals could be the cue for clumping behavior.

Our results demonstrate that upper subduction zone venting can have a significant effect on distributions and occurrences of benthic invertebrates and shelf fishes. Nehalem Bank is a soft-bottom bank similar to others off Oregon. However, the extensive past venting there has produced rock outcrops of a variety of morphologies in the midst of a more or less soft bottom region. These outcrops are of three basic types: donuts (chimneys), jumbles, and flat slabs (Kulm and Suess, submitted). The rock jumbles clearly provided a different habitat used by rockfishes and encrusting epifauna in large numbers.

The fish (typically sharpchin rockfish and rosethorn rockfish) often extended their ranges out over the nearby mud. The donuts and flat slabs (which typically appeared as small ledges protruding from the sediment) harbored few fish. If any fish were present, there were only one or two sheltering alongside the rock. These results are not unexpected. They are similar to the fish distributions described by Pearcy et al. (in press) from Heceta Bank, Oregon. In both situations an isolated patch of hard substrate can attract and apparently maintain an isolated group of rockfish.

However, the widespread occurrence of calcium carbonate slabs and chimneys, a product of active vents in the past, has probably changed the patterns of occurrence of a variety of fish species, primarily rockfishes, and hard substrate invertebrate epifauna. Active liquid and gas venting at shallow depths may be occurring now elsewhere on the Oregon shelf. If this is the case, venting could have additional effects on the structure and

functioning of benthic assemblages at the shelf edge by the introduction of methane and  $H_2S$ -based chemosynthetic food webs.

#### ACKNOWLEDGMENTS

We thank the captain and crew of the R/V Aloha, the R/V McGaw and the diving personnel of the DSV Mermaid-II and DSV Delta for their helpful support during these studies. We acknowledge the helpful discussions and invaluable field support of L.D. Kulm and E. Suess of the geological group. We thank NOAA's Undersea Research Office (Contract No. 50-DGNR-7-00155) for our first chance to observe and study in situ the rugged, rocky shelf edge environments off Oregon, and we thank the Oregon State University Sea Grant College Program for research support.

#### LITERATURE CITED

Barnes, R. D. 1980. Invertebrate Zoology. Philadelphia, PA, Saunders College. 1089 pp.

Boulegue, J., E. L. Benedetti, D. Dron, A. Mariotti, and R. Letolle. 1987. Geochemical and biogeochemical observations on the biological communities associated with fluid venting in Nanakai Trough and Japan Trench subduction zones. Earth and Planet. Sci. Lett., Vol. 83, pp. 343-355.

Carey, A. G., Jr. 1972. Food sources of sublittoral, bathyal and abyssal asteroids in the Northeast Pacific Ocean. Ophelia, Vol. 10, pp. 35-47.

Cavanaugh, C. M. 1985. Symbiosis of chemoautotrophic bacteria and marine invertebrates from hydrothermal vents and reducing sediments. In: M. L. Jones (ed.) Hydrothermal Vents of the Eastern Pacific: An Overview, Biol. Soc. of Washington Bull. 6, pp. 373-388.

Hyman, L. H. 1955. The Invertebrates: Echinodermata. New York, N. Y., McGraw-Hill. 763 pp.

Kulm, L. D., E. Suess, J. C. Moore, B. Carson, B. T. Lewis, S. D. Ritger, D. C. Kadko, T. M. Thornburg, R. W. Embley, W. D. Rugh, M. G. Langseth, G. R. Cochrane, and R. L. Scammon. 1986. Oregon subduction zone: Venting, fauna and carbonates. Science, Vol. 231, pp. 561-566.

Kulm, L. D., E. Suess, and P. D. Snavely, Jr. 1988. Fluid venting structures on the northern Oregon continental shelf. In: Michael P. De Luca and Ivar Babb (eds.), Global Venting, Midwater, and Benthic Ecological Processes. National Undersea Research Program Research Report 88-4, pp. 151-176. Rockville, MD, NOAA Undersea Research Program.

Kulm, L. D. and E. Suess. Relationship between carbonate deposits and fluid venting: Oregon accretionary prism. (Submitted).

Pearcy, W. D., D. L. Stein, M. A. Hixon, and E. K. Pikitch. Submersible observations of deep-reef fishes of Heceta Bank, Oregon. Fish Bull., (In press).

Ritger, S., B. Carson, and E. Suess. 1987. Methane-derived authigenic carbonates formed by subduction-induced pore water expulsion along the Oregon/Washington margin. Geol. Soc. America Bull., Vol. 8, pp. 147-156.

Schroeder, N. A. M., Kulm, L. D., Muehlberg, G. E. 1987. Carbonate chimneys on the outer continental shelf: Evidence for fluid venting on the Oregon margin. Oregon Geol., Vol. 49, pp. 91-98.

Suess, E., B. Carson, S. D. Ritger, J. C. Moore, L. D. Kulm, and G. R. Cochrane. 1985. Biological communities at vent sites along the subduction zone off Oregon. In: M.L. Jones, (ed.), The Hydrothermal Vents of the Eastern Pacific: An Overview. Biol. Soc. of Washington Bull. 6, pp. 474-484.

APPENDIX 1. Species list of mega-epifaunal invertebrates  
collected on the Oregon continental shelf edge (200-220 m),  
1962-1987.

---

CNIDARIA

Anthozoa

Alcyonaria

Anthomastus ritteri \*

Pennatulacea

Stylatula elongata

Actiniaria

Paractinostola faeculenta

Liponema sp. \*

Actinostola sp.

Anemone Type N

ECHINODERMATA

Astroidea

Heterozonias alternatus

Luidia foliolata \*

Pseudarchaster parelii alasensis

Orthasterias koehleri

Dipsacaster anoplus

Nearchaster aciculatus

Thrissacanthias pectinatus

Pedicellaster magister

Solaster endeca ?

Solaster borealis \*

Hippasteria spinosa

Stylasterias forreri

Rathbunaster californicus

Crossaster papposus

Zoroaster sp.

Mediaster aequalis

Echinoidea

Allocentrotus fragilis \*

Brisaster latifrons \*

Holothuroidea

Parastichopus californicus \*

Pentamera populifera

Molpadias intermedia

Psolus chitonoides \*

Ophiuroidea

Ophiura sarsii

Ophiura lutkenii

Unioplus macrospis

Ophiopholis bakeri

Ophiomusium jolliensis

Ophiophthalmus diplasia \*

Appendix 1. (Cont'd.)

Crinoidea

Florometra serratissima \*

MOLLUSCA

Gastropoda

Buccinum strigillatum  
Antiplanes perversa  
Natica clausa  
Fusitriton oregonensis  
Armina californica  
Tritonia sp.

Bivalvia

Solemya johnsoni

Cephalopoda

Japatella sp.

ARTHROPODA

Decapoda

Pagurus ochotensis  
Parapagurus mertensii  
Paguristes turgidus  
Pagurus tanneri  
Pandalus danae  
Pandalus jordani  
Cragnon communis Schmitt  
Spirontocaris macrophthalmia  
Spirontocaris bispinosa  
Lopholithodes foraminatus \*

Chionoecetes tanneri

Munida quadrispina

Chorilia longipes

Mursia gaudichaudii

Pycnogonida

Collossendis sp.

Nymphon sp.

Cirripedia

Scalpellum sp.

ANNELIDA

Polychaeta

Aphrodite sp.

BRACHIOPODA

Laqueus californicus \*

\* Tentatively identified from Nehalem Bank.



FLUID VENTING STRUCTURES ON THE  
NORTHERN OREGON CONTINENTAL SHELF

LaVerne D. Kulm<sup>1</sup>, Erwin Suess<sup>1</sup>, and Parke D. Snavely, Jr.<sup>2</sup>

<sup>1</sup>College of Oceanography  
Oregon State University  
Corvallis, OR 97331

<sup>2</sup>U.S. Geological Survey  
Branch of Pacific Marine Geology  
Menlo Park, CA 94025

ABSTRACT

The Oregon subduction zone is actively venting pore fluids from the accretionary prism which produce vent sites consisting of one or more of the following features: (1) benthic animal communities harboring chemosynthetic bacteria, (2) carbonate deposits, and (3) anomalously high methane concentrations. Carbonate deposits, which are apparently formed by precipitation from oxidized methane and CO<sub>2</sub>-charged fluids, occur on the upper continental slope and outer continental shelf off northern Oregon. Using the submersible Mermaid and the ROV Recon-IV, extensive areas of carbonate crusts, slabs, chimneys, and irregular edifices were mapped on the seafloor in water depths ranging from 92 to 382 m. These carbonate structures are covered with abundant living benthic organisms, especially crinoids. The ROV television camera photographed one circular chimney structure situated within the substrata of the seafloor. It rises 15-20 cm above the seafloor and has a sediment-free vertical opening of 15-20 cm in diameter, suggesting that it is an active vent site. It is similar to a circular chimney, with an open plumbing network, that was recovered by commercial fishermen in a trawl net from the same area. In addition, one 200 lb, irregular carbonate edifice was recovered by the support vessel Aloha in a trawl in the vicinity of the ROV trackline. The lower portion of the chimney-like structure was buried in the sediment and the upper portion contains a profusion of cemented tubes which are exceedingly complex in shape, but clearly indicate a plugged plumbing system. The bulk of the chimney as well as the walls of the plumbing system consist of aragonite and/or Mg-calcite cemented glauconitic sand, quartz and minor amounts of clay minerals. Glauconite is common in the surrounding shelf sediments. The irregular carbonate edifice is highly depleted in  $\delta^{13}\text{C}$  (-48.27 to -53.31 PDB) and has positive  $\delta^{18}\text{O}$  (+4.19 to +4.84 PDB) values. These chimney structures apparently grow both within the bottom sediment and above the sediment-water interface depending upon the rate of clastic sedimentation surrounding the structures.

## INTRODUCTION

In 1985, while dragging for bottom fish along the northern Oregon coast, the fishing vessel Kodiak recovered three chimney-like rocks located in a water depth of about 247 m on the outer edge of the continental shelf (Figs. 1,2; Schroeder et al. 1987). Interestingly, these chimneys are similar to carbonate chimney structures observed on the lower continental slope off central Oregon with the aid of the submersible Alvin in August 1984 (Kulm et al. 1986) at sites of fluid venting in the Oregon subduction zone. The shelf chimneys were the first occurrence of possible fluid venting structures in the shallow waters of the continental shelf off Oregon, and they are among a growing number of features for fluid venting recently reported from shallow water areas of the active and passive margins of the United States (Paull et al. 1984; Brooks et al. 1984; Kulm et al. 1986; Childress et al. 1986), North Sea (Hovland et al. 1987) and Japan (Le Pichon et al. 1987). Both the venting sites off Oregon and Japan are associated with subduction zones.

Previous experience has shown that these venting sites can only be studied in detail with the use of a submersible. Direct observation, sampling and experiments are necessary to conduct studies of the fluid venting processes and manifestations of such processes. The submersible Mermaid and a Remotely Operated Vehicle (ROV) Recon-IV were utilized to survey the suspected venting area off northern Oregon during August 11-21, 1987. This underwater survey was the first of a two-year dive program on the Oregon continental shelf.

This was an integrated geological and biological study of fluid venting sites in the oldest portion of the accretionary prism on the upper slope and outer continental shelf. The specific geological objectives of this study were to (1) locate actively venting carbonate chimneys on the outer shelf, (2) determine the configuration and position of the chimneys in relation to the geologic structure of seafloor, (3) compare the physical, chemical and mineralogical characteristics of the shelf chimneys with those found in deeper water on the continental slope, and (4) determine the nature and source of fluids that flow through the shelf chimneys. The first three objectives were partially completed in the fall of 1987 two months after the end of the field program. The fourth objective will be the focus of the second field season scheduled for late summer of 1988. The biological objectives are described elsewhere (Carey et al. 1988).

## METHODS

In August 1987 the submersible Mermaid and support vessel Aloha were contracted by NOAA's Office of Undersea Research to survey the northern Oregon continental shelf area to locate

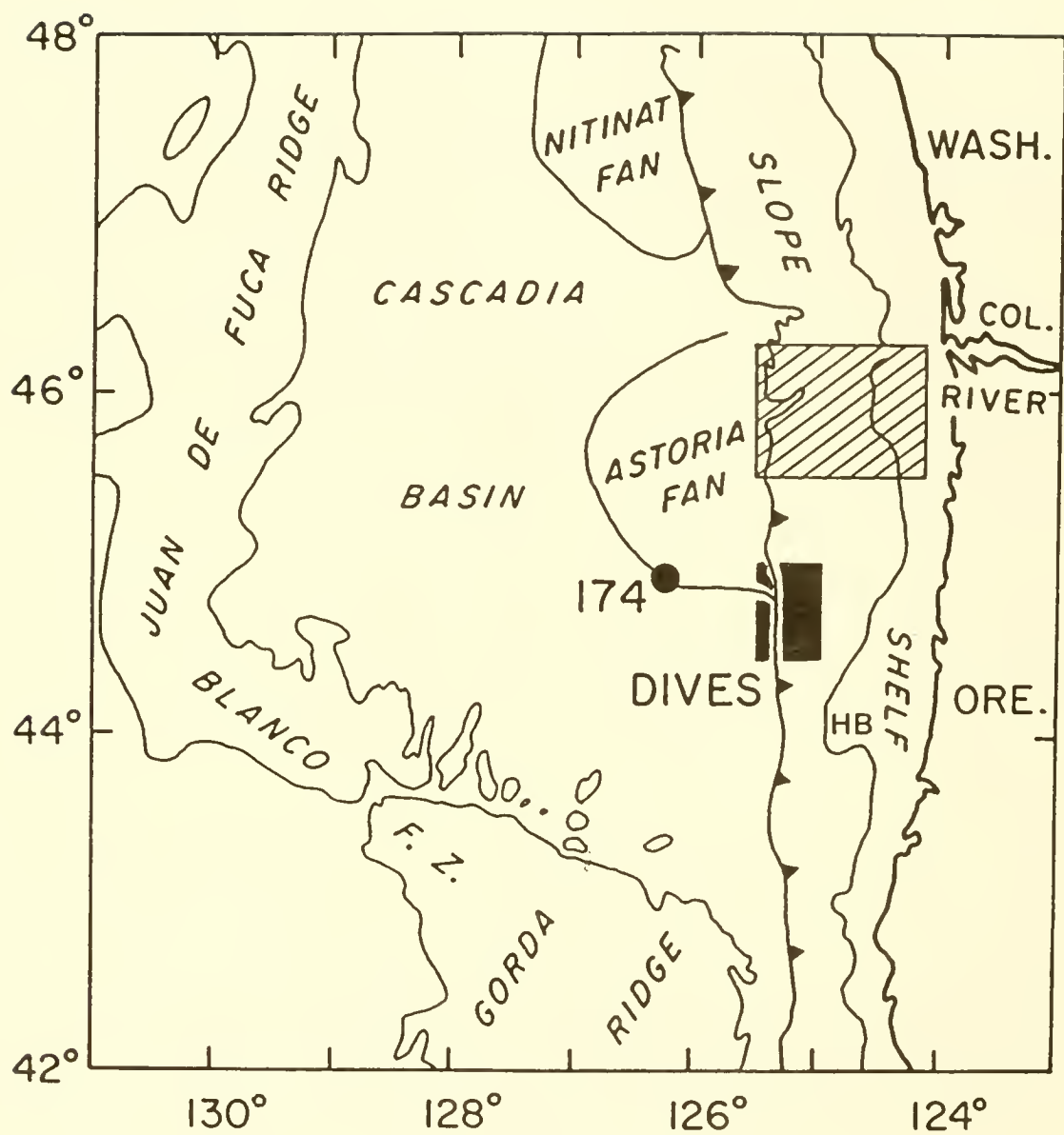


Figure 1. Location map of Oregon continental margin (shelf and slope), Juan de Fuca plate (Cascadia Basin), and spreading Juan de Fuca and Gorda ridges. Subduction zone (saw teeth on upper plate) located on the continental slope. Location of Deep Sea Drilling site 174 on Astoria Fan shown by solid dot. Alvin dive area (labeled dives) is shown by the black box. Study area is shown as lined box (see also fig. 2). (After Schroeder et al. 1987).

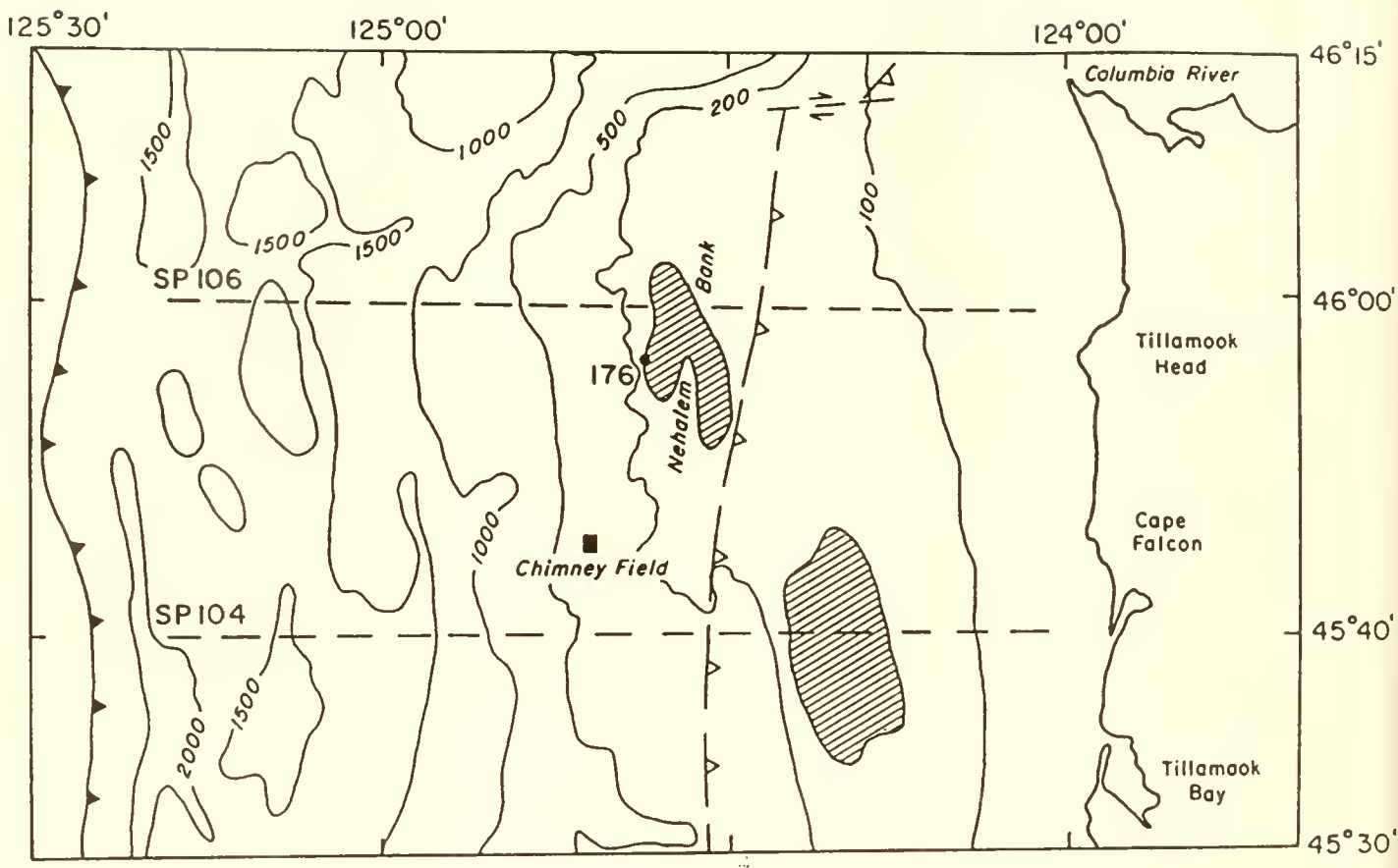


Figure 2. Geologic map of study area (modified from Peterson et al. 1986, see fig. 1) showing the location of the carbonate chimneys (solid square) on the outer shelf. Note the thrust boundaries between Juan de Fuca plate and Oregon margin (solid barbs on upper plate) and between the accretionary prism (west) and the Eocene volcanics with overlying younger basinal deposits (east) (dashed line open barbs). Lined pattern is exposures of Miocene to Pliocene mudstone and siltstone; DSDP drill site 176 (solid dot). Locations of seismic reflection lines SP-104 and -106 (dashed lines). Contours in meters. (After Schroeder et al. 1987).

active venting sites in the vicinity of the carbonate chimneys recovered earlier. Due to inclement weather conditions and equipment failures only three dives, one off northern Oregon and two off central Oregon in the vicinity of Heceta Bank (Fig. 1), were completed during the nine-day dive program. However, four deployments of the ROV were made successfully with the Recon-IV, two on the northern Oregon shelf and two in the vicinity of Heceta Bank. The ROV deployments were limited to moderate sea conditions because of the lack of an acoustic tracking system which determines the position of the ROV relative to the surface vessel.

#### GEOLOGIC SETTING

Deformation and uplift of the North American plate during the past 60 my, which is caused by the converging Juan de Fuca plate, has developed a structurally and stratigraphically complex continental margin (Kulm and Fowler 1974; Snavely et al. 1980). Clastic sediments are scraped off from the subducting oceanic plate forming an accretionary prism which is comprised of a series of fold and thrust ridges, with intervening basins, striking subparallel to parallel to the Oregon-Washington margin (Fig. 3; Kulm et al. 1973; Kulm and Fowler 1974; Barnard 1978; Snavely et al. 1980). The most recently deformed ridges (<2 Ma) lie farthest seaward at the toe of the continental slope (Fig. 4; Kulm and Fowler 1974; Kulm and von Huene et al. 1973a) and the ridges become successively older and more complexly deformed farther landward.

Submarine banks occur along the outer edge of the continental shelf (Kulm and Fowler 1974; Snavely et al. 1980) and form some of the most strikingly folded and faulted areas of the continental margin. The chimneys described in this paper are located on Nehalem Bank, on the outermost edge of the shelf (Fig. 3). An accretionary prism Oligocene to Miocene in age underlies this portion of the bank and underthrusts the Eocene volcanics to the east (Snavely et al. 1980; Peterson et al. 1986). Miocene to Pleistocene sedimentary deposits overlie the prism and contain unconformities that are late Miocene to late Pliocene in age (Kulm and Fowler; 1974).

#### RELEVANT PREVIOUS STUDIES

##### Continental Slope

In 1984 sites of fluid venting were observed on the lower continental slope off central Oregon using the submersible Alvin (Kulm et al. 1986). Each site is located on the crest of a a Pleistocene thrust ridge about 110 km to the south of the shelf chimney field at a water depth of 2036 m (Fig. 4). Vent-type animals (harboring chemosynthetic bacteria), authigenic carbonate chimneys and slabs, and anomalous concentrations of methane

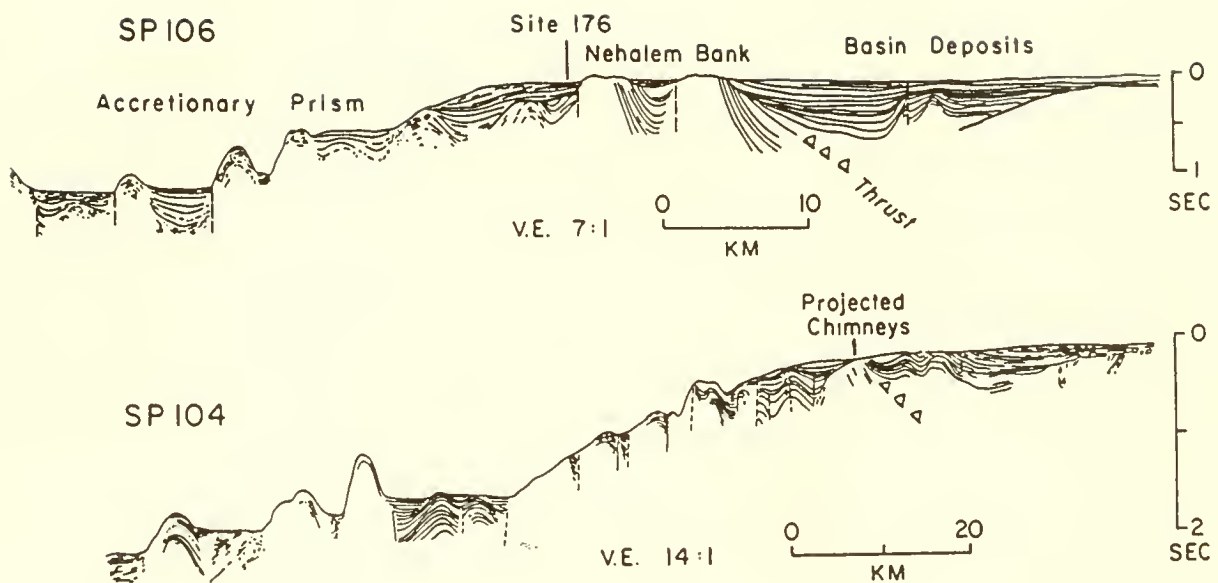


Figure 3. Line drawing interpretations of Oregon State University single channel seismic reflection lines SP-104 and -106 showing shelf basin deposits and accretionary prism. Dashed line with open barbs shows thrust boundary between the two features. See figure 2 for location. Drill site 176 and Nehalem Bank are indicated on SP-106. Note projected location of carbonate chimneys over accretionary prism on SP-104. (After Schroeder et al. 1987).

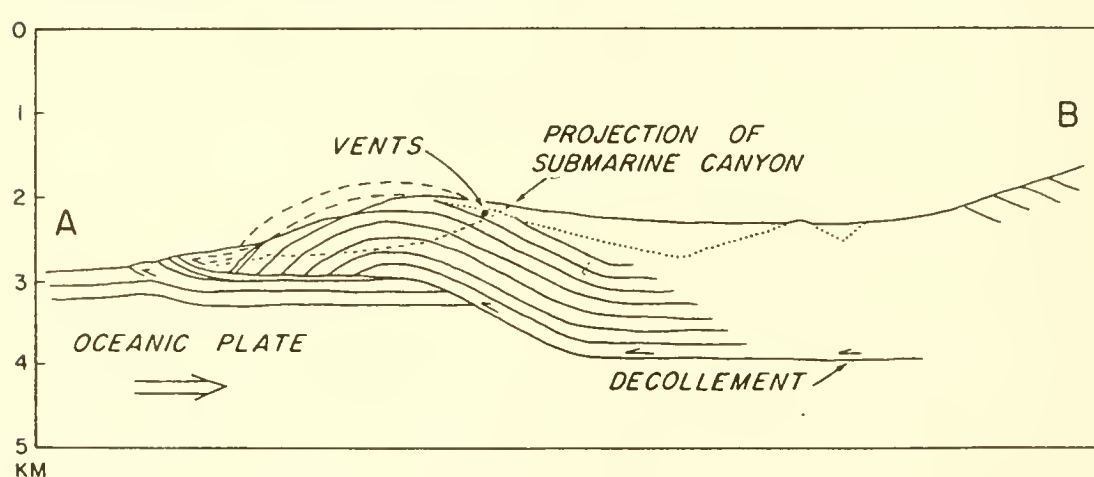
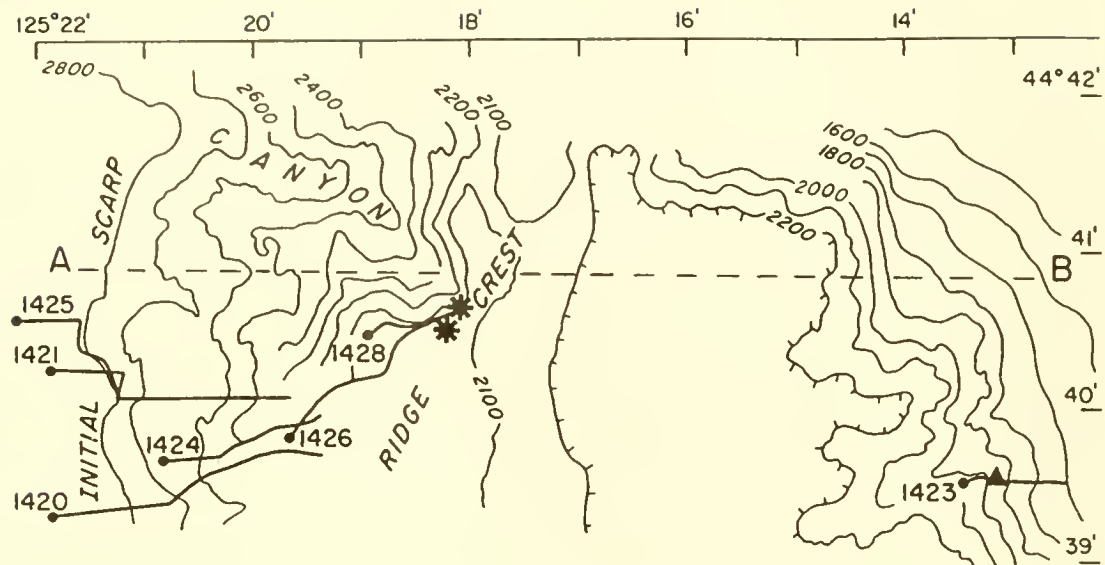


Figure 4. (Top diagram) Alvin submersible transects and Sea Beam bathymetry map across the lower continental slope (see fig. 1, dive area). Contours in meters; numbered dives commence at the solid dots. Asterisks indicate fluid venting sites and carbonate chimneys (i.e., northern site 1428 and southern site 1426 on marginal ridge); triangle indicates carbonate chimneys at site 1423 on the second ridge. (Bottom diagram) Interpretive structural depth section of the deformation front along profile A-B (dashed line across contour map at top). (From Kulm et al. 1986, their fig. 2.)

characterize most of these sites (Fig. 5; Suess et al. 1985; Kulm et al. 1986; Ritger et al. 1987). Methane concentrations generally range from 180 to 420 nl/liter with maxima of 1300 nl/l in the free water at 1 m above the seafloor, which are 3 to >10 times higher than those found in the ambient waters on the adjacent abyssal plain (Kulm et al. 1986). The expelled fluids are derived from the pore waters that migrate upward through the sediments of the accretionary prism beneath the vents. The clastic sediments of Astoria Fan, which were accreted to the continental slope during late Pleistocene time, are the ultimate source of the methane-enriched fluids (Fig. 1).

Carbonate slabs and crusts are found a few centimeters beneath the sediment surface at each vent site or completely cover the sediments, forming large carbonate surfaces. Isolated, conical carbonate chimneys rise from 1- 2 m above these sediment-covered vent sites (Fig. 5). One isolated carbonate chimney was located above a sharp-crested ridge on the second thrust ridge landward of the marginal ridge (Fig 4). Numerous cavities, grooves and flutes, which have smoothly rounded edges, give the chimneys a 'sculptured' appearance (Ritger et al. 1987). Each chimney is covered with numerous organisms, consisting of corals and sponges. The two slope chimneys contain magnesian calcite, dolomite and aragonite with minor amounts of detrital clays, silt and sand (Ritger et al. 1987).

At each vent site, where the authigenic carbonates are forming, methane-enriched waters were being expelled from the underlying accretionary prism (Ritger et al. 1987). According to the stable carbon isotope data the carbonates are derived from a reservoir that is extremely depleted in carbon 13. Values of  $\delta^{13}\text{C}$  of all carbonate samples collected on the margin range from  $-34.9\text{ ‰}$  to  $-66.7\text{ ‰}$  PDB; this indicates a methane-derived carbon source (Ritger et al. 1987). The two slope chimneys analyzed have a  $\delta^{13}\text{C}$  value of  $-32.5$  and  $-32.6\text{ ‰}$  and  $\delta^{18}\text{O}$  values of  $+5.4$  to  $+6.2\text{ ‰}$ , which indicate that the carbonates are marine and formed close to equilibrium with the ambient bottom water temperature. This confirms other evidence that the temperature of the venting fluid is only slightly elevated, if at all different, from that of the bottom water.

### Continental Shelf

The chimneys recovered on the outer continental shelf in 1985 range in height from 1 to 2 m (Table 1; Figs 6,7; Schroeder et al. 1987). The conical chimneys (Fig. 6, chimneys 1,3) are very similar in shape and size to those found on the lower slope. Each chimney has a hollow center, or vertical cavity, along with at least one large cavity in the side wall; numerous smaller tubes penetrate the walls. Chimney 2 is unique because of its cylindrical shape; it contains more small tubes and cavities than the conical ones. A secondary tube that runs parallel to the

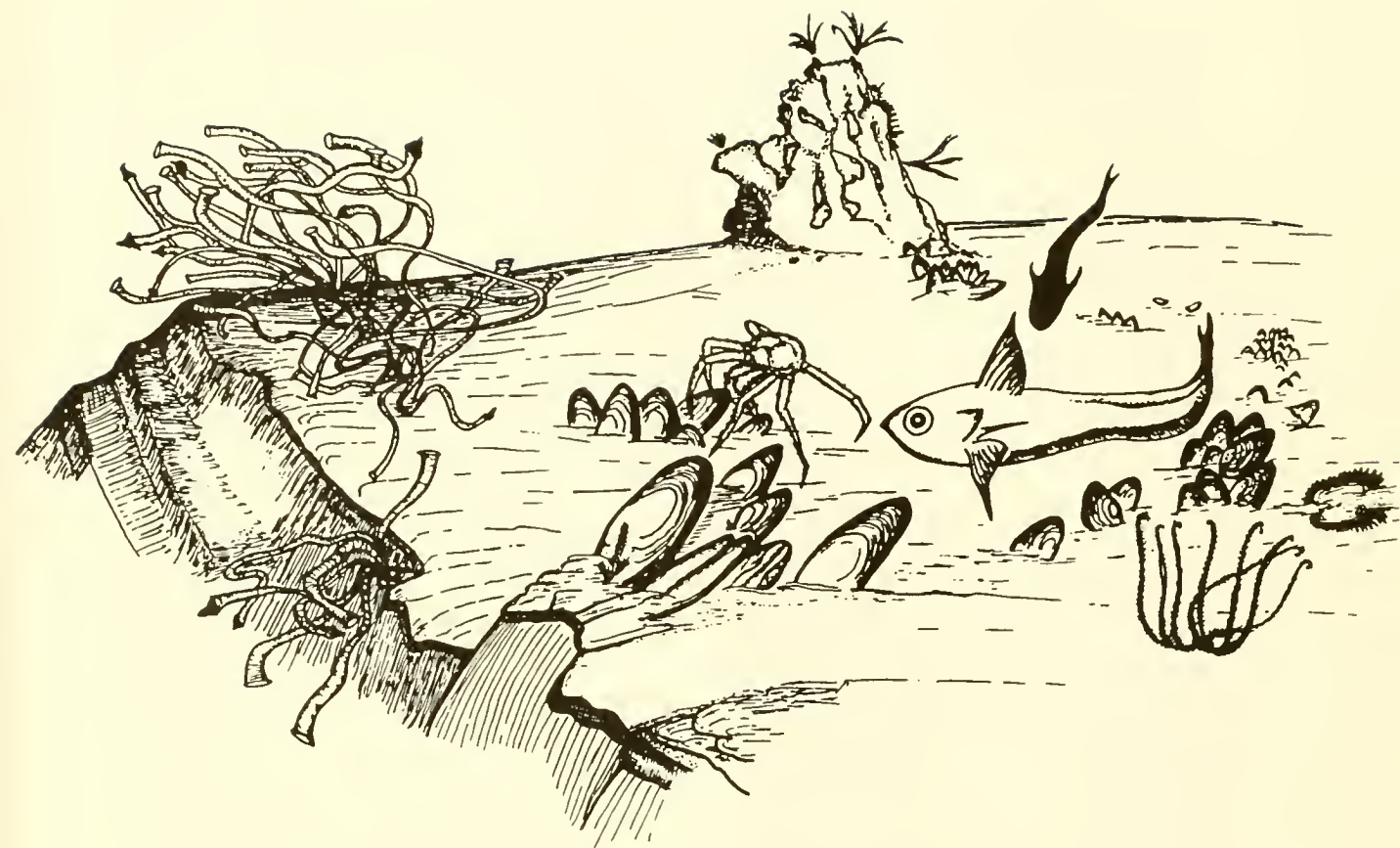


Figure 5. Composite sketch of fluid venting site 1428 on marginal thrust ridge (see fig. 4 for location). Colonies of tube worms occupy the ledge above the canyon wall, and several clusters of giant white clams are aligned along presumed zones of fluid expulsion. Cone-shaped carbonate chimney structure, with attached corals, is seen at the top of the sketch. Venting sites are about  $20 \text{ m}^2$  areal extent. (From Suess et al. 1985, their fig. 1.)

Table 1. Physical characteristics of the carbonate chimneys recovered from the outer continental shelf off northern Oregon. Dimensions given in metric system (m and cm) and weight in English system (lb).

Characteristic	Chimney #1(a)	Chimney #2(b)	Chimney #3(c)	Shelf Chimney(d)	Edifice(e)
Shape	conical	cylindrical	conical	cylindrical	irregular
Weight estimate	900 lb	400 lb	500 lb		200 lb
Height	1.0 m	1.7 m	90 cm	15-20 cm	63 cm
Top diameter	40 cm	30 cm	30-50 cm	25-30 cm	33 cm
Base diameter	75 cm	30 cm	40-60 cm		52 cm
Wall thickness	10-30 cm	3-15 cm	30-16 cm	5-10 cm	solid
Vertical vent hole diameter					
top	10 cm	13 cm	10 cm	15-20 cm	none
base	30 cm	13 cm	18 cm	none	same
Color*	mostly lt gr N-7 Br Gy 5YR 5/1**	same	same	same	same
Biological artifacts	abundant	abundant	common	none	common

(a-c) from Schroeder et al., 1987

(d-e) this study

\* Geological Society of America color chart

\*\* In vent holes

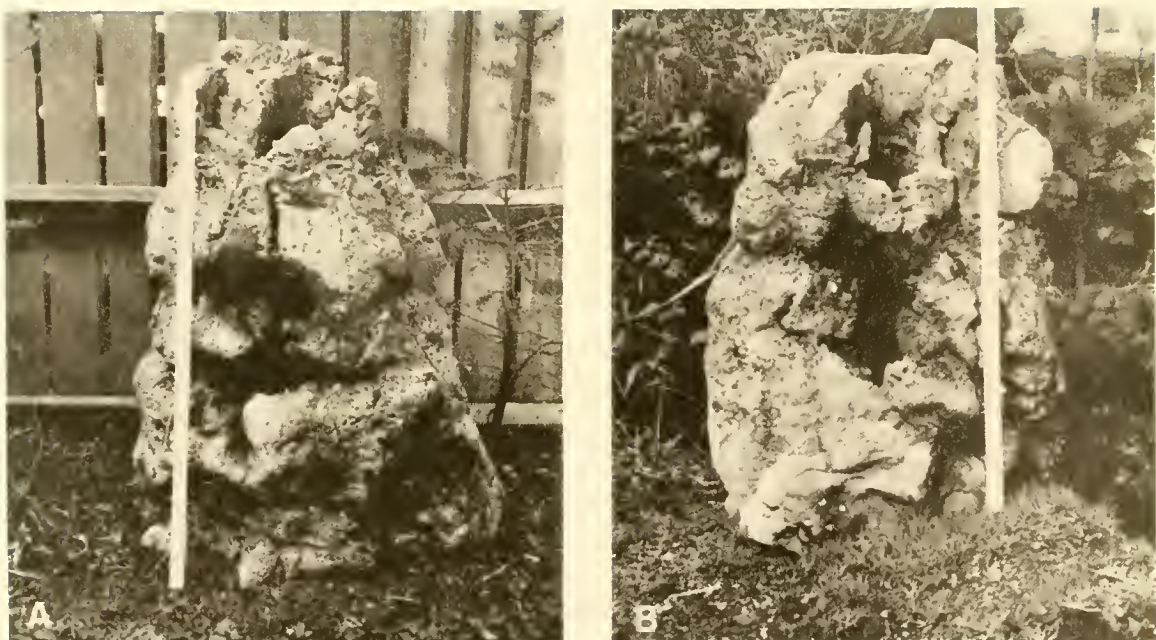


Figure 6. Conical carbonate chimneys (A = chimney #1 and B = chimney #3) dragged from the outer continental shelf off northern Oregon. See figure 2 for location designed chimney field. Note cone-like shape and large internal cavities viewed through openings in the side walls and top. See table 1 and text for detailed description of chimneys. Scale is 1-meter ruler. (After Schroeder et al. 1987).

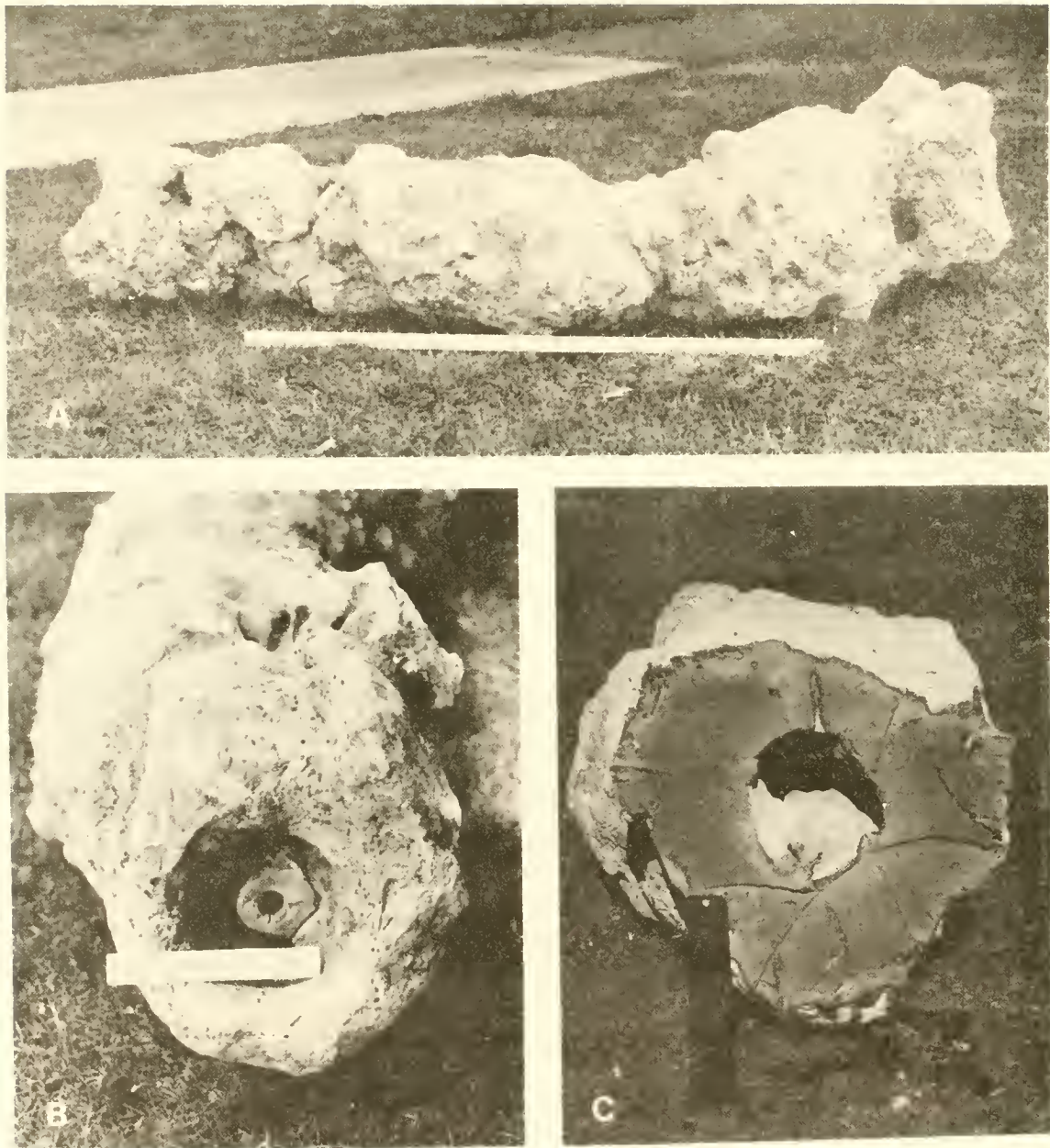


Figure 7. (A) Cylindrical carbonate chimney #3, lying on its side, dragged from same location as conical chimneys (see fig. 2). We have no indication which end is the top or bottom of the chimney, but for sampling purposes the top and bottom were arbitrarily chosen. (B) End view of cylindrical chimney; note internal cavity with its well-rounded, open plumbing tube that runs parallel to the main chamber. Scale is 6-inch ruler. (C) Cross-sectional cut of the smaller of the two ends of cylindrical chimney; burrowing animals produce grooves in dense carbonate lithology. See table 1 and text for detailed description of chimney. Scale is 6-inch ruler. (After Schroeder et al. 1987).

main cavity extends the length of the chimney. Skeletons of encrusting corals and sponges are still attached to the chimneys. Dolomite (69 -89% carbonate), SiO<sub>2</sub> (14-22%), and Al<sub>2</sub>O<sub>3</sub> (4-6%) are the chief components of the shelf chimneys (Schroeder et al. 1987). Tests of foraminifera as well as scattered quartz and feldspar grains occur within the carbonate matrix.

The stable isotopic composition of the three shelf chimneys is quite similar (Table 3). Negative  $\delta^{13}\text{C}$  values (-16.9 to -21.9 ‰) show that the carbon in these carbonates is moderately depleted in carbon-13. Interestingly, the large positive  $\delta^{18}\text{O}$  values (+7.62 to +7.87 ‰) are much heavier than those found in other authigenic carbonates on the lower and middle continental slope on the Oregon margin (Ritger et al. 1987), suggesting a different source of fluids within the accretionary prism.

## RESULTS

### Field Observations and Sampling: Northern Oregon Shelf

One submersible dive, two ROV deployments, and two otter trawls were conducted on the northern Oregon shelf and upper slope in the vicinity of Nehalem Bank (Fig. 8). Collectively, these observation and sampling devices outlined extensive areas of carbonate deposits which occur in a great variety of sizes and shapes. The first ROV traverse (#1) covered the southern side of the uplifted bank from water depths of 382 to 92 m. This traverse showed the frequent occurrence of flat-lying carbonate slabs and crusts on the seafloor and a perfect example of a cylindrical chimney rising above the seafloor. Many irregular carbonate edifices, the size of large boulders, were also encountered along the traverse. These features are all covered with abundant benthic organisms, especially crinoids (see Carey et al. 1988).

The crusts and slabs are generally several centimeters to tens of centimeters thick, have an irregular shape and are about one meter across at the widest dimension. The slabs clearly rise above the surrounding sediment for several tens of centimeters. They are whitish in color along their edges which strongly suggests they are composed of carbonate. Several of these structures have holes on their surfaces and are free of sediment while others appear to have a thin covering of sediment. One slab was recovered with the submersible. Crinoids are attached to most slabs and crusts in great numbers.

One perfectly circular chimney was clearly identified in ROV traverse #1 (see Table 1, shelf chimney). It rises from 15 to 20 cm above the surrounding seafloor and is 25 to 30 cm across. This chimney has a vertical opening of 15 to 20 cm in diameter which is completely free of sediment. It appears to be, at least partially, embedded within the sedimentary strata of the

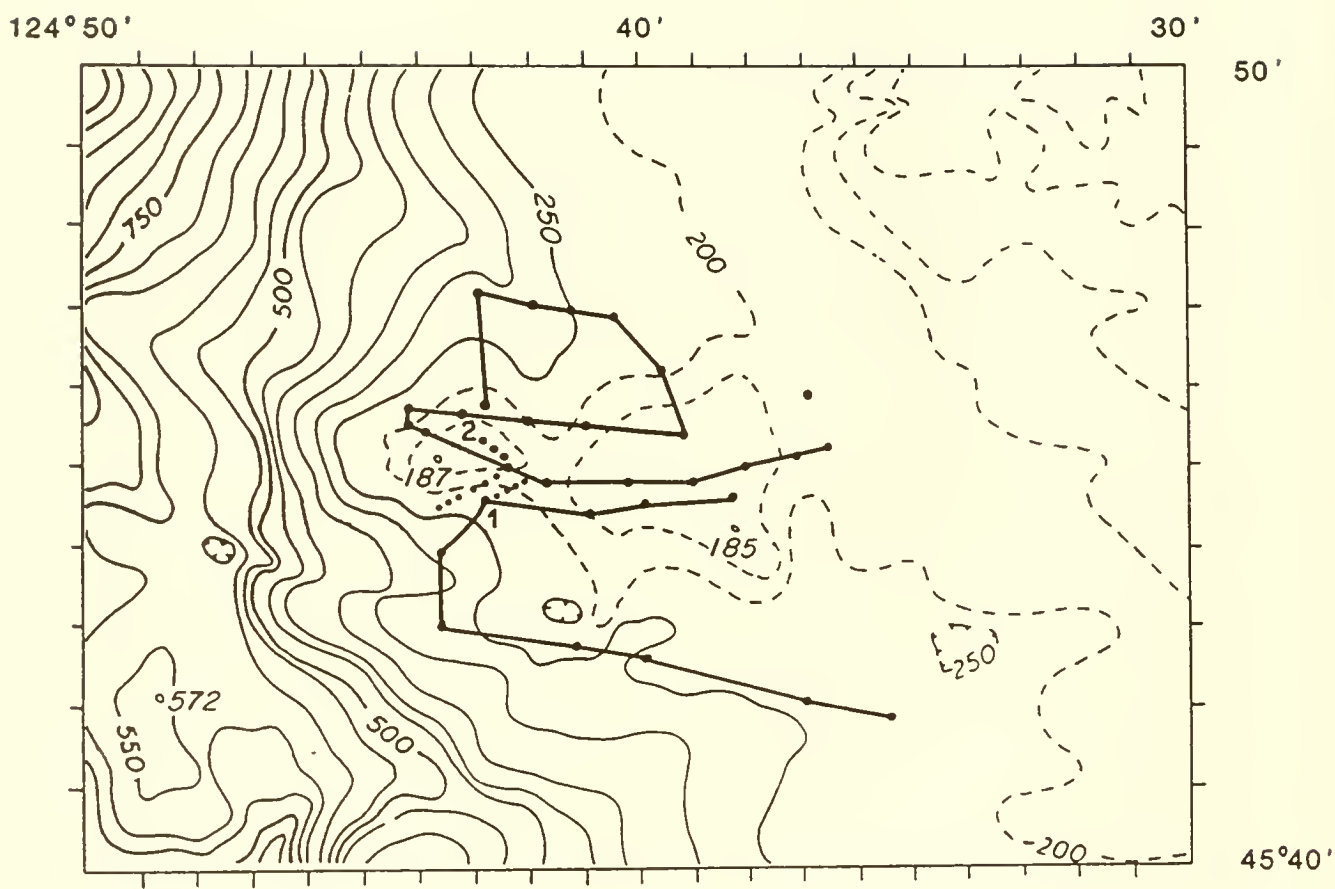


Figure 8. Bathymetry map of the submersible and ROV survey area. Solid lines are fathometer tracklines from the R/V Aloha cruise 8708-I. Dotted lines are tracklines of ROV #1 and #2 deployments (see text for discussion); track commences at the number of each track. Contours are in meters.

seafloor, but the extent of its subsurface penetration could not be determined from the video observation only.

Other carbonate edifices rise up to 0.6 meter above the seafloor and many have a constricted stem just above the sediment-water interface and a bulbous thicker structure above it with numerous intertwined tube sections which appear to be conduits for venting fluids. (Using these criteria, we were able to differentiate normal sedimentary boulders and rock fragments on the seafloor from those constructional carbonate features related to fluid vents.) The surfaces of the carbonate edifices are covered with numerous holes, borings and sharp protrusions which harbor benthic organisms, such as chitons, worms and solitary and encrusting corals.

One of these carbonate edifices was recovered intact in an otter trawl (Fig. 9). This structure (weighing 200 lbs) showed a clear demarkation line separating a chalky, whitish upper section covered with knobs and irregular protrusions to a sulfide-stained black lower section having essentially the same surface features. Iron oxide stains near the color boundary indicate that it marks the oxic-reducing transition which, in the area of investigation, roughly coincides with the sediment-water interface. This indicates that the lower portion of the structure was buried in the sediment; the buried section is reminiscent of the cylindrical chimneys recovered by the fishing vessel Kodiak. However, in the upper portion of the edifice there is a profusion of cemented tubes which are exceedingly complex in shape, but they clearly indicate a plugged (cemented) plumbing system. Several generations of interior and exterior cement can be recognized, notably a white fibrous carbonate cement which fills the last remaining voids within the tubes (Fig. 10). Another generation of cement is a 5-mm thick botryoidal cement with amber colored laminae which covers the exterior of the tubes and the interstices between adjoining tube segments (Fig. 11).

The bulk of the chimney as well as the walls of the plumbing system consist of aragonite and/or Mg-calcite cemented glauconite sand. The insoluble fraction of two representative samples ranges from 29 to 68 wt.-%, and consists of well-sorted glauconitic grains (0.063 to 0.25 mm in diameter) and some small fraction of clays (Table 2). The dark glauconitic groundmass generally consists of aragonite and Mg-calcite or just aragonite. The gray cement is usually Mg-calcite while the white cement is aragonite.

The stable isotopic composition of the irregular carbonate edifice shows that samples 1 through 5 taken from this chimney structure (Fig. 9) are highly depleted in carbon-13 and range from  $\delta^{13}\text{C}$  -48.27 to -53.31 PDB (Table 3). The oxygen values are positive, ranging from  $\delta^{18}\text{O}$  +4.19 to +4.84 PDB (Table 3). The highly depleted carbon-13 values indicate a methane and  $\text{CO}_2$ -

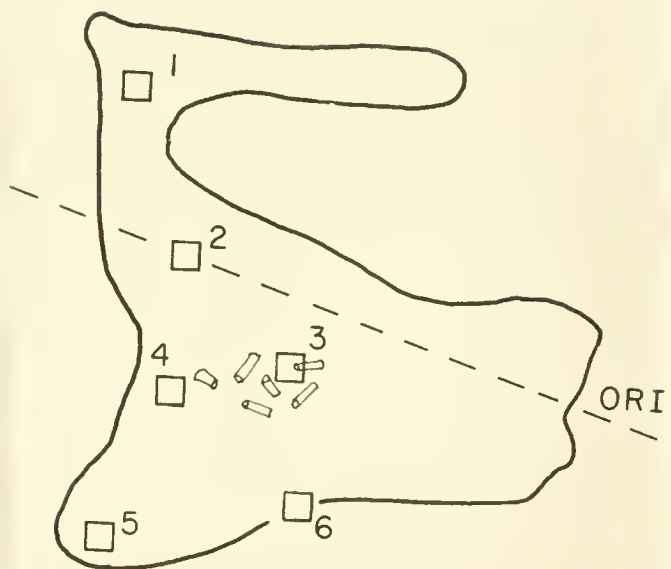


Figure 9. (Left) Irregular carbonate edifice recovered from the outer continental shelf off northern Oregon in Aloha trawl in 1987. (Right) Sketch of edifice showing samples (1-6) taken for geochemical analyses. Note small cemented tubes illustrated in sketch (sample 3). ORI is the oxic reducing interface (see text for explanation). Analyses are given in tables 2 and 3.

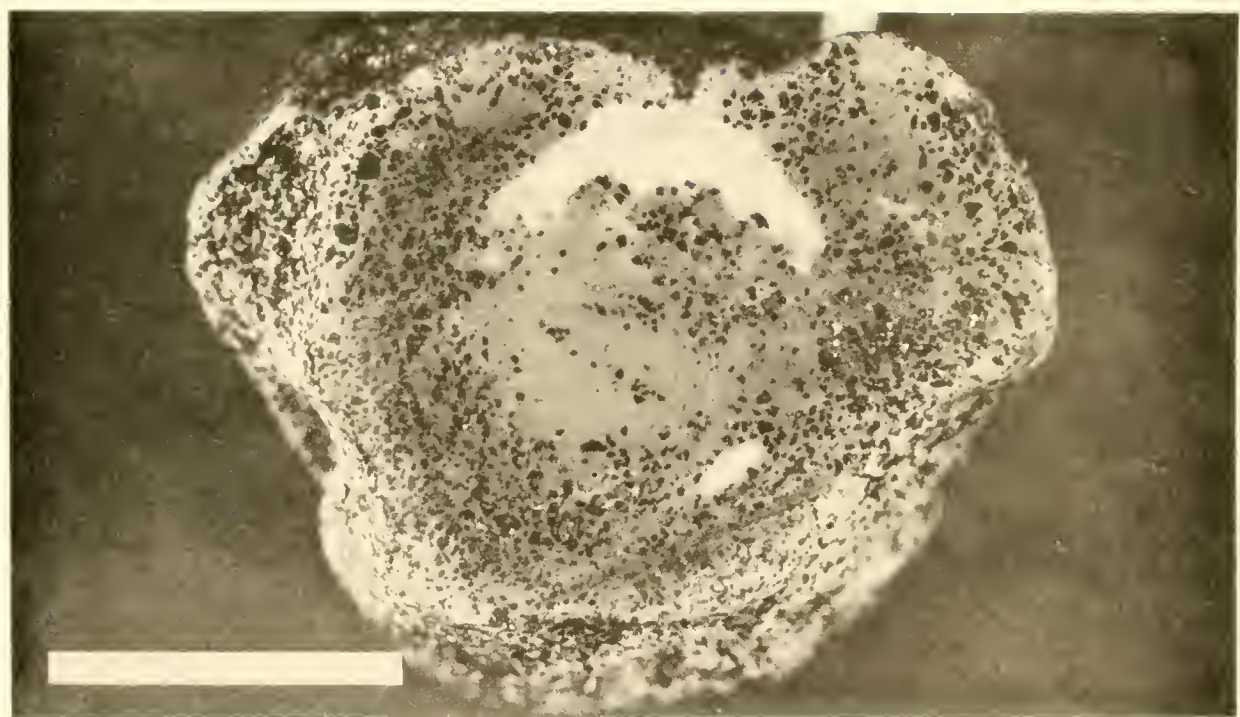


Figure 10. Cemented vent tube from carbonate edifice (see sample 3, fig. 9; subsamples 3a-exterior wall of cemented black groundmass, 3b-interior tube gray cement, 3c-interior tube white cement, table 3). White bar is 1 cm in length.



Figure 11. Exterior black glauconitic groundmass of carbonate edifice (see sample 4, fig. 9; subsample 4b-exterior white cement, table 3). White bar is 1 cm in length.

Table 2. Insoluble residues of cemented groundmass of irregular carbonate structure from Aloha trawl.

Grain Size (Micron)	Sample 2 E Chalky White Groundmass (Wt - %)	Sample 4 D H <sub>2</sub> S Stained Groundmass (Wt - %)	Dominant Mineralogy
>250	7.8	12.6	Glauconite
150-250	13.4	20.7	Glauconite
150- 63	5.4	7.8	Glauconite
< 63	2.2	27.4	Clay
Total Glauconite	26.6	41.1	
Total Clay	2.2	27.4	
Total Carbonate	71.2	31.5	Mg-Calcite Aragonite

Table 3. Analyses of irregular carbonate edifice obtained from Aloha trawl.

Sample Description	Principal mineralogy	$\Delta O^{18}$ ( $^{\circ}$ /oo PDB)	$\Delta C^{13}$ ( $^{\circ}$ /oo PDB)
1. Weathered surface, chalky cemented glauconite sand			
a. Groundmass dominating	Aragonite	+4.20	-49.91
b. Cement dominating	Aragonite	+4.37	-50.63
2. Weathered surface, gray oxic-reducing boundary			
a. Groundmass, soft, whitish	Aragonite, Mg-Calcite	+4.42	-51.59
b. Groundmass, fresh interior, hard, black	Aragonite, Mg-Calcite	+4.49	-51.24
c. Gravelly groundmass with white cement	Aragonite	+4.32	-48.27
3. Cemented tube segment			
a. Fresh tube wall, black cemented sandy groundmass	Aragonite, Mg-Calcite	+4.56	-51.54
b. Interior cement, gray	Mg-Calcite	+4.84	-52.23
c. Interior cement, white	Aragonite	+4.30	-51.75
4. Groundmass, black with "laminated" exterior cement			
a. Fresh interior groundmass, black	Aragonite, Mg-Calcite	--	--
b. Exterior cement, white	Aragonite	+4.19	-51.96
5. Fresh groundmass, black with yellowish fibrous cement			
a. Fresh groundmass, black	Aragonite, Mg-Calcite	+4.42	-51.80
b. Exterior cement	Aragonite	+3.95	-53.31

bearing source for the precipitating fluids that created this carbonate structure.

#### Field Observations and Sampling: Central Oregon Shelf

Two submersible dives and two ROV deployments were conducted in the area around the northern end of Heceta Bank (see Fig. 1, symbol HB) where clams known to harbor chemosynthetic bacteria were recovered during earlier trawling expeditions by benthic biologists (A.G. Carey) at Oregon State University. No carbonate structures were encountered in this area. The seafloor was covered with sediments to the north of the bank and benthic animals, especially sea pens, were quite abundant here. Several dives made on Heceta Bank in another submersible program did not reveal any carbonate structures. Therefore, we conclude that this area of the Oregon shelf probably does not contain any obvious carbonate structures which might be related to fluid venting.

#### DISCUSSION

##### Comparison of Chimney Structures

From the ROV observations on the northern Oregon shelf we know that the cylindrical carbonate chimney observed from the ROV on the seafloor in 1987 is virtually identical in shape and diameter to the cylindrical chimney which was recovered in a trawl net from the outer continental shelf in 1985 (see Table 1). The large sediment-free opening (15 to 20 cm) that was observed within the chimney suggests that fluid venting is actively occurring through this structure. A previous study shows that all chimneys dredged from this area possess an internal plumbing system consisting of large cavities as well as small tubes (Schroeder et al. 1987). This plumbing network allows the methane-enriched and CO<sub>2</sub>- charged fluids, which are apparently derived from permeable sand zones or fault zones within the underlying strata, to flow through the chimneys and precipitate the authigenic carbonate that forms the chimney walls. The new chimney structure appears to be embedded within the sedimentary rocks of the seafloor to some unknown depth. In this case, the flow probably emanates from a hole in the top of the chimney and carbonate precipitation occurs uniformly over the external portions of the structure that protrude from the seafloor. From the distribution of open tubes within the cylindrical chimney obtained in the trawl (Fig. 7), it is clear that the precipitation patterns may also produce a rather complex and elaborately intertwined plumbing system (Schroeder et al. 1987). While the high seas at the surface and the lack of an acoustic tracking system on the ROV, precluded us from scanning the opening of the embedded chimney for internal tubes, we believe that it was technically feasible to accomplish such a task.

## Distribution of Carbonate Crusts, Slabs and Edifices

The two ROV surveys clearly showed, for the first time, that authigenic carbonates occur in a great variety of configurations over an extensive area of the upper slope and outer continental shelf off northern Oregon. Previous dredge and dart core samples from this region of the Oregon margin occasionally recovered calcareous mudstones, but no carbonate slabs (Kulm and Fowler 1974; Kulm et al. 1984). Direct observation with the ROV and submersible allows mapping of the distribution pattern of the carbonates to locate the most likely areas of active fluid venting.

## Composition of Carbonates

The carbonate mineral composition of the irregular edifice is quite different from that of the three other chimneys recovered from the same area on the continental shelf. The former structure consists largely of aragonite and Mg-calcite while the latter structures consist of dolomite. This wide range in carbonate composition was also reported from the several venting areas on the continental slope off Oregon (Ritger et al. 1987).

The carbonate edifice recovered in the Aloha trawl is highly depleted in carbon-13 (average -51.29) compared to the conical and cylindrical carbonate chimneys (average -19.77) recovered by the commercial trawling vessel Kodiak from the same area of the outer continental shelf. Both the oxygen and carbon isotopes suggest that the sources of fluids for the two types of chimney structures are different. There appears to be a rather broad range in carbonate mineralogy and stable isotopic composition in both the shelf chimneys and the slope chimneys. In the next field program in 1988, we shall determine under what geochemical and geological conditions each of the different chimney compositions occurs in the active venting areas on both the shelf and slope. We shall attempt to sample the fluids being expelled at each vent site as described below.

## Fluid Flow Measurements

Preparations were made prior to the cruise to sample the fluids flowing from any of the venting structures (e.g., carbonate chimneys, slabs, edifices) that might be found on the shelf. A new automated rosette water sampler enclosed in a benthic chamber was constructed by the investigators for sampling these fluids. Unfortunately, only one submersible dive was completed in the northern shelf and this was before the chimney and slab structures were discovered by the ROV. While this water sampling device was not used on this cruise, it was deployed successfully two weeks later at a vent site on the lower

continental slope with the aid of the submersible Alvin. Two time series measurements of fluid flow were completed using the chemical changes of the captured fluids (Suess et al. 1987). On one of these deployments, fluid flow was measured with a flow meter attached to the water sampler. It is highly probable that an equally successful deployment could have been achieved had the weather conditions been better and the technical layout and equipment performance of the Mermaid and Aloha been optimized.

### Formation and Origin of the Carbonate Chimneys

Two hypotheses had been proposed for the origin of the chimney structures: (1) upward growth of the chimney above the seafloor, and (2) chimney formation below the seafloor within the sediment column with later exhumation by uplift and erosion (Ritger et al. 1987; Schroeder et al. 1987). Based upon the present study, we now think that the chimney grows upward approximately at the same rate as the clastic sediments are deposited at the sediment-water interface around the chimney. The continuing fluid flow essentially keeps the precipitating carbonate walls free of fine clastic debris, although the three chimneys recovered from the shelf do contain sand and silt-sized quartz, glauconite and feldspar. If the rate of clastic sedimentation is slow and fluids continue to flow through the chimney, it will grow upward well above the sediment-water interface producing a much longer cylindrical chimney structure (i.e., similar in length to the one recovered by the fishing vessel Kodiak, Fig. 7). On the other hand, if the rate of sedimentation is fast, the upward growth of the chimney might not keep pace with the clastic sedimentation and the structure will be buried. In this case, the escaping fluid may find a more circuitous route to the surface and in the process forms the complexly intertwined plumbing structure noted in the irregular carbonate edifice recovered in this project (Fig. 9). It is clear that some of the shelf chimneys were formed within the seafloor and that they probably represent relatively recent venting of methane and dissolved carbonate-bearing fluids from the underlying Oligocene to Miocene accretionary prism.

### CONCLUSIONS

1. Extensive carbonate deposits were discovered on the seafloor on the upper continental slope and outer continental shelf off northern Oregon. This carbonate deposition is occurring in a depositional environment dominated by clastic sedimentation, which implies a unique set of geochemical processes in the area
2. These carbonate deposits include a large variety of structures, such as crusts, slabs, chimney and irregular edifices, which are covered with abundant living benthic organisms. The lack of terrigenous sedimentation on many of the

features, the numerous open holes, and the sediment-free opening of one chimney indicate that carbonate deposition is presently active in this area.

3. We propose that the carbonate structures are formed through aragonite, Mg-calcite, and dolomite precipitation from methane and dissolved carbonate-rich fluids that emanate from these structures. An open plumbing network is initially created and maintained by the deposition of the carbonate within and on top of the terrigenous substrata that comprise the seafloor. In some structures, the plumbing tubes are eventually cemented with carbonate causing the venting fluids to seek alternate routes of expulsion around the structure. The ultimate source zones for these fluids are most likely located within the Oligocene to Miocene accretionary prism underlying the outer continental margin.

#### ACKNOWLEDGMENTS

We gratefully acknowledge the financial support of NOAA's Office of Undersea Research in providing the submersible Mermaid with its support vessel Aloha and ROV Recon-IV in this study. The research support for this study was provided by the Oregon State University Sea Grant Program.

#### LITERATURE CITED

Barnard, W. D. 1978. The Washington continental slope: Quaternary tectonics and sedimentation. Mar. Geol., Vol. 27, pp. 79-114.

Brooks, J. M., M. C. Kennicutt II, R. R. Fay, T. J. McDonald, and R. Stassen. 1984. Thermogenic gas hydrates in the Gulf of Mexico. Science, Vol. 22, pp. 965-967.

Childress, J. J., T. J. Fisher, J. M. Brooks, M. C. Kennicutt II, R. R. Bidigare, and A. Anderson. 1986. A methanotrophic marine molluscan (Bivalvia, Mytilidae) symbiosis: Mussels fueled by gas. Science, Vol. 233, pp. 1306-1308.

Hovland, M., M. R. Talbot, M. R. Qvale, S. Olausson, and L. Aasberg. 1987. Methane-related carbonate cements in pockmarks of the North Sea. J. Sedimen. Petrol., Vol. 57, pp. 881-892.

Kulm, L. D., E. Suess, J. C. Moore, B. Carson, B. T. Lewis, S. D. Ritger, D. C. Kadko, T. M. Thornburg, R. W. Embley, W. D. Rugh, G. J. Massoth, M. G. Langseth, G. R. Cochrane, and R. L. Scamman. 1986. Oregon subduction zone: venting, fauna, and carbonates. Science, Vol. 231, pp. 561-566.

Kulm, L. D., P. W. Loubere, and J. S. Peper. 1984. Geology of the continental margin and Cascadia Basin. In: L. D. Kulm et al. (eds.), Atlas of the Ocean Drilling Program, Western North America Continental Margin and Adjacent Ocean Floor off Oregon and Washington, Region IV, Joint Oceanographic Institutions, Inc., Marine Sciences International, Woods Hole, MA, sheet 29.

Kulm, L. D. and G. A. Fowler. 1974. Oregon continental margin structure and stratigraphy: a test of the imbricate thrust model. In: C. A. Burk and C. L. Drake (eds.), The Geology of Continental Margins, New York, N.Y., Springer-Verlag, pp. 261-283.

Kulm, L. D., R. A. Prince, and P. D. Snavely, Jr. 1973. Site survey of the northern Oregon continental margin and Astoria Fan. In: Initial Reports of the Deep Sea Drilling Project, U.S. Government Printing Office, Washington, D.C., Vol. 18, pp. 979-987.

Le Pichon, X., T. Iiyama, J. Boulegue, J. Charvet, M. Faure, K. Kano, S. Lallemand, S. Okada, C. Rangin, A. Taira, T. Urabe, and S. Uyeda. 1987. Nankai Trough and Zenisu Ridge: a deep-sea submersible survey. Earth and Planet. Sci. Lett., Vol. 83, pp. 285-299.

Paull, C. K., B. Hecker, R. Commeau, R. P. Freeman-Lynde, C. Neuman, W. P. Corso, S. Golubic, J. E. Hook, E. Sikes, and J. Curray. 1984. Biological communities at the Florida Escarpment resemble hydrothermal vent taxa. Science, Vol. 226, pp. 965-967.

Peterson, C. P., L. D. Kulm, and J. J. Gray. 1986. Geologic map of the ocean floor off Oregon and the adjacent continental margin. State of Oregon Department of Geology and Mineral Industries, Geological Map Series, GMS-42.

Ritger, S., B. Carson, and E. Suess. 1987. Methane-derived authigenic carbonates formed by subduction-induced pore water expulsion along the Oregon/Washington margin. Geol. Soc. Amer. Bull., Vol. 98, pp. 147-156.

Schroeder, N. A. M., L. D. Kulm, and G. E. Muehlberg. 1987. Carbonate chimneys on the outer continental shelf: evidence for fluid venting on the Oregon margin. Oreg. Geol., Vol. 49, No. 8, pp. 91-96.

Snavely, P. D. Jr., H. C. Wagner, and D. L. Lander. 1980. Interpretation of the Cenozoic geologic history, central Oregon continental margin: Cross-section summary. Geol. Soc. Amer. Bull., Vol. 91, pp. 143-146.

Suess, E., L. D. Kulm, and M. J. Whiticar. 1987. Fluid flow and methane fluxes at the Oregon subduction zone. Abstract, EOS Transactions, Amer. Geophys. Union (in press).

Suess, E., B. Carson, S. D. Ritger, J. C. Moore, M. L. Jones, L. D. Kulm, and G. R. Cochrane. 1985. Biological communities at vent sites along the subduction zone off Oregon. In: M. L. Jones (ed.), The Hydrothermal Vents of the Eastern Pacific: An Overview, Biol. Soc. Washington, No. 6, pp. 475-484.

ENERGY AND CARBON SOURCES FOR ENDOSYMBIOSES  
BETWEEN BACTERIA AND MARINE INVERTEBRATES

James J. Childress and Charles R. Fisher  
Marine Science Institute and  
Department of Biological Sciences  
University of California  
Santa Barbara, CA 93106

ABSTRACT

The major sessile invertebrate species living around the hydrocarbon seeps on the Louisiana Slope were collected alive using the Johnson Sea-Link submersible in June of 1987. Specimens collected were either frozen for later studies, studied on board the RV Seward Johnson or brought alive to UC Santa Barbara for live maintenance and further study. Extensive studies have been carried out on these materials to determine the carbon and energy sources utilized by the endosymbionts. These tests have indicated that the symbionts of the mytilid mussel are methanotrophs which use methane as both an energy and carbon source. In contrast all of the other symbioses from this environment which we have studied appear to have endosymbionts which derive energy from the oxidation of reduced sulfur compounds and carbon from the fixation of inorganic carbon. Several lines of evidence indicate that the endosymbionts provide much, if not all, of the carbon utilized by the hosts in some of these symbioses.

INTRODUCTION

Shortly after the discovery of the deep-sea hydrothermal vents in 1977 (Corliss et al. 1978), biologists realized that the major sessile animal species contained chemoautotrophic bacterial symbionts within their bodies (Cavanaugh et al. 1981; Felbeck 1981; Felbeck, Childress, and Somero 1981). This initial realization was quickly followed by the discovery of similar symbioses in other reducing habitats as well as in other invertebrate taxa (Cavanaugh 1985; Felbeck, Childress, and Somero 1981; Southward et al. 1981). In the flurry of searching for new symbioses, the nutritional bases of the various symbioses were only superficially described. However, the energy source for all of the symbioses appeared to be reduced sulfur compounds. The remarkable discovery of vent-type taxa around hydrocarbon seeps on the Louisiana Slope (Brooks et al. 1985) raised the question of the energy and carbon sources of the animals in this hydrocarbon rich environment.

The nutrition of these symbioses can be approached from several perspectives. First there is the question of the energy and carbon sources of the symbionts. Second is the interaction of the hosts with the inorganic substrates including the possible derivation of energy from inorganic substrates by the hosts (Powell and Somero 1986). Third is the degree to which the hosts obtain reduced carbon compounds from their symbionts and from their environment. The nature of the symbiont nutrition can be inferred from a variety of information including assays for key enzymes in the pathways of oxidation of reduced inorganic compounds and the fixation of inorganic carbon, ratios of stable carbon isotopes, autotrophic CO<sub>2</sub> fixation, elemental sulfur contents and symbiont ultrastructure. Additional information about the symbiont nutrition as well as its relationship to the host nutrition can be obtained from studies of the metabolism and growth of the host with symbiont energy and carbon sources. This study describes our efforts to date to determine the nutritional basis of the major sessile invertebrates living around the hydrocarbon seeps.

## METHODS

The animals studied were collected with the manipulator of the Johnson Sea Link submersible. They were brought to the surface in a closed box which protected them from the warm surface temperatures. Once at the surface the animals were kept alive in cold seawater until used. Samples to be frozen were placed in cryovials and then in liquid nitrogen.

### Enzyme Assays

Enzyme assays were done on samples which had been frozen in liquid nitrogen and stored at -70° C. The weighed tissue was homogenized with a ground-glass tissue-grinder in 0.2mM Tris/HCl (pH 7.5) with 1% Triton X100 (1:7 tissue:buffer). This crude homogenate was assayed for RuBP carboxylase activity by the 14 C-incorporation method (Wishnick and Lane, 1971) as modified by Felbeck (1981) and methanol dehydrogenase activity by the spectrophotometric method of Anthony and Zatman (1965). ATP sulfurylase and APS reductase activities were assayed using the methods described by Felbeck (1981).

### Histology

For transmission electron microscopy pieces of gill from freshly recovered animals were fixed in 3% glutaraldehyde in 0.1M phosphate-buffered 0.35M sucrose pH 7.3, and stored in this fixative at 4x C for up to two weeks. The tissues were then washed in buffered sucrose, post-fixed in 1% osmium (on ice) for 1 hour, dehydrated through a graded ethanol series, and embedded in Spurrs embedding medium. Thin sections were cut using an LKB

Ultratome V, stained with uranyl acetate and lead citrate, and examined with a Philips 300 transmission electron microscope.

#### NaH<sup>14</sup>CO<sub>3</sub> Incubations

To test for substrate stimulation of carbon fixation by tissues, small pieces (0.2-0.6 g wet weight) of gill or preparations of vestimentiferan trophosome were incubated with a variety of substrates in 10 ml glass syringes, at 7.5°C, with NaH<sup>14</sup>CO<sub>3</sub> (ICN Radiochemicals, Irvine, Ca., specific activity = 54 mCi/m mol). Gills were dissected from the mussels and cut into small pieces without damaging individual filaments. The pieces of gill were rinsed in 0.45 fm membrane filtered seawater (MFSW) and then preincubated for one hour in MFSW with the substrate to be tested. Following preincubation, the gill pieces were placed in 10 ml glass syringes containing fresh MFSW and the desired substrate (and/or inhibitor). After an additional 10-20 minutes the incubations were initiated by the addition of NaH<sup>14</sup>CO<sub>3</sub> (200fCi/ml) to a final activity of 0.5-2.0 fCi/ml. At the end of the incubation period the NaH<sup>14</sup>CO<sub>3</sub> fixation was stopped by removing the gill pieces from the syringes, quickly blotting them dry, and freezing the pieces in cryovials in liquid nitrogen. Viability of the gill tissue throughout the incubation period was confirmed by visual observation (under a dissecting microscope) of ciliary currents on the surface of other pieces of gill tissue removed from the same animals.

Trophosome was dissected free from the anterior portion of the trunk of the vestimentiferans and tissue containing bacteria was separated from the major blood vessels and gonads also present in this organ. A portion of the tissue (0.49-0.71 g) was quickly weighed on a motion compensated shipboard balance system (Childress and Mickel 1980) and then submerged in 20 ml of deoxygenated (nitrogen purged), pH 7.5 vestimentiferan saline solution. The tissue was gently homogenized for 5-10 seconds in a chilled, loose fitting Dounce type ground glass tissue homogenizer, to rupture the bacteriocytes and disperse the symbionts. A portion of this homogenate was fixed in buffered glutaraldehyde and integrity of the bacteria was later confirmed microscopically in the laboratory. To commence the incubations, NaH<sup>14</sup>CO<sub>3</sub> was added to the trophosome preparation and 3 ml of the preparation was drawn into each of 6 syringes which already contained 7 ml of dilute (~50%) Riftia pachyptila blood or vestimentiferan saline solution, variable concentrations of sulfide (4-3000fM), and a marble for mixing the incubation medium. To confirm that stimulated carbon fixation was through autotrophic pathways, 10 mM D. L. glyceraldehyde (a feedback inhibitor of RuBP carboxylase) was added to one syringe in each series (Stokes and Walker 1972).

The specific activity in each syringe was determined by measuring the total inorganic <sup>14</sup>C activity and the concentration

of inorganic carbon (primarily  $\text{CO}_2 + \text{HCO}_3^-$ ) in the incubation media. To determine the activity of inorganic carbon, replicate 50  $\mu\text{l}$  aliquots were placed in scintillation vials containing 0.1 ml of hyamine hydroxide. Ten ml of Fluorosol (National Diagnostics) was added to each sample, and the disintegrations per minute determined by scintillation counting in a Beckman LS 6800 liquid scintillation counter and corrections made for background and counting efficiency (~ 92%). The total inorganic carbon pool in the seawater or saline incubation media was determined by gas chromatography (Childress, Arp, and Fisher 1984). Rates of total inorganic carbon fixation were calculated from these measurements (Strickland and Parsons 1972).

#### Elemental Sulfur Determination

For the analysis of elemental sulfur, pieces of tissue (0.1 - 4.0 g wet weight) were dried for 18 hours in a 60°C drying oven and then extracted for 24 hours with cyclohexane in a micro-soxhlet apparatus. The extract was cleaned up by passage through a fluorosil column and concentrated by allowing most of the solvent to evaporate. Sulfur in the extract was quantified by gas chromatography according to the method of Richard et al. (1977). Ten  $\mu\text{l}$  of cyclohexane was injected onto the column. The injector temperature was 240°C and the initial column temperature was 150°C programmed to 220°C over the course of the separation. A six foot glass column with a 2 mm bore, packed with 5% SP2401 on 100/120 mesh Supelcoport was used to separate the sulfur. The sulfur was detected and quantified using a thermal conductivity detector. The detection limit for elemental sulfur was ca. 0.001% of the dry weight of the sample (depending somewhat on sample size). The identity of the separated sulfur was confirmed by the distinctive smell of sulfur vapor coming out of the gas chromatograph.

#### Metabolism Measurements

The net fluxes of  $\text{CO}_2$ ,  $\text{O}_2$ ,  $\text{CH}_4$ , and other gases were measured for pieces of gill, trophosome preparations and whole animals to test for methane consumption. The gases were analyzed by gas chromatography of 0.5ml aliquots. The gill and trophosome incubations were prepared as described previously and were carried out in glass syringes. The whole animal incubations were carried out in a flowing water respirometer system (Anderson, Childress, and Favuzzi 1987).

#### RESULTS

The bulk of the results are presented in Table 1. The undescribed hydrocarbon seep mytilid which has been shown to contain methanotrophic symbionts (Childress et al. 1986) has a very different pattern of properties than do the other species tested. It is the only species tested which has endosymbionts

Table 1. Enzyme activities, elemental sulfur (S<sup>0</sup>) content, stable carbon isotope ratio ( $\delta^{13}\text{C}$ ), presence of symbiotic bacteria (S.B.), and methane consumption (CH<sub>4</sub>) in organisms from the Louisiana slope and the Galapagos Rift hydrothermal vents. Assays were conducted on symbiont containing tissues (bivalve gills and vestimentiferan trophosome). One unit of enzyme activity will convert 1  $\mu\text{mol}$  of substrate to product. RuBP, ribulose-bisphosphate carboxylase; ATP, ATP sulfurylase; APS, adenosine-5'-phosphosulfate reductase; methanol, methanol dehydrogenase; sulfide, sulfide oxidase;  $^{14}\text{C}$ , sulfide stimulated fixation of inorganic carbon, CH<sub>4</sub>, methane consumption of gill or trophosome tissue, ND, not detected; N, no; Y, yes; NT, not tested; WW, wet weight; and EM, electron microscopy.

Animal	Enzyme activity (units/g WW/min)						S <sup>0</sup> (% WW)	$^{14}\text{C}$	$\delta^{13}\text{C}$	S.B. (E.M.)	CH <sub>4</sub>					
	RuBP	ATP	APS	CH <sub>3</sub> OH	Sulfide											
Louisiana slope animals																
Mollusca																
Lucinidae																
<u>Pseudomiltha</u> sp.	0.43	10.25	0.95	ND	2.03	0.15	Y	-34.3	Y	N						
Mytilidae																
undescribed	0.018	ND	ND	0.53	0.85	ND	N	-52.1	Y	Y						
Vesicomyidae																
<u>Vesicomya</u> <i>cordata</i>	NT	29.58	ND	ND	NT	ND	NT	-39.8	Y	NT						
<u>Calyptogena</u> <i>ponderosa</i>	NT	NT	NT	NT	NT	4.4	NT	-37.4	Y	NT						
Vestimentifera																
Lamellibrachiidae																
<u>Lamellibrachia</u> sp.	3.08	1.93	0.74	ND	3.46	4.4	Y	-36.9	Y	N						
Undescribed family																
undescribed sp.	4.23	1.08	1.54	ND	3.56	0.8	Y	-38.6	Y	N						
Galapagos Rift hydrothermal vent animals																
Mollusca																
Mytilidae																
<u>Bathymodiolus</u> <i>thermophilus</i>	0.003	2.7	ND	ND	0.92	ND	N	-35.6	Y	N						
Vesicomyidae																
<u>Calyptogena</u> <i>magnifica</i>	0.032	2.47	NT	ND	5.83	1.2	Y	-32.7	Y	N						
Vestimentifera																
Riftiidae																
<u>Riftia</u> <i>pachyptila</i>	0.50	57.74	23.3	ND	27.89	4.83	Y	-12.8	Y	N						

with methanol dehydrogenase, the second enzyme in the pathway for the oxidation of methane. It is also the only species which shows methane consumption, and as Fisher et al. (1987) have shown the rate of consumption is proportional to the activity of this enzyme in individual mussels. The seep mussel is also the only species among those examined whose bacteria have the internal membranes characteristic of Type I methanotrophic bacteria (Anthony 1982). In addition the seep mussel gills lack the enzymes characteristic of sulfur oxidation (adenosine triphosphate sulfurylase and adenosine-5'-phosphosulfate reductase), lack elemental sulfur, and have only trace activities of RuBP carboxylase (an enzyme characteristic of autotrophic carbon fixation); these factors indicate that the seep mussel symbionts are not sulfur-oxidizing chemoautotrophs.

The other three bivalves and the two vestimentiferans from the seeps appear to harbor sulfur-oxidizing chemoautolithotrophic symbionts. The enzyme activities, the presence of elemental sulfur, carbon fixation stimulated by sulfide, and electron microscopy provide evidence that both vestimentiferans and the lucinid clam, Pseudomiltha sp., contain chemoautotrophic, sulfur bacterial symbionts. The evidence for the vesicomyid clams is not as conclusive since we have not yet analyzed the enzyme activities in tissues frozen alive in liquid nitrogen. The absence of specific enzyme activities is thus of little significance. Nonetheless, the high level of elemental sulfur in the gills of C. ponderosa and the high levels of ATP sulfurylase in V. cordata gills suggest that sulfur oxidizing symbionts are present in the living clams. The sulfide oxidase activities in all animals assayed are at the level expected for invertebrates exposed to a sulfide environment (Powell and Somero 1986).

The absence of methane consumption in live animals and the absence of methanol dehydrogenase activity in the symbiont containing tissues clearly indicates that the three vent species (shown in Table 1) do not harbor methanotrophic symbionts. The presence of substantial activities of RuBP carboxylase and ATP sulfurylase, elemental sulfur in symbiont containing tissues, and sulfide stimulation of carbon fixation in these same tissues leaves little doubt that these symbionts are chemoautolithotrophic sulfur oxidizers. The mussel B. thermophilus is however more problematic since it lacks a strong indication of sulfur chemoautotrophy and is clearly not hosting methanotrophs (Fisher et al. 1987).

## DISCUSSION

The data presented here demonstrate the necessity of using as many criteria as possible to characterize the nutrition of symbionts in chemoautotrophic symbioses in the absence of the ability to culture the symbionts. Any one or even several

criteria may show aberrant values in particular symbioses due to biological, environmental or methodological variability. But when a range of carefully selected criteria are used, a pattern usually stands out indicating the nutritional basis of the symbionts.

It is particularly interesting to note that on the Louisiana slope, although one species has methanotrophic symbionts, the others appear to use sulfide as their energy source even though methane appears to be available to at least some of them (Childress 1986). The apparent rarity of methane based symbioses is somewhat puzzling at this time. However, it may simply indicate that there are relatively few habitats which have a sufficient abundance of methane to support symbionts located within the tissues of an animal. In contrast, the hosts of sulfur oxidizing bacteria have a variety of mechanisms for concentrating sulfide from their environments allowing them to live at very low sulfide concentrations in some cases (Childress 1987).

While the nature of the symbionts is coming into focus in these symbioses, the nature of the functional relationship between the symbionts and their hosts has proven much more elusive. There is little direct evidence concerning the benefits which the hosts derive from these symbioses. The seep animals have proven particularly useful for such studies because since they live at only modest depths they can be kept alive without pressure systems. This opens the possibility of making rapid progress in understanding these symbioses. In the case of the seep mussel for example we are able to keep individuals alive for more than a year in the laboratory. This has allowed us to undertake studies on the growth of this species with methane as the sole energy and carbon source as well as studies to determine this species ability to ingest and use particulate food.

#### ACKNOWLEDGMENTS

These studies were supported by NSF grants OCE83-11256 and OCE86-10514, as well as Johnson Sea Link dives funded by the National Undersea Research Program of NOAA.

#### LITERATURE CITED

Anthony, C. 1982. The Biochemistry of Methylotrophs. London, England, Academic Press. 431 pp.

Anthony, C. and L. J. Zatman. 1965. The microbial oxidation of methanol. The alcohol dehydrogenase of Pseudomonas sp. M27. Biochem. J., Vol. 96, pp. 808-812.

Anderson, A. E., J. J. Childress, and J. A. Favuzzi. 1987. Net uptake of  $\text{CO}_2$  driven by sulphide and thiosulphate oxidation in the bacterial symbiont-containing clam Solemya reidi. J. Exp. Biol., Vol. 133, pp. 1-31.

Belkin, S., D. C. Nelson, and H. W. Jannasch. 1986. Symbiotic assimilation of  $\text{CO}_2$  in two hydrothermal vent animals, the mussel Bathymodiolus thermophilus and the tube worm Riftia pachyptila. Biol. Bull., Vol. 170, pp. 110-121.

Brooks, J. M., M. C. Kennicutt II, C. R. Fisher, S. A. Macko, K. Cole, J. J. Childress, R. R. Bidigare, and R. D. Vetter. 1987. Deep-sea hydrocarbon seep communities: Evidence for energy and nutritional carbon sources. Science, Vol. 228, pp. 1138-1142.

Cavanaugh, C. M. 1983. Symbiotic chemoautotrophic bacteria in marine invertebrates from sulfide-rich habitats. Nature, Vol. 302, pp. 58-61.

Cavanaugh, C. M. 1985. Symbioses of chemoautotrophic bacteria and marine invertebrates from hydrothermal vents and reducing sediments. In: M. L. Jones (ed.), The Hydrothermal Vents of the Eastern Pacific: An Overview. Bull. Biol. Soc. Washington, Vol. 6, pp. 373-388.

Cavanaugh, C. M., S. L. Gardiner, M. L. Jones, H. W. Jannasch, and J. B. Waterbury. 1981. Prokaryotic cells in the hydrothermal vent tube worm Riftia pachyptila Jones: possible chemoautotrophic symbionts. Science, Vol. 213, pp. 340-342.

Childress J. J. and T. J. Mickel. 1980. A motion compensated shipboard precision balance system. Deep-Sea Res., Vol. 27, pp. 965-970.

Childress, J. J., C. R. Fisher, J. M. Brooks, M. C. Kennicutt II, R. R. Bidigare, and A. E. Anderson. 1986. A methanotrophic marine molluscan (Bivalvia: Mytilidae) symbiosis: Mussels fueled by gas. Science, Vol. 233, pp. 1306-1308.

Felbeck, H. 1981. Chemoautotrophic potential of the hydrothermal vent tube worm, Riftia pachyptila Jones (Vestimentifera). Science, Vol. 213, pp. 336-338.

Felbeck, H., J. J. Childress, and G. N. Somero. 1981. Calvin-Benson cycle and sulfide oxidation enzymes in animals from sulfide-rich habitats. Nature, Vol. 293, pp. 291-293.

Fiala-Mdioni, A., C. Mtivier, A. Henry, and M. Le Pennec. 1986. Ultrastructure of the gill of the hydrothermal-vent mytiliid Bathymodiolus sp. Mar. Biol., Vol. 92, pp. 65-72.

Fisher, C. R., J. J. Childress, R. S. Oremland, and R. R. Bidigare. 1987. The importance of methane and thiosulfate in the metabolism of the symbionts of two deep-sea mussels. Mar. Biol., Vol. 96, pp. 59-71.

Kennicutt, M. C. II., J. M. Brooks, R. R. Bidigare, R. R. Fay, T. L. Wade, and T. J. McDonald 1985. Vent-type taxa in a hydrocarbon seep region on the Louisiana slope. Nature, Vol. 317, pp. 351-353.

Powell, M. A. and G. N. Somero. 1985. Sulfide oxidation occurs in the animal tissue of the gutless clam, Solemya reidi. Biol. Bull., Vol. 169, pp. 164-181.

Powell, M. A. and G. N. Somero. 1986a. Adaptations to sulfide by hydrothermal vent animals: sites and mechanisms of detoxification and metabolism. Biol. Bull., Vol. 171, pp. 274-290.

Powell, M. A. and G. N. Somero. 1986b. Hydrogen sulfide oxidation is coupled to oxidative phosphorylation in mitochondria of Solemya reidi. Science, Vol. 233, pp. 563-566.

Richard J. J., R. D. Vick and G. A. Junk. 1977. Determination of elemental sulfur by gas chromatography. Envir. Sci. Tech., Vol. 11, pp. 1084-1086.

Southward, A. J., E. C. Southward, P. R. Dando, G. H. Rau, H. Felbeck, and H. Flgel. 1981. Bacterial symbionts and low  $^{13}\text{C}/^{12}\text{C}$  ratios in tissues of Pogonophora indicate unusual nutrition and metabolism. Nature, Vol. 293, pp. 616-620.

Stokes, D. M. and D. A. Walker. 1972. Photosynthesis by isolated chloroplasts: Inhibition by DL-glyceraldehyde of carbon dioxide assimilation. Biochem. J., Vol. 128, pp. 1147-1157.

Strickland, J. D. H. and T. R. Parsons. 1972. A practical handbook of seawater analysis, 2nd ed. Bull. Fish. Res. Bd. Can., Vol. 167, pp. 1-310.

Wishnick, M. and M. D. Lane. 1971. Ribulose diphosphate carboxylase from spinach leaves. Methods in Enzymology, Vol. 23, pp. 570-577. New York, Academic Press.



INITIAL MICROBIOLOGICAL AND CHEMICAL INVESTIGATIONS  
OF PELE'S VENT, LOIHI SEAMOUNT

David M. Karl<sup>1,2</sup>  
Andrew Brittain<sup>3</sup>  
and  
Bronte Tilbrook<sup>1</sup>

<sup>1</sup> Department of Oceanography  
University of Hawaii  
Honolulu, Hawaii 96822

<sup>2</sup> Division of Oceanic Biology  
Hawaii Institute of Geophysics  
University of Hawaii  
Honolulu, Hawaii 96822

<sup>3</sup> Department of Microbiology  
University of Hawaii  
Honolulu, Hawaii 96822

INTRODUCTION

The discovery of deep-sea hydrothermal vents and their associated bacterial and animal assemblages (Lonsdale 1977; Corliss, Dymond, Gordon, Edmond, von Herzen, Ballard, Green, Williams, Bainbridge, Crane, and van Andel 1979; Galapagos Biology Expedition Participants 1979) has led to a decade of exploration and in-situ experimentation. In 1977, Lonsdale first observed the relationship between the distribution and abundance of deep-sea animal communities and the discharge of hydrothermal vent fluids. His deep-sea bottom photographs taken at the Galapagos Rift revealed freshly-produced oceanic basalts covered with hydrothermal mineral precipitates and an unexpected presence of large benthic invertebrates. Lonsdale formulated two independent, but not mutually exclusive, hypotheses to explain these observations. First, he suggested that the clustering of suspension feeding animals around active hydrothermal vents might be due to the entrainment of bottom water by the rising buoyant plumes. This localized bottom water current could sustain the deep-sea vent community by delivering a steady supply of suspended particulate matter. In this ecosystem model, the particulate materials consumed by the benthic invertebrates living at hydrothermal vents would be derived from phytoplankton production in the surface waters. The deep-sea vent community would, therefore, be supported ultimately by energy supplied to the ocean in the form of solar radiation. As an alternate hypothesis, Lonsdale suggested that vent-associated chemoautotrophic bacteria living at the expense of reduced

inorganic substrates present in the hydrothermal fluids might represent a localized source of food for the vent-associated animal community. In this ecosystem model, the particulate materials consumed by the benthic invertebrates would be derived from bacterial production in the hydrothermal waters rather than from plankton production in the surface waters of the ocean. The deep-sea vent community would, therefore, be supported ultimately by energy supplied to the ocean in the form of geothermal energy. This "heat-based" system, maintained by the radioactive decay of long-lived isotopes of uranium, thorium and potassium and coupled to bacterial chemolithoautotrophic growth at the expense of geothermally reduced chemical compounds, would then represent an alternative to conventional sunlight-photosynthesis based communities. At the time of the discovery of deep-sea vents, all life processes on earth were thought to be sustained ultimately by photosynthetic processes.

These two fundamentally independent hypotheses regarding the distribution and abundance of animal life at deep-sea vents have provided the incentive and initiative for a decade of extensive hydrothermal vent investigation. While the buoyant plume ("thermal advection") hypothesis has received some support (Enright, Newman, Hessler, and McGowan 1981) it is unlikely that this process, by itself, could supply the amount of utilizable organic matter that would be required by the dense, metabolically-active vent animal communities. Furthermore, direct measurements of the  $\delta^{13}\text{C}$  and natural  $^{14}\text{C}$  content of selected vent animal tissues indicated that the utilization of photosynthetically derived organic matter is quantitatively insignificant (Williams, Smith, Druffel, and Linick 1981; Rau 1981, 1985). These results have focused attention on the second hypothesis, and the potential for bacterial chemolithoautotrophy (i.e., the reduction of inorganic carbon at the expense of reduced inorganic compounds) at deep-sea hydrothermal vents.

The initial microbiological investigations conducted at the Galapagos Rift provided evidence for the presence of high concentrations of bacterial cells in the discharged hydrothermal vent fluids (Corliss et al. 1979 [samples analyzed by J. Baross]; Jannasch and Wirsén 1979; Karl, Wirsén, and Jannasch 1980; Jannasch and Wirsén 1981). These data supported, but by no means confirmed, the hypothesis of localized chemolithoautotrophic bacterial production. However, since 1980, most scientists have tacitly accepted as fact the previously mentioned hypothesis. If true, it could have important implications for oceanic carbon cycles and would establish a global precedent for a non-solar based food web. It is, therefore, a hypothesis of fundamental importance and clearly deserving of a rigorous experimental evaluation. One of the authors, David M. Karl, has recently summarized the extant data base on bacterial production at deep-sea hydrothermal vents with particular emphasis on the bacterial chemolithoautotrophy production hypothesis (Karl 1987).

Following the initial discovery of microorganisms and macrofauna at the Galapagos Rift spreading center, similar mid-ocean ridge hydrothermal vent communities were discovered along the East Pacific Rise (at 10°57'N, 12°49'N, 20°50'N and 18°31'S), the Juan de Fuca-Endeavor-Explorer Ridge system (at 46°N, 130°01'W; 46°53'N, 129°17'W; 45°57'N, 130°01'W; 47°57'N, 129°04'W; and 49°44'N 130°18'W) and the mid-Atlantic Ridge (at 26°N and 23°22'N). These so-called "hard lava" hydrothermal vent systems have numerous shared geochemical characteristics resulting from the circulation of seawater through mid-ocean ridge crustal materials. However, they also vary considerably with respect to the nature and extent of heat dissipation and in the structure and organization of their associated animal communities.

In addition to the hydrothermal vents which have been investigated at sediment-starved mid-ocean ridge spreading centers, active hot springs have also been discovered at several sediment-rich sites including the Guaymas Basin (a sediment covered ridge axis; 27°02'N, 111°22'W), the Manus Basin (a back-arc basin of the New Britain arc-trench system; 3°10'S, 150°17'E), the Okinawa Trough (a back-arc basin of the Ryukyu arc system; 27°34'N, 127°09'E) and, most recently, at Loihi Seamount (an active hot-spot volcano in the Hawaiian Archipelago; 18°55'N, 155°16'W). The existence of hot-spot hydrothermal fluid discharge is significant in that deep-sea vents and associated biological assemblages need not be restricted to oceanic plate boundaries. This paper reports the results of our initial microbiological and chemical investigations of samples collected from the summit of Loihi Seamount.

## METHODS

### Habitat Description

Loihi Seamount is a seismically active submarine volcano that marks the southernmost extent of the Hawaiian island chain and the probable site of an emerging Hawaiian island (Fig. 1). It is one of the two known active hotspot submarine volcanoes of the Pacific Ocean; the other is the Macdonald Seamount of the Austral Island chain. Persistent swarms of earthquakes, characteristic of those associated with Hawaiian volcanism, occur near the summit of Loihi.

Detailed photographic surveys and dredging operations at the summit of Loihi initially provided evidence for the presence of fresh, glass-encrusted pillow lava, talus, and pockets of sand and gravel as well as several fields of hydrothermal iron oxides and nontronite (Malahoff, McMurtry, Wiltshire, and Yeh 1982; DeCarlo, McMurtry, and Yeh 1983). In 1983, Horibe, Kim and Craig reported elevated concentrations of methane ( $\text{CH}_4$ ) and helium-3 in the water column above Loihi indicating the presence of active

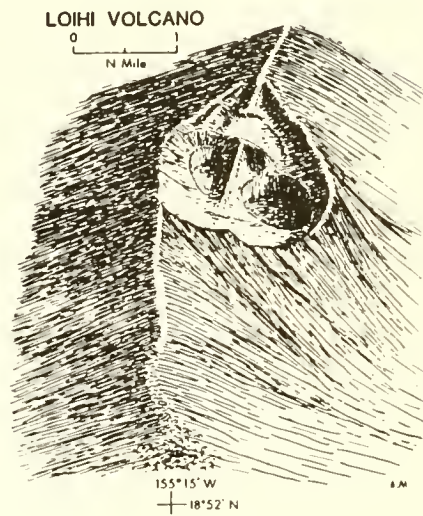
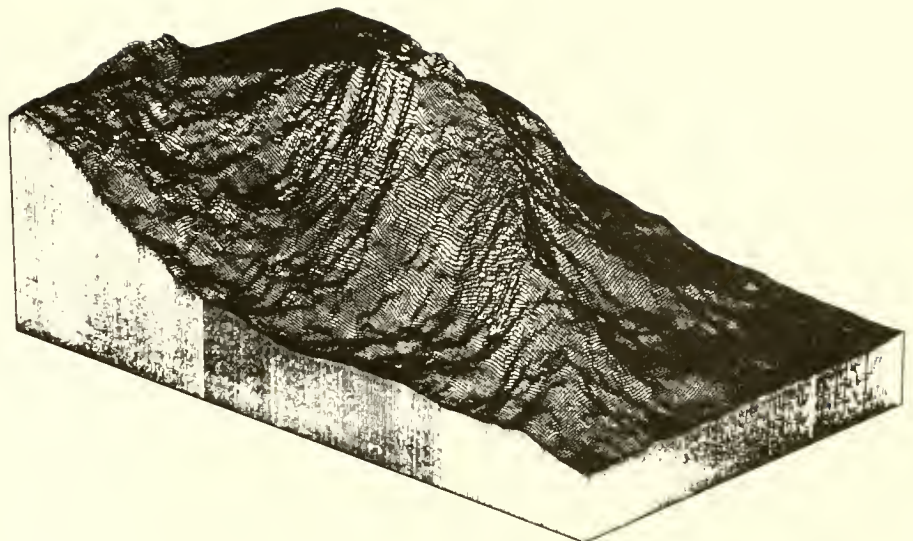


Figure 1. Top: Fishnet image of Loihi Seamount. This oblique view of Loihi from the southeast is based on a February 1987 bathymetric survey using the Sea Beam system on the R/V Atlantis II. Note the two depressions (pit craters) at the summit of Loihi which are over 300 m deep. A prominent rift zone extends towards the southeast. A lesser rift zone trends towards the north. Vertical exaggeration is 3:1. Image courtesy of Michael Garcia, Hawaii Institute of Geophysics. Bottom: Map of the summit of Loihi Seamount showing the characteristic pit craters and major rift zone (from Malahoff, McMurtry, Wiltshire, and Yeh (1982)).

hydrothermal venting. In September 1985, an interdisciplinary group of scientists aboard the R/V Hakuho Maru conducted a comprehensive hydrographic and geochemical study of the water column above the summit of Loihi Seamount. During that cruise a hydrothermal plume rich in dissolved methane, helium (with a high  $^3\text{He}/^4\text{He}$  ratio), excess carbon dioxide and high concentrations of Fe, Mn, Ni, and Co was detected (Sakai, Tsubota, Nakai, Ishibashi, Akagi, Gamo, Tilbrook, Igarashi, Kodera, Shitashima, Nakamura, Fujioka, McMurtry, Malahoff, and Ozima 1977). These results indicated the presence of an active hydrothermal system at or near the summit of Loihi.

In February 1987, two active hydrothermal vent fields were located, mapped and sampled by scientists aboard the deep-sea research submersible Alvin. On that expedition, we obtained several water and bacterial mat samples from the larger of the two fields in an area that we named Pele's Vent. In August 1987 we returned to Pele's Vent during a NOAA-NURP sponsored research expedition using the deep-sea research submersible Pisces V.

#### Sample Collection

Hydrothermal fluids flowing from Pele's Vent were collected on Alvin dives #1797-1800 and Pisces V dives #25-29 using either a small volume (approximately 700 ml) piston-driven titanium sampler specially-designed for hydrothermal vent research (Von Damm, Edmond, Grant, Measures, Walden, and Weiss 1985), standard 5-1 Niskin bottles attached to the basket of the respective submersible or a 2-1 Niskin baggie sampler adapted with a 2-m tygon tube for directional sampling. Bacterial mats were also sampled using either a standard Alvin tube core or the suction produced by the opening of the 2-1 Niskin baggie samplers. The complete sample log is given in Table 1.

#### Sample Processing and Chemical Analyses

##### Dissolved methane and total dissolved inorganic carbon measurements

Gas sampling was routinely the first of several subsampling procedures. Water samples for the measurement of dissolved methane and total dissolved inorganic carbon were transferred into 60 ml ground glass stoppered bottles immediately and poisoned with 0.5 ml of a saturated  $\text{HgCl}_2$  solution. During sampling, care was taken to avoid gas exchange or trapping bubbles in the sample bottles during sealing. The samples were returned to the laboratory for analysis.

Dissolved methane was determined using a modification of the gas stripping method described by Swinnerton, Linnenbom, and Cheek (1962) and Swinnerton and Linnenbom (1967). Dissolved gases were purged from a 23 ml subsample with methane-free

Table 1. Sample log from Loihi Seamount Microbiology Research Program

Dive#	Date	Samples Collected	Measurements/Experiments
<u>Alvin EXPEDITION 1987</u>			
1797	2/13	3 Niskin bottles	nutrients, dissolved gases, microscopy, ATP
1798	2/14	1 Niskin bottle, 2 titanium bottles	nutrients, dissolved gases, microscopy, ATP
1799	2/15	4 Niskin bottles, 2 titanium bottles, 1 core sample	nutrients, dissolved gases, microscopy, ATP, CH <sub>4</sub> oxidation experiments, <sup>3</sup> H-adenine assimilation experiments
1800	2/16	2 Niskin bottles, 2 titanium bottles	nutrients, dissolved gases, microscopy, ATP, CH <sub>4</sub> oxidation experiments, <sup>3</sup> H-adenine assimilation experiments
<u>Pisces V EXPEDITION 1987</u>			
25	8/29	1 Niskin bottle	nutrients, dissolved gases, microscopy, CH <sub>4</sub> oxidation experiments
26	8/31	1 titanium bottle, 2 Niskin baggies	nutrients, dissolved gases, microscopy, CH <sub>4</sub> oxidation experiments, bacterial enrichments
27	9/1	1 Niskin bottle, 2 titanium bottles	nutrients, dissolved gases, microscopy, CH <sub>4</sub> oxidation experiments
28	9/2	1 titanium bottle	nutrients, dissolved gases microscopy, CH <sub>4</sub> oxidation experiments, bacterial growth experiments
29	9/3	1 Niskin bottle, 1 titanium bottle	nutrients, dissolved gases, microscopy, bacterial enrichments, CH <sub>4</sub> oxidation experiments, bacterial growth experiments

helium. The gases were concentrated on Porapak Q cooled with liquid nitrogen, and then injected into a gas chromatograph equipped with a flame ionization detector. Calibrations were made by injecting known volumes of a gas standard (23 ppm CH<sub>4</sub> in helium). Precision of the analysis was  $\pm 5\%$ .

Dissolved inorganic carbon measurements were made on 3.5 ml samples taken from the same bottles as the methane samples. The samples were analyzed using a gas chromatograph following the gas stripping method described by Weiss and Craig (1973). Samples were calibrated against standards prepared gravimetrically from Na<sub>2</sub>CO<sub>3</sub> solutions as described by Wong (1970). The precision of replicate analyses was  $\pm 0.5\%$ .

After sampling, a gas phase formed in several of the sealed bottles. Partitioning of methane and carbon dioxide into this gas phase can alter their dissolved concentrations. This was especially noticeable in the warmest waters sampled (i.e., those with dissolved Si approximately twice that of ambient bottom seawater). Consequently, we restrict our statistical analysis of the relationships between dissolved gas concentrations and dissolved silica to those samples containing  $< 160 \mu\text{m}$  Si. Concentrations of methane and total carbon dioxide in the warmer vent fluids are estimated by extrapolation of the linear trends observed in the CH<sub>4</sub> or  $\Sigma\text{CO}_2$  versus Si relationships to the Si concentrations measured in the 30-35°C vent samples (as follows).

#### Dissolved nutrients

Individual vent water samples and control (non-vent) deep (1000 m) seawaters were processed immediately upon their arrival on the support vessel (R/V Atlantis II for Alvin dives or R/V Kila for Pisces V dives). For the Alvin dive series, subsamples (125 ml) for dissolved nutrients ( $[\text{NO}_3^- + \text{NO}_2^-]$ , NH<sub>4</sub><sup>+</sup>, PO<sub>4</sub><sup>-3</sup>, Si[OH]<sub>4</sub>) were filtered through pre-combusted (450°C, 3 hr) Whatman glass fiber filters (GF/F type) and placed into acid-washed polyethylene bottles and stored frozen (-20°C). Inorganic nutrients were measured by the Hawaii Biogeochemical Analytical Facility using standard Technicon II autoanalyzer techniques for the analysis of seawater. We also compared the total nutrient content of filtered versus unfiltered vent water samples and concluded that filtration (GF/F filter) had no significant effect on the nutrient determinations at Pele's Vent.

Technically speaking, the spectrophotometric methods used in this study measure soluble reactive phosphorus (SRP) rather than total dissolved phosphate and reactive silica rather than total dissolved silica. The latter may be of special interest in the analysis of samples collected from deep-sea vents due to the possible presence of Si, either as polymerized Si or as micro-particulate ( $< 0.4 \mu\text{m}$  diameter) Si which would escape detection by our autoanalyzer methods. For this reason we also

measured total Si by atomic absorption spectrometry (McMurtry, Karl, Tilbrook, and Sedwick 1987). Our analyses revealed that there was an excellent correspondence between reactive Si (by autoanalyzer) and total Si (by atomic absorption) for samples with total Si < 600  $\mu$ M. At higher concentrations, the autoanalyzer methods underestimated the total dissolved Si contained in the vent water samples. All nutrient determinations were made within 1 week of sample collection.

We also attempted to measure dissolved organic nitrogen (DON) and dissolved organic phosphorus (DOP) in Pele's Vent water samples but these analyses were unsuccessful because of the precipitation of dissolved Fe during the 60°C UV oxidation procedure.

#### Particulate ATP

The particulate materials contained in Pele's Vent water samples (100-250 ml) were concentrated onto Whatman glass fiber filters (GF/F type) and the filters were immediately placed into a test tube containing 5 ml of boiling phosphate buffer (60 mM, pH 7.4; Karl and Craven 1980). The samples were extracted for 5 minutes, and stored frozen for subsequent laboratory analysis of adenosine-5'-triphosphate (ATP) by the firefly bioluminescence assay procedure (Karl and Holm-Hansen 1978).

#### Chemical composition of bacterial mat

Bacterial mats (approximately 5 g wet weight) were concentrated by low speed (500 x g) centrifugation, rinsed twice (by resuspension and centrifugation) with distilled water and dried for 48 hours at 60°C. The dried samples were pulverized with a mortar and pestle to a fine powder and stored at -20°C in a dessicator jar until analyzed. Triplicate subsamples (1-2 mg) for organic carbon analysis were carefully weighed using a Cahn electrobalance and measured by high temperature (1100°C) combustion using a Hewlett-Packard Model 185 CHN analyzer. Acetanilide ( $C_8H_9NO$ ) was used as the primary standard.

A frozen subsample of the fresh bacterial mat was also sent to Dr. Greg Rau (National Aeronautics and Space Administration, Moffett Field, CA) for stable carbon isotope analysis. In his laboratory, a portion of the mat sample was washed with 0.25 M HCl (to remove carbonates) and dried for several days at 50°C. Subsamples were placed into precombusted quartz tubes, mixed with organic-free CuO and Cu particles (30 mesh), sealed and combusted at 800°C for 6 hr. The resulting CO<sub>2</sub> was purified cryogenically and the stable C isotope ratios were measured using a Nuclide 6-60 ratio mass spectrometer.

For phosphorus determinations, 10 mg subsamples of the dried mat material were placed into three clean glass test tubes and

were leached with either: (1) 0.5 N acetic acid/sodium acetate (pH 5) buffer, (2) 0.2 M oxalic acid/ammonium oxalate (pH 3) buffer, or (3) hot 8 M HCl (Froelich, Bender, and Heath 1977). The three classes of P released by these procedures are operationally defined as  $\text{CaCO}_3$ -associated plus loosely bound P (acetate extract), hydrogenous metal-associated P (oxalate extract) and total P (HCl extract). The latter treatment would also include mineral-P. After a reaction period of 4 hours, the tubes were centrifuged (1500 x g), diluted 1000-fold in distilled water and measured using the SRP procedures given previously. Only a small residue (1-5% of the original material) was observed in the HCl extracted sample. This colorless fine-grained particulate matter is believed to be siliceous material.

The remaining two preparations contained approximately 5-10 percent and 90-100 percent of the original mass of the pulverized material for the oxalate and acetate preparations, respectively. Samples of the dried, pulverized bacterial mat were also prepared for analysis by electron microprobe and for x-ray diffraction.

#### Microbiological Measurements and Metabolic Rate Determinations

Bright-field, epifluorescence and electron microscopy

A subsample (100 ml) of each vent water and bacterial mat sample collected at Pele's Vent was immediately preserved in electron microscopy grade glutaraldehyde (final concentration, 2%) and stored at 4°C for subsequent laboratory processing. For bright-field viewing, wet mounts of the bacterial mats were prepared and examined at 100, 400, and 1000x magnification with a Zeiss Standard 18 compound microscope equipped with planapo objectives. Photographs were taken with a 35 mm Olympus camera and Kodak high speed ektachrome film. For epifluorescence microscopy, a 5 ml portion of each preserved sample was stained with acridine orange (0.05% final concentration), filtered onto an irgalan-black stained 0.2  $\mu\text{m}$  Nuclepore membrane filter and viewed at 1000x magnification with a Zeiss Standard 18 epifluorescence microscope equipped with a 100 W mercury lamp, neofluar objectives and an A-0 filter set (Hobbie, Daley, and Jasper 1977). Quantitative cell counts were determined for selected Pele's Vent water samples.

For transmission electron microscopy (TEM) of the bacterial mat samples, a portion of the glutaraldehyde-fixed particulate material was first collected by high speed centrifugation (10,000 x g), embedded in noble agar (2% wt/vol), washed in a cacodylate buffered filtered seawater solution (0.1 M, pH 7.7), post-fixed in an  $\text{OsO}_4$  (1%) cacodylate-seawater solution, desalinated in graded seawater/distilled water solutions (to 0% seawater), dehydrated in graded distilled water/ethanol solutions (to 100% ethanol), embedded in an epoxy resin and

polymerized at 65°C for 5 days. Ultrathin sections were cut using an LKB Nova ultramicrotome and collected on formvar and carbon-coated 200 mesh copper grids. Sections, both stained (uranyl acetate and lead acetate) and unstained, were viewed and photographed on a Hitachi scanning/transmission electron microscope (Model H-600).

For scanning electron microscopy (SEM) of the bacterial mat samples, a portion of the glutaraldehyde-fixed particulate material was desalinated by consecutive immersion in a graded series of seawater/distilled water solutions (to 0% seawater) immediately followed by sample dehydration by consecutive immersion in a graded series of distilled water/ethanol solutions (to 100% ethanol). After dehydration, the ethanol was exchanged with liquid carbon dioxide during the critical point drying procedure. Prior to examination the samples were mounted onto aluminum pedestals and coated, by vacuum evaporation, with a layer of either gold (in preparation for high resolution viewing) or carbon (in preparation for x-ray elemental analysis). The samples were viewed at 100-20,000x magnification using an ISI scanning electron microscope (Model SS-40), and images were recorded on Polaroid P/N55 type film. Energy dispersive x-ray fluorescence spectroscopy was performed using a Princeton Gamma Tech spectrophotograph.

#### Methane oxidation experiments

Bacterial methane oxidation was assessed during both the Alvin and Pisces V dive programs. Preliminary experiments were performed to measure the potential for methane oxidation using  $^{14}\text{C}$ -labeled methane as a tracer. Water samples collected on Alvin dives #1799 and #1800, a bacterial mat sample and a deep-sea water (1000 m) control were used for these experiments. Twenty-five ml of each sample was placed into a glass serum bottle which was stoppered with a gas-tight rubber septum. One ml (50  $\mu\text{Ci}$ ) of  $^{14}\text{C-CH}_4$  (5 mCi  $\text{mmol}^{-1}$ , Cat. #17339, ICN Radiochemicals) was injected into each serum bottle and the samples were inverted (to eliminate potential loss of  $^{14}\text{C-CH}_4$  and  $^{14}\text{C-CO}_2$ ) and incubated at 25°C. Following incubation periods of 7.5 and 18 hours, exactly 10 ml of each sample was transferred, by syringe, to a second serum bottle containing a gas tight serum stopper, a plastic well and a piece of fluted filter paper as described by Hobbie and Crawford (1969). After the addition of NaOH hydroxide (100  $\mu\text{l}$  of 1 M NaOH) to the filter paper, one ml of 5 M HCl was added to each sample. Following a 6 hour passive distillation period, the serum bottles were opened and the filter paper wicks (now containing the  $^{14}\text{CO}_2$  released from the acidified solutions) were removed, placed into glass vials containing 10 ml of Aquasol-2 (New England Nuclear) and their radioactivities measured using a Packard Model 4640 liquid scintillation counter. The acid-insoluble particulate materials were collected onto Whatman glass fiber filters (GF/F) and

processed for  $^{14}\text{C}$  incorporation into nucleic acids and protein (Karl 1982).

During the Pisces V expedition, we continued our initial assessment of  $\text{CH}_4$  oxidation potential by comparing the rates of  $\text{CH}_4$  oxidation in a variety of water samples collected from Pele's Vents. For each water sample that was collected, one subsample was immediately fixed with  $\text{HgCl}_2$  (as previously mentioned) for measurement of the initial  $\text{CH}_4$  and  $\text{CO}_2$  concentrations and a replicate subsample was placed into a sealed glass-stoppered bottle and incubated at  $25^\circ\text{C}$  for a period of 30 days, after which the final  $\text{CH}_4$  and  $\text{CO}_2$  concentrations were determined. At the end of the experiment, several selected water samples (those which had demonstrated significant  $\text{CH}_4$  oxidation activity) and the deep-water control were processed for  $^{14}\text{C-CH}_4$  oxidation activity as described previously.

#### Adenine incorporation experiments

Pele's Vent water samples (500 ml) collected on Alvin dives #1799 and #1800, bacterial mats collected on dive #1800 and a deep-water control sample were incubated in polycarbonate bottles at  $25^\circ\text{C}$  for 8 and 18 hours in the presence of 100  $\mu\text{Ci}$   $^{3}\text{H}$ -adenine (15 Ci  $\text{mmol}^{-1}$ ; New England Nuclear, Cat. #NET-250). At each time point, 250 ml of the sample was filtered through a Whatman glass fiber filter (GF/F) and the filters were stored frozen for subsequent determination of radioactivity incorporated into RNA, DNA, and protein (Karl 1982).

Pele's Vent water samples collected on Pisces V dives #28 and #29 and a control deep-water sample were analyzed for total rates of microbial RNA and DNA synthesis. Portions (175 ml) of each water sample were incubated with 10  $\mu\text{Ci}$  of  $^{3}\text{H}$ -adenine (see aforementioned) at  $25^\circ\text{C}$  for 16 hours. Following incubation, subsamples were extracted for ATP and were processed for RNA/DNA (Karl and Winn 1984). Rates of RNA and DNA synthesis ( $\text{pmol l}^{-1} \text{hr}^{-1}$ ) were estimated from the incorporation rates ( $\text{nCi hr}^{-1}$ ) and the direct measurement of the intracellular specific radioactivity of the ATP pool ( $\text{nCi pmol}^{-1}$ ) according to the methods described previously (Karl 1981).

#### Effects of temperature on bacterial activity

Portions (25 ml each) of a Pele's Vent water sample collected on Pisces V dive #28 were placed into a series of 16 polycarbonate incubation bottles and, in groups of four, were allowed to equilibrate for 1 hour in temperature controlled water baths at  $4^\circ$ ,  $25^\circ$ ,  $37^\circ$  and  $60^\circ\text{C}$ . Radiolabeled substrates including,  $^{3}\text{H}$ -thymidine (10  $\mu\text{Ci}$ ; 65 Ci  $\text{mmol}^{-1}$ , New England Nuclear, Cat. #NET-027Z),  $^{3}\text{H}$ -adenine (10  $\mu\text{Ci}$ ; see previously mentioned for isotope description),  $^{3}\text{H}$ -glutamic acid (10  $\mu\text{Ci}$ ; 50 Ci  $\text{mmol}^{-1}$ , New England Nuclear, Cat. #NET-490) and

$^{14}\text{C}$ -acetate (10  $\mu\text{Ci}$ ; 50 mCi  $\text{mmol}^{-1}$ , New England Nuclear, Cat. #NEC-553) were added individually to one of the four bottles at each temperature. The samples were incubated for 18 hours at which time the particulate materials were collected onto Whatman glass fiber filters (GF/F) and stored frozen until analyzed for incorporation into total acid insoluble material (Karl 1982).

### Enrichment culture experiments

Eight different elective culture media (Table 2) were used in an attempt to characterize the physiological groups of bacteria at Pele's Vent. Dilution-to-extinction procedures were employed to determine the relative numerical importance of each group. Two water samples from Pisces V dive #29 and scrapings from a rock recovered from the active vent field were serially diluted with sterile artificial seawater, inoculated into the various media and incubated at 22°C under the conditions indicated (Table 2).

## RESULTS AND DISCUSSION

### General Appearance of Pele's Vent Field: First Impressions

Pele's Vents are situated in the southwest portion of the summit of Loihi Seamount at a water depth of 980 m. The area of active hydrothermal fluid discharge is restricted to the flank of a relatively small volcanic cone approximately 10-15 m below the summit elevation. The active field is less than 0.5  $\text{km}^2$  and is characterized by numerous individual vents discharging waters heated to a temperature of at least 30°C. The vent orifices are distinguished by a white precipitate (Fig. 2a) which has been determined to contain high concentrations of elemental sulfur (G. McMurtry, pers. comm.). The sulfur deposition is most likely the result of bacterial oxidation of reduced sulfur species contained in the discharged waters. The vent fluid is exceptionally clear and nearly devoid of suspended particulate matter.

At least four potential habitats exist for the growth of hydrothermal vent bacteria. The first is the subsurface vent system itself which is technically difficult to sample except by obtaining discharged hydrothermal fluids. It should be kept in mind that the chemical composition of this suspected growth habitat is unknown but is likely to differ substantially from the fluids collected at the points of discharge where rapid mixing with ambient bottom water is known to occur. Likewise, the bacteria sampled from the hydrothermal vent fluids may not be truly representative of the assemblages growing in the interstices of the volcanic edifice. The second habitat is the region immediately surrounding the vent loci where the presumably anoxic hydrothermal fluids are mixed with oxygenated

Table 2. Enrichment culture media used for the analysis  
of water and rock samples collected on Pisces V dive #29

Target Organism	Electron Donor	Electron Acceptor	Carbon Source	Incubation Atmosphere	Reference
<b>Chemoautotrophs</b>					
NH <sub>4</sub> <sup>+</sup> oxidizer	NH <sub>4</sub> <sup>+</sup>	O <sub>2</sub>	CO <sub>2</sub>	20% O <sub>2</sub> 80% N <sub>2</sub>	Watson (1965)
NO <sub>2</sub> <sup>-</sup> oxidizer	NO <sub>2</sub> <sup>-</sup>	O <sub>2</sub>	CO <sub>2</sub>	20% O <sub>2</sub> 80% N <sub>2</sub>	Watson and Waterbury (1971)
Fe oxidizer	Fe <sup>+2</sup>	O <sub>2</sub>	CO <sub>2</sub>	2% O <sub>2</sub> 98% N <sub>2</sub>	Tuovinen and Kelley (1973)
S oxidizer	dithionite	O <sub>2</sub>	CO <sub>2</sub>	2% O <sub>2</sub> 98% N <sub>2</sub>	Taylor et al. (1971)
<b>Chemoheterotrophs</b>					
SO <sub>4</sub> reducer	ethanol	SO <sub>4</sub>	ethanol	100% N <sub>2</sub>	Stanier et al. (1976)
proteo- lytic	nutrient broth, gelatin	O <sub>2</sub>	nutrient broth, gelatin	20% O <sub>2</sub> 80% N <sub>2</sub>	---
N <sub>2</sub> fixer	glucose	O <sub>2</sub>	glucose	20% O <sub>2</sub> 80% N <sub>2</sub>	---
<b>Phagotroph</b>					
protozoa	bacteria	O <sub>2</sub>	bacteria	20% O <sub>2</sub> 80% N <sub>2</sub>	Cynar et al. (1985)

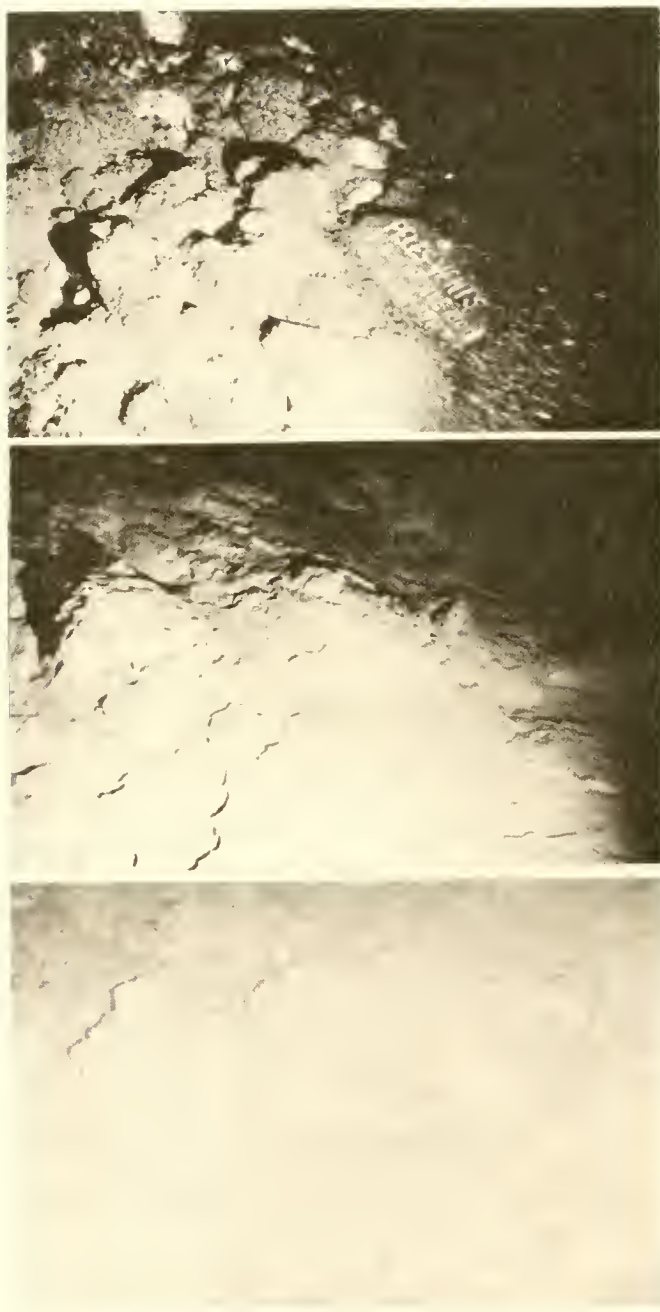


Figure 2. Characteristic bacterial habitats at Pele's Vent hydrothermal field. Top: View of Pele's Vent field showing the plaque placed at the site on Alvin dive #1800. The white precipitates at the top (center and left) identify the areas of active fluid flow. Middle: View of area peripheral to the active hydrothermal vent field where we observed extensive reddish-brown bacterial carpets. Bottom: View of zone of organic matter deposition (indicated by white fluff-like material) in an area downslope from the active vent field.

deep-sea waters. It is within this characteristic hydrothermal vent habitat of well-defined anoxic-to-oxic chemical gradients that much of the chemolithoautotrophic bacterial production is thought to occur. A third major habitat is the region of bacterial mat formation which appears to be in the periphery of the main hydrothermal vent field. At these locations, extensive bacterial mats completely cover the bottom substratum with a thick carpet of organic matter (Fig. 2b). Finally, we also observed an area further down the flank of the volcanic cone which contained a high concentration of what appeared to be organic detritus arranged in "windrow-like" formations (Fig. 2c). This leads us to suspect that material deposited in this area of the seafloor was transported by currents and gravity from an active vent field. We have made numerous observations of this material but have, to date, been unsuccessful at obtaining any samples for chemical and microbiological analyses.

#### Dissolved Nutrient Concentrations

Hydrothermal fluids collected at Pele's Vents are enriched in reactive Si,  $\text{NH}_4^+$  and SRP and depleted in  $[\text{NO}_3^- + \text{NO}_2^-]$ , relative to ambient bottom seawater collected from that site (Table 2). The enrichment of reactive Si is characteristic of hydrothermal vents, in general, and it is used as a geochemical thermometer due to the highly significant positive correlation between Si concentration and vent water temperature (Corliss, Dymond, Gordon, Edmond, von Herzen, Ballard, Green, Williams, Bainbridge, Crane, and van Andel 1979). When SRP,  $[\text{NO}_3^- + \text{NO}_2^-]$  and  $\text{NH}_4^+$  concentrations are plotted versus Si for the Loihi Seamount data, the relationships are described adequately by a single mixing curve (Figs. 3-5). These results suggest that the numerous fluid discharges which comprise the Pele's Vent hydrothermal habitat have a common end-member solution. In fact, the single water sample that was collected from the deeper hydrothermal vent field to the south of Pele's Vent also fit the same linear relationship indicating that the hydrothermal emissions from at least two separate Loihi Seamount hydrothermal vents have similar chemical compositions.

A second consistent trend in the nutrient data set was that the SRP versus Si, and the  $[\text{NO}_3^- + \text{NO}_2^-]$  versus Si relationships for Pele's Vents were not significantly different for water samples collected in February and August (Figs. 3 and 4). These results indicate that the concentrations of  $[\text{NO}_3^- + \text{NO}_2^-]$  and SRP may be stable, at least over time periods of months. The  $\text{NH}_4^+$  versus Si curves (Fig. 5), however, indicate that the  $\text{NH}_4^+$  content per unit Si (or per unit of total heat) was approximately two times higher during the February expedition. At the present time these data are not comprehensive enough to be used as reliable evidence for a temporal alteration in dissolved  $\text{NH}_4^+$  at Pele's Vent. Nevertheless, our results clearly indicate that the vent waters are a source of reduced N and SRP to the surrounding

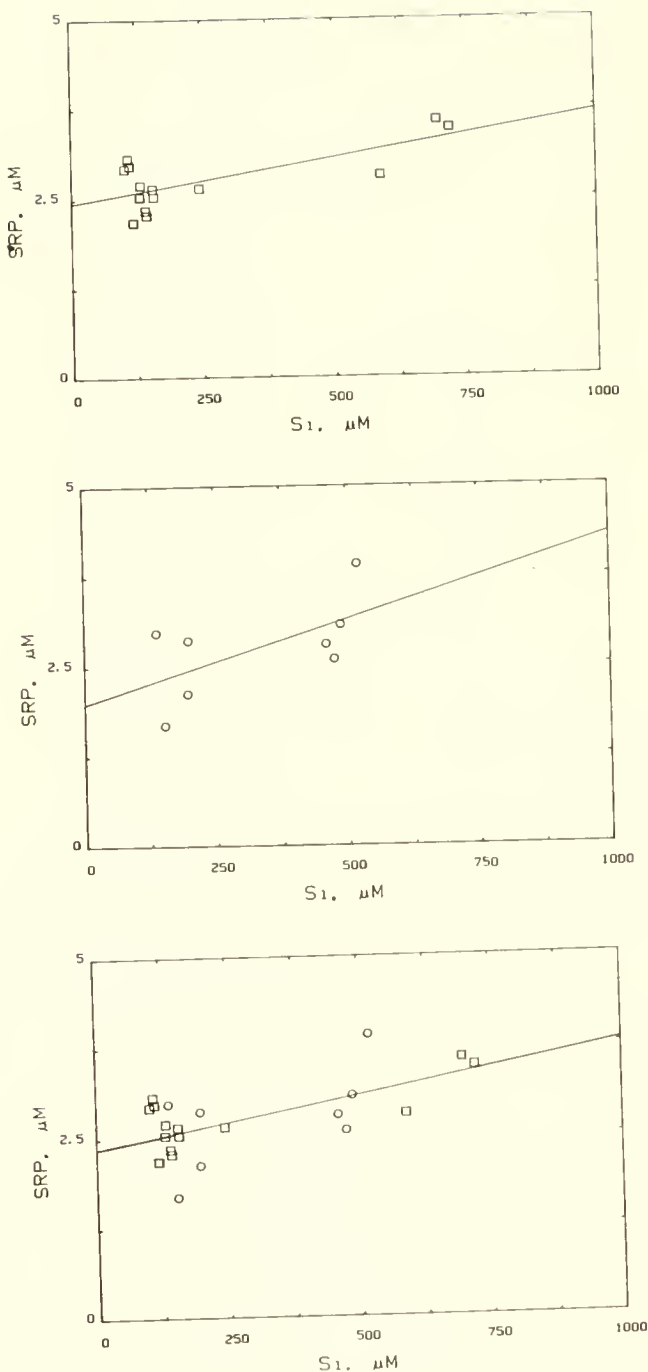


Figure 3. SRP versus Si relationships for water samples collected at Pele's Vent. The upper figure presents the data collected during the Alvin dive expedition. The middle figure presents the data collected during the Pisces V dive expedition. The bottom figure is the combined data base. The linear regression analyses were:  $SRP = 2.45 + 0.00124Si$  (Alvin);  $SRP = 1.98 + 0.00233Si$  (Pisces V); and  $SRP = 2.36 + 0.00144 Si$  (Alvin + Pisces V).

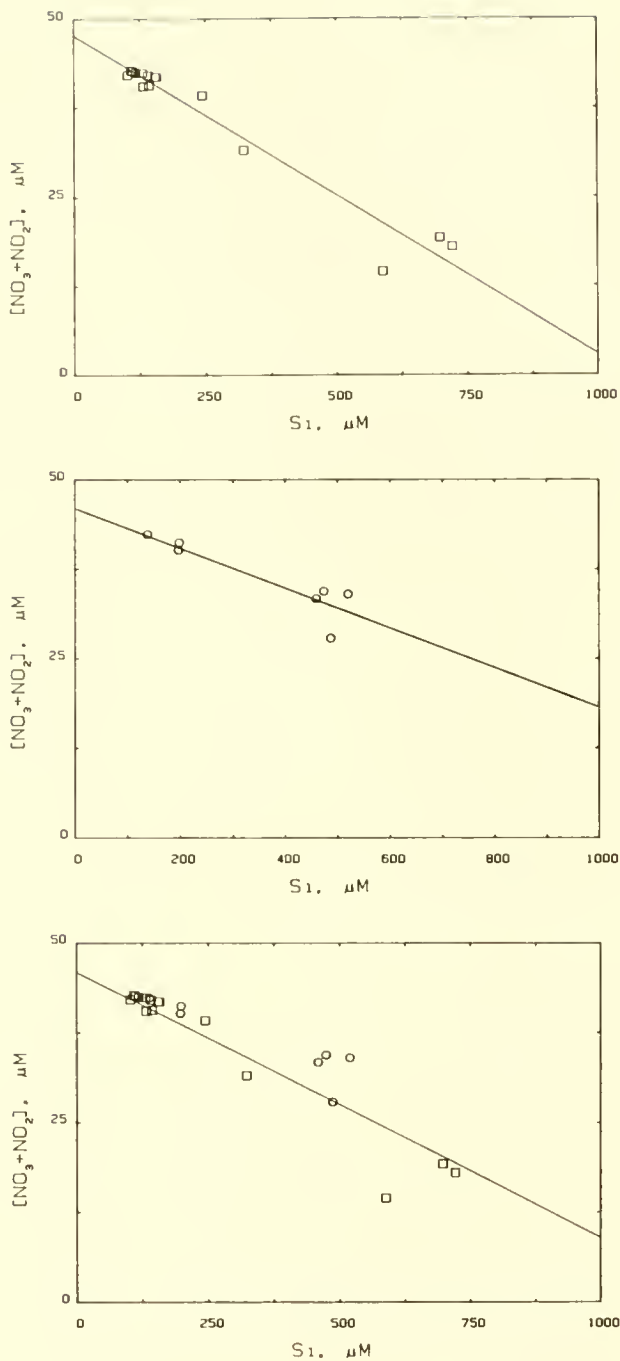


Figure 4.  $[NO_3^- + NO_2^-]$  versus  $Si$  relationships for water samples collected at Pele's Vent. The upper figure presents the data collected during the Alvin dive expedition. The middle figure presents the data collected during the Pisces V dive expedition. The bottom figure is the combined data base. The linear regression analyses were:  $[NO_3^- + NO_2^-] = 47.66 - 0.045Si$  (Alvin);  $[NO_3^- + NO_2^-] = 46.23 - 0.028Si$  (Pisces V);  $[NO_3^- + NO_2^-] = 45.94 - 0.037Si$  (Alvin + Pisces V).

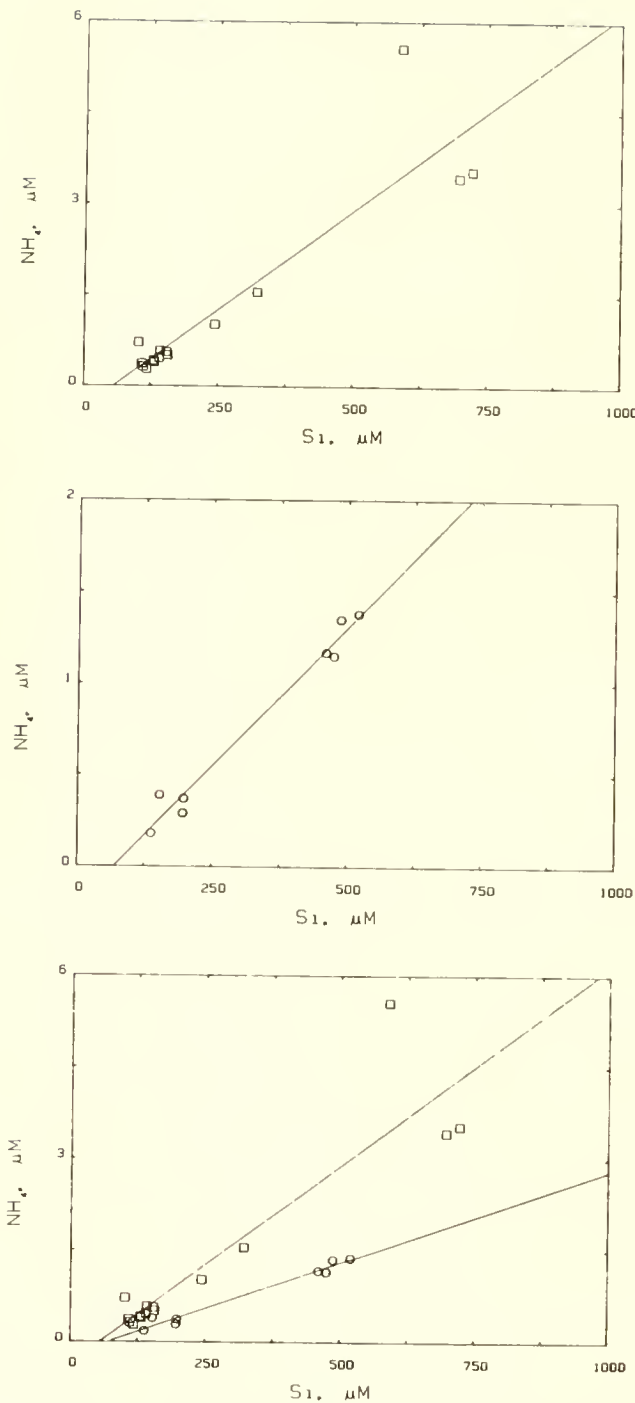


Figure 5.  $\text{NH}_4^+$  versus Si relationships for water samples collected at Pele's Vent. The upper figure presents the data collected during the Alvin dive expedition. the middle figure presents the data collected during the Pisces V dive expedition. The bottom figure is the combined data base. The linear regression analyses were:  $\text{NH}_4^+ = -0.37 + 0.0065\text{Si}$  (Alvin);  $\text{NH}_4^+ = -0.21 + 0.0030\text{ Si}$  (Pisces V).

deep water. It should be mentioned, however, that there appears to be a net loss of fixed N in the hydrothermal system because the input of each mole of  $\text{NH}_4^+$  is offset by a loss of 6-7 moles of  $[\text{NO}_3^- + \text{NO}_2^-]$ . Presumably the N balance is accounted for by gaseous constituents not measured in our initial study. From a microbiological perspective the reduced form of nitrogen ( $\text{NH}_4^+$ ) has the potential to serve as an energy source for certain bacteria, so its presence in the hydrothermal vent system is significant.

It is not easy to compare our results on the dissolved nutrient content of Pele's Vent water samples to other hydrothermal systems (Table 3). Of the numerous publications on the chemistry of hydrothermal solutions, relatively few data are presented on the concentrations of  $[\text{NO}_3^- + \text{NO}_2^-]$ ,  $\text{NH}_4^+$  and SRP. Of the data which are available for comparison, a depletion of oxidized nitrogen has also been observed at the Galapagos Rift (Corliss, Dymond, Gordon, Edmond, von Herzen, Ballard, Green, Williams, Bainbridge, Crane, and van Andel 1979), at 21°N on the East Pacific Rise (Edmond and von Damm 1985) and at the Guaymas Basin (Edmond and von Damm 1985; Karl, Taylor, Novitsky, Jannasch, Wirsén, Pace, Lane, Olsen, and Giovannoni 1987) hydrothermal vents. For Pele's Vents we predict a total depletion of  $[\text{NO}_3^- + \text{NO}_2^-]$  at a Si concentration of 1.2 mM (Fig. 4), a value which corresponds to a temperature of approximately 30-35°C. The  $[\text{NO}_3^- + \text{NO}_2^-]$  measured in the discharged fluids, then, must be derived from mixing of vent waters with ambient bottom seawater.

The enrichment of  $\text{NH}_4^+$  in Pele's Vent (Fig. 5) is consistent with the data previously reported for high-temperature ( $>300^\circ\text{C}$ ) vent fluids collected at both the Explorer Ridge (Tunnicliffe, Botros, de Burgh, Dinet, Johnson, Juniper, and McDuff 1986) and the Guaymas Basin (von Damm, Edmond, Measures, and Grant 1985; Karl, Taylor, Novitsky, Jannasch, Wirsén, Pace, Lane, Olsen, and Giovannoni 1987), but conflicts with the extensive data base obtained from the 21°N East Pacific Rise vents. It is conceivable that the different trends which have been observed in the concentrations of dissolved  $\text{NH}_4^+$  are due to mechanisms other than strict seawater-basalt interactions. It has been suggested previously that the presence of elevated  $\text{NH}_4^+$  concentrations in vent water samples collected from Guaymas Basin is the result of thermolytic degradation of sedimented organic matter (von Damm, Edmond, Measures and Grant 1985). The absence of  $\text{NH}_4^+$  in the 21°N hydrothermal solutions is due to the absence of pelagic sediments at the mid-ocean ridge. It is conceivable that the hydrothermal solutions sampled at Pele's Vent are also reacting with a sediment phase at Loihi Seamount.

The systematic increase in SRP for the water samples collected at Pele's Vent appears to be unique to Loihi Seamount. While there is some scatter in our present data set, we feel

Table 3. Dissolved nutrient concentrations in Pele's Vent hydrothermal solutions

Dive	Sample	SRP	$[\text{NO}_3^- + \text{NO}_2^-]$	$\text{NH}_4^+$	Si
#	#	( M)	( M)	( M)	( M)
<u>Alvin EXPEDITION</u>					
1797	1	2.18	42.44	0.28	117.8
	3	2.70	40.52	0.39	131.8
	4	2.97	42.67	0.32	111.4
1798	1	2.54	41.85	0.51	156.8
	2	3.07	42.73	0.37	108.6
1799	1	2.35	42.08	0.46	141.0
	2	2.54	42.39	0.42	130.8
	3	2.65	41.85	0.56	154.9
	4	2.65	39.20	1.02	243.9
	5	2.81	14.48	5.56	588.1
	6	---- <sup>1</sup>	31.55	1.55	321.7
1800	1	3.57	19.27	3.43	696.9
	2	3.46	18.00	3.54	721.0
	3	2.28	40.64	0.58	142.9
	4	2.93	42.10	0.72	102.1
<u>Pisces V EXPEDITION</u>					
25	1	2.86	41.23	0.37	197.7
26	1	2.80	33.40	1.17	458.9
27	1	2.59	34.42	1.15	473.9
	2	3.91	34.04	1.38	519.1
	3	3.07	27.88	1.35	486.6
28	1	2.97	42.37	0.18	137.7
29	1	1.68	---- <sup>1</sup>	0.39	152.8
	2	2.12	40.19	0.29	196.5
BOTTOM SEAWATER					
	4	2.93	42.10	0.72	102.1

<sup>1</sup> sample lost or contaminated in analysis

confident that the waters discharged from Pele's Vent are a source of phosphorus to the deep ocean habitat surrounding the Hawaiian archipelago. In addition to the SRP contained in the discharged hydrothermal solutions, we have also measured (to be discussed later) a significant enrichment of phosphorus in association with the bacterial carpets. At the present time we believe that the "excess" P contained in the Pele's Vent habitat must be derived ultimately from the reaction between heated seawater and Hawaiian basalts, which are characteristically enriched in P relative to mid-oceanic ridge basalts (Byers, Garcia, and Muenow 1986; M. Garcia, unpublished data from Loihi).

#### CH<sub>4</sub> and CO<sub>2</sub> Content of Pele's Vent

Water samples collected from Pele's Vent were enriched in both CH<sub>4</sub> and  $\Sigma$  CO<sub>2</sub> relative to ambient bottom seawater (Table 4 and Fig. 6). The presence of a high CH<sub>4</sub> concentration in Pele's Vent was fully expected based on previous reports of elevated CH<sub>4</sub> concentrations in hydrothermal plumes sampled at Loihi Seamount (Horibe, Kim, and Craig 1983; Sakai, Tsubota, Nakai, Ishibashi, Akagi, Gamo, Tilbrook, Igarashi, Kodera, Shitashima, Nakamura, Fujioka, McMurtry, Malahoff, and Ozima 1987; Gamo, Ishibashi, Sakai, and Tilbrook 1987), and from the presence of CH<sub>4</sub> in hydrothermal vents on the East Pacific Rise (Welhan and Craig 1979, 1983; Lilley, Baross, and Gordon 1983) and the Galapagos Rift (Lilley, de Angelis, and Gordon 1982). The concentrations of both gases were positively correlated with dissolved Si, suggesting a hydrothermal origin (Fig. 6). From these linear relationships, the 30°C Pele's Vent water (the warmest vent temperature measured) should contain approximately 7  $\mu$ M CH<sub>4</sub> and 300 mM  $\Sigma$  CO<sub>2</sub>. The latter estimate is in excellent agreement with direct measurements of  $\Sigma$  CO<sub>2</sub> in the 30°C waters collected using gas tight samples and total gas extraction procedures (Craig, Welhan, and Hilton 1987). This extrapolated  $\Sigma$  CO<sub>2</sub> content is in excess of two orders of magnitude greater than the  $\Sigma$  CO<sub>2</sub> concentration of ambient bottom seawater.

The concentrations of CH<sub>4</sub> measured for the water samples collected at Pele's Vent are similar to the range of values previously measured for the low-temperature vents at the Galapagos Rift spreading center (Lilley, de Angelis, and Gordon 1982). When CH<sub>4</sub> ( $\mu$ M) was plotted versus dissolved Si ( $\mu$ M) for three separate Galapagos vent fields, the slopes of the linear regression analyses were  $1.4 \times 10^{-2}$ ,  $4.9 \times 10^{-3}$  and  $3.9 \times 10^{-3}$  for the East of Eden, Mussel Bed and Rose Garden sites (Lilley, de Angelis, and Gordon 1982). These data indicate that, for a given Si (i.e., heat) content, the Galapagos Rift vents vary by a factor of 3-4 with respect to their CH<sub>4</sub> enrichment. These substantial variations in the dissolved CH<sub>4</sub>-Si relationships among vent fields from the same locale may indicate variations in the rates of methane oxidation for regions having characteristically different biota. For Pele's Vent the slope of

Table 4. Dissolved methane and total carbon dioxide content of Pele's Vent water, February 1987

Dive #	Niskin Bottle #	CH <sub>4</sub> (nM)	$\Sigma$ CO <sub>2</sub> (mM)	Si ( $\mu$ M)
A-1797	1	64.2	4.21	117
A-1797	4	148.1	6.99	132
A-1798	3	11.5	2.63	108
A-1798	4	348.8	15.16	157
A-1799	1	230.3	11.90	155
A-1799	3	240.3	17.20	141
A-1800	2	196.7	13.70	142
A-1800	4	7.2	2.38	102

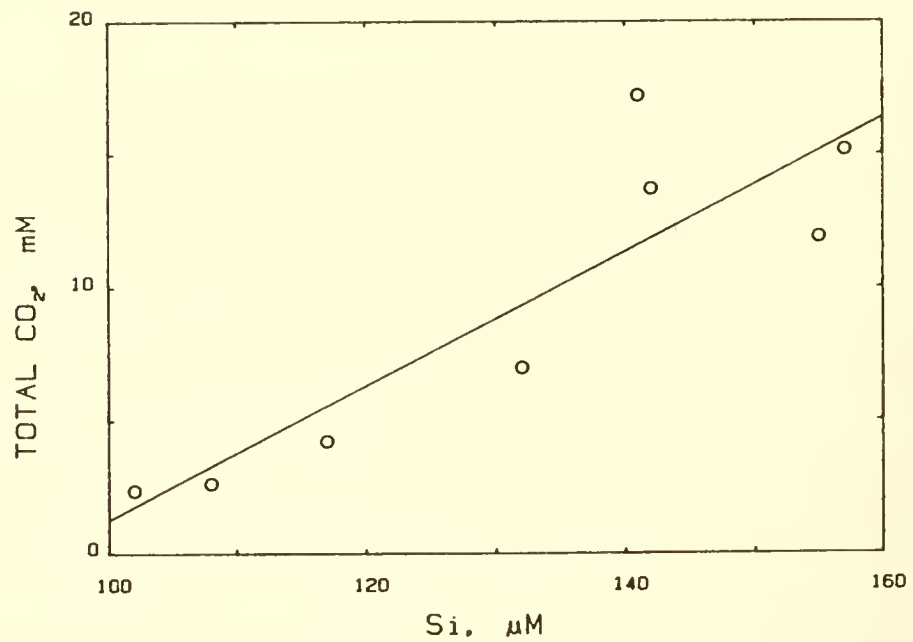
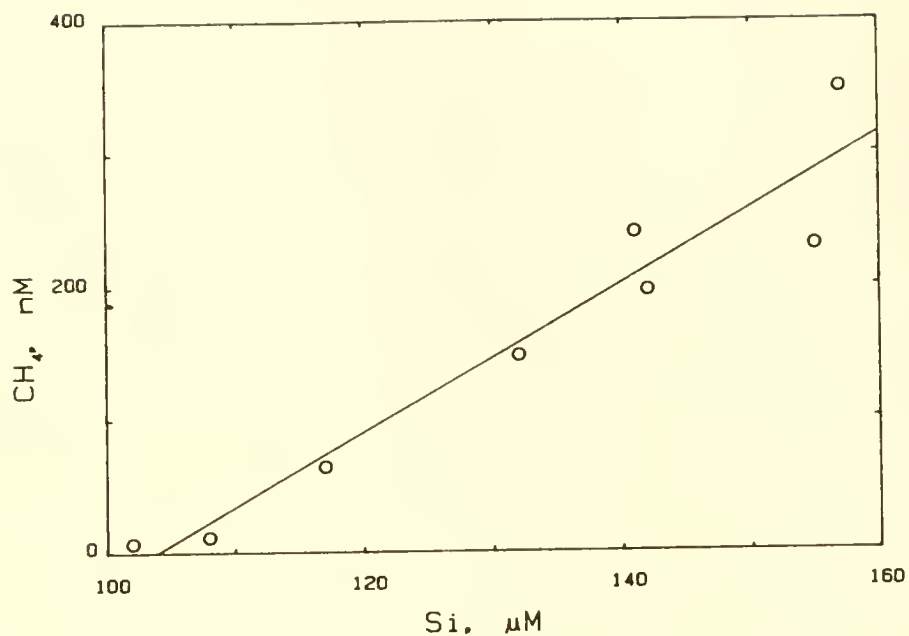


Figure 6. Methane and Total  $\text{CO}_2$  versus Si relationships for samples collected from Pele's Vent during the Alvin dive expedition. The linear regression analyses were:  
 $\text{CH}_4 = -5.82 + 5.60\text{Si}$  and  $\text{CO}_2 = -23.95 + 0.252\text{Si}$ .

our  $\text{CH}_4$  (nM) versus  $\text{Si}$  ( $\mu\text{M}$ ) regression (Fig. 6a) was  $5.6 \times 10^{-3}$ , a value which is in the range of the previously published Galapagos Rift data.

The  $\text{CH}_4/\text{excess } \Sigma \text{CO}_2$  molar ratio estimated for the water samples collected from Pele's Vent is  $2.3 \times 10^{-5}$  (Fig. 7), compared to a value of  $3 \times 10^{-4}$  that was predicted from the  $\text{CH}_4/\text{pH}$  relationships of Loihi Seamount hydrothermal plumes (Sakai, Tsubota, Nakai, Ishibashi, Akagi, Gamo, Tilbrook, Igarashi, Kodera, Shitashima, Nakamura, Fujioka, McMurtry, Malahoff, and Ozima 1987). It is highly unlikely that there is either  $\text{CH}_4$  production or net  $\text{CO}_2$  uptake in the hydrothermal plume that might account for the different ratios. One possible explanation is that the  $\text{CH}_4/\text{excess } \Sigma \text{CO}_2$  ratio of Pele's Vent may not be characteristic of Loihi Seamount as a whole. In support of this interpretation, Gamo, Ishibashi, Sakai and Tilbrook (1987) have suggested that there exist at least two identifiable and chemically-distinct hydrothermal plumes at Loihi. Relative to the content of  $^3\text{He}$ , the deep plume had approximately 3-4 times more  $\text{CH}_4$  than the plume detected at shallower depths (1000-1050 m). This chemical distinction is also evident in the  $\text{CH}_4-\text{pH}$  relationships (Gamo, Ishibashi, Sakai, and Tilbrook 1987). Two mixing lines, representing two end-member fluid compositions, are evident; the shallow plume again has less  $\text{CH}_4$  (relative to pH [i.e.,  $\text{CO}_2$ ]) than the deep plume.

At Pele's Vent, there are at least two potential sources for hydrothermal  $\text{CH}_4$ : (1) abiogenic sources, including volatile release from mantle sources, thermocatalysis of deposited organic matter, and high-temperature exchange reactions with the basalt-seawater system (i.e.,  $4\text{H}_2 + \text{CO}_2 \rightarrow \text{CH}_4 + 2\text{H}_2\text{O}$ ) and (2) biogenic reactions involving the activities of thermophilic, methanogenic bacteria. Welhan and Craig (1983) suggest that the observed enrichments of  $\text{CH}_4$  in hydrothermal fluids are the result of direct extraction of  $\text{CH}_4$  from basalt by circulating seawaters. Their conclusion is based upon several lines of evidence, including: the association of  $\text{CH}_4$  with  $^3\text{He}$  and excess  $\Sigma \text{CO}_2$  which are known to be derived from ridge crest basalts, the lack of known sources of organic matter for thermocatalysis, the general absence of  $\text{C}_2^+$  hydrocarbon homologues in vent solutions, the  $\delta^{13}\text{C}$  enrichment of vent-derived  $\text{CH}_4$ , and the similarity in the  $\text{CH}_4/^3\text{He}$  ratios of the EPR hydrothermal fluids and mid-ocean ridge basalts.

On the other hand, the  $\text{CH}_4$  measured at Pele's Vent and enriched in hydrothermal solutions in general could, at least in part, be formed as a result of the reduction of  $\text{CO}_2$  by the activities of methanogenic bacteria. Baross, Lilley and Gordon (1982) have demonstrated the production of  $\text{CH}_4$  (and other "biogenic" gases) at  $100+2^\circ\text{C}$  by  $21^\circ\text{N}$  EPR hot water and sulfide-chimney associated bacterial communities. Because their

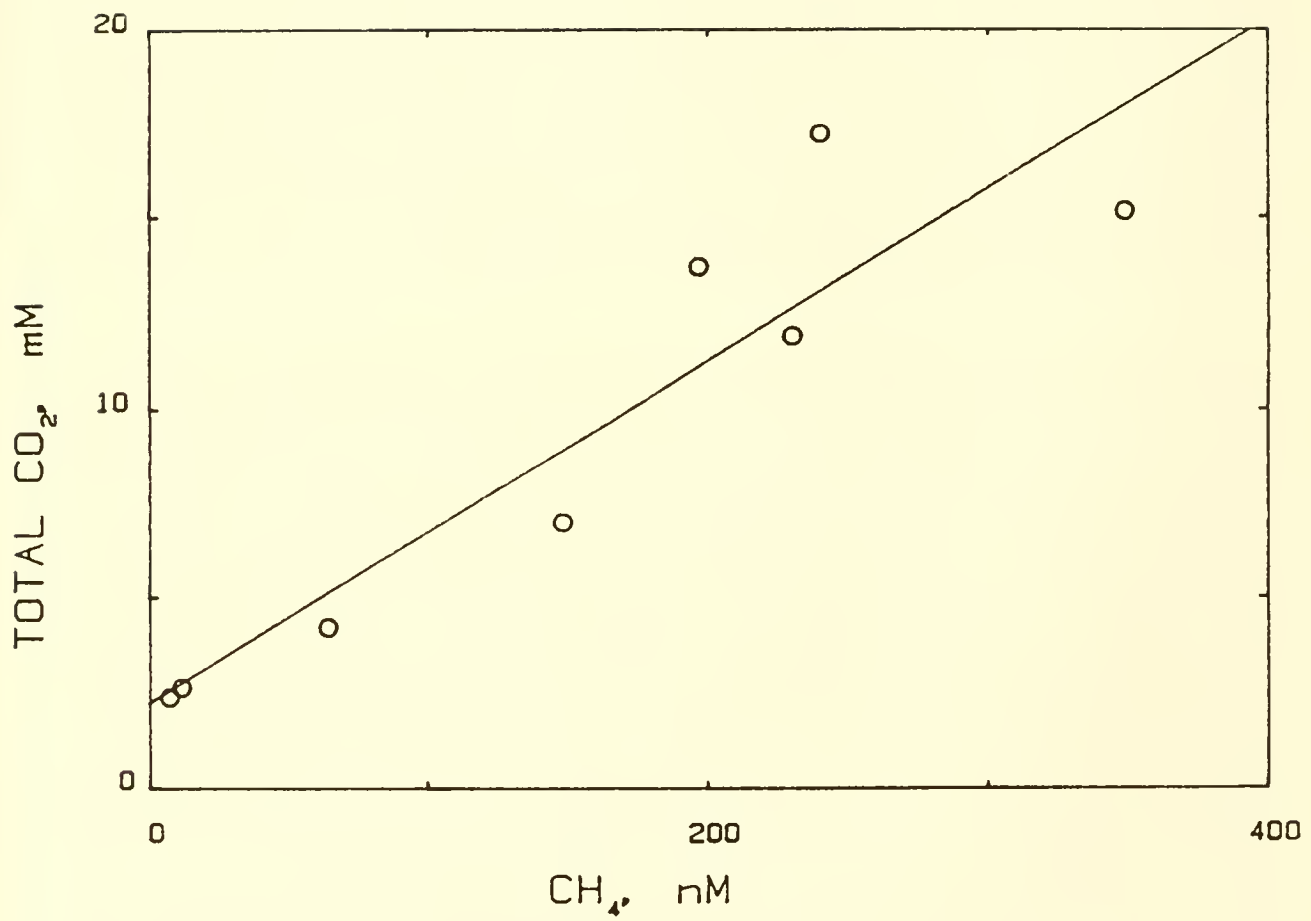


Figure 7. Total  $\text{CO}_2$  versus  $\text{CH}_4$  concentrations measured at Pele's Vent. The linear regression analysis was:  $\text{CO}_2 = 2.235 + 4.514\text{CH}_4$ .

experiments were performed in the laboratory under enrichment culture (artificial growth medium) conditions, the in-situ rates of CH<sub>4</sub> production cannot be estimated. Furthermore, they also detected the presence of active bacterial CH<sub>4</sub> oxidation at 100°C, consequently the net effect of microbial activity on CH<sub>4</sub> concentrations in hydrothermal systems cannot be easily predicted. Nevertheless, the potential for biological CH<sub>4</sub> production does appear to exist in certain deep-sea hydrothermal systems.

The process of oxidation of CH<sub>4</sub> by specific bacterial species is well-documented (Crawford and Hanson 1984). It is probable that the CH<sub>4</sub> derived from the hydrothermal systems at Loihi Seamount is also oxidized either by bacterial populations located at or near the vent fields, or by bacteria contained within the hydrothermal plumes. Based on calculations performed by Welhan and Craig (1979), the CH<sub>4</sub> flux from the world-ocean ridge system (estimated from <sup>3</sup>He flux) is sufficient to replace the entire pool of deep-sea CH<sub>4</sub> in a period of approximately 30 years. This implies a rapid bacterial consumption rate beneath the thermocline (Welhan and Craig 1979, 1983). Our experimental results from Pele's Vent indicate a significant potential for bacterial CH<sub>4</sub> oxidation in samples collected from discharged hydrothermal fluids and bacterial mats (Table 5). These results suggest that CH<sub>4</sub> oxidation does occur at Pele's Vents.

During the Pisces V field expedition, we continued to investigate the process of CH<sub>4</sub> oxidation by measuring the net changes (i.e., balance between CH<sub>4</sub> oxidation and CH<sub>4</sub> production) which occur in the total CH<sub>4</sub> concentrations of Pele's Vent water samples during prolonged incubation (30 d) at 25°C, 1 atm. Our results indicate a significant net decrease in dissolved CH<sub>4</sub> for all but one of the hydrothermal vent samples analyzed (Table 6). We then used these water samples to measure the presence and activity of methane oxidizing bacteria using <sup>14</sup>CH<sub>4</sub>, as described previously. In these latter experiments, we measured the radioactivity incorporated in cell materials (nucleic acids and protein) as well as the radioactivity that was respired as CO<sub>2</sub> (Table 7). Our results indicated that all of the samples from which we had detected substantial CH<sub>4</sub> oxidation by chemical determinations also displayed oxidation using the radiochemical method. The most active samples (#25/Niskin and #29/Niskin) were the two samples which initially contained the highest concentrations of CH<sub>4</sub> (Table 6). It is interesting to point out that >90% of the radioactivity resulting from the metabolism of <sup>14</sup>CH<sub>4</sub> was respired as <sup>14</sup>CO<sub>2</sub> with only a minor fraction being incorporated in cellular macromolecules.

#### Bacterial Biomass and Metabolic Activity at Pele's Vent

Warm waters (up to 30°C) emitted from Pele's Vents contained elevated concentrations of ATP with enrichment factors (i.e., ATP

Table 5. Oxidation of  $^{14}\text{CH}_4$  to  $^{14}\text{CO}_2$  by Pele's Vent bacteria.  
Samples were collected during the Alvin expedition, February  
1987.

Dive #/Sample Type	Incubation Time (hr)	$^{14}\text{CO}_2$ produced (nCi per l)
1799 - Niskin	7.5	6.27
	18	11.46
1800 - Niskin	7.5	22.73
	18	26.60
1800 - mat	7.5	16.86
	18	43.68
control - deep water	7.5	2.05
	18	5.36

Table 6. Changes in  $\text{CH}_4$  and  $\Sigma \text{CO}_2$  content of Pele's Vent water samples following incubation for 30 d at 25°C, 1 atm.

Dive #/Sample Type	initial $\text{CH}_4$ (nM)	final $\text{CH}_4$ (nM)	% change
#25 - Niskin	582.4	10.0	-98.3
#26 - Titanium	312.1	96.5	-69.1
#27 - Niskin	65.8	59.0	-10.3
#27 - Titanium	212.2	284.1	+33.9
#29 - Niskin	452.8	35.2	-92.2
#29 - Titanium	279.3	6.1	-97.8
bottom seawater	2.34	2.39	+2.1

Table 7. Metabolism of  $^{14}\text{CH}_4$  by bacteria collected from Pele's Vent and distribution of radioactivity in respired  $\text{CO}_2$  and incorporated nucleic acids (NA) and protein. The % values given in parentheses represent the % of the total  $^{14}\text{C}$  assimilated that is represented by each of the individual metabolic compartments.

---

Dive # Sample Type <sup>1</sup>	Total $^{14}\text{CH}_4$ assimilated (nCi per l)	$^{14}\text{CO}_2$ (nCi per l)	$^{14}\text{C-NA}$ (nCi per l)	$^{14}\text{C-Protein}$ (nCi per l)
#25 Niskin	280.2 (100%)	252.4 (90%)	19.5 (7%)	8.3 (3%)
#26 Titanium	42.7 (100%)	41.1 (96%)	0 (0%)	1.6 (4%)
#27 Titanium	61.0 (100%)	59.4 (97%)	0 (0%)	1.6 (3%)
#29 Niskin	232.7 (100%)	229.1 (98%)	0.3 (0.1%)	3.2 (1.4%)
#29 Titanium	26.1 (100%)	26.1 (100%)	0 (0%)	0 (0%)

---

<sup>1</sup> The samples used were from the experiment described in Table 6 following the 30 d incubation. For the  $^{14}\text{CH}_4$  oxidation study, the samples were incubated for 6 d at 25°C.

in vent water to ATP in ambient bottom seawater) ranging from 1.2 to 23. The highest ATP concentration measured for a freshly collected vent water sample was 118 ng  $1^{-1}$  (Alvin dive #1797). This ATP concentration is 3-4 times greater than the ATP contained in surface waters near Hawaii (Winn and Karl 1984) and documents a local enrichment of microbial biomass in Loihi Seamount hydrothermal vent fluids. The ATP concentrations and enrichment factors measured at Pele's Vent are similar to those previously reported for a variety of hydrothermal vent ecosystems (summarized by Karl 1987). Incubation of Pele's Vent water samples for periods ranging from days to weeks at 25°C resulted in the growth of a substantial population of bacteria (up to 2500 ng ATP  $1^{-1}$ ) indicating the potential for sustained bacterial growth and biomass production. During these incubation periods, the growing microbial assemblages actively incorporated the radioactivity from  $^3\text{H}$ -adenine and  $^3\text{H}$ -thymidine into both cellular nucleic acids and protein. Over short-term incubation periods (<1 d), the biomass-specific (i.e., per unit ATP) incorporation of  $^3\text{H}$ -adenine into cellular DNA was up to an order of magnitude greater for samples collected from Pele's Vent than for ambient bottom seawater (when incubated at 25°C, 1 atm.). Water samples collected at Pele's Vent also had elevated concentrations of bacterial cells relative to ambient bottom seawater (Table 8). Enrichment factors ranged from 3.1 to 14.4 for the samples analyzed, a range similar to that presented previously for ATP concentrations.

During the Pisces V expedition, we sought to learn more about the environmental conditions where bacterial growth in the Pele's Vent hydrothermal system is likely to occur. We adopted the protocol of Karl (1985), previously employed at the Galapagos Rift and 21°N hydrothermal vent sites, in order to evaluate the temperature-metabolic activity relationships for vent derived microorganisms. The results of these experiments would help us to determine the upper limits for temperature, and to predict the fate of hydrothermal bacterial assemblages discharged into the relatively cool (4°C) bottom seawaters.

For Pele's Vent water samples we observed a striking dependence on temperature for the uptake and assimilation of a variety of nucleic acid precursors (adenine and thymidine) and potential growth substrates (acetate and glutamic acid; see Table 9). These data confirm the importance of temperature as an important environmental variable. Our results indicate that the microorganisms sampled from Pele's Vent have temperature optima of at least 37°C, and probably higher. The assimilation of glutamic acid was greatest at 60°C and for adenine and thymidine the population response at 60°C was 80-90% of the maximum measured at 37°C (Table 9). In this respect, Pele's Vent populations are more thermophilic than the microbial communities at either the Galapagos Rift or from the low temperature (<35°C) vents at 21°N on the East Pacific Rise (Karl 1985). The

Table 8. Acridine orange direct counts of bacterial cell numbers for water samples collected at Pele's Vent during the Pisces V expedition (August 1987)

Dive #	Sample Type	bacteria (cells per ml)	Enrichment Factor <sup>1</sup>
25	Niskin	$7.4 \times 10^4$	8.2
26	Titanium #1	$1.3 \times 10^5$	14.4
27	Titanium #1	$2.8 \times 10^4$	3.1
27	Titanium #2	$4.7 \times 10^4$	5.2
	bottom seawater	$9.0 \times 10^3$	---

<sup>1</sup>Enrichment Factor = cells in vent sample/cells in control bottom seawater sample

Table 9. Effects of temperature on the metabolism of four different organic substrates by micro-organisms sampled from Pele's Vent. The data are presented either as total amounts of radioactivity incorporated into acid insoluble cellular materials ( $^3\text{H}$ -adenine,  $^3\text{H}$ -thymidine,  $^3\text{H}$ -glutamate) or as respiration plus incorporated radioactivity ( $^{14}\text{C}$ -acetate and  $^{14}\text{C}$ -methane). The values given in parentheses indicate the percentage of the total metabolic activity relative to the maximum rate observed for that particular substrate.

Substrate <sup>1</sup>	Total Radioactivity, pCi per ml <sup>-1</sup>			
	4°C	25°C	37°C	60°C
$^{14}\text{C}$ -acetate	21.3 (2.4%)	43.3 (4.9%)	886.8 (100%)	33.2 (3.7%)
$^3\text{H}$ -adenine	122.2 (27.5%)	253.5 (57.0%)	445.0 (100%)	364.3 (81.9%)
$^3\text{H}$ -glutamate	79.7 (9.0%)	332.8 (37.4%)	732.2 (82.4%)	888.8 (100%)
$^3\text{H}$ -thymidine	32.5 (5.8%)	306.2 (43.2%)	708.6 (100%)	563.5 (79.5%)

<sup>1</sup> Details of the site of labeling, specific radioactivities and experimental design are given in the text.

assimilation versus temperature data for acetate (Table 9) suggest that this organic substrate is perhaps utilized by a specialized sub-population which displayed a much more narrow tolerance with respect to temperature. Similar experiments were also performed to determine the temperature optimum for the metabolism of  $^{14}\text{CH}_4$ . Using the Niskin bottle collected sample from Pisces V dive #25 (see Tables 6 and 7) we determined a metabolic maximum at  $37^\circ\text{C}$  with 62.2% of this maximum  $^{14}\text{CH}_4$  oxidation activity still remaining at an incubation temperature of  $60^\circ\text{C}$ . In this regard the temperature dependence of  $\text{CH}_4$  oxidation was similar to that measured for the nucleic acid precursors (see Table 9). On the basis of these experiments we conclude that the Pele's Vent bacterial populations are adapted for growth at warm ( $35-60^\circ\text{C}$ ) temperatures and probably decrease their rates of metabolism by factors of 20-100 fold when they are injected into the cold ( $4^\circ\text{C}$ ) ambient bottom seawater surrounding the vent field.

#### Enrichment Culture Results

Our first attempts at pure culture isolation were, in general, unsuccessful. The enrichment cultures failed to recover any organisms with the exception of proteolytic bacteria. Our selective medium (see Table 2) recovered gelatinase positive bacteria with a most probable number of  $750 \text{ cells ml}^{-1}$  for the rock scraping suspension and  $550 \text{ cells ml}^{-1}$  for the titanium sample from dive #29. The negative results obtained with the other enrichment culture media should not be interpreted as conclusive evidence for the absence of the "target" organisms. As with any enrichment experiment, negative results cannot preclude the presence of a particular group of microorganisms but could alternately reflect improper incubation or enrichment conditions. This is especially true for the unique habitat of Pele's Vent. Improper conditions, with respect to temperature, pH-alkalinity, dissolved gases, eH or specific organic or inorganic growth factors could have significantly affected the potential growth of the vent bacteria. The presence of heterotrophic bacteria able to hydrolyse protein is not startling. Our investigation of the temperature of maximum growth might help in future studies to define the actual habitat for these organisms while other conditions could be studied to help in defining proper enrichment conditions for the other micro-organisms present. The effects of high concentrations of dissolved  $\text{CO}_2$  and its effect on bacterial metabolism may also need to be evaluated in future experiments.

#### Structure and Composition of Bacterial Mats

One of the most conspicuous features of Pele's Vent is the extensive reddish-brown bacterial mat, or more precisely carpet, which covers large areas of the hydrothermal habitat (Fig. 2b). When viewed under bright-field (Fig. 8) or scanning electron



Figure 8. Bright-field microscopic images of the bacterial mat sampled from Pele's Vent.

microscopy (Fig. 9) the detailed structure of the mat is clearly visible. The primary morphology is that of long, thin filaments approximately 1-2  $\mu\text{m}$  in diameter and up to 200-500  $\mu\text{m}$  in length. No filament branches were observed in any of our preparations. Transmission electron microscopic analyses indicated that these filaments were actually tubular in shape with relatively uniform wall diameters of 0.2-0.3  $\mu\text{m}$  (Fig. 10). Of approximately 1000 cross-sections that were analyzed, only 1-2% of the filaments had recognizable cellular materials inside of the electron dense walls (an example is presented in Fig. 10); the majority appeared to be empty. At the present time we do not know whether this is a result of poor preservation of these bacterial structures or whether these initial results adequately describe the relative proportion of "live" versus "fossil" filaments. In addition, there was also a relatively large and morphologically diverse assemblage of bacteria that were either attached to or otherwise associated with the bacterial filaments. Because we made no attempt to quantify these attached cells we are not certain whether they comprise a significant portion of the total mat biomass.

We further investigated the nature of the filamentous matrix to determine the bulk chemical and mineralogical composition of these materials. These analyses included scanning electron microscopy-energy dispersive x-ray fluorescence spectroscopy (SEM-EDS) of individual filaments, x-ray diffraction, electron microprobe analysis and bulk chemical analysis for phosphorus and organic carbon. The latter analyses revealed that the mats were only  $1.8 \pm 0.07\%$  organic carbon (by weight) indicating the presence of a large inorganic component. The  $^{13}\text{C}/^{12}\text{C}$  carbon isotope ratio (expressed as  $\delta^{13}\text{C}$ ) was  $-24.3\text{ o/oo}$  (G. Rau, pers. comm.).

The P content of the bacterial mat, as determined by chemical analysis, was 2.4% by weight. This exceeds the total organic carbon value and indicates that most of the P must be inorganic rather than cell-associated (the average C:P [wt/wt] ratio of bacteria under P sufficient growth conditions is expected to be 30-50). From the results of our chemical leaching experiments, we conclude that <2% of the P associated with the bacterial mat is "CaCO<sub>3</sub>-bound" (i.e., <2% is extracted in acetate buffer, pH 5.0), <2% is "mineral-P" (difference between oxalate buffer, pH 3.0 and 8 M HCl extractions) and that the majority (>95%) of the P must be termed "hydrogenous." Our results support Berner's (1973) hypothesis regarding the sorption or coprecipitation of P onto hydrothermal ferric oxyhydroxides. These results are also consistent with the experimental results of Froelich, Bender and Heath (1977) for samples collected from the East Pacific Rise, and with the stated implications for rapid P accumulation in hydrothermal sediments. However, at Loihi Seamount it is possible that the origin of the P that is accumulating in the metalliferous



Figure 9. Scanning electron microscopic images of the bacterial mat sampled from Pele's Vent.

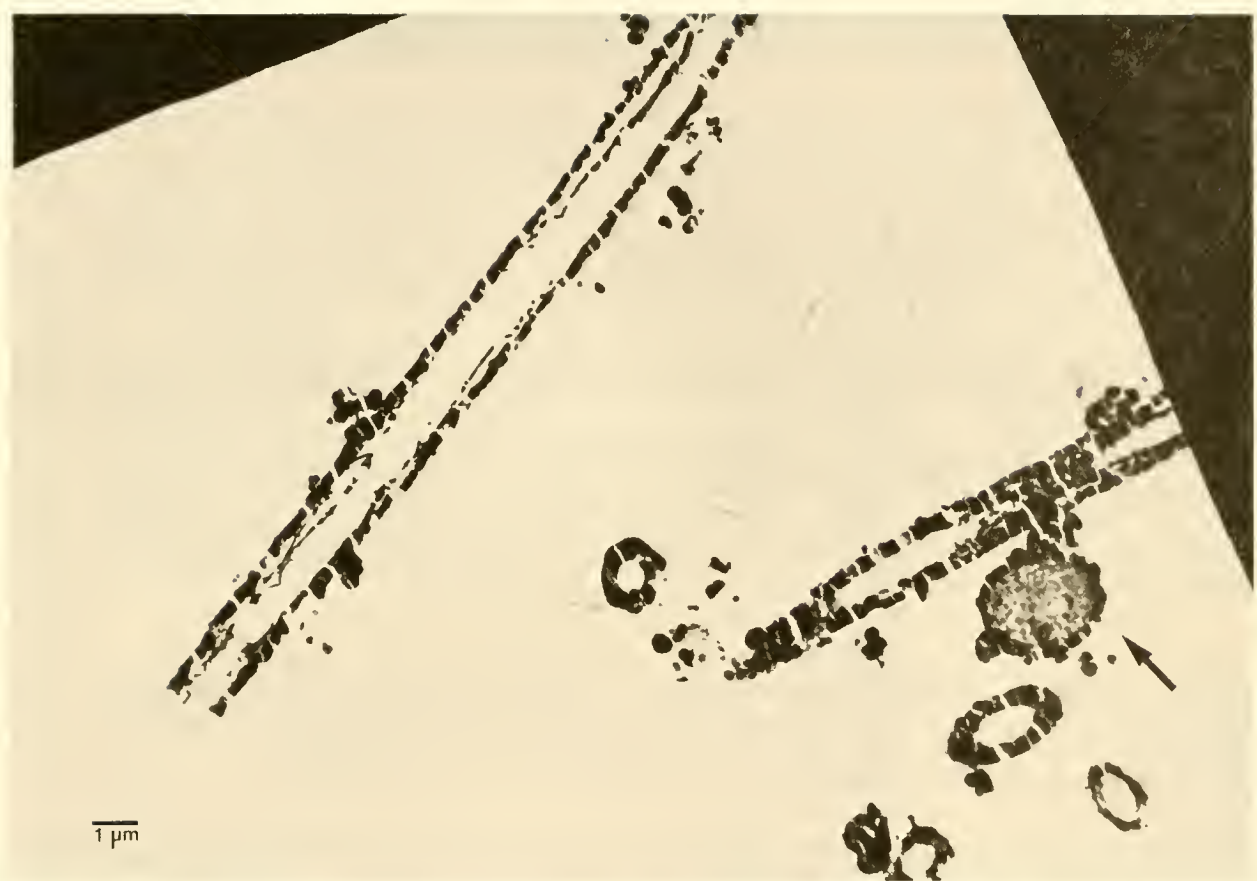


Figure 10. Transmission electron microscopic image of the filaments which comprise the bacterial mat. The arrow points to the presence of cytoplasm in a cross section of one of the individual filaments.

deposits is from the hydrothermal solutions themselves (see Fig. 3) rather than being derived from seawater.

The SEM-EDS analysis (Fig. 11) indicated that the bacterial mat was comprised predominantly of Fe with significant contributions from P and Ca. Si also appeared as a minor constituent of bulk sample excitation (i.e., sample magnification of <100 x) but was not present as a compositional constituent of a higher magnification (and excitation) of individual filaments.

These results were confirmed by quantitative microprobe analyses which revealed that the mat had an Fe:P ratio (by weight) of 6-7 to 1 (M. Garcia, pers. comm.). The percent P content, as determined by microprobe, was generally higher than that estimated by chemical methods. X-ray diffraction (XRD) analysis of the bacterial mat material indicated the general absence of crystalline material in the dried preparations. The Ca peak (Fig. 11) is most likely due to the presence of contaminating seawater as trace amounts of halite (NaCl) and bassanite ( $\text{CaSO}_4 \cdot 0.5 \text{ H}_2\text{O}$ ) were detected in the XRD analysis (J. Schoonmaker, pers. comm.). The presence of amorphous Fe (oxides/hydroxides) is consistent with the suggestion of a microbiological origin of the filamentous structures. Metal associations, especially amorphous Fe, are also known to occur in other biological/ microbiological hydrothermal vent deposits (Alt 1986; Juniper, Thompson, and Calvert 1986).

Ferrous iron oxidation is well known in the microbial world (e.g., Thiobacillus ferrooxidans, Sulfolobus acidocaldarius, Leptospirillum ferrooxidans, Gallionella ferruginea, Leptothrix ochracea, Siderocapsa geminata, Sphaerotilus natans, Metallogenium; Cullimore and McCann 1977, Ehrlich 1981, Ghiorse 1984). Not all iron-oxidizing bacteria couple the oxidation to CO<sub>2</sub> reduction and in some cases the oxidation of iron is only an indirect metabolic process (i.e., non-enzymatic). However, obligate chemolithoautotrophic growth utilizing Fe+2 has been demonstrated for selected species. Waters collected from Pele's Vent at Loihi Seamount contain >700  $\mu$ moles dissolved Fe l<sup>-1</sup> (G. McMurtry, pers. comm.). The molar Fe/Mn ratio decreases in the Loihi hydrothermal vent system from approximately 50 in the warmest anoxic waters (30°C) to a value of 20 at lower water temperatures (2-5°C). These data suggest iron deposition is perhaps mediated by micro-organisms.

#### Absence of Benthic Macrofauna at Pele's Vent

A hallmark of nearly all hydrothermal vent systems studied to date is the presence of dense populations of benthic invertebrates which thrive on the localized source of bacterial production. These deep-sea oases contrast sharply with the depauperate nature of non-vent deep-sea benthic populations, a

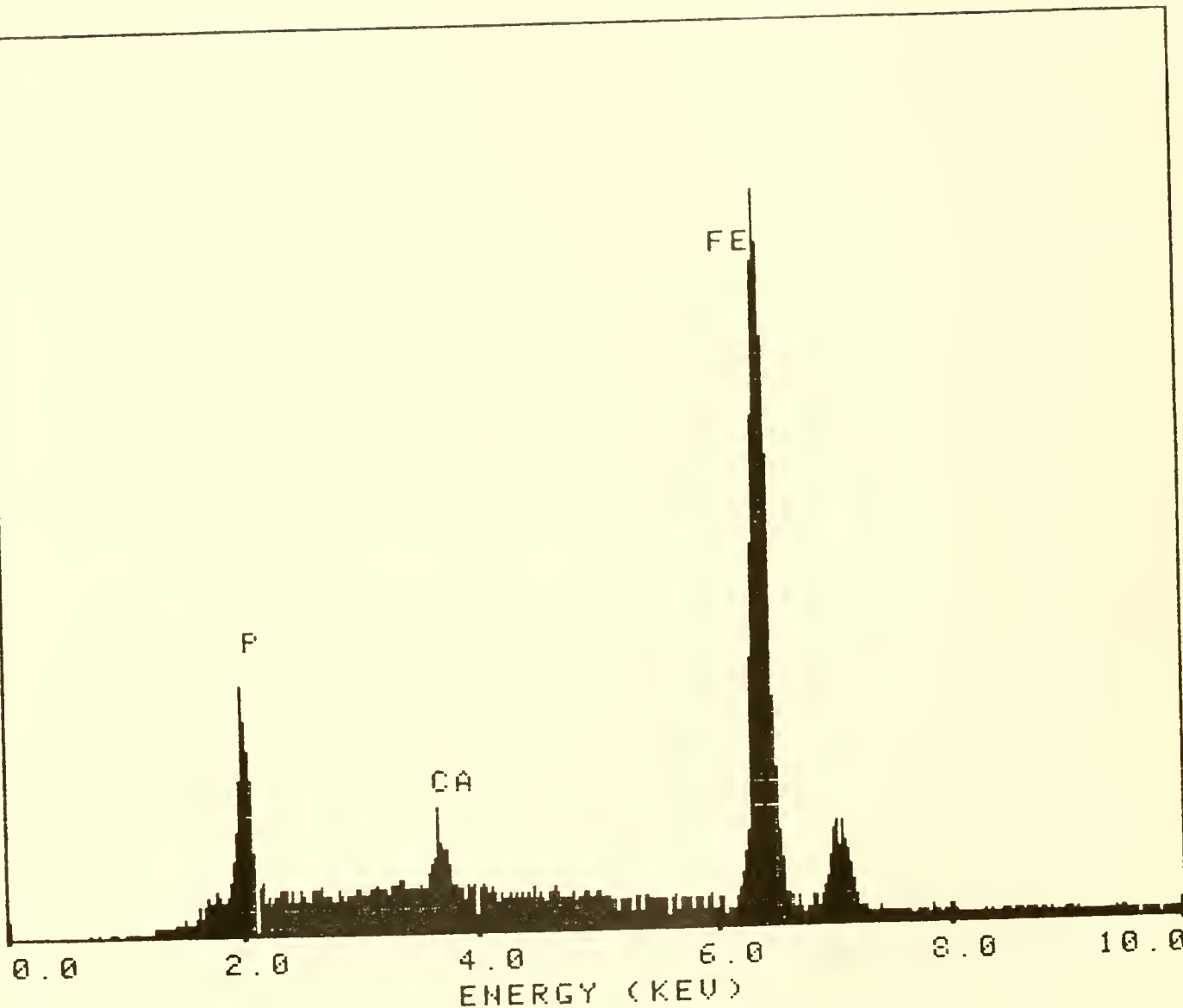


Figure 11. Energy dispersive X-ray analysis of Pele's Vent bacterial mat. The major peaks correspond to the presence of Fe, Ca, and P. The peak to the immediate right of the Fe (Ka) is the secondary (KB) peak from that same element.

difference which has been attributed to the amount and rate of food supply. The biomass (expressed as wet weight) of animals at most vent ecosystems can exceed 20-30 kg m<sup>-2</sup> (Hessler and Smithey 1983, Laubier and Desbruyeres 1984). Although the list of characteristic vent organisms continues to grow, at least 40 new species from 16 previously unknown families of invertebrates have now been described (summarized by Grassle 1985, 1986). In addition to these predominantly sessile benthic organisms, there is also a vent-associated fish fauna (Cohen and Haederich 1983); however, the vertebrates as a group display a lower degree of endemism than that observed among the invertebrate fauna. Despite the ubiquitous presence of animal communities at deep-sea vents, their distribution and abundance is far from uniform. Distinct zonation patterns, perhaps in response to the physical/chemical characteristics of the discharged hydrothermal fluids, are commonly encountered (Hessler and Smithey 1983; Tunnicliffe, Juniper and de Burgh 1985).

Another feature of the hydrothermal vent communities is the large difference in relative abundance of dominant organisms occurring in otherwise similar habitats. For example, at the Galapagos Rift spreading center, several characteristically different ecosystems, each dominated by a different vent species, have been observed along a 10-20 km segment of the rift zone (Galapagos Biology Expedition participants 1979). A similar observation was recorded for several individual hydrothermal vent fields along a 1 km portion of the Explorer Ridge (Tunnicliffe, Botros, de Burgh, Dinet, Johnson, Juniper and McDuff 1986).

Pele's Vent field and other hydrothermal areas on Loihi Seamount are in conspicuous contrast to other characteristic deep-sea vents by the absence of a luxuriant benthic community. Although it is conceivable that a Loihi vent-associated benthic community actually does exist but has thus far eluded both the saturation bottom photography surveys (Malahoff, McMurtry, Wiltshire and Yeh 1982; A. Malahoff and R. Grigg, pers. comm.) and the Alvin and Pisces V dive tracts, a more probable conclusion is that a Loihi Seamount vent community is, in fact, absent.

This is of particular interest because bacterial populations, which presumably comprise the base of other deep-sea hydrothermal vent food webs, are present in high concentrations at Pele's Vent. It has been suggested that submarine hydrothermal activity may be too infrequent to support a specialized benthic community of animals (Malahoff, McMurtry, Wiltshire and Yeh 1982); however, it is now well known that the communities at other hydrothermal vent sites have evolved in spite of discontinuous venting and variable hydrothermal fluid discharge.

At the present time there is no data base for comparison of Loihi to other seamounts which lack the volcanically induced disturbance, metalliferous sediment deposition and hydrothermal fluid discharge which characterize our study site. Consequently it is difficult to evaluate whether recruitment, *per se*, is a factor in the establishment of seamount faunas or whether the depauperate Loihi fauna is directly related to the fact that it is geologically active with a resultant instability of the substratum (Grigg 1988).

Another possible explanation for the absence of fauna at the Pele's Vent site is the toxicity of the hydrothermal solutions themselves. As discussed previously, the  $\Sigma \text{CO}_2$  content of the vent waters is in excess of two orders of magnitude greater than ambient bottom seawater. This results in a lowering of the pH to a value of approximately 5.4 (Edmond, Campbell, Palmer, Falkner and Bowers 1987), a value which could be toxic to most invertebrates. The high concentrations of dissolved trace metals (Edmond, Campbell, Palmer, Falkner and Bowers 1987; Sedwick and McMurtry 1987) may also contribute to solution toxicity. Finally, the fact that Loihi Seamount is a relatively young geological feature compared to the mid-ocean ridge habitats also needs to be considered. It is conceivable that Loihi Seamount constitutes a very early stage in the lengthy processes of dispersal, recruitment and natural selection that are required to establish a successful hydrothermal vent animal community.

## CONCLUSION

In conclusion we have discovered, explored and sampled active hydrothermal vents on the summit of Loihi Seamount, Hawaii at an area referred to as Pele's Vent. The active vent field is characterized by iron-rich nontronite deposits, warm ( $30^\circ\text{C}$ ) hydrothermal fluids, extensive bacterial mats and by the conspicuous absence of large benthic animals. Our initial experiments have revealed the presence of elevated concentrations of reactive Si,  $\text{NH}_4^+$ , SRP,  $\Sigma\text{CO}_2$  and  $\text{CH}_4$  in the discharged vent fluids, relative to ambient bottom seawater. Bacteria present in the warm discharged vent fluids were shown to be metabolically-active at temperatures up to at least  $60^\circ\text{C}$ . Bacterial methane oxidation potential was also measured in water sampled from Pele's Vent. Bacterial mats observed in certain regions of the vent field are comprised of long filaments coated with Fe precipitates. It is hypothesized that these tubular structures are actively formed by the growth of Fe-oxidizing bacteria. This hypothesis will require a comprehensive *in-situ* experimental evaluation. In the words of Rison and Craig (1983), "Loihi volcano, born in the shadow of the world's greatest, if least known, mountains has possibly revealed an important secret, but it is young and needs to be understood." We agree with their

assessment. Our initial microbiological and chemical studies at Loihi Seamount have generated a detailed and ambitious research prospectus that may take at least a decade to address adequately.

#### ACKNOWLEDGMENTS

We thank the officers and crew members of the R/V Atlantis II and R/V Kila and especially the pilots and support personnel for the Alvin and Pisces V submersibles for their assistance and expertise, T. Walsh for inorganic nutrient analyses, T. Carvallo and A. Berger for their assistance in the electron microscopic and EDS analyses, J. Schoonmaker for the XRD data, M. Garcia for the electron microprobe data, G. Tien, U. Magaard and T. Tagami for technical assistance, R. Grigg for helpful comments and L. Wong for manuscript preparation. This research was a joint effort of the University of Hawaii Loihi Research team (G. McMurtry, A. Malahoff, R. Grigg and D. Karl). The research described herein was supported, in part, by the National Undersea Research Program (NURP) of the National Oceanic and Atmospheric Administration (NOAA), and by grants from NOAA-Seagrant Project R/OM-2 (University of Hawaii Seagrant Program) and the National Science Foundation (OCE 83-51751) both awarded to the senior author. Contribution #1923 of the Hawaii Institute of Geophysics.

#### LITERATURE CITED

Alt, J. C. 1986. A Hydrothermal/Bacterial Iron Deposit from a Seamount Near 21°N, East Pacific Rise. Geol. Soc. Amer., Abstr. #95618.

Baross, J. A., M. D. Lilley, and L. I. Gordon. 1982. Is the CH<sub>4</sub>, H<sub>2</sub> and CO Venting from Submarine Hydrothermal Systems Produced by Thermophilic Bacteria? Nature, Vol. 298, No. 5872, pp. 366-368.

Byers, C. D., M. O. Garcia, and D. W. Muenow. 1986. Volatiles in Basaltic Glasses from the East Pacific Rise at 21°N: Implications for MORB Sources and Submarine Lava Flow Morphology. Earth Planet. Sci. Lett., Vol. 79, No. 1/2, pp. 9-20.

Cohen, D. M. and R. L. Haedrich. 1983. The Fish Fauna of the Galapagos Thermal Vent Region. Deep-Sea Res., Vol. 30, No. 4A, pp. 371-379.

Corliss, J. B., J. Dymond, L. I. Gordon, J. M. Edmond, R. P. von Herzen, R. D. Ballard, K. Green, D. Williams, A. Bainbridge, K. Crane, and T. H. van Andel. 1979. Submarine Thermal Springs on the Galapagos Rift. Science, Vol. 203, No. 4385, pp. 1073-1083.

Craig, H., J. A. Welhan and D. R. Hilton. 1987. Hydrothermal Vents in Loihi Caldera: Alvin Results. EOS, Trans., Amer. Geophys. U., Vol. 68, No. 44, p. 1553 (Abstract).

Crawford, R. L. and R. S. Hanson (eds.). 1984. Microbial Growth on Cl Compounds. Proceedings of the 4th International Symposium. Washington, D.C., American Society for Microbiology, 343 pp.

Cullimore, D. R. and A. E. McCann. 1977. The identification, cultivation and control of iron bacteria in ground water. In: F. A. Skinner and J. M. Whelan (eds.), Aquatic Microbiology. Soc. for Applied Bacteriology Symposium, Vol. 6, pp. 219-261. London, Academic Press.

Cynar, F. J., K. W. Estep and J. McN. Sieburth. 1985. The Detection and Characterization of Bacteria-Sized Protists in Protist-Free Filtrates and Their Potential Impact on Experimental Marine Ecology. Microbial Ecol., Vol. 11, No. 4, pp. 281-288.

De Carlo, E. H., G. M. McMurtry and H.-W. Yeh. 1983. Geochemistry of Hydrothermal Deposits from Loihi Submarine Volcano, Hawaii. Earth Planet. Sci. Lett., Vol. 66, pp. 438-449.

Edmond, J. M., A. C. Campbell, M. R. Palmer, K. K. Falkner, and T. S. Bowers. 1987. Chemistry of Low Temperature Vent Fluids from Loihi and Larson's Seamounts. EOS, Trans., Amer. Geophys. U., Vol. 68, No. 44, pp. 1553-1554 (Abstract).

Edmond, J. M. and K. L. Von Damm. 1985. Chemistry of ridge crest hot springs. In: M. L. Jones (ed.), The Hydrothermal Vents of the Eastern Pacific: An Overview. Bull. Biolog. Soc. Washington, No. 6, pp. 43-47.

Ehrlich, H. L. 1981. Geomicrobiology. New York, N.Y., Marcel Dekker. 393 pp.

Enright, J. T., W. A. Newman, R. R. Hessler, and J. A. McGowan. 1981. Deep-Ocean Hydrothermal Vent Communities. Nature, Vol. 289, No. 5795, pp. 219-220.

Froelich, P. N., M. L. Bender, and G. R. Heath. 1977. Phosphorus Accumulation Rates in Metalliferous Sediments on the East Pacific Rise. Earth and Planet. Sci. Lett., Vol. 34, No. 3, pp. 351-359.

Galapagos Biology Expedition Participants. 1979. Galapagos '79: Initial Findings of a Deep-Sea Biological Quest. Oceanus, Vol. 22, No. 2, pp. 2-10.

Gamo, T., J. Ishibashi, H. Sakai, and B. Tilbrook. 1987. Methane Anomalies in Seawater Above the Loihi Submarine Summit Area, Hawaii. Geochim. Cosmochim. Acta., Vol. 51, No. 10, pp. 2857-2864.

Ghiorse, W.C. 1984. Biology of Iron- and Manganese-Depositing Bacteria. Annual Rev. Microbiol., Vol. 38, pp. 515-550.

Grassle, J. F. 1985. Hydrothermal Vent Animals: Distribution and Biology. Science, Vol. 229, No. 4715, pp. 713-717.

Grassle, J. F. 1986. The Ecology of Deep-Sea Hydrothermal Vent Communities. Advan. Mar. Biol., Vol. 23, pp. 301-362.

Grigg, R. W. 1988. Loihi Seamount: No macrofauna associated with hydrothermal vents. EOS, Trans. Amer. Geophys. U., (in press) (Abstract).

Hessler, R. R. and W. M. Smithey, Jr. 1983. The distribution and community structure of megafauna at the Galapagos Rift hydrothermal vents. In: P. A. Rona, K. Bostrom, L. Laubier, and K. L. Smith, Jr. (eds.), Hydrothermal Processes at Seafloor Spreading Centers, NATO Conference Series IV, pp. 735-770. New York, N.Y., Plenum Press.

Hobbie, J. E. and C. C. Crawford. 1969. Respiration Corrections for Bacterial Uptake of Dissolved Organic Compounds in Natural Waters. Limnol. Oceanog., Vol. 14, No. 4, pp. 528-532.

Hobbie, J. E., R. J. Daley, and S. Jasper. 1977. Use of Nuclepore Filters for Counting Bacteria by Fluorescence Microscopy. Appl. Environ. Microbiol., Vol. 33, No. 5, pp. 1225-1232.

Horibe Y., K. Kim, and H. Craig. 1983. Off-Ridge Submarine Hydrothermal Vents: Back-Arc Spreading Centers and Hotspot Seamounts. EOS, Trans., Amer. Geophys. U., Vol. 64, No. 45, pp. 724 (Abstract).

Jackson, E. D., E. A. Silver, and G. B. Dalrymple. 1972. Hawaiian-Emperor Chain and Its Relation to Cenozoic Circumpacific Tectonics. Geol. Soc. Amer. Bull., Vol. 83, No. 3, pp. 601-618.

Jannasch, H. W. and C. O. Wirsen. 1979. Chemosynthetic Primary Production at East Pacific Sea Floor Spreading Centers. BioScience, Vol. 29, No. 10, pp. 592-598.

Jannasch, H. W. and C. O. Wirsen. 1981. Morphological Survey of Microbial Mats Near Deep-Sea Thermal Vents. Appl. Environ. Microbiol., Vol. 41, No. 2, pp. 528-538.

Juniper, S. K., J. A. J. Thompson and S. E. Calvert. 1986. Accumulation of Minerals and Trace Elements in Biogenic Mucus at Hydrothermal Vents. Deep-Sea Res., Vol. 33, No. 3, pp. 339-347.

Karl, D. M. 1981. Simultaneous Rates of Ribonucleic Acid and Deoxyribonucleic Acid Syntheses for Estimating Growth and Cell Division of Aquatic Microbial Communities. Appl. Environ. Microbiol., Vol. 42, No. 5, pp. 802-810.

Karl, D. M. 1982. Selected Nucleic Acid Precursors in Studies of Aquatic Microbial Ecology. Appl. Environ. Microbiol., Vol. 44, No. 4, pp. 891-902.

Karl, D. M. and C. D. Winn. 1984. Adenine metabolism and nucleic acid synthesis: Applications to microbiological oceanography. In: J. E. Hobbie and P. J. leB. Williams (eds.), Heterotrophic Activity in the Sea, pp. 197-215. New York, N.Y., Plenum Press.

Karl, D. M. 1985. Effects of temperature on the growth and viability of hydrothermal vent microbial communities. In: M. L. Jones (ed.), The Hydrothermal Vents of the Eastern Pacific: An Overview. Bull. Biol. Soc. Washington, No. 6, pp. 345-353.

Karl, D. M. 1987. Bacterial production at deep-sea hydrothermal vents and cold seeps: Evidence for chemosynthetic primary production. In: Ecology of Microbial Communities, Soc. Gen. Microbiol. Vol. 41, pp. 319-360. England, Cambridge University Press.

Karl, D. M. and D. B. Craven. 1980. Effects of Alkaline Phosphatase Activity on Nucleotide Measurements in Aquatic Microbial Communities. Appl. Environ. Microbiol., Vol. 40, No. 3, pp. 549-561.

Karl, D. M. and O. Holm-Hansen. 1978. Methodology and Measurement of Adenylate Energy Charge Ratios in Environmental Samples. Mar. Biol., Vol. 48, No. 2, pp. 185-197.

Karl, D. M., G. T. Taylor, J. A. Novitsky, H. W. Jannasch, C. O. Wirsen, N. R. Pace, D. J. Lane, G. J. Olsen, and S. J. Giovannoni. 1988. A Microbiological Study of Guaymas Basin High Temperature Hydrothermal Vents. Deep-Sea Res., Vol. 35, No. 5, pp. 777-791.

Karl, D. M., C. O. Wirsen and H. W. Jannasch. 1980. Deep-Sea Primary Production at the Galapagos Hydrothermal Vents. Science, Vol. 207, No. 4437, pp. 1345-1347.

Laubier, L. and D. Desbruyeres. 1984. Les Oasis du Fond les Oceans. La Recherche, Vol. 15, pp. 1506-1517.

Lilley, M. D., J. A. Baross, and L. I. Gordon. 1983. Reduced gases and bacteria in hydrothermal fluids: The Galapagos spreading center and 21°N East Pacific Rise. In: P. A. Rona, K. Bostrom, L. Laubier, and K. L. Smith, Jr. (eds.), Hydrothermal Processes at Seafloor Spreading Centers, NATO Conference Series IV, pp. 411-449. New York, N.Y., Plenum Press.

Lilley, M. D., M. A. de Angelis, and L. I. Gordon. 1982. CH<sub>4</sub>, H<sub>2</sub>, CO and N<sub>2</sub>O in Submarine Hydrothermal Vent Waters. Nature, Vol. 300, No. 5887, pp. 48-50.

Lonsdale, P. 1977. Clustering of Suspension-Feeding Macrobenthos Near Abyssal Hydrothermal Vents at Oceanic Spreading Centers. Deep-Sea Res., Vol. 24, No. 9, pp. 857-863.

Malahoff, A., G. M. McMurtry, J. C. Wiltshire and H. W. Yeh. 1982. Geology and Chemistry of Hydrothermal Deposits from Active Submarine Volcano Loihi, Hawaii. Nature, Vol. 298, No. 5871, pp. 234-239.

McMurtry, G. M., D. M. Karl, B. Tilbrook and P. Sedwick. 1987. Chemistry and Microbiology of Loihi Seamount Hydrothermal Vent Fields. EOS, Trans. Amer. Geophys. U., Vol. 68, No. 44, p. 1553 (Abstract).

Rau, G. H. 1981. Hydrothermal Vent Clam and Tube Worm 13C/12C: Further Evidence of Nonphotosynthetic Food Sources. Science, Vol. 213, No. 4505, pp. 338-340.

Rau, G. H. 1985.  $^{13}\text{C}/^{12}\text{C}$  and  $^{15}\text{N}/^{14}\text{N}$  in hydrothermal vent organisms: Ecological and biogeochemical implications. In: M. L. Jones (ed.), The Hydrothermal Vents of the Eastern Pacific: An Overview. Bull. Biol. Soc. Washington, No. 6, pp. 243-247.

Rison, W. and H. Craig. 1983. Helium Isotopes and Mantle Volatiles in Loihi Seamount and Hawaiian Island Basalts and Xenoliths. Earth Planet. Sci. Lett., Vol. 66, pp. 407-426.

Sakai, H., H. Tsubota, T. Nakai, J. Ishibashi, T. Akagi, T. Gamo, B. Tilbrook, G. Igarashi, M. Kodera, K. Shitashima, S. Nakamura, K. Fujioka, M. Watanabe, G. McMurtry, A. Malahoff, and M. Ozima. 1987. Hydrothermal Activity on the Summit of Loihi Seamount, Hawaii. Geochem. J., Vol. 21, No. 1, pp. 11-21.

Sedwick, P. N. and G. M. McMurtry. 1987. Transition Metals in Loihi Seamount Hydrothermal Solutions. EOS, Trans. Amer. Geophys. U., Vol. 68, No. 44, p. 1554 (Abstract).

Stanier, R. Y., E. A. Adelburg, and J. Ingram. 1976. The Microbial World. Englewood Cliffs, N. J., Prentice Hall. 871 pp.

Swinnerton, J. W. and V. J. Linnenbom. 1967. Determination of C1 to C4 Hydrocarbons in Seawater by Gas Chromatography. J. Gas Chromatogr., Vol. 5, pp. 570-573.

Swinnerton, J. W., V. J. Linnenbom and C. H. Cheek. 1962. Determination of Dissolved Gases in Aqueous Solutions by Gas Chromatography. Anal. Chem., Vol. 34, pp. 483-485.

Taylor, B. F., D. S. Hoare and S. Hoare. 1971. Thiobacillus denitrificans as an Obligate Chemolithotroph: Isolation and Growth Studies. Archiv. fur Mikrobiol., Vol. 78, No. 3, Berlin, Springer-Verlag, pp. 193-204.

Tunnicliffe, V., M. Botros, M. E. de Burgh, A. Dinet, H. P. Johnson, S. K. Juniper, and R. E. McDuff. 1986. Hydrothermal Vents of Explorer Ridge, Northeast Pacific. Deep-Sea Res., Vol. 33, No. 3, pp. 401-412.

Tunnicliffe, V., S. K. Juniper and M. D. de Burgh. 1985. The hydrothermal vent community on Axial Seamount, Juan de Fuca Ridge. In: M. L. Jones (ed.), The Hydrothermal Vents of the Eastern Pacific: An Overview. Bull. Biol. Soc. Washington, No. 6, pp. 453-464.

Tuovinen, O. H. and D. P. Kelly. 1973. Studies on the Growth of Thiobacillus ferrooxidans. Archiv. fur Mikrobiol., Vol. 88, No. 4, Berlin, Springer-Verlag, pp. 285-298.

Von Damm, K. L., J. M. Edmond, B. Grant, C. I. Measures, B. Walden and R. F. Weiss. 1985. Chemistry of Submarine Hydrothermal Solutions at 21°N, East Pacific Rise. Geochim. Cosmochim. Acta., Vol. 49, No. 11, pp. 2197-2220.

Von Damm, K. L., J. M. Edmond, C. I. Measures and B. Grant. 1985. Chemistry of Submarine Hydrothermal Solutions at Guaymas Basin, Gulf of California. Geochim. Cosmochim. Acta., Vol. 49, No. 11, pp. 2221-2237.

Watson, S. W. 1965. Characteristics of the Nitrifying Bacterium *Nitrosocystis oceanus* Sp. N. Limnol. Oceanogr., Vol. 10, p. R274.

Watson, S. W. and J. B. Waterbury. 1971. Characteristics of Two Marine Nitrite Oxidizing Bacteria, *Nitrospina gracilis* Nov. Gen. Sp. and *Nitrococcus mobilis* Nov. Gen. Sp. Archiv. fur Mikrobiol., Vol. 77, No. 3, Berlin, Springer-Verlag, pp. 203-230.

Weiss, R. F. and H. Craig. 1973. Precise Shipboard Determination of Dissolved Nitrogen, Oxygen, Argon, and Total Inorganic Carbon by Gas Chromatography. Deep-Sea Res., Vol. 20, No. 4, pp. 291-303.

Welhan, J. A. and H. Craig. 1979. Methane and Hydrogen in East Pacific Rise Hydrothermal Fluids. Geophys. Res. Lett., Vol. 6, No. 11, pp. 829-831.

Welhan, J. A. and H. Craig. 1983. Methane, hydrogen and helium in hydrothermal fluids at 21°N on the East Pacific Rise. In: P. A. Rona, K. Bostrom, L. Laubier, and K. L. Smith, Jr. (eds.), Hydrothermal Processes at Seafloor Spreading Centers, NATO Conference Series IV, pp. 391-409. New York, N.Y., Plenum Press.

Williams, P. M., K. L. Smith, E. M. Druffel, and T. W. Linick. 1981. Dietary Carbon Sources of Mussels and Tubeworms from Galapagos Hydrothermal Vents Determined from Tissue <sup>14</sup>C Activity. Nature, Vol. 292, No. 5822, pp. 448-449.

Winn, C. D. and D. M. Karl. 1984. Microbial Productivity and Community Growth Rate Estimates in the Tropical North Pacific Ocean. Biol. Oceanogr., Vol. 3, No. 2, pp. 123-145.

Wong, C. S. 1970. Quantitative Analysis of Total Carbon Dioxide in Sea Water: A New Extraction Method. Deep-Sea Res., Vol. 17, pp. 9-17.

SULFIDE, SEDIMENT, AND BIOLOGICAL ZONATION  
AT ASHES VENT FIELD, AXIAL VOLCANO

Alexander Malahoff, Anne M. Arquit, and Gary M. McMurtry  
Hawaii Institute of Geophysics  
University of Hawaii, Honolulu, HI 96822

ABSTRACT

A young, high-temperature hydrothermal vent field consisting of two polymetallic sulfide chimneys 5 m high was sampled along a fault complex associated with the southwestern wall of the summit caldera of Axial Volcano during four Alvin dives in 1984. Temperatures up to 270°C were measured within the orifice of one of the chimneys, which was then broken off and recovered for analysis. Both black and white "smoke" were emanating from the chimney that was sampled. The chimney has formed directly on top of lobate lava flows that occur about 200 m east of the caldera wall at 1,550 m water depth, making this vent one of the shallowest active high-temperature vents studied to date. The vent is surrounded by clumps of vestimentiferan worms and is surrounded on all sides by an elongate field of yellowish iron smectite sediment and chimney structures. This low-temperature field of hydrothermal precipitates is 150 m wide and extends about 1,300 m along the base of the caldera wall.

Chemical analyses of the hydrothermal deposits from the metal sulfides of the chimney to the outer zones of the low-temperature field show a range of elemental assemblages that can be explained by thermo-chemical gradients in the near-vent region. Chemical zonation within the high-temperature chimney is indicated by mineralogical banding and is confirmed by chemical gradients such as the observed increase of gold from 750 parts per billion (ppb) in the center to 2,800 ppb at the outer edge of the chimney. The sulfides sampled on the floor of the caldera are relatively small volume but have a high gold content compared to other deposits precipitated along mid-ocean rift valleys. These findings support the hypothesis that there are larger volume, lava-hosted sulfide deposits at depth that are subject to dissolution by upward-moving hydrothermal fluid along the fissures associated with the normal fault forming the caldera wall. This suggested concentration mechanism could repeat over several cycles, following each successive burial of sulfides by fresh lava flows.

INTRODUCTION TO ZONATION STUDIES

Axial Volcano straddles the Juan de Fuca Ridge at 45°56'N (Fig. 1). Active hydrothermal venting was first discovered in the summit caldera of the volcano during the Canadian-American

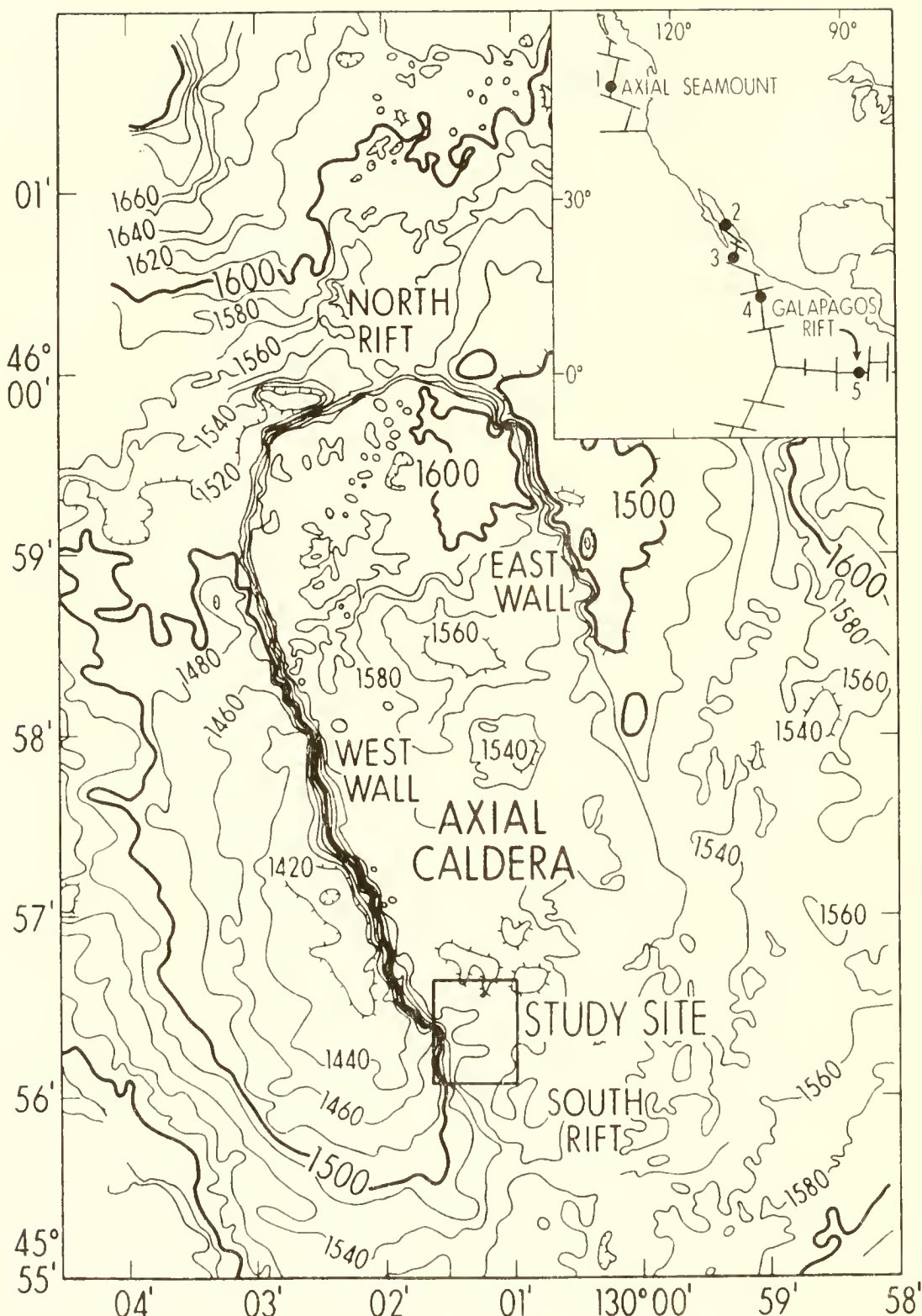


Figure 1. Location of Axial Volcano at  $45^{\circ}58'N$  on the Juan de Fuca Ridge. SeaBeam bathymetry in 20 m contours is shown.

Seamount Expedition (CASM) in 1983. The CASM vent is found at the northern end of the caldera, where fissures associated with the northern Juan de Fuca Rift Valley intersect the caldera wall (Chase et al., 1985). Rather than with fissures generated by rifting processes, Ashes Vent Field is linked to normal faulting that created the caldera, probably following lava drainback from a shallow magma chamber (Fig. 2).

Samples and photographs necessary for geologic mapping and a detailed study of the biogeography of the area were obtained during four exploratory Alvin dives (1411 through 1414) to Ashes Vent Field in 1984. Towed camera photographs were also used. The dive site in the vent field was selected on the basis of available SeaMarc I and SeaBeam data for the area. Following the first dive, a transponder was deployed allowing short baseline ranging from the R/V Atlantis II during subsequent dives. A suite of sediment samples surrounding the active hot vents was collected in 1986 using the Canadian submersible Pisces IV. The database consists of approximately 14,000 bottom photographs, as well as mineralogical (XRD and SEM) and elemental (instrumental neutron activation, ICP-AES and AAS) analyses on the chimney and seven sediment samples.

The focus of research has been on both active smoker chimneys and the transition zone between vent and nonvent environments within the caldera. Two sulfide chimneys about 5 m high were observed precipitating on top of a field of broken lobate lava flows in 1984. In the immediate vicinity of the chimneys, clumps of vestimentiferan worms and patches of clams were noted. The clams were concentrated in depressions between lobate flows and along cracks in sheet flows. Surrounding the locus of observed high temperature venting is a low-temperature field of hydrothermal precipitates that forms a zone about 150 m wide, extending 1,300 m along the strike of the caldera boundary fault. Chemical analyses of hydrothermal deposits, including both chimney and hydrothermal sediments of the transition zone, show a range of elemental assemblages that can be explained by variable thermo-chemical environments. Photographic data indicate that physical environmental gradients also affect the biogeography of epibenthic organisms.

#### STRUCTURE AND GEOLOGY OF THE AXIAL CALDERA HYDROTHERMAL VENTS

Structural analyses of the SeaMarc I image are shown in Figure 3. Analysis of this image previously described by Crane et al. (1985) are shown in the form of identifiable fissures, faults, and structural lineaments. SeaMarc I was towed at 200 m above the ocean floor in an earlier study; the image extends beyond the walls of the caldera as mapped by SeaBeam (Fig. 1), providing good sidescan imagery of the caldera walls, but poor coverage of the floor of the caldera directly beneath the tow track of SeaMarc I. The SeaMarc I imagery and its tectonic

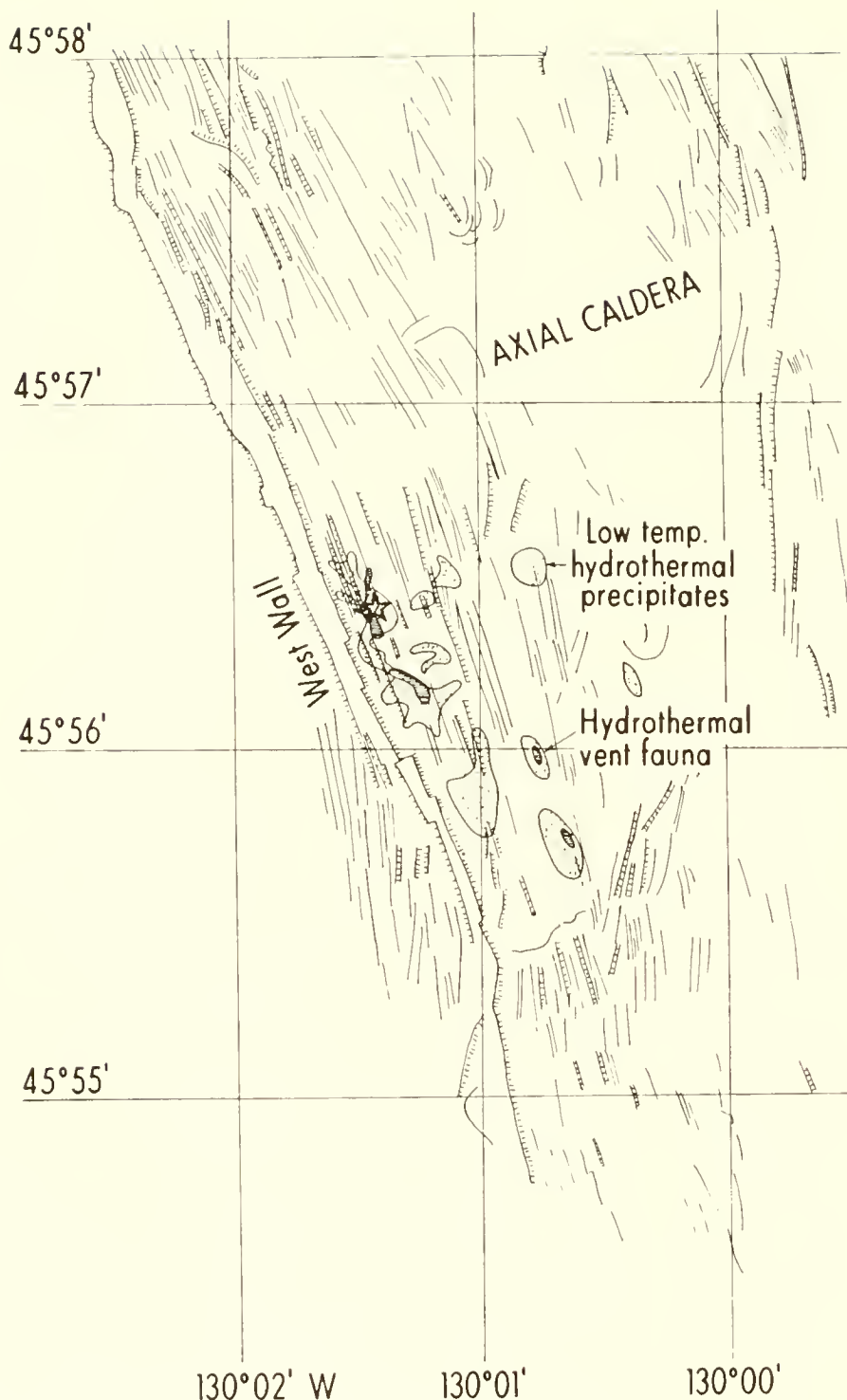


Figure 2. Tectonic features in the vicinity of Ashes Vent Field; also shown are the distribution of vent organisms and low temperature hydrothermal precipitates around the high temperature black smoker chimneys (star).

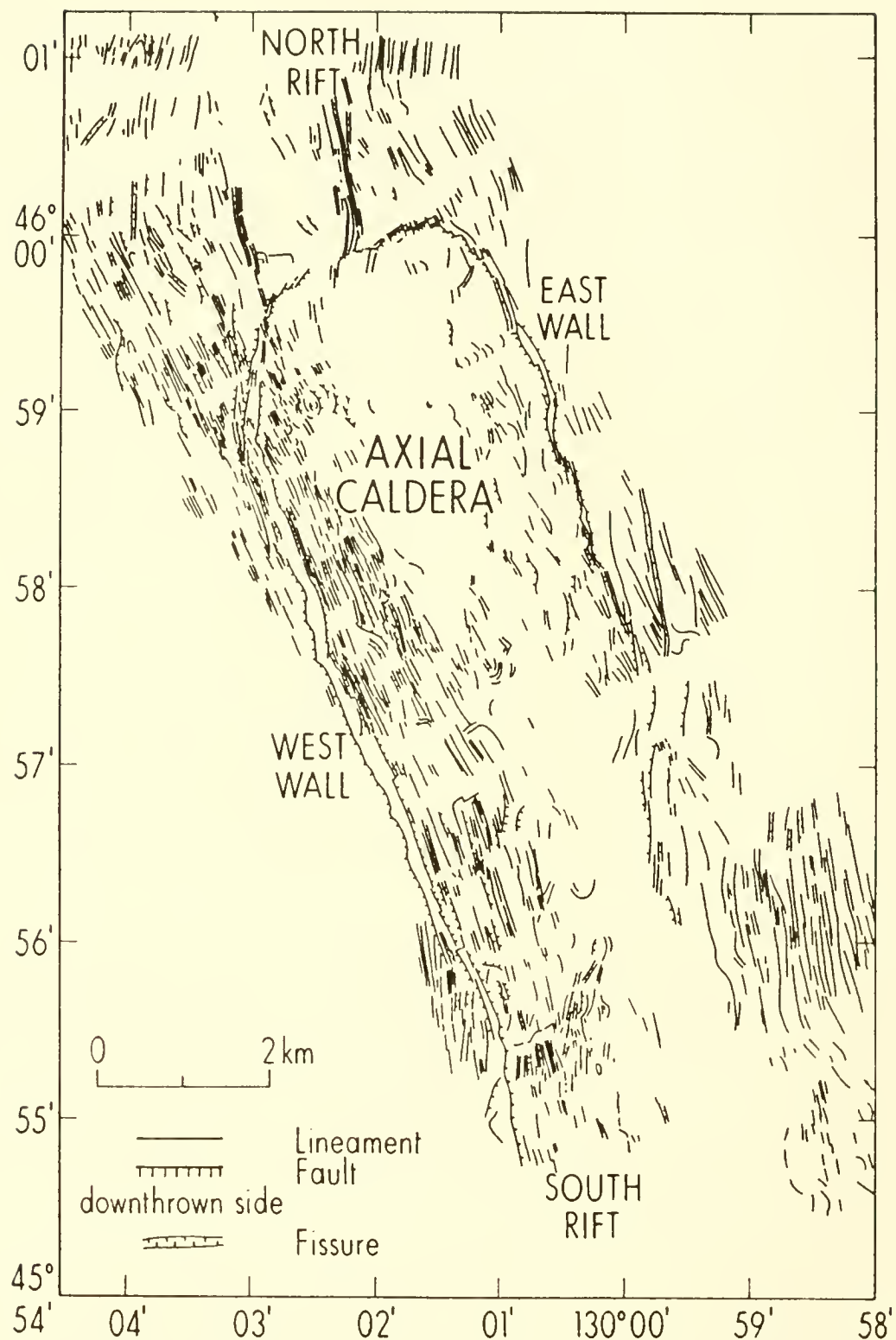


Figure 3. Structure of Axial Volcano based on SeaMarc I imagery.

interpretation show the caldera to have well-defined east, west, and north walls that from SeaBeam bathymetry appear to be about 100 m high in the northeastern corner of the caldera and about 30 m high along the eastern wall. The northern end of the caldera is marked by two fissures. The CASM vent site is associated with the eastern one, which is the major fissure of the northern rift of the volcano. The southern end of the caldera has a poorly defined margin, presumably because the caldera floor was tilted down toward the southeast during the phase of magma withdrawal that developed the current morphology of the caldera.

Although it straddles the Juan de Fuca Ridge, Axial Volcano is a volcano with a hot-spot source (Hammond and Delaney, 1985). The morphology and structural setting for the hydrothermal activity observed in the summit caldera of Axial Volcano have striking similarities to the geothermal systems active in Hawaiian calderas that were formed by the Hawaiian Hotspot, such as Mauna Loa and Kilauea. Geothermal activity in the Hawaiian calderas is associated with normal faults and talus cones along the margin of the caldera floor, much the same as what has been observed and mapped for Axial Volcano.

Photographs taken by a tethered camera system using the R/V Discoverer in 1983 show the floor of the caldera to be covered largely with sheet and lobate flows. Fresh pillow mounds in lobate flow terrain were observed in photographs collected during the detailed photo survey of Ashes Vent Field conducted in 1984. The base of the caldera wall is covered with talus and marked by a shallow depression 1 to 2 m deep. The high-temperature vents are located within a small hydrothermal field on top of lobate lava flows intermixed with broken sheet flows and pillows.

#### SULFIDE ZONATION

A 20-cm-long section of the top of one of the high temperature chimneys, venting both black and white "smoke" at a maximum measured temperature of 270°C, was sampled with Alvin for analysis. This sample was cut into seven horizontal sections through the chimney (Fig. 4). Results of  $^{238}\text{U}$ -series gamma-ray spectrometry on Slab #1 yield an estimated rate for the horizontal (i.e., away from the vent orifice) growth of the chimney of 3.9 mm per year (Kim and McMurtry, in review). Using this growth rate, the 55 mm radius of the chimney corresponds to approximately 14 years of growth.

Slab #1 of the chimney was selected for mineralogical and chemical analyses. Optical and electron microscopy of the section revealed seven concentric mineralogical bands that were then subsampled for chemical analysis (Fig. 4). A thorough interpretation of these results is in preparation. Semi-quantitative x-ray diffraction shows that pyrite and sphalerite

ALVIN 1411-3A  
270°C White Smoker Chimney

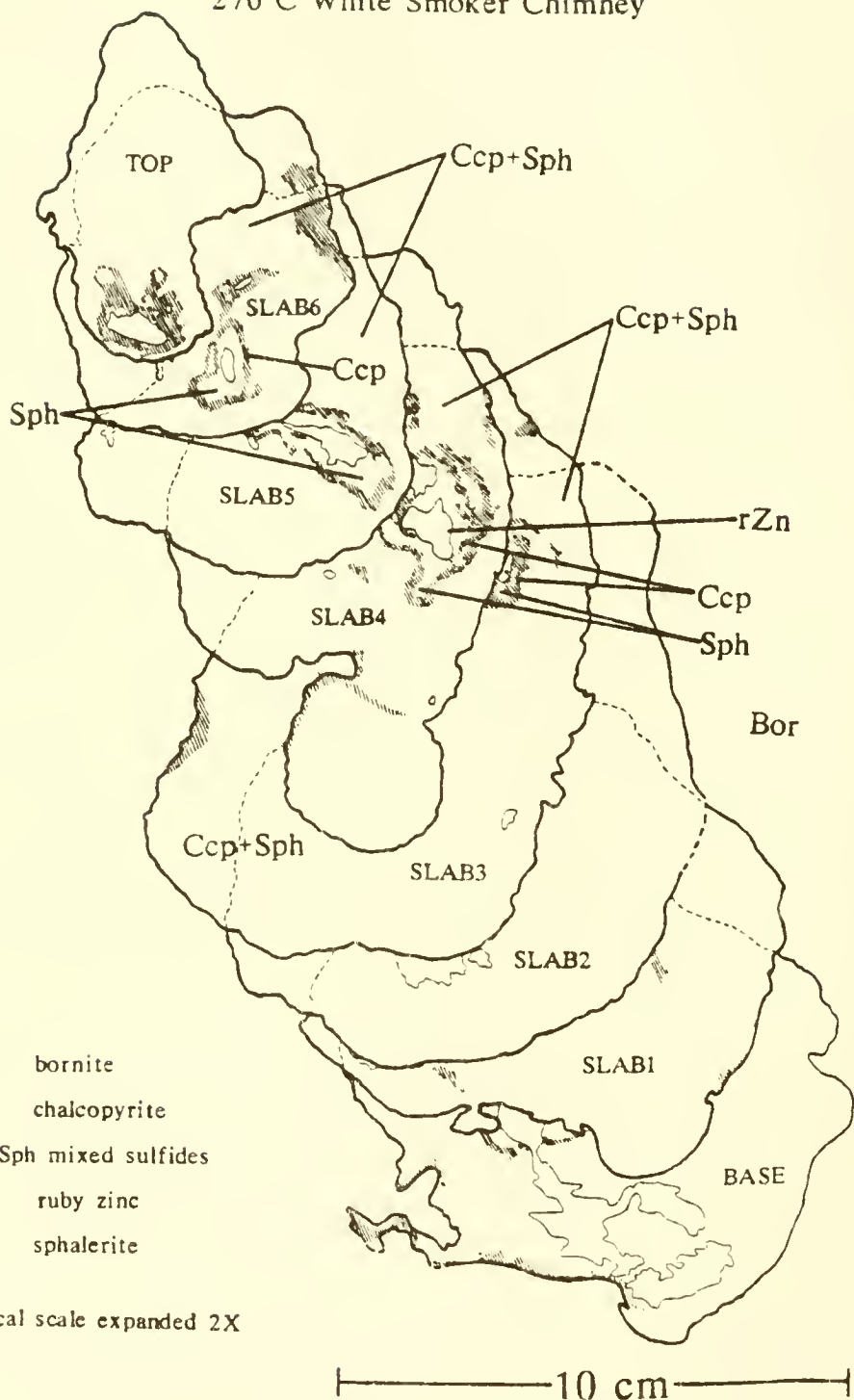


Figure 4. Schematic diagram showing a) how the smoker chimney was subsampled, and b) mineralogical banding.

are the major mineral phases present, with pyrite dominant near the inner core of the chimney (presumably in the highest temperature regime) and sphalerite becoming the major phase in the outer half of the chimney. Chalcopyrite is also present in the inner sections of the core (Fig. 4). Consequently, concentrations of Fe and Cu decrease steadily from core to outer surface, and Zn increases. The gold content also increases steadily toward the edge of the chimney, from 750 ppb to 2,800 ppb in the outer zone. Although high with respect to the few parts per billion gold concentrations typical of other ridge crest sulfides, the gold content of the Ashes chimney falls within the range reported for samples from the CASM vent field, at the northern end of the Axial Volcano caldera ( $\leq$ 6,700 ppb), and a mature vent field on the Explorer Ridge, farther to the north ( $\leq$ 1,500 ppb).

#### SEDIMENT ZONATION

A split from one sediment push core (Core 1141) and six slurp gun samples were collected from the Ashes Vent Field with Pisces IV in 1986. Despite the limited selection of samples available, four sediment types are distinguishable, based on results of x-ray diffraction; 1) anhydrite, 2) zinc, iron, and copper sulfides, 3) iron smectite (nontronite), and 4) x-ray amorphous silica (+ iron oxide). The dominant sulfide phase present is sphalerite, with pyrite, chalcopyrite, marcasite, and wurtzite also present in lesser quantities. This combination of mineral phases corresponds with the components found in the chimney sample, suggesting that sediment in the immediate vicinity of the high temperature vents is derived from the hydrothermal plume. Mass wasting and redeposition can apparently be ruled out, because no basal mound of sulfide debris has developed around the two small chimneys, which are built directly on top of lobate flows.

This suite of near-vent sediments ( $\leq$ 300 m from the smoker chimneys) is apparently distributed zonally, with near-source anhydrite and/or sulfide-rich sediment grading to various combinations of iron silicate, iron oxide, and amorphous silica in the low temperature hydrothermal sediment zone. The sediment suite collected at Ashes does not include the manganese oxide component commonly associated with mid-ocean ridge hydrothermal vent systems. It is likely that the relatively insoluble Mn is transported farther than 300 m away from the vent exit site before deposition and was, therefore, not sampled. Detailed results of chemical analyses of the sediment samples are in preparation. This distribution of sediment samples gives an indication of the variable, yet extreme, chemical regimes encountered within a typical composite (i.e., both high and low temperature) vent field. Anhydrite and sulfide components are indicative of the  $>350^{\circ}\text{C}$  fluid regime encountered immediately beneath the seafloor and within vent orifices; whereas in situ

nontronite chimneys mark regions of  $<60^{\circ}\text{C}$  venting in distal zones of lower velocity flow. Such variability is observed within 200 m of the locus of high temperature venting in Ashes Vent Field.

#### BIOLOGICAL ZONATION

In addition to geochemical zonation recorded in hydrothermal vent chimney samples and sediment, biological zonation is also observed along gradients of temperature and water chemistry radiating from hydrothermal sources. Vent habitats encountered within Ashes Vent Field range from diffuse, low temperature seeps to black smokers venting fluid in excess of  $270^{\circ}\text{C}$ .

Both biological and geological information obtained from photographs of the Ashes Vent Field (R/V Discoverer, 1983; Alvin, 1984; Angus, 1984) have been included in a computer data base and mapped with respect to reconstructed bottom track lines on a SeaBeam base map of the site. These data suggest that for both vent and nonvent organisms, species distribution and megafaunal abundance are zoned similarly to sediment type (i.e., with distance from a vent source). Dense thickets of tube worms and bacterial mat communities extend to 100 m from the highest temperature venting recorded; clams, to 200 m; and yellow-orange hydrothermal nontronite and iron oxide sediment, to at least 500 m from the hot vents (Arquit et al., 1985).

No bacterial mats or high abundances of megafaunal communities are associated with the zone of hydrothermal sediment surrounding the high temperature vents. About 4.7 percent of Alvin photographs taken in the Ashes Vent Field in 1984 (i.e., 137 of 2,920) contain more than 300 hexactinellid sponges per frame; of these photos having elevated sponge densities, however, only 17.5 percent include any low temperature hydrothermal nontronite sediment. Preliminary results show that maximum sponge densities occur beyond this seemingly barren sediment zone, at least 250 m from the vent source, and then drop to average caldera-wide values as more typical benthic living conditions are encountered 700 to 1,000 m from the locus of high temperature venting. The local density of other megafauna identified in photographs can also be described in terms of distance from venting centers.

Nonparametric statistical analysis of information gathered from photographic data indicate that other factors (e.g., community dynamics, local geology, substrate, sediment type and thickness, morphology, and surface texture of lava flows) must be important controls on organism distributions as well. Additional data from Alvin dives and camera tows taken within Ashes in 1985 and 1986 (courtesy Marine Resources Research Division, NOAA/PMEL, Newport, OR) are currently being added to this data base to fine-tune initial observations. The excellent navigation and

altimetry of the new data will allow accurate estimates of organism densities to be computed from abundance counts.

#### A MODEL FOR THE ASHES HYDROTHERMAL VENT SYSTEM

This preliminary survey shows that the total volume and number of sulfide chimneys within Ashes Vent Field is small compared to other vent fields along the mid-ocean ridge, such as the Explorer Ridge (Tivey and Delaney, 1986), southern Juan de Fuca (Normark et al., 1987), Galapagos (Malahoff, 1985), and segments of the East Pacific Rise (Spiess et al., 1980). The CASM Vent Field at the northern end of Axial Volcano's summit caldera is also small, in comparison. It is possible that frequent volcanic activity within the summit caldera of the volcano prohibits the formation of extensive surficial sulfide deposits by regularly covering successive sulfide structures with fresh lava flows. Large deposits, however, may still be precipitating beneath the surface. Previous research has indicated that larger deposits are probably formed as a result of multiple hydrothermal cycles (Lowell and Rona, 1985). Given such a model system, surficial hydrothermal vent fields would be underlain by an inter-layered series of prior hydrothermal deposits and lava flows, all formed along the same major fault system. The unusually high gold content of the sulfide chimney suggests secondary enrichment, a process that would be facilitated by hydrothermal fluid leaching old sulfide deposits during convective circulation.

Results of the current study suggest that regional topography channels mixing vent water along the strike of the faults that form the walls of the volcano's summit caldera, affecting the pattern of sedimentation in the vent field. Organism distributions are explained, in part, by local geology and by vent processes. Regional tectonics control the emplacement of polymetallic sulfide deposits and the nature and distribution of diffuse warm water seepage. Observed zonation attributable to hydrothermal vent processes occurs on a wide range of scales, from individual mineral grains in sulfide samples to the biogeography of vent and nonvent organisms at a single vent field; chemical and mineralogical zonation is even evident on a small regional scale, as hydrothermal imprints preserved in the local sedimentary record.

This paper is Hawaii Institute of Geophysics Contribution No. 2051.

#### REFERENCES

Arquit, A. M., A. Malahoff, and G. M. McMurtry, 1985. Chemical and biological halos of a hydrothermal vent system, Axial Caldera, Juan de Fuca Ridge. EOS, Vol. 66, No. 18, p. 401 (Abstract).

Chase, R. L., J. R. Delaney, J. L. Karsten, H. P. Johnson, S. K. Juniper, J. E. Lupton, S. D. Scott, V. Tunnicliffe, S. R. Hammond, and R. E. McDuff, 1985. Hydrothermal vents on an axis seamount of the Juan de Fuca Ridge. Nature, Vol. 313, No. 5999, pp. 212-214.

Crane, K., F. Aikman, R. Embley, S. Hammond, A. Malahoff, and J. Lupton, 1985. The distribution of geothermal fields on the Juan de Fuca Ridge. J. Geophys. Res., Vol. 90, pp. 727-744.

Hammond, S. R., and J. R. Delaney, 1985. Evolution of Axial Volcano, Juan de Fuca Ridge. EOS, Vol. 66, No. 46, pp. 925-926.

Kim, K. H., and G. M. McMurtry, 1988. Radial growth rates and  $^{210}\text{Pb}$  ages of hydrothermal massive sulfides from the Juan de Fuca Ridge. In review.

Lowell, R. P., and P. A. Rona, 1985. Hydrothermal models for the generation of massive sulfide ore deposits. EOS, Vol. 66, No. 18, p. 402 (Abstract).

Malahoff, A., 1985. Hydrothermal vents and polymetallic sulfides of the Galapagos and Gorda-Juan de Fuca Ridge systems. In: M. L. Jones (ed.), Hydrothermal Vents of the Eastern Pacific: An Overview. Biol. Soc. Wash. Bull. No. 6, pp. 19-41.

Normark, W. R., J. L. Morton, and S. L. Ross, 1987. Submersible observations along the southern Juan de Fuca Ridge: 1984 Alvin program. J. Geophys. Res., Vol. 92, No. B11, pp. 283-11, 290.

Spiess, F. N., K. C. Macdonald, T. Atwater, R. Ballard, A. Carranza, D. Cordoba, C. Cox, V. M. Diaz-Garcia, J. Francheteau, J. Guerrero, J. Hawkins, R. Haymon, R. Hessler, T. Juteau, M. Kastner, R. Larson, B. Luyendyk, J. D. Macdougall, S. Miller, W. Normark, J. Orcutt, and C. Rangin, 1980. East Pacific Rise: hot springs and geophysical experiments. Science, Vol. 207, p. 1421.

Tivey, M. K., and J. R. Delaney, 1986. Growth of large sulfide structures on the Endeavour Segment of the Juan de Fuca Ridge. Earth Planet. Sci. Lett., Vol. 77, pp. 303-317.



## SESSION SUMMARY: DEEP WATER ECOLOGY

Larry Madin  
Woods Hole Oceanographic Institution  
Woods Hole, MA 02543

The five papers presented in this chapter include two research projects of an experimental nature in the benthic environment, and three reports on work of a more observational nature in midwater.

Mullineaux's study of larval settlement patterns within known flow regimes is a pioneering extension of laboratory and shallow water research into the deep sea. In the last decade, studies of settlement behavior have moved out of benchtop beakers into experimental flumes, shallow water environments and now the open ocean. Along the way, a new understanding of the flow regime above the bottom and around hard substrates has radically altered our concept of the forces that determine larval settling patterns, and consequently the spatial distribution and composition of benthic communities. The crucial combination in these studies is simultaneous observation of the flow regime around the substrate, and the actual pattern of larval settling. Mullineaux has used a sophisticated current meter to record the larger scale properties of the bottom currents, and alabaster dissolution plates to register the fine scale flow which actually impinges on the settlement substrates.

A study of this nature requires precise placement of the settling plates and other instruments on an appropriate bottom, and recovery of the equipment without damaging the plates or dislodging the settled larvae. Clearly, a manned submersible is the only way this could have been accomplished at these depths. The success of this effort illustrates how well experimental techniques developed in shallow water for SCUBA divers can be transplanted to the deep sea, using modern submersibles and auxiliary equipment.

The second benthic study, by Grassle, Snelgrove, Weinberg and Whitlatch, also demonstrates use of the submersible to carry out experimental manipulations on the deep sea floor. As Mullineaux's work is concerned with colonization of hard substrates, Grassle is interested in colonization of the sediments, and factors affecting the abundance and diversity of the infauna.

Spatial and temporal variability of the food supply to the deep benthos is one of these factors. Against a background "rain" of fine particulate matter from the water column, there are episodic arrivals at the bottom of larger chunks of food,

ranging in size from shrimps to whales. In the Sargasso Sea around Bermuda, Sargasso weed is sometimes stripped of its floats in rough weather and sinks below the surface, eventually reaching the bottom. In the experiments reported here, local enrichments of the sediments were produced by burying clumps of Sargassum in shallow pits in a sand bottom near Bermuda, then sampling the sediments later to compare the numbers and diversity of organisms in the enriched sediments with those from control areas. After 37 days, abundances of some of the opportunistic species had increased sharply in the enriched sediment, creating a community composition like those seen in disturbed environments elsewhere.

Use of submersibles for observation in the water column dates back to Beebe in the 1930's, but only recently have scientists been able to use more quantitative techniques and bring back specimens. In the last 10 years, the number of known species of midwater plankters, especially gelatinous ones, has been dramatically increased, and in situ observations have changed our perceptions of the kinds of organisms that live in this largest of earthly habitats. Comparable advances in understanding behavioral interactions and trophic structure are now beginning to be seen as manned operations in midwater enter a second decade. Two major efforts in midwater biology, supported in part by NOAA/NURP, are described in this chapter.

Larson and co-authors report on a series of dives made in 1986 and 1987 in the submarine canyons off the New England coast. These are the first submersible explorations of these productive regions, and were carried out by a group of systematic and behavioral specialists led by Richard Harbison. Most of their emphasis is on gelatinous zooplankton and midwater fish, two conspicuous components of the midwater community. The paper summarizes patterns of distribution found for dominant species within these groups, concluding that most were truly mesopelagic in distribution. Ctenophores and siphonophores were common and diverse, although they are rarely seen in net collections because of their fragility. The Sea-Link's sophisticated collecting equipment permitted collection of numerous specimens of these delicate organisms, including some probable new species.

The papers by Madin and Hamner et al. stem from the Beebe Project, a multidisciplinary study of the water column and benthos (Grassle's work was part of this project) at stations near Bermuda. The first field season of this project was in July 1987. Due to weather and logistical problems, the number of dives accomplished was fewer than planned, and most of the participants consider the 1987 results as preliminary.

Madin's paper discusses the objectives of the pelagic component of the project, and describes a midwater mooring developed for studying behavior of mesopelagic plankton and nekton. From transcripts of the recorded comments of observers,

he summarizes the patterns of depth distribution seen for gelatinous plankton and crustaceans on the 11 dives made in 1987. The abundance of animals was less in this oceanic environment than Larson et al. reported from the canyons, but similarities in species occurrences and distributions were apparent. A number of probable new species were collected during these dives also, including a large and unusual medusa found near the bottom.

The midwater studies discussed here have been largely observational, with backup on film and videotape of visual sightings. Quantification of these observations is a serious problem in midwater, because there is usually no frame of reference outside the submersible to provide a scale for the abundance or distribution of organisms. Spatial relationships between objects are difficult to record, and human observers have trouble keeping more than one organism in view at a time. Hamner, Prewitt and Kristof describe equipment for recording video images in three dimensions, so that a stereoscopic field of view can be reconstructed later for visual or automated analysis. A preliminary version of this equipment was used on the Pisces VI during the Beebe project to record 3-D images of sharks on the bottom. Applied to midwater observations, the system will permit the detailed analysis of density of organisms, their positions relative to one another and the speed and pattern of their movements, all within a defined volume of water. Hamner et al. describe two sets of hardware under development, as well as some general considerations for stereoscopic video systems and automated motion analysis.



# EFFECTS OF BOUNDARY-LAYER FLOW ON THE SETTLEMENT OF ORGANISMS ONTO FLAT PLATES: PRELIMINARY RESULTS FROM CROSS SEAMOUNT

L. S. Mullineaux, C. A. Butman, and C. M. Fuller  
Dept. of Ocean Engineering  
Woods Hole Oceanographic Institution  
Woods Hole, MA 02543

## ABSTRACT

Boundary-layer flow conditions may influence the supply of invertebrate larvae to benthic habitats, and their behavior during settlement. The response of larvae of deep-water, encrusting organisms to different flow conditions was investigated by deploying two thicknesses of settlement plates on the summit of Cross Seamount, central north Pacific (410 m water depth). Currents were measured 1.8 m above the study site during the 48-day experiment. These measurements were combined with dissolution rates of alabaster disks and previous laboratory flume studies to describe the flow patterns expected over the settlement plates. Settlement of organisms (mostly benthic foraminifers) onto 1-cm-thick Lexan plates was significantly greater than onto 0.15-cm thick plates, possibly because of advantageous settlement environments in eddies formed at the edges of thick plates. Ferromanganese coated plates were also deployed to see if larvae actively selected substrates similar to their natural habitat.

## INTRODUCTION

The initial settlement of larvae can be an important stage in structuring benthic communities, especially those living on hard substrates (Osman, 1977; Underwood, Denley and Moran, 1983; Grossberg, 1982; Keough, 1984a; Connell, 1985; Gaines and Roughgarden, 1985; Gaines, Brown and Roughgarden, 1985). In many habitats, early colonists determine subsequent successional events, and the species composition may be more strongly influenced by larval settlement than by competition or predation (e.g. Keough, 1984b).

Field and laboratory experiments on settlement onto sediment (Eckman, 1983; Butman, Grassle and Webb, submitted) and onto hard substrates (Crisp, 1955; Christie, 1973; DeWolf, 1973; Munteanu and Maly, 1981; Wethey, 1985) have suggested that the boundary-layer flow regime can have a major effect on transport and settlement of larvae and other propagules. The temporal and spatial scales of these types of investigations often determine the relative importance of hydrodynamic and other processes affecting larval settlement (Butman, 1986; 1987). Although very little is known about settlement of deep-sea larvae, it is

probable that, on some scales, hydrodynamic processes play an important role in initial settlement and subsequent colonization in the deep sea.

For many years, studies of settlement onto hard substrates were conducted almost exclusively in shallow water, with the exceptions of experiments on wood-boring bivalves (Turner, 1973; 1977) and a series of deep-water biodeterioration studies (DePalma, 1962; Muraoka, 1964; 1966a; 1966b; 1966c). The scarcity of research on settlement and colonization of deep-sea hard substrates is surprising since several studies of softbottom communities have shown that dispersing colonists may have an important influence on community structure in the deep sea (Grassle, 1977; Desbruyeres, Bervas and Khripounoff, 1980; Levin and Smith, 1984; Smith, Jumars and DeMaster, 1986). A recent experiment conducted at 1300 m in the Catalina Basin near Southern California showed that initial settlement of foraminifers and metazoans onto hard substrates (manganese nodules and ceramic models of nodules) was strongly influenced by the elevation of the substrate off the seafloor. This pattern may have been due to larval responses to the difference in flow characteristics directly over the seafloor and 20 cm above it (Mullineaux, 1987a; 1988). The study also suggested that several metazoan species may be actively selecting ferromanganese substrates over ceramic models. The indications that deep-sea larvae respond to flow conditions during settlement, and that initial colonization of deep-water habitats may be quite different than shallow water environments, motivated the choice of study site and the experimental design of the present study.

The major goal of this study is to investigate the response of hard-substrate larvae to different flow regimes in a deepwater environment. The experimental substrates were flat plates, chosen for their hydrodynamic simplicity, as the flow regime over them could be adequately described and quantified with laboratory flume measurements. When a flat plate is placed in steady, unidirectional flow, a boundary layer develops and thickens as a function of distance from the leading edge. For a very thin flat plate, the thickness of the boundary layer depends only on the velocity of the oncoming flow, the distance from the leading edge and the viscosity and density of seawater, and can be calculated from empirical equations. At the leading edge of a thick plate, however, the plate acts as a bluff body, and can cause the flow to separate. This separation is due to an adverse pressure gradient which develops over the plate, forming an eddy downstream of the leading edge. In this case, the boundary-layer thickness can be predicted from equations only downstream from the eddy, where the boundary layer has reattached.

Experiments were conducted at the deep-water site on Cross Seamount to address several specific questions. The responses

of deep-water larvae to boundary-layer flow conditions were tested by measuring gradients in settlement downstream from the leading edges of plates, and by comparing leading-edge settlement on plates predicted to be with and without eddies. Behavioral responses of larvae to substrate composition were also tested with plates composed of different materials. These plates were designed to determine whether deep-sea larvae actively selected naturally occurring substrates, and to compare the magnitude of larval responses to substrate composition with responses to flow. The plates used for the flow and composition tests were elevated above the seafloor to isolate them from flow disturbances caused by small topographic irregularities. Additional plates were set directly on the seafloor in order to collect demersal larvae that were potentially excluded from the elevated plates.

#### STUDY SITE

Cross Seamount is a flat-topped, submerged peak located 60 km to the southeast ( $18^{\circ}0' N$ ,  $158^{\circ}17' W$ ) of the Hawaiian Islands. The summit rises to within 375 m of the surface and the base is at a depth of greater than 4500 m (topography illustrated in Malahoff, 1985). The site chosen for this study was near the center of the summit at a depth of 410 m. All experiments and current measurements were conducted on an oblong, rippled sand flat, approximately 85-m long and 35-m wide. Ripple orientation was generally north-south. Observers in the Pisces V submersible noted that ripples were asymmetrically shaped and estimated that ripple height was less than 2 cm and ripple spacing averaged 5 cm. Small boulders and outcrops of ferromanganese crust surrounded the site, but the nearby surface relief was no greater than 20-30 cm (with the exception of one large basalt block, 1-m tall and 3-m long).

A sand flat, rather than a site covered with ferromanganese crust, was selected as the study site for its hydrodynamic simplicity. A flat site was needed to ensure that the experimental substrates rested horizontally on the bottom, with the collecting surfaces oriented parallel with the flow. This particular site was expansive enough to distance the substrates from nearby surface topography which could shed eddies, or otherwise complicate the flow regime. Experiments and measurements were conducted near the center of the sand flat and well away from the large basalt block. Ripples and other small surface relief do influence boundary-layer flows (Schlichting, 1936), but at this site they were relatively small and regularly spaced. A few centimeters above the seafloor, the influence of the ripples is probably reflected in the flow as bed roughness, rather than as individual flow disruptions.

## METHODS

### Larval Settlement Plates

The settlement substrates were made of Lexan, which is a non-toxic plastic used in many kinds of experiments on chemically sensitive marine organisms, such as larvae and phytoplankton. Disk-shaped plates (24 cm in diameter) were used in order to present a similar leading edge to all oncoming flows. Four different types of plates were created: thick-elevated, thin-elevated, thick-benthic, and thick-elevated-manganese. The thick plates were 1-cm thick and the thin plates were 1.5-mm thick. Elevated plates were supported 6 cm above the seafloor on three legs. Thick-benthic plates were set directly on the seafloor. Thick-manganese plates were covered with a fine powder (silt-size particles) of ferromanganese crust that had been collected (unpreserved) previously at a nearby site on Cross Seamount. The powder was affixed to the plates with Tile Clad, a non-toxic adhesive in general use for marine aquaria.

The two plate thicknesses were selected on the basis of laboratory studies, performed in the 20-m Flume at Woods Hole Oceanographic Institution (see Butman, Chapman, Geyer, and Trowbridge, in press, for description of flume). Flow over a plate was visualized by releasing dye upstream from its leading edge. Visualizations were connected at boundary shear velocities ( $u_*$ ) between 0.3 and 1.0  $\text{cm s}^{-1}$  which are within the range of those found in the deepsea ( $u_*$  is commonly less than 1  $\text{cm s}^{-1}$  in deep-sea boundary layers; Chriss and Caldwell, 1982; Grant, Williams and Gross, 1985). In this range of shear velocities, the flow separated and formed a recirculating eddy at the leading edge of a 1-cm-thick plate supported 6 cm above the flume bottom. No flow separation occurred over the 1.5-mm-thick plate, and a well-behaved boundary layer developed downstream from the leading edge. The eddy over the thick plate was very small at low shear velocities, but extended up to 3 cm downstream from the leading edge at higher values of  $u_*$ . The boundary layer reattached downstream from the eddy and attained a thickness similar to the boundary layer over the thin plate. Eddies forming at the edge of benthic-thick plates (those sitting on the flume bottom) were smaller than the eddies over elevated-thick plates (supported 6 cm above the flume bottom) at corresponding shear velocities.

If larvae do respond to the flow regime over substrates, then two settlement patterns can be predicted from these flume observations. Larvae would be expected to settle in densities that vary as a function of distance from the leading edge of a plate, due to the growth of the boundary layer downstream. They also may settle in different densities at the leading edge of a thick plate (due to the presence of an eddy) than at the leading edge of a thin plate.

## Deployment of Experiments

Five replicates of the four types of plates (thick-elevated, thin-elevated, thick-benthic and thick-elevated-manganese) were deployed by the submersible *Pisces V* at the study site in an array of five linear transects, each containing all four plate treatments. The transects were intended to be set out in a rectangular randomized block array, but the irregular shape of the sand flat constrained their deployment. In order to keep the plates at least 2 m from each other and 5 m from the edges of the site, some transects were laid out parallel, and others perpendicular, to the long axis of the site. Despite this lack of symmetry in the blocks, the arrangement of transects ensured that replicates of a treatment were spread out over the sand flat, and were not subject to potential biases from their positions in the site. Plates were suspended with fine nylon line (<1 mm in diameter) to polypropylene loops for deployment and recovery. The line created very little flow disturbance near the plate and the polypropylene loop floated at least 30 cm above the plate.

All plates were deployed within two days of each other, remained on the site for 46 to 50 days and were recovered within two days of each other. An average deployment duration of 48 days is used in the following analyses. The maximum error from this approximation is < 5%, and since plates were deployed and recovered in blocks (transects), the error in duration time does not bias the treatments systematically. A total of 14 plates were recovered intact, including three sets complete with all four treatments.

The plates were preserved in 10% buffered formalin in seawater and were later transferred to 80% ethanol for inspection. All eukaryotic organisms visible under a dissecting microscope were counted and identified to the lowest taxonomic group possible. Individuals were counted in each of 144 subareas on a plate (which was divided into 12 radial sectors, and 12 1-cm wide concentric rings) for future analyses.

## Flow Measurements

Flow patterns at the Cross Seamount study site were measured at three scales. Transects of XBT (expendable bathythermograph) profiles were taken over the summit of the seamount on both the deployment and recovery cruises, and CTD (conductivity, temperature, density) profiles were measured over the study site during the recovery cruise. These measurements were collected in order to infer mesoscale flow patterns over the entire seamount. Current velocities in the benthic boundary layer at the study site were measured (using a 300 s averaging interval) for 48 days with a Neil Brown SACM (Smart Acoustic Current Meter) moored 1.8 m off the seafloor.

Time-integrated patterns of boundary shear stress were measured on the scale of individual settlement plates by quantifying the dissolution of flat disks of alabaster (crystalline calcium sulfate). The disks were 15 cm in diameter and 1-cm thick, so even though they were slightly smaller than the thick settlement plates, they had the same shape and leading-edge thickness. They were glued to plastic bases, and coated with Tile Clad along the edges, so that only the upper surface of the alabaster was exposed to seawater. Disks were deployed on the seafloor at the site for 2- and 3-day durations. Total dissolution of a disk was measured by weighing it before and after deployment. Dissolution patterns with respect to the edge of a disk were quantified by placing a grid of 90 points over the disk and measuring (in millimeters) the amount of alabaster dissolved from the upper surface at each point on the grid. Although calculations of  $u_*$  can be made from flush-mounted alabaster plates (Santschi, Bower, Nyffeler, Azevedo and Broecker, 1983; Opdyke, Gust and Ledwell, 1987); the applicability of these empirical equations to thick plates remains to be tested. The disks used in the Cross Seamount study were made intentionally with thick edges, so that shear stress patterns could be compared directly with larval settlement patterns on the Lexan plates. Thus, it was the spatial patterns of dissolution on the alabaster plates, rather than quantitative estimates of  $u_*$ , that were of primary interest in this study.

## RESULTS

### Larval Settlement Patterns

The mean number of attached individuals found on three replicate plates of the four treatments are listed in Table 1. Foraminifers were much more abundant than metazoans on all plate treatments. Settlement onto the thick-elevated plates was significantly higher than onto any of the other plates (Model I ANOVA and Student Neumann Keuls *a posteriori* test of the log ( $x+1$ )-transformed abundance data;  $P < 0.05$ ), and settlement onto both the thick-elevated plate types (Lexan and manganese covered) was greater than onto the thick-benthic plates.

### Flow Environment

The results of two sets of XBT profiles, taken in transects over the summit of Cross Seamount during the deployment and recovery cruises, indicated that the upper mixed layer was 70-m thick and the steepest part of the thermocline was between 200-300 m water depth. No signature of the seamount was detected in isotherms on the west-to-east transect taken during the deployment cruise. On the recovery cruise, however, a south-to north transect showed isotherms doming over the seamount summit (with vertical displacements of up to 30 m), indicating an interaction between the seamount and the general oceanic currents.

Table 1. Number of individuals attached to plates (mean and standard deviation for three replicates), after a 48 day deployment on Cross Seamount

Plate treatment	Foraminifers inds/452 cm <sup>2</sup>	Metazoans inds/452 cm <sup>2</sup>
Thick-elevated	294 (150)	3.6 (3.5)
Mn-thick-elevated	182 ( 22)	6.3 (2.1)
Thin-elevated	146 ( 13)	5.7 (4.7)
Thick benthic	121 ( 12)	5.0 (4.0)

The 46-day record from the current meter showed that near-bottom currents at the study site fluctuated semidiurnally, both in speed and direction. The current speed (recorded as 300-s averages) reached a minimum of  $28 \text{ cm s}^{-1}$ , and averaged approximately  $10 \text{ cm s}^{-1}$ . The flow was omnidirectional, but with a strong bias towards west-northwest. A thermometer mounted on the current meter recorded semidiurnal temperature fluctuations between  $7.5$  and  $9.6^\circ\text{C}$ .

Dissolution patterns on all six alabaster disks showed greater dissolution of the upper surface near the edges than near the center (Mullineaux and Butman, submitted). The patterns were not symmetric, however, and dissolution was consistently higher along one edge than along the opposite edge. Total dissolution (measured as total weight loss) of four disks placed within a meter of each other was much less variable than dissolution of two disks placed 8 m apart (Table 2). The low weight loss of one disk that was strapped to the submersible during one dive indicates that relatively little dissolution (less than 3 g) occurs during a transit between the study site and the surface. The disks, therefore, predominantly reflect shear stress at the study site, rather than shear stress during transit.

## DISCUSSION

Current meter measurements over the summit of Cross Seamount indicate that the benthic environment is subject to relatively strong currents varying at semidiurnal frequencies. This record is similar to currents recorded at Horizon Guyot, where the semidiurnal fluctuations are thought to be due to internal tides (Noble and Mullineaux, submitted). The XBT, CTD, and current meter results obtained in the present study are being analyzed for evidence that the benthic flow environment at Cross Seamount is sensitive to interactions between the seamount and general oceanic currents (Mullineaux and Butman, submitted).

The pattern of greater dissolution at the edges of alabaster disks than at the center suggests that the boundary shear stress near the edges was greater than in the center (see Opdyke, Gust and Ledwell, 1987 for a discussion of the relation between dissolution and shear stress). This may have been a consequence of the thin boundary layer near the leading edge, and/or the recirculating eddy at the leading edge. The asymmetry of this pattern is consistent with the directional bias in near-bottom currents measured by the current meter. If the currents had been omnidirectional, the expected dissolution patterns would have been radially symmetric, with the greatest dissolution occurring around the entire perimeter of the disk. If larvae are indeed responding to boundary shear stress over the settlement plates, then the settlement patterns should be correspondingly asymmetric.

Table 2. Dissolution of alabaster (crystalline calcium sulfate) disks. Four disks were set out for 3 days during the deployment cruise (D1-4), and two disks were set out for 2 days during the recovery cruise (R1-2). D1-4 were spaced 1-m apart and R1-2 were spaced 8-m apart. \*R3 was carried to the study site and back by submersible, but was not deployed.

Disk	Dissolution (g)	Deployment (h)	Spacing (m)
D1	19.92	70	1
D2	19.90	70	1
D3	16.11	70	1
D4	19.89	70	1
R1	25.48	46	8
R2	27.75	46	8
R3	2.94	5*	

The significantly greater numbers of organisms settling on thick-elevated than thin-elevated plates suggests that eddies at the leading edges of thick plates enhance settlement. This trend is also seen in the difference in settlement on the thick-elevated-manganese and thin-elevated plates. Several different interpretations, however, can be made of the low faunal densities found on thick-benthic plates. One is that the benthic plates were positioned lower in the boundary layer in slower oncoming flows, so that the leading-edge eddies were consistently smaller than those over elevated plates. If the size of the eddy influenced settlement, then fewer larvae may have settled on the benthic plates. On the other hand, settlement onto the thin plates was greater than onto the benthic thick plate, and no leading-edge eddy should have formed over the thin plate in flow conditions observed at the study site. Thus, it is possible that the higher boundary shear stress over elevated plates had more influence on settlement than the presence/absence of an eddy. A third explanation, that has nothing to do with settlement, is that the benthic plates were grazed by predators unable to access the elevated plates. Mucus trails found on one of the benthic plates (not used in this analysis) lend some support to this explanation.

Detailed spatial analyses of organisms attached to individual plates will help resolve the difference between responses of larvae to turbulence generated by a leading edge from responses to downstream gradients in boundary shear stress (Mullineaux and Butman, submitted). In addition, analyses of the species composition of settled organisms will address questions on the species-specific responses of deep-water larvae to ferromanganese-encrusted substrates.

#### ACKNOWLEDGMENTS

This research was supported by contract N00014-87-K0007 from the Office of Naval Research, a grant of submersible time from NOAA, and the Coastal Research Center at Woods Hole Oceanographic Institution. We thank the pilots and crew of the Pisces V submersible for their technical assistance and enthusiasm. W. Terry generously loaned the current meter and P. Boutin assisted with the mooring design. This is contribution 6694 of the Woods Hole Oceanographic Institution.

## LITERATURE CITED

Butman, C. A., 1986. Larval settlement of soft-sediment invertebrates: Some predictions based on an analysis of near-bottom velocity profiles. In: J. C. J. Nihoul (ed.), Marine Interfaces Ecohydrodynamics, Proc. 17th Intl. Liege Colloq. Ocean Hydrodynamics. Amsterdam, Elsevier Publishers, Elsevier Oceanography Series, Vol. 42, pp. 487-513.

Butman, C. A., 1987. Larval settlement of soft sediment invertebrates: The spatial scales of pattern explained by active habitat selection and the emerging role of hydrodynamical processes. Oceanogr. Mar. Biol. Ann. Rev., Vol. 25, pp. 113-165.

Butman, C. A., R. J. Chapman, W. R. Geyer, and J. W. Trowbridge. (in press). The 17-Meter Flume: Description, operating constraints and user's manual. WHOI Technical Report.

Chriss, T. M., D. R. Caldwell. 1982. Evidence for the influence of form drag on bottom boundary layer flow. J. Geophys. Res., Vol. 87, No. C6, pp. 4148-4154.

Christie, A. O. 1973. Spore settlement in relation to fouling by Enteromorpha. In: R. F. Acker, B. F. Brown, J. R. DePalma, and W.P. Iverson (eds.), Proc. 3rd International Congress on Marine Corrosion and Fouling, pp. 674-681. Evanston, Ill., Northwestern Univ. Press.

Connell, J. H. 1985. The consequences of variation in initial settlement vs. post-settlement mortality in rocky intertidal communities. J. Exp. Mar. Biol. Ecol., Vol. 93, pp. 11-45.

Crisp, D. J. 1955. The behavior of barnacle cyprids in relation to water movement over a surface. J. Exp. Biol., Vol. 32, pp. 569-590.

DePalma, J. R. 1962. Marine fouling and boring organisms in the Tongue of the Ocean, Bahamas, exposure II. Informal Manuscript Report No. 0-64-62, U.S. Naval Oceanographic Office, Marine Sciences Department, 13 numb. leaves, unpublished manuscript.

Desbruyeres, D., J. Y. Bervas and A. Khripounoff. 1980. Un cas de colonisation rapide d'un sediment profond. Oceanologica Acta. Vol. 3, pp. 285-291. Paris, Gauthier-Villars.

DeWolf, P. 1973. Ecological observations on the mechanisms of dispersal of barnacle larvae during planktonic life and settling. Neth. J. Sea Res., Vol. 6, No. 1-2, pp. 1-129.

Eckman, J. E. 1983. Hydrodynamic processes affecting benthic recruitment. Limnol. Oceanogr., Vol. 28, pp. 241-257.

Gaines, S. and J. Roughgarden. 1985. Larval settlement rate, a leading determinant of structure in an ecological community of the marine intertidal zone. Proc. Natl. Acad. Sci., Vol. 82, pp. 3707-3711.

Gaines, S., S. Brown and J. Roughgarden. 1985. Spatial variation in larval concentrations as a cause of spatial variation in settlement for the barnacle Balanus glandula. Oecologia, Vol. 67, pp. 267-272. Springer, Germany.

Grant, W. D., A. J. Williams III, T. F. Gross. 1985. A description of the bottom boundary layer at the Hebble Site: Low frequency forcing, bottom stress and temperature structure. Mar. Geol., Vol. 66, pp. 219-241.

Grassle, J. F. 1977. Slow recolonization of deep-sea sediment. Nature, Vol. 265, No. 5595, pp. 618-619.

Grosberg, R. K. 1982. Intertidal zonation of barnacles: The influence of planktonic zonation of larvae on vertical distribution of adults. Ecology, Vol. 63, pp. 894-899.

Keough, M. J. 1984a. Dynamics of the epifauna of the bivalve Pinna bicolor: Interactions among recruitment, predation, and competition. Ecology, Vol. 65, No. 3, pp. 677-688.

Keough, M. J. 1984b. Effects of patch size on the abundance of sessile marine invertebrates. Ecology, Vol. 65, No. 3, pp. 423-427.

Levin, L. A. and C. R. Smith. 1984. Response of background fauna to disturbance and enrichment in the deep sea: A sediment tray experiment. Deep-Sea Res., Vol. 31A, pp. 1277-1285.

Malahoff, A. 1985. Active and extinct submarine volcanoes of the southern Hawaiian ridge--morphology and mineral formation. In: L. Magaard, R. Pujalte, and V. Gaynor (eds.), HOE: The Hawaiian Ocean Experiment. Hawaii Inst. Geophys. Sp. Pub., pp. 171-188.

Mullineaux, L. S. 1987a. Epifaunal communities on manganese nodules. Ph.D. dissertation, University of California San Diego, Scripps Institution of Oceanography, 202 pp.

Mullineaux, L. S. 1987b. Organisms encrusting manganese nodules and crusts: Distribution and abundance at three North Pacific sites. Deep-Sea Res., Vol. 34, No. 2, pp. 165-184.

Mullineaux, L. S. 1988. The role of settlement in structuring a hard substratum community in the deep sea. J. Exp. Mar. Biol. Ecol., Vol. 120, pp. 247-261.

Munteanu, N. and E. J. Maly. 1981. The effect of current on the distribution of diatoms settling on submerged glass slides. Hydrobiologia, Vol. 78, pp. 237-282. The Hague, Dr. W. Junk Publishers.

Muraoka, J. S. 1964. Deep-ocean biodeterioration of materials Part I. Four months at 5640 feet. Technical Report R-329, U.S. Naval Civil Engineering Laboratory, Port Hueneme, CA, 45 pp.

Muraoka, J. S. 1966a. Deep-ocean biodeterioration of materials Part III. Three years at 5300 feet. Technical Report R-428, U.S. Naval Civil Engineering Laboratory, Port Hueneme, CA, 62 pp.

Muraoka, J. S. 1966b. Deep-ocean biodeterioration of materials Part IV. One year at 6800 feet. Technical Report R-456, U.S. Naval Civil Engineering Laboratory, Port Hueneme, CA, 60 pp.

Muraoka, J. S. 1966c. Deep-ocean biodeterioration of materials Part V. Two years at 5640 feet. Technical Report R-495, U.S. Naval Civil Engineering Laboratory, Port Hueneme, CA, 59 pp.

Opdyke, B. N., G. Gust and J. R. Ledwell 1987. Mass transfer from smooth alabaster surfaces in turbulent flows. Geophys. Res. Lett., Vol. 14, No. 11, pp. 1131-1134.

Osman, R. W. 1977. The establishment and development of a marine epifaunal community. Ecol. Monogr., Vol. 47, pp. 37-63.

Santschi, P. H., P. Bower, U. P. Nyffeler, A. Azevedo and W. S. Broecker. 1983. Estimates of the resistance to chemical transport posed by the deep-sea boundary layer. Limnol. Oceanogr., Vol. 28, No. 5, pp. 899-912.

Schlichting, H. 1936. Experimental investigation of the problem of surface roughness. Ingenieur-Archiv, Vol. VII, No. 1, Technical Memorandums, National Advisory Committee for Aerodynamics, Washington.

Smith, C. R., P. A. Jumars and D. J. DeMaster. 1986. In situ studies of megafaunal mounds indicate rapid sediment turnover and community response at the deep-sea floor. Nature, Vol. 323, pp. 251-253.

Turner, R. D. 1973. Wood-boring bivalves, opportunistic species in the deep sea. Science, Vol. 180, pp. 1377-1379.

Turner, R. D. 1977. Wood, mollusks, and deep-sea food chains. Bull. Amer. Malacolog. Union 1976, pp. 13-19. Houston, Texas, American Malacological Union, Inc.

Underwood, A. J., E. J. Denley and M. J. Moran. 1983. Experimental analyses of the structure of mid-shore rocky intertidal communities in New South Wales. Oecologia, Vol. 56, pp. 202-219. Berlin, Springer-Verlag.

Wethey, D. 1986. Ranking of settlement cues by barnacle larvae: Influence of surface contour. Bull. Mar. Sci., Vol. 39, No. 2, pp. 393-400.

MIDWATER COMMUNITY STUDIES OFF NEW ENGLAND  
USING THE JOHNSON SEA-LINK SUBMERSIBLES

Ronald J. Larson<sup>1</sup>, G. Richard Harbison<sup>1</sup>, Phillip R. Pugh<sup>2</sup>,  
John A. Janssen<sup>3</sup>, Robert H. Gibbs<sup>4</sup>, James E. Craddock<sup>5</sup>,  
Claudia E. Mills<sup>6</sup>, Richard L. Miller<sup>7</sup>, and Ronald W. Gilmer<sup>1</sup>

1 - Harbor Branch Oceanographic Institution, Fort Pierce, FL

2 - Institute of Oceanographic Sciences, Wormley, England

3 - Biology Department, Loyola University, Chicago, IL

4 - Fish Division, U.S. National Museum, Washington, D.C.

5 - Woods Hole Oceanographic Institution, Woods Hole, MA

6 - Friday Harbor Laboratories, Friday Harbor, WA

7 - Biology Department, Temple University, Philadelphia, PA

ABSTRACT

The midwater community off New England was studied using manned submersibles. Twenty-three dives were made in three submarine canyons SE of Woods Hole in 800 m of water. We found a diverse community present. Gelatinous zooplankton (medusae, siphonophores and ctenophores) were represented by 38 species, several are undescribed. The vertical distributions of most were determined and it was discovered that they were mostly mesopelagic (occurring below 400 m). Ctenophores were both diverse and numerous in contradiction to the results of studies using nets. The siphonophore Nanomia cara, which showed evidence of a 150 m diel vertical migration, was most abundant. Crustacean micronekton consisted mostly of Meganyctiphanes norvegica, Sergestes sp., and Themisto gaudichaudii. These species all vertically migrated 100 m or more and were sometimes very numerous in midwater strata or near the bottom. Midwater fishes were found in the mesopelagic but some migrated into the upper 100 m at night. It is concluded that predation by visually orienting predators in surface waters may be the primary factor which determines vertical distributions. Nevertheless, the mesopelagic is not a good refuge from predators because there are large numbers of gelatinous predators there.

INTRODUCTION

Although a large number of studies have been done on the midwater fauna of the North Atlantic little is known about the species composition and vertical distribution of most taxa in

this community. The major reason for this is that midwater trawls fail to capture a significant part of the fauna. Active nekton, e.g., squids and larger fishes are able to avoid the nets. Many gelatinous zooplankton are either damaged beyond recognition or they pass through the net because of their fragility. Here, we report the first detailed description of the vertical distribution of midwater animals based on direct in-situ observations made using the Johnson Sea-Link submersibles.

The study reported here was conducted near the shelf edge off New England, just south of Woods Hole, in 800 m of water. This region is referred to as the Slope Water Region (Backus and Craddock, 1977; Backus et al., 1977) and is known to be a mixture of shelf water and Gulf Stream water (Iselin, 1936).

## METHODS

Twenty-three dives were made to depths of 800 m using the Johnson Sea-Link I and II manned submersibles (described by Youngbluth, 1984). Nine dives were made from 30 August to 6 September 1986 and 14 dives from 2 to 9 August 1987 in three submarine canyons (Atlantis, Hydrographer, and Veatch) south of the Grand Banks off the New England coast (Fig. 1). The dives were of 3-4 hours duration. They were made to depths ranging from 400 to 800 m and usually included the entire water column. It should be stressed that more time was spent at the deepest depths and thus some bias is present in the data. Dives were made between 1200 and 1500 hrs, and 2000 and 2300 hrs EDST so that diel vertical migrations could be documented.

During each submersible dive observations on the fauna as well as depth and temperature were narrated onto audio tape by audio recorder. Color video was recorded on 3/4-inch tape. Following each dive videotapes were reviewed and discussed by observers and the sound track transcribed. Specimens, even very fragile ones, were successfully collected using several kinds of samplers (described by Youngbluth, 1984). Because of the large volume of the samplers, specimens experienced relatively small temperature changes (<5°C) when brought to the surface. Specimens were kept in shipboard incubators at ambient temperatures until studied (usually within 1-3 h). Representative specimens were photographed and preserved, where possible. The data reported here are limited to the macrozooplankton (>2 cm long), because smaller specimens could not be adequately visually quantified.

Scuba dives were made in the upper 20 m to document the epipelagic fauna.

Water temperatures in the upper 800 m ranged from 4.8 to 18°C with a well marked thermocline in the top 25 m (Fig. 2).

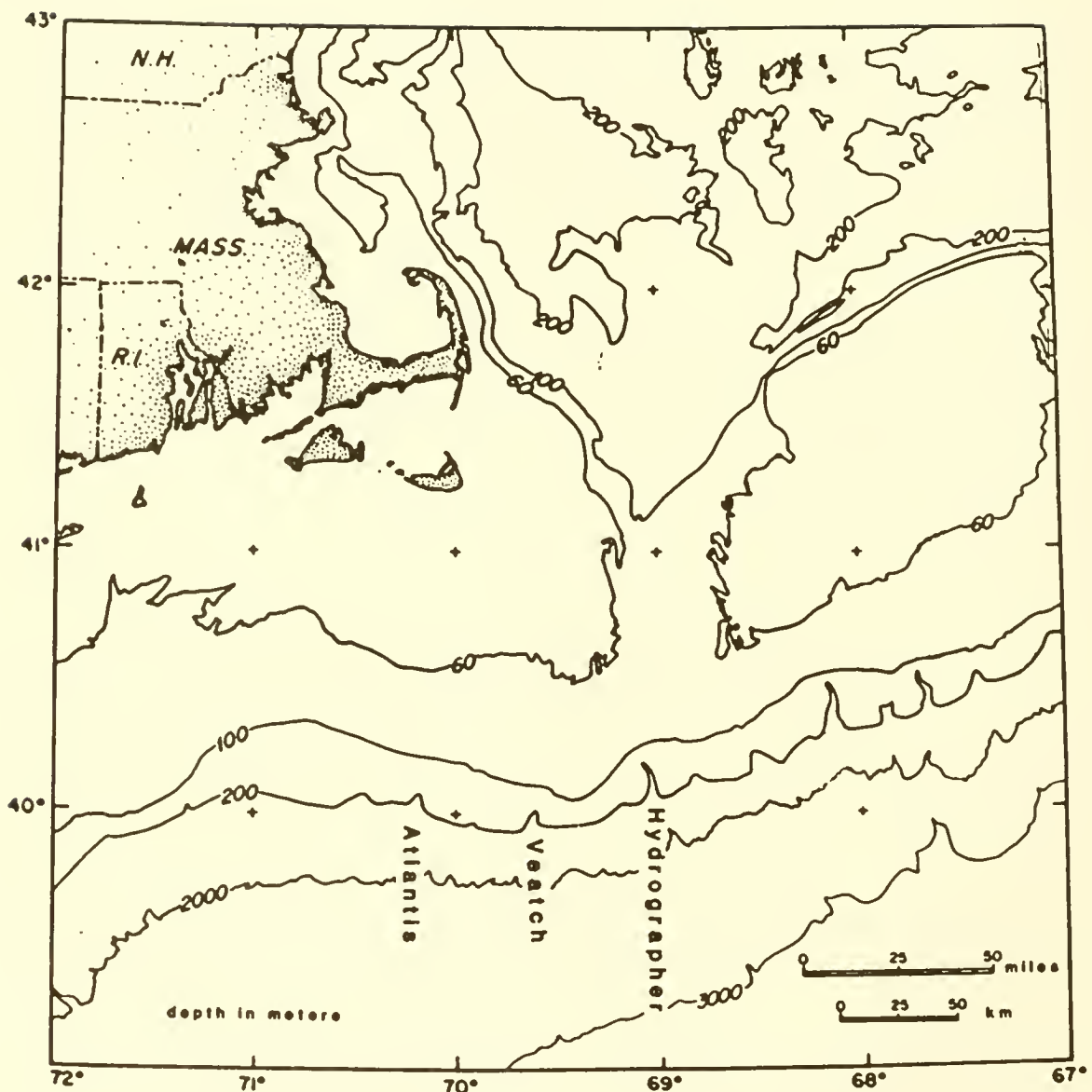


Figure 1. Chart showing locations of Atlantis, Veatch and Hydrographer canyons where dives were made.

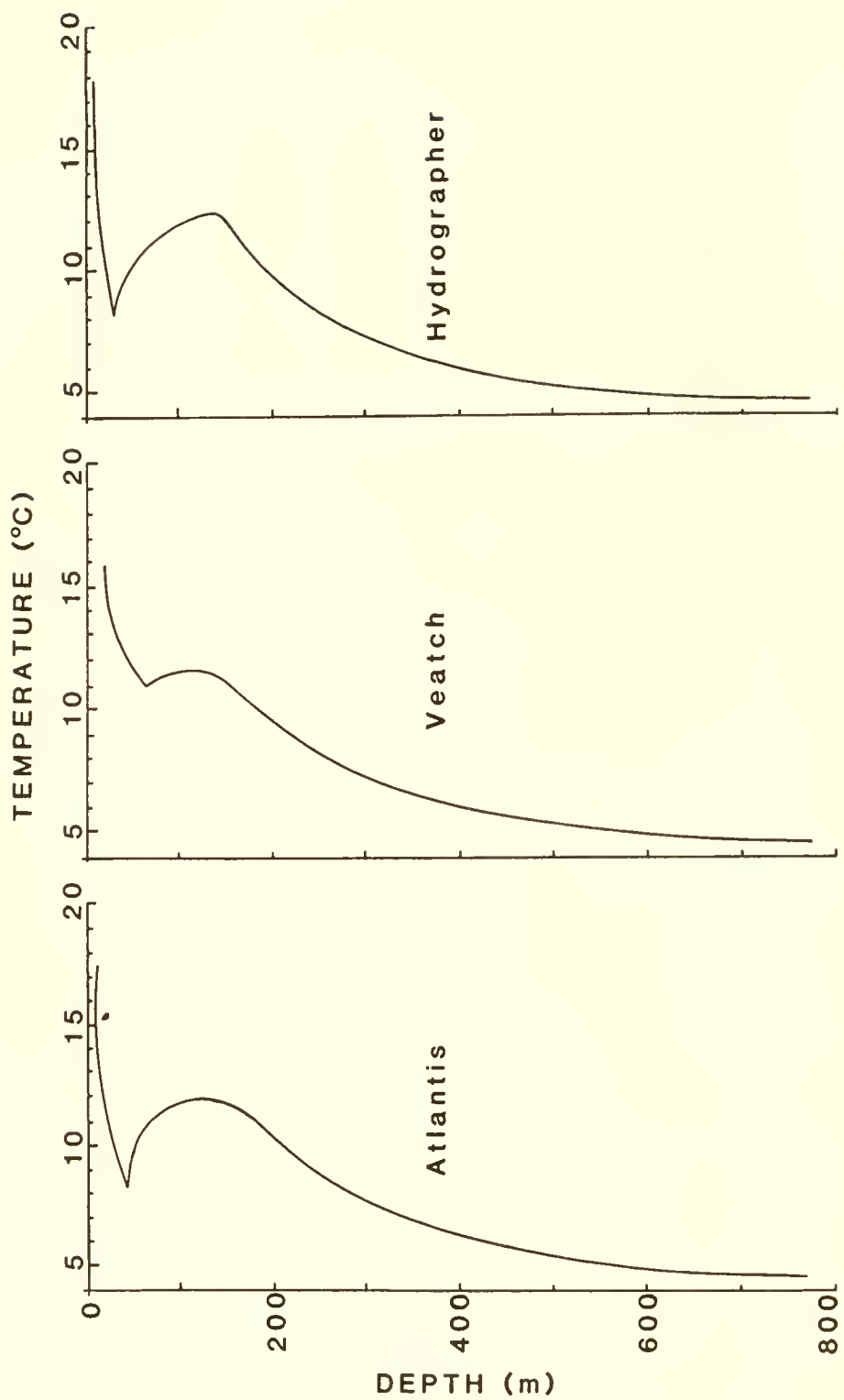


Figure 2. Temperature versus depth profiles for Atlantis, Veatch and Hydrographer canyons.

In Atlantis and Hydrographer Canyons, and to a lesser extent in Veatch Canyon, at about 40 m there was a temperature inversion where temperatures increased with depth to 150 m but thereafter decreased. Below 400 m temperatures changed only slightly (4.8-7°C). Salinities were not measured.

## RESULTS

Thirty-eight species of gelatinous macrozooplankton were observed and collected (Table 1). Medusae, with 16 taxa, represented the largest group. Of these, two species of hydromedusae, Pantachogon haeckeli and Halicreas minimum, were most abundant. No new species were found, however two rare medusae were collected i.e., Poralia rufescens and Halitrepes maasi.

Siphonophores were represented by 13 species, several of which are undescribed. Nanomia cara and Forskalia spp. dominated. N. cara was the most numerous coelenterate observed. It was sometimes very abundant in midwater strata and near the bottom. The physonect Agalma okenii was the only coelenterate that was commonly seen in the surface waters by scuba divers.

Ctenophores were represented by 9 species. Several species are new to science. Bathocyroe fosteri and Beroe cucumis were most common.

Macro-crustaceans were dominated by three species, the euphausiid Meganyctiphanes norvegica. The sergestid shrimp Sergestes sp. and the amphipod Themisto (Parathemisto) gaudichaudii. M. norvegica was often very numerous in well defined depth strata and near the bottom. Neither Themisto nor Sergestes were limited to specific depth strata although their abundance was depth dependent. Large calanoid copepods were seen, mostly below 600 m but were not collected or identified.

Pelagic molluscs were represented by a number of unidentified squids and the commonly seen cranchiid Megalocranchia sp. and by the pteropods Clione limacina, Limacina helicoides, and ?Cymbulia.

Representatives of at least 13 families and many genera and numerous species of fishes were seen, video taped, and or collected. Myctophids (many taxa), hatchet fishes (Sternopychidae, several taxa), paralepidids (mostly Notolepis rissoii), and snipe eels (Nemichthyidae, mostly Nemichthys scolopaceus) were most abundant. Other important taxa were Stomias boa ferox (Stomiidae) and Melanostigma atlanticum (Zoarcidae).

Table 1. List of midwater organisms identified from submersible dives off New England

HYDROMEDUSAE:

Aeqina citrea  
Aeqinura grimaldii  
Chromatonema rubrum  
Colobonema sericeum  
Halicreas minimum  
Halitrepes maasi  
Pandea rubra  
Pantachogon haeckeli  
Solmissus incisa  
Solmundella bitentaculata

SIPHONOPHORES:

Apolemia spp.  
Bathyphysa conifera  
Chuniphyes moerae  
?Cordagalma cordiformis  
Forskalia spp.  
Halistemma rubrum  
Lensia conoidea  
Lychnagalma utricfularia  
Marrus orthocanna  
Nanomia cara  
physonect n. sp. #1  
physonect n. sp. #2  
Praya dubia

SCYPHOMEDUSAE:

Atolla vanhoeffeni  
Atolla wyvillei  
Nausithoe atlantica  
Pelagia noctiluca  
Periphylla periphylla  
Poralia rufescens

PTEROPODS:

Clione limacina  
?Cymbulia sp.  
Limacina helicoides

SQUIDS:

Order Teuthoidea  
Megalocranchia sp.  
Stolothethis leucoptera  
squids undetermined species

AMPHIPODS:

Mimonectes sp.  
Themisto (Parathemisto)  
guadichaudii  
Phronima sp.

EUPHAUSIIDS:

Meganyctiphanes norvegia

DECAPODS:

Notostomus robustus  
Sergestes sp.

Fam. Paralepididae  
Notolepis rissoii  
?Paralepis sp.

Fam. Bathysauridae  
Bathysaurus sp.

Fam. Myctophidae

CTENOPHORES:

Aulococtena acuminata  
Bathocyroe fosteri  
Beroe cucumis  
Bolinopsis infundibulum  
cydippid n. sp. #1 (red)  
cydippid n. sp. #2 (orange)  
lobate n. sp. #1  
Mertensia ovum  
Thalassocalyce inconstans

FISHES:

Fam. Scyliorhinidae  
Apristurus sp.  
  
Fam. Bathylagidae  
Bathylagus ?euryops  
  
Fam. Sternopychidae  
Argyropelecus aculeatus

Table 1. (Cont'd.)

A. <u>qiqas</u>	<u>Ceratoscopelus maderensis</u>
A. <u>hemiqymnus</u>	many unidentified
Fam. Gonostomatidae	Fam. Macrouridae
<u>Cyclothona</u> spp.	early juveniles
? <u>Gonostoma</u> sp.	
others	
Fam. Stomidae	Fam. Caristiidae
<u>Chauliodus sloani</u>	<u>Caristius</u> sp.
<u>Photonectes</u> sp.	
or <u>Malarosteus</u> sp.	
<u>Stomias boa ferox</u>	Fam. Zoarcidae
Fam. Nemichthyidae	<u>Melanostigma atlanticum</u>
<u>Nemichthys scolopaceus</u>	
others	
Fam. Serrivomeridae	Fam. Synaphobranchidae
<u>Serrivomer beanii</u>	<u>Synaphobranchus</u> sp.
	others

## Vertical Distributions

Vertical distribution data for all dives were lumped together because there were insufficient data to determine if it varied among submarine canyons or from year to year.

The medusae were mostly found at depths in excess of 600 m (Fig. 3). Only a single macro-medusa (>2 cm diameter) species i.e. Pelagia noctiluca was found above 300 m and only three species occurred above 600 m while 15 species were found below this depth. There were no eurybathyl species. Pantachogon haeckeli occurred over the greatest depth range (425-800 m). The medusae as a group showed no evidence of a diel vertical migration.

Siphonophores were somewhat more eurybathyl than medusae. Two species i.e., Forskalia sp. and Nanomia cara, were found at depths of 100-170 m to 800 m. Nine species occurred above 600 m and only four species were not found above this depth. N. cara apparently showed a diel vertical migration of about 150 m.

During the day the mean depth of minimum occurrence was 480 m but at night it was only 330 m.

Ctenophores showed a somewhat different depth distribution. Two species i.e., Beroe cucumis and Bolinopsis infundibulum were eurybathyl, occurring from near the surface to 800 m. Four species were observed above 450 m and five species were only seen at greater depths. Ctenophores did not vertically migrate to any extent.

The only mollusc species for which we have depth data is Limacina helicoides a dark-purple pteropod which was seen below 580 m. A number of squids were seen at depths of greater than 150 m, most were seen below 300 m.

The three common macro-crustaceans mostly occurred over a broad depth range but were not seen at the surface. Meganyctiphanes norvegica was observed from 75 to 800 m but was most numerous below 200 m. Themisto gaudichaudii and Sergestes sp. were present below 150 m but were most common at depths greater than 300 m. The mean day depths of the sometime dense layers of euphausiids was 290 m but at night it had decreased to 200 m (Table 2). Themisto populations moved from an upper limit during the day of 500 m to 370 m at night and Sergestes moved from 470 m during the day to 340 m at night. Thus, these species showed a 90 to 130 m upward movement at night.

Most of the fishes occurred below 450 m (Fig. 4). Only a few species were found above this depth by day but some migrated into surface waters at night. Hatchet fishes (Sternopychidae), myctophids, paralepidids and snipe eels showed some evidence of a

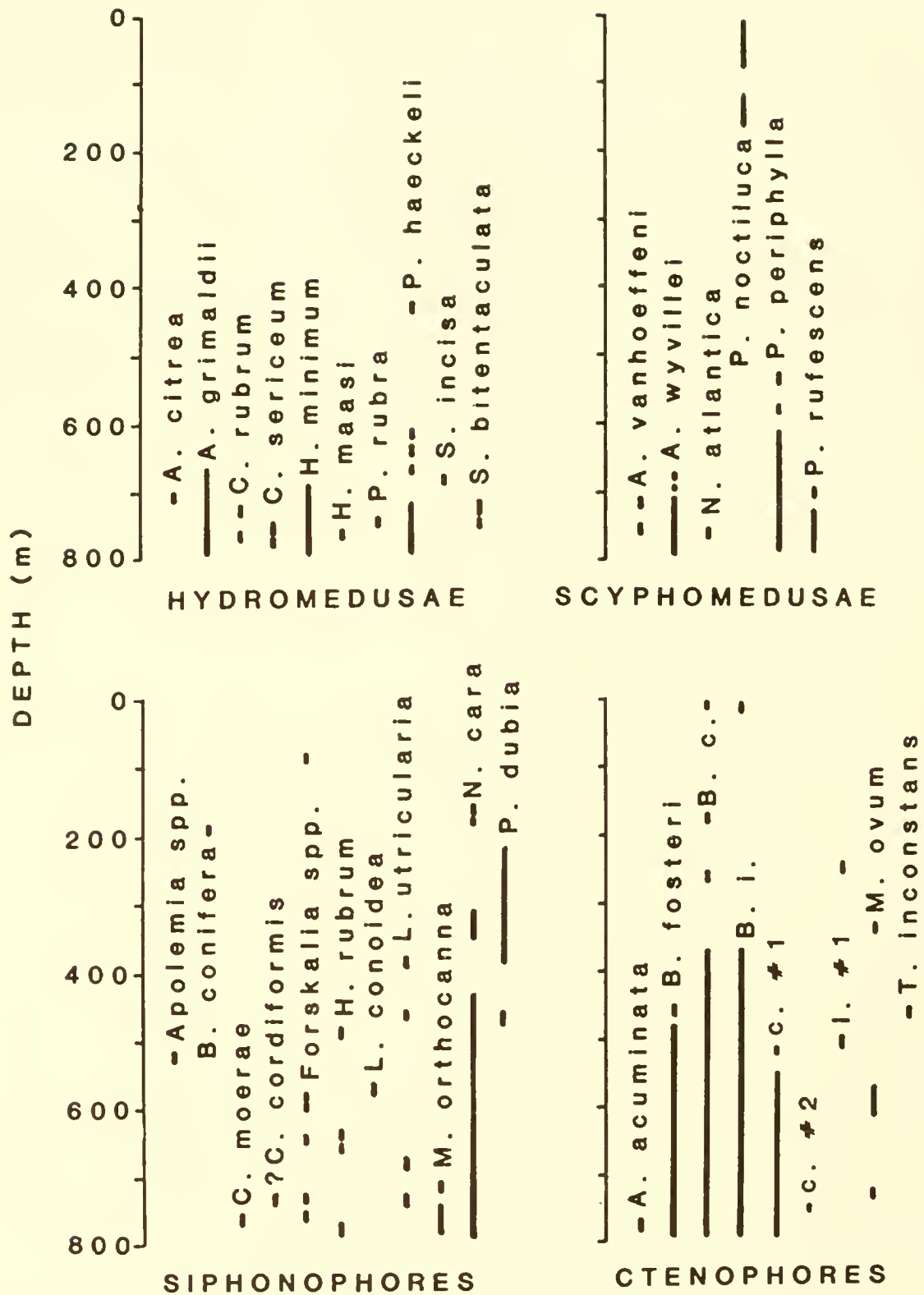


Figure 3. Bathymetric distributions of gelatinous macroplankton. Solid lines = individuals seen more or less throughout entire range. Dashes = individuals mostly confined to strata.

Table 2. Day versus night depth ranges for midwater crustaceans

TAXON	DAY DEPTH (M) $\bar{X}$ (RANGE)	NIGHT DEPTH (M) $\bar{X}$ (RANGE)
<u><i>Meqanvctiphanes</i></u> <u><i>norvegica</i></u>	290 (240-370)	200 (150-300)
<u><i>Sergestes</i></u> sp.	470 (340-580)	340 (120-460)
<u><i>Themisto gaudichaudii</i></u>	500 (240-660)	370 (110-610)

N = 10 pairs of day/night observations

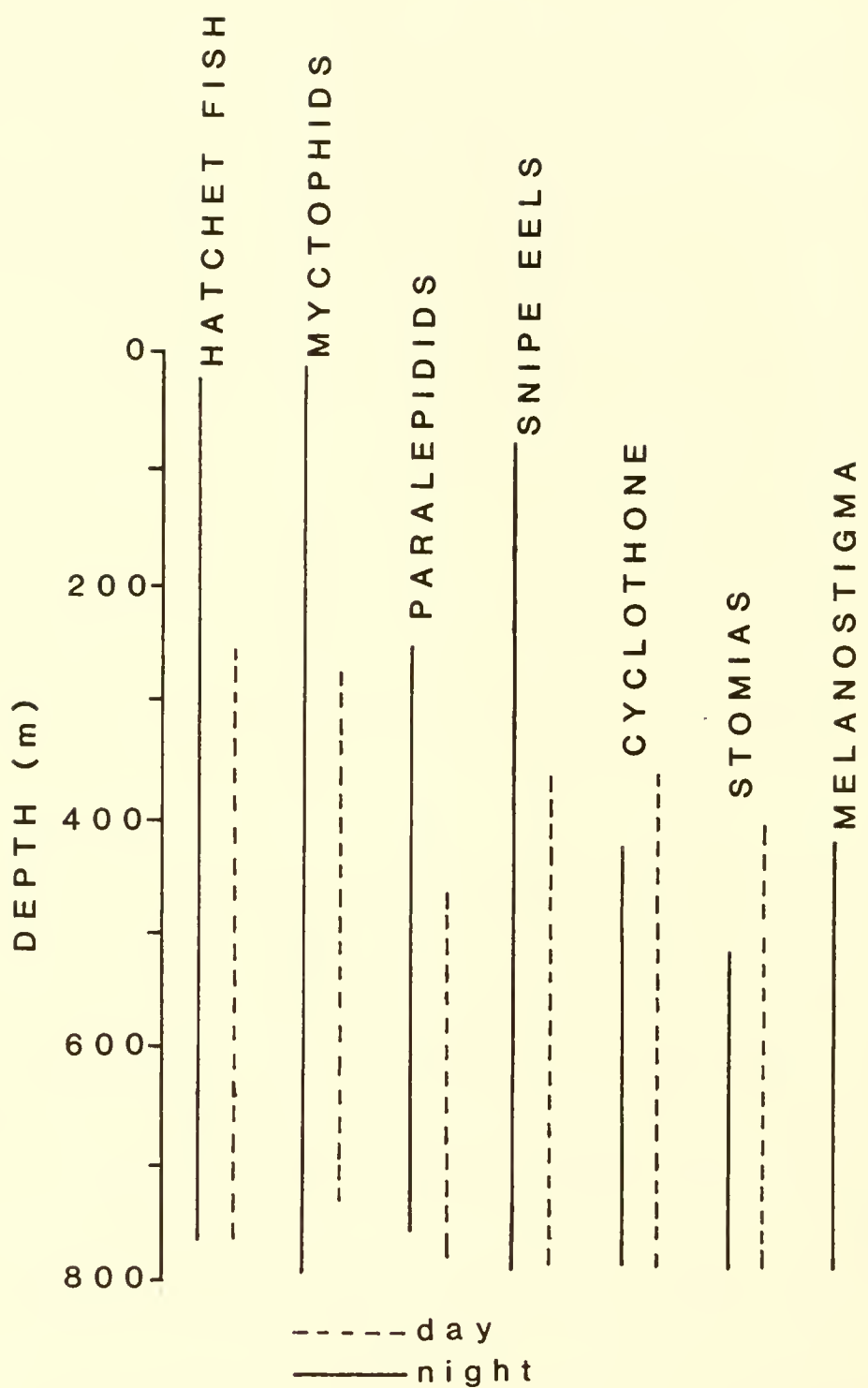


Figure 4. Day and night vertical distributions of dominant fishes.

diel vertical migration. Hatchet fishes and myctophids were found below 250 m by day but were found in the upper 100 m at night. Snipe eels (Nemichthyidae) were found deeper than 350 m by day but move up into the upper 100 m at night. Paralepidids were found somewhat deeper, >450 m, by day but were found above 250 m at night.

Melanostigma atlanticum, which we nicknamed the "Cheerio" fish because it was mostly seen motionless, curled in a circle, also showed some evidence of a diel vertical migration. During the day it was found at a minimum depth of 600 m but this decreased to 400 m at night. Other common fishes, e.g., Cyclothona spp. and Stomias boa ferox apparently did not vertically migrate or they had a reverse migration since their minimum day depth was slightly shallower than their night depth.

There is some evidence to suggest that some midwater taxa may be more abundant just above the bottom (Wishner, 1980; Smith, 1983). During 1987 we found that on some dives there was an increased number of gelatinous zooplankton near the bottom. Nanomia, an undescribed red cydippid, Beroe, and trachymedusae were sometimes most numerous near the bottom. On several dives Nanomia were so numerous within 10 m of the bottom that many could be seen at any time. Euphausiids sometimes occurred in dense swarms near the bottom at depths of 400 to 600 m. Also the numbers of fishes was sometimes higher near the bottom where midwater and benthopelagic species co-occurred.

## DISCUSSION

For the invertebrate macroplankton and micronekton it was evident that the fauna was dominated, both in terms of species and individuals, by those that were found at depths in excess of 400 m. Only about 20% of the species were observed at depths of less than 300 m and 50% were only seen below 600 m.

Only a single species (Pelagia noctiluca) was found to only occur in surface waters (<300 m). Most of the species which were found in the upper 100 m were eurybathic species e.g., Beroe cucumis, Bolinopsis infundibulum, Meganyctiphanes norvegica, which also were found much deeper and generally were more abundant at greater depths. Thus the midwater invertebrate macroplankton and micronekton fauna in slope waters south of Georges Bank was mostly mesopelagic and although some species occupied a relatively broad depth range the fauna was most diverse at greatest depths.

For medusae, the results of two previous studies of the midwater fauna of the North Atlantic can be compared with the present study. Thurston (1977) and Roe et al. (1984) working in the eastern North Atlantic, at 53-60° N 20° W and 44° N 13° W respectively, both employed discrete depth open-closing midwater

trawls to examine vertical distributions. The overall vertical distributions are similar for the three geographic areas although there are differences. The major difference in the studies is that even though Roe et al., (1984) worked at 44° N their data showed a more shallow distribution for most medusae (the exception was Periphylla periphylla which was taken at the surface at 53-60° N) than does ours at 40°N. All three studies found highest species diversity and greatest numbers of individuals at depths of 600 m and greater. Some of the differences among these studies is due to numbers of samples taken and their depths.

Thurston (1977) and Roe et al. (1984) found evidence for diel vertical migrations, up to 200 m, for a number of midwater medusae including Atolla vanhoeffeni, Pantachogon haeckeli, and Periphylla periphylla. But others e.g., Atolla wyvillei and Halicreas minimum did not migrate.

The most abundant midwater coelenterate off the Grand Banks was the physonect Nanomia cara. Previously N. cara was known to be abundant at shallower depths in this region (Rogers et al., 1978) but its importance at mesopelagic depths was unknown.

We found evidence that midwater siphonophores undertook diel vertical migrations of up to 150 m. Previous studies in the North Atlantic have documented similar diel migrations but this was mainly for calycophorans (Pugh, 1977, 1986).

Because of the extreme fragility of ctenophores almost nothing is known about their existence in midwater (Madin and Harbison, 1978; Harbison, 1986). For example, in one of the most comprehensive studies of the midwater community in the North Atlantic, Roe et al., (1984) only listed a single ctenophore species, Beroe cucumis. Until about a decade ago only three ctenophore species were definitely known to occur in the deep-sea (Madin and Harbison, 1978). However recently, direct observations using submersibles (Madin and Harbison, 1978; Youngbluth, 1984; Mackie, 1985; Harbison, 1986) has shown that the number of midwater ctenophores is large and, in fact, Harbison (1986) states that "the vast majority of ctenophores live in the deep-sea." Our results supports Harbison's conclusion.

Here we found that midwater fishes were mainly below 400 m, day and night. Backus et al., (in preparation) working in the same area found that midwater fish were concentrated in the 400-800 m zone regardless of time of day. We also noted that at night, hatchet fishes, myctophids, and snipe eels occurred above 100 m. Other studies have documented mesopelagic concentrations of midwater fishes and diel vertical migrations (Badcock, 1970; Clarke, 1973, 1974; Roe, 1974; Pearcy et al., 1977; Howell and Krueger, 1987; Karnella, 1987). In some regions 50% of the

midwater fauna may vertically migrate (Young, 1983) but in others the proportion is much less (Pearcy et al., 1977). Although the exact causes of diel vertical migrations are unknown there is good evidence that they are mediated by light and are related to feeding behavior (Zaret and Suffern, 1976).

Possibly if we could determine what factors affect midwater vertical distributions we might be able to better understand vertical migrations. The major environmental parameters which affect vertical distributions are light, temperature, and abundance of prey and predators (Roe, 1974; Merrett and Roe, 1974; Zaret and Suffern, 1976; Enright, 1977; Young, 1983; Larson, 1986; Pugh, 1986). It appears that physical factors, most importantly temperature, may determine the overall vertical limits of a given midwater species but biological parameters, mainly food availability and predation pressure, determine the normal range. Vertical migrators must be able to cope with a broad range of temperatures, up to 25°C in the tropics. They probably do this so that they can feed on the more abundant zooplankton in the upper 100 m (Roe, 1972).

Although light is important in determining vertical distributions it mostly acts indirectly through feeding success and predation (however, we have observed the lethal effects of light on siphonophores). As a result the mesopelagic may act as a partial refuge from visual predators. However, even in the lower mesopelagic where vision may be limited, tentaculate, gelatinous predators are abundant and they may be significant causes of mortality.

Direct observations on the behavior and associations between midwater organisms are needed to provide essential data for understanding the vertical distributions and ecology of midwater organisms. Our results will be the subject of future papers.

This contribution is number 16 of Direct Studies of Mesopelagic Communities.

#### LITERATURE CITED

Backus, R. H. and J. E. Craddock. 1982. Mesopelagic faunal provinces and sound-scattering levels in the Atlantic Ocean. In: N. R. Anderson and B. J. Zahuranec (eds.), Ocean sound scattering production. Mar. Sci., Vol. 5, , pp. 529-547.

Badcock, J. 1970. The vertical distribution of mesopelagic fishes collected on the SOND cruise. J. Mar. Biol. Assoc. U.K., Vol. 50, pp. 1004-1044.

Clarke, T. A. 1973. Some aspects of the ecology of lanternfishes (Myctophidae) in the Pacific near Hawaii. Fish. Bull., Vol. 71, pp. 401-434.

Clarke, T. A. 1974. Some aspects of the ecology of stomiatoid fishes in the Pacific near Hawaii. Fish. Bull., Vol. 72, pp. 337-351.

Enright, J. T. 1977. Diurnal vertical migration: Adaptive significance and timing. Part 1. Selective advantage: A metabolic model. Limnol. Oceanogr., Vol. 22, No. 5, pp. 856-872.

Harbison, G. R. 1986. Toward a study of the biogeography of pelagic ctenophores. In: A. C. Pierrot-Bults, S. van der Spoel, B. J. Zahuranec, and R. K. Johnson (eds.), Pelagic Zoogeography. Unesco Tech. Paper. Mar. Sci., No. 49, pp. 112-117. Paris, UNESCO.

Harbison, G. R., Madin, L. P. and N. R. Swanberg. 1978. On the natural history and distribution of oceanic ctenophores. Deep-Sea Res., Vol. 25, pp. 233-256.

Howell, W. H., and W. H. Krueger, 1987. Family Sternopychidae, marine hatchetfishes and related species. In: R. H. Gibbs and W. H. Krueger (eds.), Biology of the midwater fishes of the Bermuda Ocean Acre. Smithsonian Cont. Zool. No. 452, p. 3250.

Iselin, C. O. 1936. A study of the circulation of the western North Atlantic. Pap. Phys. Oceanogr. Meteorol., Vol. 4, pp. 1-101.

Karnella, C. 1987. Family Myctophidae, lanternfishes. In: R. H. Gibbs and W. H. Krueger (eds.), Biology of the midwater fishes of the Bermuda Ocean Acre. Smithsonian Cont. Zool. No. 452, pp. 50-168.

Larson, R. J. 1986. Pelagic Scyphomedusae (Scyphozoa: Coronatae and Semaeostomeae) of the Southern Ocean. In: L. Kornicker (ed.), Biology of the Antarctic Seas XVI. Ant. Res. Ser., Vol. 41, pp. 59-165.

Mackie, G. O. 1985. Midwater macroplankton of British Columbia studied by submersible PISCES IV. J. Plank. Res., Vol. 7, No. 6, pp. 753-777.

Madin, L. P. and G. R. Harbison. 1978. Bathocyroe fosteri (gen. nov., sp. nov.), a mesopelagic ctenophore observed and collected from a submersible. J. Mar. Biol. Assoc. U.K., Vol. 58, pp. 559-564.

Merrett, L., and H. S. J. Roe. 1974. Patterns and selectivity in the feeding of certain mesopelagic fishes. Mar. Biol., Vol. 28, pp. 115-126.

Pearcy, W. G., E. E. Krygier, R. Mesecar, and F. Ramsey. 1977. Vertical distribution and migration of oceanic micronekton off Oregon. Deep-Sea Res., Vol. 24, pp. 223-245.

Pugh, P. R. 1977. Some observations on the vertical migration and geographic distribution of siphonophores in the warm waters of the North Atlantic Ocean, pp. 362-378. In: Proc. Symp. on Warm Water Zooplankton. Spec. Pub. NIO. Paris, UNESCO.

Pugh, P. R. 1986. Trophic factors affecting the distribution of siphonophores in the North Atlantic Ocean. In: A. C. Pierrot-Bults, S. van der Spoel, B. J. Zahuranec, and R. K. Johnson (eds.), Pelagic Zoogeography. Unesco Tech. Paper Mar. Sci., No. 49, pp. 230-234. Paris, UNESCO.

Roe, H. S. J. 1972. The vertical distributions and diurnal migrations of calanoid copepods collected on the SOND Cruise, 1965. 1. The total population and general discussion. J. Mar. Biol. Assoc. U.K., Vol. 52, pp. 277-314.

Roe, H. S. J. 1974. Observations on the diurnal vertical migrations of an oceanic animal community. Mar. Biol., Vol. 28, pp. 99-113.

Roe, H. S. J., and J. Badcock. 1984. The diel migrations and distributions within a mesopelagic community in the north east Atlantic. 5. Vertical migrations and feeding of fish. Prog. Oceanogr., Vol. 13, pp. 389-424.

Roe, H. S. J., P. T. James, and M. H. Thurston. 1984. The diel migrations and distributions within a mesopelagic community in the north east Atlantic. 6. Medusae, ctenophores, amphipods and euphausiids. Prog. Oceanogr., Vol. 13, pp. 425-460.

Rogers, C. A., D. C. Biggs, and R. A. Cooper. 1978. Aggregation of the siphonophore Nanomia cara in the Gulf of Maine: Observations from a submersible. Fish. Bull., Vol. 76, pp. 281-284.

Smith, K. L. 1982. Zooplankton of a bathyal benthic boundary layer: In situ rates of oxygen consumption and ammonium excretion. Limnol. Oceanogr., Vol. 27, No. 3, pp. 461-471.

Swanberg, N. 1974. The feeding behavior of Beroe ovata. Mar. Biol., Vol. 24, pp. 69-76.

Thurston, M. H. 1977. Depth distributions of Hyperia spinicera Bovallius, 1889 (Crustacea: Amphipoda) and medusae in the North Atlantic Ocean, with notes on the associations between Hyperia and coelenterates. In: M. Angel (ed.), A voyage of discovery: George Deacon 70th anniversary volume. Oxford, England, Pergamon Press, pp. 499-536.

Wishner, K. F. 1980. The biomass of the deep-sea benthopelagic plankton. Deep-Sea Res., Vol. 27A, pp. 203-216.

Young, R. E. 1983. Oceanic bioluminescence: An overview of general functions. Bull. Mar. Sci., Vol. 33, No. 4, pp. 829-845.

Youngbluth, M. J. 1984. Water column ecology: In situ observations of marine zooplankton from a manned submersible. In: N.C. Fleming (ed.), Divers, submersibles and marine science. Mem. Univ. Occas. Pap. Biol., Vol. 9, pp. 1-118.

Zaret, T. M. and J. S. Suffern. 1976. Vertical migration in zooplankton as a predator avoidance mechanism. Limnol. Oceanogr., Vol. 21, No. 6, pp. 804-813.



THE EFFECT OF PLANT MATERIAL ON A BENTHIC COMMUNITY OF THE  
BERMUDA CONTINENTAL SLOPE

J. Frederick Grassle<sup>1</sup>, Paul V. R. Snelgrove<sup>1</sup>,  
James R. Weinberg<sup>1</sup>, and Robert B. Whitlatch<sup>2</sup>

1 - Woods Hole Oceanographic Institution

2 - University of Connecticut

ABSTRACT

Aggregations of organic material have been shown to be important in determining the composition of deep-sea benthic communities on the continental margin. Using the submersible Pisces, a bottom station was established on the continental slope northwest of Bermuda. Sargassum seaweed collected from surface waters near Bermuda was placed in the sediments to determine the effect of this organic addition on the bottom community. In a period of 37 days the addition of Sargassum resulted in sharp population increases of several relatively opportunistic benthic species.

INTRODUCTION

The small invertebrate fauna of the deep-sea floor rivals rain forest insect faunas in the number of species found in each local collection (Grassle and Maciolek in prep.). The complex patterns of biogenic structures (such as burrows, stalks and tubes) and uneven distribution of organic material settling from the water column introduce the temporal and spatial heterogeneities required to maintain a large number of species. The surface of deep-sea sediments is uneven (from activities of organisms as well as geologic processes) and the flow of water over shallow depressions and burrows ensures a patchy distribution of organic particles settling to the bottom. In contrast to continental shelves and coastal embayments, the bottom sediments are not homogenized by storm waves or intense currents in most deep-sea areas. In these circumstances sediment structures can last for more than a single generation of even the most long-lived deep-sea species.

Despite the complexity of seafloor habitats, it is a relatively easy environment in which to conduct experiments *in situ*. This is because each treatment is a single event, unlikely to be confounded by fluctuations in the physical environment. Dead carcasses of nektonic organisms, clumps of Sargassum weed, and gelatinous clumps of salp bodies from surface blooms produce sharp changes in the abundance of benthic organisms (Grassle and Morse-Porteous 1987). Because of the need for precise placement of samples within and outside experimental treatments, the

submersible Alvin has been the most efficient vehicle for conducting experiments on the seafloor. The difficulty of scheduling Alvin dives separated by several-month intervals and the availability of relatively inexpensive submersibles for use on the continental slope led us to join the NOAA-sponsored Beebe expedition to the Bermuda slope and use the IUC submersible, Pisces VI.

## METHODS

We planned an ambitious series of experiments for Pisces dives to the Bermuda slope. The support ship, TWIN DRILL, was anchored at  $32^{\circ}23'N$  and  $64^{\circ}57'W$  and the station was just beyond the anchor at 763 m depth. In our first few dives, tracer particles of several kinds were spread on the bottom for studies of feeding behavior and bioturbation of the sediments (Whitlatch). Animals were labelled with tetracycline and placed on the seafloor to study growth rates (Weinberg). Effects of fish and shark scavengers on the benthic communities around baits were also to be studied (Grassle and Snelgrove). Because of problems with weather we were only partially able to complete a study of the effects of Sargassum on the benthic community.

Floating Sargassum was collected from Bermudian waters by Robert Burns of the Bermuda Biological Station. The algae was kept frozen until deployment on the sea bottom using the Pisces VI. Only encrusting animals remained on the algae and these were killed during freezing. The Sargassum was carried to the bottom in plastic bags and placed in the sediment depressions left after taking 15 by 15 cm box cores. The box core samples were used to characterize the community at the experimental site and were used as controls for the Sargassum treatment. After a period of 37 days the Sargassum and surrounding sediment was cored using the same box corer. The Sargassum was mixed in with the sediment and none of the animals were observed clinging to the Sargassum. The terrain at the experimental site was flat, however the general topography at this depth (763 m) was very rugged with many sink holes and crevasses in the terrain between steep carbonate buttresses.

We had planned to sample six treatment areas and take samples from the surrounding community when the Sargassum was placed and when it was retrieved. Although this was not achieved because of difficulties with weather and logistics, we were able to obtain some results.

## RESULTS

### Megafauna

The fauna observable on the sediment surface (megafauna sensu Grassle et al. 1975) at 800 m depth on the northwest Bermuda slope was rich and varied. Fishermen regard the area as highly productive and the steeply sloping carbonate buttresses may funnel organic material to the comparatively rare flat areas where sediments accumulate. Throughout the area sediments were marked with many holothurian and sea urchin trails and several kinds of burrows including some containing callianassid shrimp. Brittle stars, echinoids (*Hygrosoma?*), holothurians, anemones (cerianthids and *Actinoscyphia*) and shrimp were abundant. Fish included viper fish (*Chauliodus?*), *Benthosarus*, macrourids, eels, and sharks.

Brisingid starfish and whip corals were among the most obvious animals on the hard surfaces.

### Macrofauna

A maldanid polychaete *Mastobranchus* sp. A was the most common animal in the macrofaunal benthos (Table 1a). This family of polychaetes does not feed at the sediment surface and is abundant in the deep sea at sites rich in organic material such as the upper slope off New England (Maciolek and Grassle in prep.). The other species are in genera common in most deep-sea environments, however it is unusual for the predatory bivalve *Cuspidaria* to be among the ten most abundant species. Five of the ten species are probably predators on meiofauna and perhaps small macrofauna. An increased abundance of predators may be another feature of relatively organic-rich deep-sea environments (Turner 1977).

### Response of macrofaunal populations to Sargassum addition

Each of the species listed in Table 1b was found in both cores. Two of the taxa *Capitella* spp. and *Hesionidae* spp. were entirely juveniles and could not be separated using external morphology. Densities of the seven most abundant species in the *Sargassum* cores are greater than any of the species in the background community. The increases in all but one of the abundant species in the *Sargassum* cores were much greater than the background densities. The two gastropods, the isopod and the polychaete *Ophryotrocha* were not present among the three cores without *Sargassum*. The core with lower numbers of *Capitella* and *Ophryotrocha* contained a 5.4 cm-long gastropod, *Conus* nr. *fosteria*. This species may be feeding on these polychaetes. Of the ten abundant species in the background cores only

Table 1. Average densities of species whose abundance is more than 3% of the fauna before (a) and after (b) the addition of Sargassum. Actual counts from each of the five 225 cm<sup>2</sup> box cores are shown.

p = polychaete, s = aplacophoran, b = bivalve, a = amphipod, i = isopod, g = gastropod, o = oligochaete.

	Ave. #/sq m	#/core n = 3	% contri- bution	Sargassum #/core n = 2
a. Before <u>Sargassum</u> treatments (background fauna)				
<u>Mastobranchus</u> sp. A. (p)	163	5,1,5	8.6	0,0
<u>Pholidostrepia</u> spp. (s)	148	1,0,9	7.8	1,4
<u>Cuspidaria</u> nr. <u>atlantica</u> (b)	133	6,0,3	7.0	1,0
<u>Thyasira obsoleta</u> (b)	104	6,0,1	5.5	0,0
<u>Caulieriella</u> sp. A. (p)	104	6,1,0	5.5	2,0
<u>Litocorsa</u> nr. <u>stremna</u> (p)	89	1,2,3	4.7	0,1
<u>Harpinia</u> sp. A (a)	89	2,3,1	4.7	3,6
<u>Syllis</u> sp. A (p)	74	1,1,3	3.9	2,1
<u>Spionidae</u> spp. (p)	74	1,3,1	3.9	2,1
<u>Pseudomesus</u> sp. A. (i)	59	3,0,1	3.1	1,0
TOTAL		1,896/sq m		

	Ave. #/sq m	#/core n = 2	% contri- bution	Background #/core n = 3
b. After <u>Sargassum</u> treatments				
<u>Capitella</u> spp. (p)	889	9,31	20.6	0,1,0
<u>Cocculina</u> nr. <u>leptalia</u> (g)	356	8,8	8.3	0,0,0
<u>Disconnectes</u> sp. A (i)	356	10,6	8.3	0,0,0
<u>Ophryotrocha</u> sp. B (p)	333	1,14	7.7	0,0,0
<u>Dorvillea</u> sp. A (p)	244	8,3	5.7	0,1,1
<u>Cyclostrema</u> nr. <u>valvatoides</u> (g)	178	7,1	4.1	0,0,0
<u>Hesionidae</u> spp. (p)	179	4,4	4.1	0,2,0
<u>Harpinia</u> sp. A (a)	156	5,2	3.6	2,3,1
<u>Oligochaeta</u> sp. A (o)	133	3,3	3.1	1,0,0
TOTAL		4,311/sq m.		

Mastobranchus sp. A and Thyasira obsoleta are absent from the two Sargassum-treatment cores.

The two Sargassum cores had a mean of 32 species and the three background cores had a mean of 25 species, however, the background density was less than half. More samples would be needed to compare species diversity.

## DISCUSSION

### Experimental design

The experimental design was planned to include more replicates, samples from the background community when the experimental treatments were recovered, and controls in which the sites were cored without the addition of Sargassum. Although this design was not achieved, alternatives to the explanation that the observed effect is the result of organic enrichment are not likely. Similar increases as a result of natural aggregations of Sargassum were observed at 3600 m depth on the continental rise (Grassle and Morse-Porteous 1987). In hundreds of cores without obvious organic enrichment taken at several upper slope stations south of New England (Maciolek and Grassle in prep.) and off the southeast U.S. (Blake and Grassle, in prep.), increases of this magnitude have not been apparent. Sediment disturbance in the absence of organic enrichment is likely to lead to a reduction rather than an increase in fauna (Smith 1986, Grassle and Morse-Porteous 1987).

### Comparison with other studies of plant material on the sea floor

Three of the taxa are the same as those responding to natural increases in Sargassum at 3600 m depth south of New England: Ophryotrocha sp. A, Capitella spp. and Hesionidae spp. (Grassle and Morse-Porteous 1987). The predatory gastropod species Cyclostrema nr. valvatooides has been observed by Turner (1977) on an experimental concentration of wood blocks at slope depths in the Tongue of the Ocean, Bahama Islands. Cocculinid gastropods have previously been observed on seagrass blades from abyssal depths in the Caribbean (Wolff 1976). Eurycopid isopods (Disconectes) have not previously been observed associated with plant material.

### Community characteristics

There are too few samples to compare species diversity, however the pattern of relative abundance in the Sargassum samples is characteristic of disturbed environments (Fig. 1). The most common species in deep-sea communities is generally

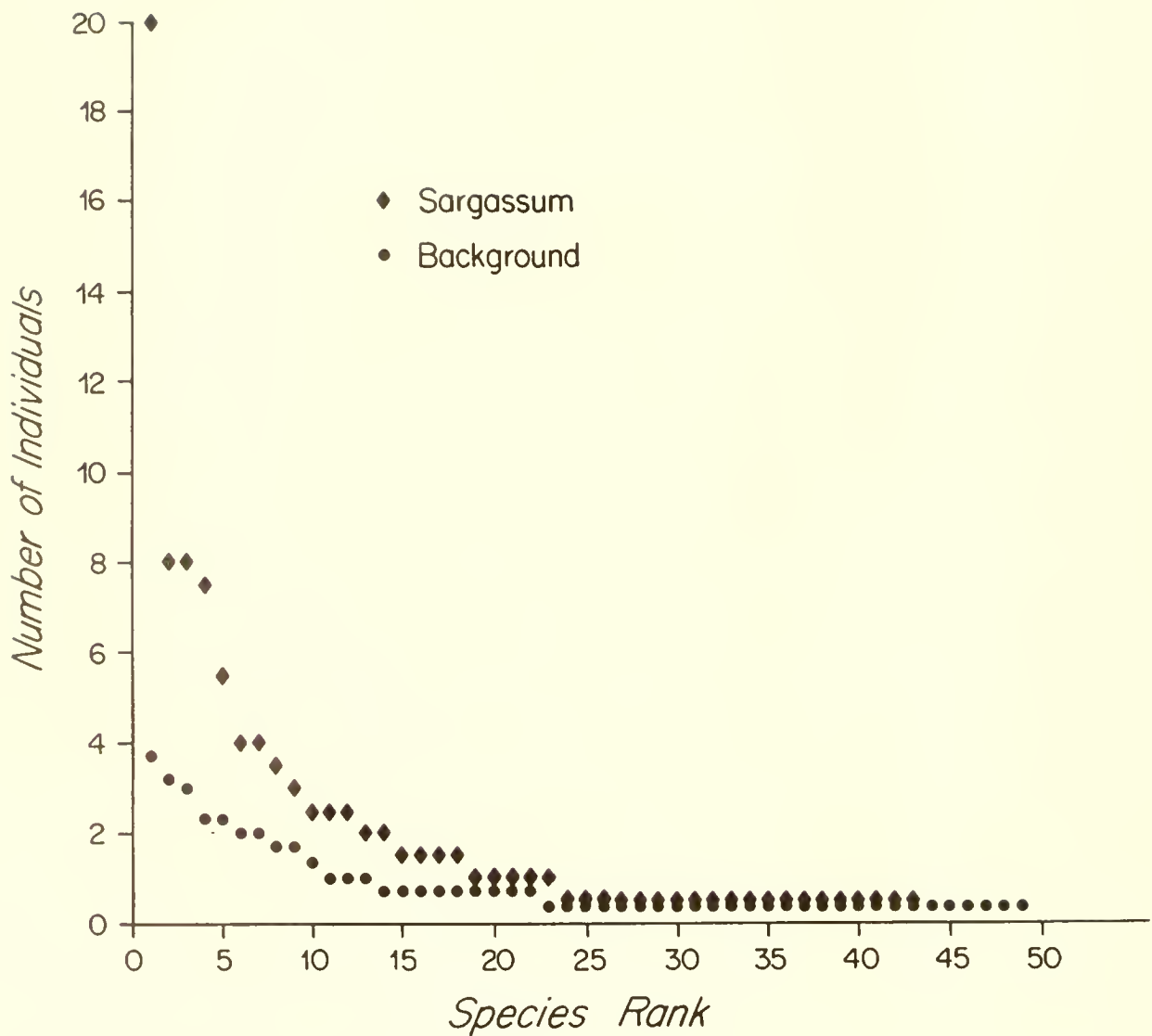


Figure 1. Average number of individuals per  $225 \text{ cm}^2$  for each species ordered by rank from the most common to the least common.

less than 10% of the total fauna (Grassle and Morse-Porteous 1987). In disturbed environments the most common species contributes significantly more than 10% of the individuals. Examples are the high current regime at the HEBBLE site (Thistle et al. 1985) where the most common species is 50-64% of the fauna, the mounds produced by burrowing animals that have a macrofauna consisting of 67% of a single species (Smith et al. 1986), and decomposing Sargassum on the northeastern U.S. continental rise where the most common species is 33% of the fauna.

#### ACKNOWLEDGMENTS

This work was supported by the NOAA Beebe Project and NSF grants OCE-8702836 and OCE-8311201.

#### LITERATURE CITED

Grassle, J. F. and L. S. Morse-Porteous. 1987. Macrofaunal colonization of disturbed deep-sea environments and the structure of deep-sea benthic communities. Deep-Sea Res., Vol. 34, No. 12, pp. 1911-1950.

Smith, C. R. 1986. Nekton falls, low-intensity disturbance and community structure of infaunal benthos in the deep sea. J. Mar. Res., Vol. 44, No. 3, pp. 567-600.

Smith, C. R., P. A. Jumars and D. J. DeMaster. 1986. In situ studies of magafaunal mounds indicate rapid sediment turnover and community response at the deep-sea floor. Nature, Vol. 323, No. 6085, pp. 251-253.

Thistle, D., J. Y. Yingst and K. Fauchald. 1985. A deep-sea benthic community exposed to strong near-bottom currents on the Scotian Rise (western Atlantic). Mar. Geol., Vol. 66, No. 1/4, pp. 91-112.

Turner, R. D. 1977. Wood, mollusks, and deep-sea food chains. Amer. Malac. Bull. 1977, pp. 13-19.

Wolff, T. 1976. Utilization of seagrass in the deep sea. Aquat. Bot., Vol. 2, No. 2, pp. 161-174.



## BEEBE PROJECT: ZOOPLANKTON STUDIES IN THE 1987 FIELD SEASON

Laurence P. Madin  
Woods Hole Oceanographic Institution  
Woods Hole, MA 02543

### ABSTRACT

Zooplankton research was conducted on 11 dives with the Johnson Sea-Link during the Beebe Project off Bermuda in 1987. The work included documentation of abundance and vertical distribution, collection of new or unusual species, and observations of behavior. A lighted platform was deployed at the site to attract midwater animals, but weather prevented completion of these experiments. Observations on vertical and diel distribution showed evidence of vertical migration in narcomedusae, euphausiids, sergestids and squid. Some near surface, gelatinous species were found throughout the water column, whereas other mesopelagic forms were found only below 300 m. A distinctive fauna of red-pigmented organisms from several groups occurred below 700 m. Several new species were seen or collected, including a scyphomedusa in the genus Deepstaria.

### INTRODUCTION

#### Origin and Organization of the Beebe Project

The Beebe Project in 1987 was a multidisciplinary investigation of benthic and pelagic ecology in waters 1000 meters deep off Bermuda. Funded mainly by NOAA's Office of Undersea Research, with additional support from the National Geographic Society and several private donors, the project brought together 6 primary investigators and their assistants, two submersibles and three support ships for a series of dives in July and early August, 1987.

The 1987 program was the third incarnation of the Beebe Project. It began in 1984, to commemorate the 50th anniversary of the bathysphere dives made by William Beebe off Bermuda. At that time Emory Kristof of the National Geographic Society and William M. Hamner of UCLA hoped to recreate Beebe's dives, using the Johnson Sea-Link. The Project was revived in 1986 with a different focus, when Emory Kristof and Eugenie Clark of the University of Maryland used the Pisces VI to bait and photograph deep sea sharks near Bermuda for a magazine article (Clark et al., 1986). An expanded Beebe Project, to include studies on sharks, benthic ecology and midwater organisms, was planned during a 1986 conference on Low Cost Submersibles at the University of Rhode Island, and subsequently proposed to NOAA/OUR, with Larry Madin (Woods Hole Oceanographic Institution) and Bruce Robison (University of California, Santa Barbara) as Co-Principal Investigators.

Two projects in 1987 used the Pisces VI, leased from International Underwater Contractors and supported by their vessel Twin Drill. Fred Grassle (WHOI) established bottom stations northwest of Bermuda for time course experiments to examine the effect of Sargassum falls on the diversity of the benthic fauna (Grassle et al., 1988). The Pisces also was used by Eugenie Clark and Emory Kristof to continue their studies of six-gill sharks. Kristof and Hamner used a new 3-D video camera system to obtain dramatic footage of shark feeding behavior (Hamner et al., 1988). Related work on the six-gill sharks was carried out by Frank Carey (WHOI) who placed acoustic tags on two sharks caught on longlines, and tracked their movements over several days.

The midwater program of the Beebe Project was conducted by William and Peggy Hamner, Madin, and Robison using the Johnson Sea-Link II and the R.V. Edwin Link from Harbor Branch Oceanographic Institution. Although part of the project, Marsh Youngbluth (HBOI) was unable to participate in 1987 due to cruise conflicts.

#### Pelagic Biology Program

Research on midwater zooplankton and micronekton was planned to include studies of vertical distribution, feeding and swimming behavior, and patterns of aggregation of fish, crustaceans and gelatinous animals. By diving repeatedly at the same site, we hoped to characterize the vertical distribution of the fauna, and monitor changes from one day to the next. In order to provide a reference point in midwater, a lighted platform was moored at 300 m. Its lights could be used to illuminate organisms with back- and side-lighting, and to act as an attractant for the aggregation of planktonic animals responsive to artificial light. The Sea-Link could then be used as a darkened blind from which to observe animals around the platform. Unfortunately, weather conditions caused about half the planned dives to be cancelled, including most of the dives at the platform.

In this paper, the author will describe the design, deployment and operation of the midwater platform, summarize the observations on depth distribution of midwater zooplankton, and discuss some of the behavioral observations made. In a separate contribution, Hamner et al. (1988) discuss the design and use of stereoscopic video systems for midwater studies. A new and unusual medusa collected during the dives is described by Larson et al. (1988b).

## METHODS

### Field Operations

Midwater dives were made with the Johnson Sea-Link II, equipped with a 24-canister suction collector, 8 detritus samplers, a color video camera with dual laser-beam size scale, a U-matic videocassette recorder, and a 35 mm Benthos camera and strobe. Details of the design and operation of this equipment are given by Youngbluth (1984). Collected specimens were maintained in refrigerated aquaria on deck or in the lab for observation and photography, then preserved in formalin.

### Observational Data

All dives (except 1419) were made with observers in both the front and rear compartments of the submersible. Their observations on the occurrence, abundance and behavior of organisms were recorded on individual audio recorders. These were subsequently transcribed and combined into a database to facilitate sorting of observational data according to location, depth or type of animal. On each dive we made stops during the descent at 30, 150, 300, 450, 600, and 780 m, for a 5 minute transect to count and identify the animals present. The itinerary for the rest of the dive depended on what was seen, but all dives went to the bottom at some point.

## RESULTS

### Dives Accomplished

We were able to make only 11 of the planned 21 dives, due to weather limitations and damage to the Sea-Link which occurred on recovery of dive 1422. The twelfth dive (1429) was used to film shark-baiting by the Pisces VI. Dates, times, depths and positions of these dives are given in Table 1.

### Design and Operation of the Midwater Platform

The purpose of the midwater platform was to provide a station moored in the water column to which the sub could return on successive dives, and which would support lights, bait packages, and other experimental apparatus for the duration of the field season. The mooring was designed and built at W.H.O.I. by Madin and Russ Peters, with engineering consultation with members of the W.H.O.I. Department of Ocean Engineering.

The platform was constructed on a fiberglass framework previously used for a bottom-landing tripod (Fig. 1). For midwater mooring, the pyramid was inverted to provide an attachment point at the bottom vertex for the anchor, and a flat top surface of about  $1.5 \text{ m}^2$ . Glass spheres for flotation were

Table 1. Johnson Sea-Link II Dives in July, 1987. Times are local (Atlantic), maximum depth in meters. First observer listed was in front, second in rear.

DIVE	DATE	TIME	DEPTH	OBSERVERS	LOCATION
1418	11	2030-2230	646	Madin, Peters	32°23'N 64°58'W
1419	12	1437-2027	646	Robison, none	32°23'N 64°58'W
1420	13	1250-1634	646	W.Hamner, Madin	32°23'N 64°58'W
1421	13	2126-2400	646	Madin, Reisenbichler	32°23'N 64°58'W
1422	14	1300-1500	646	Robison, P.Hamner	32°23'N 64°58'W
1423	16	1315-1640	604	W.Hamner, P.Hamner	32°23'N 64°58'W
1424	18	2300-0300	856	Madin, W.Hamner	32°13'N 64°49'W
1425	19	1035-1415	901	Robison, Reisenbichler	32°18'N 64°39'W
1426	19	1930-2255	922	W.Hamner, P.Hamner	32°16'N 64°44'W
1427	20	1300-1640	928	Madin, W.Hamner	32°16'N 64°44'W
1428	21	0805-1150	916	Robison, Madin	32°18'N 64°41'W
1429	21	1822-2030	916	Calaiyanos, Loates*	32°18'N 64°41'W

\*Nick Calaiyanos, cinematographer for National Geographic Society; Glen Loates, wildlife artist.

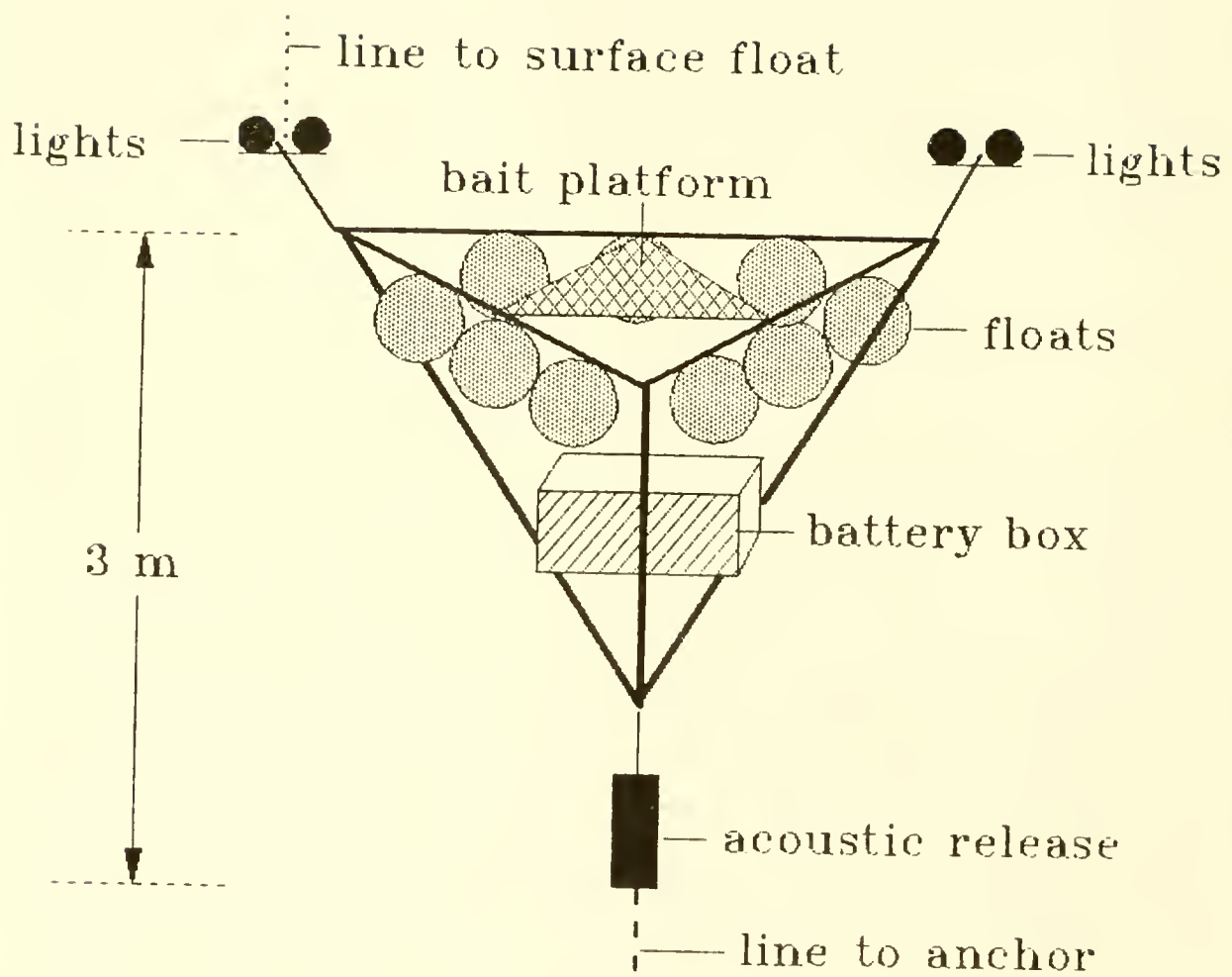


Figure 1. Diagram of the midwater platform moored at 300 m north of Bermuda.

built into the interior of the pyramid. The positively buoyant platform was connected with a Benthos acoustic release to 300 m of 3/8" wire and a 1000 kg anchor of scrap steel. A polypropylene line ran from the platform to a surface float for location of the mooring by the submersible.

Two sets of 12 V lights were mounted on two top corners of the pyramid, a low power pair of 20 watt lamps, and a high power pair of 100 watt lamps. These were powered from a battery box containing 6 12-volt deep-cycle batteries immersed in mineral oil. Each pair of lights could be switched on and off from the surface ship through acoustically controlled auxiliary circuits in the Benthos acoustic release. The low power lights were intended to be turned on from the surface before a dive to attract zooplankton and micronekton to the platform. Once activated, they would remain on for 4 hours, but could be turned off from the submersible via a switch mounted on the platform. The high power lights were intended to illuminate organisms when the submersible was at the platform. They were turned on and off acoustically from the surface, with visual confirmation by the submersible.

A hook on the platform was provided to hang baited traps. One trap was deployed on dive 1422, but nothing was found in it when the platform was recovered.

The submersible was launched on July 12 from the Twin Drill at 32°23'N adjacent to the bottom station established by Grassle. When first visited on Dive 1420, it was found to be moored at exactly 1000 ft (330 m), with the anchor secure on a small patch of level bottom. Efforts to turn on the low power lights from the ship were unsuccessful, evidently because of a relay malfunction at the platform. The high power lights were turned on and found to provide excellent illumination of small, transparent zooplankton. On dive 1421, we were unable to locate the platform at night. The platform was located again on dive 1423, when the high power lights were found still burning after an earlier attempt to find the mooring. After 60 hours of continuous operation the batteries were nearly exhausted. A change in the weather forced us to move to the south side of Bermuda after dive 1423, and we were unable to make any further dives at the platform. It was recovered on July 21 by the Twin Drill, disassembled in Bermuda and shipped back to Woods Hole.

Despite these problems, we felt that the concept of a station moored in midwater was adequately tested, and with improvements, it will be a useful tool for future programs.

## Abundance and Vertical Distribution of Zooplankton

We had no absolutely quantitative means of recording the abundance, sizes or distances of animals seen from the submersible. However, observers recorded their visual observations on audio tape. From transcriptions of these recordings, I have made a preliminary summary of our observations on the occurrence and distribution of the major groups of zooplankton. Table 2 gives the depth range observed and the approximate average number of organisms reported for each group on day and night dives. These numbers only indicate the relative abundance of different major groups, and are not comparable to data from net tows. Observers neither saw everything present nor recorded everything they saw. Estimates of abundance were sometimes absent or vague, especially for small, common organisms like colonial radiolarians, amphipods, and copepods. All the abundance figures should be considered quite conservative. Observations by Robison on dives 1419, 1422, 1425 and 1428 were not available at this writing, but will be added to a later analysis.

### **Radiolaria and Foraminifera**

Colonial radiolarians were often abundant near the surface, but rarely extended below a few hundred meters. They are presumably restricted to the photic zone because of their zooxanthellae. Phaeodarian radiolarians in the genus Coelothamnus (Swanberg et al., 1986) were seen occasionally at greater depths. Forams were reported throughout the water column; larger individuals were usually seen deeper. They were never as abundant as the colonial radiolarians.

### **Medusae**

Narcomedusae were the most abundant type, mainly the genera Solmissus and Solmundella, found in the deeper water column, and Aeginura, seen just above the bottom. The narcomedusae were seen shallower at night than during the day. Few trachymedusae were reported, but small ones could easily have been overlooked. Other hydromedusae were leptomedusae or unspecified types. Coronates were the predominant scyphomedusae; about equal numbers of Atolla and Periphylla were reported, always below 700 m (the corona at 225 m in Table 2 was a Linuche). Other scyphomedusae included Pelagia, both deep and shallow, and a new species of Deepstaria (Larson et al., submitted) seen over the bottom at 900 m.

### **Siphonophores**

Most siphonophores were identified only as physonect or calycophoran types, although species of Agalma, Apolemia, Nanomia, Forskalia and Hippopodius were noted. Somewhat more

Table 2. Summary of diel and vertical distribution of zooplankton observed from the Johnson Sea-Link on 5 day and 4 night dives. Min. and Max. Depth are shallowest and deepest depths (meters) at which animals in each category were reported. Mean No. is the approximate average number of each animal group reported on each dive.

ANIMALS	DAY			NIGHT			Mean No.
	Min Depth	Max Depth	Mean No.	Min Depth	Max Depth		
<b>Radiolaria</b>							
colonial	11	601	>50	23	135	>100	
phaeodiarian	450	841	2	856	856	<1	
<b>Foraminifera</b>	150	811	15	90	781	15	
<b>Medusae</b>							
trachymedusae	150	541	1	541	751	1	
narcomedusae	300	901	5	135	856	4	
other Hydro-	42	811	1	450	922	1	
coronates	225	916	3	751	856	3	
other Scypho-	30	601	1	-	-	-	
<b>Siphonophores</b>							
physonect	30	916	6	30	601	3	
calycophoran	156	841	2	375	511	1	
unspecified	150	601	3	201	922	2	
<b>Ctenophores</b>							
cydippid	90	901	6	180	901	3	
lobate	33	841	5	300	922	3	
thallasocalycid	300	601	2	300	601	1	
cestid	15	691	2	30	631	3	
<b>Crustaceans</b>							
amphipods	30	901	>50	0	911	>100	
copepods	150	916	>50	315	922	>50	
euphausiids	300	901	>50	60	856	>10	
sergestids	450	928	30	75	922	>10	
other "shrimp"	51	928	10	901	922	3	
<b>Chaetognaths</b>	30	871	>50	30	922	>10	
<b>Molluscus</b>							
pteropods	108	108	<1	856	856	1	
heteropods	45	300	<1	-	-	-	
squid	480	751	20	75	856	10	
<b>Tunicates</b>							
larvaceans/houses	60	841	3	300	915	10	
salps	30	841	2	180	526	1	

physonect forms were reported than calycophoran, and species of Nanomia were common around 300 m. Siphonophores in general were found throughout the water column, but deep red physonects were only seen close to the bottom at about 900 m. Some Apolemia were 1-2 m in total length, but no very large siphonophores were seen. Two unknown and possibly undescribed specimens were collected and subsequently given to P. R. Pugh (Institute of Oceanographic Sciences, U.K.) for examination.

### Ctenophores

Ctenophores were fairly abundant and widely distributed. Colorless cydippid species were seen through the whole depth, and at least three deep red species, previously observed but still undescribed, were seen only below 700 m (see also Larson et al., 1988). Most of the cydippids seen had their tentacles extended in fishing position. The lobate ctenophores Ocyropsis and Eurhamphaea, common epipelagic forms, were seen all the way to the bottom at 900 m. On dive 1428, large numbers of Eurhamphaea vexilligera were swimming just above the bottom. A single Deiopea kaloktenota and a few specimens of the mesopelagic Bathocyroe fosteri were reported below 500 m, as well as larger unidentified lobate ctenophores. Several specimens of Thalassocalyce inconstans were seen or collected, always deeper than 300 m. Although originally described from the epipelagic (Madin and Harbison, 1978), this genus is probably mesopelagic. Cestum veneris, the common epipelagic cestid, was seen throughout the water column.

### Crustaceans

Hyperiid amphipods and copepods were abundant on most dives, occurring throughout the water column. During the day they were attracted to the lights of the sub only below 300 m, but at night would swarm around lights at the surface. This aggregation accounts for high numbers in Table 2. The amphipods included species of Themisto and Phrosina, with a few specimens of Scina reported below 700 m. Many copepods and euphausiids were also attracted to the lights, and swarms might be monotypic or mixed. An unusual copepod, not yet identified, was seen at depths greater than 500 m. Red-orange in color, it swam vertically, and had a long strand trailing posteriorly from the telson. We were unable to collect a specimen, but the strand appeared to be a fecal string like those carried by some mysids (Youngbluth et al., 1981).

Euphausiids and sergestids showed distinct diel differences in distribution, occurring much shallower at night. Euphausiids included species of Stylocheiron and Euphausia, some of which were carrying eggs. The shallower sergestids were colorless or white, possibly juvenile stages; larger red and half-red specimens were seen only below 700 m. Other shrimp noted

included decapods like Acanthephyra. Again, the red ones were seen only below 700 m.

### Chaetognaths

No diel pattern of distribution was seen for chaetognaths. Although usually scattered, they were occasionally seen in groups and appeared to be attracted to the lights. A few bright red ones were noted below 800 m.

### Molluscs

A few atlantid heteropods and Pterotrachea were reported from shallow depths. Pteropods seen included one Gleba at 108 m, and several gymnosomes at 856 m. Squid were common on most dives, occurring below about 500 m during the day and much shallower at night. Often we saw only puffs of ink as evidence of their presence, but squid also swam directly at the lights and hull of the sub. At least one large specimen was observed for several minutes while eating a fish.

### Tunicates

Tunicates did not seem particularly abundant. Larvacean houses were scattered through the water column, and salp chains occurred sporadically. The migratory Salpa aspera was seen near the bottom; most other salps, including Salpa cylindrica and Pegea sp., were in the top 300 meters. W. Hamner observed a large red Pyrosoma during a dive in the Pisces VI after the Sea-Link dives were over.

### Behavioral Observations

#### Attraction of crustaceans to artificial light

We intended to use the lights on the midwater platform to attract animals over periods of several hours. During the one dive when we observed the platform lights, few crustaceans were seen, perhaps because it was moored too shallow. Later dives were away from the platform because of weather. We noted aggregation of hyperiid amphipods, copepods, euphausiids, squid and sometimes chaetognaths around the sub's lights on almost every dive. On dive 1421, I recorded the time course of aggregation by crustaceans (mainly amphipods) when the sub's lights were switched on after a period of darkness. The number of animals seen (Fig. 2) is plotted against time elapsed since turning on the lights. The form of this plot is similar to those given by Ste. Marie and Hargrave (1987) for amphipods and other deep-sea scavengers attracted to bait packages on the sea floor. When we are able to measure swimming speeds of the amphipods, it will be possible to estimate the distances from which they were attracted to the light from the time course of their arrival.

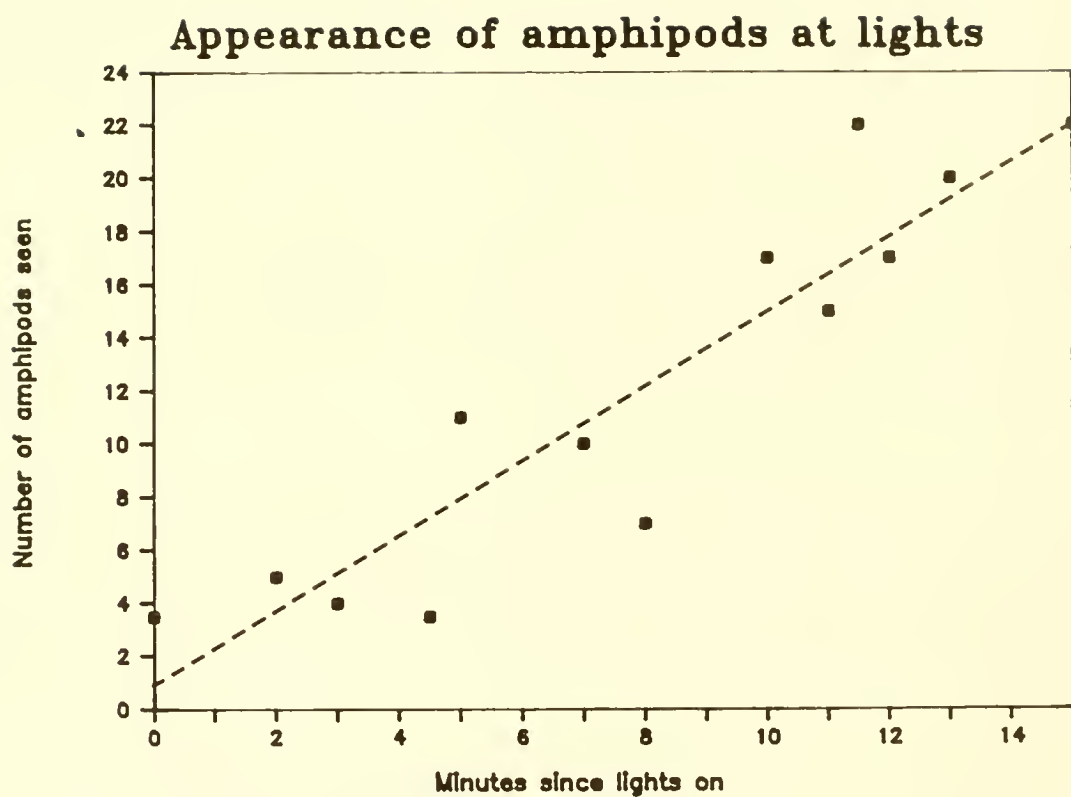


Figure 2. Time course of appearance of hyperiid amphipods to lights of the submersible. The regression line is given by the equation: No. of amphipods = 1.41 (elapsed time, min) + 1.04; N = 13,  $R^2 = .085$ .

## Organisms at the benthic-pelagic interface

Dives 1424 to 1428 were made south of Bermuda over a bottom 900 to 950 meters deep. Here, we found the "red fauna," including medusae, siphonophores, ctenophores, crustaceans and chaetognaths below 700 to 800 meters. Just above the bottom there was often a distinct concentration of zooplankton and fish. Some of these animals may have been driven down by the descent of the sub, but the gelatinous forms showed no such behavior. The red-brown narcomedusa Aeginura was seen only at this depth, drifting just over the bottom with its tentacles hanging down. An undescribed physonect siphonophore, also pigmented red, behaved similarly.

The most dramatic of the benthopelagic animals was a specimen of Deepstaria, about 60 cm in diameter and colored a deep red-brown. This scyphomedusa, a new species in the genus, was seen drifting less than 1 meter above the bottom with its large bell opened downward. We recorded its swimming behavior on videotape, and accidentally triggered its prey capture mechanism while attempting to collect it in the detritus sampler. On contacting a protruding knob of the sampler with the edge of its bell, the medusa contracted around it, enclosing the knob so tightly we could only remove it with the suction collector. We inferred that the medusa captures its prey, perhaps including benthic organisms which swim up off the bottom, by engulfing them in the bell and then ingesting them with the oral arms. A description of the species and its behavior is given by Larson et al. (1988b).

## DISCUSSION

The data presented here are limited by the reduced number of dives we were able to make, and the lack of an opportunity since July 1987 for all observers to participate in analysis of the videotapes. Although these results are only preliminary, some patterns in distribution of macrozooplankton are evident in the summary given previously.

Little restriction in vertical distribution is apparent at high taxonomic levels, like siphonophores or crustaceans as a whole (Table 2), but lower taxa were often limited in range. The vertical distribution of these groups will be refined further when species and genus identifications from the videotapes have been completed.

The distribution of radiolaria appears to reflect their trophic niches, with the photosynthetic colonial radiolaria almost entirely in the top 200 m, and the detritivorous phaeodarians mainly below 800 m.

Among medusae, only the narcomedusae, coronates and Deepstaria were restricted as groups to deeper water. There was evidence of vertical migration in narcomedusae, but not in the other mesopelagic medusae. Both physonect and calycophoran siphonophores were widely distributed as groups, although Apolemia and the unknown red physonects were seen only below 700 m. Many surface-living lobate and cestid ctenophores were found to be eurybathyal in distribution, but the truly mesopelagic genera, including red cydippids, were seen only below 300 m. Larson et al. (1988a) report a broadly similar vertical distribution for gelatinous organisms in waters off New England. They rarely saw medusae above 600 m, but found siphonophores and ctenophores to be widely distributed. Two unidentified species of pigmented cydippid ctenophores, perhaps like the ones we collected, were seen only below 550 m.

The abundance of crustaceans seen from a submersible is always affected by their attraction to the lights. However, estimates of depth distribution based on shallowest and deepest sightings are probably fairly reliable. We found a clear pattern of diel vertical migration for the euphausiids and sergestids, but amphipods and copepods were patchily distributed day and night.

Although we were unable to conduct experiments in attraction and aggregation from the midwater platform, observations from the submersible showed that the time-course of attraction to a light source can be quantified and expressed in the same way as attraction to bait (St. Marie and Hargrave, 1987). During the second and third years of this project, we plan to make more use of moored lights and baits in midwater to study the dynamics of attraction and aggregation.

The distribution of the "red fauna" between about 700 m to the bottom at 900 m was the most distinct discontinuity we observed. With representatives from all the zooplankton taxa, this group does not appear to migrate, and is presumably limited to this depth range by one or more common factors. The red-to-brown pigmentation suggests that obscurity in the blue-green ambience of bioluminescence is of primary importance to this entire community.

Our field work in 1987 has confirmed our belief that in-situ observation and documentation is essential to understand mesopelagic animals and the processes which bind them into a community. With further field time in the oceanic environment we hope to develop more specific models of the distribution, trophic roles and behavioral patterns of the midwater zooplankton and micronekton.

## ACKNOWLEDGMENTS

Thanks to R. Peters and K. Reisenbichler for technical assistance, and the crew of the Johnson Sea-Link and R. V. Edwin Link for able support. The Beebe Project was supported by a grant from the NOAA National Undersea Research Program, with additional support from the National Geographic Society and the National Science Foundation.

## LITERATURE CITED

Clark, E., E. Kristof and D. Lee. 1986. Luring Deep-Sea Life. Nat. Geo., Vol. 170, No. 5, pp. 681-691.

Grassle, J. Frederick, Paul V. R. Snelgrove, James R. Weinberg, and Robert B. Whitlatch. 1988. The effect of plant material on a benthic community of the Bermuda continental slope. In: Michael P. De Luca and Ivar Babb (eds.), Global Venting, Midwater, and Benthic Ecological Processes. National Undersea Research Program Research Report 88-4, pp. 283-289. Rockville, Md., NOAA Undersea Research Program.

Hamner, W. M., C. T. Prewitt and E. Kristof. 1988. Quantitative analysis of the abundance, swimming behavior, and interactions of midwater organisms. In: Michael P. De Luca and Ivar Babb (eds.), Global Venting, Midwater, and Benthic Ecological Processes. National Undersea Research Program Research Report 88-4, pp. 307-317. Rockville, Md., NOAA Undersea Research Program.

Larson, R. J., G. R. Harbison, P. R. Pugh, J. A. Janssen, R. H. Gibbs, J. E. Craddock, C. E. Mills, R. L. Miller and R. W. Gilmer. 1988a. Midwater community studies off New England using the Johnson Sea-Link submersibles. In: Michael P. De Luca and Ivar Babb (eds.), Global Venting, Midwater, and Benthic Ecological Processes. National Undersea Research Program Research Report 88-4, pp. 265-281. Rockville, Md., NOAA Undersea Research Program.

Larson, R. J., L. P. Madin and G. R. Harbison. 1988b. In situ observations of deepwater medusae in the genus Deepstaria, with a description of D. reticulum, sp. nov. J. Mar. Biol. Ass. U.K., Vol. 68, pp. 689-699.

Madin, L. P. and G. R. Harbison. 1978. Thalassocalyce inconstans, new genus and species, an enigmatic ctenophore representing a new family and order. Bull. Mar. Sci., Vol. 28, No. 4, pp. 680-687.

Sainte-Marie, B. and B. T. Hargrave. 1987. Estimation of scavenger abundance and distance of attraction to bait. Mar. Biol., Vol. 94, pp. 431-443.

Swanberg, N., P. Bennet, J. L. Lindsey and O. R. Anderson. 1986. The biology of a Coelodendrid: A mesopelagic phaeodarian radiolarian. Deep-Sea Res., Vol. 33, pp. 15-25.

Youngbluth, M. J. 1982. Utilization of a fecal mass as food by the pelagic mysis larva of the penaeid shrimp Solenocera atlantidis. Mar. Biol., Vol. 66, pp. 47-51.

Youngbluth, M. J. 1984. Manned submersibles and sophisticated instrumentation: Tools for oceanographic research. In: Proceedings of SUBTECH '83 Symposium. London, England, Society for Underwater Technology, pp. 335-344.



QUANTITATIVE ANALYSIS OF THE ABUNDANCE,  
SWIMMING BEHAVIOR, AND INTERACTIONS OF MIDWATER ORGANISMS

W. M. Hamner<sup>1</sup>, C. T. Prewitt<sup>2</sup>, and E. Kristof<sup>3</sup>

<sup>1</sup>Department of Biology  
University of California  
Los Angeles, CA 90024

<sup>2</sup>Geophysical Laboratory  
2801 Upton St. N.W.  
Washington, D.C. 20008

<sup>3</sup>National Geographic Society  
Washington, D.C. 20036

ABSTRACT

Prior efforts to record spatial and temporal distributions of animals *in situ* from submersibles have been based on visual counts or limited to two-dimensional video or photographic records, but 2-D optics are inadequate for quantitative investigations of objects in a 3-D medium. We describe here the 3-D stereo-videoGRAMMETRIC system that we used aboard the Pisces VI submersible off Bermuda in 1987 to record and measure the behavior of midwater organisms and deep-water sharks and compare it with a diver-operated system for shallow water. We discuss some of the laboratory equipment needed to obtain quantitative measurements from these video tapes of the abundance, movements, and interactions of large numbers of animals in a volume of tens of cubic meters. The basic components of a complete underwater image analysis facility are reviewed.

INTRODUCTION

In oceanic research the need to measure distances, shapes and volumes in three-dimensional (3-D) space is critical, whether it be for behavioral studies or for investigations associated with the measurement of physical objects. For many years distance and objects beneath the surface of the sea have been measured and mapped acoustically, but for short range measurements underwater, optical techniques are far more accurate than acoustics. Optical measurement of underwater objects requires that one obtain high quality underwater images in a form that will permit subsequent extraction of point locations in 3-dimensional space. This essay describes the rationale behind the approach that we have taken to record and view the behavior of marine animals at sea.

The numbers and kinds of animals in midwater can be quantified by any number of standard visual or two-dimensional optical techniques. For example, for animals that are not particularly abundant in midwater (e.g. large medusae) we routinely obtain information on density by making horizontal transects at specific depths and recording the number of individuals of particular species that pass through a premeasured area in front of the submarine. Knowledge of the size of this area, speed of the submersible, and duration of the transect gives density. When the animals of interest are more common, one can obtain instantaneous measurements of density by estimating nearest neighbor distances (Hamner and Carleton, 1979; Mackie and Mills, 1983). Unfortunately, measurement of density alone constitutes only a small part of the quantitative information that we wish to record. Density is a mean figure for the number of objects within a given volume; it tells us nothing about the actual location of the objects within that volume. Furthermore, zoologists invariably are interested in the behavior of the animals that they observe, and they need information not only on "how many" or "where," but also on "what" the animals do within the observational arena over time.

In order to extract quantitative information from video tapes on the location of animals and their behavior through time within a three-dimensional volume, optical information must be recorded stereoscopically in order to calculate x-, y-, and z-coordinates. Use of 2-D optics has repeatedly been demonstrated as futile for quantitative investigations of objects or organisms in a 3-D medium such as air or water unless the optics are supplemented with additional information on depth. For example, in the laboratory depth information on the structure of fish schools has been obtained via the use of shadows in conjunction with standard 2-D photography (Cullen et al., 1965; Partridge et al., 1980). But in the field the only way to collect 3-D optical information (besides laser ranging) is via stereoscopic photography (Dill et al., 1981; Potel and Wassersug, 1981; Klimley and Brown, 1983).

#### THE ROLE OF 3-D OPTICS IN MIDWATER RESEARCH

Because of the enormous expense and limited time available for exploration of the midwater realm via manned submersibles or remote vehicles, it is absolutely necessary to obtain as complete a record as possible of each dive on film or on video tape for subsequent analysis in the laboratory. The footage obtained must contain 3-D information and it must be in a form that permits subsequent comfortable viewing by the investigator for long periods of time. The format must be compatible with frame-by-frame computer-automated image analysis because of the immense amount of optical information that is encoded on the film or video tape for any given dive.

The initial decision regarding optical data acquisition relates to the choice between movie film and video tape to record the objects or events of interest. Except for special projects or for situations that require the highest possible resolution, film is far too expensive a medium for recording an entire dive. Video tapes, on the other hand, are inexpensive, available for instant replay, and reusable. Hours of behavioral observations can be permanently recorded or edited immediately. Furthermore, video information is coded electronically and viewed with computer compatible equipment.

Translation from the NTSC video format to RGB computer signals is far easier than translation of analog 16 mm photographs into the digitized format required for computer analysis. The resolution of electronic images is, of course, limited by the design of the video camera, recorder, and monitor, but the current level of resolution is now acceptable for many purposes and the level of resolution in video systems improves each year.

### 3-D Video Optical Systems

One may record 3-D information underwater via an optical system that is either single or dual band. Single band formats are usually simple add-on mirror or prism devices which can be used with standard cameras and projectors. They are relatively inexpensive and avoid the problems of synchronization and optical calibration, yet some of these simple systems have serious inherent disadvantages. We do not use a single band system (a single camera) because this approach creates a 3-D image by using field dividing devices that produce a peculiar vertical field, that have fixed interaxial distance, and do not work well with wide angle lenses (Lipton, 1982). Because of the optical properties of water we often use wide angle lenses to collect data underwater. Furthermore, "...field-dividing devices employing a prism or mirror optic placed over a single objective, known as frame or field dividers (mistakenly called beam splitters), often produce unwanted asymmetry of illumination (vignetting). Since all lenses have illumination intensity and, generally, correction of aberration - in terms of conventional point symmetry, symmetrical about the center of the frame or field - any superimposition of such a split field must produce fields that are matched in terms of illumination and aberration. This is why it is preferable to use dual objectives in stereoscopic photography and projection systems" (see Lipton, 1982).

We currently use two different three-dimensional optical systems for mid-water research in manned submersibles and for shallow water research by scuba divers. Both are color video, dual band 3-D optical systems. For the self-contained scuba diver operated system, two video cameras are mounted in parallel

at approximately human interocular distance between centers of lenses (70 mm) to produce the left and right video images that are recorded on separate left and right VHS recorders. The advantages of this system for shallow water work are that the small, relatively inexpensive cameras and recorders can be packaged in one portable underwater housing and that one does not suffer a major financial loss if the housing floods. This shallow water system produces excellent 3-D images that can be viewed comfortably for long periods of time.

For deeper water investigations that employ untethered manned submersibles we use a system marketed by Stereographics Corporation and designed in part by Lipton (1982). Two video cameras are mounted parallel to each other in separate housings outside the submarine and the images ported inside to a single tape recorder onto which the video signals are multiplexed. The images are presented alternately on a single monitor within the submarine via stereo image alternation using electro-optical shutters at the screen surface and on the glasses worn by the video operator in the submarine, thereby separating the left and right images and creating stereopsis. The advantage of this system for use in submersibles is that the operator can view the images as they are recorded and thereby insure that the best possible information is collected during the dive. The single monitor and recorder are compact, which is an important consideration inside a submarine. The disadvantage of the single monitor-recorder solution is that the equipment necessary to multiplex two video signal electronically onto one video frame is expensive. This system also produces excellent 3-D images that can be viewed for long periods of time without eyestrain. Both systems have sufficient resolution to permit subsequent stereophotogrammetric reconstruction and measurement.

### 3-D calibration of cameras

Potel and Wassersug (1981) stated that "...the real power of the generalized 3-D analysis will come in describing ...geometry ...in natural habitats. A set of stable anchor lines with markers (or fixed landmarks, such as coral heads) and two cameras are the essential equipment necessary to collect data. The Cameras are positioned anywhere. All that the investigator needs to know is the 3-D positions of six reference markers on the anchor lines. If the reference markers can be seen in each image, it is even possible to film the scene with non-stationary movie cameras, subsequently calibrating the perspective views in each frame."

This protocol certainly would permit 3-D photography in the field, but at sea, placement of fixed anchor lines is not possible. We have proceeded instead using the approach of Klimley and Brown (1983), who calibrated their 3-D still cameras prior to use, thereby obviating the need for fixed reference

points within each photograph. Knowledge of the distances between the two cameras and from camera lens to film plate and measurement of the size and horizontal displacement in the paired images of a reference object of known size and distance from the cameras permit accurate measurement of any 3-D object in space. If the cameras are stationary, accurate speeds in 3-D space, etc. can be recorded; if the cameras track a given individual, this animal becomes the reference point and movements of other individuals are calculated in relation to the moving reference point. Recalibration of the cameras is not necessary as long as the cameras are not moved in relation to one another.

### 3-D video projection

The motion picture industry has used two methods to display 3-D images to audiences of more than one person. The anaglyphic method uses complementary colored filters over the left and right projector lenses to superimpose both images on a screen. The viewer wears one red and one green lens to isolate the appropriate image for each eye. But proper anaglyphic projection is extremely difficult because it is technically tricky to balance the color densities of the red and green. The result is invariably a binocular asymmetry in color, resulting in eye strain. Further, two-color mixing processes produce an image with unnatural color. Several years ago the television industry enjoyed a brief flurry of interest in 3-D anaglyphic cable television, but problems of viewing were not resolved and interest in that format quickly waned (Lipton, 1982).

The second common method of viewing 3-D images uses linearly polarized images for the right and left eyes, with the planes of polarization for the two eyes at right angles. Polarizing lenses worn by the viewer occlude the image of the contralateral projection lens, producing one discrete image for each eye, perceived by the brain and processed as are our own retinal images. The optics work fine if the viewer is seated properly in relation to the screen and the head is not tilted sideways. Lateral movement of the head moves the glasses out of alignment with the fixed axes of polarization of the projected image, resulting in distorted 3-D images and rapid eye fatigue due to unnatural tracking patterns of accommodation and convergence.

During the last several years circular polarizing filters have become available, and these "...provide excellent extinction over a wide range of angular rotation, thus providing the opportunity to view 3-D comfortably with great freedom of head motion and position." (Walworth et al., 1984). We utilize this projection technique to view in 3-D the paired video tapes recorded with our shallow water system. The paired images are projected stereoscopically in the laboratory by two video projectors with left and right circular polarizers fitted over

the respective lenses and the superimposed images are viewed on an aluminized screen that preserves polarized light. The viewers wear circular polarized glasses and the human brain then reconstructs a stereoscopic image from the left and right 2-D images that impinge on the left and right retinas.

There is a third method of viewing 3-D images, not as well known nor often employed by the film industry. This is the eclipse method of projection, wherein "...shutters are placed in front of both left and right projection lenses and shutters are used in the spectacles worn by the audience. When the left shutter is opened at the projector, the left is opened at the viewing device, and so on. In this way the observer sees only the image meant for the appropriate eye" (Lipton, 1982). The eclipse method is also called Stereo Image Alternation (SIA) and is "...the most successful stereoscopic system used for stereoscopic viewing of projected overlapping diapositives" (Moffitt and Mickhail, 1980). The image to each eye is electronically synchronized with the projector and therefore no optical confusion results. "The main advantage of the SIA system over the anaglyph and polarization systems is the more brilliant image on the viewing platen. The SIA system is also most suitable for viewing color diapositives." (See Moffitt and Mickhail, 1980.) Eclipse projection has not been widely used in the commercial film industry because the optical shutters previously available were electronically sophisticated and, until quite recently, were too costly to supply to an audience with the propensity to take them home after the show. The newest generation of liquid crystal shutters, however, are relatively cheap, comfortable, and the screen can be viewed from any of a variety of angles by a reasonably large number of people, limited only by the number of optical shutters provided.

### Computer Analysis of 3-D Images

Once the events that transpired on the dive have been appropriately recorded, the data must be analyzed. Four problems are associated with data analysis: the volume of data, analysis of motion, 3-D spatial reconstruction, and complete image analysis. We quote extensively from Potel and Wassersug (1981):

"The first problem involves the volume of data ... Given the large number of [animals observed during a dive] it is necessary to record accurately the positions of all individual organisms [so that their interactions can be accurately evaluated]. Knowledge of spatial distribution of organisms precedes statistical evaluation. Thus, the first intrinsic problem ...is the enormous amount of positional information that has to be recorded."

"The second intrinsic problem...is the analysis of motion. Continuous motion can be reduced to discrete events by a still camera, [but]...meaningful analysis of changes in position requires a more dynamic record, such as that provided by video or motion picture cameras...A scientist with a movie camera can record in a few seconds more raw information on film about the motion of a single object than he can quantify and analyze by hand in months..."

"A third intrinsic problem is that of the third spatial dimension. A frequent simplifying assumption is that oceanic organisms can be studied as a two dimensional problem just as one might study land-based animals. But except in the shallowest of water the spatial arrangement of [oceanic animals]...is inherently three-dimensional...Thus, the proper study of [oceanic animals]...involves determining the positions of individual organisms in three dimensions."

"A fourth problem involves the necessity on occasion to analyze each picture completely for its full information content. In classical signal-processing-based computer image analysis a photograph or video image must be digitized point for point or pixel by pixel. For a standard JVC video chip this requires some 500,000 entries, each evaluated in terms of pixel density (commonly 98 shades of grey). The image then must be processed for noise removal, edge detection and edge linking, statistics and shape metrics, and image classification. Obviously such a task is impossible to accomplish manually because of the time required to enter such an enormous data set physically into the computer. At present only the largest and most expensive computers such as the Cray can do full-image analysis in real time. Minicomputers can accomplish all of the tasks required but must deal with them sequentially and much more slowly because of the magnitude of the computations involved."

#### Automated Tracking of Objects in 3-D Space in Real Time: Sacrifice of Information for Time

Historically, two computing systems have been used to track behavior of marine or fresh water organisms. The system in use at the University of Chicago, called the Galatea system, can resolve all of the problems noted previously (Potel et al., 1979; 1980), but the Galatea system is limited by the fact that the data still must be manually digitized. (Also it is one of a kind and not available commercially.) However, one cannot afford to rely on operator data input. If one were to manually digitize the movements of 20 fish in three-dimensional space, and record their positions via stop-frame analysis at 30 frames per second, it would require over a half-million file entries to digitize 10 minutes of data. At one entry every three seconds (far faster

than most could manage), it would take about six months to digitize 10 minutes of video footage. Unless the data can be for the most part digitized automatically, a study of the video tapes that should constitute a record of every submersible dive would just take too much time.

The second prototype digitizing system (apparently not in current operation), the Bugsystem, was constructed some 15 years ago (Graves, 1977; Koltes, 1984; see also Miller et al., 1982). The Bugsystem is more sophisticated than the Galatea system in that a computer is used to recognize specific images and it then automatically tracks the movements of those images over time. The operator does not manually introduce data into the computer. This system recognizes specific objects by preprocessing each video frame for contrast discontinuities, then outlining the object and summarizing its position in space as a single centroid. This machine therefore sacrifices visual information in order to track movements of objects in real time. We currently use a commercially available descendant of the Bugsystem, the ExpertVision Integrated Motion Analysis System, which is capable of 3-D tracking of objects recorded by multiple cameras placed at any angle and through any transparent media or mixtures thereof (such as an air-water interface).

Even though we have stressed the need for automatic data analysis, the need still exists for non-automated, human interactive capabilities. In short, machines make mistakes. During the process of automatically tracking a given individual like a shrimp or squid within a school the ExpertVision system gets confused when images are occluded and/or adjacent tracks become too precisely aligned. In this event the scientist can usually determine what actually happened by reviewing the original 3-D video tape again and again at slower and slower speeds. This is because humans use much more visual information than that provided by stereopsis in order to judge distance. For example, we use retinal image size, linear perspective, overlapping, aerial perspective (haze), light and shadows and directional reflection, color, textural gradients of acuity, motion parallax, accomodation, convergence, disparity, and stereopsis, whereas the computer relies on stereopsis alone for z-coordinate calculations (Lipton, 1982). What all this means is that the biologist must be able to intrude into the digitizing process and interact with the computer via an appropriate computer compatible language to edit the files as they accumulate (Potel et al., 1980). The ExpertVision System permits interactive editing of data files.

#### Complete Analysis of Stereopaired Images: Sacrifice of Time for Information

We have been able to track the movements in 3-dimensional space of animals ranging in size from approximately 5 mm (large

copepods in the laboratory) to 5 meters (6-gill sharks in the Atlantic at 6,000 ft.). This is a major breakthrough in underwater imaging, but the nature of our approach to image analysis (which sacrifices information content to track in real time) limits our use of the original stereopaired video tapes. We cannot now extract photogrammetric data from the tapes for automated measurement because our motion analysis program must reduce successive images of each individual to a series of points (centroids) moving in 3-D space. For example, although we can track the movements of the 6-gill sharks around baits of tuna at 6,000 ft. with great precision using 3-D cameras mounted on the Pisces submarine, we do not have the computer capability for automated measurements of body lengths, shapes, and surfaces needed in order to compare the individual sharks recorded on the tapes. In short, the digitized data taken from the stereometric paired tapes cannot distinguish whales from submarines nor can one measure the sizes or plot the shapes of those objects, which is the starting point for all modern 3-D image analysis. We intend to develop this capability in the future because measurement of objects is absolutely critical for all aspects of underwater science, from analysis of the behavior of fish to mapping the shape of natural or man-made objects.

Image analysis is now accomplished automatically by a computer through almost instantaneous "frame grabbing" techniques. Still, each data set is very large and the digitized information from the original images quickly fills the memory even of large computers. Intermediate sized minicomputers commonly frame-grab 2 to 4 video images at once, but complete analysis of each image can last minutes or hours depending on the analytical task required. The result is that if one wants complete image analysis (as is required for any photogrammetric application) one must sacrifice real-time processing in order to obtain a complete pixel by pixel analysis. It is important to stress that the original video sequences from which we obtain information on movements of marine animals in 3-dimensional space are recorded under water with stereometric video cameras, aligned and calibrated in such a way that we could also use the full information content of the tapes for photogrammetric reconstruction. Several image analysis computers are now available that apparently can do these tasks.

### Information Analysis

Most biologists are unfamiliar with the mathematics involved in 3-D statistics and 3-D reconstruction, but these are commonly used in the discipline of x-ray crystallography. We will use these tools for reconstruction and predictive modelling of aggregation and behavior in three-dimensional space, and use computer animation to test the applicability of our models. We will discuss this aspect of the subject in a later publication (Prewitt and Hamner, in preparation).

## SUMMARY

A complete underwater image facility should incorporate five components:

- 1) High-quality 3-D underwater dual band optics for data collection.
  - A. Shallow water system: compact, diver operated, no immediate 3-D replay.
  - B. Deep-water system; cameras mounted on submarine; internal immediate 3-D review capability.
- 2) 3-D video viewing system.
  - A. Dual-band 3-D video projection theater.
  - B. Single or dual-band 3-D video monitor display.
- 3) Automated tracking of objects in 3-dimensional space and in real time.  
Sequential-frame motion analysis of digitized objects (e.g. ExpertVision/SUN computer system).
- 4) Photogrammetric reconstruction and full image analysis of stereopaired images.  
Image analysis computer (e.g. PIXAR).
- 5) Mathematical modelling and 3-D computer animation.

## ACKNOWLEDGMENTS

We have quoted extensively from Lipton's Foundations of the Stereoscopic Cinema: A study in Depth and have paraphrased from that excellent source with several of Lipton's shorter phrases remaining intact. We thank him for his comments on our text. We thank J. Mardesich of JayMar Engineering Services for design and construction of the shallow water 3-D housing.

## LITERATURE CITED

Cullen, J. M., E. Shaw, and H. A. Baldwin. 1965. "Methods for measuring the three-dimensional structure of fish schools." Animal Behavior, Vol. 13, pp. 534-543.

Dill, L. M., R. L. Dunbrack, and P. F. Major. 1981. "A new stereophotographic technique for analyzing the three-dimensional structure of fish schools." Environ. Biol. Fishes, Vol. 6, pp. 7-13.

Graves, J. 1977. "Photographic method for measuring spacing and density within pelagic fish schools at sea." Fish. Bull., Vol. 75, pp. 230-234.

Hamner, W. M. and J. H. Carleton. 1979. "Copepod swarms: Attributes and role in coral reef ecosystems." Limnol. Oceanogr., Vol. 24, No. 1, pp. 1-14.

Klimley, A. P. and S. T. Brown. 1983. "Stereophotography for the field biologist: Measurement of lengths and three-dimensional positions of free-swimming sharks." Mar. Biol. Vol. 74, pp. 175-185.

Koltes, K. H. 1984. "Temporal patterns in three-dimensional structure and activity of schools of the Atlantic silverside Menidia menidia." Mar. Biol., Vol. 78, pp. 113-122.

Lipton, L. 1982. Foundations of the Stereoscopic Cinema: A Study in Depth. New York, N.Y., Van Nostrand, Reinhold, 343 pp.

Mackie, G. O. and C. E. Mills. 1983. "Use of the Pisces IV submersible for zooplankton studies in coastal waters of British Columbia." Can. J. Fish. Aquat. Sci., Vol. 40, No. 6, pp. 763-776.

Miller, D. C., W. H. Lang, J. O. B. Greaves, and R. S. Wilson. 1982. Investigations in aquatic behavioral toxicology using a computerized video quantification system. In: J. G. Pearson, R. B. Foster, and W. E. Bishops (eds.), Aquatic Toxicology and Hazard Assessment: Fifth Congress. American Society of Testing and Materials Special publication 766, pp. 206-220.

Moffitt, F. H. and E. M. Mickhail. 1980. 3rd ed. New York, N.Y., Harper and Row, 648 pp.

Partridge, B. L., T. J. Pitcher, J. M. Cullen and J. Wilson. 1980. "The three-dimensional structure of fish schools." Behav. Ecol. Sociobiol., Vol. 6, pp. 277-288.

Potel, M. J., R. E. Sayre, and A. Robertson. 1979. "A system for interactive film analysis." Computers in Biol. Medicine, Vol. 9, pp. 237-256.

Potel, M. J., R. E. Sayre, and S. A. MacKay. 1980. "Graphics input tools for interactive motion analysis." Computer Graphics and Image Processing, Vol. 14, pp. 1-23.

Potel, M. J. and R. J. Wassersug. 1981. "Computer tools for the analysis of schooling." Environ. Biol. Fish., Vol. 6, pp. 15-19.

Walworth, J., S. Bennett and G. Trapani. 1984. "Three-dimensional projection with circular polarizers." Optics in Entertainment II. SPIE, Vol. 462, pp. 64-68.



SESSION SUMMARY: OCEAN SERVICES/BIOLOGICAL PRODUCTIVITY

Ivar Babb  
National Undersea Research Center  
University of Connecticut at Avery Point  
Groton, CT 06340

The six papers presented in the final session of the symposium deal with two major research themes supported by the National Undersea Research Program (NURP) and illustrate the diversity of its science program. NURP augments NOAA's mandate to provide information of an applied science nature by defining a major research theme of Ocean Services. This category fills a niche that exists because of the inadequacy of conventional oceanographic techniques information of high resolution and small scale. Conversely, research of a pure science nature that NURP supports is exemplified by the papers that focus on the topic of Biological Productivity.

The first Ocean Services paper of Cunningham and Colwell reflects NURP's commitment to scuba diving as a productive means to conduct in situ research. The paper summarizes our knowledge of the hazards that threaten the scuba diver in polluted waters and has direct applicability by alerting divers to the nature of hazards present in these waters and precautions that can minimize their impact.

Two Ocean Services papers were presented that utilized the unique capabilities of manned submersibles and ROV's to assess the efficiency and impact of two distinct types of fishing gear. The paper by Bublitz presents preliminary observations of the behavior of the Alaskan flatfish species in response to commercial trawls. These observations indicate that the initial reaction of the fish were to audible stimuli, but that the field of binocular vision played an important secondary role in determining fish behavior. The paper of Cooper et al. summarizes the results of a 3-year study of the abundance and potential impacts of lost gillnets in the Gulf of Maine. Recommendations are provided to better manage this gear impact problem.

The first paper dealing with Biological Productivity, by Watanabe et al., described the progress of a successful mariculture project designed to raise freshwater tilapia in saltwater cages at the Caribbean Marine Research Center (CMRC). Another presentation of CMRC's involvement with the productivity of important living resources was by Wicklund et al. that summarizes information on the life cycles of the queen conch, Strombus gigas. The final paper of Hay et al. provides insight into the complex interactions between the seaweed Halimeda and herbivorous reef fish. This seaweed appears to rely on chemical defenses to protect its nutritionally valuable new tissue.



## HAZARDS TO DIVERS IN POLLUTED WATERS

Kelly Cunningham and Rita R. Colwell

Department of Microbiology

University of Maryland

College Park, MD 20742

### INTRODUCTION

Obvious examples of exposure of divers to chemical and microbiological pollutants include underwater repair or construction in sewage outfalls, chemical disposal tanks or nuclear reactors. Divers participating in research studies may enter polluted waters to place animals for bioaccumulation studies or tidal gauges for hydrographic studies. Pollutants encountered by divers derive from a wide variety of sources, including sewage treatment plants, industrial waste outfalls, agricultural and urban runoff, and waterway spills of petroleum products. Phoel (1981) cited an incident which occurred in 1980 involving an explosion at the Elizabeth, New Jersey chemical waste storage site. Approximately 20,000 55-gallon drums containing acids, solvents, pesticides, explosives and carcinogens were destroyed and the contents of the drums washed into the Bayonne Bay, along with the water used to fight the fire. This is an extreme example; however, the total number of chemical spills into the nation's waterways each year is estimated at 15,000 (Tejada, 1985). In addition to chemical pollution, hazards also include bacteria, viruses and protozoans which enter waterways with human sewage disposal.

It has often been assumed that pollutants entering a water system are diluted and dispersed. As a consequence, little consideration has been given to the effects of pollutants on divers. Pennella, (1981) described the common medical problems faced by Navy divers to be ear and eye infections, infected cuts and gastrointestinal infections, but he also notes, with respect to diving in hazardous waters, "To date the operational diver has been ill-equipped to work in this environment."

### DIVER CONTAMINATION

Several studies have been carried out to investigate the contamination of divers during diver operations. Coolbaugh et al. (1981) reported results from the assessment of bacterial contamination of divers during exercises in Norfolk, VA, Seattle, WA, and New York, NY. Sampling at the NOAA Atlantic Marine Center, Norfolk, VA, included 16 divers who wore four different combinations of diving gear: standard neoprene foam wet suit with standard mask (SCUBA); Unisuit with AGA full-face mask; Unisuit with Superlight-17 hood/mask; and Unisuit with Kirby-Morgan helmet. Before and after each dive, divers' nose, throat,

ears, and mask were swabbed with sterile cotton-tipped swabs. Samples were transferred to culture media, and assessments of bacterial contamination of divers was based on two criteria: approximate quantification of viable organisms at each body site sampled, and identification of potential pathogens that were present only after the dive. All three of the divers in SCUBA masks were contaminated after the dive, with Aeromonas sobria and Aeromonas hydrophila being the predominant post-dive isolates. In contrast, of the 13 divers wearing AGA, Superlight-17 or Kirby-Morgan type masks which offer more protection, only one showed post contamination of the ear.

Similar sampling procedures were used at the NOAA Pacific Marine Center, Seattle, WA. Results were similar to the Norfolk study, i.e., when wet suits with hoods were worn, heavy post-dive ear contamination occurred. Consequently, one diver developed severe ear infection caused by Pseudomonas aeruginosa. The authors postulated that increased humidity and heat inside the suit promoted rapid growth of the divers' normal flora.

The studies of Coolbaugh et al. (1981) and Brook et al. (1982) highlight several important aspects of diving in polluted waters. First, standard wet suits offer little protection against hazards encountered in polluted waters. Second, while more protective gear such as the Unisuit or variable volume dry suit do lower the possibility of contamination, divers may still be colonized with pathogens from the water and come into contact with toxic chemicals dumped into waterways. Thirdly, a paradox is created by the need to protect divers with sufficiently impermeable suits and hoods while the data presented indicates that the heat and humidity build up inside of protective diving gear promotes rapid growth of normal skin flora which may also be unhealthy for a diver.

#### POTENTIAL PATHOGENS

Marine waters containing enterococci levels of greater than three cells per 100 ml have been cited as unfit for swimming (Cabelli, 1979). But the enterococci are merely indicator organisms and, therefore, do not allow determination of the specific nature of the pollution in these "unfit" waters. Numerous studies have been carried out, however, to quantify precisely and identify pathogens in waters which are used for diving operations (Allen et al., 1979; Attwell et al., 1981; Cavari et al., 1981b; Gottlieb, 1981; Seidler et al., 1979; Daily et al., 1981a; Seidler et al., 1980a). Daily et al. (1981a) studied pathogens isolated from the Anacostia River, which was then the site of the U.S. Naval School of Diving and Salvage and from the New York Bight, site of NOAA diving exercises. Isolates included Aeromonas, Vibrio parahaemolyticus, V. cholerae, Escherichia coli, Klebsiella, Salmonella, Enterobacter and from the New York Bight, group F Vibrio, a potentially highly virulent

Vibrio species (Seidler et al., 1980b). Isolates also included two genera of obligate anaerobes, Bacteroides and Clostridium, several of which were shown to be cytotoxic for Y-1 adrenal cells. Fecal coliform counts from these waters numbered from  $1 \times 10^2$  to  $5 \times 10^3/100$  ml, indicating significant levels of pollution. These investigators also examined the ears, noses, throats and equipment of divers after the divers had been exposed for 30 minutes to Anacostia River water. This survey was conducted in August and October when the water temperature was 20°C and 13°C respectively.

In August, when the water temperature was higher, 90% of the divers' ears and masks were found to become colonized. With a drop in water temperature, the colonization rates were lower, except for the divers' ears which again were colonized in 90% of the divers. The differences probably reflect changes in the microbial populations during the different seasons. Also reported was the observation that exposure to polluted water for only 30 minutes resulted in significant change in the skin flora of the divers, such that it reflected the flora of the diving environment. This has obvious implications for divers who are required to enter heavily polluted waters.

#### Protozoans

Some exposure to potentially pathogenic protozoans in polluted water is likely (Daggett, 1981). There are two genera of amphizoic amoebae of primary concern to divers: Naegleria and Acanthamoeba. There is not a large number of human cases involving Naegleria or Acanthamoeba, but most cases have been associated with water, in particular, thermally polluted freshwater. The only known pathogenic Naegleria species is N. fowleri, which causes primary amoebic encephalitis. This amoeba infects humans by entry through the nose, and, therefore, poses a risk to divers, if the polluted water leaks through the facemask during a dive.

Reported cases of Acanthamoeba include eye infections, respiratory infections, and granulomatous amoebic encephalitis (Daggett, 1981; Martinez et al., 1980; Powers et al., 1978). Entry into the body may be via inhalation, nasal route, ingestion, or through a wound. Acanthamoeba isolated by Sawyer et al. (1977) from sediment collected from the Baltimore Harbor were found to be pathogenic when tested in the laboratory. Sawyer (1980) has also found that Acanthamoeba can be isolated from clean sediment as well as active ocean dump sites. It has been reported that sites from which Acanthamoeba are readily isolated often are sites of elevated coliform counts (Daggett, 1981).

In addition to the amphizoic amoebae, two obligately parasitic protozoans, which may be a hazard for divers, are Entamoeba histolytica and Giardia lamblia. Both organisms cause

intestinal disease and, in both cases, the cysts must be ingested to contract disease. Of importance concerning the risk to divers, cysts of E. histolytica can survive municipal chlorine levels, temperatures of 0°C for several weeks and temperatures close to 30°C for up to three days (Albach and Booden, 1978). They are, therefore, hardy organisms which persist in the environment and may pose a problem if ingested by a diver, especially via splashback through the regulator. E. histolytica and G. lamblia exposure would be most likely to occur in areas where sewage effluent enters because of the intestinal habitat of these protozoans.

### Actinomycetes

Actinomycetes are branched, spore-forming bacteria with elongated mycelia. They are found in the upper layers of soil, but have also been isolated from freshwater (Al-Diwany and Cross, 1978) and from estuarine (Walker and Colwell, 1975) and marine (Weyland, 1969) environments. Most actinomycetes in aquatic habitats are allochthonous organisms washed in with land runoff (Al-Diwany and Cross, 1978). The spores are deposited eventually into the sediment (Cross and Johnson, 1971) and, thereby, Actinomycetes become especially abundant in sediments. These organisms may also be associated with sewage effluent (Lechevalier and Lechevalier, 1974), and with coastal dredge material dumped at sea (Attwell et al., 1981). Actinomycetes species may be obligate pathogens, e.g., Mycobacterium tuberculosis or M. leprea; or they may be opportunists, e.g. Arachnia and Actinomyces spp. However, Actinomycete infections acquired from contact with natural waters are likely to be caused by members of the genus Nocardia, Actinomadura or Streptomyces (Pulverer and Schaal, 1978).

Nocardia enter the body through wounds or via inhalation and may result in systemic or pulmonary nocardiosis. Actinomadura and Streptomyces may enter through skin lesions and give rise to actinomycetoma. The best protection for divers against an Actinomycete infection is to wear protective suits when working in polluted waters and to avoid disturbing the sediment when working near the bottom, since spores of these organisms are prevalent in the sediment.

### Anaerobes

The significance of obligate anaerobes in disease of divers has not been studied as thoroughly as has that of the facultatively anaerobic bacteria. However, Bacteroides and Clostridium sp. are potentially pathogenic for humans. Therefore, if present in polluted waters, they can present a risk to divers. Daily et al. (1979 and 1981c) collected samples from the New York Bight and Anacostia River to determine if obligate anaerobes were present in sufficiently large numbers to represent

a health risk for divers. Anaerobes from these sites included Bacteroides, Clostridium, Butyribibrio, and Propionibacterium, with the majority of the anaerobic isolates belonging to the genera Bacteroides and Clostridium.

Total anaerobic counts were made (obligate and facultative) and differentiation was done by replica plating, i.e., incubating one plate in a 10% CO<sub>2</sub> atmosphere and the other under total anaerobic conditions. In the Anacostia River, total anaerobic counts (TAC) and obligate anaerobic counts (OAC) varied from  $2 \times 10^2$  to  $9 \times 10^3$  cells/ml and 10 to  $1.8 \times 10^3$  cells/ml, respectively, in the water column. The highest TAC and OAC occurred during the summer, when temperatures were warmer and the dissolved oxygen values were lower, e.g., 1-5 ppm. Sediment TAC and OAC showed similar variation, but were higher than the water column counts.

Cultures were also analyzed for cytotoxicity, using the Y-1 adrenal cell tissue culture assay, and for enterotoxin-like activity in rabbit ligated ileal loops. Several of the isolates were found to be cytotoxic, although weakly so, and several elicited fluid accumulation in ligated loops, indicating potential enterotoxigenicity. Based on these findings, obligate anaerobes should be considered a potential health hazard for divers entering polluted waters.

#### Vibrio

There are many species of the genus Vibrio which can be isolated from aquatic habitats. Vibrios which pose a potential risk to divers include V. cholerae, both O1 and non-O1 serotypes, V. vulnificus and group F vibrios. Kaper et al. (1979) recovered 65 isolates of V. cholerae non-O1 from Chesapeake Bay water, sediment and shellfish. Salinity appeared to be the primary factor controlling distribution of V. cholerae, with isolates being recovered only in waters ranging from 4-17 ppt. V. cholerae non-O1 serotype could be isolated at all times of the year, and thus there was no strong seasonal influence on the distribution of these vibrios. A majority of the isolates were positive in the rabbit ligated ileal loop and mouse lethality tests. Therefore, it is not surprising that non-O1 V. cholerae have been implicated in cases of diarrhea (Zafari et al., 1973; McIntyre et al., 1965), septicemia and encephalitis (Fearington et al., 1974). In the Kaper et al. study (1979), no correlation was detected between incidence of fecal coliforms and V. cholerae non-O1. Thus, coliform counts, which are often used to indicate the level of pollution in a body of water, are not necessarily indicative of the presence of V. cholerae. It should be pointed out that the numbers of V. cholerae non-O1 found in the Chesapeake Bay were on the order of 1-10/liter, significantly less than that required for infection if direct ingestion of Bay water were to occur. However, in nutrient enriched waters, such as areas of the Chesapeake Bay exposed to agricultural runoff,

the number of bacteria are typically higher. Under such conditions, V. cholerae could conceivably multiply to a level presenting a risk to divers.

More recently, Colwell et al. (1981) isolated the more virulent Vibrio cholerae serotype O1 from water samples of the Chesapeake Bay and Louisiana salt marshes and sewers. The O1 strains demonstrated positive reactions for fluid accumulation in rabbit ileal loops. Several strains also elicited positive Y-1 adrenal cell assays. In DNA probe analyses, an E. coli labile toxin (LT) DNA probe lit up one of the O1 strains that were tested, indicating the presence of the cholera toxin gene. As with non-O1 V. cholera, the O1 isolates were present in samples collected from areas relatively free of fecal coliforms. Therefore, levels of pollution as indicated by coliform counts do not necessarily provide an accurate estimate of the safety of the waters for either recreational or commercial diving.

Vibrio vulnificus is another species of vibrio which may pose a threat to divers. V. vulnificus has been isolated from seawater, sediment, plankton, and animal samples collected from a variety of locations from Miami, Florida to Cape Cod, Massachusetts (Oliver et al., 1983). It is a ubiquitous microorganism, occurring in widely different geographical areas and has been isolated from a variety of environmental samples, although in relatively low numbers. Of the V. vulnificus isolates tested by Oliver et al. (1983), 82% were lethal for mice upon injection. Although mice pathogenicity does not necessarily imply human pathogenicity, the environmental isolates of V. vulnificus should be considered potential human pathogens. Oliver (1981) also noted that, in cases where V. vulnificus infection was acquired through an open cut, the infections were always associated with seawater. V. vulnificus can be remarkably virulent, causing death if it infects a wound or is ingested. Onset of infection is rapid, with symptoms occurring within 12-16 hours and death can occur within 24 hours.

The organism causes extensive vascular tissue damage, leading to a great amount of fluid accumulation. In cases of V. vulnificus infection acquired by ingesting contaminated seafood, the data indicate that elevated serum iron levels are required to predispose an individual to the infection. In contrast, in case studies where individuals acquired V. vulnificus infection via wound contamination, the victims were relatively healthy to begin with (Oliver, 1981). Thus, while the number of reported cases of V. vulnificus infection is not high, the fatality rate is rather high, and divers should be aware of the risk of such infections if diving with an open wound.

Seidler et al. (1980b) reported the isolation of a bacterium resembling the genus Aeromonas, but requiring salt, from the New York Bight. DNA hybridization experiments and G+C

base composition determinations showed this organism to be more closely related to Vibrio than Aeromonas species. Further characterization showed the bacterium to be indistinguishable from group F organisms isolated from cases of human diarrhea in Indonesia and Bangladesh. Nine of 16 group F strains from the New York Bight showed responses for virulence in both the Y-1 adrenal cell and the rabbit ileal loop assays. Group F vibros, therefore, represent yet another potential human pathogen in coastal waters.

#### Aeromonas

Aeromonads are ubiquitous waterborne microorganisms. Several studies have been undertaken to determine the distribution of Aeromonas spp. in the Chesapeake Bay and its tributaries (Kaper et al., 1981; Seidler et al., 1979; Seidler et al., 1980a; Cavari et al., 1981a). In each study, it was demonstrated that counts of Aeromonas increased with increasing temperature and were highest during the summer months, dropping off with declining temperatures in the fall and winter. From studies of heterotrophic activity Cavari et al. (1981a; 1981b) determined that one reason Aeromonas counts drop off in cold weather is that they are physiologically unable to compete with other microorganisms under such conditions. Furthermore, Seidler et al. (1980a) showed that Aeromonas counts tended to be higher in sediment than in the water column, reaching 300 cells/ml in the water column, compared with  $4 \times 10^5$  cell/g sediment in the Anacostia River in August. Numbers of Aeromonas spp. also exhibit an inverse correlation with salinity and dissolved oxygen, (Kaper et al., 1981; Seidler et al., 1980a) and are, thus, more prevalent in hypoxic waters of medium to low salinity.

Kaper et al. (1981) and Seidler et al. (1980a) have shown that counts of Aeromonas in the Chesapeake Bay and Anacostia River demonstrate significant correlation with total and fecal coliforms. However, Kaper also cites cases whereby A. hydrophila was isolated from samples devoid of fecal coliforms, providing further evidence that traditional coliform counts are insufficient indicators of microbial pollution.

Regarding toxicity of environmental isolates of Aeromonas, Kaper et al. (1981) cite positive Y-1 adrenal cell assays for 71% of 116 isolates tested. In addition, the strains which were cytotoxic also produced fluid accumulation in ligated loops, albeit in low concentrations. Similarly, Seidler et al. (1980a) reported that 39% of A. hydrophila strains and 37% of A. sobria strains isolated from polluted waters produced cytotoxin. Investigating the question of whether a particular subpopulation or biotype of Aeromonas is more likely to be virulent, Daily et al. (1981b) determined that A. sobria is a human pathogen of significance. Furthermore, subpopulations of Aeromonas in the environment may be distinguished on the basis of virulence

factors, including piliation, cytotoxin production, protease, lipase, enterotoxin production and hemolysin. The more virulent environmental isolates of Aeromonas (LD50 for mice less than  $10^7$  cfu), generally possessed these virulence factors, whereas in the less virulent isolates (LD50 for mice greater than  $10^7$  cfu), these were generally lacking (Daily et al., 1981b).

Aeromonas sp. have been reported to be associated with a variety of clinical manifestations: septicemia (Ketover et al., 1973); meningitis (Quadri et al., 1976); endocarditis (Davis et al., 1978); wound infection (Hanson et al., 1977); and acute diarrheal disease (Ljungh et al., 1977). Moreover, infections are frequently acquired as a result of exposure to waters harboring Aeromonas species (Fulghum et al., 1978; Hanson et al., 1977; Joseph et al., 1979). Often Aeromonas species are considered to be secondary opportunistic pathogens. However, there are documented cases in which Aeromonas spp. were isolated as the primary pathogen in a human infection. Joseph et al., (1979), cite a case in which two species of Aeromonas, A. sobria and A. hydrophila, were primary pathogens isolated from a leg wound sustained by a diver conducting operations in the Anacostia River. Both the A. sobria and A. hydrophila were beta hemolytic for sheep erythrocytes and cytotoxic for Y-1 adrenal cells. Also, whole cells of A. sobria caused fluid accumulation in ligated rabbit ileal loops.

A follow-up survey at the site where the diver acquired the infection yielded 193 Aeromonas isolates, of which 25% were cytotoxic (Joseph et al., 1979; Seidler et al., 1979). In addition, Seidler et al. (1979) reported that biotypes and antibiograms of Aeromonas spp. from the Anacostia River were similar or identical to those which infected the diver's leg wound.

In a similar case, a previously healthy young man acquired cellulitis after sustaining a laceration while diving in a shallow water lake in the vicinity of an agricultural drainage ditch (Hanson et al., 1977). A. hydrophila was isolated in large numbers from the wound and was also shown to be the dominant bacterial species in the lake where the injury occurred. Fecal coliform counts along the shoreline of the lake were in the marginally acceptable range and, therefore, wound contamination by A. hydrophila can occur in water with acceptable numbers of pollution indicator organisms.

#### Legionella

Legionella was first described as an important pathogen in 1977, following the L. pneumophila outbreak among the legionnaires attending a convention in Philadelphia. Legionella are nutritionally fastidious organisms with an active amino acid metabolism. Morphologically they are indistinguishable from

other rod-shaped Gram negative bacteria. The disease associated with Legionella is a severe pneumonia, with symptoms including high fever, abscess formation, diarrhea, neurologic symptoms and possible kidney and liver damage, (Weiss, 1981). In the environment, Legionella are present in soil and in water. L. bozemani was isolated from a Navy diver who died of acute bronchopneumonia, following a diving exercise (Bozeman et al., 1968; Brenner et al., 1980). A similar isolate was recovered from a fatal case of pneumonia in a patient who had been thrown from a boat into murky swamp water, where he swam for 15-20 minutes before being rescued. The victim was on antileukemic and immunosuppressive therapy (Thomason et al., 1979). Thus, Legionella spp. may pose a potential threat to divers and a serious threat to the immunocompromised individual.

#### Viable But Non-Culturable Bacteria

It has been reported by Grimes et al. (1986) that allochthonous enteric pathogens can survive for long periods of time in seawater despite the high salt concentration, low temperature and reduced nutrient concentration of seawater. Under such conditions, bacteria can enter into a dormant phase during which they remain viable and potentially virulent. The direct viable count (DVC), a technique developed by Kogure et al. (1979) is useful in detecting allochthonous bacteria in the marine environment that do not die when introduced into seawater. Although the bacterial cells become non-culturable, they retain virulence, as shown by positive response in rabbit ligated ileal loops (Colwell et al., 1985). Similarly, an environmental isolate of Salmonella enteritidis was shown by Roszak et al. (1984) to become non-culturable within 48 hours after being inoculated into a sterile Potomac River water microcosm. Xu et al. (1982) documented the persistence of viable E. coli and V. cholerae, even when the organisms were no longer detectable by conventional culture methods. Rollins and Colwell (1986) reported that Campylobacter jejuni also converts to a non-culturable state under adverse conditions. The implication regarding diving hazards is that while viable but non-culturable cells cannot be detected by conventional techniques, they still pose a potential hazard to divers, evidenced by their return to a virulent state upon passage through an animal system.

#### PRECAUTIONS

It is clear that military and commercial divers who must enter polluted waters may be exposed to a wide variety of pathogens including protozoans and both culturable and non-culturable bacteria. Preventative measures should be taken to reduce the risk of contracting waterborne infections.

A commonly used measure against ear infection is acetic acid application. Brook et al. (1982) carried out a study in

which 4 drops of 2% acetic acid were instilled in the left ears of 14 of 26 divers before diving and 8 of 16 members of a control group who wore diving hoods but remained out of the water. A comparison revealed that 43.8% of the untreated individuals showed an increase in bacterial counts in the ears after diving, whereas 13.6% of the treated individuals showed a similar increase. Thus, acetic acid application can be an effective prophylactic against ear infection associated with diving.

Further preventative measures can be taken to prevent contamination of divers who regularly enter polluted waters. Phoel (1981) recommends that divers who regularly work in polluted water maintain current immunization for diphtheria, tetanus, smallpox, and typhoid fever. Phoel (1981) also gives the following protocol for disinfection of divers. After a dive, the diver should be washed off while still dressed in the dive gear, using either fresh or sea water from the ship's water system. Scrubbing with detergent and hot fresh water make the procedure more efficient. After removing the dive dress, the diver should scrub his hands with an antibacterial soap and then shower. The suit should be washed in 50% bleach and hot fresh water for 20 minutes, rinsed in fresh water, and hung at room temperature to dry. In a study of divers in the New York Bight, a disinfection procedure was employed after the dives, i.e., divers were sprayed with betadine while still fully suited (Coolbaugh et al., 1981). No organisms were recovered from the suit exterior after the disinfection procedure.

Helmets and suits specifically designed to protect divers from microbiological and chemical pollution can improve diving safety. During the mid-1970s, a working group was formed whose purpose was to improve diving safety by selecting and developing new procedures and equipment to protect divers from hazardous materials encountered while diving. The group consisted of the EPA, U.S. Navy, U.S. Coast Guard, the Department of Energy, Undersea Medical Society, University of Maryland and NOAA. Advice from commercial diving companies was also considered.

Smooth-skinned dry suits are now available, which are more amenable to decontamination than the commonly used, coarse-textured foam neoprene suits. Series exhaust valves are available on some commercial helmets and masks which eliminate the problem of water splashback through the exhaust system by trapping water in a cavity between the two valves of the system.

The most comprehensive development in diving safety is the double-layered positive pressure suit under suit (SUS). The SUS combines a foam neoprene dry inner suit worn under a conventional dry suit to protect the diver from leakage and from hyperthermia. Before diving, clean water at a pressure slightly greater than the outside water pressure is pumped into the space between the suit layers. If a leak occurs in the suit, the result is that

clean water flows out rather than the outside water flowing in. The water layer also acts to stabilize the ambient temperature around the diver and acts as a thermoregulator, with a working range of 30-130°F. The primary drawback to the SUS is the need for a clean water supply at the appropriate temperature.

#### CONCLUSION

Increased attention must be paid to the potential threat of acquiring infections with future complications as a result of diving in microbiologically and chemically polluted waters. The combined effect of chemical and microbiological pollutants must be considered since chemicals can irritate a diver's skin or mucosal surfaces and increase the probability of acquiring a bacterial infection. There is clearly a real threat to the health of divers who must work in polluted waters. However, an improved understanding of the hazards and appropriate pre- and post-dive precautions will protect both the divers and support personnel.

#### ACKNOWLEDGMENT

Grateful acknowledgment is made to the National Oceanic and Atmospheric Administration Grant No. NA86AA-D-SG006 for support of the study reported here.

#### LITERATURE CITED

Albach, R. A., T. Booden. 1978. "Amoebae." In: J. P. Kreier (ed.), Parasitic Protozoa II. Intestinal Flagellates, Histomonads, Trichomonads, Amoeba, Ooplinds, and Ciliates. New York, N.Y., Academic Press, pp. 455-506.

Al-Diwany, L. J., T. Cross. 1978. Ecological Studies on Nocardio-forms and Other Actinomycetes in Aquatic Habitats. In: M. Mordarski, W. Kurylowicz, and J. Jeljaszewicz (eds.), Nocardia and Streptomyces. Stuttgart and New York, Gustav Fischer Verlag, pp. 153-160.

Allen, D. A., R. J. Seidler, J. W. Deming, R. R. Colwell, O.P. Daily and S. W. Joseph. 1979. Potential Pathogens Associated with Diving Operations in Polluted Waters. Abstracts of the Annual Meeting of the American Society for Microbiology, p. 230.

Attwell, R. W., R. R. Colwell and J. Coolbaugh. 1981. Actinomycetes, a Possible Hazard Encountered in Diving Operations. Mar. Technol. Soc. J., Vol. 15, No. 2, pp. 36-40.

Bozeman, F. M., J. W. Humphries, J. M. Campbell. 1968. A New Group of Rickettsia-like Agents Recovered from Guinea Pigs. Acta. Virol., Vol. 12, pp. 87-93.

Brenner, D. J., A. G. Steigerwalt, G. W. Gorman et al. 1980. Legionella bozemanii sp. nov. and Legionella dumoffii sp. nov.: Classification of Two Additional Species of Legionella Associated with Human Pneumonia. Curr. Microbiol., Vol. 4, pp. 111-116.

Brook, Itzhak, J. C. Coolbaugh, and R. G. Williscroft. 1982. Effect of Diving and Diving Hoods on the Bacterial Flora of the External Ear Canal and Skin. J. Clin. Microbiol., Vol. 15, No. 5, pp. 855-859.

Cabelli, V. J., A.P. Dufour, M. A. Levine, L. J. McCabe and P.W. Haberman. 1979. Relationship of Microbial Indicators to Health Effects at Marine Bathing Beaches. Amer. J. Publ. Health, Vol. 69, pp. 690-696.

Cavari, B. Z., D. A. Allen and R. R. Colwell. 1981a. Use of Heterotrophic Activity Measurements for Studying the Temperature Effect on the Survival of Aeromonas spp. and for Rapid Screening of Water for Pollution. Mar. Technol. Soc. J., Vol. 15, No. 2, pp. 30-35.

Cavari, B. Z., D. A. Allen and R. R. Colwell. 1981b. Effects of Temperature on Growth and Activity of Aeromonas spp. and Mixed Bacterial Populations in the Anacostia River. Appl. Environ. Microbiol., Vol. 41, No. 4, pp. 1052-1054.

Colwell, R. R., P. R. Brayton, D. J. Grimes, D. B. Roszak, S.A. Huq and L. M. Palmer. 1985. Viable but Non-Culturable Vibrio cholerae and Related pathogens in the Environment: Implications for Release of Genetically Engineered Microorganisms. Bio/Tech., Vol. 3, pp. 817-820.

Colwell, R. R., R. J. Seidler, J. Kaper, S. W. Joseph, S. Garges, H. Lockman, D. Maneval., H. Bradford, N. Roberts, E. Remmers, I. Huq and A. Huq. 1981. Occurrence of Vibrio cholerae Serotype O1 in Maryland and Louisiana Estuaries. Appl. Environ. Microbiol., Vol. 41, No. 2, pp. 555-558.

Coolbaugh, J. C., O. P. Daily, S. W. Joseph and R. R. Colwell. 1981. Bacterial Contamination of Divers During Training Exercises in Coastal Waters. Mar. Technol. Soc. J., Vol. 15, No. 2, pp. 15-21.

Cross, T., D. W. Johnson. 1971. Thermoactinomyces vulgaris II. Distribution in Natural Habitats. In: A. N. Barker, G. W. Gould and J. Wolf (eds.), Spore Research. London, Academic Press, pp. 315-330.

Daggett, Pierre-Marc. 1981. Protozoa from Polluted Waters; Potential Human Pathogens. Mar. Technol. Soc. J., Vol. 15, No. 2, pp. 27-29.

Daily, O. P., J. D. Gillmore, J. E. Perry, L. M. Petrone, S. W. Joseph, R. J. Seidler and R. R. Colwell. 1979. Anaerobic Bacteria Isolated from Polluted Waters. Abstracts of the Annual Meeting of the American Society for Microbiology, p. 230.

Daily, O. P., S. W. Joseph, J. D. Gillmore, R. J. Seidler, D. A. Allen, and R. R. Colwell. 1981a. Water-Borne Microbial Pathogens: Potential Human Health Hazards in Marine Environments. In: A. J. Bachrach and M. M. Matzen (eds.), Underwater Physiology VII, Proceedings of the Seventh Symposium on Underwater Physiology. Bethesda, Md., Undersea Medical Society, Inc., pp. 817-824.

Daily, O. P., S. W. Joseph, J. C. Coolbaugh, R. I. Walker, B. R. Merrell, D. M. Rollins, R. J. Seidler, R. R. Colwell and C. R. Lissner. 1981b. Association of Aeromonas sorbia with Human Infection. J. Clin. Microbiol., Vol. 13, No. 4, pp. 769-777.

Daily, O. P., S. W. Joseph, J. D. Gillmore, R. R. Colwell and R. J. Seidler. 1981c. Identification, Distribution and Toxigenicity of Obligate Anaerobes in Polluted Waters. Appl. Environ. Microbiol., Vol. 41, No. 4, pp. 1074-1077.

Davis, W. A., J. G. Kane, and V. F. Garagusi. 1978. Human Aeromonas Infections: A Review of the Literature and a Case Report of Endocarditis. Medicine, Vol. 57, pp. 267-277.

Fearington, E. L., C. H. Rand, Jr., A. Mewborn and J. Wilkerson. 1974. Non-cholera Vibrio Septicemia and Meningoencephalitis. Ann. Intern. Med., Vol. 81, p. 401.

Fulghum, D. D., W. R. Linton, Jr., and D. Taplin. 1978. Fatal Aeromonas hydrophila infection of the Skin. South. Med. J., Vol. 71, No. 6, pp. 739-741.

Gottlieb, Sheldon F. 1981. Assessing the Potential of Microbial Hazards of Diving in Polluted Waters. Mar. Technol. Soc. J., Vol. 15, No. 2, pp. 12-13.

Grimes, D. J., R. W. Attwell, P. R. Brayton, L. M. Palmer, D. M. Rollins, D. B. Roszak, F. L. Singleton, M. L. Tamplin and R. R. Colwell. 1986. The Fate of Enteric Pathogenic Bacteria in Estuarine and Marine Environments. Microbiol. Sci., Vol. 3, No. 11, pp. 324-329.

Hanson, P. G., J. Standridge, F. Jarrett and D. G. Maki. 1977. Fresh Water Wound Infection Due to Aeromonas hydrophila. J. Am. Med. Assoc., Vol. 238, No. 10, pp. 1053-1054.

Joseph, S. W., O. P. Daily, W. S. Hunt, R. J. Seidler, D. A. Allen and R. R. Colwell. 1979. Aeromonas Primary Wound Infection of a Diver in Polluted Waters. J. Clin. Microbiol., Vol. 10, No. 1, pp. 46-49.

Kaper, J. B., H. Lockman, R. R. Colwell. 1981. Aeromonas hydrophila: Ecology and Toxigenicity of Isolates from an Estuary. J. Appl. Bacteriol., Vol. 50, No. 2, pp. 359-377.

Kaper, J., H. Lockman, R. R. Colwell and S. W. Joseph. 1979. Ecology, Serology, and Enterotoxin Production of Vibrio cholerae in Chesapeake Bay. Appl. Environ. Microbiol., Vol. 37, No. 1, pp. 91-103.

Ketover, B. P., L. S. Young, and D. Armstrong. 1973. Septicemia Due to Aeromonas hydrophila: Clinical and Immunological Aspects. J. Infect. Dis., Vol. 127, pp. 284-290.

Kogure, K., U. Simidu, and N. Taga. 1979. A Tentative Direct Microscopic Method for Counting Living Marine Bacteria. Can. J. Microbiol., Vol. 25, No. 3, pp. 415-420.

Lechevalier, M. P., H. A. Lechevalier. 1974. Nocardia amarae sp. nov. An Actinomycete Common in Foaming Activated Sludge. Internat. J. Systematic Bacter., Vol. 24, No. 2, pp. 278-288.

Ljungh, A., M. Popoff, and T. Wadstrom. 1977. Aeromonas hydrophila in Acute Diarrhoeal Disease: Detection of Enterotoxin and Biotyping of Strains. J. Clin. Microbiol., Vol. 6, No. 2, pp. 96-100.

Martinez, A. J., C. A. Garcia, M. Halks-Miller, R. Arce-Vela. 1980. Granulomatous Amoebic Encephalitis Presenting as a Cerebral Mass Lesion. Acta. Neuropathol., Vol. 51, pp. 85-91.

McIntyre, O.R., J. E. Feeley, W. B. Greenough III, A. S. Benenson, S. I. Hassan and S. A. Saad. 1965. Diarrhea Caused by Non-Cholera Vibrios. Am. J. Trop. Med. Hyg., Vol. 14, pp. 412-418.

Oliver, J. D., R. A. Warner and D. R. Cleland. 1983. Distribution of Vibrio vulnificus and Other Lactose Fermenting Vibrios in the Marine Environment. Appl. Environ. Microbiol., Vol. 45, No. 3, pp. 985-998.

Oliver, J. D. 1981. The pathogenicity and Ecology of Vibrio vulnificus. Mar. Technol. Soc. J., Vol. 15, No. 2, pp. 45-52.

Pennella, J. J. 1981. U.S. Navy Diving in Polluted Waters. Mar. Technol. Soc. J., Vol. 15, No. 2, pp. 10-11.

Phoel, W. C. 1981. NOAA's Requirements and Capabilities for Diving in Polluted Waters. Mar. Technol. Soc. J., Vol. 15, No. 2, pp. 4-9.

Powers, J. S., R. Abbot, M. Boyle, et al. 1978. Primary Amoebic Meningo-Encephalitis - California, Florida, New York. Mrb. Mort. Wk. Rept., Vol. 27, pp. 333-334.

Pulverer, G., K. P. Schaal. 1978. Pathogenicity and Medical Importance of Aerobic and Anaerobic Actinomycetes. In: M. Mordarski, W. Kurylowicz, J. Jeljaszewicz (eds.), Nocardia and Streptomyces. Stuttgart and New York, Gustav Fisher Verlag, pp. 417-427.

Quadri, S. M. H., L. P. Gordon, R. D. Wende, and R. P. Williams. 1976. Meningitis Due to Aeromonas hydrophila. J. Clin. Microbiol., Vol. 3, No. 2, pp. 102-104.

Rollins, D. M., R. R. Colwell. 1986. Viable but Non-Culturable Stage of Campylobacter jejuni and Its Role in Survival in the Natural Aquatic Environment. Appl. Environ. Microbiol., Vol. 52, No. 3, pp. 531-538.

Roszak, D. B., D. J. Grimes and R. R. Colwell. 1984. Viable but Non-Recoverable Stage of Salmonella enteritidis in Aquatic Systems. Can. J. Microbiol., Vol. 30, No. 3, pp. 334-338.

Sawyer, T. K., G. S. Visvesvara, and B. A. Harke. 1977. Pathogenic Amoebas from Brackish Water and Ocean Sediments with a Description of Acanthamoeba hatchetti n. sp. Science, Vol. 196, pp. 1324-1325.

Sawyer, T. K. 1980. Marine Amoebae from Clean and Stressed Bottom Sediments of the Atlantic Ocean and Gulf of Mexico. J. Protozool., Vol. 27, No. 1, pp. 13-32.

Seidler, R. J., D. A. Allen, H. Lockman, R. R. Colwell, S. W. Joseph and O. P. Daily. 1979. Characterization of Aeromonas from the Lower Anacostia River. Abstracts of the Annual Meeting of the American Society for Microbiology, p. 230.

Seidler, R. J., D. A. Allen, H. Lockman, R. R. Colwell, S. W. Joseph and O. P. Daily. 1980a. Isolation, Enumeration and Characterization of Aeromonas from Polluted Waters Encountered in Diving Operations. Appl. Environ. Microbiol., Vol. 39, No. 5, pp. 1010-1018.

Seidler, R. J., D. A. Allen, R. R. Colwell, S. W. Joseph and O. P. Daily. 1980b. Biochemical Characteristics and Virulence of Environmental Group F Bacteria Isolated in the United States. Appl. Environ. Microbiol., Vol. 40, No. 4, pp. 715-720.

Tejada, S. 1985. Safe Diving in Polluted Waters. EPA Journal, March, pp. 28-29.

Thomason, B. M., P. P. Harris, M. D. Hicklin et al. 1979. A Legionella-like Bacterium Related to WIGA in a Fatal Case of Pneumonia. Ann. Intern. Med., Vol. 91, No. 5, pp. 673-676.

Walker, J. D., R. R. Colwell. 1975. Factors Affecting Enumeration and Isolation of Actinomycetes from Chesapeake Bay and Southeastern Atlantic Ocean Sediments. Mar. Biol., Vol. 30, pp. 193-201.

Weiss, Emilio. 1981. The Legionella Group of Bacteria in the Environment and in Human Disease. Mar. Technol. Soc. J., Vol. 15, No. 2, pp. 22-26.

Weyland, H. 1969. Actinomycetes in North Sea and Atlantic Ocean Sediments. London. Nature, Vol. 223, p. 858.

Xu, H. S., N. Roberts, F. L. Singleton, R. W. Attwell, D. J. Grimes and R. R. Colwell. 1982. Survival and Viability of Non-culturable Escherichia coli and Vibrio cholerae in the Estuarine and Marine Environment. Microb. Ecol., Vol. 8, No. 4, pp. 313-323.

Zafari, Y., A. Z. Zarifi, U. S. Rahmanzadeh and N. Fakhar. 1973. Diarrhoea Caused by Non-Agglutinable Vibrio cholerae (Non-cholera vibrio). Lancet, Vol. ii, pp. 429-430.

RECENT PROGRESS IN EXPERIMENTAL SALTWATER  
TILAPIA CULTURE IN THE CARIBBEAN

Wade O. Watanabe<sup>1</sup>, Robert I. Wicklund<sup>1</sup>, Bori L. Olla<sup>2</sup>,  
and Douglas H. Ernst<sup>1</sup>

<sup>1</sup> Caribbean Marine Research Center  
100 E. 17th Street, Riviera Beach, FL 33404, and  
Lee Stocking Island, Exuma Cays, Bahamas

<sup>2</sup> Cooperative Institute for Marine Resources Studies  
National Marine Fisheries Service  
Hatfield Marine Science Center  
Newport, OR 97365

ABSTRACT

The Caribbean Marine Research Center is conducting research aimed at developing technology for mariculture production of tilapias (a euryhaline finfish group) as an inexpensive food source for Caribbean Islands and similar regions where freshwater resources are limiting. Florida red tilapia hybrids (Oreochromis urolepis hornorum x O. mossambicus), found highly adaptable to seawater, were selected for mariculture development, and studies are underway to develop hatchery, nursery and growout methods. A pilot-scale hatchery supporting experimental research and extension projects has been in operation since April 1987 on Lee Stocking Island (Exuma Cays, Bahamas).

Experimental studies have included: 1) the determination of the effects of salinity on growth and reproduction in Florida red tilapia; 2) the development of seawater acclimation methods which minimize the requirement for freshwater during the hatchery phase of production and which maximize survival and growth in seawater; 3) an assessment of the utility of organic fertilizers (i.e., chicken manure) in lieu of prepared feeds for fingerling production in seawater tanks; and 4) the assessment of survival and growth of Florida red tilapias reared in floating cages at a marine site in the Bahamas. A feasibility study on saltwater cage culture of Florida red tilapia in Haiti is also in progress. Results of completed studies and preliminary findings of experiments in progress are summarized.

INTRODUCTION

The Caribbean Marine Research Center (CMRC) is a private, non-profit research organization located on Lee Stocking Island, Exuma Cays, Bahamas. Since July 1984, CMRC has undertaken a program of research aimed at developing technology for marine aquaculture of tilapias (a euryhaline, freshwater finfish group),

as an inexpensive source of animal protein for Caribbean Islands and similar regions where freshwater resources are limiting (Watanabe, Wicklund, Olla, Ernst and Ellingson, in press). Although not indigenous marine species, tilapias were identified as the finfish group best meeting important criteria established by CMRC including, acceptance as food fish, ease of breeding and rearing, ability to utilize a variety of inexpensive feeds of both plant and animal origin, and adaptability of culture methods to lesser developed regions. In addition, euryhaline tilapias are generally able to tolerate a wide range of salinities, suggesting a potential for culture in brackishwater or marine systems. Suitability for high-density culture in cages was also considered an important attribute that would permit farming in coastal waters, thereby minimizing costs associated with construction and maintenance of land-based production systems.

The blue tilapia, Tilapia aurea (O. aureus), was initially selected for seawater culture trials in the Bahamas. In a preliminary study conducted in October 1984, fingerling T. aurea averaging 21.2 g were reared for 90 days in 1.0-m<sup>3</sup> floating cages placed in concrete seawater (34-37 ppt) ponds on Lee Stocking Island (McGeachin, Wicklund, Olla and Winton, 1987). Disease, high mortalities, and poor growth, indicated that T. aurea was not a suitable species for cage culture in full seawater.

Subsequent studies revealed that Florida red tilapia, a hybrid strain originally derived by crossing Oreochromis urolepis hornorum (female) with O. mossambicus (male) (Ernst, Ellington, Olla, Wicklund, Watanabe, and Grover, in press), were highly tolerant of seawater, and studies on culture methodology were initiated. Experimental work has sought to obtain basic information on the biology of the Florida red tilapia hybrid with respect to salinity tolerance as well as to assess production performance in seawater. Work has also begun to extend saltwater cage culture of Florida red tilapia to other areas of the Caribbean Basin, beginning in Haiti. In this paper, recent progress in experimental saltwater culture of Florida red tilapia is summarized.

#### THE EFFECTS OF SALINITY ON GROWTH OF FLORIDA RED TILAPIA

##### Growth of juvenile, monosex males at different salinities

Little information is available on the influence of salinity on growth in tilapias. The effects of salinity on growth of Florida red tilapia, previously unknown, were studied in juvenile, monosex males under controlled photoperiod (12 L: 12 D) and temperature (28°C). A high euryhaline capacity of the Florida red tilapia strain was evidenced by faster growth rates in brackish and seawater than in freshwater, although results appeared to be modified by stocking density. At a high density (20 fish/200-l tank), growth in freshwater was comparable to growth at 10 ppt

and above. Growth under 36 ppt at a low density (10 fish/tank) was lower than that at a high density. At an intermediate density (15 fish/tank), however, there was a clear trend toward increased growth with salinity due to increased food consumption and declining conversion ratios with salinity (Watanabe, Ellingson, Wicklund and Olla, 1988). These results support previous reports of faster growth in brackish- and seawater than in freshwater in certain tilapias including *O. mossambicus* (Canagaratnam, 1966; Jurss, Bittorf, Vokler and Wacke, 1984) and Taiwanese red tilapia hybrids (*O. mossambicus* x *O. niloticus*) (Liao and Chang, 1983).

#### The influence of behavior on growth at different salinities

The apparent density-dependent differences in growth response to salinity observed in these studies suggested that behavioral factors influenced these results. Further investigations revealed that agonistic encounters among fish as well as percentages of fish with damaged fins (due to agonistic encounters) declined with salinity, suggesting that growth response to salinity was influenced by inhibitory effects of territorial aggression, which was mitigated by increasing salinity (Watanabe, French, Ellingson, Wicklund and Olla, 1988). This suggested that aggression impairs growth by lowering food consumption (appetite) and increasing conversion ratios. Hence, as aggression was mitigated by increasing salinity, growth was improved. That behavioral interactions may exert inhibitory effects on growth which vary with salinity, was previously suggested for Taiwanese red tilapia (Liao and Chang, 1983).

#### Growth in seawater pools under maximum feeding

Survival and growth of monosex male Florida red tilapia (1.3 g mean weight) in seawater pools (23-m<sup>3</sup>) under conditions of maximum feeding with a prepared diet (30% protein) were studied. A mean body weight of 467 g was attained after 170 days at a survival rate of 90% (Ernst, Ellingson, Olla, Wicklund, Watanabe, and Grover, in press). Mean specific growth rates decreased as a function of fish size from 9.2%/day to 0.8%/day during the 170 day period, and exceeded reported values for Taiwanese red tilapia hybrids in freshwater. A high growth capacity in seawater from fingerling through market stages was demonstrated.

#### PILOT HATCHERY FOR SALTWATER TILAPIA CULTURE

The methods that have been developed at CMRC for culture of Florida red tilapia in seawater are relatively simple: spawning occurs naturally in brood tanks maintained at low salinity (3-6 ppt groundwater) and yolk-sac-absorbed fry are collected following release by mouthbrooding females. The fry are then sex-reversed by hormone (17 alpha-ethynyltestosterone) treatment to transform genotypic females to phenotypic males (Guerrero, 1975). Monosex culture prevents unwanted reproduction at an early age which

results in overcrowding and stunting and minimizes the possibility of reproduction outside of the hatchery and the likelihood of unwanted introductions. After sex-reversal, fry are gradually acclimated to seawater over a period of 1 week, then transferred to nursery tanks for a period of rapid growth prior to stocking in sea cages.

Construction of a new pilot-scale hatchery to support experimental research as well as extension projects in the Caribbean was completed in April 1987 on Lee Stocking Island. The design and operation of the hatchery, consisting of six 34-m<sup>3</sup> broodfish tanks, twelve 6.5-l egg incubators, sixteen 560-l rearing tanks for sex reversal of fry, and eight 4.9-m<sup>3</sup> tanks for seawater acclimation of sex-reversed fry, were described in detail by Ernst (in press). The hatchery incorporates a system for recirculation of water through biofilters, a critical design feature in the Bahamas where limited groundwater resources must be conserved. Multiple recirculation systems permit simultaneous testing of separate salinity regimes for broodstock holding and sex-reversal so that optimal salinities for maintaining broodstock and rates for acclimation of fry to seawater may be determined experimentally. Spawning, incubation of eggs and sex-reversal of fry may be conducted at any salinity up to that of full seawater (36-37 ppt).

During the period April 9 to July 27, 1987, a total of 796,613 and 536,668 eggs and fry were collected from hatchery broodfish units maintained under salinities of 3-6 ppt and 18 ppt, respectively (Ernst, unpublished data).

#### DEVELOPMENT OF METHODS FOR ADAPTATION OF FLORIDA RED TILAPIA TO SEAWATER

Gradual acclimation of fry to seawater following sex reversal (approximately 35 days post-hatching) has been found to generally result in good survival and growth in seawater. However, the requirement for low-salinity water for maintaining broodstock and for early rearing increases infrastructure costs for recirculation of water and restricts the siting of future hatcheries to areas where low-salinity water is available. Considerable research emphasis at CMRC has been placed on the development of seawater acclimation methods that minimize the requirement for low-salinity water during the hatchery phase of production and that maximize survival and growth in seawater.

#### Selection of optimal life stage for seawater transfer

Low-salinity water requirements during the hatchery phase of production may be reduced by acclimating stocks to seawater at early stages of development. Early acclimation may be accomplished by initiating seawater transfer during the early fry stages or by incubating and hatching eggs at elevated salinities (Watanabe, Kuo and Huang, 1985a,b). This approach may be limited by the fact that,

in tilapias, salinity tolerance varies ontogenetically, suggesting that seawater survival and growth may be affected by the age or size at which seawater acclimation is begun (Watanabe, Kuo and Huang, 1985b). Preliminary results of studies on responses of Florida red tilapia transferred to seawater at different times of the sex reversal period suggest that survival was relatively poor among groups acclimated to seawater before 35 days post-hatching (Watanabe, unpublished data). Corresponding effects on growth are under study. Additional studies are required to determine the relationships between salinity tolerance and age and body size to provide a practical basis for determining optimal time for transfer to seawater.

#### Production of seedstock in brackish- or seawater

An alternative approach to reducing low-salinity water requirements for holding broodstock and early rearing is to maintain and spawn broodstock at elevated salinities. There is evidence suggesting that in tilapias, exposure to a saline environment at the early embryonic stages may confer adaptive advantages to these individuals which improve growth and survival in seawater (Watanabe, Kuo and Huang, 1985a). This approach is generally limited by the fact that, in tilapias, normal reproduction is inhibited by increasing salinity (Watanabe and Kuo, 1985; Ridha, Al-Ahmad and Al-Ahmad, 1985).

The effects of salinity on reproductive performance of Florida red tilapia were studied. Adult breeders were maintained in laboratory aquaria at salinities of 1, 9, 18, 27 and 36 ppt under controlled photoperiod (14 L: 10 D) and temperature (28°C). Egg production and spawning was observed at all salinities, although an inhibitory effect of salinity on reproductive performance was evidenced by a marked decline in fertilization and hatching success at salinities above 18 ppt (Watanabe, Burnette, Olla, and Wicklund, in press). Nevertheless, viable yolksac-absorbed fry were produced at all salinities, including full seawater (36 ppt). These results suggest that although seed production at salinities as high as 36 ppt is possible, productivity declines at salinities higher than 18 ppt. Seed production at high salinity may be practical in areas where low-salinity water is lacking.

#### Seawater survival and growth of progeny spawned at different salinities

A study comparing survival and growth of progeny spawned in brackishwater (18 ppt) with those spawned in freshwater (2 ppt) showed that survival and growth were not significantly different between these groups under a mean water temperature of 27°C. However, when temperatures abruptly declined to below 25°C, survival and growth remained significantly higher in brackishwater-spawned progeny (Watanabe, French, Ernst, Olla, and Wicklund, in press). These results suggest that seawater survival and growth are

not impaired in progeny spawned at salinities as high as 18 ppt, and that brackishwater-spawned progeny possess a higher capacity for survival and growth in seawater than freshwater-spawned progeny when environmental temperatures approach lower tolerance limits.

Seawater survival and growth of progeny spawned at salinities higher than 18 ppt has not been studied. Available information suggests that advantages of spawning at high salinities will be gained at the cost of lowered seed production at these salinities.

#### DEVELOPMENT OF COST-EFFECTIVE FEEDS FOR SEAWATER CULTURE

An approach to reducing costs associated with use of prepared diets during nursery culture in land-based systems, is the indirect utilization of cheap animal wastes as fertilizer for production of natural planktonic foods. To assess the feasibility of this approach, growth of Florida red tilapia receiving a prepared diet was compared to fish reared in seawater pools enriched with chicken manure. Growth of fish in the fed pools continued at an exponential rate to day 80, while growth in manured pools became asymptotic by about day 30, indicating that food availability in manured pools was growth limiting (Ernst, Ellingson, Olla, Wicklund, Watanabe, and Grover, in press). Significant differences in fish growth among manured pools were evident, suggesting that food availability varied significantly between manured pools. Plankton and fish gut-content analyses supported the conclusion that identical methods of manuring do not necessarily produce identical biological communities and fish growth (Grover, Olla, O'Brien, and Wicklund, in press). Further research is needed to determine fish densities at which a sustainable yield of the food resource and acceptable fish growth rates could be maintained. Supplementary feeding with prepared diets in manured systems may also be practical.

#### REARING EXPERIMENTS IN FLOATING SEA CAGES

In May 1986, a pilot study was conducted to assess survival and growth of Florida red tilapia in floating cages placed in a seawater (37-40 ppt) channel near Barraterre on Great Exuma, Bahamas (Watanabe, Wicklund, Olla, Ernst and Ellingson, in press). The technical feasibility of rearing Florida red tilapia at high densities in floating sea cages using prepared diets was demonstrated in this study.

A detailed cage production study involving 9,600 sex-reversed fingerlings (10.1 g mean weight) and twenty-eight 1-m<sup>3</sup> experimental cage units was initiated at Barraterre in August 1987. The effects of feed rate and stocking density on growth from fingerling through market stages, using a commercially available diet (Purina Tilapia Chow, 32% protein), are being assessed. After 43 days of culture, mortalities were negligible, and mean body weights among the experimental groups ranged from 48.6 to 78.2 g, while food conversion ratios (dry weight: wet weight) ranged from 1.4 to 2.6

(Clark, unpublished data). Fish will be reared for 90 days; these data will provide a basis for estimating present production costs.

#### APPLICATION STUDIES IN THE CARIBBEAN

In Haiti, natural fish stocks have been depleted by heavy exploitation. A previous aquaculture demonstration project in la Gonave, Haiti has shown that blue tilapia (O. aureus) are acceptable as food fish and bring competitive prices at the marketplace (Stickney and Kohler, 1986). Lack of freshwater and machinery for pond construction were primary constraints toward production of significant numbers of fish.

The Caribbean Marine Research Center has recently initiated a feasibility study on saltwater cage culture of Florida red tilapia in Haiti. Twenty-five marine or brackishwater sites in four bays along the northern coast of Haiti, including Baie du l'Acul, Baie de Cap Haitien, Baie de Caracol and Baie de Ft. Liberte, were identified as potentially suitable for cage culture of Florida red tilapia (Rust, Wicklund, and Olla, in press). Environmental conditions including protection from prevailing wind and wave action, temperature (27-31°C), dissolved oxygen (3.6-6.3 ppm), salinity (16.0-40.2 ppt), and turbidity (1->7 m) at these sites were found acceptable for tilapia culture.

A study on production of Florida red tilapia in sea cages is currently in progress at Baie de Ft. Liberte. In addition to determining the technical feasibility of seawater cage culture in Haiti, social, cultural and economic factors affecting the extension of this technology to coastal communities are being assessed (Brass and Olla, in press).

#### ACKNOWLEDGMENTS

We thank G. Wenz, L. Ellingson, K. French, A. Clark, B. Bell, and G. Van Zandt for logistic and technical support. This research was supported by a grant from the Office of Undersea Research, National Oceanic and Atmospheric Administration, U.S. Department of Commerce and by the Perry Foundation, Inc.

#### LITERATURE CITED

Brass, J. and B. L. Olla. Social, cultural and economic considerations for saltwater cage culture of Florida red tilapia in northern Haiti. Paper presented at the Fortieth Annual Gulf and Caribbean Fisheries Institute, 9-13 November 1987, Curacao, Netherland Antilles (in press).

Canagaratnam, P. 1966. Growth of Tilapia mossambica. (Peters) in different salinities. Bull. Fish. Res. Station Ceylon, Vol. 19, pp. 47-50.

Ernst, D. H. Design and operation of a hatchery for seawater production of tilapia in the Caribbean. Proceedings of the Thirty-Ninth Annual Gulf and Caribbean Fisheries Institute, November 1986, Bermuda (in press).

Ernst, D. H., L. J. Ellingson, R. I. Wicklund, W. O. Watanabe, and J. J. Grover. Production of Florida red hybrid tilapia in fed and manured seawater pools. Aquaculture (in press).

Grover, J. J., B. L. Olla, M. O'Brien, and R. I. Wicklund. Food habits of Florida red hybrid tilapia fry in manured seawater pools in the Bahamas. Prog. Fish-Cult. (in press).

Guerrero, R. D. III. 1975. Use of androgens for the production of all-male Tilapia aurea (Steindachner). Trans. Amer. Fish. Soc., Vol. 104, No. 2, pp. 342-348.

Jurss, K., Th. Bittorf, Th. Vokler and R. Wacke. 1984. Biochemical investigations into the influence of environmental salinity on starvation of the tilapia, Oreochromis mossambicus. Aquaculture, Vol. 40, pp. 171-182.

Liao, I.-C. and S.-L. Chang. 1983. Studies on the feasibility of red tilapia culture in saline water. In: L. Fishelson and Z. Yaron (compilers). Proceedings of the International Symposium on Tilapia in Aquaculture, Nazareth, Israel, 8-13 May 1983. Tel Aviv University, Tel Aviv, Israel, pp. 524-533.

McGeachin, R. B., R. I. Wicklund, B. L. Olla and J. R. Winton. 1987. Growth of Tilapia aurea in seawater cages. J. World Aquaculture Soc., Vol. 18, No. 1, pp. 31-34.

Ridha, M., T. A. Al-Ahmad and A. A. Al-Ahmad. 1985. Tilapia culture in Kuwait: Spawning experiments, 1984. KISR Technical Report 1875, Kuwait Institute for Scientific Research, 19 pp.

Rust, M. B., R. I. Wicklund, and B. L. Olla. Potential for saltwater cage culture of the Florida red hybrid tilapia along the northeast coast of Haiti: Part 1 - Environmental conditions. Paper presented at the Fortieth Annual Gulf and Caribbean Fisheries Institute, 9-13 November 1987, Curacao, Netherland Antilles (in press).

Stickney, R. R. and C. C. Kohler. 1986. Overfishing: The Haiti Experience. Naga. The ICLARM Quarterly, Vol. 9, No. 3, pp. 5-7.

Watanabe, W. O. and C-M. Kuo. 1985. Observations on the reproductive performance of Nile tilapia (Oreochromis niloticus) in laboratory aquaria at various salinities. Aquaculture, Vol. 49, pp. 315-323.

Watanabe, W. O., C-M. Kuo and M-C. Huang. 1985a. Salinity tolerance of Nile tilapia fry (Oreochromis niloticus). spawned and hatched at various salinities. Aquaculture, Vol. 48, pp. 159-176.

Watanabe, W. O., C-M. Kuo and M-C. Huang. 1985b. The ontogeny of salinity tolerance in the tilapias Oreochromis aureus, O. niloticus, and an O. mossambicus x O. niloticus hybrid, spawned and reared in freshwater. Aquaculture, Vol. 47, pp. 353-367.

Watanabe, W. O., K. M. Burnette, B. L. Olla, and R. I. Wicklund. The effects of salinity on reproductive performance of Florida red tilapia. J. World Aquacult. Soc. (in press).

Watanabe, W. O., L. J. Ellingson, R. I. Wicklund, and B. L. Olla. 1988. The effects of salinity on growth, food consumption and conversion in juvenile, monosex male Florida red tilapia. In: R. S. V. Pullin, T. Bhukasawan, K. Tonguthai, and J. L. Maclean (eds.), The Second International Symposium on Tilapia in Aquaculture. ICLARM Conference Proceedings 15, Department of Fisheries, Bangkok, Thailand, and International Center for Living Aquatic Resources Management, Manila, Philippines.

Watanabe, W. O., K. E. French, L. J. Ellingson, R. I. Wicklund, and B. L. Olla. 1988. Further investigations on the effects of salinity on growth in Florida red tilapia: Evidence for the influence of behavior. In: R. S. V. Pullin, T. Bhukasawan, K. Tonguthai, and J. L. Maclean (eds.), The Second International Symposium on Tilapia in Aquaculture. ICLARM Conference Proceedings 15, Department of Fisheries, Bangkok, Thailand, and International Center for Living Aquatic Resources Management, Manila, Philippines.

Watanabe, W. O., K. E. French, D. H. Ernst, B. L. Olla, and R. I. Wicklund. Salinity during early development influences growth and survival of Florida red tilapia in brackish- and seawater. J. World Aquacult. Soc. (in press).

Watanabe, W. O., R. I. Wicklund, B. L. Olla, D. H. Ernst, and L. J. Ellingson. Potential for saltwater tilapia culture in the Caribbean. Proceedings Thirty-Ninth Annual Gulf and Caribbean Fisheries Institute, November 10-14, 1986, Bermuda (in press).



PRELIMINARY STUDIES ON THE EARLY LIFE HISTORY OF THE  
QUEEN CONCH Strombus gigas IN THE EXUMA CAYS, BAHAMAS

Robert I. Wicklund, Lucinda J. Hepp, and Geraldine A. Wenz  
Caribbean Marine Research Center  
Lee Stocking Island, Exuma Cays, Bahamas, and  
Riviera Beach, Florida 33404

ABSTRACT

The Caribbean Marine Research Center has initiated a study on the life history of the queen conch Strombus gigas in the Exuma Cays, Bahamas. Nursery grounds of S. gigas in the southern Exumas are described. Surveys of a major nursery area conducted from October through November 1984 resulted in a count of 570,000 juvenile 0+ and 1+-year-class conch within a total area of 386,000 m<sup>2</sup>. Average density of the conch within the area was 1.48/m<sup>2</sup>. Average densities within grass beds and adjacent sand shoals were 1.72/m<sup>2</sup> and 0.76/m<sup>2</sup>, respectively. Modes of length-frequency curves were 8.0 cm for May 1985 and 11.0 cm for February 1986. Seasonal distribution and behavior of deepwater adults are also described.

INTRODUCTION

The queen conch (Strombus gigas) is one of the most important marine species in the Caribbean region. It has been second only to finfish as a harvested resource for the past century (Brownell and Stevely 1981). Its popularity as a food source, however, has resulted in depletion of the species in southern Florida, the Bahamas and most of the Caribbean and Bermuda. The species has been so depleted in Florida that the State has closed the fishery completely. In the Exuma Cays, Bahamas, adult queen conch are no longer found in shallow waters where they were once abundant (Richard Ellis, pers. comm.). Most adult conch in this area are located in relatively deep channels (>6 m) and offshore, out of reach of most breath-hold divers.

A paucity of data concerning the life history of the queen conch existed until recently (Berg 1976; Brownell et al. 1976; Hesse 1979; Jory 1982; Ballantine and Appeldoorn 1983; Wood and Olson 1983; Appeldoorn 1985; Iversen et al. 1986; Iversen et al. 1987). The recent development of hatchery techniques has provided a better understanding of the early life stages of S. gigas (Brownell et al. 1976; Iversen 1983; Siddall 1983; Appeldoorn and Sanders 1984).

Randall (1964) made some early observations concerning predation on juvenile and adult queen conch and their migration. Recent studies suggest predation to be the most important factor

in juvenile queen conch mortality (Jory 1982; Iversen et al. 1986).

Relatively little is known, however, about the factors controlling recruitment, habitat selection, density dependency and survival during the first months of settlement. In this paper we present preliminary biological information on the life history of S. gigas from the southern Exuma Cays, Bahamas, during 1984, 1985 and 1986.

### Study Site

The southern Exuma Cays lie on the southwestern edge of Exuma Sound on the Great Bahama Bank, 110 miles southeast of Nassau, Bahamas (Fig. 1). The overall study area is in the vicinity of Lee Stocking Island ( $23^{\circ}45'N$ ,  $76^{\circ}10'W$ ), site of the Caribbean Marine Research Center (CMRC). Most of the study sites on the western side of the Cays have strong tidal currents, particularly between islands, resulting in shifting sand banks. Temperatures range from about  $21^{\circ}C$  in February to  $30^{\circ}C$  in August and September. Salinity ranges from 36 ppt to an occasional 40 ppt. The bottom is characterized by stable subtidal sand and seagrass flats, comprised primarily of turtlegrass (Thalassia testudinum) and high concentrations of the calcareous algae Rhipocephalus, Penicillus and Halimeda species. Mounds produced by the shrimp Callianassa are common in the same area.

The bottom is stabilized by an organic mat consisting primarily of algae, diatoms and the rhizomes of T. testudinum. The stabilized grassflats contain ooids, pellets, grapestones and fine-grain carbonates (Kendall and Dill 1987).

The eastern side of the Cays is characterized by a typically open ocean profile (2 m - >30 m), coral reefs, sand flats and smooth rising relic coral reef mounds.

Norman's Pond Cay (Fig. 2, Site A) is characterized by an old salt production pond (about 80 acres) with an effluent channel on the western side of the Cay. Sand and beachrock lie north and south of the channel entrance. A partial dike at the entrance to the channel maintains water level in the pond about two feet above the surrounding sea during the ebbing and low tides, resulting in an outward flow most of the day. For a short period during high tide, when the level of the sea is above the dike, the flow is into the pond.

The site of the Children's Bay Cay S. gigas nursery area (Fig. 2, Site B) is characterized by a large bed of T. testudinum adjacent to an unstable ooid shoal to the west and a moderately deep channel (>7 m) to the east. The nursery ground is primarily in a grass bed at a depth of 3-5 m which extends onto a shallow sand shoal (1-2 m).

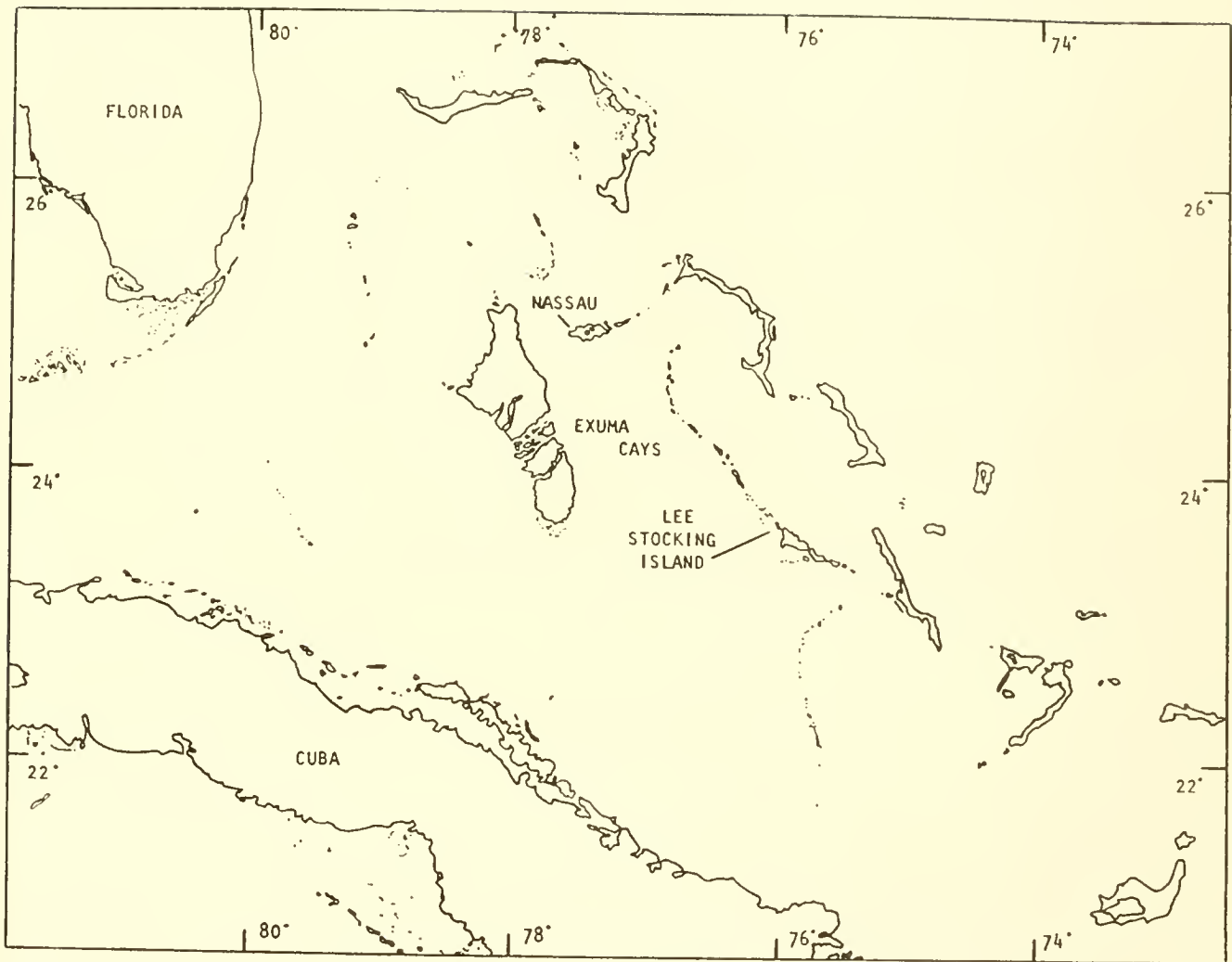


Figure 1. Lee Stocking Island.

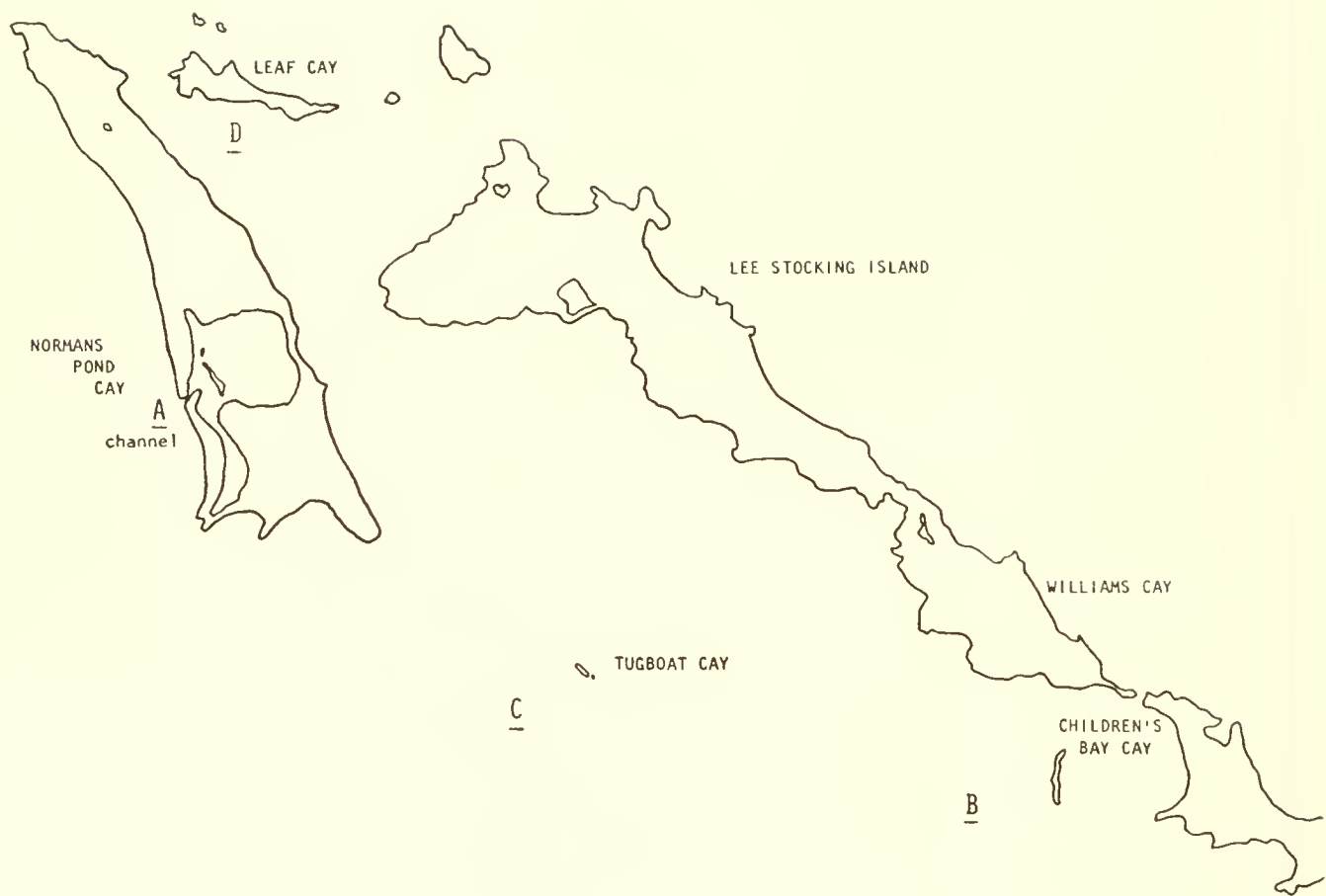


Figure 2. Study sites.

The Tugboat Cay site (Fig. 2, Site C) extends from the Cay to about 1/2 mile northwest onto a sand shoal and 1 mile west. Its major bottom characteristic is sporadic patches of T. testudinum and coarse sand pebbles with a mean depth of about 4 m. Tidal currents reach about 1 knot.

The Leaf Cay site (Fig. 2, Site D) is a small patch of T. testudinum on the southwest side of the Cay in 4 m surrounded by deeper water. This is a minor nursery lying to the west of a major inlet.

## METHODS

Standard scuba diving techniques were used to observe and measure juvenile conch. Plastic spaghetti tags were cut and tied around the spires of the conch shell.

Conch were measured along the anterior-posterior axis of the shell. Population density estimates of juvenile conch at the Children's Bay Cay site were obtained by; (1) measuring distances and direction between buoys set on the outer perimeters of the bed with a rangefinder instrument, (2) estimating area of the bed geometrically, and (3) counting and measuring conch within 20 circles each measuring 31.9 m<sup>2</sup>. Fifteen of the samples were taken on grass beds and five on the adjacent sand shoal.

Surveys of a shallow-water population of S. gigas at Norman's Pond Cay were conducted by counting all conch in blocks, each measuring 39 m north and south alongshore and 2 m east and west seaward (Fig. 3).

## RESULTS AND DISCUSSION

### Juvenile Queen Conch

#### Norman's Pond Cay

Distribution of juvenile conch (0+ and 1+ year class) at Norman's Pond Cay in July 1984 appeared to be related to the effluent from the salt pond which flows from the channel either north or south alongshore most of the day. Ambient water temperature was about 30°C and effluent temperature was about 2°C above ambient during the afternoon.

Approximately 2500 conch counted on July 18-28, 1984, were centered at the entrance to the channel and spread directly seaward about 22 m from the entrance and along the shoreline north and south (Fig. 3). The conch were often exposed along the beach at low tide. This behavior has also been reported by Iversen et al. (1987).

	A	B	C	D	E	F	G	H	I	J	K	L
1	16	13	18	32	47	38						
2	24	5	11	19	9	5						
3	28	12	28	15	12	11						
4	62	61	40	23	8	4	0					
5	7	36	9	9	2	2	0					
6	103	81	88	47	51	45	45	53	59	37	21	0
7	24	26	21	27	44	15	7					
8	42	50	36	24	29	8	2					
9	72	68	38	7	32	7	12					
10	86	56	47	23	17	9	2					
11	39	64	23	37	6	3	2					
12	47	51	34	12	1							
13	26	38	13	6	3							
14	50	27	11	1	1							
15	7	1	2	0	0							

Figure 3. Distribution and number of juvenile S. gigas surveyed at the entrance channel to the Old Salt Pond located at Norman's Pond Cay, Bahamas, 18-24 July 1984.

By August 18th the conch started moving away from the channel entrance to the north and south. On September 9th only two conch were observed at the channel entrance, but heavy concentrations were found along the shallow shore on both sides. Ambient water temperature was 31.6°C, shoreline temperature was 31.6°C, and effluent temperature was 33.3°C.

On October 7th most conch were concentrated in two large clusters on the south side of the inlet. Waterflow from the channel at this time was northward alongshore. Ambient temperature was 26°C; effluent temperature reached 27°C by noon. This was the last observation of the Norman's Pond Cay population of conch due to an almost complete harvest by local fishermen soon after October 7th.

We presume that the association of juvenile S. gigas with the salt pond effluent was related to higher temperature and possibly higher nutrient content of effluent water (which was normally a murky green color), particularly during the late spring to early fall months. However, in July 1984 we observed that during the ebbing tide, when the channel water flows seaward, the conch moved away from the entrance as illustrated in Table 1.

We believe this movement of conch away from the channel during the outgoing tide was due to either the strong current coming from the channel or abnormally high temperatures of effluent water occasionally found at midday.

During late summer, when temperatures of the pond effluent reached 33.3°C, the conch moved away from the channel completely but remained along the shoreline.

In October 1984 westerly storms and winds brought relatively high wave action onto Norman's Pond Cay. We observed that for one week following this action, many of the young S. gigas were partially buried or gathered around small coral heads. Presumably this behavior was in response to the high energy waves in shallow water that could wash the conch onto the beach. Only a few dead conch were found stranded on the beach after the storm. Appeldoorn (1985) reported that burial of S. gigas and S. costatus was greater during periods of turbulence in Puerto Rican waters.

#### Children's Bay Cay

Our pilot studies were centered around a large S. gigas nursery area adjacent to Children's Bay Cay just south of Lee Stocking Island during 1985 and 1986. This nursery area is characterized by Thalassia grass, coral rubble, stabilized sand and adjacent shifting ooid shoals. Depth ranges between 3 and

Table 1. Number of Conch at Norman's Pond Cay Channel Entrance and Adjacent Sites at High and Low Tide -July 1984.

	High Tide	Low Tide
North	29	95
Entrance	184	95
South	50	110

5 m and tidal currents move west and east at about 1 knot at the peak flow.

Since 1985 this area has remained populated with juveniles rarely exceeding 120 mm, although an occasional lipped adult was found in the nursery area. As of May 1985 no individuals measured under 60 mm. This is consistent with reports that juvenile S. gigas under 80 mm bury and are out of sight during the day (Randall, 1964; Appeldoorn and Ballantine, 1982).

Density of juvenile S. gigas in the Children's Bay Cay nursery area appeared fairly constant throughout the year. During October 29 through November 4, 1985, we counted 570,000 juvenile S. gigas in an area of 386,000 m<sup>2</sup>.

Mean density was 1.48/m<sup>2</sup> (N=946). Densities within the two distinct habitats of the nursery area were 1.72/m<sup>2</sup> (N=824) for the Thalassia grassbeds and 0.76/m<sup>2</sup> (N=122) on the adjacent ooid sand shoal. Comparative density measurements in the Berry Islands, Bahamas, ranged from 1.5/10 m<sup>2</sup> at Little Cockroach Cay to 19.6/10 m<sup>2</sup> at Bird Cay Channel (Iversen et al. 1987).

With the exception of Bird Cay Channel, the densities of juvenile S. gigas in the Children's Bay area of the Exuma Cays are among the highest reported anywhere. Densities of 0.001/m<sup>2</sup> and 0.9/m<sup>2</sup> have been reported for S. gigas populations in the Virgin Islands (Woods and Olsen 1983) and in the Turks and Caicos (Hesse 1979), respectively.

The size distribution of juvenile S. gigas in the Children's Bay Cay nursery area ranged from 6.0-12.5 cm in May 1985 to 7.0-15.0 cm in January 1986. The modes of the length-frequency curves were 8.0 cm for May 1985 and 11.0 cm for February 1986. Iversen's (1987) estimates of average length by ages suggest that the main population measured at Children's Bay Cay was 1 year old. This agrees with age-size estimates in Puerto Rico (Berg 1976) and Venezuela (Brownell, 1977), but is under Von Bertalanffy growth curve analyses of populations in the Virgin Islands (Berg 1976; Brownell et al. 1976) and Cuba (Alcolado 1976).

One-hundred and fifty-two juvenile conch were tagged at the Children's Bay Cay site with 48 returns including 8 captured twice. Most of the recaptures were made within 1-2 months of the initial tagging and all within a short distance of the site. Mean growth rate calculated from all of the returned tags was 0.12 mm/day and 0.37 cm/month. Iversen et al. (1987) reported growth rates from the Berry Islands as 0.44-1.63 cm/month for the summer and 0.18-0.30 cm/month for the rest of the year. Table 2 summarizes the tagging returns for this site.

Table 2. Summary of tag returns.

## Children's Bay Cay Site

<u>Tagging Date</u>	<u>Size (cm)</u>	<u>Recovery Date</u>	<u>Size (cm)</u>	<u>Recovery Date</u>	<u>Size (cm)</u>	<u>Growth mm/day</u>
5-02-85	9.5	6-12-85	10.0			0.12
	8.5	7-10-85	9.0			0.007
	9.5	7-10-85	10.2	8-22-85	10.7	0.01/0.11
	9.5	6-12-85	9.5			0.00
	9.5	6-11-85	10.5			0.25
	8.5	6-12-85	9.0			0.12
	9.0	6-18-85	9.0			0.00
	9.5	6-11-85	9.5			0.00
	5.5	7-10-85	6.5			0.14
	9.5	6-12-85	10.5			0.24
	8.0	6-12-85	Dead			----
	10.0	8-22-85	Dead			----
5-13-85	9.5	6-12-85	9.5	7-10-85	10.0	0/0.18
	9.0	6-11-85	9.5			0.17
	10.0	10-21-85	Dead			----
	9.5	6-12-85	10.0			0.16
	9.5	7-10-85	10.0			0.08
	8.5	6-11-85	8.5	7-10-85	9.0	0/0.17
	9.5	7-10-85	10.0			0.08
	8.0	6-12-85	8.5			0.16
	9.5	8-22-85	10.5			0.09
	9.0	6-11-85	9.0			0.00
	8.0	6-12-85	8.5			0.16
	8.5	6-12-85	9.0			0.16
5-15-85	8.5	6-11-85	9.0			0.18
	9.0	10-21-85	11.0			0.13
	6.5	10-14-85	Dead			----
	8.5	6-12-85	9.0			0.17
	8.5	6-11-85	9.0			0.17
	9.0	6-12-85	9.5	8-12-85	10.5	0.17/0.16
	9.5	6-11-85	9.5	7-10-85	10.0	0/0.17
	8.0	6-11-85	9.0			0.37
	9.5	6-11-85	9.5			0.00
	9.0	6-11-85	10.0	10-21-85	10.5	0.37/0.04
	8.5	7-10-85	9.5	8-8-85	10.0	0.18/0.17
	8.0	6-11-85	8.5			0.18
	8.5	6-12-85	9.0			0.18
10.5	8.5	6-11-85	9.0	7-10-85	9.5	0.18/0.17
	8.5	9-26-85	Dead			----

Mean growth rate = 0.12 mm/day

We believe that the Children's Bay Cay site is important to the recruitment of conch into the southern Exuma Cays. Our observations indicated that the numbers of 1-year-old juvenile S. gigas remain relatively stable suggesting that new conch recruit into the area each year. The conditions that allow conch to thrive here are not understood. Obviously, food availability, good water quality, bottom sediment suitable to allow the youngest conch to bury and avoid predation, and currents that carry the pelagic veligers to nursery areas are all important to the success and survival of the juveniles. The Children's Bay Cay site offers rich Thalassia grassbeds that provide food for the conch and strong tidal currents that move water in and out of Exuma Sound.

#### Leaf Cay

A small population of juvenile S. gigas was found adjacent to Leaf Cay just north of Lee Stocking Island. This group was fairly isolated and warrants only a brief mention here. Measurements made from July 1985 to January 1986 showed a size distribution ranging from 8.0-13.5 cm, similar to that of the Children's Bay Cay population. Modes of the length-frequency curves ranged from 10.0 cm in July 1985 to 11.5 cm in January 1986.

On June 4 and 10, 1985, 97 juvenile S. gigas were tagged at the Leaf Cay site. Fifty-nine were recaptured in the same area, including 14 captured twice. Mean growth rates calculated from tagging data were 0.14 mm/day and 0.41 cm/month. Tagging returns and growths from Leaf Cay are summarized in Table 3.

#### Tugboat Cay

One of the largest juvenile conch populations in the vicinity of Lee stocking Island was found west of Tugboat Cay. Although we do not have density figures for this area, it was generally observed that densities were not as high as in the Children's Bay Cay population, the Tugboat Cay nursery area being larger and the range of sizes and ages much wider. In August 1985 sizes at Tugboat Cay (N=78) ranged from 8.4-14.7 cm (Fig. 5). During the same month, sizes at Children's Bay Cay (N=100) ranged from 8.0-12.5 cm (Fig. 4). A bimodal size distribution curve of juvenile S. gigas was evident at various times from July 1985-January 1986 (Fig. 5) due to occasional sampling of a population of smaller conch toward the eastern end of the Tugboat area. At the Tugboat Cay site conch ranged from 1 year to adult, the dominant ages being 1- and 2-year olds with significant numbers of 3+ also found. Nowhere else in the area between Leaf Cay and south of Children's Bay Cay have we found significant numbers of 2- to 3-year-old conch as were found at Tugboat Cay. Considering its close proximity, the Children's Bay Cay 1- to 2-year-old conch could migrate to the Tugboat Cay site.

Table 3. Summary of tag returns.

## Leaf Cay Site

Tagging Date	Size (cm)	Recovery Date	Size (cm)	Recovery Date	Size (cm)	Growth mm/day
6-04-85	10.5	7-08-85	10.5			0.00
	9.5	7-08-85	10.0			0.15
	9.5	7-08-85	10.0			0.15
	11.5	8-09-85	12.2			0.09
	9.7	7-08-85	10.0			0.09
	9.7	7-08-85	9.8			0.03
	8.5	7-08-85	9.2	12-13-85	11.0	0.20/0.11
	10.0	7-08-85	10.3	8-09-85	10.7	0.09/0.12
	8.5	7-08-85	9.2			0.20
	10.0	7-08-85	10.7			0.20
	9.5	7-08-85	10.5			0.29
	10.0	7-08-85	10.7			0.20
	11.2	7-09-85	11.2	8-15-85	11.3	0/0.02
	10.5	7-08-85	11.0			0.17
6-10-85	10.0	7-08-85	10.5			0.17
	8.5	7-08-85	9.0	8-09-85	9.2	0.17/0.06
	9.5	7-08-85	10.0	8-09-85	10.2	0.17/0.06
	10.0	7-08-85	10.5			0.17
	8.5	7-08-85	9.5			0.35
	9.5	7-09-85	10.0			0.17
	10.5	7-09-85	10.5			0.00
	9.0	7-08-85	9.5			0.18
	9.5	7-08-85	10.1	8-15-85	10.1	0.21/0
	10.0	7-08-85	10.5			0.17
	10.0	7-08-85	10.5			0.17
	10.5	7-08-85	11.0	8-09-85	11.3	0.17/0.09
	10.5	7-08-85	10.5			0.00
	10.0	7-08-85	10.5			0.17
	10.0	7-08-85	10.5	8-09-85	10.8	0.17/0.09
	10.0	7-09-85	10.5			0.17
	9.5	11-06-85	11.8			0.15
	11.0	7-08-85	11.3	8-15-85	12.3	0.10/0.26
	10.5	8-15-85	10.9			0.06
	9.5	7-08-85	10.0	12-13-85	Dead	0.17
	9.5	7-08-85	9.7			0.11
	11.0	7-08-85	11.6			0.21
	9.5	7-08-85	10.0			0.17
	9.5	7-01-85	10.0	7-08-85	10.0	0.24/0
	10.2	7-08-85	10.7			0.17
	9.2	7-09-85	9.8			0.20
	10.2	7-09-85	10.7			0.17
	9.5	7-08-85	Dead			----
	10.5	7-01-85	11.0	7-08-85	11.0	0.24/0
	9.3	7-09-85	9.5			0.17

Mean growth rate = 0.14 mm/day

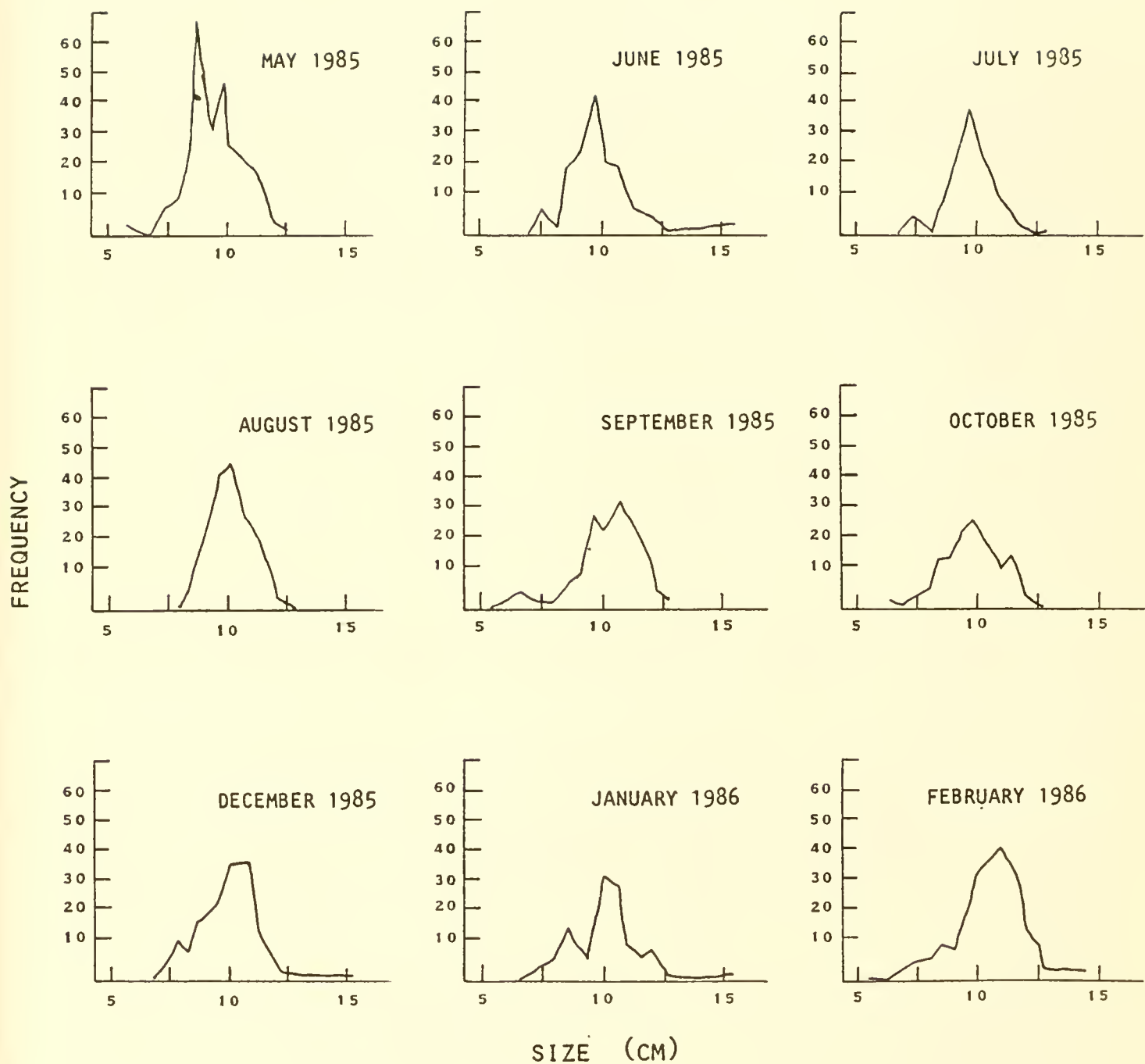


Figure 4. Size frequencies of juvenile Strombus gigas, Children's Bay Cay site, Exuma Cays, Bahamas -- 1985-86.

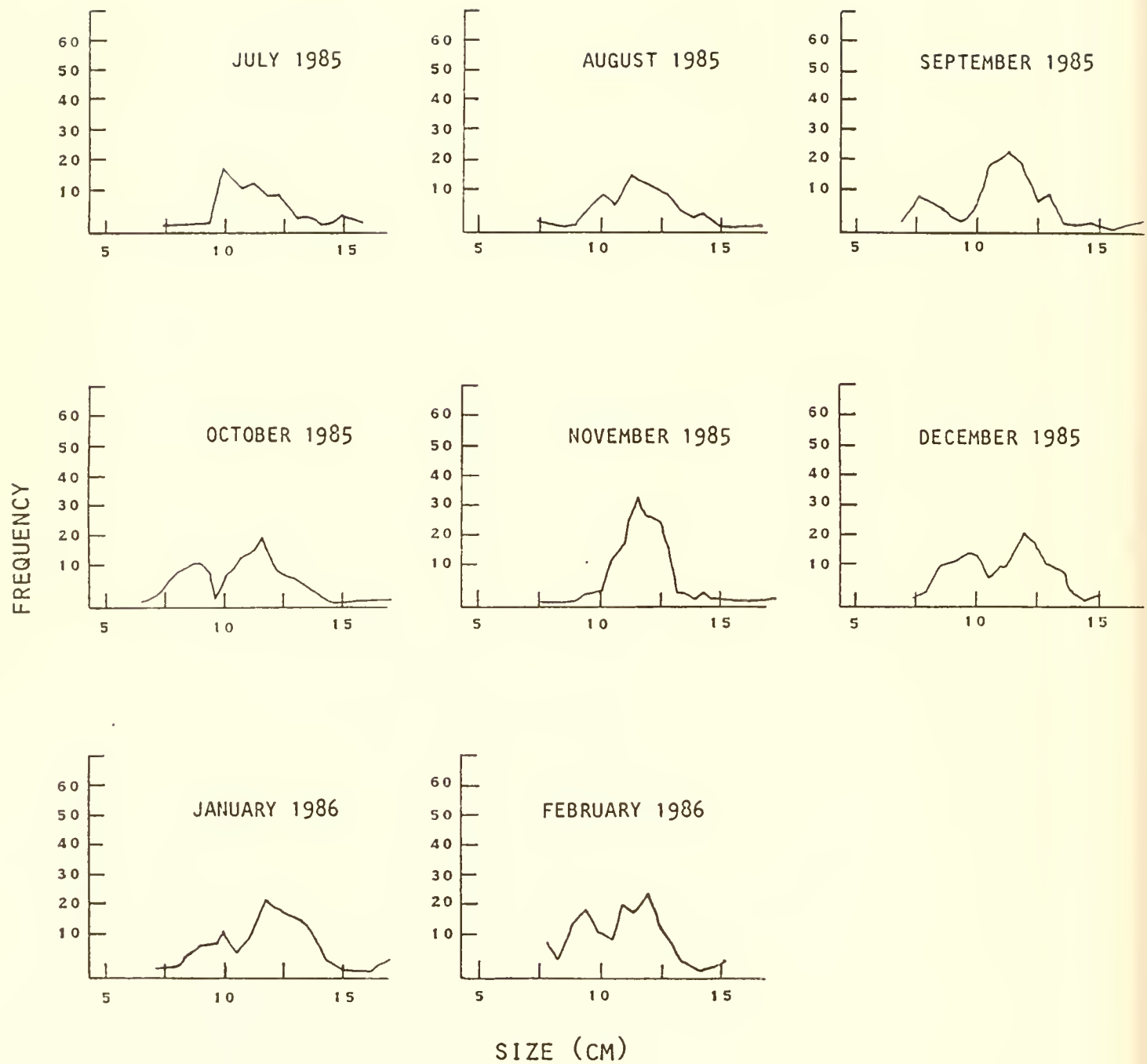


Figure 5. Size frequencies of tagged juvenile *Strombus gigas*, Tugboat Cay, Exuma Cays, Bahamas, 1985-86.

### Adult Queen Conch

#### Horseshoe Reef, Lee Stocking Island

Adult queen conch in the Exuma Cays are now only found in relatively deep water (>6 m), generally in channels with high concentrations of Thalassia and offshore on sand and relic coral reef outcroppings.

The most significant adult population in the Lee Stocking Island area is an offshore spawning stock found at a depth of 15-23 m on the Exuma Sound side of the Island and ranging in size from 17.7-26.8 cm. They are found mainly during late spring through early fall on carbonate sand bottom partially covered by a thin algal mat adjacent to a deepwater reef (Horseshoe Reef) running parallel to, and about 1/2 mile from, the beach. This reef, with a steep vertical profile of about 5 m, is a barrier which prevents the conch from moving further inshore. During the winter months most of the offshore group have been observed on top of relic patch reefs. These large mounds have little living hard coral but are covered by algae and soft corals. The algae most likely provide food to the conch during the winter. During August 1987 some individuals remained on the offshore mounds (Allan Stoner, CMRC, pers. comm.). We believe that a sizeable portion of the Children's Bay Cay, Tugboat Cay and other nursery conch populations in the area are recruited from the offshore spawning groups. The depth of the offshore conch population protects them from most fishing pressure allowing their numbers to remain constant and ensuring spawning success.

Studies of conch by other investigators indicate that their spawning season ranges from March to September (Randall 1964; D'Asaro 1965; Brownell 1977) and that they migrate offshore in the winter (Randall 1964; Hesse 1979). We observed spawning behavior in this deepwater population on the sand bottom throughout spring and summer in 1985, 1986, and 1987. One small shallow water (<5 m) spawning group was also observed near the eastern shore of Norman's Pond Cay in July 1987.

In summary, the area around Lee Stocking Island is a major nursery ground for juvenile S. gigas and an excellent site for research on the species. We suggest that this site be the focus of future research concentrating on the following: 1) recruitment of young into the nursery areas, 2) description of factors necessary for the survival of the youngest conch, 3) predation, and 4) food availability.

#### ACKNOWLEDGMENTS

This research was supported by the Office of Undersea Research, National Oceanic and Atmospheric Administration, U.S.

Department of Commerce (Grant Number NA85AA-D-UR034). Special thanks go to Myffie Lewis, a student from New Zealand, who set up and conducted the Norman's Pond Cay survey, Gay Van Zandt for her wordprocessing and review of this paper, and Lisa Ellingson for her illustrations. We also thank Drs. Wade Watanabe and Allan Stoner for their review and comments. This work could not have been conducted without the support of the Department of Fisheries, Bahamas Ministry of Agriculture and Fisheries.

#### LITERATURE CITED

Alcolado, P. M. 1976. Crecimiento, variaciones morfológicas de la concha y algunos datos biológicos del cabo, Strombus gigas, L. (Molusca; Mesogastropoda). Acad. Cienc. Cuba, Ser. Oceanol., Vol. 34, 36 pp.

Appeldoorn, R. S., and I. M. Sanders. 1984. Quantification of the density-growth relationship in hatchery-reared juvenile conchs (Strombus gigas Linne and S. costatus Linne). J. Shellfish Res., Vol. 4, No. 1, pp. 63-66.

\_\_\_\_\_. 1985. Growth, mortality and dispersion of juvenile laboratory-reared conchs, Strombus gigas and S. costatus, released at an offshore site. Bull. Mar. Sci., Vol. 37, pp. 785-793.

Ballantine, D. L., and R. S. Appeldoorn. 1983. Queen conch culture and future prospects in Puerto Rico. Proc. Gulf Carib. Fish. Inst., Vol. 35, pp. 57-63.

Berg, C. J., Jr. 1976. Growth of the queen conch, Strombus gigas, with a discussion of the practicality of its mariculture. Mar. Biol. (Berl.), Vol. 34, pp. 191-199.

Brownell, W. N. 1977. Reproduction, laboratory culture, and growth of Strombus gigas, S. costatus and S. pugilis in Los Roques, Venezuela. Bull. Mar. Sci., Vol. 27, pp. 668-680.

\_\_\_\_\_, C. J. Berg, Jr., and K. C. Haines. 1977. Fisheries and aquaculture of the conch, Strombus gigas, in the Caribbean. In: H. B. Stewart, Jr., (ed.), Cooperative Investigations of the Caribbean and Adjacent Regions. Caracas, Venezuela, 12-16 July 1976, pp. 59-69. FAO Fish. Rep. 200.

\_\_\_\_\_, and J. M. Stevely. 1981. The biology, fisheries and management of the queen conch, Strombus gigas. Mar. Fish. Rev., Vol. 43, No. 7, pp. 1-12.

D'Asaro, C. N. 1965. Organogenesis, development and metamorphosis in the queen conch, Strombus gigas, with notes on breeding habits. Bull. Mar. Sci., Vol. 15, pp. 359-416.

Hesse, K. O. 1979. Movement and migration of the queen conch, *Strombus gigas*, in the Turks and Caicos Islands. Bull. Mar. Sci., Vol. 29, pp. 303-311.

Iversen, E. S. 1983. Feasibility of increasing Bahamian conch production by mariculture. Proc. Gulf Carib. Fish. Inst., Vol. 35, pp. 83-88.

\_\_\_\_\_, D. E. Jory, and S. P. Bannerot. 1986. Predation on queen conchs, *Strombus gigas*, in the Bahamas. Bull. Mar. Sci., Vol. 39, pp. 61-75.

\_\_\_\_\_, E. S. Rutherford, S. P. Bannerot, and D. E. Jory. 1987. Biological data on Berry Islands (Bahamas) queen conchs, *Strombus gigas*, with mariculture and fisheries management implications. Fish. Bull., Vol. 85, No. 2, pp. 229-310.

Jory, D. E. 1982. Predation by tulip snails, *Fasciolaria tulipa*, on queen conchs, *Strombus gigas*. M.S. Thesis., University of Miami, Coral Gables, FL. 73 pp.

Kendall, C. G. St. C., and R. F. Dill. 1987. Guidebook to the giant subtidal stromatolites and carbonate facies of Lee Stocking Island, Bahamas. Special Publication, Dept. Geol., University of South Carolina, 151 pp.

Randall, J. E. 1964. Contributions to the biology of the queen conch, *Strombus gigas*. Bull. Mar. Fish. Rev., Vol. 47, No. 4, pp. 1-10.

Siddal, S. E. 1983. Biological and economic outlook for hatchery production of juvenile queen conch. Proc. Gulf Carib. Fish. Inst., Vol. 35, pp. 46-52.

Wood, R. S., and D. A. Olsen. 1983. Application of biological knowledge to the management of the Virgin Islands conch fishery. Proc. Gulf Carib. Fish. Inst., Vol. 35, pp. 112-121.



DIEL PATTERNS OF GROWTH, NITROGEN CONTENT, HERBIVORY,  
AND CHEMICAL VERSUS MORPHOLOGICAL DEFENSES:  
CAN TROPICAL SEAWEEDS REDUCE HERBIVORY BY GROWING AT NIGHT?

Mark E. Hay<sup>1</sup>, Valerie J. Paul<sup>2,5</sup>, Sara M. Lewis<sup>3</sup>,  
Kirk Gustafson<sup>2</sup>, Jane Tucker<sup>4</sup>, and Robbin N. Trindeell<sup>1</sup>

<sup>1</sup>University of North Carolina at Chapel Hill,  
Institute of Marine Sciences,  
Morehead City, NC 28557

<sup>2</sup>Scripps Institution of Oceanography,  
La Jolla, CA 92093

<sup>3</sup>Aiken Laboratory, Harvard University  
Cambridge, MA 02138

<sup>4</sup>Ecosystems Center,  
Marine Biological Laboratory,  
Woods Hole, MA 02543

<sup>5</sup>Present address: University of Guam Marine Laboratory,  
UOG Station, Mangilao, Guam 96923

#### ABSTRACT

Tropical seaweeds in the genus Halimeda reduce losses to grazing by capitalizing on diel patterns of herbivore activity. These seaweeds produce new, more herbivore-susceptible growth at night when herbivorous reef fishes are inactive. Plant portions more than 48 hr old are low in food value, well defended morphologically (calcified and high in ash content), and relatively resistant to herbivory. Younger plant portions represent 3-4.5 times the food valued (nitrogen or organic content) of older portions but are only moderately more susceptible to herbivores due to their high concentrations of the terpenoid feeding deterrents halimedatrial and halimedatetraacetate. Halimedatrial significantly deters grazing by both parrotfishes (Scaridae) and surgeonfishes (Acanthuridae) and occurs in high concentrations (2-4.5% of plant ash-free dry mass) in plant portions that are 4-12 hr old, intermediate concentrations (0.3-2.3%) in portions that are 16-26 hr old, and low concentrations (0.3%) in older plant portions. The related compound halimedatetraacetate is absent from the youngest plant portions, shows a rapid increase in concentration (from 0 to 1%) in plant material that is approximately 16 hr old, and then rapidly declines to low levels (0.1 to 0.2%) in older plant portions. Thus, newly produced tissues are nutritionally valuable but contain high concentrations of defensive chemicals. As these tissues age, morphological defenses increase, the tissue

becomes less valuable as a food for herbivores, and chemical defenses decrease. Additionally, new growth of Halimeda remains unpigmented until just before sunrise. Thus, the valuable, nitrogen-containing molecules associated with photosynthesis are not placed in the new, and more herbivore susceptible, growth until light is available and they can start producing income for the plant.

Experiments in a coral-reef microcosm, where diel patterns of light and water chemistry could be altered, indicated that Halimeda's growth pattern is cued by the timing of light-dark cycles rather than by co-occurring diel changes in water chemistry.

Although the growth patterns of Halimeda seem unusual, similar patterns appear to occur in numerous other seaweeds and in microalgae such as diatoms and dinoflagellates.

## INTRODUCTION

Herbivory plays a major role in determining the distribution and abundance of primary producers in many marine communities (Lubchenco and Gaines, 1981). This is especially true on coral reefs where herbivores are abundant, diverse, and directly affect the species composition and biomass accumulation of benthic algae and seagrasses (Hay, 1985; Carpenter, 1986; and Lewis, 1986). Even though it is clear that herbivory is one of the major factors affecting algal biomass on tropical reefs, ecologists have only recently begun to investigate seaweed characteristics that may deter herbivores. Spatial escapes (Hay, 1984b, 1985; Lewis, 1986; and Taylor et. al., 1986), seasonal temporal escapes (Lubchenco and Cubit, 1980), chemical deterrents (Paul and Fenical, 1986; Paul and Hay, 1986; Hay et al., in press a, b), morphological deterrents (Littler and Littler, 1980; Lubchenco and Cubit, 1980; Hay, 1981b; Steneck and Watling, 1982; Steneck, 1986; and Lewis et al., 1987), and potential deterrents associated with nutritional inadequacy (Lubchenco and Gaines, 1981) have all been discussed as important components of seaweed-herbivore interactions. The potential importance of diel escapes, when associated with rapidly mobilizable defenses, has not been investigated.

When herbivore activity is temporally predictable, plants may reduce losses to consumers by producing vulnerable portions only during periods of minimal herbivore activity. Examples of this phenomenon include: (1) plants that produce seeds in mass at intervals of several years, thus exceeding the ability of local granivores to consume all seeds (Janzen, 1976); (2) plants that produce new, and unprotected, growth early in the season before insect herbivores reach high densities; as herbivores become more abundant these plants may defend their foliage by an increased production of chemical deterrents (Feeney, 1970); and

(3) seaweeds that grow as upright blades during periods when grazers are inactive, but grow as herbivore-resistant, encrusting or creeping forms during periods when herbivores are active (Lubchenco and Cubit, 1980; and Lewis et al., 1987). These previous studies have focused on seasonal or year-to-year variability in consumption. In this study, we show that some tropical seaweeds reduce losses to grazers by exploiting diel patterns of herbivore activity. These seaweeds produce new, nitrogen rich, and more vulnerable, growth only at night when herbivorous reef fishes are inactive. Immediately after production, the new, nutritionally valuable, tissue contains high concentrations of terpenoid compounds that deter grazing by the most common herbivorous fishes. Over the next 2-3 days, morphological defenses increase, the tissue becomes less valuable as a food source, and chemical defenses decrease. Although nocturnal growth appears to occur in numerous genera of tropical, chemically-defended seaweeds in the order Caulerpales, we focused our investigations exclusively on species in the genus Halimeda. Halimeda is an ecologically and geologically important component of several tropical habitats and is one of the most abundant seaweeds in the tropics (Hillis-Colinvaux, 1980; Drew, 1983; Davies and Marshall, 1985; and Drew and Abel, 1985). We ask the following questions:

- 1) Do seaweeds in the genus Halimeda initiate new growth primarily at night?
- 2) Does this nocturnal production of new growth coincide with a diel decrease in the overall rate of herbivory on Halimeda?
- 3) Is young Halimeda tissue more susceptible to herbivory than older tissue?
- 4) How do nutritional value (nitrogen and organic content) and secondary metabolite concentration of Halimeda vary with tissue age?
- 5) Do the terpenoid metabolites produced by Halimeda deter grazing by common reef herbivores? and,
- 6) Are the patterns documented for Halimeda unique or do they occur in other organisms?

#### Organisms and study sites

Species in the genus Halimeda grow by the addition of new segments at the apex (Fig. 1). This makes quantifying new growth particularly easy since very simple field procedures can be used to mark older segments and count the addition of new segments with time (Drew, 1983). Halimeda and related genera produce calcium carbonate at rates of  $32-185 \text{ g m}^{-2}\text{yr}^{-1}$  (Bach, 1979; and Drew, 1983) and account for more than half of the carbonate production in tropical reef and lagoon systems (Stockman et al., 1967; Milliman, 1974; Neumann and Land, 1975; Bach, 1979; and Wefer, 1980). The unconsolidated carbonated sediments produced by these seaweeds are often quantitatively more important in contributing to the bulk of reefs than are the

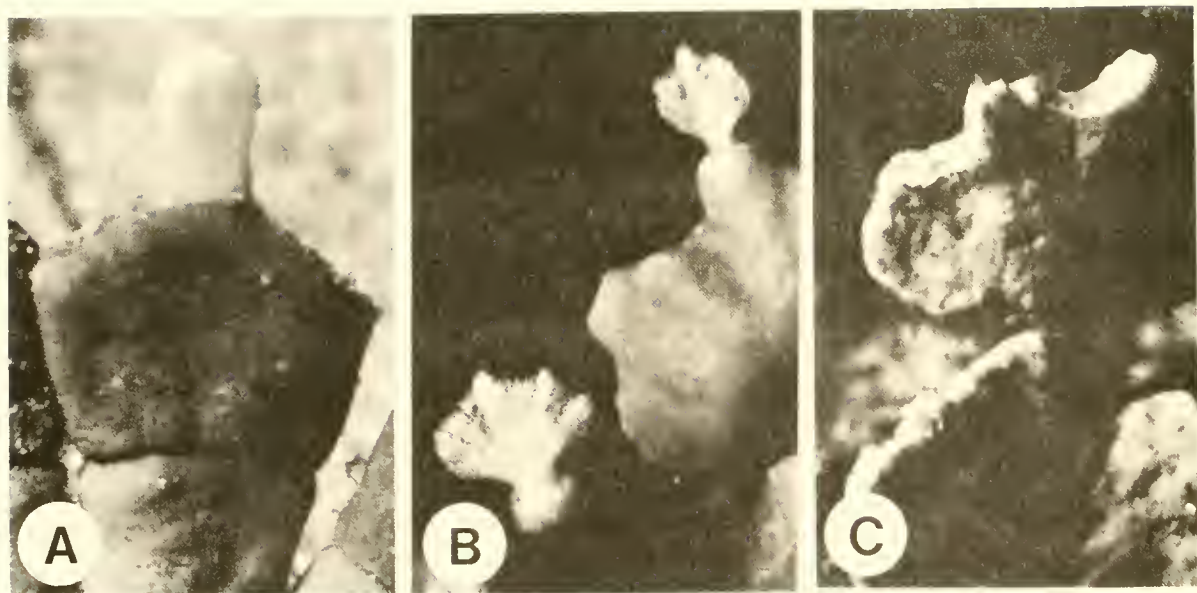


Figure 1. Terminal branches of *Halimeda* showing (A) unpigmented tips as they appear at about 0000 hr, (B) expanding but unpigmented tips as they appear at about 0400 hr (older terminal segments may produce 1, 2, or occasionally 3 new segments), and (C) an older segment whose developing tips have each been bitten off.

carbonates bound in framework organisms such as corals and encrusting coralline algae (Milliman, 1974).

The ability of Halimeda to maintain high standing stocks on reefs where other seaweeds are rapidly eaten to extinction has generally been attributed to its calcified thallus and its ability to synthesize numerous novel terpenoid metabolites (see Paul, 1985 for the structures of these compounds) that appear to function as herbivore feeding deterrents (Paul and Fenical, 1983; Hay, 1984b; Paul, 1985; Paul and Fenical, 1986; and Targett et al., 1986). The consequences of nocturnal segment production for Halimeda-herbivore interactions have not been investigated.

The majority of this study was conducted from the National Oceanic and Atmospheric Administration's Hydrolab facility located in Salt River Canyon, St. Croix, U.S. Virgin Islands ( $17^{\circ}47'N$ ,  $64^{\circ}45'W$ ). The habitats near this facility have been described previously (Adey et al., 1977). Most of our observations and experiments were made on populations of Halimeda incrassata that occurred abundantly on the sandy canyon floor at a depth of 18-21 m. Some herbivory assays were conducted on the nearby reef slope at a depth of 15 m or in areas of the back reef at a depth of 2-3 m. Herbivorous parrotfishes (Scarus taeniopterus, S. iserti, Sparisoma aurofrenatum, and S. viride) and surgeonfishes (Acanthurus coeruleus and A. bahianus) were common in the back-reef habitat; on the deeper reef slope, parrotfishes were the most common herbivores. Sea urchins are rare in these habitats, and spatial patterns of herbivory on the reef at Salt River Canyon, St. Croix are typical of those occurring on most Caribbean reefs that are not subject to heavy fishing (Hay, 1984a).

Observations and experiments on a second Halimeda species, H. simulans, were conducted in a shallow (1-3 m deep) mangrove-lined bay next to the Hydrolab shore base in St. Croix. In this habitat, H. simulans and documentation of its diel pattern of segment production were conducted on a 20-24 m deep sand plain at Coki Point, St. Thomas, U.S. Virgin Islands ( $18^{\circ}21'N$ ,  $64^{\circ}52'W$ ).

We investigated the proximate causes of nocturnal segment initiation in Halimeda using a large (7000 l) coral-reef microcosm at the Smithsonian Institution's National Museum of Natural History in Washington, D.C. A simplified schematic of the microcosm is shown in Figure 2; the system has been described in detail by Adey (1983). A wave generator produces turbulence within the microcosm and powerful metal-halide bulbs provide intense light that facilitates seaweed growth. Diel variations in water chemistry are similar to those that occur on natural coral reefs (Adey, 1983). The microcosm supports several hundred species of organisms found on Caribbean reefs. Halimeda opuntia grows particularly well in the microcosm and undergoes the same

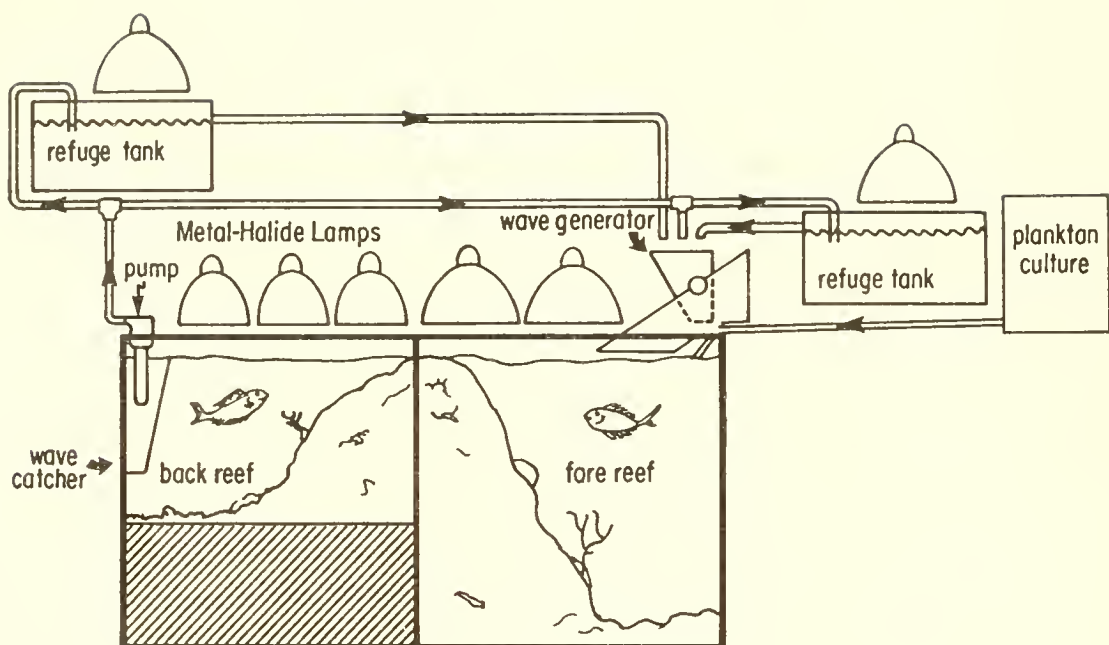


Figure 2. A simplified illustration of the Smithsonian Institution's coral reef microcosm and refuge tanks. The figure is modified from an earlier one by Brawley and Adey (1981).

diel pattern of segment production (M. Hay, personal observation) that we document for H. incrassata and H. simulans in the Virgin Islands. By using the microcosm and its connected refuge tanks, we were able to reverse day-night photoperiods and assess the importance of light cycles versus diel changes in water chemistry in regulating segment production.

## METHODS

Diel patterns of segment production in Halimeda incrassata growing near the Hydrolab in St. Croix were documented by collecting 30 haphazardly selected plants every 4 hrs for 56 hrs and investigating each branch tip on each plant to see if it contained a new bud (a small white protuberance of less than 1 mm wide), an expanding but unpigmented tip (larger than the bud, with the shape of a segment, but still white), or a relatively mature, pigmented segment (see Fig. 1). At each sampling period, plants were taken into the Hydrolab where newly forming buds, immature tips, and mature segments (4-6 segments below the apex) were blotted dry on paper towels and carefully cut from the plant using a razor blade or small scissors. Each type of segment material was stored in small vials that were taken to the surface within 4 hrs of collection and either extracted for chemical analyses in a mixture of 25% methanol and 75% dichloromethane or dried and frozen for analyses of nitrogen and organic content. These samples were later analyzed for nitrogen content, ash content, and concentration of three secondary metabolites commonly produced by the genus Halimeda. In order to get enough material for an adequate determination of nitrogen, ash, and secondary metabolite content, we had to pool the new buds from several plants and the immature tips from several plants (usually about 10). Independent replicates for each time interval were obtained by making collections on 4 separate days. While processing these samples, some replicates were lost due to spillage or a breakdown of the high performance liquid chromatography (HPLC) equipment used for quantifying concentration of secondary metabolites. This resulted in less than 4 replicates for some time intervals.

During the 56 hrs when we quantified diel patterns of segment production, we simultaneously quantified herbivory on Halimeda incrassata. Two mature branches of H. incrassata were affixed into sections of 3-strand rope so that 5 segments on each branch were exposed to grazers. These ropes were placed on the sand plain at a depth of 21-24 m and on the reef slope at a depth of 15 m. Grazing was quantified as the number of segments eaten on each rope during each 4 hr interval. Grazed branches were replaced at each 4 hr monitoring interval and all branches were replaced every 12-24 hrs. Fifteen separate ropes were placed on the sand plain at intervals of 3-4 m. Twenty-one ropes were placed on the reef slope in a similar manner.

Diel pattern of segment production in Halimeda simulans was quantified by collecting 65 plants every 3-4 hrs from a 20-25 m deep sand plain near Coki Point, St. Thomas, U.S. Virgin Islands. The proportion of branches having initial buds or expanding but unpigmented tips was determined as described previously for H. incrassata.

To follow the time course of production and expansion of individual segments, we marked 23 individual Halimeda incrassata plants by placing numbered surveyor's flags next to their bases. As new buds were just becoming apparent (1200-1600 hrs), we marked 5-13 branches per plant by loosely attaching very small cable ties around the base of a mature segment that was beginning to produce a bud. This is a slight modification of Drew's (1983) previously proven method for following growth in Halimeda. The growth of expanding segments on each plant was monitored every 4 hrs for the next 51 hrs by placing a small centimeter rule behind each branch tip and recording its width to the nearest mm. The fatigue associated with continuously monitoring the plants for more than 2 days caused us to miss some plants at some sampling intervals; our sample size thus varied from 16-23 plants.

Nitrogen content of Halimeda incrassata segments of different ages was determined by CHN analysis. The organic content of segments of different ages was determined by drying them to a constant mass at 60°C and then determining their ash free dry mass after maintaining them at 450°C for 24 hrs.

Concentrations of the 3 abundant secondary metabolites produced by Halimeda, halimedatrial, epihalimedatrial, and halimedatetraacetate (see Paul, 1985), were determined by high performance liquid chromatography (HPLC). The retention time and peak size for known amounts of each metabolite had been determined previously under identical solvent and flow rate conditions (45% ethyl acetate in isooctane). Each extract from each compound was measured by cutting out and weighing the peak; this provided concentration data by reference to the peak sizes for known amounts of each compound. The identity of the peaks was confirmed by proton nuclear magnetic resonance spectrometry (NMR).

Although we made every effort to minimize the time between collection of the plants and determination of compound concentration, concentrations were usually not determined until several hours following collection. This delay was necessitated by the time required for blotting and clipping the plant tips, transporting these from the Hydrolab to the shore-based chemists, and the extraction and purification procedures performed prior to HPLC analysis. Since secondary metabolites produced by Halimeda are somewhat unstable (V. Paul, personal observation), we suspect our concentration data are low despite our attempts to stabilize these compounds by rapid extraction, chromatographing over

florisil, and keeping the extract frozen until just before it was injected into the HPLC. In 3 crudely quantified HPLC assays that we performed immediately after collecting tips from H. incrassata, we found halimedatrial concentrations ranging from 2-6% of blotted wet mass. These concentrations are higher than our rigorously quantified measurements but are similar to immediately analyzed extracts of Halimeda from the Pacific (Paul and Van Alstyne, in press). Thus, our concentration data may be low but the observed patterns of relative concentration would not have been affected since all samples were treated similarly.

To evaluate the susceptibility of young versus old Halimeda segments to herbivores, we paired branches of Halimeda incrassata having newly formed apical segments (approximately 20 hrs old) with branches having apical segments that were more than 48 hrs old (the shortest time in which we ever saw a new segment come to resemble an old one) and transplanted these onto the reef slope at a depth of 15 m. On our "young" branches, the top 2-3 segments appeared to have been produced recently as evidenced by their bright green color and soft texture, which appear to be a consequence of their incomplete calcification. All of the segments on our "old" branches appeared to be fully calcified. Each branch was 5 segments in length. The basal segment of each branch was wedged between the strands of a length of 3-strand rope and ropes were attached to pieces of coral on the reef. A distance of 2-3 m separated each rope. Thirty-seven ropes were placed on the reef at 1200 hrs and retrieved at 1000 hrs the next day. Grazing was measured as the number of segments consumed. Herbivores removed all of both plants on 2 ropes and none of either plant on 17 ropes; these replicates were excluded from the paired-sample analysis since they provided no information on the relative susceptibility of new versus old branches.

A similar test using branches of Halimeda simulans was performed in the 2-3 m deep bay near the Hydrolab shore base. Thirty-eight ropes with paired branches were set out at 1800 hrs and retrieved at 0930 hr the next day. At this site grazing was slight and was due primarily to very small scarids that did not remove entire segments. Here we counted the number of new versus old apical segments showing bite marks. To identify the fishes responsible for grazing in this habitat, we took time lapse movies (1 frame/min) of a dense patch of H. simulans from 1500-1000 hrs using an underwater 8 mm camera and electronic strobe mounted on a tripod.

We tested the effects of halimedatrial on herbivorous fish feeding by comparing the consumption of palatable plants coated with either (1) halimedatrial dissolved in diethyl ether or (2) diethyl ether alone (i.e., a control). Two palatable seaweeds were used, the seagrass Thalassia testudinum, which is preferred by parrotfishes, and the red alga Acanthophora spicifera, which is preferred by surgeonfishes (Lewis, 1985). Using these two

seaweeds allowed us to separately test the effects of halimedatrial on parrotfishes versus surgeonfishes. Halimedatrial was coated on the plants as 1% of their blotted wet mass (our initial HPLC analysis of fresh, young tips of Halimeda had indicated that halimedatrial comprised 2-6% of their blotted wet mass). Since this compound is hydrophobic, it adheres to the plant after the ether evaporates. The plant can then be placed in seawater with minimal loss of the halimedatrial. McConnell et al. (1982) developed this method for similar compounds and demonstrated that 88-100% of these types of hydrophobic compounds remain on coated plants after several hours in seawater. Following our assays, we extracted the uneaten portions of our treatment plants and confirmed by thin layer chromatography (TLC) that halimedatrial was still present and had not degraded to some other compound. We attempted similar tests with halimedatetraacetate but at the end of our assays we could not confirm its presence by TLC.

Paired groupings of halimedatrial-treated and control plants were placed on either shallow (2-3 m) back reef (assay for surgeonfishes) or the deeper (15-18 m) reef slope (assay for parrotfishes). For assays with either Thalassia or Acanthophora, 4 halimedatrial-coated plants or 4 control plants (6 cm long) were placed in a single 3-strand rope. Ropes with treatment plants and ropes with control plants were paired by placing them within 0.5-1 m of each other on the reef. For Thalassia assays we used 14 rope pairs; for Acanthophora assays we used 10 pairs. During the first hour of each test, each of 4 or 5 divers watched two pairs of ropes and recorded the number of separate fish grazing from the ropes, the number of bites taken from each, and whether the grazers were parrotfishes or surgeonfishes. After the first hour, all ropes were checked approximately hourly and a pair was removed whenever half or more of the plant material on either rope had been consumed. Some pairs were removed after only 1 hr, some remained for 7 hrs. Consumption was measured as the proportion (in cm) of each blade that was consumed (see Hay, 1984a). During our observations, Thalassia was fed on exclusively by the red band parrotfish Sparisoma aurofrenatum; Acanthophora was eaten exclusively by surgeonfishes, primarily Acanthurus bahianus and to a lesser extent by A. coeruleus.

The proximate effects of light cycles and diel changes in water chemistry on the timing of segment production were evaluated by altering the timing of day-night periods within different portions of the Smithsonian's coral-reef microcosm (see Fig. 2). By placing the refuge tanks on light-dark cycles that were opposite those of the large microcosm and rapidly cycling water from the microcosm through the refuge tanks, we were able to place Halimeda plants in a nighttime environment characterized by a daytime chemical regime. Water from the lighted microcosm (7000 l) was supplied at a rate that filled the refuge tanks (150 l) every 8 minutes; we assumed that the relatively small

biomass of algae in the refuge tanks would have no measurable effect on the chemistry of water being turned over at this rate. Since the changes in timing of light-dark cycles were sometimes complex, and since remembering the methodology of each experiment is crucial for evaluating the results, the specific methodologies and results of these experiments are given together in the results section.

## RESULTS

### Diel patterns of *Halimeda* growth

Production of new segments. The developmental sequence of newly forming *Halimeda* segments is shown in Figures 1 and 3. Very small (<1 mm wide) segment buds begin to form in the afternoon (1200-1600 hrs) with initiation of buds decreasing rapidly after sunset (Fig. 3). Developing tips expand rapidly over the course of only a few hours but remain unpigmented (Fig. 1) until just before sunrise when the segments rapidly change from white to green. This pattern occurs for both *Halimeda incrassata* and *H. simulans* (Fig. 3). We did not quantify the pattern for other *Halimeda* species but field observations on numerous reefs in the Caribbean Sea and Indian and Pacific Oceans suggest that most *Halimeda* species, and perhaps related genera like *Caulerpa*, *Udotea*, *Penicillus*, and *Rhipocephalus*, follow this basic pattern of nocturnal production of new growth (M. Hay and V. Paul, personal observation). We have, however, noted two exceptions to this pattern. Firstly, in St. Croix, *Halimeda copiosa* appeared to initiate segment production at the same time as other *Halimeda* species but it was common for some of the newly formed apical segments to remain unpigmented for much of the next day. Secondly, on Pacific reefs around Guam, newly produced *Halimeda macroloba* segments are commonly white during the first day after production and some plants occasionally produce new segments during the day (V. Paul personal observation).

If segments of *H. incrassata* at our study site were being produced throughout the 24 hr cycle, heavy fish grazing on segments produced during the day could cause the appearance of nocturnal production. We tested this hypothesis by separately caging 56 *Halimeda incrassata* plants occurring at 21 m depth on the sand plain and periodically noting their pattern of segment production. These caged plants followed the same pattern shown in Figure 3; new segments were never produced during the day. To assess the effects of small day-active grazers that would not have been excluded by our cages, we conducted experiments in the coral-reef microcosm at the Smithsonian Institution's National Museum of Natural History (see Fig. 2). Segment production of *Halimeda opuntia* in the microcosm follows the basic temporal pattern shown in Figure 3 (M. Hay, personal observation). When 10 portions of *H. opuntia* were moved from the large microcosm (7000 l) to two small refuge tanks (150 l) that had been cleaned

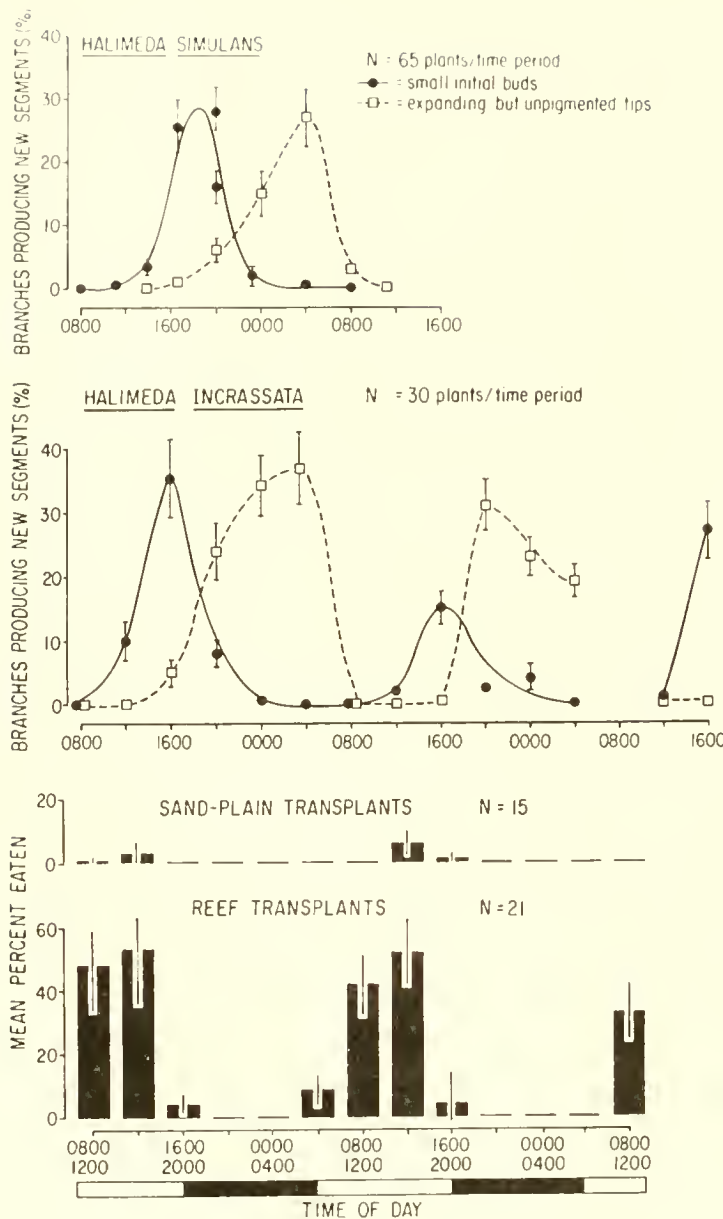


Figure 3. Diel pattern of segment production in Halimeda simulans at Coki Point, St. Thomas (top panel) and in (H. incrassata) at Salt River Canyon, St. Croix (middle panel). Solid and dashed lines in the upper graphs were fitted by eye. The histograms (bottom panel) show diel patterns of grazing on branches of H. incrassata placed on the Salt River Canyon sand plain at a depth of about 24 m or on the reef slope at a depth of 15 m. Error bars show  $\pm 1$  standard error. Shaded bars below the x-axis indicate periods of darkness.

of all obvious herbivores, none of these portions produced new segments during the day and 9 of the 10 produced new segments that night. Control portions that had been transplanted back into the microcosm showed the same pattern; none produced segments during the day and 10 of 10 produced new segments that night.

#### Growth of new segments

The sequence of development shown in Figure 3 is based on the average number of branch tips having each type of terminal segment at each sampling period; it does not clearly show how rapidly an average segment expands or how long the expansion of newly formed segments continues. We examined the time course of segment expansion by individually marking H. incrassata branches at the earliest visible stage of segment initiation and measuring the width of the newly forming segments and taking notes on their general appearance every 4 hours for the next 48-51 hrs. Production of very small (<1 mm wide), unpigmented buds began between 1300-1600 hrs (Fig. 4). Width of these newly forming segments increased approximately linearly for 24-28 hr after initiation and then leveled off. Between 0400 and 0600 hr the new tips began to show pigmentation and by 0800 hr all tips were pigmented and resembled mature segments except for their lack of obvious calcification and their smaller size (2.5 mm wide versus 4 mm wide in older segments).

#### Effects of light on the timing of segment production

To test the effect of changing light regimes on segment production, we performed the following experiments. After 8 hrs of light, we cut ten 50 cm<sup>2</sup> diameter cores from mats of Halimeda opuntia growing in the Smithsonian microcosm and transplanted these from the large microcosm into two separate refuge tanks (5 per tank) that were connected by water flow with the large microcosm (see Fig. 2). In one of these tanks the plants were subjected to continuous light; in the other tank they were subjected to continuous darkness (all plants had previously been acclimated to 16 hr light:8 hr dark periods). During the next 24 hr, 4 of the 5 plants kept in constant light produced normal segments at the same time that Halimeda populations in the large microcosm (now dark) were producing segments; no plants placed in constant darkness produced any new segments. Water flow to both refuge tanks had been adjusted so that turnover time was about 8 minutes. Thus, water chemistry in both tanks should have been similar since all water for both came directly from the large microcosm. Thirty-six hours after the initial transplanting, light cycles in both refuges were set on a reverse 16 hr light:8 hr dark cycle so that the dark cycle in the refuges coincided with the light cycle in the large microcosm. Thus, during the dark cycle in the refuges, plants received water with daytime chemical characteristics from the large microcosm. We allowed

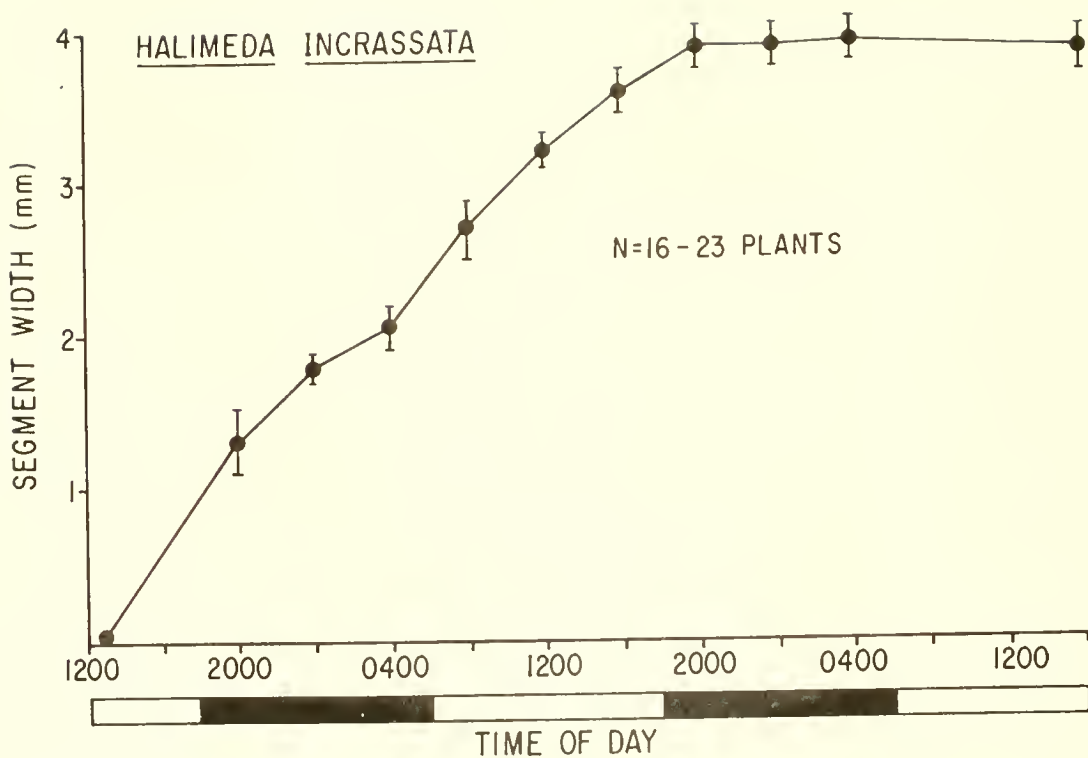


Figure 4. Change in width ( $\bar{X} \pm 1\text{SE}$ ) of newly forming segments of Halimeda incrassata as a function of time of day. Since multiple branch tips on one plant could not be considered independent replicates, we considered the mean width of tips on each plant a replicate. Plots are thus based on the average segment width per plant.

the plants to acclimate to this new light regime for 24 hr and then monitored their pattern of segment production. By the second day, 7 of the 10 transplants were producing segments in the dark (daytime in the large microcosm); none of the 10 control plants in the large microcosm were producing segments at this time.

#### Nutritional value and secondary metabolite production

Nitrogen and organic content. We estimated the nutritional quality of different aged segments of *Halimeda incrassata* from the sand-plain at St. Croix by evaluating their nitrogen content and organic content as a function of time of day (Fig. 5). During the night and early morning (2100-0800 hr), new segments are rich in nitrogen with values ranging from 3.4 to 4.2% of algal dry mass. The maximum concentration of 4.2% occurs as a small nitrogen spike at about 0600 hr (Fig. 5) when the new segments are rapidly becoming pigmented. This spike may result from an increased abundance of chlorophyll molecules and of various enzymes involved in photosynthesis since these contain nitrogen. Our visual observations of segment color, as well as TLC and HPLC analyses, indicated that pigments were rapidly entering the segments at this time and not merely coming to the surface where they would cause an obvious color change. Pigments, and possibly other cellular constituents, appear to move from older to newly developing segments just before and during sunrise. During the first daylight period encountered by the new segment (0800-1800 hr), nitrogen content drops by 22%; by the next morning (0630 hr), nitrogen content has dropped by about 43%. Segments that are several days old have only 25% of the nitrogen content of newly forming tips (Fig. 5).

Almost all of the change in nitrogen content per dry mass of plant shown in Figure 5 resulted from the increasing ash content of the segment and not from changes in the concentration of nitrogen relative to the organic content of the segment. When nitrogen content is expressed as a function of the ash free dry mass of the segments (Fig. 5), nitrogen concentration is relatively constant through time.

Organic content of segments shows a decline with age that is similar to that seen for nitrogen concentration (Fig. 5). Newly produced tips (1500-0630 hr) have only 25-45% ash content, new segments (0800-0630 hr) contain 45-67% ash, and old segments are 82% ash. Thus, the newly produced, uncalcified tips that are being expanded at night have nitrogen concentrations 370-450% higher than old segments and concentrations of organic material that are 300-410% higher than old segments.

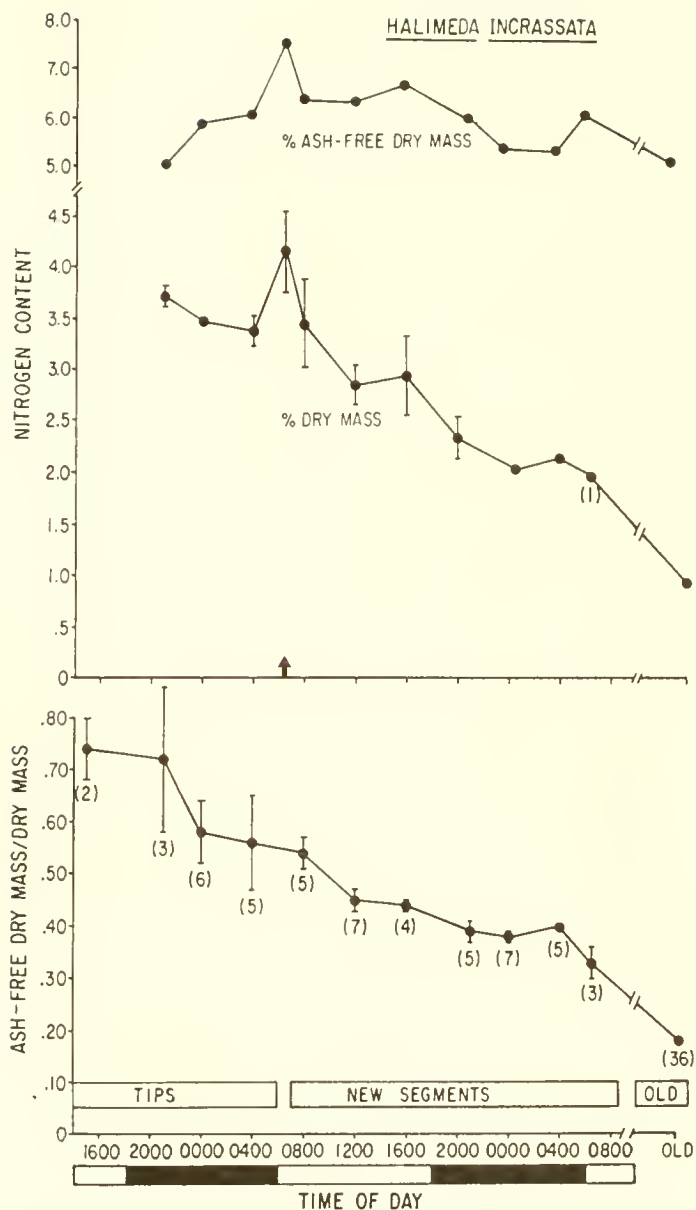


Figure 5. Nitrogen (top graph) and organic (bottom graph) content of newly forming segments of *Halimeda incrassata* as a function of time of day (=age). Graphs plot  $\bar{X} \pm 1SE$ . N for each mean in the lower graph is given in parentheses. N for nitrogen content as a function of dry mass is 2 except where noted. "Old" segments were collected 4-6 segments below the apex. Their true age is unknown but given the rate of segment production noted in other studies at this site (V. Paul and M. Hay, personal observation), minimum segment age was probably 4 days. The nitrogen content as a % of segment ash-free-dry mass/dry mass ratios (lower graph). The arrow on the x-axis in the upper figure indicates the approximate time during which the new segments become pigmented.

## Concentration of secondary metabolites

The concentration of common secondary metabolites produced by Halimeda also varied with segment age (Figs. 6 and 7, and Table 1). The concentrations of halimedatrial and ephihalimedatrial as a function of time and segment type are shown separately in Table 1. We know little about the biosynthesis of these two compounds, but their concentrations per ash-free dry mass of plant material were almost identical for all times and segment types. For this reason and because the compounds differ only stereochemically in structure (Paul, 1985), we pooled these two compounds to produce the top panel in Figure 6. With increasing segment age, the halimedatrials (halimedatrial and ephihalimedatrial combined) decrease as a percentage of the ash-free dry mass of the segments (Fig. 6); they constitute up to 4% of the ash-free dry mass of newly forming segments but constitute only 0.3% of the ash-free dry mass of old segments. Differences in concentrations between tips (2000-0400 hr), young segments (0800-1800 hr) and old segments (several days old) were large and significant ( $p < .05$ , Kruskal-Wallis Test and a nonparametric parallel of the Student-Newman-Keuls (see Zar, 1974) after randomly reducing all sample sizes to  $N=9$ ). Halimedatetraacetate did not occur in newly developing tips of H. incrassata (Fig. 6 lower panel). The 0400 hr samples showed no halimedatetraacetate; by 0800 hr, halimedatetraacetate concentration had risen to approximately 1% of the ash-free dry mass of the young segments. Its concentration then decreased in older segments. The concentration of halimedatetraacetate differed significantly between tips, young segments, and old segments ( $p < .05$ , Kruskal-Wallis Test and a nonparametric parallel of the Student-Newman-Keuls), with the maximum concentration occurring in young segments that had been formed the previous night. Since the rapid rise in halimedatetraacetate occurs at about sunrise when pigments are being pumped into the newly formed segments, it seems probable that halimedatetraacetate is being moved from the older to the younger segments or that biosynthesis of the tetraacetate is dependent upon photosynthesis.

For Halimeda simulans, we conducted only preliminary analyses on the timing of changes in secondary compound concentration. However, the available data suggest that patterns for H. simulans (Fig. 7) are similar to those documented for H. incrassata.

## Herbivory on Halimeda

Diel patterns. The rapid nocturnal expansion of the newly formed and uncalcified segments coincides with a predictable decrease in grazing that starts in the afternoon and continues throughout the night (Fig. 3). Grazing in the sandplain habitat was much less intense (0-6%/4 hr) than on the reef slope (as much

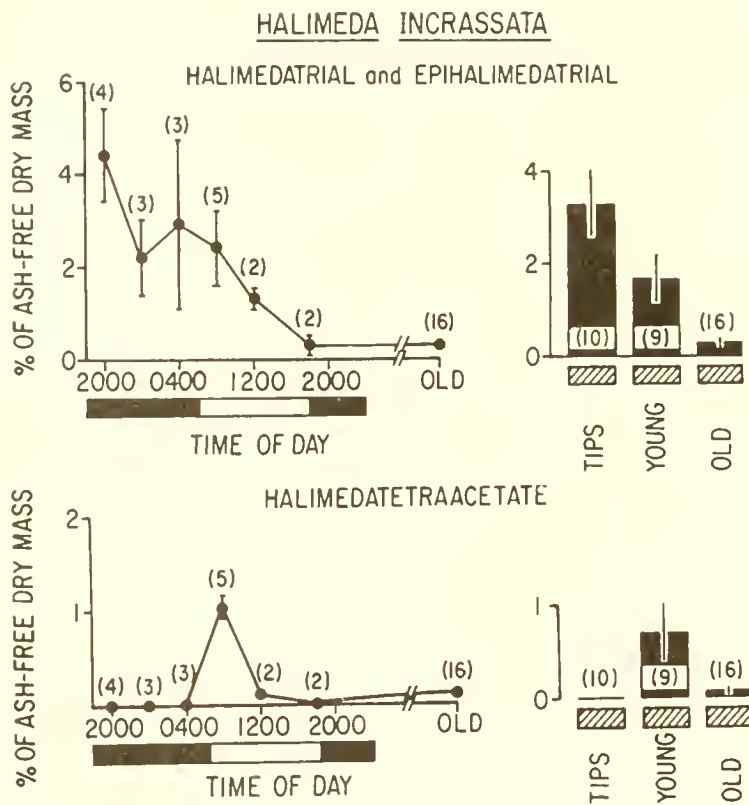


Figure 6. The concentration ( $\bar{X} \pm 1SE$ ) of halimedatrials (halimedatrial and epihalimedatral combined) (top panel) and halimedatetraacetate (bottom panel) in newly forming segments of *Halimeda incrassata* as a function of time of day (=age). Concentration is expressed as a percentage of the ash-free-dry mass of the plant portions extracted. The histograms on the right combine all small and unpigmented segments (2000-0400 hr) as tips, all new but pigmented segments (0800-1800 hr) as young segments, and all mature and heavily calcified segments (at least several days old) as old segments. Hatched bars below the histograms connect segment types that do not differ significantly ( $p > .05$ , Kruskal-Wallis Test and a nonparametric parallel of the Student-Newman-Keuls Test). Numbers in parentheses show N for each mean; vertical bars show  $\pm 1SE$ .

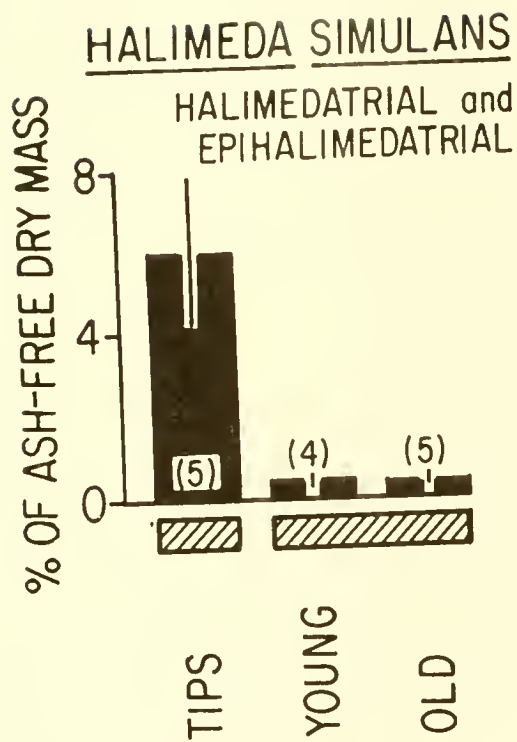


Figure 7. The concentration of halimedatrials in different aged sections of Halimeda simulans from the shallow lagoon near the Hydrolab shore base. Statistical evaluation was by the Kruskal-Newman-Keuls Test (Zar, 1974). Hatched bars below the histograms connect segment types that do not differ significantly ( $p > .05$ ).

Table 1. Concentration of halimedatrial and epihalimedatrial in newly developing segments of Halimeda incrassata as a function of time of day. Because we know little about their biosynthesis and because their structures differ only stereochemically, these compounds were combined to produce Figures 6 and 7.

		HALIMEDATRIAL	EPIHALIMEDATRIAL
		% of Ash-Free Dry Mass	% of Ash-Free dry Mass
(N)		$\bar{X} \pm 1SE$	$\bar{X} \pm 1SE$
<u>A</u>			
<u>Time</u>			
2000 hr	(4)	2.2 $\pm$ 1.0	2.2 $\pm$ 0.8
0000 hr	(3)	1.0 $\pm$ 0.3	1.2 $\pm$ 0.4
0400 hr	(3)	1.8 $\pm$ 1.0	1.1 $\pm$ 0.8
0800 hr	(5)	1.2 $\pm$ 0.4	1.2 $\pm$ 0.4
1200 hr	(2)	0.8 $\pm$ 0.2	0.4 $\pm$ 0.1
1800 hr	(2)	0.2 $\pm$ 0.1	0.1 $\pm$ 0.1
Old	(16)	0.2 $\pm$ 0.2	0.1 $\pm$ 0.0
<u>B</u>			
<u>Segment Type</u>			
Tips	(10)	1.7 $\pm$ 0.5	1.6 $\pm$ 0.3
Young	(9)	0.8 $\pm$ 0.2	0.8 $\pm$ 0.2
Old	(16)	0.2 $\pm$ 0.0	0.1 $\pm$ 0.0

as 53%/4 hr), but the temporal pattern was similar in both habitats (Fig. 3). Detectable losses to herbivores occurred only during the day.

#### Grazing on young versus old segments

When branches of H. incrassata with young (<24 hr old) apical segments were paired with branches having older (>48 hr old) apical segments and transplanted onto the reef slope, significantly more segments were consumed from branches with young apical segments than from branches with older apical segments ( $p < .05$ , Wilcoxon Paired-Sample Test, Fig. 8). On average, branches with new apical segments lost 39% more segments than branches with old apical segments. When similar assays were conducted using H. simulans in the shallow, mangrove-lined bay near the Hydrolab shore base, grazing by small fishes was concentrated on the newer segments. Sixteen percent of the new apical segments (6 of 38) showed grazing scars typical of small parrotfishes; none of the older apical segments (0 of 38) showed similar bite marks. The newer segments were therefore significantly more prone to attack by these small herbivores ( $p = .013$ , Fisher's Exact Test). Time lapse movies made in this area showed that almost all grazing was done by small brown and white striped parrotfishes which our field observations indicated were juvenile Scarus species.

#### Halimedatrial as an herbivore deterrent

When halimedatrial was coated onto Thalassia blades as 1% of their wet mass (our initial HPLC-derived estimates indicated that halimedatrial comprised 2-6% of the blotted wet mass of developing tips) and these blades were transplanted onto the reef, halimedatrial significantly reduced losses by 36% (Fig. 9) relative to ether-coated controls ( $p = .005$ , Wilcoxon Paired-Sample Test). Field observations showed that the Thalassia transplants at this site were fed on primarily by the red band parrotfish Sparisoma aurofrenatum. When similar assays were conducted using the red alga Acanthophora spicifera, it was fed on only by surgeonfishes, and halimedatrial reduced grazing by 47% (Fig. 9,  $p = .025$ , Wilcoxon Paired-Sample Test). Following these field assays, remaining portions of the coated plants were extracted and analyzed by TLC. Halimedatrial was still present on the plants and had not degraded to some other compound. Since TLC is not a quantitative method, the concentration of the remaining compound could not be determined.

Direct observation of parrotfish feeding during these experiments indicated that coated blades did not differ significantly ( $.10 > p > .05$ , Contingency Table Analysis) from control blades in their probability of being bitten at least once during the course of our assays (Table 2). However, once bitten, a parrotfish was significantly ( $.025 > p > .01$ , Paired-Sample t-Test)

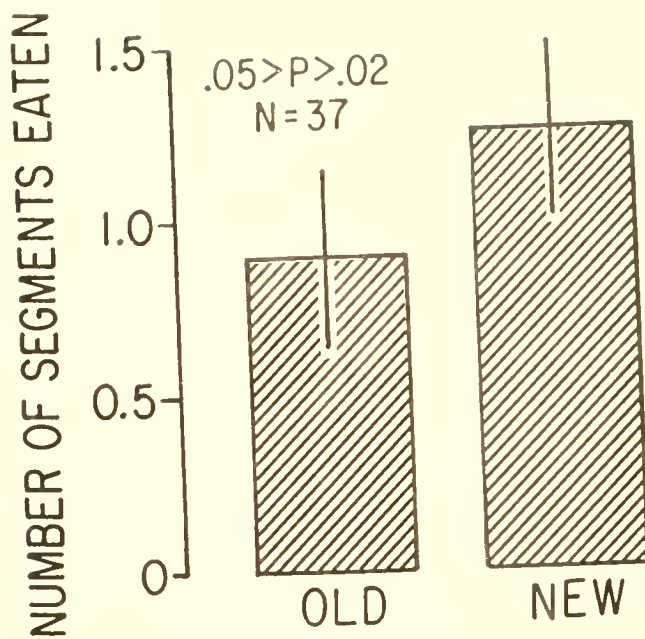


Figure 8. Grazing on halimeda incrassata branches with terminal segments that were approximately 20 hr old (new) versus branches with terminal segments that appeared several days old (old). Vertical bars through the histograms show  $\pm 1SE$ . On 19 of the 37 ropes, herbivores removed all of both plants (2 ropes) or none of either plant (17 ropes); these replicates were excluded from Wilcoxon Paired-Sample Test since they provided no information on the relative susceptibility of new versus old branches. The sample size used to generate the p-value in the figure was thus 18.

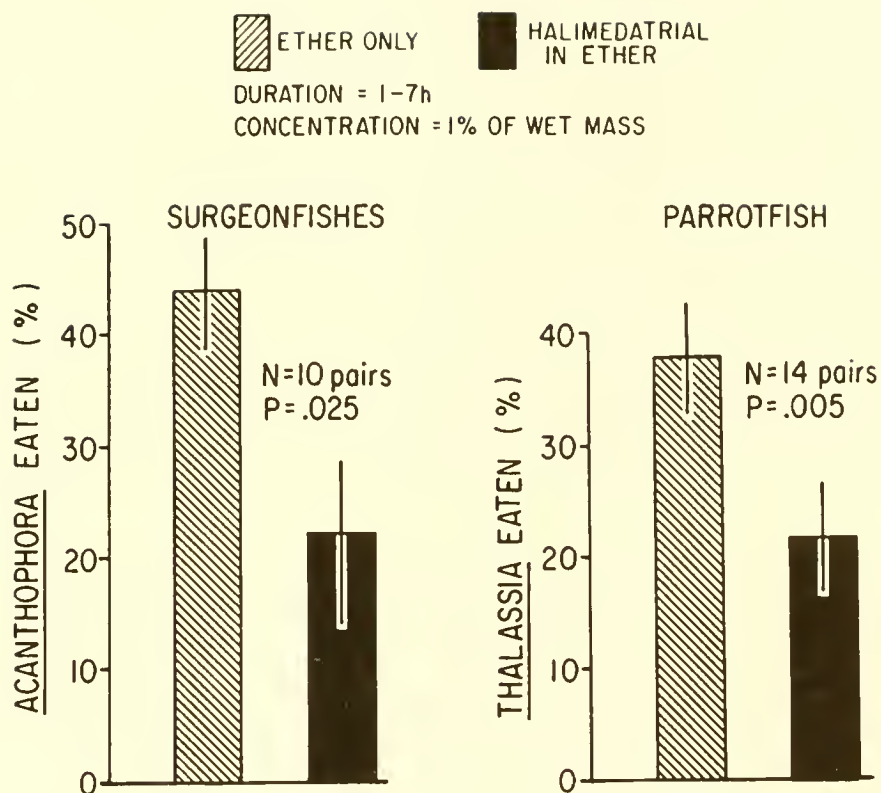


Figure 9. The effects of halimedatrial on feeding by herbivorous parrotfish and surgeonfishes. Statistical evaluations are by Wilcoxon Paired-Sample Test. The seagrass Thalassia testudinum was used as the assay seaweed in tests with the parrotfish; the red alga Acanthophora spicifera was used in tests with surgeonfishes.

more likely to take additional bites from a control blade than from a treatment blade. Fish that initially bit control blades usually took several bites; fish that initially bit treatment blades usually swam away without feeding more (Table 2). Surgeonfishes showed a significant ability to avoid treated blades without biting them (.025>p>.01, Contingency Table Analysis) and also took fewer bites from treated blades (.01>p>.005, Paired-Sample t-Test).

## DISCUSSION

### Nocturnal growth

Studies assessing diel variation in the growth of seaweeds are rare. The limited data presently available show that photosynthesis and growth are synchronous in most species and that elongation of the thallus is a light-dependent process. Stromgren (1977a, b) investigated growth in length of five brown seaweeds common to the west coast of Norway by using a laser diffraction method (Stromgren, 1975) to measure very small changes in length with great accuracy. He found growth rates, measured over a few hours, to be stimulated by both increasing light intensities and increasing day length up to some saturation intensity or period of illumination. When placed in the dark, some species could use stored material to continue to grow in length but growth rates were always greatly reduced. One species, *Fucus serratus*, showed significant shrinkage during periods of darkness (Stromgren, 1977a). More recent studies of both red (Rhodophyta) and brown (Phaeophyta) seaweeds from the southern California intertidal show similar patterns (Stromgren, 1984).

The nocturnal initiation of new growth in Halimeda (Fig. 3) is clearly different from these previously documented patterns even though expansion of new segments continues throughout the next day (Fig. 4). Our casual observations of numerous siphonous green seaweeds from tropical habitats suggest that similar growth patterns may occur in Udotea, Penicillllus, Caulerpa, Rhipocephalus, and Avrainvillea.

Nocturnal increases in growth-related processes are not unique to seaweeds. Many terrestrial plants in habitats subject to severe water stress possess crassulacean acid metabolism (CAM) which allows them to acquire carbon at night and fix it during the day. This temporal separation of carbon acquisition and fixation results in large savings of water for terrestrial plants but obviously will not be of value for subtidal seaweeds. Additionally, several terrestrial plants that do not use CAM appear to increase in length at night. They produce new cells during the day but do not expand them until after dark when turgor pressure increases due to decreased evapotranspiration (F. Putz, personal communication). Again, this daily pattern of

Table 2. Effect of Halimeda metabolites on grazing by (A) parrotfishes (primarily the red band parrotfish Sparisoma aurofrenatum) and (B) the surgeonfishes Acanthurus bahianus and A. coeruleus. Assays for parrotfish grazing used Thalassia testudinum as the test plant and were conducted on the reef slope at a depth of 15-18 m. Assays for surgeonfish grazing used Acanthophora spicifera as the test plant and were conducted on the back reef at a depth of 2-3 m. All compound concentrations were at 1% of algal wet mass. 14 control-treatment pairs were used for the parrotfish assay and 10 for the surgeonfish assay. We observed 17 parrotfish and 12 surgeonfish graze from our plants.

# Blades Bitten Experimental/Control	Contingency Table p-value	Paired Samp.	
		Bites/Blade ( $\bar{x} \pm 1SE$ ) Experimental/Control	t-Test p-value
<b>(A) Parrotfish</b>			
Grazing	7      12      .10>p>.05	$0.5 \pm 0.2$	$2.5 \pm 0.7$ .025>p>.01
<b>(B) Surgeonfish</b>			
Grazing	3      9      .025>p>.01	$2.2 \pm 1.3$	$8.6 \pm 2.1$ .01>p>.005

elongation appears to be related to diel changes in water availability and could not account for nocturnal growth in submerged seaweeds.

#### Proximate factors affecting nocturnal segment production

Timing of segment production in Halimeda opuntia was sensitive to changes in the timing of the light-dark cycle. Plants that were transplanted from the large microcosm into the small refuge tanks (Fig. 2) and subjected to reversed day/night cycles produced new segments during the dark cycle even though the water in the refuge tank would have had daytime chemical characteristics since it was coming from the lighted microcosm. This indicates that light levels are more important proximate cues than diel changes in water chemistry. However, it takes some time for plants to readjust to changing light cycles. When plants were removed from the microcosm at the midpoint of their normal light cycle, those placed in the dark did not produce new segments in the next 24 hr while those held in constant light produced new segments on their expected schedule even though it was not dark at this time. These investigations need to be expanded but these preliminary data suggest that onset of the dark cycle is the primary proximate cue synchronizing segment formation. If darkness comes too early (after 8 instead of 16 hr), no segments are produced. This suggests that some critical amount of stored reserves may need to be accumulated before segment production can be initiated regardless of other cues received by the plant.

Nocturnal growth of Halimeda could have arisen in response to (1) physiological advantages associated with nocturnal water chemistry, (2) advantages associated with a short term (10-12 hr) escape from day-active herbivores, or (3) some unique and, as yet, unrecognized physiological need of Halimeda.

Experiments in the microcosm show that timing of segment production responds to changes in the timing of the day-night cycle even if plants in the dark cycle exposed to water chemistry are not directly controlling the timing of segment production. However, it is still possible that diel changes in water chemistry could significantly affect the rate of growth as opposed to the timing at which it occurs. Plants in the microcosm were only recorded as producing or not producing new segments at given time intervals. Potential differences in the rate of production under different types of light cycles and chemical conditions were not investigated. Although we cannot rigorously exclude the possibility that diel changes in water chemistry interact with Halimeda physiology to select for nocturnal growth, we feel that other factors may have been more important selective agents.

## Ultimate factors selecting for nocturnal segment production

Herbivore avoidance may have played an important role in selecting for the nocturnal timing of Halimeda growth shown in Fig. 3. All of our data suggest that nocturnal production of new segments results in lowering losses to day-active herbivorous fishes which have been shown to be the herbivores of primary importance on many coral reefs (Randall, 1961; Hay, 1981a, 1984a, 1985; Hay et al., 1983; Lewis, 1986).

Mature portions of most Halimeda species appear to be well protected from herbivory. Of more than 100 algal species that have been exposed to guilds of herbivores (primarily fishes) on 16 different reefs in the Caribbean Sea and Indian Ocean, species of Halimeda are consistently among the species least susceptible to removal (Ogden, 1976; Hay, 1981a, 1984b; Lobel and Ogden, 1981; Littler et al., 1983; Lewis, 1985, 1986; Paul and Hay, 1986). Decreased vulnerability appears to result from multiple defensive characteristics that include: (1) adult tissues composed of 22% (H. cuneata) to 85% (H. opuntia) calcium carbonate by dry weight (Hillis-Colinvaux, 1980); (2) production in Halimeda of toxic diterpenoid trialdehydes (Paul and Fenical, 1983; Paul, 1985); and (3) an aggregated growth form in some species (H. opuntia) that decreases herbivore access and may increase the probability of herbivores being attacked by their predators while feeding on the plant (Hay, 1981b; Hay et al., 1983). Although formidable, these defenses are not absolute. Some parrotfish commonly eat Halimeda, often biting the tips, (Lobel and Ogden, 1981; Wolf, 1985; N. Wolf, personal communication; D. Morrison, personal communication). We occasionally observed parrotfish feeding on the tips of Halimeda at our study sites in St. Croix and we often observed the effects of what appeared to be parrotfish grazing. Young segments were preferred to older segments by fishes on the reef slope (Fig. 8) and by fishes in the shallow lagoon. At the lagoon site, we often saw small bite marks in young segments; in addition, mature apical segments occasionally had small grazing scars that coincided with locations where new buds or tips would have occurred (see Fig. 1). Grazing scars were rare in other locations on apical segments or on mature segments on any portion of the plant. On the deep sand plain, we seldom saw evidence of grazing on mature Halimeda segments; however, during the 2 days that we repeatedly measured the width of newly forming segments (Fig. 4), some of these appeared to have been grazed by small fishes.

Several factors may explain why herbivorous fishes consume young segments more frequently than older segments. When first initiated, tips of Halimeda incrassata are not calcified and they have nitrogen and organic contents that are over 300% higher than those found in mature segments (Fig. 5). By 1200 hr when the branches with young versus old apical segments were

transplanted onto the reef slope for the herbivory assay (Fig. 8), young segments still contained 150% more organic content and 210% more nitrogen than old segments. Given the high food value of young versus old segments, it is surprising that grazing was only 39% higher on young segments (Fig. 8). We assume that the increased abundance of the halimedatrials and halimedatetraacetate (Figs 6 and 7, Table 1) in younger segments kept herbivory from more closely tracking the differences in segment food value. Halimedatrial clearly deterred grazing by both parrotfishes and surgeonfishes on the reef at St. Croix (Fig. 9, Table 2) and Targett et al. (1986) recently showed that halimedatetraacetate deterred grazing by the parrotfish Sparisoma radians in laboratory assays. Additionally, Paul and Van Alstyne (in press) have shown that halimedatrial and halimedatetraacetate both deter feeding by Pacific reef fishes and that halimedatrial is a stronger deterrent than halimedatetraacetate.

In contrast to our observations on fish feeding, Targett et al. (1986) noted that Sparisoma radians avoided the more chemically defended tips of Halimeda in favor of the less chemically rich, but more heavily calcified, basal portions of the plant. Additionally, Pacific reef fishes appear to graze new unpigmented tips less than older pigmented ones (Paul and Van Alstyne, 1987), suggesting that new tips are better defended despite their lack of calcification. These observations suggest that different fishes may respond very differently to various combinations of chemical and morphological defenses. The unusually high incidence of chemical defenses in tropical seaweeds that are calcified (Hay, 1984b; Paul and Hay, 1986) suggests that multiple defenses may be necessary for plants that live in habitats with a diverse assemblage of herbivores, several of which may be immune to any single defensive trait.

If different herbivores are differentially affected by halimedatrial versus halimedatetraacetate, then the production of the halimedatrials primarily at night and of halimedatetraacetate early in the day (Fig. 6) may correspond to the activity patterns of different herbivores. This could be a particularly interesting area for future study since different types of marine herbivores have recently been shown to have very different responses to terpenoids produced by other seaweeds (Hay et al., 1987a, b; Paul et al., 1987). The fact that halimedatrial strongly deters fish grazing (Fig. 9; Paul and Van Alstyne, 1987) yet is highest in concentration at night when herbivorous fishes are inactive is puzzling. This deserves further study and may suggest that high nocturnal concentrations of halimedatrial serve to defend the soft, new segments from night-active grazers like sea urchins or from more inconspicuous nocturnal herbivores such as amphipods, crabs, and small gastropods that are not normally considered to be capable of grazing mature, calcified segments. Additionally, preliminary investigations (V. Paul, work in progress) suggest that biosynthesis of

halimedatetraacetate requires small organic carbon compounds and is therefore coupled to photosynthesis. Halimedatrial and epihalimedatrial appear to be enzymatic products of halimedatetraacetate. Thus, the trials may be enzymatically formed at night and pumped into the nutritionally valuable new tips. At sunrise, photosynthetic activity begins and new halimedatetraacetate can be produced. Since halimedatrial is a stronger herbivore deterrent than halimedatetraacetate (Paul and Van Alstyne, 1987), this is consistent with the hypothesis that the valuable and more morphologically defended older segments are protected by a less potent compound that can be converted to the stronger forms by enzymatic action.

#### Interactions between anti-herbivore defenses and plant food value

Newly produced segments of Halimeda are soft, unpigmented, and rich in food value as evidenced by their high concentrations of nitrogen and organic contents (Fig. 5). The morphological defense of calcification (Littler and Littler, 1980; Steneck and Watling, 1982) cannot play a role during the first night since the process of calcification in Halimeda is dependent upon photosynthesis to raise internal pH and cause precipitation of  $\text{CaCO}_3$  in the semi-isolated compartments that occur between utricles (the swollen terminal portions of the filaments that coalesce to form the thallus of Halimeda) (Borowitzka, 1977). Thus, if soft new growth is to be defended during the night and early portions of the first day, then concentration of chemical feeding deterrents within the new sections may be necessary. This is the pattern shown in Table 1 and Figs. 6 and 7. The halimedatrials are abundant in the youngest tissues and significantly decrease in abundance with increasing age of the segment (Fig. 6). Halimedatetraacetate is absent in the newest tips, rapidly increases in abundance at dawn, and is low in abundance in old segments (Fig. 6). These data are consistent with the hypotheses that the plant is reducing its chemical defense of tissues as they become better defended morphologically and of less nutritional value (Fig. 5) to herbivores. These patterns are summarized qualitatively in Fig. 10.

The timing of pigmentation in newly forming segments may also be an example of how diel patterns in the allocation of scarce resources may have evolved to minimize losses to herbivores. In the field, newly forming segments of Halimeda do not become pigmented until just before sunrise. Thus, the valuable, nitrogen-containing molecules necessary for photosynthesis are not placed in the new, and more herbivore-susceptible, segments until just before the lighted period of the day when they can begin producing income for the plant. A similar pattern occurs in some terrestrial understory plants since many do not pigment their leaves until they are fully formed and structurally capable of rapid photosynthesis. It has

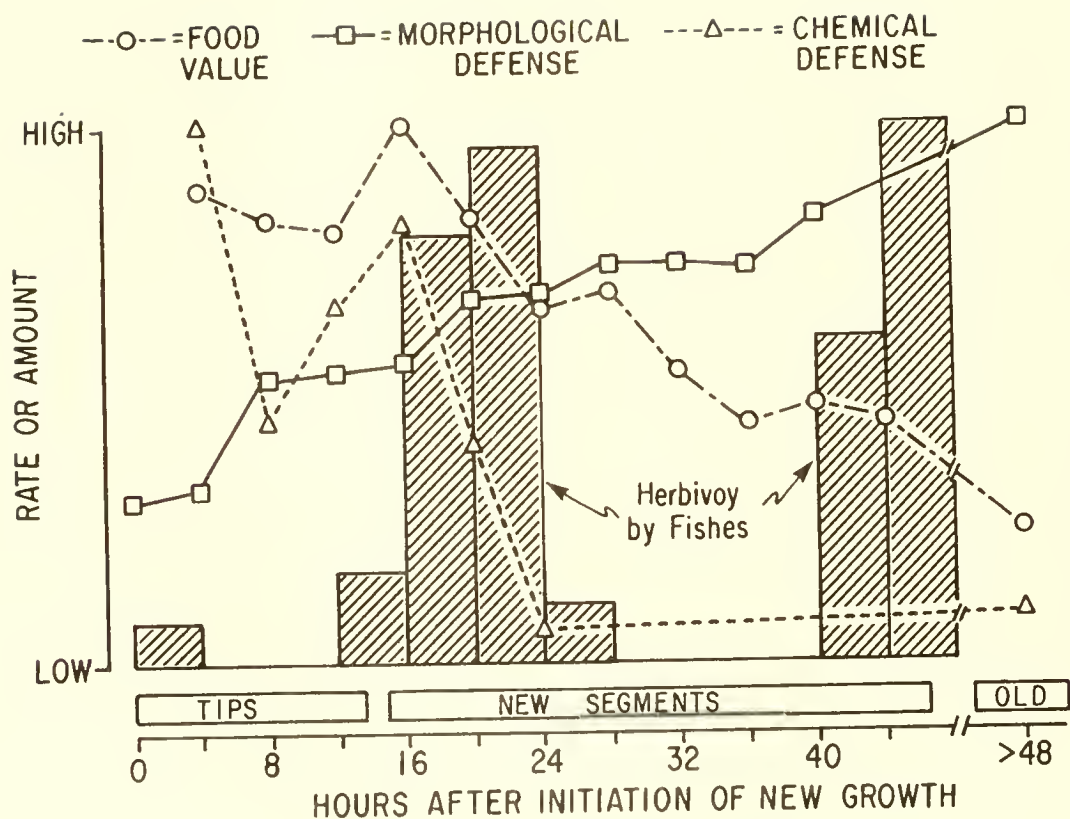


Figure 10. A qualitative summary of temporal patterns of herbivore activity, segment food value (N), chemical defense, and morphological defense (% ash). This figure assumes that new growth is initiated at 1600 hr and combines the concentrations of both halimedatrials and halimedatetraacetate into a single amount to generate the chemical defense pattern.

been hypothesized (P. Coley, personal communication) that pigmentation is delayed in these species to avoid loss of chlorophyll to herbivores before the leaves are capable of rapid production.

#### A unique curiosity or a general pattern?

Since so few other studies have assessed diel patterns in plant growth and since none have evaluated its ecological consequences, we are unable to say whether Halimeda represents an interesting but unique curiosity of nature or simply the first of many species that will eventually be found to exhibit this growth pattern. However, a few other studies on seaweeds, and many other studies on phytoplankton, suggest that the growth pattern is not unique to Halimeda and that diel patterns of growth may function to reduce herbivory in other species as well.

In contrast to the daytime growth of seaweeds documented for the temperate algae studied by Stromgren (1977a, b, 1984), Dawes and Barilotti (1969) conducted laboratory experiments showing that growth of the noncalcified, siphonous green, Caulerpa prolifera, occurred primarily at night and peaked 2-4 hr after initiation of the dark period. The presence of nocturnal growth in this siphonous, chemically defended (McConnell et al., 1982) species, which does not calcify, suggests that physiological constraints associated with calcification in Halimeda need not be responsible for its nocturnal growth pattern.

Although little information is available on diel patterns of growth in seaweeds, diel patterns of growth in dinoflagellates and diatoms have been documented on numerous occasions. Phased cell division, synchronized on light/dark cycles, is well known and common in most major taxa of phytoplankton (Sournia, 1974). Division in marine diatoms occurs at various species-specific times throughout a 24 hr cycle (Sournia, 1974) while division of photosynthetic marine dinoflagellates is generally in the late night or early morning under both laboratory and field conditions (Weiler and Chisholm, 1976; Weiler and Eppley, 1979). Individuals of several of these phytoplankton species may be more susceptible to herbivores during, or just after, cell division. For the marine diatom, Ditylum brightwellii, the probability of being consumed by the copepod, Calanus helgolandicus, increases three fold during division (Richman and Rogers, 1969). Additionally, the dinoflagellate genus Ceratium has imperfectly developed horns (proposed defensive structures) for several hours following division (Sournia, 1974). Weiler and Eppley (1979) noted that division in more than 40 species of the dinoflagellate genus Ceratium occurs at about 10 hr after darkness begins and suggested that this might reduce losses to vertically migrating herbivores. The considerable evidence that different life stages of Calanus graze with variable intensity at different times of

day (Petipa, 1964; Petipa and Makarova, 1969) suggests that synchronized division of phytoplankton could have effects on herbivory similar to those proposed for the seaweeds investigated in this study. This seems especially promising since filter feeders select food items based upon both particle size (Frost, 1977) and particle flavor (Rassoulzadegan et al., 1984; Huntley et al., 1986) and since both of these parameters may change with cell age. It is therefore possible that the processes and interactions documented in this study of Halimeda and its grazers may be similar to those occurring among other, very different, types of species. It appears that coordinating diel patterns of growth with rapidly mobilizable defenses against predators could be an important component of the ecology of many organisms.

#### ACKNOWLEDGMENTS

The majority of this work was funded by NOAA's National Undersea Research Program. Additional facilities and support were provided by the University of North Carolina's Institute of Marine Sciences, the College of the Virgin Islands, Coral World, the Marine Systems Laboratory of the Smithsonian Institution, and N.S.F grant #CHE83-15546 to W. Fenical. The divers and staff associated with Hydrolab worked extremely hard to facilitate this project; its completion would have been impossible without their support. Emmett Duffy, Jane Lubchenco, Paul Renaud, and Alan Shanks reviewed the manuscript. This is NURP publication #J-458.

#### LITERATURE CITED

Adey, W. H. 1983. The microcosm: A new tool for reef research. Coral Reefs, Vol. 1, pp. 193-201.

Adey, W., W. Gladfelter, J. Ogden and R. Dill. 1977. Field guide book to the reefs and reef communities of St. Croix, Virgin Islands. Third International Symposium on Coral Reefs, Atlantic Reef Committee, University of Miami, FL.

Bach, S. D. 1979. Standing crop, growth and production of calcareous siphonales (Chlorophyta) in a south Florida lagoon. Bull. Mar. Sci., Vol. 29, pp. 191-201.

Borowitzka, M. A. 1977. Algal calcification. Oceanogr. Mar. Biol. Annu. Rev., Vol. 15, pp. 189-223.

Brawley, S. H., W. H. Adey. 1981. The effects of micrograzers on algal community structure in a coral reef microcosm. Mar. Biol., Vol. 61, pp. 167-177.

Carpenter, R. C. 1986. Partitioning herbivory and its effects on coral reef algal communities. Ecol. Monogr., Vol. 56, pp. 345-363.

Davies, R. J., J. F. Marshall. 1985. Halimeda bioherms-low energy reefs, Northern Great Barrier Reef. Proceedings of the Fifth International Coral Reef Congress. Tahiti, Vol. 5, pp. 1-7.

Dawes, C. J., D. C. Barilotti. 1969. Cytoplasmic organization and rhythmic streaming in growing blades of Caulerpa prolifera. Amer. J. Bot., Vol. 56, pp. 8-15.

Drew, E. A. 1983. Halimeda biomass, growth rates and sediment generation on reefs in the Central Great Barrier Reef Province. Coral Reefs, Vol. 2, pp. 101-110.

Drew, E. A., K. M. Abel. 1985. Biology, sedimentology and geography of the vast inter-reefal Halimeda meadows within the Great Barrier Reef province. Proceedings of the Fifth International Coral Reef Congress. Tahiti, Vol. 5, pp. 15-20.

Feeley, P. O. 1970. Seasonal changes in oak leaf tannins and nutrients as a cause of spring feeding by winter moth caterpillars. Ecology, Vol. 51, pp. 565-581.

Frost, B. W. 1977. Feeding behavior of Calanus pacificus in mixtures of food particles. Limnol. Oceanogr., Vol. 22, pp. 472-491.

Hay, M. E. 1981a. Spatial patterns of grazing intensity on a Caribbean barrier reef: Herbivory and algal distribution. Aquat. Bot., Vol. 11, pp. 97-109.

Hay, M. E. 1981b. The functional morphology of turf-forming seaweeds: Persistence in stressful marine habitats. Ecology, Vol. 62, pp. 739-750.

Hay, M. E. 1984a. Patterns of fish and urchin grazing on Caribbean coral reefs: Are previous results typical? Ecology, Vol. 65, pp. 446-454.

Hay, M. E. 1984b. Predictable spatial escapes from herbivory: How do these affect the evolution of defense mechanisms in seaweeds? Oecologia, Vol. 64, Berlin, pp. 396-407.

Hay, M. E. 1985. Spatial patterns of herbivore impact and their importance in maintaining algal species richness. Proceedings of the Fifth International Coral Reef Congress. Tahiti, Vol. 4, pp. 29-34.

Hay, M. E., T. Colburn and D. Downing. 1983. Spatial and temporal patterns in herbivory on a Caribbean fringing reef: The effects on plant distribution. Oecologia, Vol. 58, Berlin, pp. 299-308.

Hay, M. E., J. E. Duffy, C. A. Pfister and W. Fenical. 1987a. Chemical defense against different marine herbivores: Are amphipods insect equivalents? Ecology, Vol. 68, pp. 1567-1580.

Hay, M. E., W. Fenical, and K. Gustafson. 1987b. Chemical defense against diverse coral-reef herbivores. Ecology, Vol. 68, pp. 1581-1591.

Hillis-Colinvaux, L. 1980. Ecology and taxonomy of Halimeda: Primary producer of coral reefs. Adv. Mar. Biol., Vol. 17, pp. 1-327

Huntley, M., P. Sykes, S. Rohan and V. Marin. 1986. Chemically-mediated rejection of dinoflagellate prey by the copepods Calanus pacificus and Paracalanus parvus: Mechanism, occurrence and significance. Mar. Ecol. Prog. Ser., Vol. 28, pp. 105-120.

Janzen, D. H. 1976. Why bamboos wait so long to flower. Annu. Rev. Ecol. Syst., Vol. 7, pp. 376-391.

Lewis, S. 1985. Herbivory on coral reefs: Algal susceptibility to herbivorous fishes. Oecologia, Vol. 65, Berlin, pp. 370-375.

Lewis, S. M. 1986. The role of herbivorous fishes in the organization of a Caribbean reef community. Ecol. Monogr., Vol. 56, pp. 183-200.

Lewis, S. M., J. N. Norris, R. B. Searles. 1987. The regulation of morphological plasticity in tropical reef algae by herbivory. Ecology, Vol. 68, pp. 636-641.

Littler, M. M., D. S. Littler. 1980. The evolution of thallus form and survival strategies in benthic marine macroalgae: Field and laboratory tests of a functional form model. Amer. Nat., Vol. 116, pp. 25-44.

Littler, M. M., P. R. Taylor, D. S. Littler. 1983. Algal resistance to herbivory on a Caribbean barrier reef. Coral Reefs, Vol. 2, pp. 111-118.

Lobel, P. S. and J. C. Ogden. 1981. Foraging by the herbivorous parrotfish Sparisoma radians. Mar. Biol., Vol. 64, pp. 173-183.

Lubchenco, J. and J. Cubit. 1980. Heteromorphic life histories of certain marine algae as adaptations to variations in herbivory. Ecology, Vol. 61, pp. 676-687.

Lubchenco, J. and S. D. Gaines. 1981. A unified approach to marine plant-herbivore interactions. I, Populations and communities. Annu. Rev. Ecol. Syst., Vol. 12, pp. 405-437.

McConnell, O. J., P. A. Hughes, N. M. Targett and J. Daley. 1982. Effects of secondary metabolites on feeding by the sea urchin, Lytechinus variegatus. J. Chem. Ecol., Vol. 8, pp. 1427-1453.

Milliaman, J. D. 1974. Recent Sedimentary Carbonates, Part 1: Marine Carbonate. New York, N.Y., Springer.

Neumann, A. C., L. S. Land. 1975. Lime mud deposition and calcareous algae in the Bight of Abaco, Bahamas: A budget. J. Sediment. Petrol., Vol. 45, pp. 763-786.

Ogden, J. C. 1976. Some aspects of herbivore-plant relationships on Caribbean reefs and seagrass beds. Aquat. Bot., Vol. 2, pp. 103-116.

Paul, V. J. 1985. Chemical adaptation in pantropical green algae of the genus Halimeda. Proceedings of the Fifth International Coral Reef Congress. Tahiti, Vol. 5, pp. 39-45.

Paul, V. J. and W. Fenical. 1983. Isolation of Halimedatrial: Chemical defense adaptation in the calcareous reef-building alga Halimeda. Science, Vol. 221, pp. 747-749.

Paul, V. J. and W. Fenical. 1986. Chemical defense in tropical green algae, order caulerpales. Mar. Ecol. Prog. Ser., Vol. 34, pp. 157-169.

Paul, V. J. and M. E. Hay. 1986. Seaweed susceptibility to herbivory: Chemical and morphological correlates. Mar. Ecol. Prog. Ser., Vol. 33, pp. 255-264.

Paul, V. J. and K. L. Van Alstyne. 1987. Chemical defense and chemical variation in some tropical Pacific species of Halimeda (Halimedaceae:Chlorophyta). Coral Reefs, Vol. 6, pp. 263-269.

Paul, V. J., M. E. Hay, J. E. Duffy, W. Fenical and K. Gustafson. 1987. Chemical defense in the seaweed Ochthodes secundiramea (Montagne) Howe (Rhodophyta): Effects fits monoterpenoid components upon diverse coral-reef herbivores. J. Exp. Mar. Biol. Ecol., Vol. 114, pp. 249-260.

Petipa, T. S. 1964. Diurnal rhythm of the consumption and accumulation of fat in Calanus heloglandicus (Claus) in the Black Sea. Dokl. Akad. Nauk. SSR Biol. Sci. Sect., Vol. 156, pp. 361-364.

Petipa, T. S. and N. P. Makarova. 1969. Dependence of phytoplankton production on rhythm and rate of elimination. Mar. Biol., Vol. 3, pp. 191-195.

Randall, J. E. 1961. Overgrazing of algae by herbivorous marine fishes. Ecology, Vol. 42, p. 812.

Rassoulzadegan, F., L. Fenaux and R. R. Strathmann. 1984. Effect of flavor and size on selection of food by suspension-feeding plutei. Limnol. Oceanogr., Vol. 29, pp. 357-361.

Richamn, S. and J. N. Rogers. 1969. The feeding of Calanus helgolandicus on synchronously growing populations of the marine diatom Ditylum brightwellii. Limnol. Oceanogr., Vol. 14, pp. 701-709.

Sournia, A. 1974. Circadian periodicities in natural populations of marine phytoplankton. Adv. Mar. Biol., Vol. 12, pp. 325-389.

Steneck, R. S. 1986. The ecology of coralline algal crusts: Convergent patterns and adaptive strategies. Ann. Rev. Ecol. Syst., Vol. 17, pp. 273-303.

Steneck, R. S. and L. Watling. 1982. Feeding capabilities and limitations of herbivorous molluscs: A functional group approach. Mar. Biol., Vol. 68, pp. 299-319.

Stockman, K. W., R. N. Ginsburg and E. A. Shinn. 1967. The production of lime mud by algae in south Florida. J. Sediment. Petrol., Vol. 37, pp. 633-648.

Stromgren, T. 1975. Linear measurements of growth of shells using laser diffraction. Limnol. Oceanogr., Vol. 20, pp. 845-848.

Stromgren, T. 1977a. Apical length growth of five intertidal species of Fucales in relation to irradiance. Sarsia, Vol. 63, pp. 39-47.

Stromgren, T. 1977b. The effect of photoperiod on the length growth of five species of intertidal Fucales. Sarsia, Vol. 63, pp. 155-157.

Stromgren, T. 1984. Diurnal variation in the length growth-rate of three intertidal algae from the Pacific west coast. Aquat. Bot., Vol. 20, pp. 1-10.

Targett, N. M., T. E. Targett, N. H. Vrolijk and J. C. Ogden. 1986. The effects of macrophyte secondary metabolites on feeding preferences of the herbivorous parrotfish Sparisoma radians. Mar. Biol., Vol. 92, pp. 141-148.

Taylor, P. R., M. M. Littler and D. S. Littler. 1986. Escapes from herbivory in relation to the structure of mangrove island macroalgal communities. Oecologia, Vol. 69, Berlin, pp. 481-490.

Wefer, G. 1980. Carbonate production by algae Halimeda, Penicillus and Padina. Nature, Vol. 285, pp. 323-324.

Weiler, C. S. and S. W. Chisholm. 1976. Phased cell division in natural populations of marine dinoflagellates from shipboard cultures. J. Exp. Mar. Biol. Ecol., Vol. 25, pp. 239-247.

Weiler, C. S. and R. W. Eppley. 1979. Temporal pattern of division in the dinoflagellate genus Ceratium and its application to the determination of growth rate. J. Exp. Mar. Biol. Ecol., Vol. 39, pp. 1-24.

Wolf, N. G. 1985. Food selection and resources partitioning by herbivorous fishes in mixed-species groups. Proceedings of the Fifth International Coral Reef Congress. Tahiti, Vol. 4, pp. 23-28.

Zar, J. H. 1974. Biostatistical Analysis. Englewood Cliffs, N.J., Prentice-Hall, Inc. 620 pp.



PRELIMINARY OBSERVATIONS ON THE CAPTURE  
OF FLATFISH BY TRAWLS

C. G. Bublitz  
School of Fisheries and Ocean Sciences  
University of Alaska

ABSTRACT

The remote operated submersible Manta was used to conduct behavioral studies on the capture of flatfish by commercial trawl gear. Two types of behavior patterns were exhibited during the capture process. The majority, 80%, of flatfish entered the trawl by flipping backwards over the footrope then righting themselves to a normal swimming position inside the net. Twenty percent of the flatfish captured entered the trawl by rising above the substrate, turning through 180° in the horizontal plane, and swimming into the net. These behavior patterns appear to be mediated by the visual field, in particular the field of binocular vision.

INTRODUCTION

The impact of incidental catch by the expanding North Pacific domestic trawl fishery has generated considerable concern among other domestic user groups. Traditional user groups are questioning the economic and ecological impact of these fisheries on their sector of the industry. For example, during 1985 incidental catch was estimated to have removed between \$20 and \$40 million dollars of traditional, fully utilized fish species in the Gulf of Alaska and Bering Sea. The resultant conflicts have made incidental catch an allocation issue in the North Pacific.

Incidental catch is currently being managed by the use of catch ceilings and restricted fishing. This approach has resulted in the closure of large areas of productive fishing grounds in the Bering Sea and Gulf of Alaska. In addition, once incidental catch mortality ceilings have been reached, all trawling must cease regardless of whether or not the allowable biological catch of the target species has been taken. These restrictions have impeded the development of productive near-shore whitefish grounds and slowed the development of full scale domestic shore-based whitefish processing.

The increased effort being placed on North Pacific fisheries resources requires the development of new methods to control the incidental catch problem. Quantitative analysis of fish behavior during capture by trawl gear may provide needed information for the management of this problem. Information

generated from this type of research can be applied to the development of more selective fishing gear with the objective of reducing incidental catch.

Catch selectivity is inherent in the design of fishing gear. Selectivity can be size or type specific and is dependent upon a variety of factors. These factors include direct and interactive effects of the gear which initiate or influence the behavioral patterns of target and non-target species. Factors such as the effects of visual, auditory, chemical, and pressure stimuli as well as swimming characteristics, learning, and species interaction help determine how fish react to these disturbances.

Research on the capture of fish by gill and trammel nets, set nets, pots, trawls, and longline gear have documented factors which are important in fish capture and retention. Studies such as McCombie and Berst (1969), Hamley (1975) and Marais (1985) have concentrated on the relationship between mesh size and size range of fish captured. These studies also discussed some of the physical characteristics of fish which determine how fish are captured. Rudstam et al. (1984) proposed that the probability of a certain size of fish encountering a gillnet is directly related to a fish's swimming activity. Matuda et al. (1984a,b) and Matuda and Sannomiya (1985) examined factors such as rate of entry, mouth width, leader nets, and fish schooling behavior in relation to capture.

Information generated on the capture of fish by trawl gear has documented some of the effects of various trawl components, sand clouds produced by the gear, towing speed, length of tow, and mesh size and shape on the fish capture process (Bohl 1980; Brabant et al., 1980; Rauck 1980; Sakhno and Sadokhin 1980; Shevtsov 1980; Thorsteinsson 1980; Main and Sangster 1981a,b and 1983; Briggs 1983; Robertson 1983; Jessop 1985; and Liu et al., 1985). This information has already been applied to the problem of separating species within the catch (Main and Sangster 1982a,b; Valdemarsen et al., 1985; and Briggs 1986).

Vyskrebventsev (1968) classified fish into three main groups based on their reactions to trawl gear. He linked the distance at which detection and reaction took place to the schooling tendency. Included in his classification scheme were bottom non-schooling, in which the behavior exhibited was determined by the near orientation of the gear; pelagic scattered, where fish detected gear at some distance, but no reactions took place until close visual contact was made; and typically schooling when fish assessed danger and took appropriate action before visual contact.

In addition to fish/gear interaction studies, information on biological and physiological factors such as swimming speed,

optomotor responses, and vision are important in understanding the capture process (Harden Jones 1963; Arnold 1969, 1974; Wardle 1975, 1977; Ware 1978; Batty and Wardle 1979; Anthony 1981; and Anthony and Hawkins 1983). This information has provided insight into how fish orient within the water column and how they respond to various stimuli.

The process of fish capture by trawl gear involves a complex interaction between the physical properties of the gear and behavioral aspects of the fish subject to capture. Generally, past approaches to the problem of increasing capture efficiency have been concerned with assessing the engineering parameters of the gear. The main approach used in these assessments has been comparative fishing techniques, in which "old" and "new" gear are fished together under the same conditions. This approach has resulted in valuable information on relative catching efficiencies of the different gear, in many instances this information has been directly applicable to commercial fishing operations. However, this approach does not provide direct information about the capture process involved, or on the specific factors causing the efficiency change. Additionally, it is costly and time-consuming when each experiment is carried out over as wide a range of conditions as possible.

Until recently, virtually nothing was known about the behavior of fish in the vicinity of trawls. The major factor which prevented behavioral assessments was the difficulty involved in making detailed observations of fish in the vicinity of moving gear. The development of more sophisticated techniques of underwater observation has provided new methods to approach this problem. These techniques were applied to make a quantitative assessment of how flatfish are captured and the potential of using this information to reduce the incidental catch of Pacific halibut in domestic cod trawl fisheries.

## METHODS

Underwater observations were carried out by the University of Alaska and National Marine Fisheries Service (NMFS) aboard the chartered commercial fishing vessels Royal Baron and Morning Star. Video tapes of fish during capture by trawl gear were obtained under natural light conditions using the ROV Manta equipped with an Osprey OE1323 SIT camera. Fishing operations were conducted using a Nor'Eastern Trawl Bering Sea Combination net fished at a depth of 20 fathoms. This trawl has a 138 foot chain footrope covered with 6 inch diameter cookies and intermittently spaced 14 inch diameter rubber discs. Areas of operation were the Gulf of Alaska off Kodiak Island, Alaska and the Bering Sea off Nunivak Island, Alaska. To date, behavioral analysis has been conducted only on the video tapes supplied by NMFS.

Data analysis has centered on determining and measuring those parameters useful in describing flatfish behavior near the footrope of moving trawl gear. Parameters for which quantitative measurements were made include: distance above bottom flatfish assumed during herding, distance in front of footrope maintained during herding, distance in front of the footrope at which point entry into the trawl was initiated, herding time, and height at which flatfish passed over the footrope. Qualitative evaluations were also made on the manner by which flatfish entered the trawl.

Measurements were made directly from a video screen using calipers and are reported in inches as the arithmetic mean  $\pm$  standard deviation. Measurements were taken between a point on the periphery of the fish and the corresponding point on the shadow which it cast on the substrate or reference point on the net. The point on the fish used for these measurements was the edge of the dorsal or ventral fin at the widest part of the body. The caudal fin was not used because swimming action produced considerable variation in measurements. Standard fish length and width measurements were taken at the footrope and only on those fish which were positioned so that accurate measurements could be obtained.

Edge discrimination measurements are influenced by factors such as illumination, focus, topography, contrast, and individual perception. These factors make edge or boundary discrimination prone to subjective interpretation and variation. To minimize variation, measurements were taken by only one individual. Variability of measurements was assessed by taking a series of ten replicate measurements on five separate fish. Measurements of height above bottom were found to vary by a maximum of  $\pm 0.13$  inches, distance in front of trawl by  $\pm 0.8$  inches, and height above footrope by  $\pm 0.3$  inches.

Another consideration in making quantitative evaluations was to determine inherent distortion factors imposed by the camera system and placement. Transformation from apparent to actual height above bottom was made using proportionality. Measurements of fish size and distance were made at a point relative to the footrope and again at a reference point on the footrope. Actual distance was then determined using the formula:  $H = h' (S/s')$ , where  $H$  and  $h'$  are actual and measured height respectively and  $S$  and  $s'$  are size of fish at reference point and  $h'$  respectively.

Width was used as the standard measurement for this determination. This measurement proved to be more accurate and easier to obtain than overall length because of fish orientation away from the gear. Reference measurements were

made at the footrope because the diameter of cookie and roller gear were known and used as the reference standard. The use of the roller and cookie gear as a reference standard may also impart inaccuracies on the data. Consequently, during future research, reference standards of known length will be attached to the net at key locations.

Apparent, or measured, distances in front of the footrope were transformed to actual distance using the formula:  $X = x' + [(B \tan a) - A]$ ; where: X is actual distance in front of footrope,  $x'$  is measured distance in front of footrope, B is camera height above fish,  $\tan a$  is tangent of angle at camera between vertical and camera line of sight over cookie gear, and A is the distance camera is located behind cookie gear.

The quantity and quality of data obtained to date has been impacted by several factors, most significant of which was the viewing distance limitations imposed by water clarity. Viewing distances between 10-15 feet were encountered during the sampling program. This limitation determined the number of replicates and accuracy of measurements made on fish at the periphery of viewing distance. Visual limitations and submersible positioning also prevented an assessment of fish responses to net groundlines and wing ends.

Another factor which affected the amount and type of data obtained from the video tapes was camera placement. Our analysis was conducted using video tapes obtained by the NMFS during their crab bycatch studies. These tapes had the camera positioned to observe crab rather than finfish behavior. This positioning provided only a limited view of the footrope directly in front of the camera and no view of the area behind the footrope or in the belly of the net. This limitation severely restricted a complete analysis of flatfish behavior. Data generated were mainly restricted to the area in front of and over the footrope. A few observations were obtained from the area behind the footrope when the camera occasionally panned to either side. It was not possible to follow individual fish throughout the capture process into the belly of the net, the area which is probably most important for species separation.

The final factor which may have influenced the behavior patterns observed was the effect of the submersible on flatfish entering the trawl. Due to the limited data obtained outside the submersible's influence, we have been unable to quantitatively assess this problem. However, those observations which were obtained did not indicate major changes in flatfish behavior. The submersible appeared to only influence the fish at a relatively close range. It was

assumed that the effect of the small submersible was negligible compared with the overall effects of the trawl.

To distinguish between the herding described here from herding patterns described in the literature we have used the terms active and passive herding. Active herding is defined as occurring when flatfish maintained continuous swimming without settling on the substrate. Passive herding occurs when the flatfish have the opportunity to move away from a disturbance and settle back to the substrate before being disturbed again.

## RESULTS

Flatfish, Rock Sole (Lepidopsetta bilineata), Alaska Plaice (Pleuronectes quadrituberculatus), longhead dab (Limanda proboscidea), and Yellowfin Sole (Limanda aspera), were observed during capture by trawl gear. A total of 61 fish, ranging in size from 6 to 24 inches, were observed to determine behavior during herding and trawl entry. Fish could not be identified to species on the video tapes; consequently, no species specific behavioral information is reported.

The large rubber disks on the footrope produced a significant sediment cloud behind the footrope during trawling operations. The extent of this cloud was not determined; however, webbing in the belly of the net was obscured within approximately 1.5 - 2 feet of the footrope. The height of the sediment cloud increased rapidly, reaching a height of approximately 3 feet above the webbing at about 20 feet behind the footrope.

All flatfish observed leaving the substrate were positioned with the long axis of the fish oriented in the direction of tow. Under undisturbed conditions it would be expected that the fish would be oriented in a random pattern or, if current or other physical factors determined orientation, they would be oriented in a direction not necessarily that of the tow. It is assumed the fish have either experienced passive herding, or non-herding orientation has taken place using visual or other sensory perceptions outside the visual range of the camera.

The distribution of flatfish during herding and trawl entry is shown in Figure 1. Flatfish reacted to the footrope of the trawl at relatively close range and for short time periods. Flatfish initially reacted to and were actively herded at a distance less than 48 inches from the footrope. After leaving the substrate the fish tended to drop back towards the footrope and attempted to maintain station with it. The majority of fish maintained a distance of

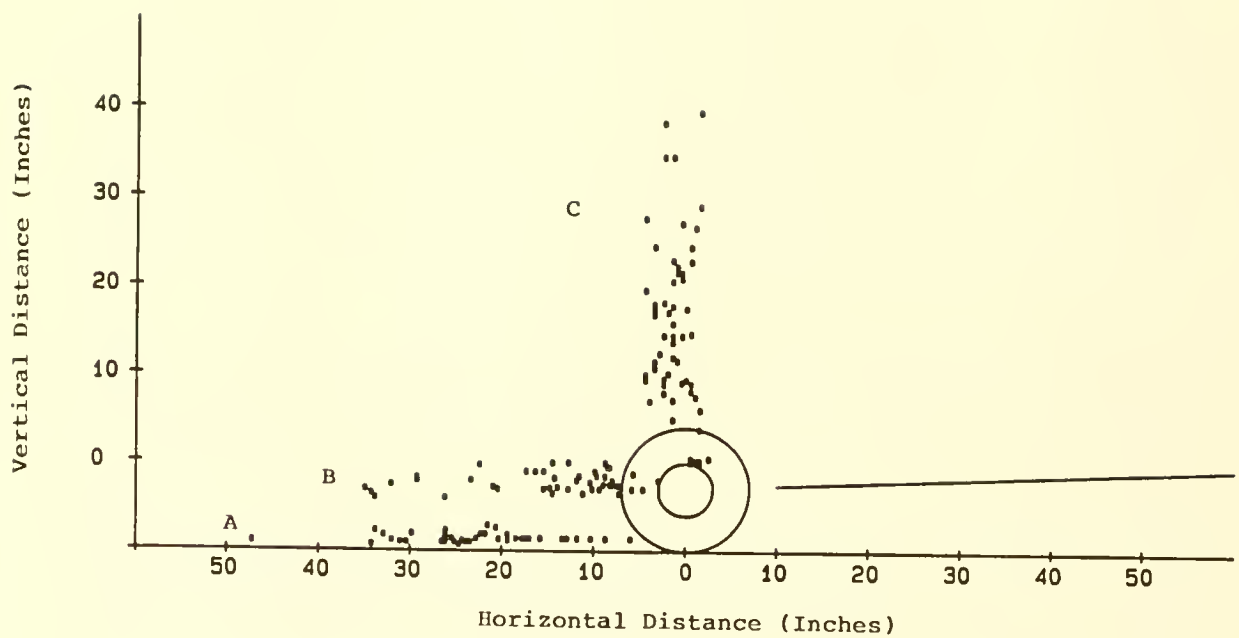


Figure 1. Position, relative to the top of cookie gear, of flatfish during herding (A), in front of footrope (B), and crossing footrope (C).

approximately 21 inches in front of the footrope. In most instances trawl entry was initiated from the point at which the fish was attempting to maintain station with the gear. During trawl entry, flatfish crossed the footrope at a height of less than 40 inches.

Two factors determine the limits of this data. First, the maximum herding distance recorded may have been determined by visibility limitations rather than actual herding distance. The maximum recorded herding distance is approximately ten feet from the camera lens. This distance is near the visual limit encountered during our operations. Herding may occur outside this limit but is undetectable by the present methodology. Second, the minimum measured distance fish approached the footrope was determined by the camera angle and position. In many cases fish were observed swimming in positions which appeared to be under the footrope. This, however, is an artifact of camera position and the fish were actually swimming in the region between the footrope and the range of camera visibility.

Observed active herding times ranged from 2 to 12.2 seconds (average 5.2 seconds  $\pm$ 3.6 seconds). During active herding, flatfish tended to swim directly away from the gear, with only an occasional fish zigzagging or traversing the footrope. In all cases the fish remained close to the bottom; in several instances the caudal fin was observed striking the substrate. The average distance above bottom maintained during herding was 1.5 inches  $\pm$ 0.56 inches. To maintain position with the gear the majority of flatfish observed swam in a burst pattern. The fish would swim rapidly away from the footrope for a short period of time followed by a gliding period during which the fish dropped back towards the footrope.

Two distinctive behavior patterns were observed when flatfish entered the trawl (Fig. 2). Eighty percent of the fish entered the trawl by turning onto their back and allowing the footrope to pass beneath the fish (sequence A). Individuals exhibiting this behavior pattern tended to be herded closer to the footrope and enter the trawl at a lower level than other fish (Fig. 3). The average herding distance for these fish was 18.3 inches  $\pm$ 6.1 inches and they crossed the footrope at an average height of 13.8 inches  $\pm$ 7.7 inches. Fish which exhibited this entry pattern ranged from 7 to 23 inches in length (average 13.8 inches  $\pm$ 4.7 inches). After crossing the footrope, fish righted themselves by executing a 180° roll. Fish crossing the footrope at a lower level tended to execute this roll sooner than fish crossing at a higher level. After crossing the footrope, and while still inverted, the fish tended to rise while swimming into the net.

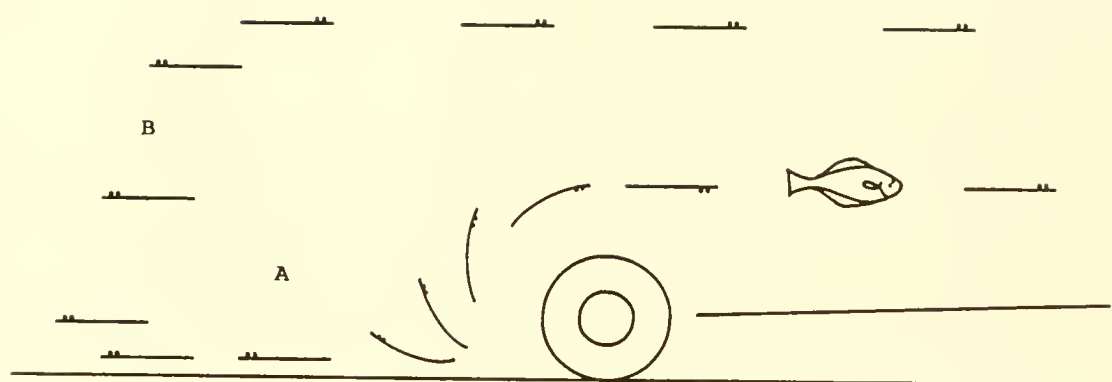


Figure 2. Entry behavior exhibited by flatfish during capture by trawl gear.

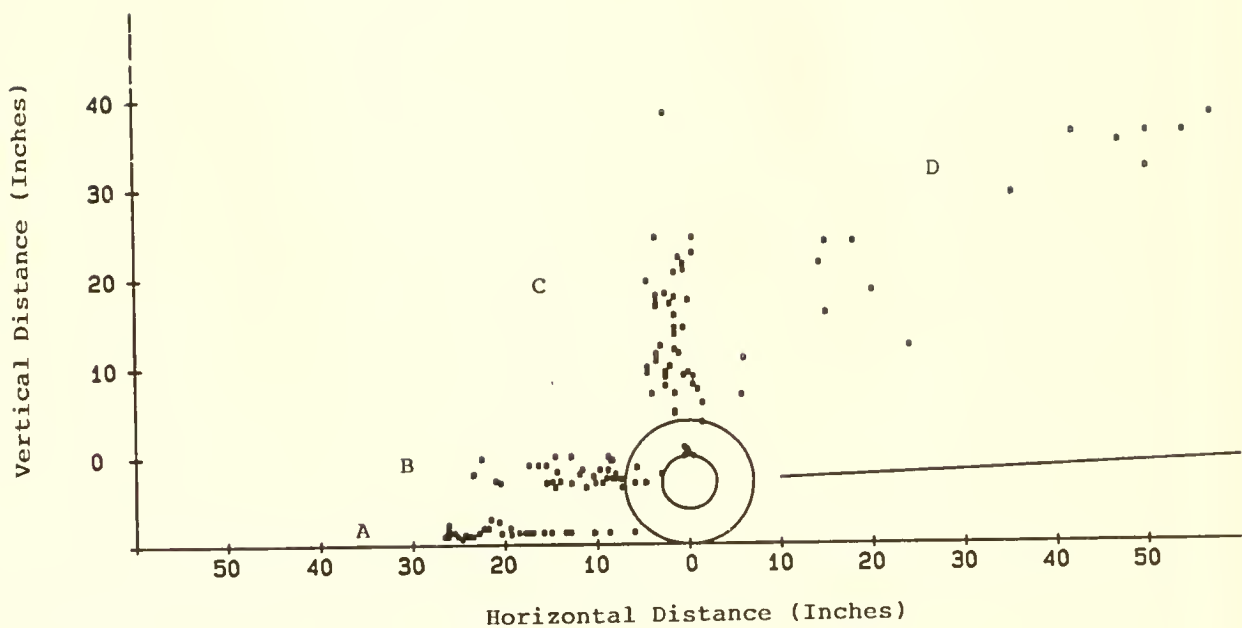


Figure 3. Position, relative to top of cookie gear, of flatfish exhibiting capture sequence A; herding (A), in front of footrope (B), crossing footrope (C), and executing 180° roll (D).

A total of 29 separate observations in front of the footrope and 15 observations behind the footrope were used to calculate a visual response field for fish exhibiting capture sequence A (Fig. 4). This visual response field is based on the maximum measured distance of the initial entry sequence and the position behind the footrope where fish righted themselves. Angles were calculated between the direction of travel and the top of the roller gear. This entry sequence was initiated (point at which the fish began its flip) at a visual angle less than or equal to  $155^{\circ}$ . After passing the footrope fish righted themselves at a visual angle between  $130^{\circ}$  and  $162^{\circ}$ .

The second type of entry sequence exhibited by flatfish (sequence B in Fig. 5) differed significantly. This behavior sequence was exhibited by 20 percent of the fish observed. In this sequence fish would rise to a height of between 14 and 39 inches above the footrope (average 23.5 inches  $\pm 6.6$  inches) and either swim with the footrope allowing it to overtake and pass beneath the fish or turn through  $180^{\circ}$  within the horizontal plane and swim into the net (Fig. 5). The distance in front of the footrope at which this sequence was initiated was between 24 and 47 inches (average 30.9 inches  $\pm 6.3$  inches). The length of the flatfish exhibiting this sequence was between 8 and 21 inches with a mean of 15.2 inches  $\pm 4.8$  inches.

A total of 13 fish exhibiting entry sequence B were observed during herding and entry to determine the visual response field of fish exhibiting this type of entry sequence (Fig. 6). The angle at which these fish initiate trawl entry was between  $152^{\circ}$  and  $164^{\circ}$ . After crossing the footrope the fish did not exhibit any unusual responses which would permit an analysis of the limit of visual contact with the footrope.

The mean length of fish exhibiting the two entry sequences were tested to determine if the entry sequences were size dependent. The t-test was used to test the null hypothesis  $H_0: u_1 = u_2$ . Based on this test the null hypothesis was accepted  $t_{0.05(2)45} = 0.93$  and it is concluded that the entry sequences are not size dependent.

## DISCUSSION

The behavior of flatfish during herding and capture by trawl gear has not been described in detail. Main and Sangster (1981b) gave a brief description of flatfish encountering the sweeps and footrope of trawl gear. They reported a tendency for flatfish to be herded at  $90^{\circ}$  to the sweeps. During herding, fish would move away from the sweeps for some distance then settle back to the substrate. When the sweeps approached, the process would be repeated.

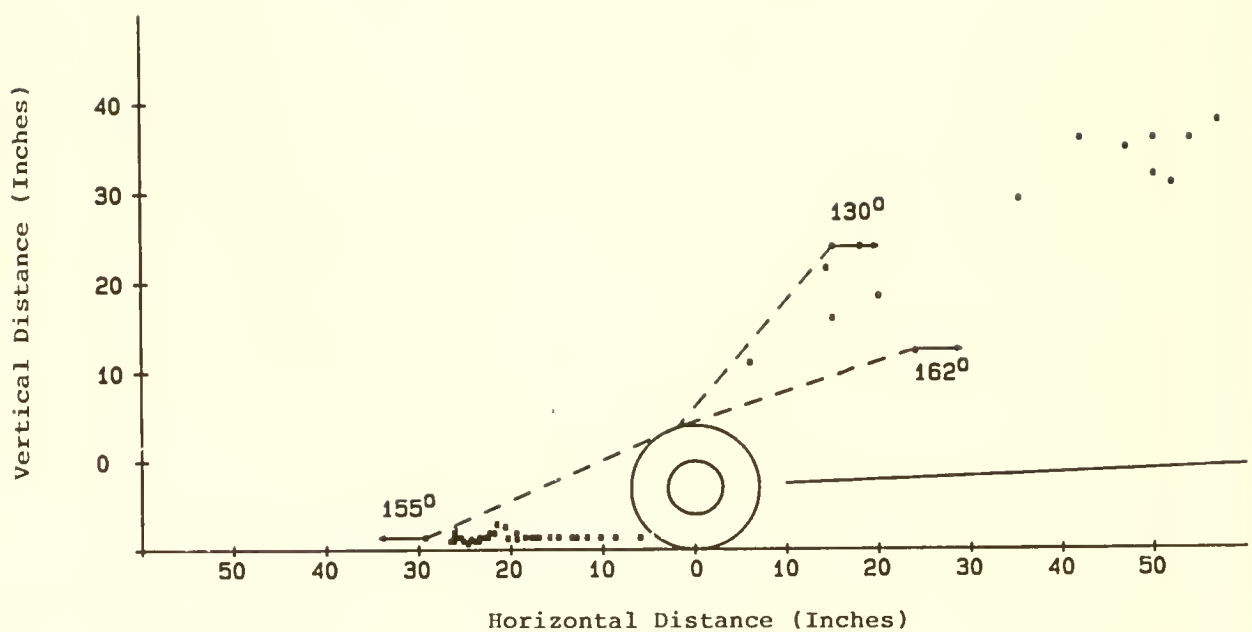


Figure 4. Visual response field of flatfish exhibiting capture sequence A, measured from maximum herding distance and points at which  $180^{\circ}$  roll executed. Arrows indicate relative direction fish is moving.

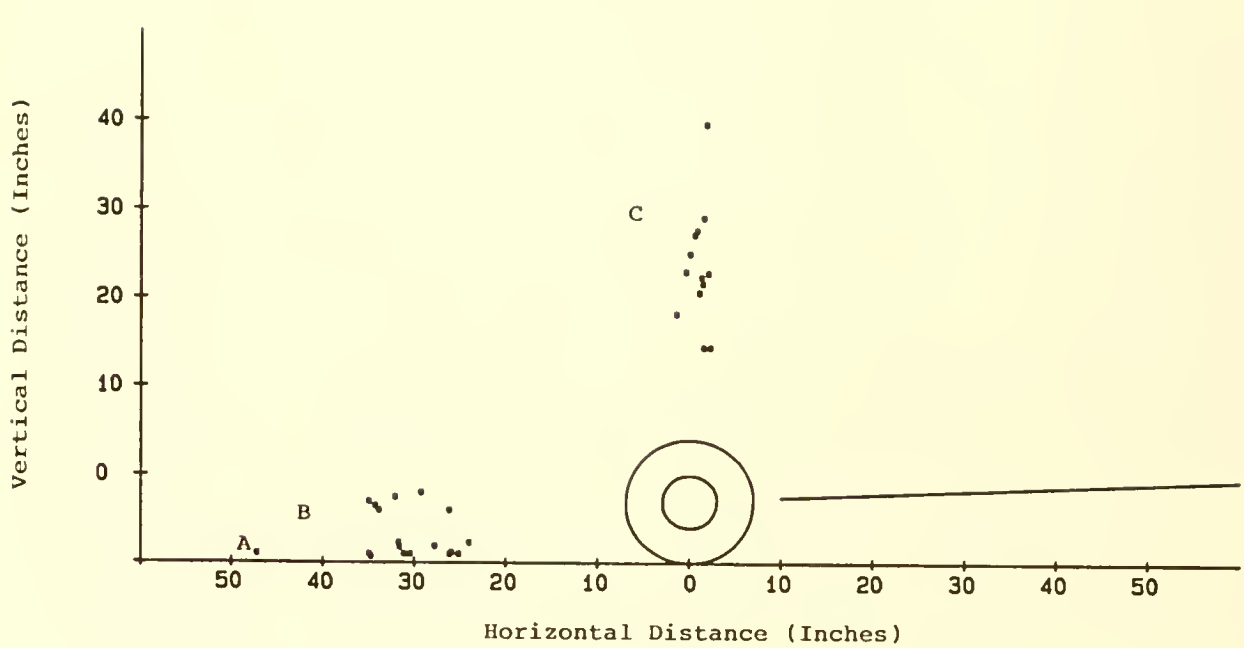


Figure 5. Position, relative to top of cookie gear, of flatfish exhibiting capture sequence B; herding (A), in front of footrope (B), and crossing footrope (C).

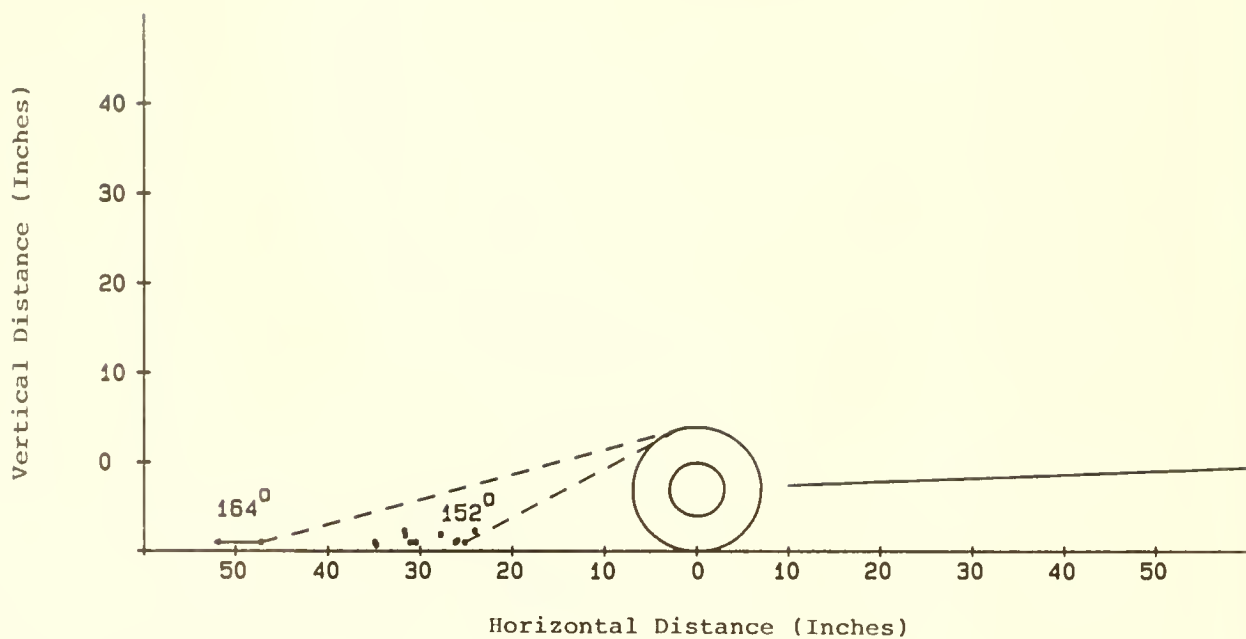


Figure 6. Visual response field of flatfish exhibiting capture sequence B, measured from maximum and minimum herding distances.

gradually moving the fish into the capture zone of the net. At the footrope fish would turn and swim with the net before entering.

Wardle (1983) described the behavior of flatfish to the ropes of the Danish seine. He observed two types of behavior and related these to rope configuration during initial and final stages of the tow. During initial stages, when rope configuration is U shaped, he found the majority of fish tended to swim in the direction of tow. During latter stages, when rope configuration is V shaped, the majority of fish tended to swim towards the mouth of the net. As in Main and Sangster's observations, fish near the footrope tended to swim in the direction of tow keeping station with the net.

All observations of flatfish made during this study were near the footrope of the trawl gear. From these observations, the mechanism by which flatfish first orient themselves to the trawl is indeterminable. However, the fact that all fish were oriented away from the advancing gear prior to leaving the substrate indicates that some stimulus, or combination of stimuli, has produced this orientation.

Two major factors, vision and sound, have been shown to influence fish behavior during fishing operations. Considerable evidence is available which indicates visual stimuli is the major factor in determining behavioral responses in close proximity to trawl gear. However, it is also well established that sound transmission underwater is detectable by fish at distances beyond visual capabilities. It seems likely, therefore, that audio stimuli may be a more important factor in determining initial orientation to the gear than visual stimuli. An additional factor, the fish's swimming ability, is critical in determining reaction distances to various stimuli, especially visual.

Kiselev (1968), observing fish schools from a manned submersible, indicated that cod and haddock became agitated by noise and all the fish oriented instantly in one direction. He did not indicate what the relative orientation to the sound was, however. Chapman (1976) reported consistent avoidance responses by gadoid fish to low frequency narrow bandwidth noise. The ability of herring to detect the direction of sounds and take evasive or selective action without visual input has been reported by Blaxter and Batty (1985), Blaxter and Hoss (1981), and Schwarz and Greer (1984).

The ability to discriminate between sounds varies with species. Most fish appear to be able to detect frequencies between 50 - 500 Hz; whereas, they are insensitive to frequencies above 2 - 3 kHz (Schwarz 1985 and Hawkins, 1986).

Fish also appear to have the ability to localize sound. Evidence has been presented that indicates fish can determine the distance to the sound source as well as its position in both the vertical and horizontal plane (Schuijf and Buwalda, 1980; Hawkins and Myrberg, 1983; Buwalda et al., 1983). Evidence has also been presented that some species, such as cod and salmon, may be capable of increasing frequency sensitivity by the presence of a frequency selective audio filter (Hawkins and Chapman, 1975; Hawkins and Johnstone, 1978).

Sounds generated by fishing gear vary greatly in intensity and frequency. Frequency ranges for vessels and gear have been measured between 25 Hz - 15 kHz. Most of this energy is generated in the range between 25 Hz - 5 kHz, particularly below 1 kHz. The frequency ranges below 1 kHz correspond well with the known hearing abilities of fish. Intensity levels, taken as far as 300 m from vessel and gear, have been measured as high as 39 dB above background noise at 250 Hz and 28 dB at frequencies below 150 Hz (Schwarz, 1985). In addition to maximum intensity levels, there is evidence to suggest that changes in intensity may be more important in determining a fish's reaction than intensity levels (Schwarz and Greer, 1984).

Initial orientation to the gear, prior to the occurrence of herding, is probably the result of sound stimuli. Trawl gear produces wide frequency audio stimuli which are constantly changing in intensity. These signals propagate through water to distances well beyond the visual limits of fish. The hearing capabilities of fish indicate these signals are detected and possibly undergo extensive and complex analysis. From this analysis fish can probably determine the relative position of the gear, possibly speed of approach, and conceivably other factors. It can be speculated that this would result in the fish orienting themselves in the most advantageous position to react to the disturbance.

Distances at which flatfish were observed reacting directly to the gear were relatively short and were probably determined by visual limitations. Light intensity and visual distance depend upon several factors, including: depth, turbidity, refractive index, dissolved organic and inorganic matter, and line of sight. Most wavelengths, and light intensity, are attenuated rapidly with depth; consequently, even at relatively shallow depths, light levels are low and monochromatic. This results in objects being seen as shades of grey and visibility being dependent upon the degree of contrast between the object and its background Guthrie (1986).

The visual capabilities of fish are well adapted to this environment. Wardle (1984) indicates that fish are likely to react visually to fishing gear at light levels as low as  $10^{-7}$  lux. Contrast discrimination in fish also appears to be acute, with the ability to discriminate between various contrasts mediated somewhat by object size (Anthony, 1981). Therefore, the distance at which an object is first seen varies, and as Wardle (1986) indicates, can lead to a variety of reactions depending upon object range, object speed, and the fish's swimming ability.

The trawl footrope, equipped with 14 inch black rubber roller gear interspersed with 6 inch black rubber cookie gear, undoubtedly presented a high contrast visual image against the sediment cloud which it produced. Previous observations have shown that trawl doors and other groundgear produce high contrast images when viewed from directly in front. This contrast is the result of the darker object being surrounded by a sediment cloud which is illuminated by downwelling light (Main and Sangster 1981a; Wardle 1986). The high contrast image presented by the footrope provides an excellent orientation point for the fish during herding.

The overall herding behavior observed in front of the footrope tended to be the same as described by previous authors; that is, the flatfish would swim in the direction of tow attempting to maintain station with the footrope. Unlike roundfish, once having crossed the footrope most flatfish did not continue to attempt maintaining station but swam directly into the net. Wardle (1983, 1986) indicated that swimming ability is the critical factor in determining when a fish enters the net. With the exception of a few larger fish all the fish observed were swimming in a burst pattern, implying that the fish were swimming at or near their maximum swimming speed. Burst swimming has been shown to produce high speeds but can only be sustained for short periods (Wardle 1975, 1977). This factor undoubtedly accounts for the relatively short herding times observed.

The herding effects of the net mouth are well known. In situ observations have shown that roundfish, depending on size, maintain station with moving nets for extended periods. Hemmings (1973) demonstrated that haddock swim within the mouth of a net even when the netting behind the mouth is completely removed. Herring schools have been observed outside a midwater trawl approaching, orienting to, and moving with the net (High and Lusz, 1966). The herding of flatfish in close proximity to the footrope is probably analogous to the herding of roundfish by the net mouth and relies on the same visual stimuli.

Herding and maintaining station with the gear has been shown to be an optomotor response. Considerable research has documented the optomotor responses of fish to moving backgrounds (Harden Jones, 1963; Arnold, 1974). These works have pointed out that the basic condition for optomotor reaction is the presence of moving orientation points in the visual field. In addition, it was shown that when responding to these orientation points the most frequently observed behavior was the full optomotor reaction, in which fish swam parallel to the moving background and at approximately the same speed.

Entry sequences appear to be positional and can be considered as escape, sequence A, or avoidance, sequence B, responses. It is unclear whether the two entry sequences observed are also directly related to swimming ability. The most common entry pattern, in which the fish flips onto its back during the entry, is initiated closer to the footrope than those exhibiting sequence B. However, it has also been shown that these sequences are not size dependent, therefore it can be concluded, not dependent upon swimming ability.

Initiating entry by turning the large flat ventral surface towards the direction of travel, sequence A, effectively accomplishes three things. First, the fish's forward momentum is reduced significantly and rapidly. In several instances the fish's forward momentum was reduced so rapidly fish were unable to avoid being struck by the footrope. Secondly, this maneuver effectively redirects the fish's momentum without significantly reducing speed. Third, the maneuver allows the fish to maintain close eye contact with the disturbance. By turning onto its back the fish is able to observe the disturbance, and in the case of the trawl, this disturbance continues away from the direction the fish is now traveling and appears to offer no further threat.

It is interesting to note that fish exhibiting sequence A behavior which crossed the footrope at a lower level righted themselves closer to the footrope than those crossing at a higher level. It is speculated that the visual field, in particular, the field of binocular vision, influences the point at which this maneuver is executed. Flatfish closer to the footrope would lose binocular contact, and depth perception, with the footrope sooner than flatfish crossing at a higher level.

Fish exhibiting entry sequence B initiated entry farther from the footrope and crossed at a higher level than those exhibiting sequence A. Those fish exhibiting this sequence also swam in a much more leisurely manner without exhibiting any rapid change in direction. The fish rose above the footrope to a height that kept maximum distance between the

disturbance and the fish before turning and entering the trawl. Eye contact was maintained with the disturbance and when no threat was offered the fish entered the trawl in a leisurely swimming manner.

In both behavior sequences the visual field plays an important role. In sequence A the field of binocular vision appears to be the critical factor in determining the response sequence. Preliminary observations of pacific halibut (Hippoglossus stenolepis), rock sole (Lepidopsetta bilineata), and yellowfin sole (Limanda aspera) indicate these flatfish have a visual angle directly rearward of between  $145^{\circ}$  and  $165^{\circ}$  in the ventral eye and between  $130^{\circ}$  and  $150^{\circ}$  in the dorsal eye. Downward visual angles, measured from the optical axis, ranged from  $40^{\circ}$  to  $50^{\circ}$  for the ventral eye and  $80^{\circ}$  to  $95^{\circ}$  for the dorsal eye (Bublitz, C. G., unpublished data). These figures indicate that rearward binocular vision is accomplished between 10 and 50 inches behind the eye, dependent upon each eye's visual field and eye rotation.

The point at which rotation from inverted to normal swimming takes place after crossing the footrope, sequence A, was observed to be between  $130^{\circ}$  and  $160^{\circ}$ . These figures compare favorably with the preliminary observations of visual angles stated above and support the theory that the limit of binocular vision may determine the point of rotation. Fish which are higher and farther back in the net may also be reacting to the loss of visual contact with the footrope.

Wardle (1983) showed that when viewed from above, objects are contrasted against a darker background than when viewed from below or at the same level. Consequently, the dark roller and cookie gear of the trawl would not present as high a contrast image from above as when viewed from in front. This reduction in contrast would likely reduce the visual distance at which flatfish could detect the footrope and thus react to it.

Flatfish exhibiting capture sequence B also maintained eye contact with the disturbance; however, in this case, contact appears to be maintained mainly through monocular vision. The visual angle within which this behavior was initiated ranged between  $152^{\circ}$  to  $164^{\circ}$ . The preliminary observations of flatfish visual field indicate flatfish may be initially reacting near the limits of binocular vision; however, once flatfish begin to rise above the substrate binocular vision is soon lost. The downward visual angles reported above indicate monocular eye contact is probably maintained throughout the behavior sequence. The distance at which fish rise above the substrate and at which they cross

the footrope indicate the fish may be swimming near the limits of visual contact, determined by contrast discrimination, with the footrope.

#### CONCLUSION

Initial orientation to trawl gear is probably a reaction to audio rather than visual stimuli. Responses to these stimuli would probably result in fish orienting themselves in the most advantageous position to react to visual stimuli produced by the gear. Herding appears to be mainly in response to the visual stimuli produced by the footrope. As with roundfish, herding times and entry into the net appear to be determined by the fish's swimming ability.

The two types of entry behavior exhibited appear to be positional rather than either size dependent or related to the relative swimming ability of the fish. The visual field, in particular the binocular field of vision, appears to play an important role in determining the relative position of reactions to the footrope. This factor probably determines the position at which fish exhibiting entry sequence A right themselves to their normal swimming position. It may also be important in determining the position at which flatfish initiate entry into the net.

#### LITERATURE CITED

Anthony, P. D. 1981. Visual contrast thresholds in cod Gadus morhua L. J. Fish. Biol., Vol. 19, pp. 87-103.

Anthony, P. D. and A. D. Hawkins. 1983. Spectral sensitivity of the cod, Gadus morhua L. Mar. Behav. Physiol., Vol. 10, pp. 145-166.

Arnold, G. P. 1969. The reactions of the plaice (Pleuronectes platessa L.) in water currents. J. Expl. Biol., Vol. 51, pp. 681-697.

Arnold, G. P. 1974. Rheotropism in fishes. Biol. Rev., Vol. 49, pp. 515-576.

Batty, R. S. and C. S. Wardle. 1979. Restoration of glycogen from lactic acid in the anaerobic swimming muscle of plaice, Pleuronectes platessa L. J. Fish. Biol., Vol. 15, pp. 509-519.

Blaxter, J. H. S. and R. S. Batty. 1985. Herring behaviour in the dark: responses to stationary and continuously vibrating obstacles. J. Mar. Biol. Ass. U.K., Vol. 65, pp. 1031-1049.

Blaxter, J. H. S. and D. E. Hoss. 1981. Startle response in herring: The effect of sound stimulus frequency, size of fish and selective interference with the acoustico-lateralis system. J. Mar. Biol. Ass. U.K., Vol. 61, pp. 871-879.

Bohl, H. 1980. Selection of cod by bottom trawl cod-ends in the central Baltic (German experiments, 1978). ICES, Fish Capture Committee, C.M. 1980/B:8.

Brabant, J. C., N. Prado, and E. Dahm. 1980. Comparative fishing trials with big meshes and rope trawls. ICES, Fish Capture Committee, C.M. 1980/B:9.

Briggs, R. P. 1983. Net selectivity studies in the northern Ireland Nephrops fishery. Fish. Rev., Vol. 2, pp. 29-46.

Briggs, R. P. 1986. A general review of mesh selection for Nephrops norvegicus L. Fish. Res., Vol. 4, pp. 59-73.

Buwalda, R. J. A., A. Schuijf and A. D. Hawkins. 1983. Discrimination by the cod of sounds from opposing directions. J. Comp. Phys., Vol. 150, pp. 175-184.

Chapman, C. J. 1976. Some observations on the reaction of fish to sound. In: A. Schuijf and A. D. Hawkins (eds.), Sound Reception In Fish. New York, N.Y., Elsevier, pp. 241-255.

Guthrie, D. M. 1986. Role of vision in fish behaviour. In: T. J. Pitcher (ed.), The Behavior of Teleost Fishes. Baltimore, Md., Johns Hopkins University Press, pp. 75-113.

Hamley, J. M. 1975. Review of gillnet selectivity. J. Fish. Res. Board Can., Vol. 32, pp. 1943-1969.

Harden Jones, F. R. 1963. The reaction of fish to moving backgrounds. J. Expl. Biol., Vol. 40, pp. 437-446.

Hawkins, A. D. 1986. Underwater sound and fish behaviour. In: T. J. Pitcher (ed.), The Behavior of Teleost Fishes. Baltimore, Md., Johns Hopkins University Press, pp. 114-151.

Hawkins, A. D. and C. J. Chapman. 1975. Masked auditory thresholds in the cod, Gadus morhua. J. Comp. Phys., Vol. 103A, pp. 209-226.

Hawkins, A. D. and A. D. F. Johnstone. 1978. The hearing of the Atlantic salmon, Salmo salar. J. Fish. Biol., Vol. 13, pp. 655-673.

Hawkins, A. D. and A. A. Myrberg. 1983. Hearing and sound communication underwater. In: B. Lewis (ed.), Bioacoustics: A Comparative Approach. New York, N.Y., Academic Press, pp. 347-405.

Hemmings, C. C. 1973. Direct observation of the behaviour of fish in relation to fishing gear. Helol. Wiss. Meeresunters., Vol. 24, pp. 348-360.

High, W. L. and L. D. Lusz. 1966. Underwater observations on fish in an off-bottom trawl. J. Fish. Res. Board Can., Vol. 23, No. 1, pp. 153-154.

Jessop, B. M. 1985. Influence of mesh composition, velocity, and run time on the catch and length composition of juvenile alewives (Alosa pseudoharengus) and blueback herring (A. aestivalis) collected by pushnet. Can. J. Fish. Aquat. Sci., Vol. 42, pp. 1928-1939.

Kiselev, O. N. 1968. Visual observations of fish in natural conditions. In: A. P. Alekseev (ed.), Fish Behavior and Fishing Techniques. Jerusalem, Israel Program for Scientific Translations. IPST Cat. No. 5938.

Liu, H. C., K. J. Sainsbury and T. S. Chiu. 1985. Trawl cod-end mesh selectivity for some fishes of North-Western Australia. Fish. Res., Vol. 3, pp. 105-109.

Main J. and G. I. Sangster. 1981a. A study of sand clouds produced by trawl boards and their possible effect on fish capture. Scottish Fish. Res. Rept. No. 20, 20 pp.

Main J. and G. I. Sangster. 1981b. A study of the fish capture process in a bottom trawl by direct observations from a towed underwater vehicle. Scottish Fish. Res. Rept. No. 23, 23 pp.

Main J. and G. I. Sangster. 1982a. A study of separating fish from Nephrops norvegicus L. in a bottom trawl. Scottish Fish. Res. Rept. No. 24, 8 pp.

Main J. and G. I. Sangster. 1982b. A study of a multi-level bottom trawl for species separation using direct observation techniques. Scottish Fish. Res. Rept. No. 26, 17 pp.

Main J. and G. I. Sangster. 1983. Fish reactions to trawl gear - a study comparing light and heavy ground gear. Scottish Fish. Res. Rept. No. 27, 17 pp.

Marais, J. F. K. 1985. Some factors influencing the size of fishes caught in gillnets in Eastern Cape estuaries. Fish. Res., Vol. 3, pp. 251-261.

Matuda, K. and N. Sannomiya. 1985. Computer simulation of fishbehavior in relation to a trap model. Bull. Jap. Soc. Sci. Fish., Vol. 51, No. 1, pp. 33-39.

Matuda, K., M. Suzuki and H. Kanehiro. 1984a. Comparison of performance of mouth of trap model by water tank experiment of fish behavior. Bull. Jap. Soc. Sci. Fish., Vol. 50, No. 4, pp. 609-615.

Matuda, K., M. Suzuki and H. Kanehiro. 1984b. Water tank experiments of fish behavior to model of set nets. Bull. Jap. Soc. Sci. Fish., Vol. 50, No. 7, pp. 1109-1114.

McCombie, A. M. and A. H. Berst. 1969. Some effects of shape and structure of fish on selectivity of gillnets. J. Fish. Res. Board Can., Vol. 26, pp. 2681-2689.

Rauck, G. 1980. Mesh selectivity studies on board a low powered German sole beam trawler. ICES, Fish Capture Committee, C.M. 1980/B:27.

Robertson, J. H. B. 1983. Square mesh cod-end selectivity experiments on whiting (Merlangius merlangus (L)) and haddock (Melanogrammus aeglefinus (L)). ICES, Fish Capture Committee, C.M. 1983/B:25.

Rudstam, L. G., J. J. Magnuson and W. M. Tonn. 1984. Size selectivity of passive fishing gear: A correction for encounter probability to gill nets. Can. J. Fish. Aquat. Sci., Vol. 41, pp. 1252-1255.

Sakhno, V. A. and K. Sadokhin. 1980. Investigation on bottom trawl selectivity in relation to the Barents sea shrimp (Pandalus borealis). ICES, Fish Capture Committee, C.M. 1980/B:7.

Schuijff, A. and R. J. A. Buwalda. 1980. Underwater localization - A major problem in fish acoustics. In: A. N. Popper and R. R. Fay (eds.), Comparative Studies of Hearing in Vertebrates. New York, N.Y., Springer-Verlag, pp. 43-78.

Schwarz, A. L. 1985. The behavior of fishes in their acoustic environment. Enviro. Biol. Fishes., Vol. 13, No. 1, pp. 3-15.

Schwarz, A. L. and G. L. Greer. 1984. Responses of Pacific herring, Clupea harengus pallasi, to some underwater sounds. Can. J. Fish. Aquat. Sci., Vol. 41, No. 8, pp. 1183-1192.

Shevtsov, S. E. 1980. Selectivity of trawl cod-ends for flounder fishery in the Baltic Sea. ICES, Fish Capture Committee, C.M. 1980/J:6.

Thorsteinsson, G. 1980. Icelandic bottom trawl and Danish seine codend selection experiments on cod, haddock, redfish and plaice in 1972-1976. ICES, Fish Capture Committee, C.M. 1980/B:3.

Valdemarsen, J. W., A. Engas and B. Isaksen. 1985. Vertical entrance into a trawl of Barents Sea gadoids as studied with a two level fish trawl. ICES, Fish Capture Committee, C.M. 1985/B:46.

Vyskrebentsev, B. V. 1968. Role of reflex stimuli in the behavior of fish near the gear. In: A. P. Alekseev (ed.), Fish Behavior and Fishing Techniques. Jerusalem, Israel Program for Scientific Translations. IPST Cat. No. 5938.

Wardle, C. S. 1975. Limit of fish swimming speed. Nature, Vol. 225, London, pp. 725-727.

Wardle, C. S. 1977. Effects of size on swimming speeds of fish. In: T. J. Pedley (ed.), Scale Effects in Animal Locomotion. New York, N.Y., Academic Press, pp. 299-313.

Wardle, C. S. 1983. Fish reactions to towed fishing gear. In: A. G. MacDonald and I. G. Priede (eds.), Experimental Biology at Sea. New York, N.Y., Academic Press, pp. 167-195.

Wardle, C. S. 1984. Fish behaviour, trawl efficiency and energy saving strategies. FIIT Working Paper, HIRT 1563 War, F. A. O., Fishing Technology Service, Rome.

Wardle, C. S. 1986. Fish Behaviour and Fishing Gear. In: T. J. Pitcher (ed.), The Behavior of Teleost Fishes. Baltimore, Md., Johns Hopkins University Press, pp. 463-495.

Ware, D. M. 1978. Bioenergetics of pelagic fish:  
Theoretical change in swimming speed and ration with  
body size. Fish. Res. Board Can., Vol. 35,  
pp. 220-228.



MANNED SUBMERSIBLE AND ROV ASSESSMENT OF GHOST GILLNETS  
ON JEFFREYS AND STELLWAGEN BANKS, GULF OF MAINE

Richard A. Cooper  
National Undersea Research Center  
University of Connecticut, Avery Point  
Groton, Connecticut 06340

H. Arnold Carr  
Massachusetts Division of Marine Fisheries  
Sandwich, Massachusetts 02563

Alan H. Hulbert  
National Undersea Research Center  
University of North Carolina  
Wilmington, North Carolina 28403

ABSTRACT

In 1984, a three-year study began to determine the abundance and likely impact of lost (ghost) demersal gillnets on two important fishing grounds in the Gulf of Maine. The surveys were undertaken using the submersibles Johnson Sea-Link II and Delta in June of each year. The *in situ* methodology for this study was established in 1984 at known ghost gillnet sites. A quantitative survey to assess ghost net density was conducted in 1985 and 1986. Twenty-four submersible transects averaging 0.5 nm resulted in a survey of 186 acres of traditional commercial gillnet fishing grounds of Jeffreys Ledge and Stellwagen Bank. Ghost gillnets found were surveyed for net dimensions, vertical profile, fouling, vertebrate and invertebrate catch, and fate of catch. One ghost net found in 1984 was surveyed again in 1985 and 1986. Another net found in June 1986 was re-examined in July 1986 using a Remotely Operated Vehicle (ROV). Extensive video documentation was acquired on each of these ghost gillnets.

INTRODUCTION

The increase in commercial and recreational fishing pressure in the New England ground fishery over the last decade has intensified the problem of gear conflict, preemption of prime fishing bottom by specific gear types and the impact of lost gear on the fishery resources. A major component of this controversy is the use of the demersal gillnet.

Commercial fishermen began utilizing demersal gillnets to catch groundfish in the Gulf of Maine in the late 1800's (Collins, 1882). Gillnets are a fixed type of fishing gear marked by

surface floats and radar detectors at each end of the net. The net body is made of monofilament webbing that usually has a vertical profile between the floatline and leadline of two meters and a mesh size of about 15 cm. Each net is 91 m (50 fathoms) long. In the Gulf of Maine demersal gillnets are usually set in a continuous string of 10 to 12 nets that total 914 to 1,097 m (500 to 600 fathoms). A single vessel generally sets five or six strings, thus occupying a considerable linear distance along the ocean floor.

Increased fishing effort is usually followed by increased gear losses, and unintended stationary fishing gear such as gillnets are subject to high loss rates. Derelict or ghost gillnets result from storms, entanglement with mobile gear and other causes. Evidence exists that these ghost gillnets continue to catch fish and crustaceans for years and may seriously affect certain fish species (Way, 1977).

These beliefs and observations developed into charges voiced by the fishing industry before the New England Fishery Management Council. The Council, in turn, requested the National Marine Fisheries Service and the National Undersea Research Program to investigate the ghost net issue and provide information on the gillnet fishery to guide its decision-making, and to take proper action, if necessary, to mitigate gear conflict and the impact of derelict gillnets.

A three year study was conducted from 1984-1986 by NMFS, the National Undersea Research Program at the University of Connecticut, and the Massachusetts Division of Marine Fisheries. Its purpose was to determine the magnitude of the ghost gillnet problem and the likely impact of these nets on groundfish (cod, pollock, haddock, flounder and lobster). The survey covered Jeffreys Ledge and Stellwagen Bank, two traditional commercial gillnet grounds that have been the center of the controversy between recreational and commercial fishermen (Fig. 1).

## METHODS

The survey was undertaken with two submersible systems: The Johnson Sea-Link II with the R/V Edward Link and R/V Seward Johnson was used in June, 1984 and June, 1985. The submersible Delta with the R/V Atlantic Twin was used in June, 1986. Both systems employed direct underwater communications and underwater tracking systems that gave the surface vessel a continuous report on the position of the submersible and therefore the positions of ghost gillnets.

The first year effort established techniques appropriate for a submersible survey and study of ghost gillnets and gillnet fishing areas. We deployed the submersible at sites that had reported ghost gillnets. When we found gillnets, we identified the

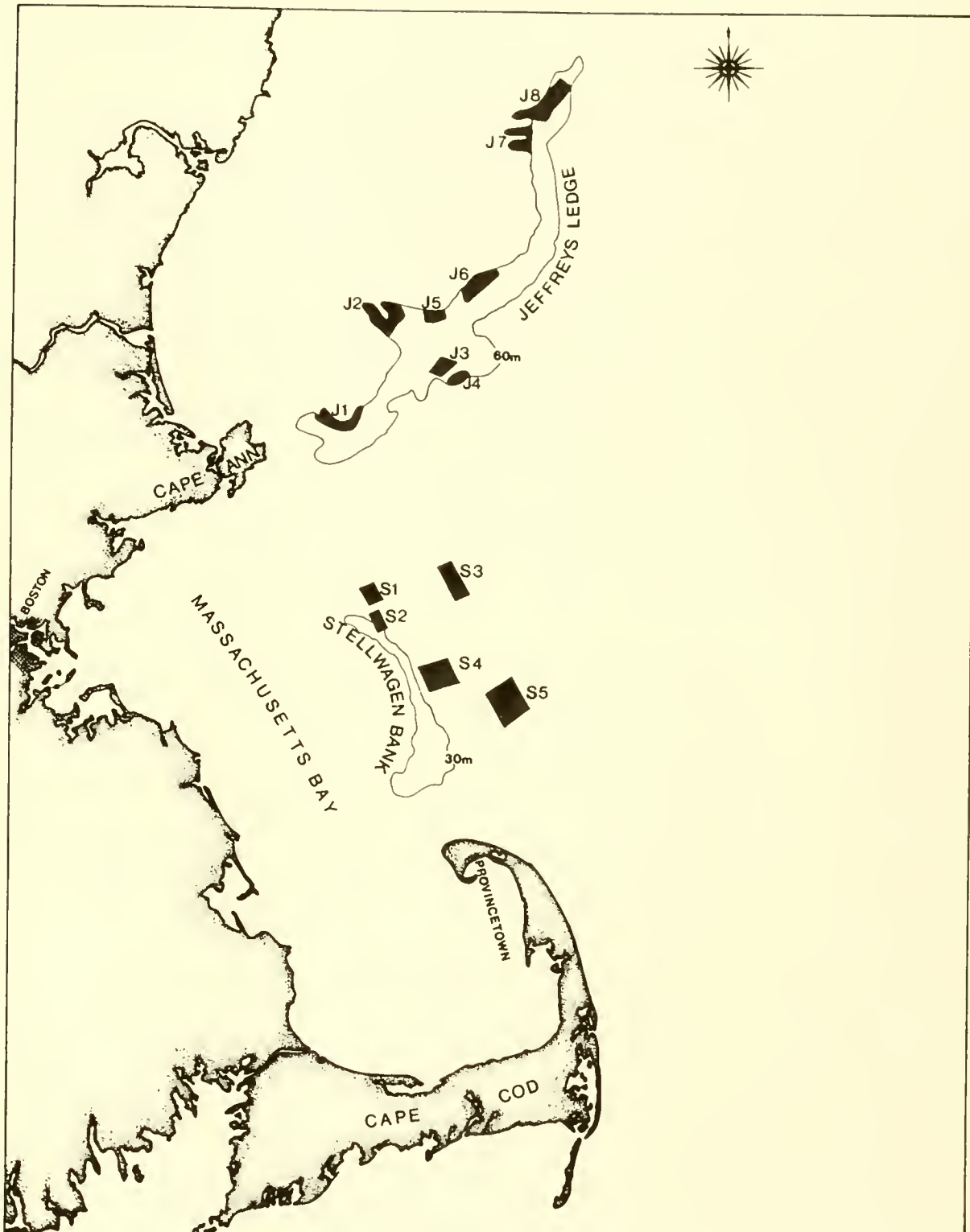


Figure 1: Location of traditional gillnet fishing areas on and within the vicinity of Jeffreys Ledge and Stellwagen Bank, Gulf of Maine. Eight (8) gillnet areas are defined for Jeffreys Ledge (J1--J8) and five (5) for Stellwagen Bank (S1-S5). Manned submersible dives were conducted within most of these gillnet areas.

location and dimensions of the net using Loran C fixes. We documented important net characteristics and the catch in the nets using still photography and color video with onsite narration by the scientific observer. The primary observations made were on net vertical profile, net integrity, fouling, species caught in the net, catch frequency by species, and fate of those species caught.

The second and third year work quantitatively surveyed Jeffreys Ledge and Stellwagen Bank, respectively. Jeffreys Ledge is a fishing area that is well-defined on a chart by depth contours. We identified eight survey areas on Jeffreys Ledge as sites that commercial gillnet fishermen traditionally fished over the past 10-15 years (Fig. 1). These sites were identified through interviews with gillnet, dragger, and recreational fishermen who fish Jeffreys. Stellwagen Bank is not easily defined by depth contours; therefore we identified this area only by the location of the traditional fishing grounds. Five survey areas were identified as traditional commercial gillnet fishing areas on or near Stellwagen Bank (Fig. 1).

The number of submersible transects in each area was determined by the number of submersible dives available in a given year and the relative size of each specific traditional gillnet area. Each submersible transect (ideally) was planned to be two nautical miles in length, but segmented into four half-mile legs, each requiring a change of direction. Each transect began at the periphery of the study area and went from a deeper depth to a shallower depth for efficient observational use of the submersible. The periphery of each area was divided into 1/4 nautical mile segments that were numbered consecutively (Fig. 2). We used a table of random numbers to determine at which segment the transects would start.

The submersible followed the ideal transect as close as possible. Position and courses were provided by the surface support vessel through frequent fixes of the submersible location. We decided that if we found many gillnets, we would modify the submersible's course alternatively left or right to survey, using full video documentation, that portion of the gillnet to its termination. We would then assume that we had surveyed 50% of each gillnet found. The submersible would then resume a course parallel to its original course and complete the transect. If one or two gillnets were found, the submersible would survey the total net and then resume a parallel transect.

During the 1985 and 1986 surveys, we returned to two nets found the first year (1984) on Jeffreys Ledge so that more data could be gathered on their profile, catch, and likely impact. These were ghost nets whose locations were known to sport fishermen. They were not included in the quantitative survey. Another survey was carried out in July 1986 using the unmanned

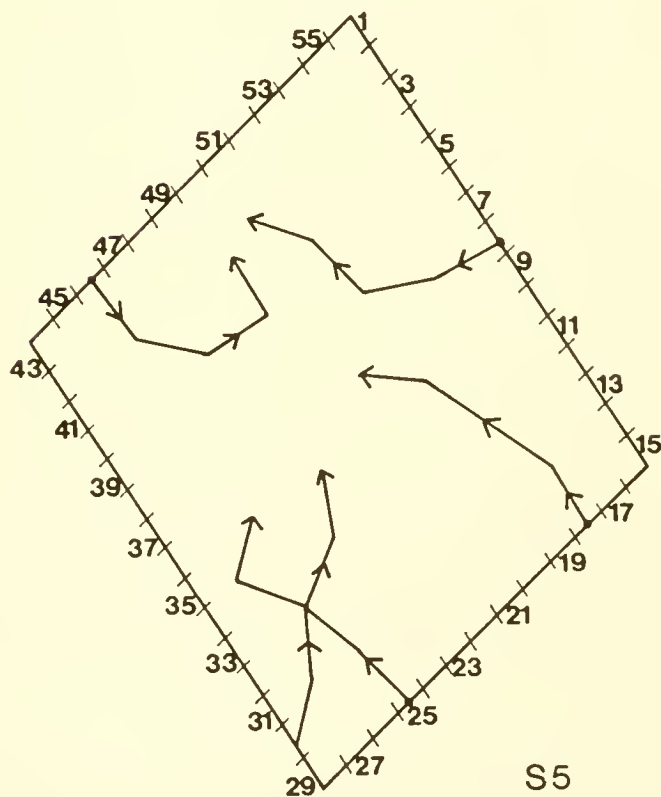
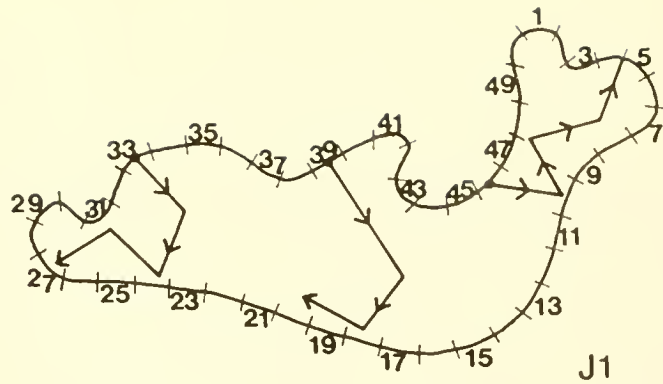


Figure 2. Schematic of two (2) traditional gillnet fishing areas J1 (Jeffreys Ledge) and S5 (Stellwagen Bank). Note the consecutively numbered 0.25 nm intervals marked along the perimeters of the fishing areas and the "idealized" 2 nm submersible transects defined to survey for ghost gillnets. Each transect was established by selecting a one or two digit number from a table of random numbers and directing the transect through the area to maximize area coverage, generally working in an upslope or constant depth direction.

vehicle Mini Rover II to re-examine a ghost gillnet found during the June, 1986 quantitative survey.

## RESULTS AND DISCUSSION

Twenty-four submersible transects were completed in the quantitative survey of ghost gillnets during June, 1985 and June, 1986, fourteen on Jeffreys Ledge and ten on Stellwagen Bank. The Jeffreys Ledge transects ranged in depth from 30 to 127 m and averaged 0.5 nm linear distance over the ocean floor. With the mean visibility at 6.4 m we surveyed approximately 0.1 nm<sup>2</sup> or 92 acres. Bottom habitats encountered on Jeffreys within the survey sites can be categorized into five distinct types:

1. Slope of ledge - clay, silt substrate with Cerianthus (anemone like anthozoan) as the dominant megabenthic fauna.
2. Slope and ledge top - scattered rocks and boulders on a silt-clay substrate.
3. Ledge top - cobble, gravel substrate with a scattering of boulders, up to 1 m in diameter.
4. Ledge top - boulder fields with occasional large boulder mounds.
5. Ledge top - granite bedrock substrate.

During the Johnson Sea-Link transects on Jeffreys Ledge, we found two 20 mm trawl wires, one 5-8 m piece of braided nylon netting, two derelict longlines, a series of overturned boulders and rocks, and one 10 m piece of gillnet. The gillnet was attached to the bottom by the leadline and floating up diagonally toward the surface. It had a vertical profile of 2 m or more (similar to an actively-fished commercial gillnet). No catch or evidence of catch was observed in or at the base of the net.

The Delta dives on Stellwagen Bank ranged in depth from 30 to 107 m and averaged a distance of 0.6 nm. The mean visibility was about 6.4 m and the total bottom surveyed was approximately 94 acres or 0.1 nm<sup>2</sup>. Bottom type was similar to Jeffreys Ledge except for a larger component of sand on the bank and a lack of granite bedrock.

The 700 m long ghost net, discovered during the June, 1986 survey on Stellwagen Bank, lay on the bottom that was primarily a boulder field at a depth of 77 m; one end of the net did reach onto a smooth silt-clay substrate. This ghost net had a vertical profile averaging 0.5 m with a maximum profile of one meter. Most of the net, including the webbing, was covered with a heavy

filamentous growth, although we did observe some irregular shaped clear mesh areas, usually with an entangled fish or shark in the center of the clear area (Fig. 3). The catch in the net was predominantly dogfish, Squalus acanthius, with more than 37 individuals caught in the net. The dogfish were in various stages from live to a stage where only the notochord remained. Other species caught and their respective numbers observed in the net were bluefish, Pomatomus saltatrix, (2 dead); lobster, Homarus americanus, (6 alive); spider crab, Lithodes sp., (2 alive); cancer crab, Cancer borealis/irroratus, (36 alive); and the skeletal remains of one large (35 pounds or more) unidentified bony fish, probably a cod, Gadus morhua or pollock, Polachius virens. Hagfish, Myxine glutinosa, were often seen preying on the dogfish and bluefish.

Figure 3 portrays a "typical" 10 m section of the 700 m ghost gillnet discovered in June 1986 on Stellwagen Bank showing a number of net conditions, i.e. stretched horizontal, wrapped around boulders and rocks, and vertical twists. The horizontal portion had a maximum verticle profile of one meter. Vertical twists rose to a vertical profile of three meters. Dogfish (1,6) were the most frequent vertebrate species caught. Dogfish remains (3) and other finfish (9) and exoskeletal remains were also observed. A filamentous growth was observed on most of the exposed webbing except in the immediate vicinity of live sharks and finfish, whose "thrashing about" movements tended to maintain a clear mesh area. Other growth on the net, especially the floatline, included the stalked ascidian (2), sponge (5) and the anemone (8). Finfish such as the sea raven (7) were found to take shelter in folds of the net without being entangled.

In July, 1986 we revisited the 700 m ghost net one month after its discovery, with the unmanned vehicle Mini Rover Mark II. A survey of 130 m of this net indicated the vertical profile, averaging 0.5 m, remained the same. There were no live or recently deceased fish or crustaceans in this portion of the net. Only the remains of several dogfish (notochords) were visible. Hagfish were still frequently observed near the net.

The most seriously impacted species we observed was the lobster. This impact relates to the economic importance of the lobster to the commercial fishing industry rather than to the actual numbers observed in the ghost net. During the two visits to the net we observed 3-7 lobsters caught. We presumed that once caught in the net they perished. However, each of these lobsters demonstrated some degree of mobility while snared in the net; with the high abundance of fouled invertebrates on the mesh of the net and the abundance of invertebrates in the immediate vicinity of the net it is entirely possible that these lobsters could feed and survive for weeks and perhaps months.

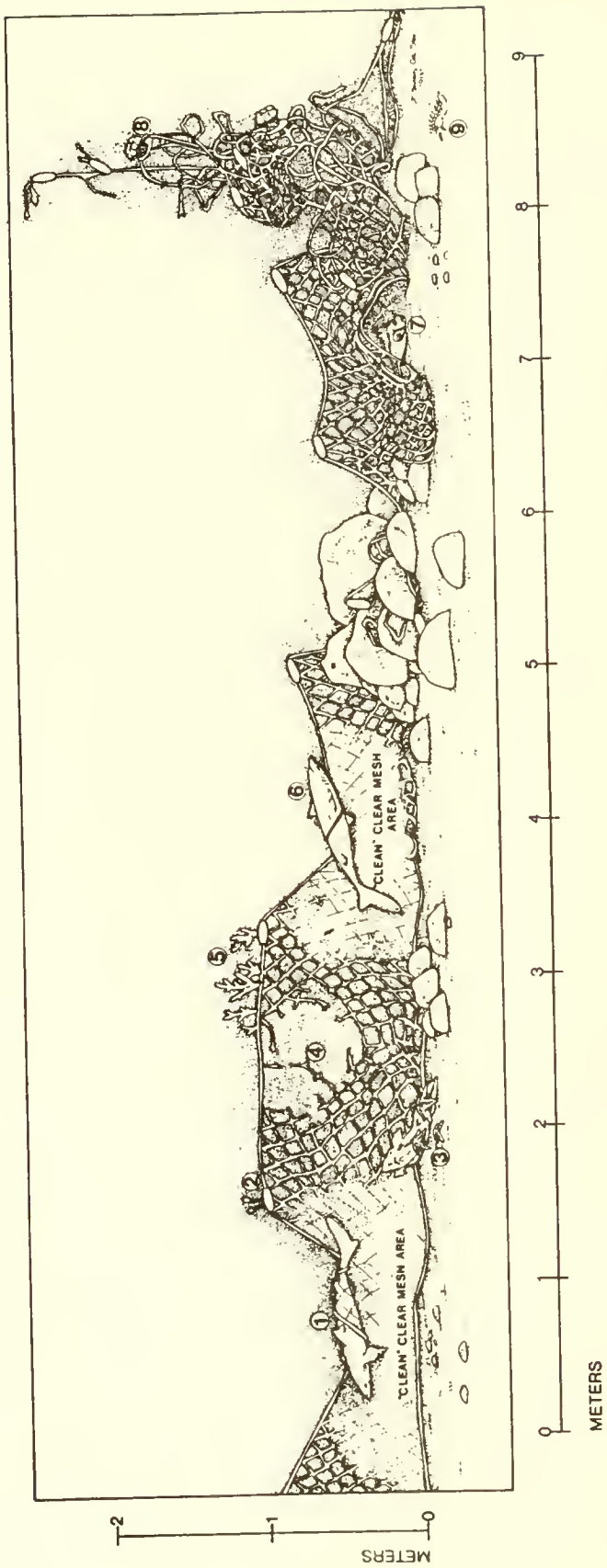


Figure 3. Schematic of a "typical" 10 m section of the 700 m ghost gillnet discovered in June, 1986 on Stellwagen Bank.

A 470 m long ghost net, first observed in June, 1984 was resurveyed for two consecutive years with Johnson Sea-Link and Delta. The vertical net profile during the first year of study varied from < 0.2 to 1.0 m and in the succeeding years from < 0.2 to 0.7 m. Dogfish was the predominant vertebrate species caught in the net; cancer crabs represented the most common invertebrate catch (Table 1). Oceanpout, Macrozoarces americanus, cunner, Tautogolabrus adspersus, and redfish, Sebastes marinus, were frequently seen near the net, but none were observed caught in the net.

Codfish were not seen in the ghost gillnet, nor were there identifiable remains of cod seen at the base of the net. Fishermen in the area notified us each year on the timing of the decrease in cod and increase in dogfish several weeks prior to our survey. Cod were not present during any of the surveys. However, if the ghost nets observed had caught cod within a month prior to our survey, at a time when cod were known to be in our study area, we would expect to find skeletal remains within or at the base of the net. We observed on only one occasion the skeletal remains of a fish belonging to the gadid family. Since cod are an economically important species associated with the New England area and one of the key species targeted by commercial gillnet fishermen, this observation is important. Impact of these ghost gillnets on juvenile groundfish, other than flatfish, should be minimal because of the size of the mesh ( $\approx 15$  cm) and its selectivity (Stewart, 1987; Kawamura, 1972).

Both the 470 m and 700 m ghost nets were stretched out in a horizontal mode. Ghost nets found in this configuration appear to have greater impact on the fishery resources than those nets that are twisted into a more vertical, "balled-up" configuration. During the first year of the study fishermen identified ten ghost gillnets which we examined; four were twisted into a vertical tight bundle, four were stretched out horizontally, and two nets (Fig. 4) had a combination of vertically-aligned twists and horizontal lengths. Within these ten nets one dogfish was observed caught in a vertical bundle: a greater number of species and individuals of a given species were found in the stretched horizontal sections.

Net-animal-substrate interactions are portrayed in Figures 3 and 4, which present typical ghost gillnet configurations and related animal associations (entangled, taking shelter, and attached to) as documented on color video. A higher than normal concentration of animals are illustrated to portray various aspects of the ghost gillnet problem. Figure 3 illustrates distinct net profiles, stretched horizontal, wrapped around boulders and rocks, and vertical twists. The horizontal stretched sections of net had a vertical profile of one meter or less. Vertical thrusts in these nets rose to a profile of 2.5 to 3.0 meters. Dogfish were the most frequent vertebrate species caught; they usually became wedged or

Table 1. Species catch frequency in the 470 m long ghost gillnet on Jeffreys Ledge observed June 1984, 1985, and 1986.

<u>Species</u>	<u>Catch Frequency</u>		
	1984	1985	1986
Dogfish	48	23	5
Skate		2	1
Wolffish	4		1
Sea raven	4		2
Pollock		1	
Bluefish		1	
Flatfish		2	
Unidentified fish		14	
Lobster	4	3	7
Cancer crabs	31+	27+	61
Spider crabs			1

gilled in the webbing, then twisted the net up by rolling which resulted in a reduced vertical profile and a webbing cleared of a filamentous growth. This filamentous growth occurred on at least 75% of the net. Stalked ascidians and sponges were attached to and growing on the net float lines; these sedentary species permit us to age (approximate minimal estimate) the ghost nets. Several species of finfish (sea raven, sculpin, wolffish) were observed taking shelter in folds of the net without becoming entangled. Two species of starfish were observed feeding on the carcasses of entrapped animals.

Figure 4 shows a typical ghost net section 7 m long with a vertical twist buoyed about 3 m above the ocean floor and a horizontal stretched section of net with an entrapped lobster (6), two groundfish fishing jigs (3), and a jagged hole 1-2 m. The lobster was caught by the telson (tail) yet demonstrated an ability to move 0.5 m in several directions giving it the ability to scavenge for food while entrapped. Numerous starfish (1) and rockcrabs (2) were attracted to the remains of animals dropping from the net. One wolffish (4) was video-taped escaping entanglement from the net; this species also is attracted to entangled fish and crustaceans in the net. The floats, frequently fouled with stalked ascidians (5), of the floatline appear to hold portions of the net up off the bottom, enabling the net to continue fishing in a reduced capacity.

An estimate of ghost gillnet abundance for Jeffreys Ledge and Stellwagen Bank was made based on the density of ghost nets found during the quantitative surveys in 1985 and 1986, the area surveyed by manned submersibles and the total area of traditional gillnet fishing grounds (Fig. 1). Ghost gillnets found in 1984, with the assistance of commercial and recreational fishermen, were not included in the assessment of ghost net abundance. The following assumptions have been made prior to calculating net abundances:

1. Traditional gillnet fishing grounds (Fig. 1) cover approximately  $64 \text{ nm}^2$  of ocean floor.
2. Area surveyed by submersibles in 1985 and 1986 equals  $0.2 \text{ nm}^2$ .
3. During the 24 submersible transects conducted in 1985 and 1986 approximately 710 m of ghost gillnets were documented (one 700 m gillnet from Stellwagen Bank and one 10 m net from Jeffreys Ledge).
4. One standard gillnet is 91 m long; generally 10 to 12 nets comprise one gillnet set.

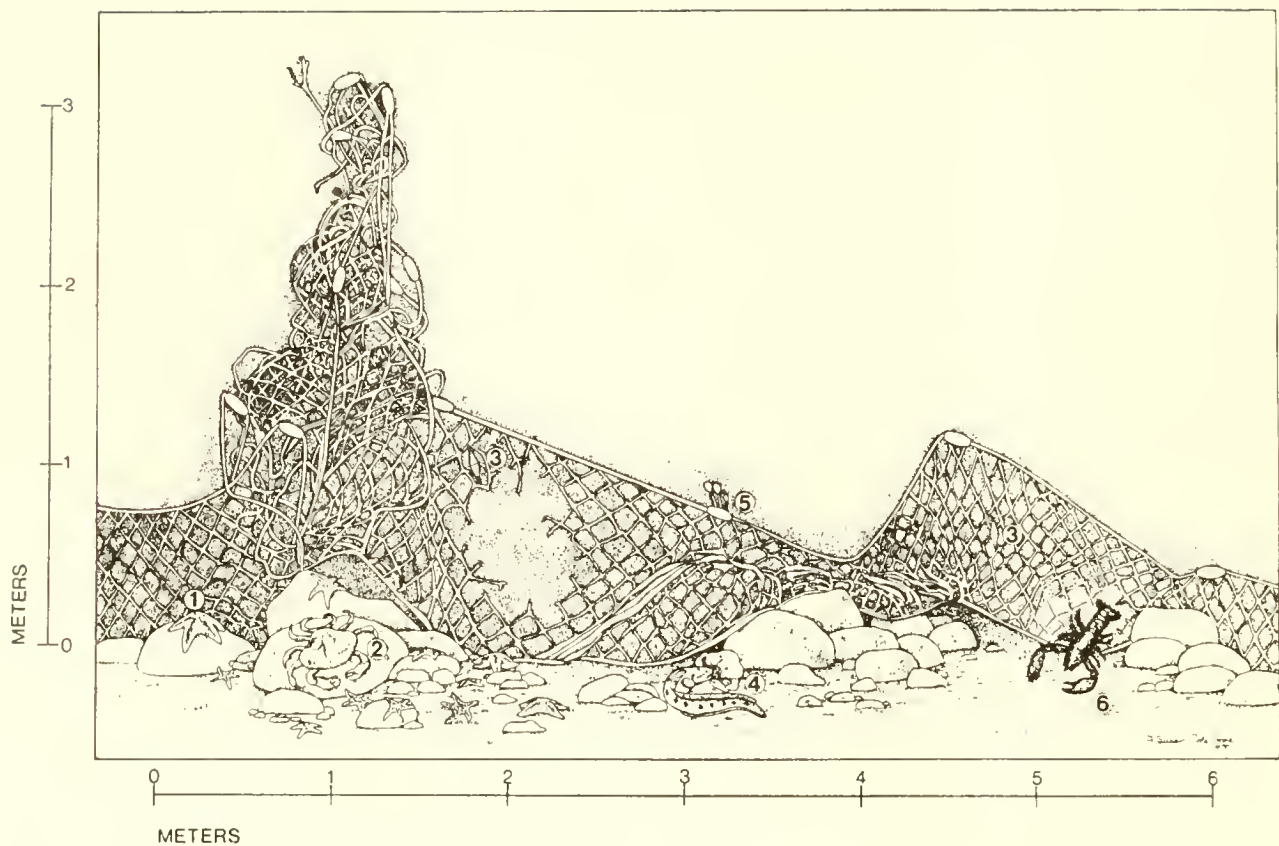


Figure 4. Typical ghost gillnet which continues to fish in a reduced capacity.

Based on the above the following calculations have been made.

$$\frac{64 \text{ nm}^2}{0.2 \text{ nm}^2} = \frac{X \text{ m ghost nets in traditional grounds}}{710 \text{ m ghost nets documented during submersible surveys}}$$

$$(0.2 \text{ nm}^2)(X) = (64 \text{ nm}^2) (710 \text{ m net})$$

X = 227,200 m ghost net or, 2,497 nets or, 250 sets at 10 nets per set; if 12 nets set then 208 sets.

We therefore estimate there are approximately 250 sets of ghost gillnets, or 2,497 nets, lying on the ocean floor of Jeffreys Ledge or within the vicinity of Stellwagen Bank. This estimate is based on the assumption that all ghost gillnets of these two commercial fishing banks are located within the 64 nm<sup>2</sup> defined as traditional commercial gillnet fishing areas. Because of the sightings of only two ghost nets during the quantitative survey and the great variation in lengths of these nets an estimate of the confidence limits about our ghost net abundance estimate of 2,497 nets is not warranted.

We believe that the net abundance estimate of 2,497 is not substantial. We expected during the process of gathering information and data prior to the submersible surveys to document many more ghost gillnets. To attain an estimate of ghost gillnet abundance with reasonably "tight" confidence limits would require a submersible survey of much greater magnitude than was conducted in 1985 and 1986 or is likely to be possible in the near future, given current costs of such operations.

Approximate age of ghost gillnets was estimated at the time of net sighting based on the degree of invertebrate fouling, specifically the sizes of the stalked ascidian, Boltenia ovifera (Figs. 3 and 4). We estimate all of the ghost nets observed from 1984 to 1986 were at least 4 years old (time since the last set) and most were probably 7 years and older. None of the nets appeared to be recently lost nets. All nets found were seen to be fixed to the bottom in such a manner that they could only be retrieved with great difficulty. We believe that most of these nets were lost around 1980 when the commercial gillnet fishery was most active and was comprised of fishermen with relatively little experience. Gillnet losses today are much less and not due to inexperience as much as conflict with mobile gear.

Based on the results of this study, our direct observations of net configuration and net-substrate-animal interactions we present the following recommendations:

1. Overall gillnet fishing procedures should be addressed to minimize net loss.
2. If a given degree of net loss (to be determined) appears unavoidable within the gillnet fishery then the use of biodegradable floats should be mandated. Floats on the gillnet maintain the verticle profile of the net and thus its continued fishing in a ghost mode.
3. Retrieval of ghost nets, given the manner in which they are fixed to the bottom, would be a very difficult and costly procedure.

#### LITERATURE CITED

Collins, J.W. 1882. Gillnets in the cod fishery: A description of the Norwegian cod nets, with directions for their use and a history of their introduction into the United States. Bull. U.S. Fish. Comm., Vol. 1, No. 2, pp. 1: 1-17.

Kawamura, G. 1972. Gillnet mesh selectivity curve developed from length-girth relationship. Bull. Jap. Soc. Sci. Fish., Vol. 38, No. 3, pp. 1119-1127.

Stewart, Peter A.M. 1987. The selectivity of slackly hung cod gillnets constructed from three different types of twine. J. Cons. Int. Explor. Mer., Vol. 43, No. 4, pp. 189-193.

Way, Eric W. 1977. Lost gillnet (ghost net) retrieval project. 1976. Industrial Development Branch, Newfoundland Region, Canada. February, 1977, pp. 1-27.

DOCUMENT  
LIBRARY

Woods Hole Oceanographic  
Institution





